Hawaii Ocean Time-series Data Report 10: 1998

September 1999

Fernando Santiago-Mandujano
Luis Tupas
Craig Nosse
Dale Hebel
Lance Fujieki
Roger Lukas
David Karl

with contributions by
Robert Bidigare
Eric Firing

University of Hawaii
School of Ocean and Earth Science and Technology
1000 Pope Road
Honolulu, Hawaii 96822
U. S. A.

SOEST 99-05

PREFACE

Scientists working on the Hawaii Ocean Time-series (HOT) program have been making repeated observations of the hydrography, chemistry and biology of the water column at a station north of Oahu, Hawaii since October 1988. The objective of this research is to provide a comprehensive description of the ocean at a site representative of the North Pacific subtropical gyre. Cruises are made approximately once a month to the HOT deep-water station (22(45'N, 158(00'W) located about 100 km north of Oahu, Hawaii. Measurements of the thermohaline structure, water column chemistry, currents, primary production and particle sedimentation rates are made on each cruise.

This document reports the data collected in 1998. However, we have included some data from 1988-1997 to place the 1998 measurements within the context of our ongoing time-series observations. The data reported here are a selected subset of the complete data set. Summary plots are given for CTD, biogeochemical, optical, meteorological, thermosalinograph, inverted echo sounder and ADCP observations. The complete data set resides on a Sun workstation at the University of Hawaii. These data are in ASCII format, and can easily be accessed using anonymous file transfer protocol (ftp) via Internet or the World Wide Web (WWW). The entire data set is available at NODC.

ACKNOWLEDGMENTS

Many people participated in the 1998 cruises sponsored by the HOT program. Special thanks are due to Karin Bjorkman, Pat Driscoll, Terrence Houlihan, Markus Karner, Scott Nunnery, Daniel Sadler, Mark Valenciano, and Don Wright which together with some of the authors (FS-M, LT, CN, DH and LF) participated in most of the 1998 cruises. We also thank them for the tremendous amount of time and effort they have put into the program. Special thanks are given to Lisa Lum for her excellent administrative support of the program, to Sharon DeCarlo for programming and data management, Javier Tuason for CTD processing and to June Firing ADCP processing. Ursula Magaard performed many of the core chemical analyses. Karin Bjorkman, Ted Walsh, and Terrence Houlihan together with some of the authors (LT and DH) performed various nutrient and biomass analyses, Don Wright performed the salinity measurements and Man Kit Tsoi provided additional technical support. We gratefully acknowledge the support from Nordeen Larson and Ken Lawson of Sea-Bird for helping us to maintain the quality of the CTD data throughout the HOT program. We also would like to thank the captain and crew members of the R/V *Moana Wave* and the UH Marine Center staff for their efforts, in particular Steve Poulos and Dave Gravatt for shipboard technical assistance on most of the cruises. Without the assistance of these and the many technicians, students and ancillary investigators, the data presented in this report could not have been collected, processed, analyzed and reported. Weather buoy data used in this report were obtained by the NOAA National Data Buoy Center (NDBC) and were provided to us by the National Oceanographic Data Center (NODC). We thank Pat Caldwell for his assistance.

This data set was acquired with funding from the National Science Foundation (NSF) and State of Hawaii general funds. The specific grants which have supported this work are

NSF grants OCE-9303094, OCE-9811921 (WOCE; Lukas and Firing) and OCE-9301368 (JGOFS; Karl, Hebel and Tupas) and the JGOFS sub-components of Michael Landry (OCE-9218152) and Robert Bidigare (OCE-9315311).

1. INTRODUCTION

In response to the growing awareness of the ocean's role in climate and global environmental change, and the need for additional and more comprehensive oceanic time-series measurements, the Board on Ocean Science and Policy (BOSP) of the National Research Council (NRC) sponsored a workshop on “Global Observations and Understanding of the General Circulation of the Oceans” in August 1983. The proceedings of this workshop (National Research Council 1984a) served as a prospectus for the development of the U.S. component of the World Ocean Circulation Experiment (WOCE). US-WOCE has the following objectives:

- To understand the general circulation of the global ocean, to model with confidence its present state and predict its evolution in relation to long-term changes in the atmosphere.
- To provide the scientific background for designing an observation system for long-term measurement of the large-scale circulation of the ocean.

In a parallel effort, a separate research program termed Global Ocean Flux Study (GOFS) focused on the ocean's carbon cycle and associated air-sea fluxes of carbon dioxide. In September 1984, NRC-BOSP sponsored a workshop on “Global Ocean Flux Study” which served as an eventual blueprint for the GOFS program (National Research Council 1984b). In 1986, the International Council of Scientific Unions (ICSU) established the International Geosphere-Biosphere Program: A Study of Global Change (IGBP), and the following year JGOFS (Joint GOFS) was designed as a Core Project of IGBP. US-JGOFS research efforts focus on the oceanic carbon cycle, its sensitivity to change and the regulation of the atmosphere-ocean CO_2 balance (Brewer et al. 1986). The broad objectives of US-JGOFS are:

- To determine and understand on a global scale the time-varying fluxes of carbon and associated biogenic elements in the ocean.
- To evaluate the related exchanges of these elements with the atmosphere, the sea floor and the continental boundaries (SCOR 1990, JGOFS Rep. #5).

In order to achieve these goals, four separate program elements were defined: Process studies to capture key regular events; Long-term time-series observations at strategic sites; A global survey of relevant oceanic properties (e.g., CO_2) and; A vigorous data interpretation and modeling effort to disseminate knowledge and to generate testable hypotheses.

In 1987, two separate proposals were submitted to the US-WOCE and US-JGOFS program committees respectively by scientists at the University of Hawaii at Manoa to establish a multi-disciplinary, deep water hydrostation in Hawaiian waters. In July 1988, these proposals were funded by the National Science Foundation and Station ALOHA was officially on the map (Karl and Lukas 1996). A sister station in the western North Atlantic Ocean, near the historical Panulirus Station, was likewise funded by the US-JGOFS program and is operated by scientists at the Bermuda Biological Station for Research, Inc. (Michaels and Knap 1996).

The primary research objectives of these ocean measurement programs are to establish and maintain deep-water hydrostations for observing and interpreting physical and biogeochemical variability. The initial design called for repeat measurements of a suite of core parameters at approximately monthly intervals, compilation of the data and rapid distribution to the scientific community.

1.1 Hawaii Ocean Time-series Program

The Hawaii Ocean Time-series (HOT) Program consists of several research components lead by scientists at the University of Hawaii at Manoa (Table 1.1). The hydrographic (WOCE) and biogeochemical (JGOFS) components are fully integrated operationally and are both involved in all aspects of planning and execution of HOT Program objectives.

TABLE 1.1. HOT Research Components in 1998

Principal Investigators	Project Title
Roger Lukas	WOCE Core Component
Eric Firing	ADCP Component
David M. Karl, Dale V. Hebel, Luis M. Tupas	JGOFS Core Component
Robert R. Bidigare	Phytoplankton community structure
Michael R. Landry	Zooplankton community structure

1.2 Scientific Objectives for HOT

The primary objective of HOT is to obtain a long time-series of physical and biogeochemical observations in the North Pacific subtropical gyre that address the goals of the US Global Change Research Program. The objectives specific to the WOCE program are to:

- Document and understand seasonal and interannual variability of water masses.
- Relate water mass variations to gyre fluctuations.
- Determine the need and methods for monitoring currents at Station ALOHA.
- Develop a climatology of short-term physical variability.

In addition to these general primary objectives, the physical oceanographic component of HOT provides CTD/rosette sampling support for the JGOFS time-series sampling program, and supports development of new instrumentation for hydrographic observations.

The objectives of HOT specific to the JGOFS program are to:

- Document and understand seasonal and interannual variability in the rates of primary production, new production and particle export from the ocean surface.
- Determine the mechanisms and rates of nutrient input and recycling, especially for N and P in the upper 200 m of the water column.
- Measure the time-varying concentrations of DIC in the upper water column and estimate the annual air-to-sea CO_2 flux.

In addition to these general primary objectives, the HOT Program provides logistical support for numerous complementary research programs (Table 1.2). A complete listing of these projects can be obtained from the HOT-JGOFS World Wide Web page (http://hahana.soest.hawaii.edu/hot/hot_jgofs.html).

TABLE 1.2. Ancillary Projects Supported by HOT in 1998

Principal Investigator(s)	Institution	Agency	Project Title
Mark Abbott and Ricardo Letelier	Oregon State University	NASA	HALE-ALOHA: bio-optics
Edward Boyle	MIT	NSF	HALE-ALOHA: Trace metals
Steven Emerson	Univ. of Washington	NSF	HALE-ALOHA: dissolved gases
Hans Jannasch	MBARI	MBARI	HALE-ALOHA: automated nutrients
Charles Keeling	UCSD Scripps Inst. of Oceanography	NSF	13C/12C Ratio of Atmosphere Carbon Dioxide and Oceanic Carbon in Relation to the Global Carbon Cycle
Paul Quay	Univ. of Washington	NOAA	13C/12C of Dissolved Inorganic Carbon in the Ocean
Francis Sansone	Univ. of Hawaii	ONR	Upper Ocean Methane Dynamics
Ken Smith	UCSD Scripps Inst. of Oceanography	NSF	Organic carbon utilization by deep-sea sediment communities
Jonathan Zehr	Rensselaer Polytech	NSF	Nitrogen Fixation Genes

1.3 HOT Study Site

There are both scientific and logistical considerations involved with the establishment of any long-term, time-series measurement program. Foremost among these is site selection, choice of variables and general sampling design, including sampling frequency. Equally important design considerations are those dealing with the choice of analytical methods for a given candidate variable (especially an assessment of the desired accuracy and precision, and availability of suitable reference materials), the hierarchy of sampling replication and, for data collected at a fixed geographical location, mesoscale horizontal variability.

We evaluated several major criteria prior to selection of the site for the HOT oligotrophic ocean benchmark hydrostation. First, the station must be located in deep water (>4000 m), upwind (north-northeast) of the main Hawaiian islands and of sufficient distance from land to be free from coastal ocean dynamics and biogeochemical influences. On the other hand, the station should be close enough to the port of Honolulu to make relatively short duration (<5 d) monthly cruises logistically and financially feasible. A desirable, but less stringent criterion would locate the station at, or near, previously studied regions of the central North Pacific Ocean, in particular Station GOLLUM. Documentation of oceanic time-series measurements in the North Pacific Ocean can be found in Karl and Winn (1991), Karl et al. (1996b), Karl and Lukas (1996) and in the HOT-JGOFS web page (http://hahana.soest.hawaii.edu/hot/hot_jgofs.html)

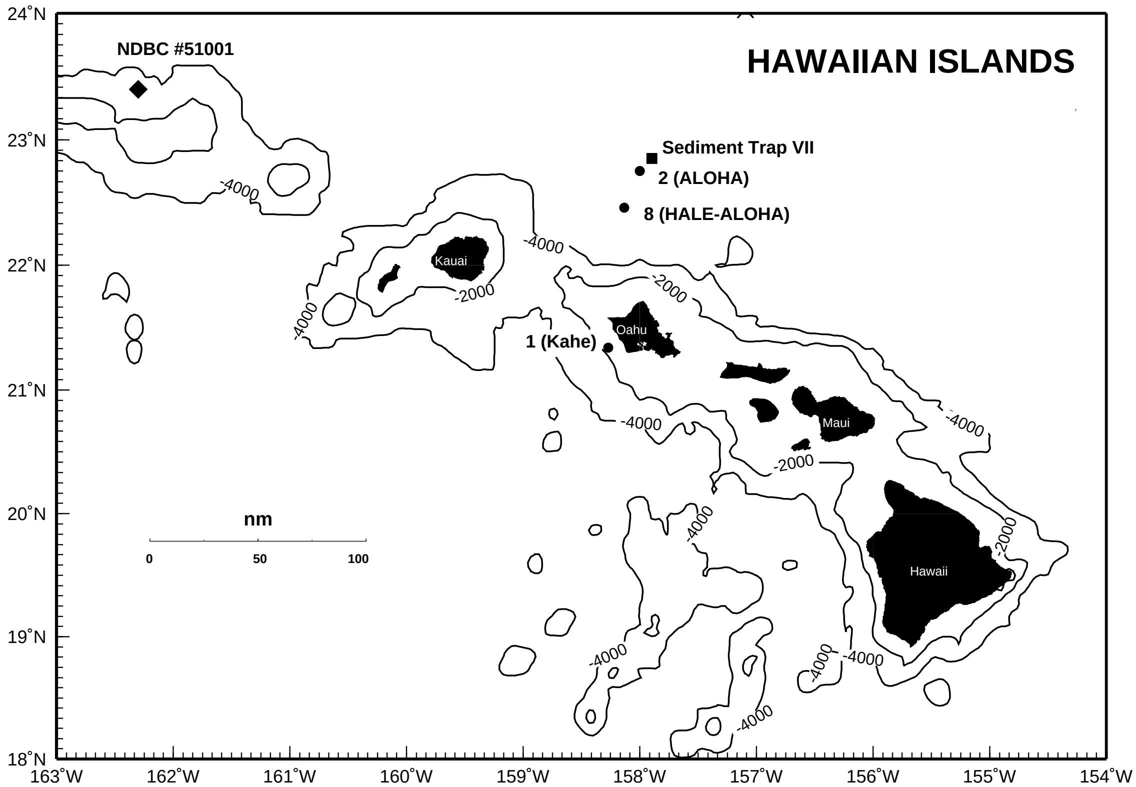

FIGURE 1.1. Map of the Hawaiian islands showing the locations of the HOT stations and the NOAA-NDBC weather buoy #51001.

After consideration of these criteria, we established our primary sampling site at 22° 45' N, 158° W at a location approximately 60 nautical miles north of the island of Oahu (Figure 1.1), and generally restrict our monthly sampling activities to a circle with a 6 nautical mile radius around this nominal site. Station ALOHA is in deep water (4750 m) and is more than one Rossby radius (50 km) away from steep topography associated with the Hawaiian Ridge. We also established a coastal station W-SW of the island of Oahu, approximately 10 km off Kahe Point (21° 20.6' N, 158° 16.4' W) in 1500 m of water. Station Kahe serves as a coastal analogue to our deep-water site and the data collected there provide a near-shore time-series for comparison to our primary open ocean site. Station Kahe is also used to test our equipment each month before departing for Station ALOHA, and to train new personnel at the beginning of each cruise. In January 1997, a physical-biogeochemical mooring was deployed to obtain continuous measurements of various atmospheric and oceanographic parameters. The mooring is located at 22° 28' N, 158° 8' W and was designated as Station HALE-ALOHA. Locations and dates of occupancy of HOT water column and bottom recording stations is available at the HOT-JGOFS web page (http://hahana.soest.hawaii.edu/hot/hot_jgofs.html).

1.4 Field Sampling Strategy

HOT program cruises are conducted at approximately monthly intervals; the exact timing dictated by the availability of research vessels. From HOT-1 (October 1988) to HOT-65 (August 1995), with the exception of HOT-42 and HOT-43 (November and December 1992), each cruise was 5 days in duration (port to port). Beginning with HOT-66 (September 1995) the standard HOT cruise was reduced by 20% to 4 days (port to port) in order to accommodate the additional mooring-based HOT field programs within a fixed per annum allocation of ship days.

From HOT-1 (October 1988) to HOT-32 (December 1991), underway expendable bathythermograph (XBT; Sippican T-7 probes) sampling was conducted at 7 nautical mile spacing on the outbound transect from Station Kahe to Station ALOHA. These surveys were later discontinued because the space-time correlation of the energetic, internal semidiurnal tides made it difficult to interpret these data. From February 1995 until December 1997 we added an instrumented, 1.5 m Endeco towfish package (Sea-Bird CTD, optical plankton counter, fluorometer) to our sampling program (Tupas et al. 1997). Upper water column currents are measured both underway and on station using a hull-mounted Acoustic Doppler Current Profiler (ADCP), when available (Firing 1996). The majority of our sampling effort, approximately 60-72 hours per standard HOT cruise, is spent at Station ALOHA. Underway near-surface measurement of a variety of physical, chemical and biological properties is made possible by sampling seawater through a pumped intake system positioned in the hull of the R/V *Moana Wave*. In May 1995, a thermosalinograph was installed in line to the ship's seawater intake system. In July 1996, the existing system was replaced with a non-contaminating PVC/ stainless steel system. Several new sensors such as an underway surface pCO_2 measuring system and a flow through fluorometer were installed in 1996.

High vertical resolution environmental data are collected with a Sea-Bird CTD having external temperature (T), conductivity (C), dissolved oxygen (DO) and fluorescence sensors and an internal pressure (P) sensor. A Sea-Bird 24-place carousel and an aluminum rosette that is capable of supporting 24 12-l PVC bottles are used to obtain water samples from desired depths.

The CTD and rosette are deployed on a 3-conductor cable allowing for real-time display of data and for tripping the bottles at specific depths of interest. The CTD system takes 24 samples sec^{-1} and the raw data are stored both on the computer and, for redundancy, on VHS-format video tapes. We also routinely collect "clean" water samples for biological rate measurements using General Oceanics Go-Flo bottles, Kevlar cable, metal-free sheave, Teflon messengers and a stainless steel bottom weight. A free-drifting sediment trap array, identical in design to the VERTEX particle interceptor trap (PIT) mooring (Knauer et al. 1979), is deployed at Station ALOHA for an approximately 2.5 day period to collect sinking particles for chemical and microbiological analyses.

Sampling at Station ALOHA typically begins with sediment trap deployment followed by a deep (> 4700 m) CTD cast and a "burst series" of at least 13 consecutive casts to 1000 m, at 3-hr intervals to span the local inertial period (~ 31 hr) and three semidiurnal tidal cycles. The drift track of the sediment trap arrays and the location of the CTD casts for each cruise are shown in Figure 1.2. The repeated CTD casts enable us to calculate an average density profile from which variability on tidal and near-inertial time scales has been removed. These average density profiles are useful for the comparison of dynamic height and for the comparison of the depth distribution of chemical parameters from different casts and at monthly intervals. This sampling strategy is designed to assess variability on time scales of a few hours to a few years. Very high frequency variability (< 6 hr) and variability on time scales of between 3-60 days are not adequately sampled at the present time, except by the inverted echo sounders (see below), and at the mooring.

Water samples for a variety of chemical and biological measurements are routinely collected from the surface to within 5 m of the seafloor. To the extent possible, we collect samples for complementary biogeochemical measurements from the same or from contiguous casts to minimize aliasing caused by time-dependent changes in the density field. This is especially important for samples collected in the upper 300 m of the water column. Furthermore, we attempt to sample from common depths and specific density horizons each month to facilitate comparisons between cruises. Water samples for salinity determinations are collected from every water bottle to identify sampling errors, and for CTD conductivity calibration. Approximately 20% of the water samples are collected and analyzed in duplicate or triplicate to assess and track our analytical precision in sample analysis.

The HOT program was initially conceived as being a deep-ocean, ship- and mooring-based observation experiment that would have an approximately 20-year lifetime. Consequently, we selected a core suite of environmental variables that might be expected to display detectable change on time scales of several days to one decade. Except for the availability of existing satellite and ocean buoy sea surface data, the initial phase of the HOT program (Oct 1988 - Feb 1991) was entirely supported by research vessels. In February 1991, an array of five inverted echo sounders (IES) was deployed in an approximately 150 km^2 network around Station ALOHA (Chiswell 1996) and in June 1992, a sequencing sediment trap mooring was deployed a few km north of Station ALOHA (Karl et al. 1996a). In 1993, the IES network was replaced with two strategically-positioned instruments: one at Station ALOHA and the other at Station Kaena. The IES at Station Kaena was retired in October 1995. Beginning in 1994, a single IES has been positioned and annually replaced at Station ALOHA. In January 1997, the Hawaii Air-sea Logging Experiment (HALE) was initiated with the deployment of a physical-biogeochemical mooring designated as HALE-ALOHA. Details of this mooring can be obtained from the HOT-JGOFS web site (http://hahana.soest.hawaii.edu/hot/hot_jgofs.html).

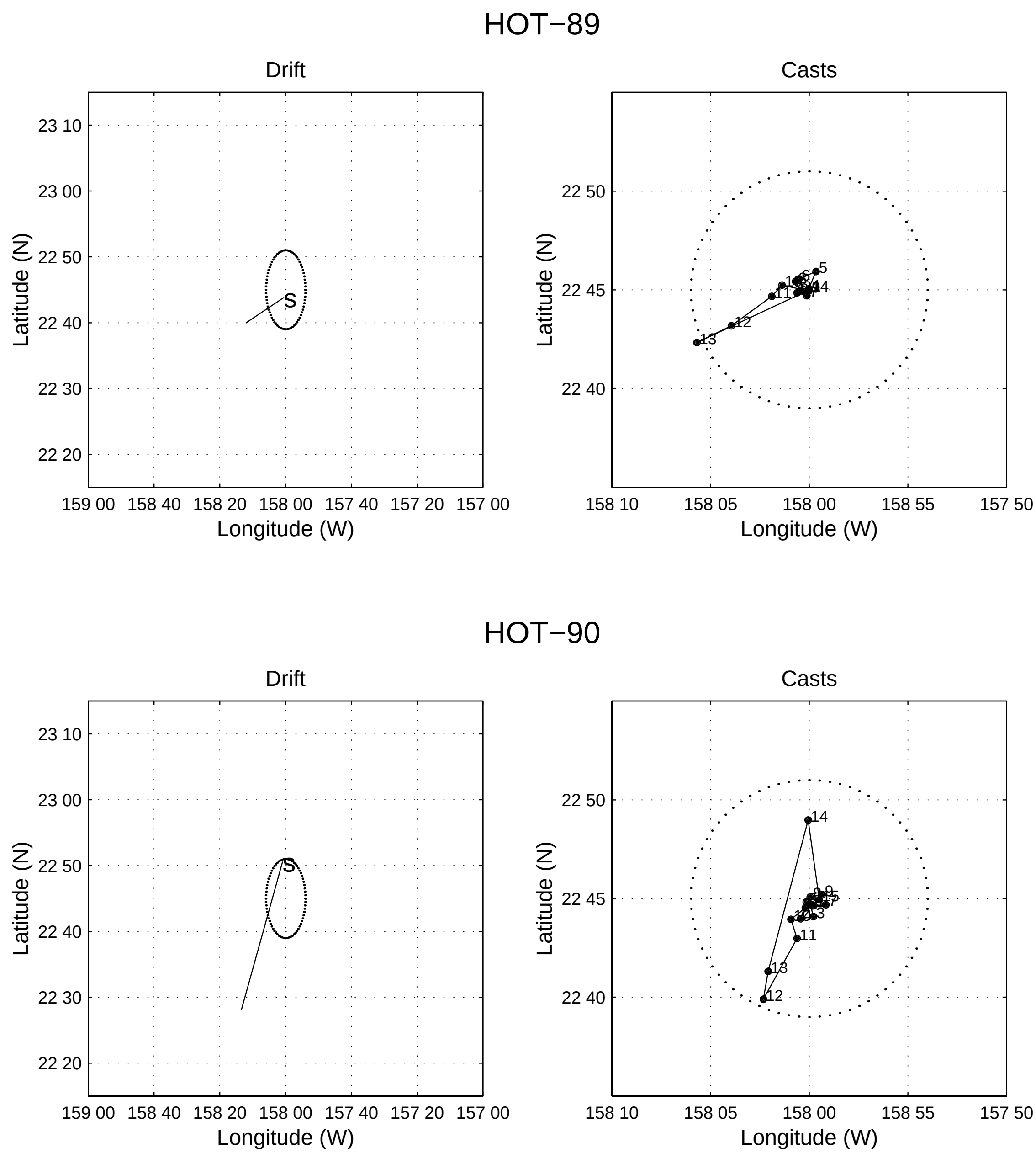

FIGURE 1.2. [Left panels] Drift track of the sediment trap array during each HOT cruise. Starting point indicated by "S". [Right panels] CTD locations during each HOT cruise in 1998. Solid line indicates cast taken in sequence and numbers show the location of each cast. Dashed line shows the 6 nautical-mile radius of the station.

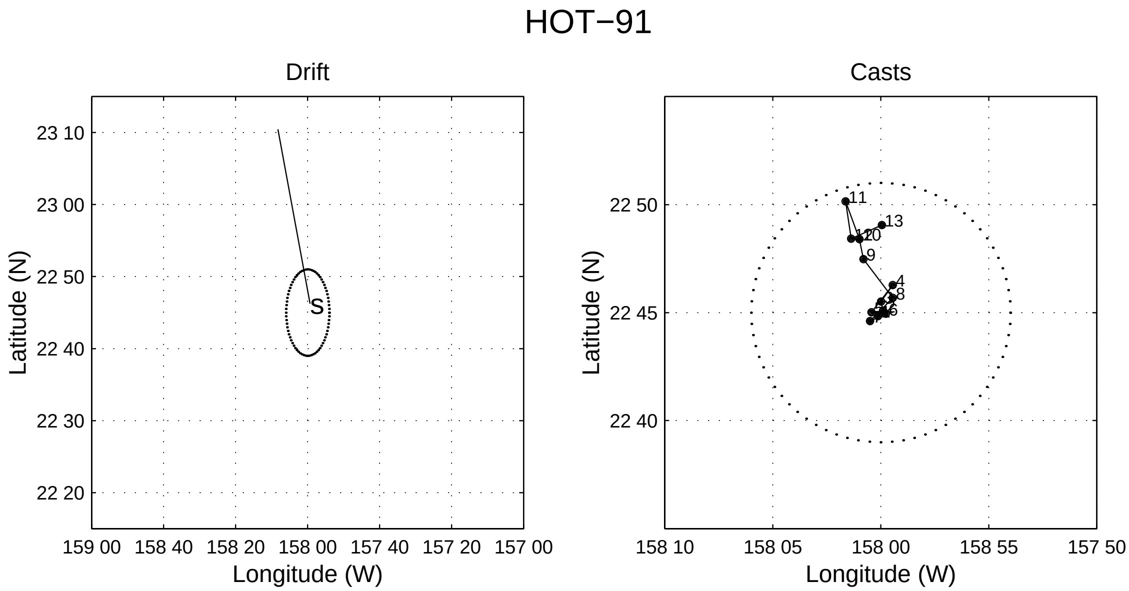

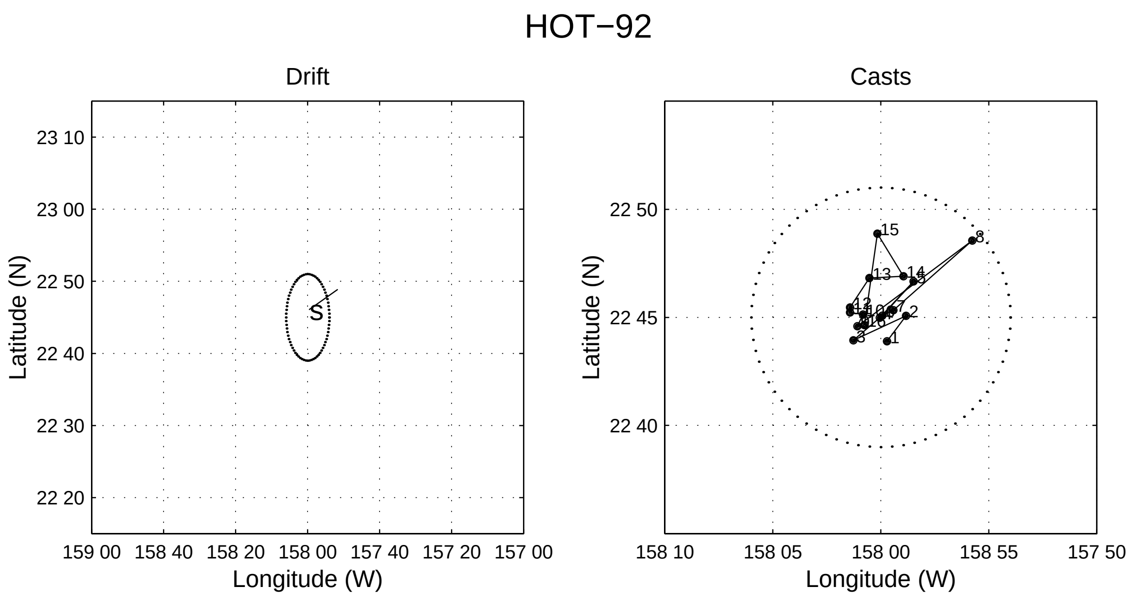

FIGURE 1.2. Continued

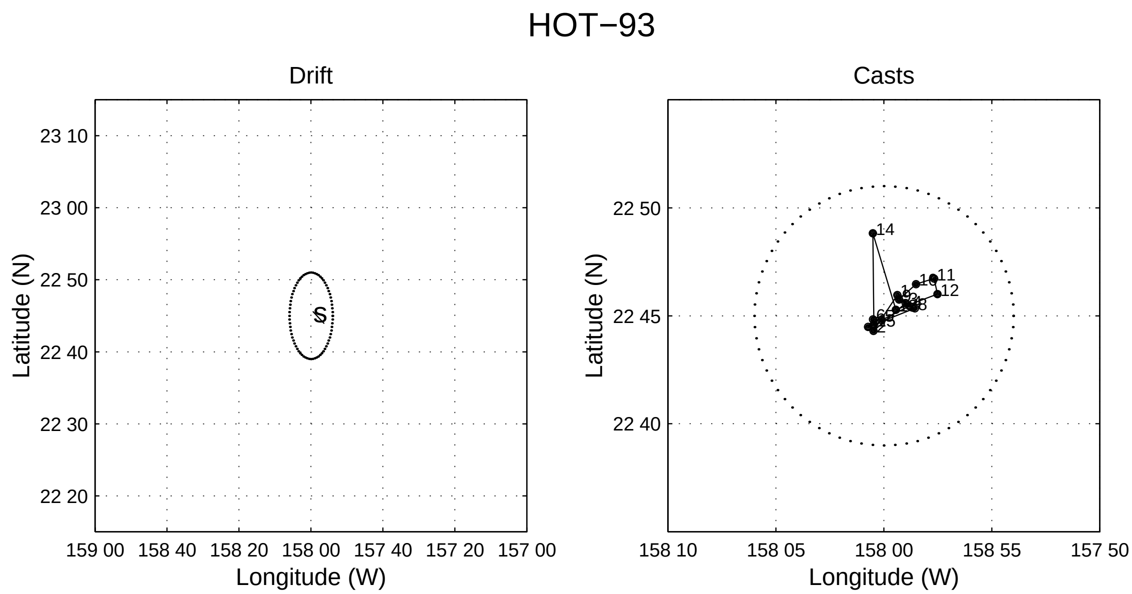

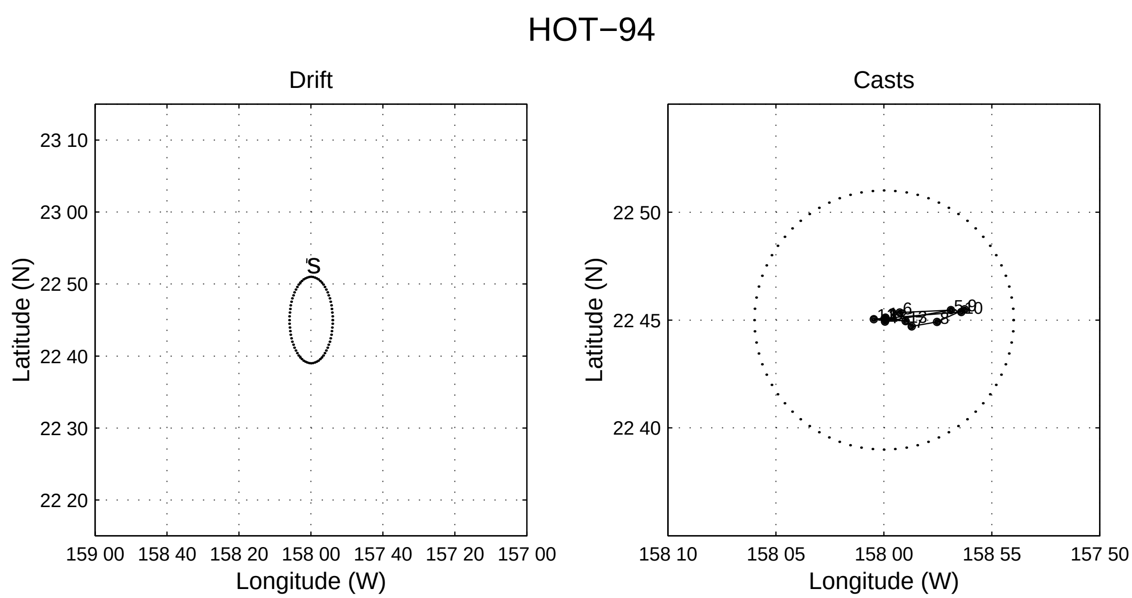

FIGURE 1.2. Continued

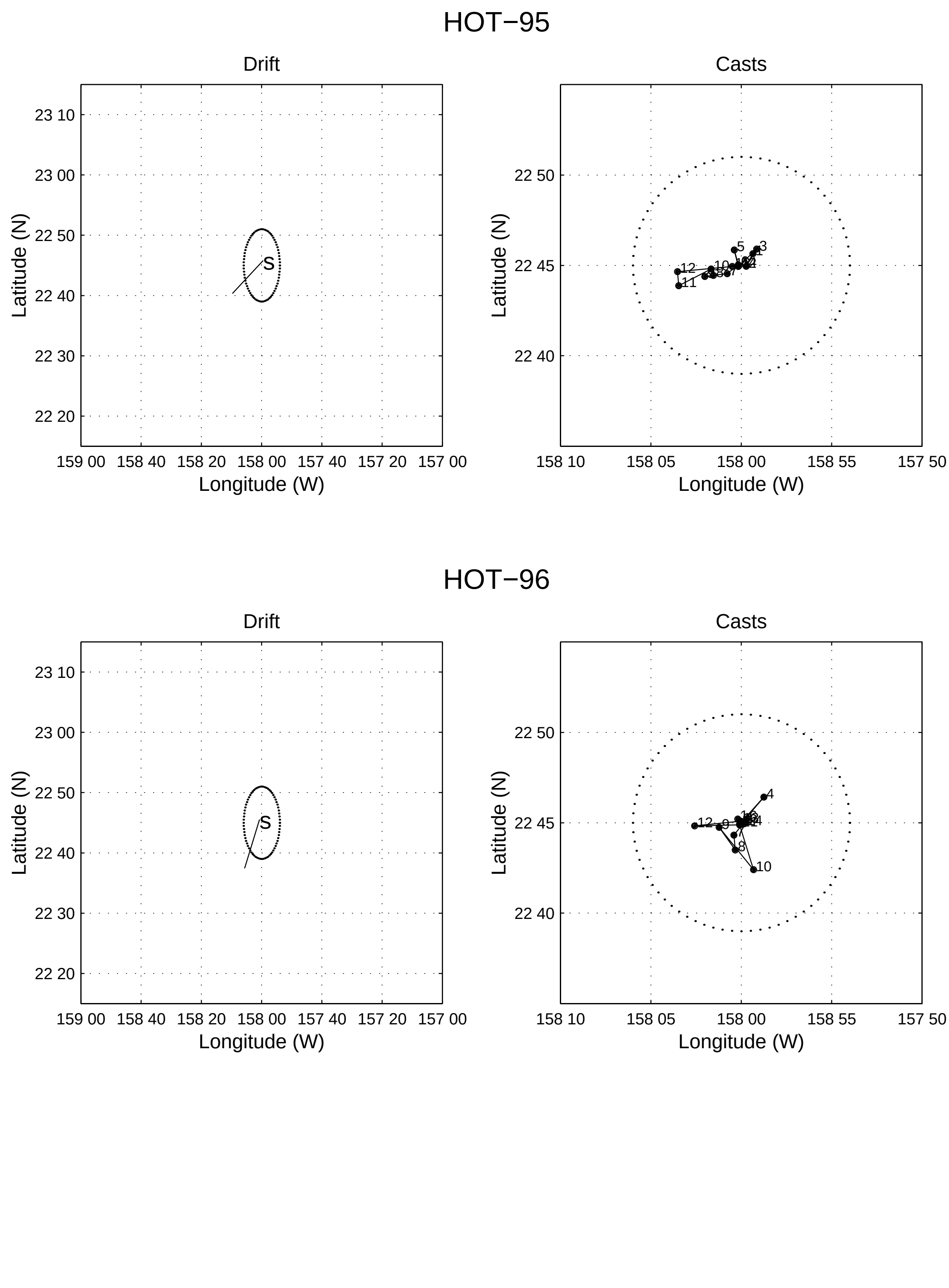

FIGURE 1.2. Continued

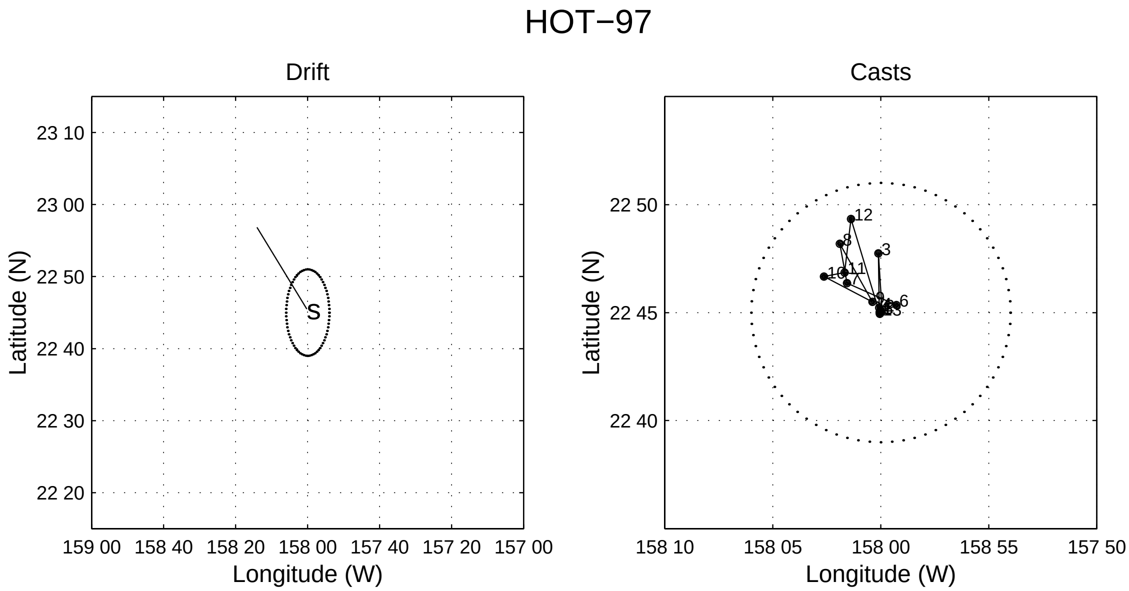

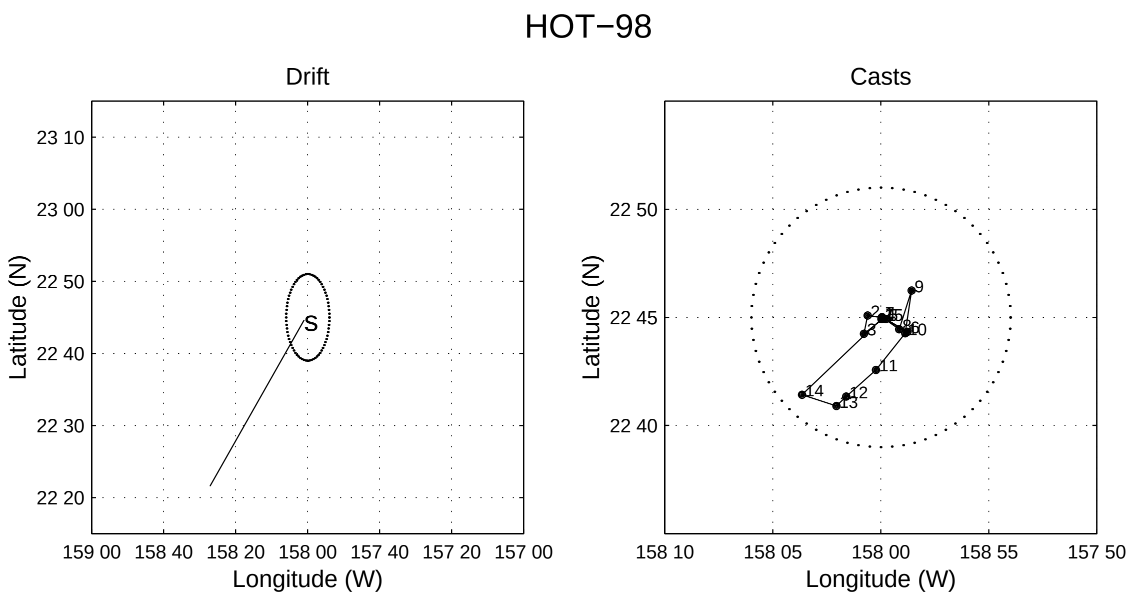

FIGURE 1.2. Continued

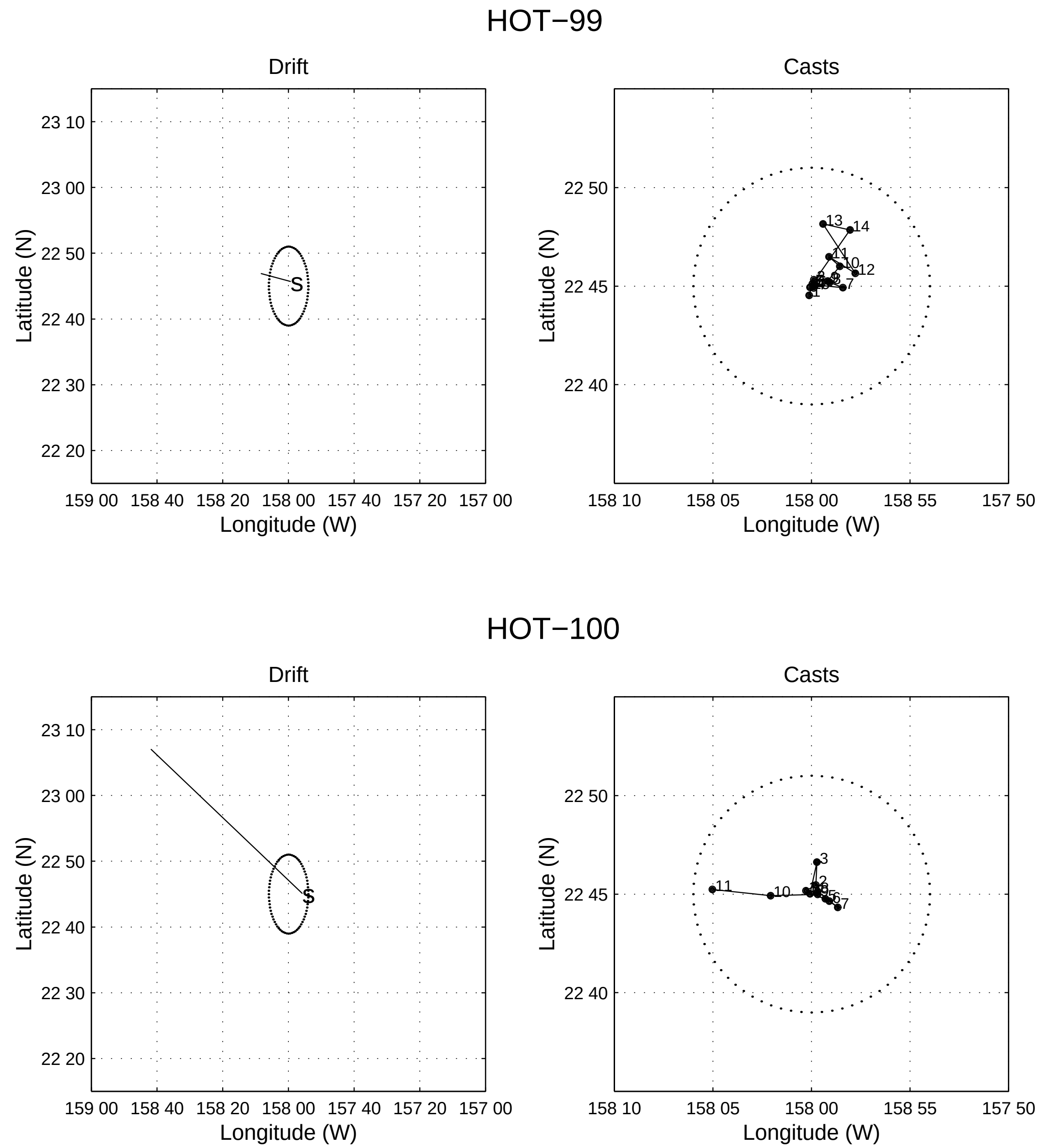

FIGURE 1.2. Continued

1.5 Core Measurements, Experiments and Protocols

The suite of core measurements provides a data base to validate existing biogeochemical models and to develop improved ones. Our list of core measurements has evolved since the inception of the HOT program in 1988, and now includes both continuous and discrete physical, biological and chemical ship-based measurements, *in situ* biological rate experiments, and observations and sample collections from bottom-moored instruments and buoys (Table 1.3). Continuity in the measurement parameters and their quality, rather than continuity in the methods employed, is of greatest interest. Detailed analytical methods are expected to change over time through technical improvements. In addition to the core data, specialized measurements and process-oriented experiments have also been conducted at Station ALOHA (Table 1.3).

TABLE 1.3. Parameters Measured at Station ALOHA

Parameter	Depth Range (m)	Analytical Procedure
I. Continuous Measurements		
Pressure (Depth)	0-4750	Pressure transducer on Sea-Bird CTD package
Temperature	0-4750	Thermistor on Sea-Bird CTD package
Conductivity (Salinity)	0-4750	Conductivity sensor on Sea-Bird CTD package, standardization with Guildline AutoSal using Wormley seawater standard
Oxygen	0-4750	YSI sensor on Sea-Bird CTD package with Winkler standardization
Fluorescence	0-1000	Sea-Tech flash fluorometer
II. Water Column Chemical Measurements		
Oxygen	0-4750	Winkler titration
Dissolved Inorganic Carbon	0-4750	Coulometry
Titration Alkalinity	0-4750	Automated Gran titration
pH	0-4750	Spectrophotometric
Nitrate Plus Nitrite	0-4750	Autoanalyzer
Soluble Reactive Phosphorus (SRP)	0-4750	Autoanalyzer
Silicate	0-4750	Autoanalyzer
Low Level Nitrate Plus Nitrite	0-200	Chemiluminescence
Low Level SRP	0-200	Magnesium-induced coprecipitation
Dissolved Organic Carbon	0-1000	High temperature catalytic oxidation
Dissolved Organic Nitrogen	0-1000	UV oxidation of total nitrogen
Dissolved Organic Phosphorus	0-1000	UV oxidation of total phosphorus
Particulate Carbon	0-1000	High temperature combustion
Particulate Nitrogen	0-1000	High temperature combustion
Particulate Phosphorus	0-1000	High temperature combustion
III. Biomass Measurements		
Chlorophyll a and Phaeopigments	0-200	Fluorometric analysis
Pigments	0-200	HPLC
Adenosine 5'-Triphosphate	0-1000	Firefly bioluminescence
Bacteria and Cyanobacteria	0-200	Flow cytometry
Meso and Microzooplankton	0-200	Net tows, elemental analysis
IV. Carbon Assimilation and Particle Flux		
Primary Production	0-200	"Clean" 14C incubations
Carbon, Nitrogen, Phosphorus	150	Free-floating particle traps

TABLE 1.3. Parameters Measured at Station ALOHA

Parameter	Depth Range (m)	Analytical Procedure
V. Currents		
Acoustic Doppler Current Profiler	10-300	Hull mounted, RDI #VM-150
Acoustic Doppler Current Profiler	10-4750	Lowered ADCP
VI. Bow Intake System		
Temperature	3	Sea-Bird remote temperature sensor
Conductivity (Salinity)	3	Sea-Bird temperature and conductivity sensors inside the thermosalinograph package
pCO_2	3	Gas equilibration, infrared detection
Fluorometry	3	Turner Designs 10-AU
VII. Optical Measurements		
Incident Irradiance	Surface	LI-COR and Biospherical collector
Upwelling and downwelling irradiance	0-175	Biospherical Profiling Reflectance Refractometer PRR-600
VIII. Moored Instruments		
Inverted Echo Sounder	4750	Acoustic telemetry, CTD calibration
Sequencing Sediment Traps	4000	Parflux MK7-21
Physical-Biogeochemical Mooring	Surface to 800	See HALE-ALOHA web site

TABLE 1.4. Chronology of 1998 HOT Cruises

Cruise	Ship	Depart	Return
89	R/V *Moana Wave*	9 January 1998	13 January 1998
90	R/V *Moana Wave*	17 February 1998	21 February 1998
91	R/V *Moana Wave*	16 March 1998	20 March 1998
92	R/V *Moana Wave*	13 April 1998	17 April 1998
HA-3B	R/V *Moana Wave*	18 April 1998	20 April 1998
HA-4A	R/V *Moana Wave*	27 April 1998	30 April 1998
93	R/V *Moana Wave*	11 May 1998	15 May 1998
94	R/V *Moana Wave*	15 June 1998	19 June 1998
95	R/V *Moana Wave*	13 July 1998	17 July 1998
96	R/V *Moana Wave*	8 August 1998	12 August 1998
97	R/V *Moana Wave*	26 September 1998	30 September 1998
98	R/V *Moana Wave*	17 October 1998	21 October 1998
HA-4B	R/V *Moana Wave*	6 November 1998	7 November 1998

TABLE 1.4. Chronology of 1998 HOT Cruises

Cruise	Ship	Depart	Return
99	R/V *Moana Wave*	9 November 1998	13 November 1998
HA-5A	R/V *Moana Wave*	16 November 1998	19 November 1998
100	R/V *Moana Wave*	7 December 1998	11 December 1998
100B	R/V *Moana Wave*	14 December 1998	16 December 1998

This report presents selected core data collected during the tenth year of the HOT Program (January-December 1998). During this period, 12 regular HOT cruises were conducted using the University of Hawaii research vessel *Moana Wave* (Table 1.4). During HOT-100 entanglement of one of the propellers by an abandoned drift net while on station necessitated a return to calm waters for removal, thus the ship came back to the lee of Oahu. The ship then returned to pick up the drifting instruments. The CTD operations interrupted during this cruise were completed during HOT-100B, which included a transit to ALOHA, with a short (19 hour) on station time, then a return to port. Four 2 to 3-day cruises were conducted to service the HALE-ALOHA mooring. The moored sediment trap was also serviced during these cruises in November 1998. University of Hawaii shipboard technical assistance personnel assisted a total field scientific crew of 53 HOT staff, students and visiting scientists (Table 1.5) in our 1998 field work.

The selected measurements reported here are part of a much larger HOT program data set on physical and biogeochemical variability at Station ALOHA that has been collected since October 1988. The complete data set is available to the community by several methods that are described in a subsequent section of this report.

TABLE 1.5. 1998 Cruise personnel

Cruise Participant	Cruises
Albrough, John	100
Baldwin, Roberta	90, 94, 97
Bartlett Jasmine	93
Benitez-Nelson, Claudia	99, 100
Bjorkman, Karin	91, 92, 93, 94, 95, 96, 97, 98, 99, 100
Calbet, Albert	96, 98, 100
Chau, Lisa	92
Christensen, Stephanie	90, 91, 97
Chun, Cecily	96
Cotton, Leslie	91
Donachie, Stuart	91, 92
Driscoll, Pat	89, 90, 91, 92, 93, 94
Falter, Jim	98
Firing, Eric	91
Fujieki, Lance	89, 90, 91, 93, 94, 95, 96, 97, 98, 99, 100
Glatts, Robert	90, 94, 97

TABLE 1.5. 1998 Cruise personnel

Cruise Participant	Cruises
Gravatt, Dave	89, 90, 91, 92, 93, 94, 95, 96, 97, 98, 99, 100
Guidry, Michael	95
Hebel, Dale	89, 90, 91, 92, 93, 94, 95, 97, 98, 99, 100
Hervig, Will	89, 98
Houlihan, Terrence	91, 92, 93, 94, 95, 96, 97, 98, 100
Karner, Markus	89, 90, 91, 92, 93, 94, 95, 97, 98, 99, 100
Landry, Michael	95
Laline, Michael	93
Lopez, Mai	89, 90
Magaard, Ursula	89, 90
Margenau, Kyle	89
Motell, Craig	92
Nosse, Craig	89, 90, 91, 92, 93, 94, 95, 96, 97, 98, 99, 100
Nunnery, Scott	91, 92, 93, 94, 95, 96, 97, 98, 99, 100
Ostrom, Nathaniel	98
Paul, Barbara	92
Popp, Brian	97
Porter, John	91
Poulos, Steve	92, 93, 96, 97, 99, 100
Ramm, Hans	89, 90
Robinson, Donna	89, 94, 95
Rock, Lyndsey	92
Rukowsky, Greg	95, 96
Sadler, Daniel	89, 92, 94, 95, 96, 97, 98, 99, 100
Santiago-Mandujano, Fernando	89, 90, 91, 92, 93, 94, 96, 97, 98, 99, 100
Sato, Toshiko	98
Selph, Karen	89
Scheinberg, Rebecca	99
Shopay, Thomas	96
Slocum, Daryl	91
Smith, Ken	90, 94, 97
Smith, Treda	95
Stahl, Sharon	89, 91, 94, 95
Tupas, Luis	89, 90, 92, 93, 94, 95, 96, 97, 98, 99, 100
Uhlman, Alfred	90, 94
Valenciano, Mark	89, 90, 91, 92, 93, 94, 95, 96, 97, 98, 99, 100
Wright, Don	89, 90, 91, 92, 93, 94, 95, 96, 97, 98, 99, 100

2. SAMPLING PROCEDURES AND ANALYTICAL METHODS

A comprehensive summary of all sampling and analytical methods currently used in the HOT program along with information on measurement accuracy and precision can be found in the "Hawaii Ocean Time-series Program Field and Laboratory Protocols" manual. This document is available on the World Wide Web (http://hahana.soest.hawaii.edu/hot/hot_jgofs.html) or can be obtained in hard copy by contacting David M. Karl [phone: (808) 956-8964; facsimile: (808) 956-5059; electronic mail: dkarl@soest.hawaii.edu]. Brief summaries of methods as well as calibration specifications and quality control / quality assurance information for 1998 are presented in this report. Hydrographic sampling methods are included in "WOCE Hydrographic Sampling Procedure. A primer for ship-board operations at the Hawaii Ocean Time-series Station," and is also available on the World Wide Web (http://www.soest.hawaii.edu/HOT_WOCE).

2.1 CTD Profiling.

Continuous measurements of temperature, salinity, oxygen and fluorescence are made with a Sea-Bird SBE-9/11Plus CTD package with dual temperature, salinity and oxygen sensors and fluorometer described in Tupas et al. (1995).

CTD casts are made at Stations Kahe and ALOHA during each cruise. A CTD cast to 1000 m is made at Station Kahe. At Station ALOHA a burst of consecutive CTD casts to 1000 m is made over 36 hours to span the local inertial period and three semi-diurnal tidal cycles. One WOCE standard cast within 10 m of the bottom is made during each cruise. During HOT-90, 92, 93, 95, 98, 99 and 100 a second deep cast was obtained at Station ALOHA. Station HALE-ALOHA was occupied during all 1998 cruises, except during HOT-99 when the moored buoy was being serviced. One CTD cast to 1000 m is regularly made about 1 nm from the buoy for calibration of Seacats and other instruments attached to the buoy array.

2.1.1 Data Acquisition and Processing

CTD data were acquired at a rate of 24 samples per second. Digital data were stored on an IBM-compatible PC and, for redundancy, the analog signal was recorded on VHS video tapes. Backups of CTD data were made onto Zip disks and later onto DAT tapes. The raw CTD data were quality controlled and screened for spikes as described in Winn et al. (1993). Data alignment, averaging, correction and reporting were done as described in Tupas et al. (1993). Salinity spike rejection parameters were modified for some cruises in 1998 because of rough conditions. Spikes occur when the CTD samples the disturbed water of its wake. Therefore, samples from the downcast are rejected when the CTD is moving upward or when its acceleration exceeds 0.5 m s^{-2} in magnitude. Cruises 89, 90, 92, 93, 98, 99 and 100 were conducted under rough sea conditions, with heavy ship rolling during some of the casts, causing large vertical velocity fluctuation of the CTD package. The acceleration cutoff value had to be increased to between 0.55 and 0.70 m s^{-2} to have points available to average in each 2-dbar bin.

The data were additionally screened by comparing the temperature and conductivity sensor pairs. These differences permitted identification of problems in the sensors. Only the data from one set of T-C sensors and one oxygen sensor, whichever was deemed most reliable, is reported here.

Temperature is reported in the ITS-90 scale. Salinity and all derived units were calculated using the UNESCO (1981) routines; salinity is reported in the practical salinity scale (PSS-78). Oxygen is reported in μmol kg^{-1}.

2.1.2 Sensor Corrections and Calibrations

2.1.2.1 Pressure

The pressure calibration strategy employed a high-quality quartz pressure transducer as a transfer standard. Periodic recalibrations of this lab standard were performed with a primary pressure standard. The transfer standard was used to check the CTD pressure transducers. The only correction applied to the CTD pressures was a constant offset determined at the time that the CTD first enters the water on each cast.

Transfer Standard Calibration.

The transfer standard was a Paroscientific Model 760 pressure gauge equipped with a 10,000 PSI transducer. This instrument was purchased in March 1988, and was originally calibrated against a primary standard. Subsequent recalibrations were performed in May 1991, September 1994, March 1996 (Karl et al., 1996). A recent calibration in November 1998 at the Scripps Institute of Oceanography (SIO) indicated that the 0 dbar offset has decreased at a rate of -0.058 dbar/year. The sensor span (0-4500 dbar) has increased to about 0.88 dbar from its value of 0.64 dbar obtained in a previous SIO calibration (May 1991). Calibrations performed at the Northwest Regional Calibration Center in 1994 and 1996 indicated a span increase of up to 1.2 dbar, this difference from the SIO results may be due to the different methods used for calibrating. The measurements from the Standard reported here were corrected by the drift between the SIO calibrations.

CTD Pressure Transducer Bench Tests.

CTD pressure transducer bench tests were done using an Ametek T-100 pump and a manifold to apply pressure simultaneously to the CTD pressure transducer and to the transfer standard. All these tests had points at 6 pressure levels between 0 and 4500 dbar, increasing and decreasing pressures. Our old pump started experiencing leakage during recent tests and was replaced with a new one in November 1998.

In the 1997 HOT data report (Tupas et al., 1998), it was explained that in older bench tests an unaccounted additional pressure head was being introduced when measuring the CTD pressure at 0 dbar, this was due to residual fluid in the CTD pipes connected to the pump. This pressure head varied from test to test and was as high as 0.6 dbar. Due to this error it is not possible to use the surface offset from older tests to determine a drift in our sensors. To correct this problem, since September 1998 our testing procedure has included a measurement of the surface CTD pressure without any pipes attached to the sensor. Another source of error affecting old bench test results is due to tilt sensitivity of the pressure sensors. Since our pressure tests are performed tilting the CTD about 45 degrees from the horizontal (for an easier access to the sensors), this has caused an additional pressure offset that has not been accounted for (the pressure offset from the upright to the test position is about -0.6 dbar for sensor #26448, and -1.15 dbar for sensor #51412). To correct for this pressure difference, our calibration procedure will include a measurement of the CTD surface pressure with the CTD in the upright position (as used at sea). According to N. Larson (Sea-Bird), the tilt sensitivity in the pressure is due to head pressure in the plumbing line, and to residual gravitational sensitivity of the sensor.

Bench tests of sensors #26448 (primary) and #51412 (backup) against the transfer standard since 1994 are shown in Table 2.1. The transfer standard measurements were corrected using the Scripps calibrations. Tests before September 1998 do not include the 0 dbar offset because of the problem explained before. Pressure transducer #26448 was used during all cruises in 1998. A constant value of -5.72 dbar was used to correct the offset at 0 dbar for all the cruises in 1998 (Note that this offset was only used for real-time data acquisition, as more accurate offset was later determined for the time that the CTD first enters the water on each cast). The 0-4500 dbar pressure span and hysteresis were not affected by the problems in the bench tests described above, and have remained constant.

The 1998 and 1999 bench tests show that the 0 dbar offset from our primary CTD compares favorably with the on-deck pressures taken before CTD casts (Fig. 2.1). After subtracting the CTD tilting offset (-0.6 dbar) and the 0 dbar offset correction offset (-5.72 dbar) we obtain: -6.4+0.6+5.72 = -0.08 dbar for the September 1998 calibration, and -6.88 +0.6+5.72 = -0.56 dbar for the January 1999 calibration. These are approximately the on-deck pressures measured during the September 1998 and January 1999 cruises (Fig. 2.1).

The on-deck pressures (Fig. 2.1) show that sensor #26448 maintained nearly constant values until mid-1997, after which it started to decrease slowly for about a year, and more rapidly after mid-1998. This decrease in the surface pressure is also seen in the January 1999 bench test compared to September 1998. A "cold dunk" test consisting in lowering the CTD in a near 0 °C bath was conducted in March 1999 as suggested by N. Larson to test for vacuum leaks in the pressure sensor. The test results indicated a possible vacuum leak, and the pressure sensor was replaced by sensor #75434 in March 1999 at Sea-Bird. This problem did not affect the data because the duration of a CTD cast is too small compared to the pressure drift rate (up to 1 dbar/year), and the problem did not affect the 0-4500 dbar pressure span and hysteresis.

The 0-4500 dbar pressure span for sensor #51412 has been nearly constant, and the hysteresis has remained small and constant.

TABLE 2.1. CTD Pressure Calibrations (units are decibars). Pressure Transducer #26448.

Calibration date	Offset at 0 dbar	0-4500 dbar offset	Hysteresis
12/16/94	-----	0.4	0.1
8/16/95	-----	0.85	0.1
1/9/96	-----	0.8	-----

TABLE 2.1. CTD Pressure Calibrations (units are decibars). Pressure Transducer #26448.

Calibration date	Offset at 0 dbar	0-4500 dbar offset	Hysteresis
8/30/96	-----	0.7	0.1
1/31/97	-----	0.5	0.1
6/12/97	-----	0.5	0.2
9/11/98	-6.4	0.65	0.15
1/27/99	-6.88	0.6	0.15
	Pressure Transducer #51412		
12/16/94	-----	0.45	0.05
8/21/95	-----	0.45	0.05
12/5/95	-----	0.65	0.07
8/30/96	-----	0.45	0.1
1/31/97	-----	0.5	0.08
6/12/97	-----	0.65	0.05
9/14/98	0.1	0.55	0.05
1/26/99	-0.2	0.55	0.05

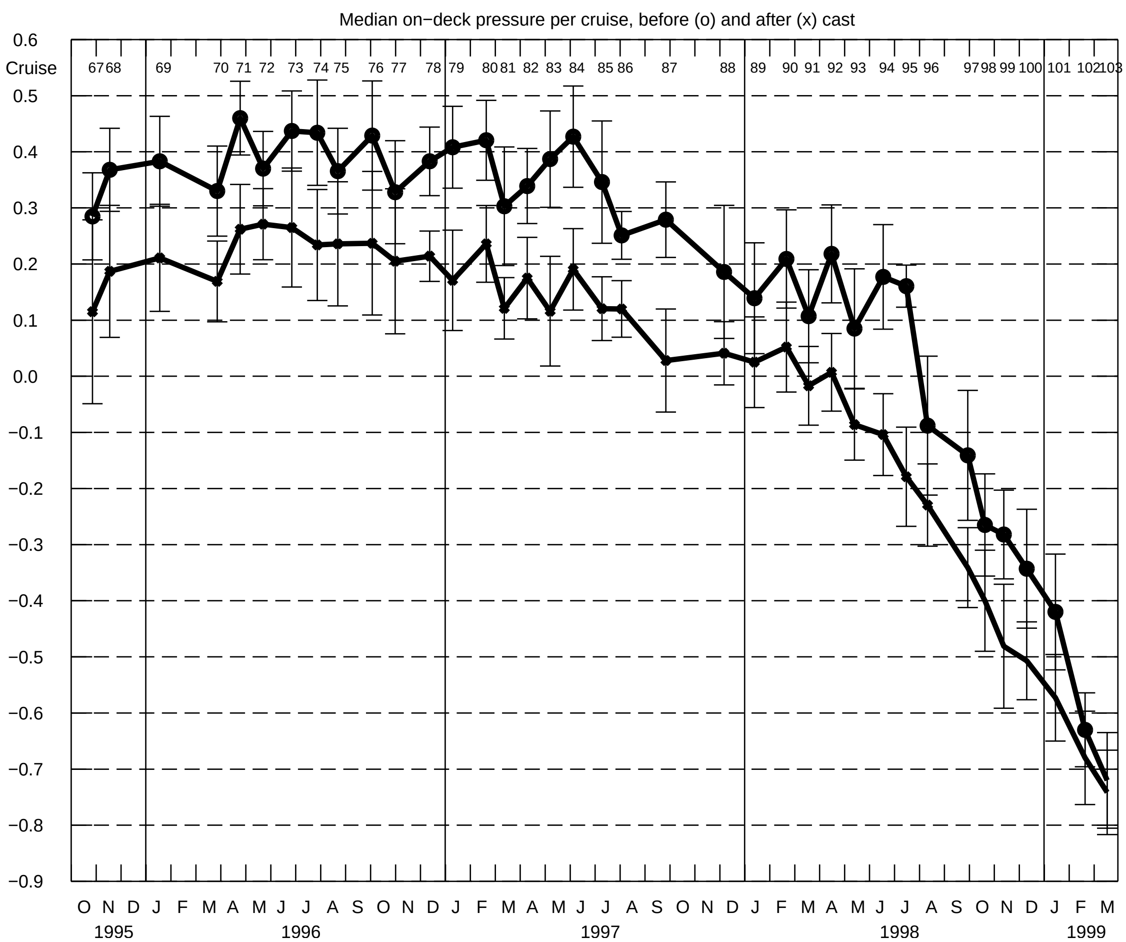

FIGURE 2.1. Median value of pressure on the ship's deck measured by the CTD pressure sensor before (circles) and after (crosses) each cast for HOT cruises 67-103. Error bars are 1 standard deviation from the mean. Cruise numbers are shown below the upper x-axis.

2.1.2.2 Temperature

Two Sea-Bird SBE-3-02/F temperature transducers, #1416 and #1591, and two new generation transducers (SBE-3-Plus) #2242 and #2472, were used in 1998 and were calibrated at Sea-Bird after every cruise, with the following exceptions. In April, only sensors #2242 and #2472 were calibrated because the others were taken on the HA-4A cruise. Sensor #2472 was acquired in November 1997, replacing #2202 which showed a large offset during the October 1997 calibration. The history of the sensors, as well as the procedures followed to obtain the sensor drift from the Sea-Bird calibrations are well-documented in Tupas et al. (1993, 1994a, 1995, 1997, 1998) and Karl et al. (1996). Calibration coefficients obtained at Sea-Bird after 1997 and used in the drift estimates are presented in Table 2.2. These coefficients were used in the following formula that gives the temperature (in °C) as a function of the frequency signal (f):

$$temperature = 1/\{a + b\,[\ln(f_0/f)] + c\left[\ln^2(f_0/f)\right] + d\left[\ln^3(f_0/f)\right]\} - 273.15$$

TABLE 2.2. Calibration coefficients for Sea-Bird temperature sensors. RMS residuals from calibration give an indication of quality of the calibration. Sensors #2045, #1496, #1392 and #2078 were used by the thermosalinograph (Sect. 2.2).

SN	YYMMDD	f0	a	b	c	d	RMS m°C
741	990126	5938.50	3.68146204e-03	6.01965237e-04	1.55235885e-05	2.03843948e-06	0.05
741	981229	5938.55	3.68145574e-03	6.01963508e-04	1.55260599e-05	2.047493850e-06	0.03
741	981125	5937.97	3.68152031e-03	6.01988032e-04	1.55794866e-05	2.08805635e-06	0.03
741	981027	5938.33	3.68148431e-03	6.01969116e-04	1.55261709e-05	2.04262958e-06	0.05
741	981006	5938.28	3.68148849e-03	6.01977884e-04	1.55521895e-05	2.06557060e-06	0.03
741	980822	5938.08	3.68150766e-03	6.01979670e-04	1.55435431e-05	2.05683602e-06	0.03
741	980727	5938.13	3.68150775e-03	6.01999228e-04	1.56025466e-05	2.10738400e-06	0.05
741	980627	5937.75	3.68154596e-03	6.01989322e-04	1.55610913e-05	2.07106315e-06	0.03
741	980529	5937.67	3.68155023e-03	6.01980837e-04	1.55864404e-05	2.11163461e-06	0.04
741	980331	5938.09	3.68150436e-03	6.01970298e-04	1.55702514e-05	2.09927114e-06	0.04
741	980227	5937.67	3.68155355e-03	6.01994040e-04	1.56127096e-05	2.13185525e-06	0.04
741	980120	5937.88	3.68152817e-03	6.01978087e-04	1.55848283e-05	2.11141726e-06	0.03
1416	990126	6232.18	3.68146341e-03	6.01818861e-04	1.50237823e-05	2.11362758e-06	0.18
1416	981229	6232.24	3.68145690e-03	6.01800604e-04	1.49753799e-05	2.08073387e-06	0.16
1416	981125	6231.56	3.68151895e-03	6.01762087e-04	1.48864384e-05	2.03319618e-06	0.19
1416	981027	6231.98	3.68148529e-03	6.01794517e-04	1.49358504e-05	2.04291623e-06	0.18
1416	981006	6231.93	3.68148972e-03	6.01792357e-04	1.49143589e-05	2.02040207e-06	0.20
1416	980822	6231.76	3.68150889e-03	6.01806098e-04	1.49466509e-05	2.04654707e-06	0.17
1416	980727	6231.76	3.68150663e-03	6.01801069e-04	1.49837213e-05	2.10659367e-06	0.18
1416	980627	6231.36	3.68154474e-03	6.01758119e-04	1.48445421e-05	1.99238010e-06	0.19

TABLE 2.2. Calibration coefficients for Sea-Bird temperature sensors. RMS residuals from calibration give an indication of quality of the calibration. Sensors #2045, #1496, #1392 and #2078 were used by the thermosalinograph (Sect. 2.2).

SN	YYM MDD	f0	a	b	c	d	RMS $m^{o}C$
1416	980507	6231.24	3.68156290e-03	6.01831419e-04	1.50667887e-05	2.16816206e-06	0.17
1416	980331	6231.78	3.68150557e-03	6.01791441e-04	1.49641821e-05	2.08469333e-06	0.18
1416	980227	6231.35	3.68155533e-03	6.01819740e-04	1.50117434e-05	2.11346853e-06	0.19
1416	980120	6231.51	3.68152843e-03	6.01783122e-04	1.49889428e-05	2.12875994e-06	0.16
1591	990126	6256.99	3.68145893e-03	6.03661084e-04	1.47770489e-05	1.72688845e-06	0.26
1591	981229	6257.08	3.68145248e-03	6.03650394e-04	1.47554000e-05	1.71456570e-06	0.28
1591	981125	6256.45	3.68151731e-03	6.03694468e-04	1.48707192e-05	1.80925704e-06	0.27
1591	981027	6256.84	3.68148109e-03	6.03664893e-04	1.47853395e-05	1.73641453e-06	0.37
1591	981006	6256.81	3.68148518e-03	6.03668878e-04	1.47948330e-05	1.74699884e-06	0.28
1591	980822	6256.62	3.68150433e-03	6.03662202e-04	1.47607625e-05	1.71317501e-06	0.28
1591	980727	6256.68	3.68150454e-03	6.03695062e-04	1.48478610e-05	1.78556464e-06	0.28
1591	980627	6256.25	3.68154297e-03	6.03691546e-04	1.48453360e-05	1.78614832e-06	0.29
1591	980507	6256.09	3.68155861e-03	6.03671918e-04	1.48260365e-05	1.78801402e-06	0.27
1591	980331	6256.65	3.68150131e-03	6.03648398e-04	1.47792829e-05	1.75237261e-06	0.28
1591	980227	6256.23	3.68155034e-03	6.03679620e-04	1.48418484e-05	1.79773651e-06	0.26
1591	980227	6256.23	3.68155034e-03	6.03679620e-04	1.48418484e-05	1.79773651e-06	0.26
1591	980120	6256.45	3.68152525e-03	6.03654640e-04	1.47921555e-05	1.75952226e-06	0.27
2242	990126	3003.50	3.68001897e-03	6.02846271e-04	1.60959418e-05	2.08066784e-06	0.10
2242	981230	3003.36	3.68005140e-03	6.02848426e-04	1.60850460e-05	2.06784447e-06	0.04
2242	981126	3003.14	3.68009202e-03	6.02855453e-04	1.61075848e-05	2.08711430e-06	0.10
2242	981027	3003.23	3.68007470e-03	6.02857883e-04	1.61273204e-05	2.10752136e-06	0.07
2242	981008	3003.11	3.68010002e-03	6.02874297e-04	1.61584819e-05	2.12083742e-06	0.08
2242	980822	3002.95	3.68012902e-03	6.02877302e-04	1.61767012e-05	2.14453430e-06	0.07
2242	980724	3003.04	3.68010958e-03	6.02868708e-04	1.61727935e-05	2.14593895e-06	0.05
2242	980528	3002.80	3.68015850e-03	6.02884146e-04	1.62401142e-05	2.21421613e-06	0.05
2242	980428	3003.05	3.68010923e-03	6.02871010e-04	1.61983175e-05	2.18259944e-06	0.06
2242	980331	3002.90	3.68013756e-03	6.02891986e-04	1.62678012e-05	2.23905207e-06	0.04
2242	980228	3002.69	3.68017837e-03	6.02889500e-04	1.62591006e-05	2.23335519e-06	0.04
2242	980204	3002.67	3.68018463e-03	6.02881695e-04	1.62314439e-05	2.20937359e-06	0.05
2242	980121	3002.68	3.68018425e-03	6.02885383e-04	1.62412759e-05	2.21882373e-06	0.05
2472	990126	2746.23	3.68001982e-03	6.13862485e-04	1.79109672e-05	2.40300002e-06	0.05
2472	981230	2746.07	3.68005216e-03	6.13866125e-04	1.79013966e-05	2.39092543e-06	0.10
2472	981126	2745.89	3.68009284e-03	6.13869148e-04	1.79107655e-05	2.40432036e-06	0.04
2472	981027	2745.97	3.68007512e-03	6.13875124e-04	1.79296967e-05	2.42302378e-06	0.03
2472	981008	2745.84	3.68010034e-03	6.13875538e-04	1.79317615e-05	2.42166775e-06	0.03
2472	980822	2745.70	3.68012921e-03	6.13880345e-04	1.79288756e-05	2.41390127e-06	0.04

TABLE 2.2. Calibration coefficients for Sea-Bird temperature sensors. RMS residuals from calibration give an indication of quality of the calibration. Sensors #2045, #1496, #1392 and #2078 were used by the thermosalinograph (Sect. 2.2).

SN	YYM MDD	f0	a	b	c	d	RMS m°C
2472	980724	2745.78	3.68011000e-03	6.13882842e-04	1.79559652e-05	2.44236880e-06	0.04
2472	980627	2745.71	3.68012358e-03	6.13888223e-04	1.79617881e-05	2.44236103e-06	0.05
2472	980528	2745.55	3.68015868e-03	6.13889005e-04	1.79907858e-05	2.48665651e-06	0.04
2472	980428	2745.75	3.68010934e-03	6.13879807e-04	1.79886334e-05	2.49378435e-06	0.04
2472	980331	2745.62	3.68013772e-03	6.13880969e-04	1.79823985e-05	2.48673862e-06	0.04
2472	980228	2745.43	3.68017840e-03	6.13880059e-04	1.79710969e-05	2.47379287e-06	0.04
2472	980204	2745.40	3.68018470e-03	6.13878686e-04	1.79623813e-05	2.46611301e-06	0.05
2472	980121	2745.41	3.68018425e-03	6.13874190e-04	1.79501401e-05	2.45706828e-06	0.04
2472	971222	2745.60	3.68014128e-03	6.13886428e-04	1.79733785e-05	2.47020437e-06	0.05
2472	971106	2745.30	3.68020047e-03	6.13883525e-04	1.79749160e-05	2.47396557e-06	0.04
2045	980728	2447.02	3.64664780e-03	5.89941753e-04	1.00854316e-05	-3.6594943e-07	0.43
1496	980716	5947.26	3.68153908e-03	5.89975419e-04	1.46589621e-05	2.88623686e-06	0.20
1392	981118	2578.63	3.64688995e-03	5.86286555e-04	9.04039578e-06	-2.3693864e-06	0.04
2078	961217	2772.55	3.68022581e-03	5.92832713e-04	1.62002729e-05	1.77796339e-06	0.03
2078	951019	2772.32	3.68029270e-03	5.92819697e-04	1.61663533e-05	1.75679211e-06	0.03

For each sensor, the final calibration consists of two parts: first, a single "baseline" calibration is chosen from among the ensemble of calibrations during the year; second, for each cruise a temperature-independent offset is applied to remove the temporal trend due to sensor drift (Table 2.3). The offset, a linear function of time, is calculated by least squares fit to the 0-30 °C average of each calibration during the year. The maximum drift correction in 1998 was less than 1.3 x 10^{-3} °C. The baseline calibration is selected as the one for which the trend-corrected average from 0-5 °C is nearest to the ensemble mean of these averages.

A small residual pressure effect on the temperature sensors documented in Tupas et al. (1997) has been removed for measurements obtained with our sensors other than #2472. A similar correction factor k = 1.33 x 10^{-3} °C / 5000 dbar was obtained at Sea-Bird for sensor #2472, and the temperatures were corrected for this effect. The corrected temperature (Tc) was calculated from the sensor temperature (T) and the pressure (P) as: Tc = T - kP.

Another correction to our temperature measurements is for the viscous heating of the sensor tip due to the water flow. This correction is thoroughly documented in Tupas et al. (1997).

Dual sensors were used during each of the 1998 cruises. The temperature differences between sensor pairs were calculated for each cast to evaluate the quality of the data, and to identify possible problems with the sensors. Means and standard deviations of the differences in 2-dbar bins were calculated from the ensemble of all casts at Station ALOHA for each cruise. Both sensors performed correctly during the 1998 cruises, showing temperature differences within expected values. The mean temperature difference as a function of pressure was typically less than 1 x 10^{-3} °C, with a standard deviation of less than 0.5 x 10^{-3} °C below 500 dbar. The largest variability was observed in the thermocline, with standard deviation values of up to 5 x 10^{-3} °C.

Sensor #1416.

This sensor was used as part of the dual-sensor configuration during cruise HA-4A. The calibrations from April 1996 throughout January 1999 were used to calculate the sensor drift and the drift corrections. A linear fit to the 0-30 °C average offset from each calibration (Table 2.2) relative to 9 April 1996 gave an intercept of 7.65 x 10^{-5} °C with a slope of 2.68 x 10^{-6} °C day^{-1}. The RMS deviation of the offsets from this fit was 1.3 x 10^{-4} °C. The 18 June 1997 calibration was used as a baseline for the cruise. When corrected for linear drift to 19 April 1998 (the midpoint of the cruise date), this calibration gave the smallest deviation in the 0-5 °C temperature range from the set of all calibrations used to determine the drift (also corrected for linear drift to 19 April 1998). The mean deviation of this calibration was 1.5 x 10^{-5} °C with a range of variation of less than 2 x 10^{-5} °C. The set of all calibrations had deviations in the range ±5 x 10^{-4} °C. The resulting drift correction for the HA-4A cruise was very small (Table 2.3).

Sensor #1591.

This sensor was used during cruise HA-4A. The calibrations from February 1997 throughout January 1999 were used to calculate a sensor drift of 4.55 x 10^{-6} °C day^{-1} with a 2.9 x 10^{-4} °C intercept and 1.7 x 10^{-4} °C RMS residual. The 27 February 1998 calibration was used as baseline for the cruises. This calibration yielded the smallest 0-5 °C mean deviation from the others, all drift-corrected to 19 April 1998 (midpoint date of the cruise). The deviation was -8.8 x 10^{-6} °C with less than 1 x 10^{-4} °C range of variation. The set of all calibrations had deviations in the range ±4 x 10^{-4} °C.

Sensor #2242.

This sensor was used during cruises HOT-89 through -100, and HA-5A. The calibrations from December 1996 through January 1999 were used to calculate a sensor drift of -1.54 x 10^{-7} °C day^{-1} with a -1.0 x 10^{-4} °C intercept and 7.4 x 10^{-5} °C RMS residual. The 27 June 1998 calibration was used as baseline for the cruises. This calibration yielded the smallest 0-5 °C mean deviation from the others, all drift-corrected to 15 May 1998 (midpoint date between the cruises). The deviation was 5.1 x 10^{-6} °C with less than 0.2 x 10^{-4} °C range of variation. The set of all calibrations had deviations in the range ±2 x 10^{-4} °C.

Because of the small drift of this sensor, the resulting drift corrections for each cruise were very small and inconsequential (Table 2.3).

Sensor #2472.

This is a new SBE-3-Plus sensor acquired in November 1997 to replace sensor #2202 which showed a calibration offset in October 1997 (Tupas et al., 1998). The calibrations from November 1997 through January 1999 were used to calculate a sensor drift of -4.18 x 10^{-6} °C day^{-1} with a -1.3 x 10^{-4} °C intercept and 1.0 x 10^{-4} °C RMS residual. This drift was used to obtain the correction for cruises HOT-80 through -100, and HA-5A. The 26 November 1998 calibration was used as baseline for the cruises. This calibration yielded the smallest 0-5 °C mean deviation from the others, all drift-corrected to 15 May 1998 (midpoint date between the cruises). The deviation was 1.0 x 10^{-5} °C with less than 0.3 x 10^{-4} °C range of variation. The set of all calibrations had deviations in the range ±2 x 10^{-4} °C. The resulting drift corrections for each cruise were very small (Table 2.3).

TABLE 2.3. Temperature (T) and Conductivity (C) sensor corrections including the thermal inertia parameter (alpha). Dual temperature and conductivity sensors were used in all cruises

Cruise	T sensor #	T correction (°C)	C sensor #	alpha	Data Reported
89	2242	-0.000026	1336	0.028	All casts
	2472	-0.001334	679	0.028	
90	2242	-0.000020	527	0.020	All casts
	2472	-0.001171	679	0.020	
91	2242	-0.000016	1336	0.028	All casts
	2472	-0.001058	527	0.028	
92	2242	-0.000011	527	0.028	All casts
	2472	-0.000941	679	0.028	
HA-4A	1416	0.000816	527	0.028	All casts
	1591	0.000232	679	0.020	
93	2242	-0.000007	527	0.028	All casts
	2472	-0.000824	679	0.028	
94	2242	-0.000002	527	0.028	All casts
	2472	-0.000678	679	0.028	
95	2242	0.000003	1336	0.028	All casts
	2472	-0.000560	527	0.020	
96	2242	0.000007	375	0.020	All casts
	2472	-0.000456	527	0.020	
97	2242	0.000014	375	0.028	All casts
	2472	-0.000247	527	0.020	
98	2242	0.000018	375	0.028	All casts
	2472	-0.000159	527	0.020	

TABLE 2.3. Temperature (T) and Conductivity (C) sensor corrections including the thermal inertia parameter (alpha). Dual temperature and conductivity sensors were used in all cruises

Cruise	T sensor #	T correction (°C)	C sensor #	alpha	Data Reported
99	2242	0.000021	375	0.028	All casts
	2472	-0.000063	527	0.020	
HA-5A	2242	-0.000022	375	0.028	All casts
	2472	0.000038	527	0.020	
100	2242	0.000025	375	0.028	
	2472	0.000054	527	0.028	All casts

2.1.2.3 Conductivity

Four sensors were used during the 1998 cruises, #1336, #679, #375, and #527. The history of the sensors is well-documented in Tupas et al. (1993, 1994a, 1995, 1997, 1998) and Karl et al. (1996). The dual sensor configurations are shown in Table 2.3. As mentioned earlier, only the data from the most reliable sensor (and its corresponding temperature sensor pair, as shown in Table 2.3) are reported here.

Sensor #1336 was calibrated at Sea-Bird on 9 April, 1998. This sensor showed large conductivity differences with respect to the secondary sensor during HOT-95 and had to be replaced. A Sea-Bird inspection showed an erratic calibration possibly due to water leaking through the epoxy jacket or a loose electrode. The conductivity cell was replaced in September 1998. Sensor #679 was calibrated on 17 July 1998.

The nominal calibrations were used for data acquisition. Final calibration was determined empirically from salinities of discrete water samples acquired during each cast. Prior to empirical calibration, conductivity was corrected for thermal inertia (α) of the glass conductivity cell as described in Chiswell et al. (1990). Table 2.3 lists the value of α used for each cruise.

Preliminary screening of bottle samples and empirical calibration of the conductivity cell are described in Tupas et al. (1993, 1994a). For cruises HOT-89 through -100, the standard deviation cutoff values for screening of bottle samples were: 0.0035 (0-150 dbar), 0.0048 (151-500 dbar), 0.0022 (501- 1050 dbar), and 0.0012 (1051-5000 dbar).

The conductivity calibration coefficients (b_0, b_1, b_2) resulting from the least squares fit ($\Delta C = b_0 + b_1C + b_2C^2$) to the CTD minus bottle conductivities (ΔC) as a function of conductivity (C) are given in Table 2.4. The quality of the CTD calibration is illustrated in Figure 2.2, which shows the differences between the corrected CTD salinities and the bottle salinities used for calibration as a function of pressure for each cruise. The calibrations are best below 500 dbar because the weaker vertical salinity gradients at depth lead to less error when the bottle and CTD pressures are slightly mismatched.

TABLE 2.4. Conductivity calibration coefficients

Cruise	Sensor #	b0	b1	b2
89	1336	0.000947	-0.000515	0.000000
	679	0.001205	-0.000625	0.000000
90	527	0.000935	-0.000322	0.000000
	679	0.001117	-0.000511	0.000000
91	1336	0.000943	-0.000454	0.000000
	527	0.000974	-0.000363	0.000000
92	527	0.001011	-0.000374	0.000000
	679	0.001220	-0.000504	0.000000
HA-4A	527	0.001579	-0.000577	0.000000
	679	0.001805	-0.000692	0.000000
93	527	0.000985	-0.000388	0.000000
	679	0.001266	-0.000535	0.000000
94	527	0.000955	-0.000383	0.000000
	679	0.001287	-0.000588	0.000000
95	1336	0.001099	-0.000380	0.000000
	527	0.001261	-0.000514	0.000000
96	375	0.000836	-0.000329	0.000000
	527	0.001018	-0.000462	0.000000
97	375	0.000866	-0.000312	0.000000
	527	0.001122	-0.000465	0.000000
98	375	0.001094	-0.000367	0.000000
	527	0.001269	-0.000470	0.000000
99	375	0.000884	-0.000345	0.000000
	527	0.001151	-0.000505	0.000000
HA-5A	375	0.001040	-0.000379	0.000000
	527	0.001302	-0.000531	0.000000
100	375	0.000893	-0.000331	0.000000
	527	0.001070	-0.000447	0.000000

TABLE 2.5. Individual cast conductivity corrections (units are Siemens m^{-1})

Cruise	Station	Cast	C correction
89	2	1	0.00002864
92	2	10	-0.00025380
92	2	11	0.00006886
92	2	12	0.00006015

TABLE 2.5. Individual cast conductivity corrections (units are Siemens m^{-1})

Cruise	Station	Cast	C correction
96	2	14	-0.00004200
97	2	3	0.00013048

The final step of conductivity calibration was a cast-dependent bias correction as described in Tupas et al. (1993) to allow for drift during each cruise or for sudden offsets due to fouling (Table 2.5). Note that a change of 1 x 10^{-4} Siemens m^{-1} in conductivity was approximately equivalent to 0.001 in salinity. Table 2.6 gives the mean and standard deviations for the final calibrated CTD minus water sample values.

Conductivity differences between sensor pairs were calculated the same way as for the temperature sensors (section 2.1.2.2). The range of variability as a function of pressure was about ±1 x 10^{-4} Siemens m^{-1}, with a standard deviation of less than ±0.5 x 10^{-4} Siemens m^{-1} below 500 dbar, from the ensemble of all the cruise casts. The largest variability was in the halocline, with standard deviations reaching up to ±5 x 10^{-4} Siemens m^{-1} between 50 and 300 dbar.

TABLE 2.6. CTD-Bottle salinity comparison for each cruise

		0-4800 dbar		500-4800 dbar	
Cruise	Sensor #	Mean	SD	Mean	SD
89	1336	-0.0000	0.0019	0.0002	0.0011
	679	0.0000	0.0019	0.0001	0.0010
90	527	0.0000	0.0014	0.0002	0.0008
	679	0.0000	0.0016	0.0003	0.0009
91	1336	0.0000	0.0015	0.0001	0.0011
	527	0.0001	0.0014	0.0002	0.0011
92	527	0.0000	0.0019	0.0005	0.0012
	679	0.0001	0.0016	0.0004	0.0010
HA-4A	527	-0.0000	0.0022	-0.0003	0.0013
	679	0.0000	0.0022	-0.0002	0.0015
93	527	0.0000	0.0017	0.0002	0.0010
	679	-0.0000	0.0017	0.0001	0.0010
94	527	0.0000	0.0018	0.0001	0.0013
	679	0.0000	0.0019	0.0001	0.0013
95	1336	0.0000	0.0018	0.0001	0.0012
	527	0.0000	0.0018	0.0001	0.0013
96	375	0.0001	0.0022	0.0003	0.0014
	527	0.0001	0.0022	0.0003	0.0014
97	375	-0.0001	0.0018	0.0003	0.0011

TABLE 2.6. CTD-Bottle salinity comparison for each cruise

		0-4800 dbar		500-4800 dbar	
Cruise	**Sensor #**	**Mean**	**SD**	**Mean**	**SD**
	527	-0.0001	0.0019	0.0004	0.0011
98	375	0.0000	0.0016	0.0001	0.0014
	527	-0.0000	0.0016	-0.0000	0.0013
99	375	0.0000	0.0020	0.0004	0.0014
	527	0.0000	0.0022	0.0004	0.0015
HA-5A	375	0.0000	0.0019	0.0002	0.0023
	527	0.0000	0.0019	0.0002	0.0023
100	375	0.0000	0.0015	0.0001	0.0013
	527	0.0000	0.0016	0.0002	0.0012

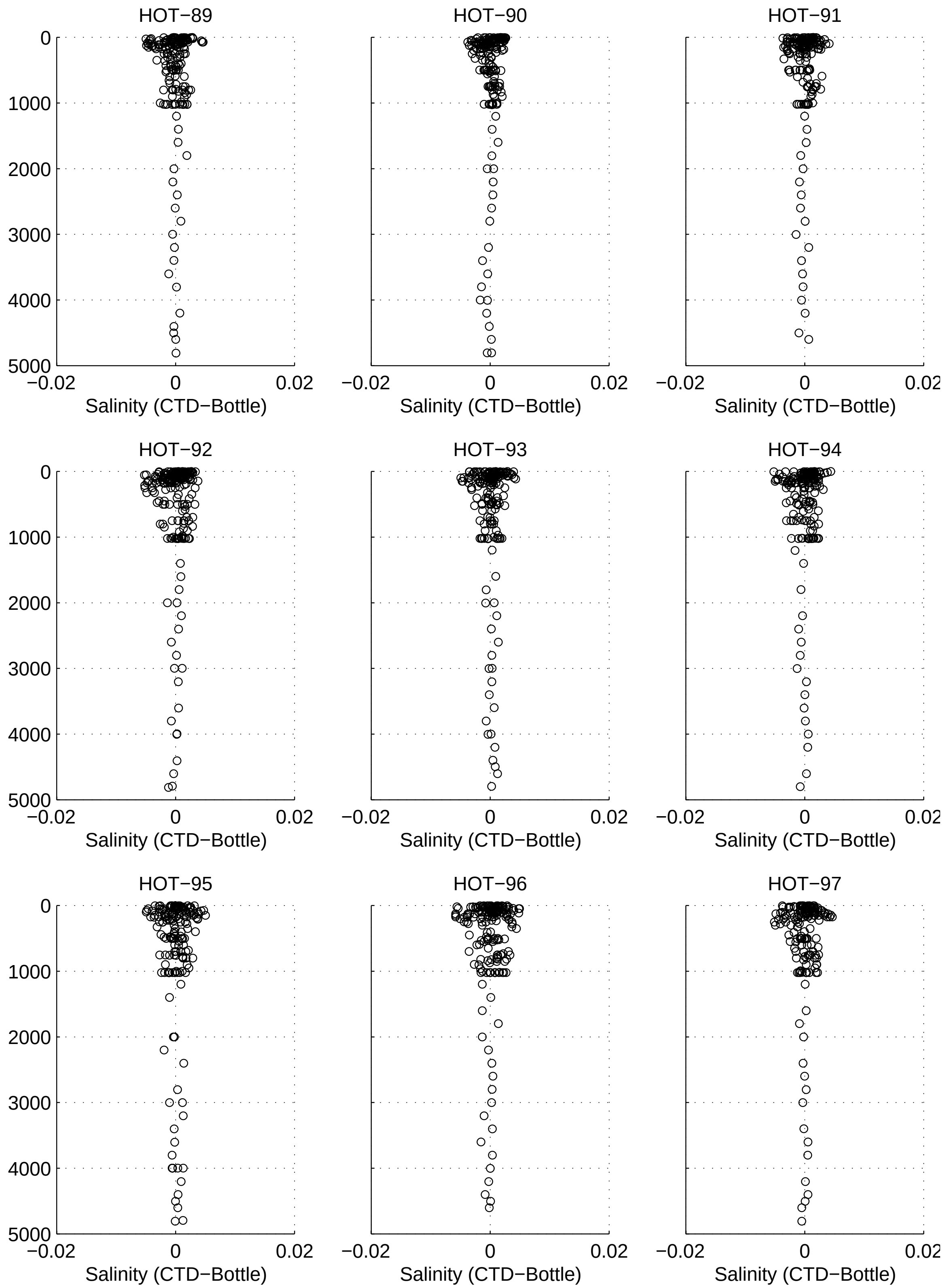

FIGURE 2.2a. Difference between calibrated CTD salinities and bottle salinities for each cruise and all casts at Station ALOHA during cruises 89 through 97.

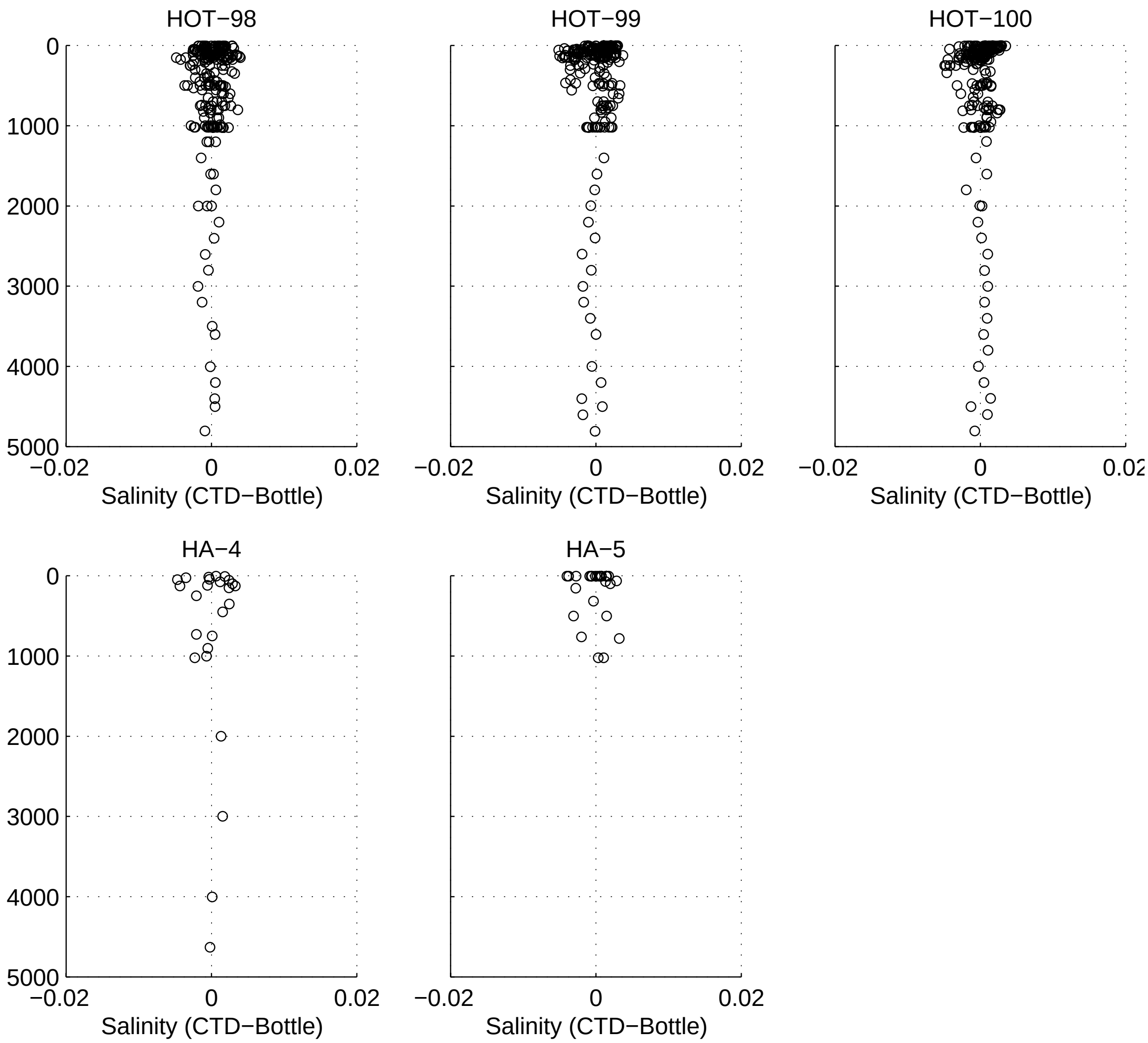

FIGURE 2.2b. Same as in a, but for cruises HOT-98 through -100, and HA-4A and -5A.

2.1.2.4 Oxygen

Two YSI Inc. probes (#13341 and #13251) were used in a dual-sensor configuration during the 1998 cruises. The history of the sensors is documented in Tupas et al. (1995, 1997, 1998) and Karl et al. (1996). The regular maintenance procedure for these sensors includes inspection of their electrolyte level and membrane before each cruise. Sensor #13341 had its membrane and electrolyte replaced prior to HOT-95 and HOT-98. Both sensors had their membrane and electrolyte replaced prior to HOT-100.

Sensor #13341 showed spikes during HOT-96 and was sent to Sea-Bird for inspection, where the sensor's head was found cracked. The sensor was refurbished in September 1998 and used in the following cruises, but it showed a slow response problem. The sensor could not be sent to Sea-Bird for inspection until February 1999 due to insufficient turnaround time between cruises. The inspection revealed that the problem with the sensor was that a low sensitivity membrane was inadvertently being used instead of the high sensitivity membrane required. Data from this sensor are not reported for the cruises affected.

Data from sensor #13251 are reported here for all the 1998 cruises, except for HOT-91, during which spikes were seen in some casts, data from sensor #13341 are reported instead. Sensor #13251 showed offsets in the data during the deep casts of HOT-97 and -99, these data were flagged suspect.

Water bottle oxygen data were screened and the sensors were empirically calibrated following procedures described previously (Winn et al. 1991; Tupas et al., 1993). Analysis of water bottle samples is described in section 2.6.1. The calibration procedure follows Owens and Millard (1985), and consists of fitting a non-linear equation to the CTD oxygen current and oxygen temperature. The bottle values of dissolved oxygen and the downcast CTD observations at the potential density of each bottle trip were grouped together for each cruise to find the best set of parameters with a non-linear least squares algorithm. Three sets of parameters were usually obtained per HOT cruise, corresponding to the casts at Stations 1, 2 and 8. Casts from HA-4A and -5A were calibrated with bottle data obtained during these cruises.

Table 2.7 gives the means and standard deviations for the final calibrated CTD oxygen minus water sample values.

TABLE 2.7a. CTD-Bottle dissolved oxygen per cruise (μ mol kg^{-1})

		Station 1, Kahe Point		Station 2, ALOHA			
		0 to 1500 dbar		0 to 4800 dbar		500 to 4800 dbar	
Cruise	**Sensor #**	**Mean**	**SD**	**Mean**	**SD**	**Mean**	**SD**
89	13251	0.02	0.89	0.09	1.35	0.05	0.94
90	13251	0.00	0.75	0.09	1.26	0.07	0.82
91	13341	0.00	0.68	0.07	1.28	0.10	1.30
92	13251	0.00	0.82	0.15	1.34	0.12	0.7
93	13251	0.01	0.80	0.16	1.10	0.22	0.76
94	13251	0.01	0.72	0.10	1.16	0.09	0.78
95	13251	0.01	0.82	-0.03	0.96	-0.08	0.63
96	13251	0.01	0.82	0.26	1.43	0.42	1.37
97	13251	0.02	1.05	0.26	1.04	0.45	1.03
98	13251	0.02	1.92	0.20	1.47	0.37	1.16
99	13251	0.02	1.09	0.20	1.71	0.32	1.32
100	13251	0.00	1.34	0.06	1.54	0.11	1.14

TABLE 2.7b. CTD-Bottle dissolved oxygen at HALE-ALOHA (μ mol kg^{-1})

Cruise	**Sensor #**	**Mean**	**SD**
89	13251	0.00	0.23
90	13251	0.00	0.44

TABLE 2.7b. CTD-Bottle dissolved oxygen at HALE-ALOHA (μ mol kg^{-1})

Cruise	Sensor #	Mean	SD
91	13341	0.00	0.12
92	13251	0.01	0.75
HA-4A	13251	0.02	0.92
93	13251	0.01	0.68
94	13251	-0.01	0.41
95	13251	0.01	0.68
96	13251	0.01	1.33
97	13251	0.00	0.79
98	13251	0.01	0.72
HA-5A	13251	0.01	1.06
100	13251	0.02	1.29

2.1.3 Discrete Salinity

Salinity samples were collected, stored and analyzed as described in Tupas et al. (1993). Samples from a large batch of “secondary standard” seawater were measured after every 24-36 bottle samples to detect drift in the salinometer for each cruise. Standard deviations of the secondary standard measurements were near ± 0.001 per cruise (Table 2.8).

Secondary standard seawater batches are made from 60 liters of seawater taken from a depth of 1000 m from Station ALOHA. Secondary standard batch #16 was prepared on January 13, 1998, batch #17 was prepared on June 24, 1998 and batch #18 was prepared on October 23, 1998.

TABLE 2.8. Precision of salinity measurements using lab standards

Cruise	Mean Salinity ±*SD*	# Samples	Substandard Batch #	IAPSO Batch #
89	34.47966 ±0.00115	23	16	p132
90	34.48078 ±0.00089	17	16	p132
91	34.48073 ±0.00075	19	16	p132
92	34.47917 ±0.00094	23	16	p132
HA-4A	34.47973 ±0.00025	3	16	p132
93	34.47961 ±0.00104	24	16	p132
94	34.49196 ±0.00084	28	17	p132
95	34.49415 ±0.00061	18	17	p132

TABLE 2.8. Precision of salinity measurements using lab standards

Cruise	Mean Salinity ±*SD*	# Samples	Substandard Batch #	IAPSO Batch #
96	34.49275 ±0.00056	26	17	p132
97	34.49166 ±0.00117	23	17	p132
98	34.48921 ±0.00112	31	18	p132
99	34.49198 ±0.00091	26	18	p132
HA-5A	34.49073 ±0.00023	3	18	p132
100	34.49052 ±0.00043	22	18	p132

2.2 Thermosalinograph.

2.2.1 Data acquisition.

SBE-21 Seacat thermosalinograph systems were used aboard R/V *Moana Wave* for the HOT-89 through HOT-100, HA-3B, HA-4A, HA-4B and HA-5A cruises. Seacat thermosalinograph sensor #2045 (comprised of one temperature and one conductivity sensor) was used for HOT-89 through HOT-93, HOT-97 through HOT-100, HA-3B, HA-4A, HA-4B and HA-5A. The HOT-94 through HOT-97 cruises used Seacat thermosalinograph sensor #1392 (also comprised of one temperature and one conductivity sensor). The thermosalinographs were installed in a pumped intake line in the hull of the R/V *Moana Wave* with an intake depth of about 3 m. Near the start of the intake line, a Sea-Bird remote temperature sensor, installed in a sea chest in the bow of the ship, recorded temperature data. This location allows for relatively undisturbed water to enter the thermosalinograph. Sea-Bird remote temperature sensor #1496 was used for HOT-89 through HOT-93, HA-3B and HA-4A. HOT-94 through HOT-100, HA-4B and HA-5A used Sea-Bird remote temperature sensor #2078. The SBE-21 Seacat thermosalinograph is used to calculate salinity using an internal temperature and conductivity sensor. Data were obtained every 10 seconds. In order to calibrate the conductivity sensor, bottle salinity samples were periodically taken from the thermosalinograph intake line. To calculate salinity, a pressure of 20 dbar was assumed to compensate for the pressure caused by the pump for the intake line (30 psi).

2.2.2 Data Processing and Sensor Calibration.

2.2.2.1 Nominal Calibration.

Temperature.

The Sea-Bird internal temperature sensors (#1392 and #2045) and external temperature sensors (#1496 and #2078) used aboard R/V *Moana Wave* were calibrated at Sea-Bird, and the calibration coefficients are given in Table 2.2. Since these sensors are the same type as used for the CTD measurements, the same procedure for drift estimation was followed (see Section 2.1.2.2). Temperature drift corrections are presented in Table 2.9.

A temperature drift rate of -3.1×10^{-6} °C day^{-1} was determined for internal temperature sensor #1392 using the 29 September 1994, 13 October 1995, 20 August 1997 and 28 August 1997 calibrations. The 29 September 1994 calibration was performed after the sensor's electronics had been reworked. This sort of work usually causes a change in the drift of a sensor so the calibrations prior to this date were not used for drift calculation purposes. Also, a calibration conducted for temperature sensor #1392 on 18 November 1998 was not used for drift calculation purposes as this calibration was not consistent with the calibration history for the instrument. The 18 November 1998 calibration was performed after problems were identified with the instrument thereby perhaps leading to its inconsistency. All the cruises which used internal temperature sensor #1392 (HOT-94 through HOT-97) calculated temperatures using the 28 August 1997 baseline calibration. Drift corrections were applied to the temperature data for sensor #1392 only for cruises which determined a drift larger than -0.001 °C.

For internal temperature sensor #2045, a drift rate of -1.7×10^{-8} °C day^{-1} was determined using the 11 October 1995, 30 July 1996 and 28 July 1998 calibrations. Temperatures were calculated with the 30 July 1996 baseline calibration. Drift corrections were not applied to the data for temperature sensor #2045 as they are very small and inconsequential.

A drift rate of 9.6×10^{-6} °C day^{-1} was determined using the 2 November 1993, 18 January 1996 and 16 July 1998 calibrations for remote temperature sensor #1496. Temperatures were calculated with the 18 January 1996 baseline calibration for sensor #1496. For remote temperature sensor #2078 a drift rate of 3.6×10^{-6} °C day^{-1} was determined using the 19 October 1995 and 17 December 1996 calibrations. Temperatures were calculated with the 17 December 1996 baseline calibration for sensor #2078.

TABLE 2.9. Thermosalinograph temperature drift corrections (°C)

Cruise	Sensor #1392	Sensor #1392	Sensor #2045	Sensor #2045
89	n/a	0.0069	No correction	n/a
90	n/a	0.0073	No correction	n/a
91	n/a	0.0076	No correction	n/a
92	n/a	0.0078	No correction	n/a
HA-3B	n/a	0.0079	No correction	n/a
HA-4A	n/a	0.0080	No correction	n/a
93	n/a	0.0081	No correction	n/a
94	No correction	n/a	n/a	0.0020
95	No correction	n/a	n/a	0.0021
96	-0.0011	n/a	n/a	0.0022
97	-0.0012	n/a	No correction	0.0024
98	n/a	n/a	No correction	0.0024
HA-4B	n/a	n/a	No correction	0.0025
99	n/a	n/a	No correction	0.0025

TABLE 2.9. Thermosalinograph temperature drift corrections (°C)

Cruise	Sensor #1392	Sensor #1392	Sensor #2045	Sensor #2045
HA-5A	n/a	n/a	No correction	0.0025
100	n/a	n/a	No correction	0.0026
100B	n/a	n/a	No correction	0.0026

Conductivity.

Sea-Bird conductivity sensor #1392 was used aboard R/V *Moana Wave* to collect thermosalinograph conductivity data for HOT-94 through HOT-97. Conductivity sensor #2045 was used for HOT-89 through HOT-93, HOT-97 through HOT-100, HA-3B, HA-4A, HA-4B and HA-5A. For sensor #1392, all conductivity data were nominally calibrated with coefficients obtained at Sea-Bird on 28 August 1997. For sensor #2045, all conductivity data were nominally calibrated with coefficients which were obtained at Sea-Bird on 30 July 1996. However, all the final salinity data reported here were calibrated against bottle data as explained below (Section 2.2.2.3).

2.2.2.2 Processing

The thermosalinograph data were screened for gross errors with upper and lower bounds of 35 °C and 18 °C for temperature and 6 Siemens m^{-1} and 3 Siemens m^{-1} for conductivity. There were no gross errors detected for any of the 1998 HOT cruises. For one mooring cruise (HA-3B), there was one gross error detected for temperature and was replaced through linear interpolation. Despite the lack of gross errors, some data can be deemed suspicious (possibly bad). These could be ascribed to such factors as biological fouling of the thermosalinograph, widely varying pump speeds, air bubbles in the thermosalinograph system, etc. Hence, a quality control system has been established so that each temperature and salinity point is given a flag to determine whether the data are good, suspect or bad to aid any data user.

HOT-92 had a large number of salinity points on April 14 and 15, 1998 flagged as suspect due to rough seas which were introducing bubbles into the thermosalinograph system. The rough seas caused a constant heaving of the ship's bow thereby introducing air bubbles into the thermosalinograph system which produced spiked and noisy salinity data. The same condition occurred on May 12, 1998 during HOT-93 and on November 17 and 18, 1998 during HA-5A. The problem of air being introduced into the thermosalinograph became so hazardous to the thermosalinograph system during HA-5A that the system had to be turned off for about 5 hours on November 17.

A 5-point running median filter was used to detect one or two point temperature and conductivity glitches in the thermosalinograph data. Glitches in temperature and conductivity detected by the 5-point median filter were immediately replaced by the median. Threshold values of 0.3 °C for temperature and 0.1 Siemens m^{-1} for conductivity were used for the median filter. No more than fifteen points were replaced after running the median filter for each cruise. A 3-point triangular running mean filter was used to smooth the temperature and conductivity data from all the cruises after they had gone through glitch detection.

2.2.2.3 Empirical Calibration

The thermosalinograph salinity was calibrated empirically by comparing it to bottle salinity samples drawn from the plumbing near the thermosalinograph. Bottle salinity samples were analyzed as described in Section 2.1.3.

For R/V *Moana Wave* the time delay between the water passing through the thermosalinograph and it reaching the bottle sampling area was determined to be about 50 seconds using autocorrelation between bottle and thermosalinograph samples. The thermosalinograph data were extracted within ± 15 seconds around the sample time minus the 50 second delay for the comparison with the bottle data.

As in previously reported cruises (i.e. Tupas et al. 1997) a cubic spline was fit to the time-series of the differences between the bottle conductivity and the thermosalinograph conductivity separately for all the 1998 cruises. The correction of the thermosalinograph conductivities was obtained from the cubic spline fit. Salinity was calculated using these corrected conductivities, thermosalinograph temperatures and a pressure of 20 dbar. The mean values for the salinity bottle minus final calibrated thermosalinograph were less than plus/minus 1 x 10^{-4} psu for each HOT cruise. Table 2.10 gives the standard deviations for the salinity bottle minus final calibrated thermosalinograph values for all 1998 cruises.

HOT-93 shows a large standard deviation (Table 2.10) compared to the other cruises. During the cruise, a drift was observed in the thermosalinograph conductivity sensor (#2045). Salinity points affected by this drift were corrected with salinity bottle data but were flagged “suspect” to caution potential data users. Sensor #2045 was sent to SeaBird for recalibration after the cruise.

TABLE 2.10. Bottle-Thermosalinograph Salinity Comparison. HA-4B conductivity data were not recorded properly and all salinity data for this cruise were flagged as “bad”

Cruise	Sensor #	Standard Deviation
89	2045	0.0031
90	2045	0.0031
91	2045	0.0045
92	2045	0.0034
HA-3B	2045	0.0079
HA-4A	2045	0.0077
93	2045	0.0144
94	1392	0.0053
95	1392	0.0050
96	1392	0.0028
97	1392/2045	0.0044
98	2045	0.0023

TABLE 2.10. Bottle-Thermosalinograph Salinity Comparison. HA-4B conductivity data were not recorded properly and all salinity data for this cruise were flagged as "bad"

Cruise	Sensor #	Standard Deviation
HA-4B	2045	n/a
99	2045	0.0011
HA-5A	2045	0.0041
100	2045	0.0013
100B	2045	0.0014

A conductivity offset was observed during HOT-97 on September 29, 1998 when conductivity sensor #1392 was being used. Salinity points affected by this offset were flagged as "suspect" and the thermosalinograph system had to be turned off for a short period of time in order to replace conductivity sensor #1392 with sensor #2045 during the cruise.

2.2.2.4 Comparison with CTD Data

The corrected thermosalinograph salinity data were compared with the downcast CTD salinity at 4 dbar for the purpose of checking the calibration. This procedure was conducted in the same manner as previously reported HOT cruises (i.e. Tupas et al. 1997). The thermosalinograph data were averaged using data sampled one minute after the acquisition time of the CTD sample. After final calibrations were performed on the thermosalinograph salinities, mean comparisons with the CTD were most of the time within ± 0.01 psu.

2.3 Inverted Echo Sounder

The history of the IESs in the HOT site is well documented in Tupas et al. (1994a, 1995, 1997, 1998) and Karl et al. (1996). One IES (#127) was deployed 4 nm north from the center of Station ALOHA during HOT-85 on 11 July 1997, and retrieved on 14 July 1998 during HOT-95. The same IES was re-deployed at the center of Station ALOHA on 9 August 1998 during HOT-96.

2.4 Meteorology

Wind speed and direction, atmospheric pressure, wet- and dry-bulb air temperature, sea surface temperature (SST), cloud cover and sea state were recorded at four-hour intervals while at Station ALOHA by the science personnel. Two arrays of meteorological instruments measuring air speed, humidity, wind velocity and precipitation at one-second intervals were available during cruises. One array was mounted on a tower near the bow of the R/V *Moana Wave*, and another on an A-frame on the back deck. Meteorological observations were also obtained every 4 hours by the ship's officers on the bridge of the R/V *Moana Wave* throughout each cruise. Additionally, hourly wind speed and direction were obtained from NDBC buoy #51001 (23.4N, 162.3W). This buoy was not operational during HOT-89 (January and part of February). The time-series of shipboard observations obtained by the science group was plotted and obvious outliers were identified and flagged. The SST-dry air temperature and wet-dry air temperature plots also helped to identify outliers. Bad data points were often replaced with the bridge data or with the tower or A-frame data. Outliers in the shipboard pressure, air temperature, SST and wind observations were detected by comparison with the buoy winds.

2.5 ADCP Measurements

Upper ocean currents were measured on all twelve HOT and the HALE-ALOHA mooring deployment and/or recovery cruises using the ADCP mounted on the R/V *Moana Wave* (RD Instruments model VM-150). Currents were also measured during the HOT-100B cruise. ADCP velocities were corrected for gyro compass errors as measured by the Ashtec 3DF GPS attitude sensor. There were no significant data recording gaps. GPS navigation (differential or PCODE) was available throughout all cruises. There was no heading correction data available for HOT-100 and 100B, as one of the receivers was down. Six other cruises had substantial single heading correction gaps (in hours): HOT-89: 1.67, HOT-92: 1.68, HOT-93: 0.67, HOT-95: 2.25, HA-3B: 2.33, and HA-5A: 0.42; all other gaps were less than 25 minutes. All heading correction gaps were filled by linearly interpolating the gyro error estimates.

Rough weather or seas on northward transits caused reduced returns on HOT-92, HOT-93, HOT-100, HA-4A, and HA-5A. These conditions resulted in velocity bias in the direction of ship's motion. Biased regions have been edited out, and will therefore appear as gaps in the plots. Gaps in the on-station data of HOT-96 and HOT-97 are due to excursions to retrieve the primary productivity array and floating sediment traps.

2.6 Biogeochemical Measurements

At Stations Kahe, ALOHA and HALE-ALOHA, water samples for chemical analyses were collected from discrete depths using 12-liter PVC bottles with teflon coated internal springs as closing mechanisms. Sampling strategies and procedures are well documented in the previous data reports and in the HOT Program Field and Laboratory Protocols manual. This report contains only a subset of the total data base which can be extracted electronically over the Internet (http://hahana.soest.hawaii.edu/hot/hot_jgofs.html). To assist in the interpretation of these data and to save users the time to estimate the precision of individual chemical analysis, we have summarized precision estimates from replicate determinations for each constituent on each HOT cruise in 1998.

2.6.1 Dissolved Oxygen

Dissolved oxygen samples were collected and analyzed using a computer-controlled potentiometric end-point titration procedure as described in Tupas et al. (1997). As in previous years we measured, using a calibrated digital thermistor, the temperature of the seawater sample at the time the iodine flask was filled. This was done to evaluate the magnitude of sample temperature error which affects the calculation of oxygen concentrations in units of μmol kg^{-1}. Figure 2.3 (upper panel) shows a plot of the difference between sample temperature and potential temperature computed from the *in situ* temperature measured at the time of bottle trip, versus pressure. The lower panel of the same figure shows a plot of the difference between oxygen concentration using on-deck and potential temperatures versus pressure. The depth dependent variability in oxygen difference is a result of the absolute magnitude of the oxygen concentration and the standard procedures we employ for sampling the water column.

Precision of the Winkler titration method is presented in Table 2.11. The mean precision of our oxygen analyses in 1998 was 0.13%. Oxygen concentrations measured over the 10 years of the program are plotted at three constant potential density horizons in the deep ocean along with their mean and 95% confidence intervals (Figure 2.4). These results indicate that analytical consistency has been maintained over the past 10 years of the HOT program.

TABLE 2.11. Precision of Winkler titration method

Cruise	CV (%)	SD (μmol l^{-1})	n
89	0.11	0.198	18
90	0.08	0.148	19
91	0.09	0.192	16
92	0.07	0.136	29
93	0.12	0.192	16
94	0.14	0.255	16
95	0.09	0.177	11
96	0.20	0.375	13
97	0.14	0.252	12
98	0.15	0.285	12
99	0.19	0.351	11
100	0.14	0.264	9

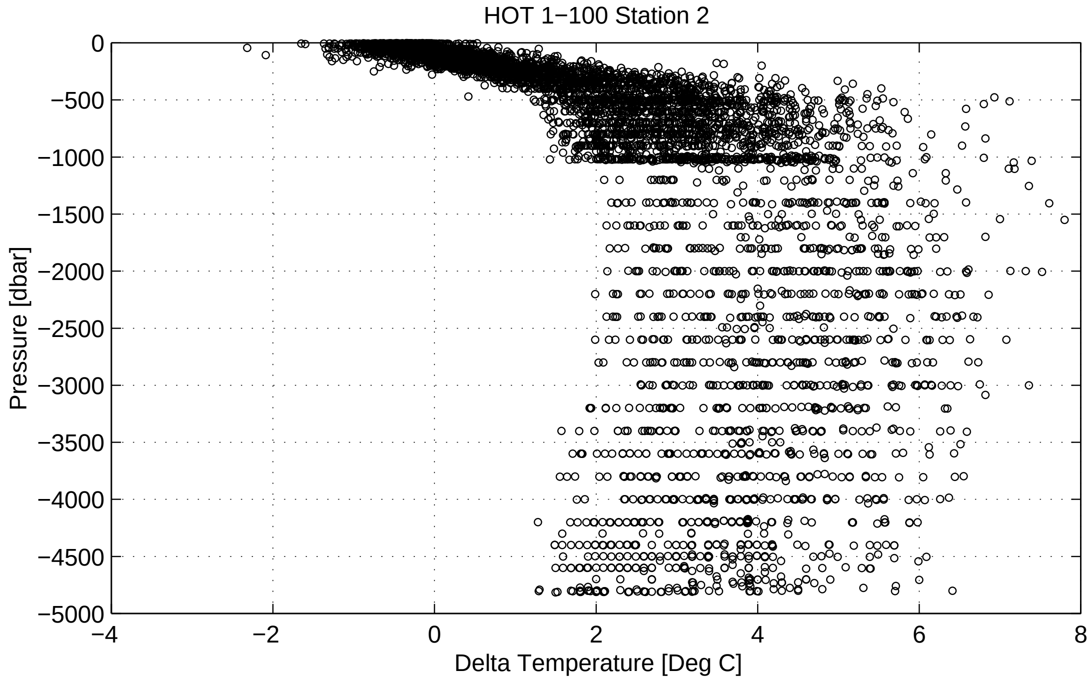

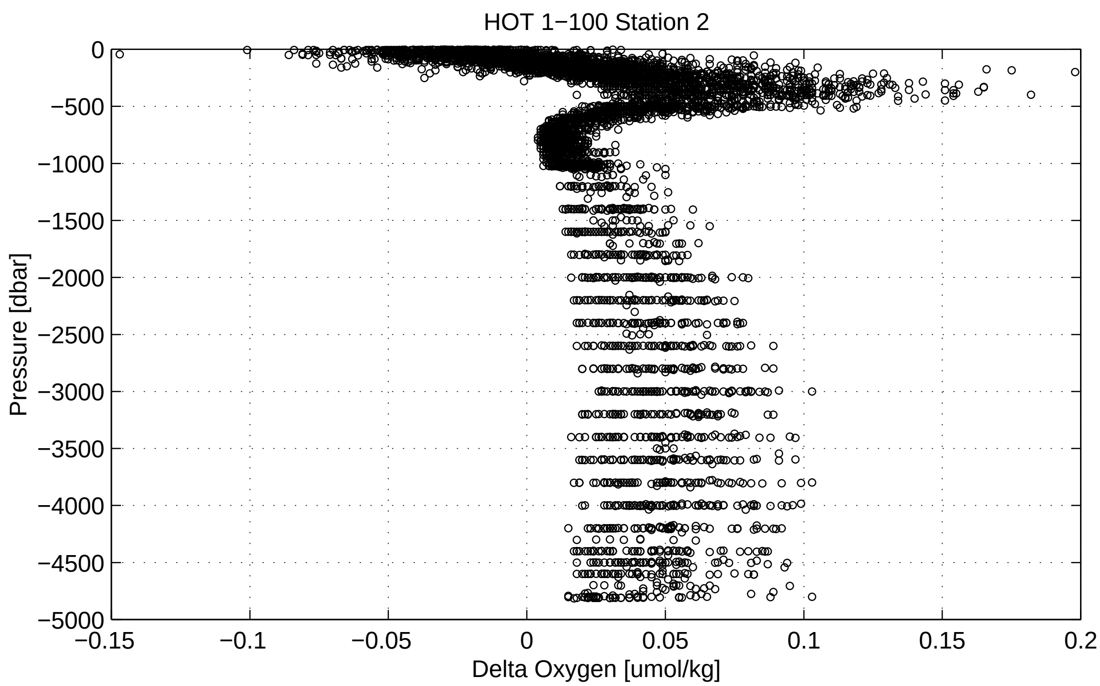

FIGURE 2.3. [Upper panel] Difference between sample temperature at the time of sample collection and potential temperature calculated from *in situ* temperature at the time of bottle trip. [Lower panel] Difference in oxygen concentration corrected for temperatures measured at the time of sample collection and potential temperature calculated from *in situ* temperature.

2.6.2 Inorganic Carbon Parameter

2.6.2.1 Dissolved Inorganic Carbon and Titration Alkalinity

Samples for dissolved inorganic carbon (DIC) were measured using a Single Operator Multi-parameter Metabolic Analyzer (SOMMA) which was manufactured at the University of Rhode Island and standardized at the Brookhaven National Laboratory. Analyses of primary DIC standards (Tupas et al. 1993) indicated that the precision of replicate samples is approximately 1 μmol kg^{-1}. Titration alkalinity was determined using the Gran titration method as described in Tupas et al. (1997). The precision of the titration procedure was approximately 5 μequiv kg^{-1}. Accuracy was established with certified reference standards obtained from Andrew Dickson at Scripps Institution of Oceanography and compared to analyses by Charles D. Keeling also at Scripps Institution of Oceanography for DIC and Andrew Dickson for alkalinity.

2.6.2.2 pCO_2

In October 1996 (HOT-76) an automated, semi-continuous system for measuring the partial pressure of carbon dioxide in seawater was installed in-line with the ship's clean-seawater intake system to measure underway surface seawater pCO_2. The system is calibrated using three standard gases of known CO_2 concentrations covering the range of 200-400 ppm (Scott Specialty Gases calibrated at SIO). A separate reference gas calibrated at 349.0 ppm is measured for quality assurance. Calibration and standardization are done at system startup and approximately every 2.5 hours. The present system consists of a shower head equilibrator operating at a flow rate of approximately 8 l min^{-1}. Equilibrated gas and bow air are both sampled every 10 minutes. The gases pass through a napthyon tube drier and a magnesium perchlorate scrubber into a LICOR 6250 infrared detector. The reference chamber is purged with reference gas after every 3 cycles of bow/equilibrator measurements. Gas flow rates into the detector are at approximately 0.5 l min^{-1}. The system output gives the CO_2 concentration of the bow-intake air and the surface seawater in ppm. The system begins operating when the ships is in clean open water and is fully operational at Station Kahe. The system is turned off after departing the last station. Measurements of pCO_2 were stopped in the middle of 1998.

2.6.2.3 pH

Beginning in 1992, pH was determined spectrophotometrically using the indicator m-cresol purple following the methods described in Tupas et al. (1993). The absorbance of the mixture was measured at wavelengths of 578 and 434 nm on a Perkin Elmer Model 3 dual-beam spectrophotometer and converted to pH on the seawater scale according to Clayton and Byrne (1993). The mean and standard deviation of the difference of sets of duplicate pH measurements was 0.0009 and 0.00077 respectively. Measurements of pH were stopped in the middle of 1998.

2.6.3 Inorganic Nutrients.

2.6.3.1 Standard Methods.

Samples for the determination of dissolved inorganic nutrient concentrations (soluble reactive phosphorus, [nitrate+nitrite] and silicate) were collected as described in Tupas et al. (1993). Analyses were conducted at room temperature on a four-channel Technicon Autoanalyzer II continuous flow system at the University of Hawaii Analytical Facility. A summary of the precision of analyses for 1998 is shown in Table 2.12. Figures 2.4-2.5 show the mean and 95% confidence limits of nutrient concentrations measured at three potential density horizons for the 10 years of the program. In addition to standard automated nutrient analyses, specialized chemical method are used to determine concentration of nutrients that are normally below the detection limits of autoanalyzer methods.

TABLE 2.12. Precision of Dissolved Inorganic Nutrient Analyses

	Soluble Reactive Phosphorus				[Nitrate + Nitrite]				Silicate			
	Analytical		Field		Analytical		Field		Analytical		Field	
HOT	CV (%)	SD μM	CV (%)	SD μM	CV (%)	SD μM	CV (%)	SD μM	CV (%)	SD μM	CV (%)	SD μM
89	0.01	0.008	0.3	0.005	0.17	0.008	0.3	0.067	0.18	0.002	3.4	0.412
90	0.01	0.008	0.5	0.010	0.10	0.005	0.5	0.052	0.16	0.002	1.1	0.308
91	0.01	0.008	0.6	0.013	0.08	0.004	0.2	0.078	0.18	0.002	3.6	0.171
92	0.01	0.007	0.7	0.016	0.08	0.004	0.3	0.043	0.15	0.002	1.0	0.128
93	0.01	0.009	0.3	0.009	0.13	0.006	0.3	0.039	0.31	0.005	4.2	0.367
94	0.01	0.005	0.6	0.012	0.12	0.005	0.4	0.075	0.19	0.002	8.3	0.339
95	0.01	0.008	0.3	0.005	0.08	0.004	0.4	0.054	0.12	0.002	2.3	0.334
96	0.01	0.009	0.5	0.008	0.09	0.004	0.3	0.042	0.18	0.002	0.4	0.259
97	0.01	0.007	0.6	0.009	0.09	0.004	0.6	0.095	0.13	0.002	0.4	0.122
98	0.01	0.005	0.6	0.016	0.05	0.003	0.2	0.029	0.15	0.002	0.3	0.098
99	0.01	0.007	1.1	0.016	0.07	0.003	0.7	0.077	0.11	0.001	1.0	0.196
100	n/a	n/a	1.0	0.020	n/a	n/a	0.4	0.107	n/a	n/a	0.5	0.499
Mn	0.011	0.008	0.59	0.012	0.094	0.005	0.38	0.063	0.168	0.002	2.21	0.269
SD	0.002	0.001	0.25	0.005	0.033	0.001	0.15	0.024	0.053	0.001	2.37	0.128

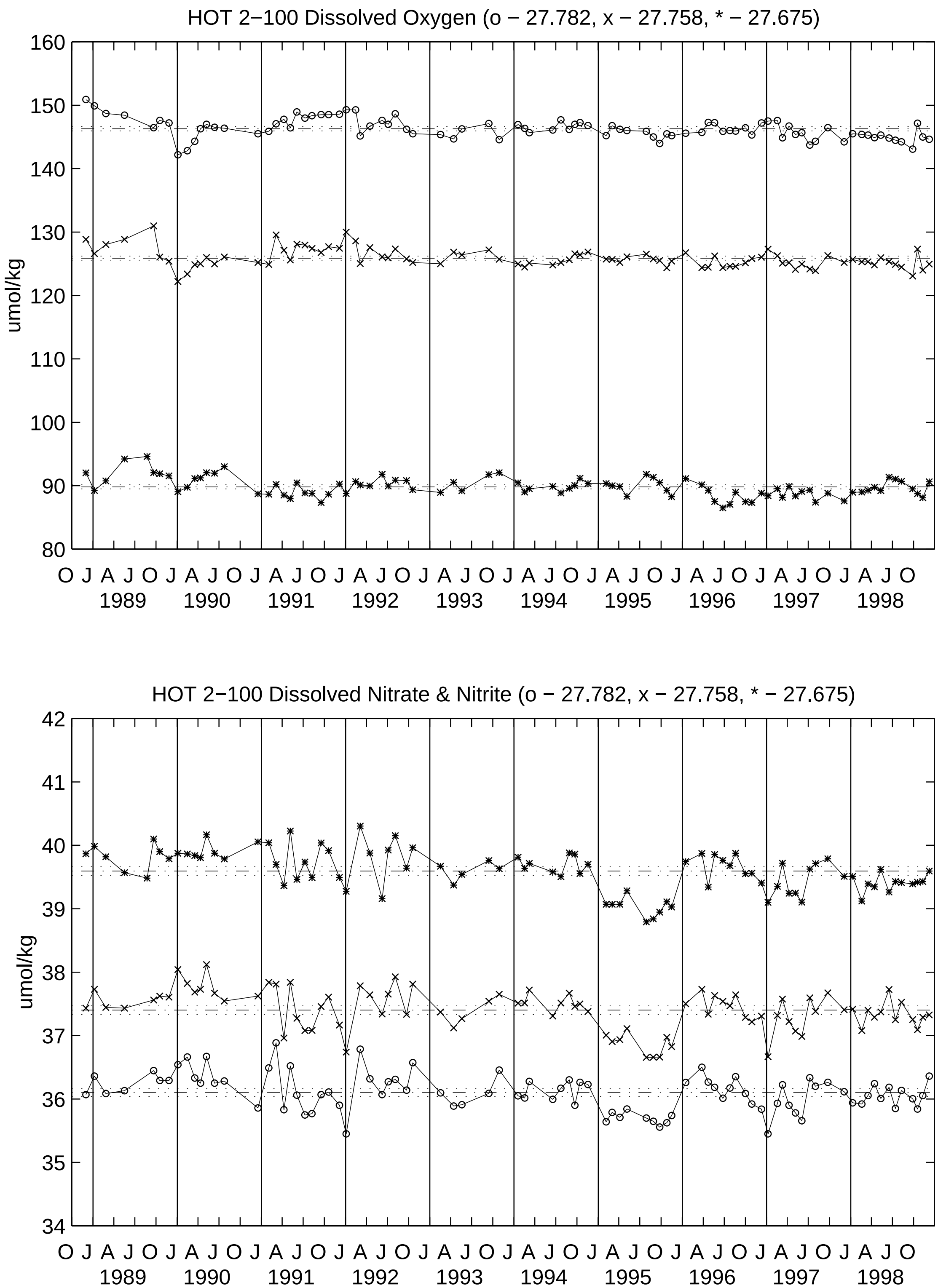

FIGURE 2.4. Concentrations at potential density horizons of 27.782, 27.758 and 27.675 at Station ALOHA. [Upper panel] Dissolved oxygen. [Lower panel] Nitrate + nitrite.

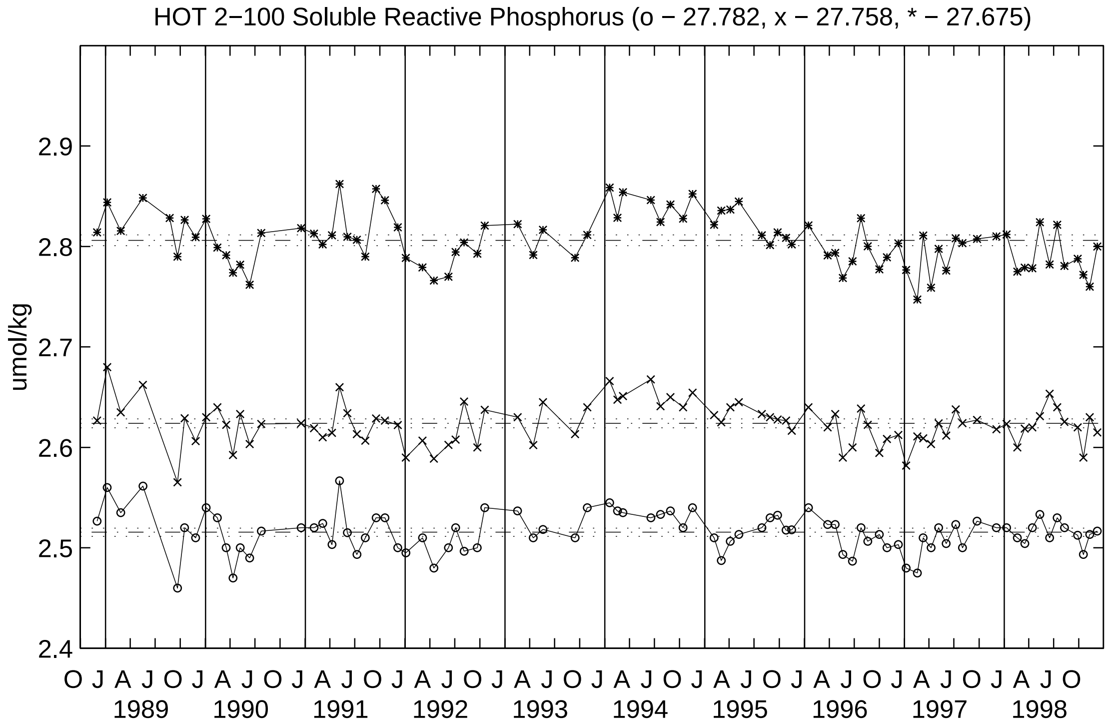

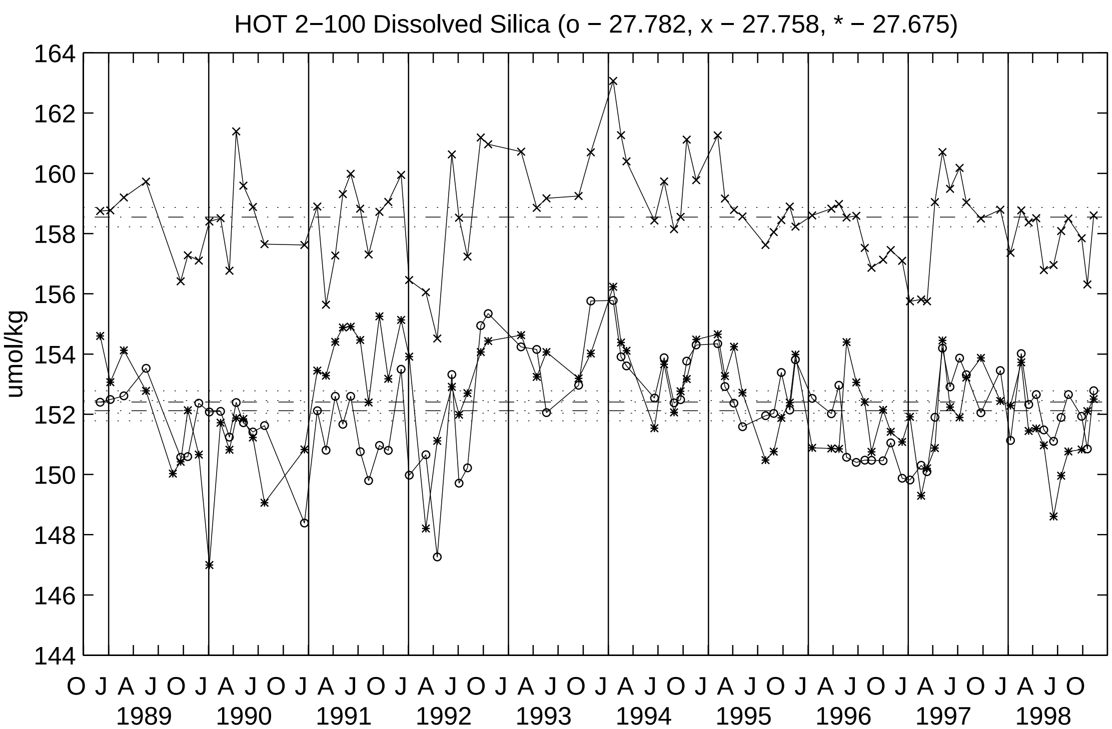

FIGURE 2.5. Concentrations at potential density horizons of 27.782, 27.758 and 27.675 at Station ALOHA. [Upper panel] Soluble reactive phosphorus [Lower panel] Silicate

2.6.3.2 High Sensitivity Methods

The chemiluminescent method of Cox (1980) as modified for seawater by Garside (1982) was used to determine the [nitrate+nitrite] content of near surface (0-200 m interval) water samples (Tupas et al. 1997). The limit of detection for [nitrate+nitrite] was approximately 2 nM with a precision and accuracy of ±1 nM (Dore et al. 1996).

Low level soluble reactive phosphorus (SRP) concentrations in the euphotic zone were determined according to the magnesium induced coprecipitation (MAGIC) method of Karl and Tien (1992). Typical precision estimates for triplicate determinations of SRP are from 1-3 % with a detection limit of 10 nmol l^{-1}. This latter measurement is also corrected for arsenate interference of the molybdenum blue colorimeteric procedure (Johnson 1971), and thus provides a more accurate estimate of SRP.

2.6.4 Dissolved Organic Matter

Dissolved organic carbon (DOC) was determined by the high temperature catalytic oxidation method using an automated DOC analyzer (Qian and Mopper 1996). Dissolved organic nitrogen (DON) was calculated as the difference between total dissolved fixed nitrogen (TDN) and [nitrate+nitrite] concentrations. DON by this definition also includes ammonium, however, ammonium in theses waters are below the detection limit of standard nutrients analysis and are estimated to be less than 100 nmol l^{-1}. Dissolved organic phosphorus (DOP) was calculated as the difference between total dissolved phosphorus (TDP) and SRP concentrations. DOP, by this definition includes inorganic polyphosphates. TDN and TDP were determined by the UV oxidation method as described in Tupas et al. (1997). A summary of the precision of these analyses is given in Table 2.13.

TABLE 2.13. Precision of dissolved organic nutrient analyses

	DON		DOP		DOC	
Cruise	Mean CV (%)	mean SD (μmol kg^{-1})	Mean CV **(%)**	mean SD (μmol kg^{-1})	Mean CV **(%)**	Mean SD (μmol kg^{-1})
89	6.3	0.309	11.7	0.015	0.8	0.453
90	12.4	0.470	9.9	0.010	3.0	1.796
91	9.8	0.314	0.9	0.002	0.8	0.407
92	8.7	0.268	35.5	0.024	0.9	0.636
93	13.2	0.263	9.6	0.012	2.2	1.573
94	8.8	0.444	8.7	0.016	3.0	1.750
95	8.6	0.346	21.8	0.018	3.4	2.316
96	6.0	0.332	8.3	0.011	1.5	1.160
97	7.9	0.392	14.4	0.016	1.3	1.167
98	9.9	0.330	25.8	0.017	2.4	1.715
99	6.3	0.219	18.5	0.018	3.3	2.517
100	7.9	0.273	24.7	0.018	1.4	0.672

2.6.5 Particulate Matter

Samples for analysis of particulate matter were prefiltered through 202 um Nitex mesh to remove large zooplankton and collected onto combusted GF/F glass fiber filters (acid washed for particulate phosphorus). Particulate carbon (PC) and nitrogen (PN) on the filters were analyzed using a Europa automated nitrogen and carbon analyzer. Particulate phosphorus (PP) was analyzed by converting the material to orthophosphate by high temperature ashing followed by acid hydrolysis and determining the orthophosphate content by colorimetry. Precision of particulate matter analysis is presented in Table 2.14.

TABLE 2.14. Precision of particulate matter analyses

	Particulate Carbon		Particulate Nitrogen		Particulate Phosphorus	
Cruise	Mean CV (%)	Mean SD (μmol kg^{-1})	Mean CV **(%)**	Mean SD (μmol kg^{-1})	Mean CV **(%)**	Mean SD (μmol kg^{-1})
89	6.6	1.308	15.0	0.530	12.5	0.035
90	6.2	1.697	5.7	0.247	1.7	0.007
91	19.3	4.632	23.2	0.778	1.6	0.004
92	NR	NR	NR	NR	22.9	0.071
93	2.3	0.460	5.0	0.177	10.1	0.025
94	4.2	1.096	5.9	0.247	26.8	0.099
95	5.0	1.344	9.2	0.354	9.3	0.039
96	7.2	3.217	12.2	0.566	11.6	0.064
97	3.5	0.884	8.1	0.318	7.6	0.032
98	10.7	2.970	5.5	0.247	20.3	0.095
99	4.4	0.884	5.2	0.177	13.8	0.053
100	4.5	0.955	4.8	0.212	8.3	0.028

2.6.6 Pigments

2.6.6.1 Standard Fluorometric Method

Chlorophyll *a* (chl *a*) and pheopigments were measured fluorometrically on a Turner Designs Model 10-AU fluorometer using 100% acetone as the extractant and standard techniques (Strickland and Parsons 1972). Analytical precision for this analysis is presented in Table 2.15. Integrated values for pigment concentrations were calculated using the trapezoid rule.

2.6.6.2 High Performance Liquid Chromatography

Chlorophyll *a* and accessory photosynthetic pigments were also measured by high performance liquid chromatography (HPLC) according to Bidigare et al. (1990). A new HPLC method following SCOR recommendation was adopted in 1994. This method is a modification of the method developed by Wright et al. (1991). The new method allows for a better separation of lutein and zeaxanthin as well as monovinyl and divinyl chlorophyll *a*.

2.6.6.3 Underway Surface Fluorometry

Beginning with HOT-76 (September 1996), a Turner Designs Model 10-AU fluorometer was installed on the R/V *Moana Wave* to measure continuous *in vivo* chlorophyll (fluorescence) from surface seawater sampled by the ship's seawater intake system. The underway measurements are calibrated by taking discrete samples from the outflow of the fluorometer and extracting the pigments according to standard methods.

TABLE 2.15. Precision of fluorometric chlorophyll *a* and pheopigment analyses

Cruise	Mean CV (%)	SD ($\mu g\ l^{-1}$)	Mean CV (%)	SD ($\mu g\ l^{-1}$)
89	3.1	0.005	4.6	0.012
90	2.2	0.004	7.4	0.049
91	7.3	0.021	6.2	0.020
92	2.9	0.006	7.0	0.014
93	3.1	0.005	7.5	0.015
94	3.5	0.005	4.8	0.010
95	3.1	0.006	5.1	0.020
96	8.2	0.015	7.5	0.022
97	2.9	0.004	7.1	0.011
98	8.8	0.015	14.6	0.033
99	3.7	0.004	3.4	0.008
100	3.3	0.004	3.3	0.007

2.6.7 Adenosine 5'-Triphosphate

Water column adenosine 5'-triphosphate (ATP) concentrations were determined using the firefly bioluminesence technique as described by Karl and Holm-Hansen (1978). The precision of ATP determinations in 1998 are given in Table 2.16.

TABLE 2.16. Precision of ATP Analyses

Cruise	Mean CV (%)	Mean SD ($\mu g\ m^{-3}$)
89	21.7	2.116
90	18.0	1.316
91	15.0	2.529
92	17.1	2.094
93	14.9	1.893
94	10.8	1.113

TABLE 2.16. Precision of ATP Analyses

Cruise	Mean CV (%)	Mean SD ($\mu g\ m^{-3}$)
95	15.4	1.722
96	15.3	2.756
97	11.4	1.567
98	13.4	2.678
99	11.3	1.730
100	14.6	1.212

2.7 Biogeochemical Rate Measurements

2.7.1 Primary Production

Photosynthetic production of organic matter was measured by a trace-metal clean, ^{14}C method. Incubations were conducted *in situ* at eight depths for at least 12 hours using a free-drifting array as described by Winn et al. (1991). Integrated carbon assimilation rates were calculated using the trapezoid rule with the shallowest value extended to 0 m and the deepest extrapolated to a value of zero at 200 m.

2.7.2 Particle Flux

Particle flux was measured at a standard reference depth of 150 m using sediment traps deployed on a free-floating array for approximately 2.5 days during each cruise. Sediment trap design and collection methods are described in Winn et al. (1991). Samples were analyzed for particulate C, N and P.

2.8 Optical Measurements

2.8.1 Solar Irradiance

Incident irradiance at the sea surface was measured on each HOT cruise with a LICOR LI-200 data logger and cosine collector. The instrument recorded data from the time the ship departed Snug Harbor and until its return.

2.8.2 Downwelling Irradiance and Upwelling Radiance

Vertical profiles of upwelling radiance and downwelling irradiance were made using a Biospherical Profiling Reflectance Refractometer (PRR-600). This instrument measures downwelling irradiance (Ed) and upwelling radiance (Lu) as well as surface irradiance from a deck unit on 7 channels. The radiance channels comply with the SeaWIFS optical parameters. The instrument is lowered by hand and depending on the subsurface currents, is deployed to a depth between 120 and 150 m.

2.8.3 Flash Fluorescence

Flash fluorescence was measured with a Sea Tech Model ST0250 flash fluorometer and the data collected with the Sea-Bird CTD system. Flash fluorescence traces were collected on as many casts as possible. Because an absolute radiometric standard is not available for flash fluorometers, instrument drift was corrected by checking the relative response of the instrument between cruises using fluorescent plastic sheeting as described in Tupas et al. (1997). A linear relationship of the form, Vn = b Vo + a, was used to convert all fluorescence data to a common voltage scale, where Vn is the normalized voltage, Vo is the output voltage and a and b are constants derived from the two deep water intervals. The constants used in 1998 were a = 1.6669 and b = 0.6503.

2.9 Microbial Community Structure

Analysis of bacterial number was made using an EPICS 753 flow cytometer (Coulter Electronics Corporation, Hialeah, FL, USA) which has been upgraded with a Cicero Data Acquisition System (Cytomation Inc., Boulder, Colorado). A consistent delivery of sample volume and sample flow rate (100 μl at 50 μl min^{-1} and 50 μl at 50 μl min^{-1} was regularly achieved using a Microsample Delivery System, Coulter Electronics Corporation, Hialeah, FL, USA). Prior to analysis by flow cytometry, samples were prepared using standard protocols (Campbell et al. 1994). Hoechst 33342 was added to each sample at a final concentration of 1μg ml^{-1} (Monger & Landry 1993). Samples were also amended with 0.57 and 0.9 μm microspheres (visible excitation, Fluoresbrite Polysciences) as well as 0.46 μm, UV-only excitable beads. Samples were illuminated simultaneously with 1 Watt of the 488 nm line, and 225 mW UV line, originating from a dual platform equipped with 5 Watt Argon lasers (90-5, Coherent Laser Products, Palo Alto CA). Fluorescence was detected using band pass interference filters for orange fluorescence (575 nm), red fluorescence (680 nm) and blue fluorescence (450 nm). Measurements from these parameters, as well as forward angle light scatter (FALS) and 90 degree light scatter (LS), were amplified into a 3-decade logarithmic scale and stored in a list mode file. Analysis of these files, using CYTOPC (Vaulot 1989), permitted the identification and enumeration of the various populations in the microbial community. The enumeration output from this analysis was corrected for volume (cells ml^{-1}). In addition, an enumeration efficiency factor, based on flow cytometer sample counting rates, was derived using 0.98 μm beads.

2.10 Zooplankton Community Structure

2.10.1 Mesozooplankton Collection

Samples for the assessment of mesozooplankton were collected using a 1 m^2 plankton net with a 202 μm Nitex mesh. The square net frame has a bottom depressor to make it dive steeply and smoothly through the depth range of the tow, and the bridle system does not cross the net mouth thereby minimizing animal avoidance. A Brancker time-depth-temperature recorder is attached to the frame to determine the depth of tow and confirm even collection at each depth. A General Oceanics flow meter is centered at the net mouth to estimate the volume of water filtered. The net is towed obliquely at a speed of 1.0-1.5 knots while deploying and retrieving the tow line at a constant speed (about 20 m min^{-1}; total line out = 200 m; 20 minute tow duration; average depth of tow 175 m. Three mid-night (between 2200-0200 local time) and three mid-day (between 1000-1400 local time) net tows are conducted on each cruise.

2.10.2 Sample Processing

Contents of the net cod ends are immediately anesthetized with carbonated water to prevent gut evacuation. The net samples are then divided using a Folsom splitter with one-half preserved in 4% buffered formaldehyde with 2 mg l^{-1} strontium sulfate to prevent acantharians from dissolving, and approximately one-fourth (depending on sample density) size fractionated through nested screens of 5, 2, 1, 0.5 and 0.2 mm Nitex mesh. The remaining one-fourth sample is prepared for live silhouette photography (Ortner et al. 1979) which provides a permanent record of delicate gelatinous forms. Each size fraction is concentrated on a preweighed Nitex screen, rinsed with isotonic ammonium formate to remove salts, sucked dry under low vacuum and flash frozen in liquid nitrogen. Frozen samples are defrosted in the dark at room temperature, weighed wet (moist) on an analytical balance before (total weight wet) and after (fraction removed) drying. Random sub-samples of the zooplankton mass are set aside for enumeration and pigment analysis. The remaining sample is dried at 60 °C, reweighed [total sample dry weight = measured dry weight/fraction of total wet weight dried] and analyzed for carbon and nitrogen.

3. CRUISE SUMMARIES

The cruise summaries presented here give an overview of the activities conducted during the 1998 HOT cruises. The official Chief Scientist's report can be found on the HOT-JGOFS and HOT-WOCE web pages.

3.1 HOT-89: Louie Tupas, Chief Scientist

The R/V *Moana Wave* departed Snug Harbor at 0900 HST on January 9, 1998 with 17 scientists on-board. All objectives of the JGOFS and WOCE programs were accomplished. All planned stations were occupied. All core samples were taken and the 36 hour CTD burst sampling period was not interrupted. All samples for ancillary projects were taken. Floating sediment trap array and primary production array deployed and recovered successfully. No samples were lost during the *in situ* incubations. ADCP measurements were made throughout the cruise. The pCO_2 system operated using the ship's uncontaminated seawater intake system. The optical plankton counter did not function despite several attempts to troubleshoot and repair the instrument. OPC work was abandoned and the schedule of work moved up by about 6 hours. Transit to Snug began at about 1600 on 12 January and cruising speed was increased to arrive at Snug by 0000 on January 13, 1998. Unloading commenced after early breakfast.

3.2 HOT-90: Dale Hebel, Chief Scientist

The R/V *Moana Wave* departed Snug Harbor at 0900 HST on February 17, 1998 with 17 scientists on-board. In addition to our routine cruise schedule we had aboard Ken Smith and his group from SIO to deploy and retrieve their FVGR for calibration of their deployed benthic Rover. Four stations were occupied at Kahe Pt. (sta. 1), Station ALOHA (sta. 2), FVGR deployment site and the HALE-ALOHA mooring location (Sta. 8).

During the cruise all underway measurement systems (thermosalinograph, ADCP, meteorological instruments, pCO_2 and fluorometer) were operable and functioned normally. Although we were able to collect all core samples and complete the 36 hr burst CTD work we did experience some problems with the CTD cable. In addition, continued electrical problems plagued the OPC preventing deployment, however we were able to use the time for a second WOCE deep cast. The weather was generally moderate with <20 knot trade winds, swells 3-6 feet and skies mostly cloudy. The ship arrived at Snug Harbor at 0800 on February 21, 1998.

3.3 HOT-91: Dale Hebel, Chief Scientist

The R/V *Moana Wave* departed Snug Harbor at 1000 HST March 16, 1998 with 17 scientists on-board. We occupied Stations Kahe Pt. (sta. 1), Station ALOHA (sta. 2), and the HALE-ALOHA mooring location (sta. 8). CTD operations were conducted at Stations 1, 2 and 8. Fifteen CTD casts were conducted at Station ALOHA and two at Station 8 in addition to 4 light casts, 6 net tows, 1 Go-Flo cast, and usual floating sediment traps and productivity operations. During the cruise the LADCP was fitted to the rosette package and depending on the circumstances either used on the new or old rosette. LADCP tests were conducted on routine hydrocasts as well as dedicated casts. All underway measurement systems (thermosalinograph, ADCP, meteorological instruments, pCO_2 and fluorometer) were operable and functioned normally. The seas were calm with light winds and skies mostly clear. The ship arrived at Snug Harbor at 0700 on March 20, 1998.

3.4 HOT-92: Louie Tupas, Chief Scientist

The R/V *Moana Wave* departed Snug Harbor at 0900 on April 13, 1998 with 17 scientists on-board. All objectives of the JGOFS and WOCE programs were accomplished. All planned stations were occupied. Weather and sea conditions were initially rough but within the limits of safety for deck operations. All core samples were taken and the 36 hour CTD burst sampling period was not interrupted. All samples for ancillary projects were taken. Floating sediment trap array and primary production array deployed and recovered successfully. No samples were lost during the *in situ* incubations. ADCP measurements were made throughout the cruise. The pCO_2 system was operated using the ship’s uncontaminated seawater intake system. The ship arrived at Snug Harbor at 0800 on April 17, 1998.

3.5 HOT-93: Dale Hebel, Chief Scientist

The R/V *Moana Wave* departed Snug Harbor at 0900 on May 11, 1998 with 14 scientists on-board. We occupied Stations Kahe Pt. (sta. 1), Station ALOHA (sta. 2), and HALE-ALOHA mooring location (sta. 8). CTD operations were conducted at Stations 1, 2 & 8. Fifteen CTD casts were conducted at Station ALOHA and one at Station 8 in addition to 7 light casts, 6 net tows, 1 Go-Flo cast, and usual floating sediment traps and productivity operations. All operations were routine with the exception of the extra light casts requested by Jasmine Bartlett of OSU. All underway measurement systems (thermosalinograph, ADCP, meteorological instruments, pCO_2 and fluorometer) were operable and functioned normal except for a period when it was discovered that the attitude feed for the ADCP was off-line. The seas were generally rough with high winds and mostly cloudy skies. Due to the rough seas a number of spikes were recorded in some of the continuous measurement systems. The ship arrived at Snug Harbor at 0740 on May 15, 1998.

3.6 HOT-94: Louie Tupas, Chief Scientist

The R/V *Moana Wave* departed Snug Harbor at 0900 on June 15, 1998 with 16 scientists on-board. All objectives of the JGOFS and WOCE programs were accomplished. All planned stations were occupied. Weather and sea conditions were initially rough but within the limits of safety for deck operations. All core samples were taken and the 36 hour CTD burst sampling period was not interrupted. All samples for ancillary projects were taken. Floating sediment trap array and primary production array deployed and recovered successfully. No samples were lost during the *in situ* incubations. ADCP measurements were made throughout the cruise. The pCO_2 system was operated using the ship’s uncontaminated seawater intake system. Ken Smith's Free Vehicle Grab Respirometer was deployed and retrieved successfully. The SIO group, however, was unable to retrieve the Rover they deployed last November. All attempts to contact it were unsuccessful. The ship arrived at Snug Harbor at 0800 on June 19, 1998.

3.7 HOT-95: Craig Nosse, Chief Scientist

The R/V *Moana Wave* departed Snug Harbor at 0915 on July 13, 1998 with 16 scientists on-board. All the primary JGOFS and WOCE objectives were accomplished and all samples for ancillary projects were taken. The IES was also successfully recovered. A 36-hour CTD burst sampling period was completed at Station ALOHA which involved twelve 1000 m casts and one deep cast to the near-bottom conducted at the end of the 36-hour period. A near-bottom deep cast was also obtained prior to the commencement of the 36-hour period. 1000 m casts were also obtained at Stations Kahe and HALE-ALOHA. One 8-bottle Go-Flo cast was made to obtain seawater for the primary productivity array which was deployed and recovered without incident. The array of floating sediment traps was also deployed and recovered without incident. The sediment traps had drifted about 15 nm west-southwest from the center of Station ALOHA. Two 4-bottle Go-Flo casts were conducted at Station ALOHA to obtain zooplankton grazing samples for M. Landry and T. Smith. S. Nunnery successfully completed 6 plankton net tows (3 during the day, 3 at night). The bottom moored IES located four nautical miles north of Station ALOHA was recovered without incident after its year-long deployment. Initial indications show that the IES appears to be in good working order. Weather conditions were somewhat rough during the transit out to Station ALOHA with 20+ knot winds and about 5-6 foot seas. However, conditions improved dramatically throughout the cruise and on the last day of the cruise, winds had diminished to below 15 knots and the sea condition diminished to 2-3 foot seas. The ADCP ran without interruption throughout the cruise, as well as the thermosalinograph, the Licor light logger and the fluorometer. It was decided by the JGOFS group not to run the pCO_2 system during the cruise. The primary meteorological sensors failed to record about 12 hours of data during the second to last day of the cruise but all other meteorological data were continuously recorded throughout the cruise. We arrived a Snug Harbor on July 17 at approximately 0730 on July 17, 1998.

3.8 HOT-96: Louie Tupas, Chief Scientist

The R/V *Moana Wave* departed Snug Harbor at 0900 on August 8, 1998 with 13 scientists on-board. All objectives of the JGOFS and WOCE programs were accomplished. All planned stations were occupied. Weather and sea conditions were initially rough but within the limits of safety for deck operations. All core samples were taken and the 36 hour CTD burst sampling period was not interrupted. All samples for ancillary projects were taken. Floating sediment trap array and primary production array deployed and recovered successfully. No samples were lost during the *in situ* incubations. ADCP measurements were made throughout the cruise. The IES was successfully deployed. The ship arrived Snug Harbor at 0800 on August 12, 1998.

3.9 HOT-97: Louie Tupas, Chief Scientist

The R/V *Moana Wave* departed Snug Harbor at 0900 on September 26, 1998 with 17 scientists on-board. All objectives of the JGOFS and WOCE programs were accomplished. All planned stations were occupied. All core samples were taken and the 36 hour CTD burst sampling period was not interrupted. All samples for ancillary projects were taken. Floating sediment trap array and primary production array deployed and recovered successfully. No samples were lost during the *in situ* incubations. ADCP measurements were made throughout the cruise. Ken Smith's Free Vehicle Grab Respirometer was successfully deployed and retrieved. Maintenance work on the ARGOS transmitter on HALE-ALOHA was accomplished. The ship arrived at Snug Harbor at 0800 on September 30, 1998.

3.10 HOT-98: Fernando Santiago-Mandujano, Chief Scientist

The R/V *Moana Wave* departed Snug Harbor at 1000 on October 17, 1998 with 15 scientists on-board. All the primary JGOFS and WOCE objectives were accomplished and all samples for ancillary projects were taken. The 36-hour CTD burst sampling was completed and fourteen 1000-m casts were obtained at Station ALOHA in addition to two deep casts. Also one 1000-m CTD cast was obtained at each of the Stations Kahe and HALE-ALOHA. One 8-bottle go-flo cast was successfully obtained at Station ALOHA, and the primary productivity array was deployed and recovered without problems. The array of floating sediment traps was also deployed and recovered without incidents; the sediment traps had drifted about 34 nm south-west upon recovery. S. Nunnery and A. Calbet successfully completed 6 plankton net tows. Weather conditions during the cruise were favorable to conduct all deck operations without problems. There were 10-20 knot easterlies and 3-5 ft. waves. The ADCP ran without interruption throughout the cruise, as well as the thermosalinograph, the pCO_2 system, the Licor light logger, the fluorometer, and the meteorological sensors. The signal from the Inverted Echo Sounder (IES) located at the center of the ALOHA Station was detected on the 12 kHz PDR. The ship arrived at Snug Harbor at 0030 on October 21, 1998.

3.11 HOT-99: Louie Tupas, Chief Scientist

The R/V *Moana Wave* departed Snug Harbor at 0900 on November 9, 1998 with 13 scientists on-board. All objectives of the JGOFS and WOCE programs were accomplished. All planned stations were occupied. Weather and sea conditions were moderate to rough but within limits of safety for deck operations. All core samples were taken and the 36 hour CTD burst sampling period was not interrupted. All samples for ancillary projects were taken. Floating sediment trap array and primary production array deployed and recovered successfully. No samples were lost during the *in situ* incubations. ADCP measurements were made throughout the cruise. Return to Honolulu was made early because the HALE-ALOHA mooring was retrieved (no HALE-ALOHA Station). The ship arrived at Snug Harbor at 1800 on November 12, 1998.

3.12 HOT-100: Dale Hebel, Chief Scientist

The R/V *Moana Wave* departed Snug Harbor at 0900 on December 7, 1998 with 15 scientists on-board. We occupied Station Kahe Pt. (sta. 1) and Station ALOHA (sta. 2), although all operations were not completed at Station ALOHA due to a drifting net which became fouled in the port propeller during CTD cast 11. This necessitated returning to the lee of Oahu for diving operations to remove the net. It was feared that the net may also entangle in the starboard propeller totally disabling the vessel. CTD operations were conducted at Stations 1 and 2. One CTD cast was conducted at Station 1 and eleven CTD casts at Station ALOHA in addition to 3 light casts, 8 net tows, 1 Go-Flo cast, and usual floating sediment traps and productivity operations. All operations were routine with the exception of additional net tows for C. B. Nelson and a rosette Go-Flo primary productivity experiment comparison. All underway measurement systems (thermosalinograph, ADCP, meteorological instruments, and fluorometer) were operable (except pCO_2) and functioned normally. The seas were moderate-rough with moderate-high winds and mostly cloudy skies. Due to the rough seas a number of spikes were recorded in some of the continuous measurement data streams and due to the overcast skies no noon sun photometer measurements were conducted. Due to the net problem we were unable to complete the 36 hr ‘burst’ sampling period, the HPLC cast, 3 net tows and experiments for A. Calbet and K. Bjorkman in addition to the CTD operations at Station 8 (HALE-ALOHA). The ship arrived at Snug Harbor at 0900 on December 11, 1998.

A short cruise (HOT-100B) was conducted to Station ALOHA with the purpose of conducting on-deck incubation experiments, and a near-bottom CTD yo-yo cast. Dave Karl was the chief scientist. The R/V *Moana Wave* departed Snug Harbor at 0830 on December 14, 1998 with 8 scientists on-board. A HPLC CTD cast at Station ALOHA, and a CTD cast at Station 8 (HALE-ALOHA) were conducted to complete the unfinished HOT-100 work. In addition a 17-hour near-bottom CTD yo-yo cast was conducted at Station ALOHA. The ship arrived at Snug Harbor at 0700 on December 17, 1998.

4. RESULTS

4.1 Hydrography

The 1998 hydrographic data described in detail below reveal an increase in salinity relative to previous years in the upper 200 dbar at Station ALOHA that started in the late months of 1997 and continued throughout 1998. Associated with this feature was an increase in potential density as compared with previous years. In the salinity maximum region (50-150 dbar), the salinity remained above 35.2 throughout 1998, reaching maximum values in November; this is in contrast with the low salinities observed in the previous year. In the bottom water, a cold anomaly developed during HOT-98 and reached record low temperatures during this cruise. Temperatures started recovering to normal values in the following cruises.

4.1.1 1998 CTD Profiling Data

Profiles of temperature, salinity, oxygen and potential density (σ_θ) were collected at Stations Kahe, ALOHA, and HALE-ALOHA. The profiles from Station ALOHA during 1998 are presented in Figure 6.1.1, together with the results of bottle determinations of oxygen, salinity and inorganic nutrients. Stack plots of CTD temperature and salinity profiles for all 1000 m casts conducted at Station ALOHA are also presented (Fig. 6.1.2). The data collected for Stations Kahe and HALE-ALOHA during 1998 are presented in Figures 6.1.3. Station HALE-ALOHA was not visited during HOT-99 because the buoy was retrieved before the cruise and re-deployed after it.

The temperature, salinity and oxygen profiles obtained from the deep casts at Station ALOHA during 1998 are presented in Figures 6.1.4-6. A cold water anomaly developed near the bottom during HOT-98 and the temperatures started recovering to normal values during the following two cruises as indicated by the potential temperature profiles (Figure 6.1.4).

4.1.2 Time-series Hydrography, 1988-1998

The hydrographic data collected during the first ten years of HOT are presented in a series of contour plots (Figures 6.1.7-22). These figures show the data collected in 1998 within the context of the longer time-series. The CTD data used in these plots are obtained by averaging the data collected during the 36-hour period of burst sampling. Therefore, much of the variability which would otherwise be introduced by internal tides has been removed. Figures 6.1.7 and 6.1.8 show the contoured time-series for potential temperature and density in the upper 1000 dbar for all HOT cruises through 1998. Seasonal variation in temperature for the upper ocean is apparent in the maximum of near-surface temperature of about 26 °C and the minimum of approximately 23°C. Oscillations in the depth of the 5 °C isotherm below 500 dbar appear to be relatively large with displacements up to 100 dbar. The main pycnocline is observed between 100 and 600 dbar, with a seasonal pycnocline developing between June and December in the 50-100 dbar range (Figure

6.1.8). The cruise-to-cruise changes between February and July 1989 in the upper pycnocline illustrate that variability in density is not always well resolved by our quasi-monthly sampling.

Figures 6.1.9-12 show the contoured time-series record for salinity in the upper 1000 dbar for all HOT cruises through 1998. The plots show both the CTD and bottle results plotted against pressure and potential density. Most of the differences between the contoured sections of bottle salinity and CTD salinity are due to the coarse distribution of bottle data in the vertical as compared to the CTD observations. Some of the bottles in Figure 6.1.12 are plotted at density values lower than the indicated sea surface density. This is due to surface density changing from cast to cast within each cruise, and even between the downcast and the upcast during a single cast.

Surface salinity is variable from cruise-to-cruise, with no obvious seasonal cycle and some substantial interannual variability. During 1998, an increase in surface salinity relative to previous years started in the late months of 1997 and continued throughout 1998. This increase is also present in deeper layers reaching 200 dbar (Fig 6.1.9).

The salinity maximum is generally found between 50 and 150 dbar, and within the potential density range 24-25 kg m^{-3}. A salinity maximum region extends to the sea surface in the later part of 1990, 1993 and during 1998, as indicated by the 35.2 contour reaching the surface. This contour nearly reaches the surface late in 1988 and 1989. The maximum shows salinities lower than normal in early 1995 and 1996, and throughout these two years the values are below 35.2 During 1997 the salinities decrease even further, with values below 35.1, to recover rapidly after February 1998 to values prior to 1995. The maximum value of salinity in this feature is subject to short-term variations of about 0.1 which is probably due to the proximity of Station ALOHA to the region where this water is formed at the sea surface (Tsuchiya, 1968). The variability of this feature is itself variable. Throughout 1989 there were extreme variations of a couple of months duration with 0.2 amplitude. The variability was much smaller and slower thereafter, except for a few months of rapid variation in earlier 1992.

The salinity minimum is found between 400 and 600 dbar (26.35-26.85 kg m^{-3}). There is no obvious seasonal variation in this feature, but there are distinct periods of higher than normal minimum salinity in early 1989, in the fall of 1990, in early 1992 and in the summer of 1996. These variations are related to the episodic appearance at Station ALOHA of energetic fine structure and submesoscale water mass anomalies (Lukas and Chiswell, 1991; Kennan and Lukas, 1995).

Figures 6.1.13 and 6.1.14 show contoured time-series data for oxygen in the upper 1000 dbar at Station ALOHA. The oxygen data show a strong oxycline between 400 and 625 dbar (26.25-27.0 kg m^{-3}), and an oxygen minimum centered near 800 dbar (27.2 kg m^{-3}). A recurrent decrease in the oxygen concentration can be seen throughout the time-series between 25 and 26.25 kg m^{-3}. This feature is accompanied by a decrease in salinity and an increase in the nutrient concentration (see discussion below). The oxygen minimum exhibits some interannual variability, with values less than 30 μmol kg^{-1} appearing frequently during the time-series. This variability can be seen in a plot of the mean oxygen in a layer spanning the oxygen minimum (27-27.8 kg m^{-3}, Fig. 6.1.23). Superimposed on this variability is a general trend towards lower values of dissolved oxygen in the intermediate waters. The surface layer shows a seasonality in oxygen concentrations, with highest values in the winter. This roughly corresponds to the minimum in surface layer temperature (Figure 6.1.7).

Figures 6.1.15-22 show [nitrate+nitrite], SRP, and silica at Station ALOHA plotted against both pressure and potential density. The nitricline is located between about 200 and 600 dbar (25.75-27 kg m^{-3}; Figs. 6.1.15-16). Most of the variations seen in these data are associated with vertical displacements of the density structure, and when [nitrate+nitrite] is plotted versus potential density, most of the contours are level. An increase in [nitrate+nitrite] can be seen between 25-26.25 kg m^{-3} (Fig. 6.1.16) in March-April 1990, January 1992, February 1993, February-March 1995, early 1996, and April-May 1997. These events can likely be attributed to mesoscale features such as eddies. It is possible for eddies to transport water with different biogeochemical characteristics from distant sources into the region of Station ALOHA. The increase of [nitrate+nitrite] during these events is accompanied by a decrease in the oxygen concentration apparent between 25-26.25 kg m^{-3} (Fig. 6.1.14). The SRP record is similar to the [nitrate+nitrite] in the upper water column (Fig. 6.1.19-20).

During 1996, the intermediate waters between 27.0-27.8 kg m^{-3} recovered from anomalously low [nitrate+nitrite] which was observed during 1995 (Fig. 6.1.17). This anomaly is apparent in a time series of mean [nitrate+nitrite] obtained from bottle data between 27.0-27.8 kg m^{-3} (Fig. 6.1.23). A decrease in [nitrate+nitrite] between 27.0-27.8 kg m^{-3} began in late 1994, with a comparable increase from mid-1995 through early 1996. The maximum decrease appears to be about 1 μmol kg^{-1} below 27.5 kg m^{-3} where nitrate concentrations are about 40 μmol kg^{-1}. This decrease appears to be real as it does have coherence over time. A precision estimate of 0.3% has been made for [nitrate+nitrite] measurements involving the high concentration samples associated with intermediate water (Dore et al., 1995). This translates to a precision of roughly 0.12 μmol kg^{-1} for samples with a concentration of 40 μmol kg^{-1}. Hence, the 1 μmol kg^{-1} decrease seen during 1995 is well within the precision level for the concentrations observed. However, the amount of the decrease could be approaching the accuracy limits of [nitrate+nitrite] measurements. The low [nitrate+nitrite] episode observed in 1995 is accompanied by an increase in oxygen concentration (Fig. 6.1.23) in the intermediate waters between 27.0-27.8 kg m^{-3}.

Intermediate water SRP (between 27.0-27.8 kg m^{-3}) starts increasing in early 1997, after a decreasing trend established in early 1994 (Fig. 6.1.18). A time series of mean SRP in this layer shows this trend clearly (Fig. 6.1.23). Decreases in phosphate in the deeper waters could persist for long periods of time as the oceanic ecosystem associated with Station ALOHA has been hypothesized to be phosphorous limited in recent years (Karl, 1995). Oxygen concentrations between 27.0-27.8 kg m^{-3} vary during the decrease of phosphate from early 1994 through 1997 (Fig. 6.1.23) without any apparent correlation.

4.2 Thermosalinograph Data

Underway measurements of near surface temperature (NST) and near surface salinity (NSS) from thermosalinograph data as well as navigation for the 1998 HOT and HALE-ALOHA cruises are presented in Figure 6.2.1a to q. Thermosalinograph data recorded while on station can be disturbed by ship effects. Namely, while the ship is stationary, the water temperature and salinity near the ship can be influenced by the ship's hull and engine temperatures. Salinity can also be influenced by the ship when on station as the ship provides a source of contamination and disturbs the water being sampled. However, significant features such as local noontime surface heating can be observed (i.e. HOT-91; Figure 6.2.1c).

Generally speaking, cooler near surface temperatures and in most cases, saltier near surface salinities were observed at Station ALOHA in comparison to the data recorded near the island of Oahu. At Station ALOHA, near surface temperatures increased on a cruise by cruise basis through the summer and fall, consistent with the usual summertime warming trend and consistent with meteorological and buoy observations (see Section 4.4). Near surface salinities at Station ALOHA increased on a cruise by cruise basis throughout the entire year. This increase is consistent with the salinity increase seen in the CTD data throughout the year from the surface to about 200 dbar (see Section 4.1).

4.3 Inverted Echo Sounder

Plots of dynamic height from the inverted echo sounders are presented in Figure 4.1. Only the IES at Station ALOHA provided data during 1998. The IES records prior to 1994 were examined and reported in Tupas et al. (1994b). It was concluded that large events with time-scales from weeks to months dominate dynamic height to such an extent that there is no clearly defined annual cycle, for instance, the highest and lowest dynamic height in 1991 occurred within the space of about a month. These events are not well sampled with the monthly spacing of the HOT cruises.

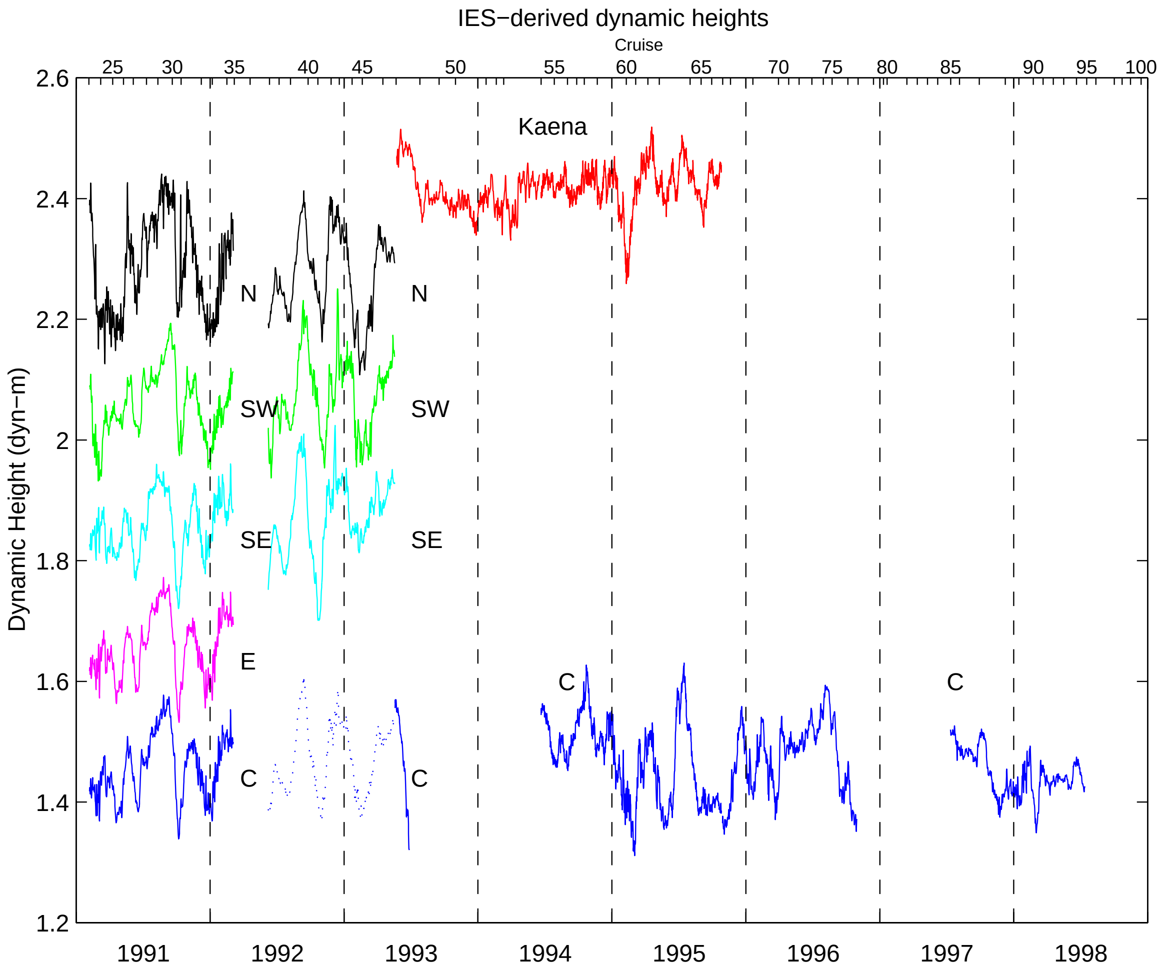

FIGURE 4.1. Dynamic height from the inverted echo sounders (IESs) after the removal of the semi-diurnal and diurnal tides and variability with time scales less than a day. The plots are staggered at 0.2 dyn-m intervals with the plot of the central IES (C) positioned at the correct y-scale. The dotted line on the C-record is an average of the N, SW and SE records between June 1992 and May 1993. All IES records have been calibrated from CTD casts at Station ALOHA. HOT cruise numbers are located at the upper x-axis.

4.4 Meteorology.

The meteorological data collected by HOT program scientists include atmospheric pressure, sea-surface temperature and wet and dry bulb air temperature. These data are presented in Figures 6.3.1 to 6.3.3. As described by Winn et al. (1991), parameters show evidence of annual cycles, although the daily and weekly ranges are nearly as high as the annual range for some variables. Wind speed and direction are also collected on HOT cruises. These data are presented in Figures 6.3.4a to l.

One National Data Buoy Center (NDBC) meteorological buoy (#51001) is located 400 km west of ALOHA at 23.4°N, 162.3°W (Fig. 1.1). This buoy collect hourly observations of air temperature, sea surface temperature, atmospheric pressure, wind speed and direction and significant wave height. The coherence of the data from Buoy #51001 with the data collected on HOT cruises was examined and reported in Tupas et al. (1993). We concluded from these analyses, that the data from this buoy can be used to get useful estimates of air temperature, sea-surface temperature and atmospheric pressure at Station ALOHA when the station is not occupied. These data are also plotted in Figures 6.3.1 to 6.3.3. As explained earlier (Section 2.6), data from the buoy were not available during January and part of February.

The thermosalinograph temperatures obtained at Station ALOHA during cruises are also plotted in Figure 6.3.1 (lower panel) and show good agreement with the sea-surface temperatures obtained at 4-hour intervals by the science personnel.

The wind vectors from buoy #51001 are plotted together with the ship observations in Figures 6.3.4b to l.

4.5 ADCP Measurements

An overview of the shipboard ADCP data is given by the plots of velocity as a function of time and depth while on station (Figures 6.4.1a to m) and velocity as a function of latitude and depth during transit to and from Station ALOHA and Station 8, combined (Figures 6.4.2a to m). As explained earlier (Section 2.5), gaps in some of the northward transit plots were caused by rough weather, and gaps in some of the on-station data are due to excursions to retrieve the primary productivity array and floating sediment traps.

4.6 Biogeochemistry

4.6.1 Dissolved Oxygen

A contour plot of dissolved oxygen in the upper 200 m of the water column from 1988-1998 analyzed from water samples collected at discrete depths is shown in Figure 6.5.1. Dissolved oxygen shows a maximum between 20 and 120 m depth and is fairly mixed in that layer. Gradients begin to form below 100 meters. The development of this maximum appears to occur during the spring and summer months and becomes mixed down in the winter.

4.6.2 Inorganic Carbon

Time-series of titration alkalinity and DIC in the mixed layer are presented in Figure 6.5.2. Titration alkalinity normalized to 35 salinity averages approximately 2305 μequiv kg^{-1} and, within the precision of the analysis, appears to remain relatively constant at Station ALOHA. This observation is consistent with the results of Weiss et al. (1982) who concluded that titration alkalinity normalized to salinity remains constant in both the North and South Pacific subtropical gyres. In contrast to titration alkalinity, the concentration of

DIC varies annually. DIC in the mixed layer is highest in March and April and lowest in September and October. This oscillation is consistent with an exchange of carbon dioxide across the air-sea interface driven by temperature dependent changes in mixed layer pCO_2.

4.6.3 Inorganic Nutrients

Euphotic zone nutrient concentrations at Station ALOHA are at or well below the detection limits of the autoanalyzer methods. Other analytical techniques and instrumentation are used to measure the nanomolar levels of [nitrate + nitrite] and SRP in the upper water column. Figures 6.5.3 show the profiles obtained from our low level nitrate analyses at Station ALOHA and HALE ALOHA. The upper 100 m is generally depleted in [nitrate + nitrite] with a few intrusions during the winter periods. At depths shallower than 100 dbar, SRP is typically less than 150 nmol kg^{-1} and on occasion, as low as 15 nmol kg^{-1} (Figure 6.5.4). SRP concentrations appear to vary by at least 3-fold in this region. Concentrations of [nitrate + nitrite] at depths less than 100 m are always less than 10 nmol kg^{-1} and are often less the 5 nmol kg^{-1}.

4.6.4 Organic Nutrients

Contour plots of dissolved organic carbon (DOC), nitrogen (DON) and phosphorus (DOP) are presented in Figures 6.5.5-7. DOC concentrations are about 100 μmol kg^{-1} at the surface and decrease rapidly to about 60 μmol kg^{-1} at about 300 m. DON is about 6 μmol kg^{-1} at the surface and gradually decreases to about 2 μmol kg^{-1} about 800 meters. DOP is about 0.3 μmol kg^{-1} at the surface and gradually decrease to about 0.1 μmol kg^{-1} at about 300 m.

4.6.5 Particulate Matter

Particulate carbon (PC), nitrogen (PN) and phosphorus (PP) concentrations in the surface ocean over the ten years of the program are shown in Figure 6.5.8. PC varies between 1.3-3.3 μmol kg^{-1}, PN between 0.08-0.65 μmol kg^{-1} and PP between 8-35 nmol kg^{-1} in the upper 100 m of the water column. PC and PN appear to have an annual cycle with the greatest particulate concentrations in summer/fall and lowest in winter. A significantly larger PN concentration was observed in the late fall of 1993 with only a slight increase in PC and a decrease in PP. The temporal distributions and magnitude of PC, PN, and PP in 1998 were similar to previous years.

4.6.6 Pigments

A contour plot of chlorophyll *a* concentrations measured using standard fluorometric techniques from 0 to 200 dbar over the ten years of the program is shown in Figure 6.5.9. As expected a chlorophyll maximum with concentrations up to 300 μg m^{-3} is observed at approximately 100 dbar. The chlorophyll *a* concentrations at depths shallower than 50 m display a clear annual cycle increasing in the fall and winter and decreasing through spring and summer which is approximately 4-6 months out of phase with the annual oscillation at the base of the euphotic zone (Winn et al. 1995).

4.6.7 Adenosine 5' Triphosphate

The concentration of particulate ATP closely resembles that of particulate matter with a maximum concentration at the surface and decreasing with depth (Figure 6.5.10). An annual cycle is evident at about 100 m where the chlorophyll maximum also occurs. There appears to be coherence in the dynamics of chlorophyll and ATP at this depth (Winn et al. 1995).

4.7 Biogeochemical Rates

4.7.1 Primary Productivity

The results of the ^{14}C incubations and pigment determinations for samples collected from Go-Flo casts in 1998 are presented in Tables 4.1 and 4.2. Table 4.1 presents the primary production and fluorometric pigment measurements made at individual depths on all 1998 cruises. Table 4.2 presents integrated values for irradiance, pigment concentration and primary production rates. The pigment concentrations and ^{14}C incorporation rates reported are the average of triplicate determinations.

Integrated primary production rates measured over all 10 years of the program are shown in Figure 6.5.11 in order to place the 1998 results within the context of the time-series data set. Rates of primary production, integrated over the euphotic zone during the ten years of the time-series program, show a seasonal cycle. Measured rates ranged from less than 200 to greater than 800 mg C m^{-2} d^{-1} with the highest rate being observed in May 1995. This variability, with a range of a factor of 4, is surprisingly large. However, the majority of the primary production estimates were between 250 and 600 mg C m^{-2} d^{-1}, and the average rate of primary production was approximately 480 mg C m^{-2} d^{-1}. Although this value is higher than historical measurements for the central ocean basins (Ryther 1969), it is consistent with more recent measurements using modern methodology (Martin et al. 1987; Laws et al. 1989; Knauer et al. 1990).

TABLE 4.1. Primary production and Pigment summary. The first two columns are cruise number and sample depth. Units are mg m^{-3} for Chl *a* and Phaeo; and mgC m^{-3} for L12 and D12.

Cr.	Z (m)	Chl *a*	Chl *a* STD	Phaeo	Phaeo STD	L12 rep #1	L12 rep #2	L12 rep #3	D12 rep #1	D12 rep #2	D12 rep #3
89	5	0.084	0.002	0.078	0.006	6.17	4.47	5.77	0.15	0.15	0.15
89	25	0.078	0.005	0.063	0.000	5.48	5.56	5.06	0.13	0.17	0.15
89	45	0.084	0.002	0.069	0.005	3.24	3.00	2.94	0.15	0.15	0.14
89	75	0.238	0.007	0.374	0.015	2.77	3.17	3.34	0.06	0.07	0.08
89	100	0.239	0.005	0.357	0.008	0.89	0.84	0.87	0.05	0.06	0.06
89	125	0.150	0.003	0.349	0.012	0.22	0.26	0.28	0.03	0.04	0.04
89	150	0.034	0.001	0.074	0.001	0.03	0.04	0.04	0.04	0.03	0.05

TABLE 4.1. Primary production and Pigment summary. The first two columns are cruise number and sample depth. Units are mg m^{-3} for Chl *a* and Phaeo; and mgC m^{-3} for L12 and D12.

Cr.	Z (m)	Chl *a*	Chl *a* STD	Phaeo	Phaeo STD	L12 rep #1	L12 rep #2	L12 rep #3	D12 rep #1	D12 rep #2	D12 rep #3
89	175	0.044	0.001	0.087	0.018	0.04	0.05	0.10	0.05	0.04	0.06
90	5	0.081	0.001	0.050	0.000	5.22	NA	5.19	0.13	0.14	0.13
90	25	0.082	0.002	0.055	0.000	4.98	4.33	5.41	0.15	0.15	0.14
90	45	0.084	0.003	0.068	0.008	4.48	45.01	4.20	0.13	0.14	0.13
90	75	0.176	0.001	0.183	0.005	3.38	3.42	3.37	0.15	0.15	0.12
90	100	0.285	0.001	0.436	0.010	2.40	2.46	2.47	0.07	0.07	0.08
90	125	0.129	0.000	0.320	0.006	0.44	0.47	0.49	0.06	0.06	0.09
90	150	0.153	0.002	0.157	0.001	0.12	0.12	0.12	0.11	0.12	0.16
90	175	0.134	0.005	0.247	0.004	0.09	0.09	NA	0.08	0.07	0.07
91	5	0.079	0.006	0.060	0.008	8.11	7.59	7.74	0.11	0.12	0.13
91	25	0.073	0.008	0.065	0.018	6.35	6.40	6.60	0.16	0.27	0.14
91	45	NA	NA	NA	NA	5.68	5.49	5.42	0.23	0.19	0.18
91	75	0.192	0.008	0.261	0.004	4.64	3.37	4.28	0.11	0.10	0.09
91	100	0.206	0.000	0.385	0.023	2.31	2.22	2.37	0.07	0.08	0.06
91	125	0.119	0.001	0.287	0.006	0.52	0.62	0.57	0.07	0.07	0.07
91	150	0.089	0.002	0.218	0.007	0.22	0.22	0.24	0.07	0.07	0.06
91	175	0.074	0.001	0.149	0.003	0.13	0.11	0.11	0.07	0.09	0.06
92	5	0.099	0.002	0.090	0.001	6.91	7.08	6.90	0.15	0.16	0.17
92	25	0.099	0.005	0.093	0.006	6.04	6.73	6.96	0.15	0.15	0.16
92	45	0.103	0.002	0.109	0.003	6.53	6.62	6.42	0.19	0.21	0.16
92	75	0.124	0.001	0.123	0.004	3.13	3.54	3.62	0.16	0.14	0.15
92	100	0.254	0.000	0.468	NA	3.73	3.42	3.78	0.08	0.08	0.01
92	125	0.144	0.002	0.202	0.030	0.49	0.58	0.65	0.11	NA	0.08
92	150	0.109	0.023	0.267	0.000	0.28	0.26	0.43	0.09	0.10	0.07
92	175	0.099	0.009	0.165	0.006	0.12	0.12	0.22	0.08	0.08	0.11
93	5	0.067	0.002	0.062	0.002	7.88	7.65	7.15	0.12	0.11	0.12
93	25	0.088	0.002	0.088	0.008	7.31	5.53	6.89	0.17	0.14	0.17
93	45	0.131	0.002	0.131	0.005	7.57	7.04	7.33	0.21	0.16	0.16
93	75	0.152	0.000	0.159	NA	4.40	4.67	4.66	NA	0.11	0.12
93	100	0.210	0.014	0.252	0.007	2.59	2.83	2.55	0.09	0.10	0.09
93	125	0.222	0.005	0.466	0.022	0.94	1.11	1.08	0.16	0.10	0.16
93	150	0.104	0.002	0.294	0.001	0.29	0.26	0.25	0.09	0.08	0.13
93	175	0.104	0.010	0.199	0.027	0.10	0.10	0.10	0.11	0.10	0.16
94	5	0.072	0.000	0.058	0.004	6.23	5.93	6.97	0.20	0.20	0.21
94	25	0.074	0.004	0.071	0.009	6.93	7.27	8.00	0.21	0.18	0.19

TABLE 4.1. Primary production and Pigment summary. The first two columns are cruise number and sample depth. Units are mg m^{-3} for Chl *a* and Phaeo; and mgC m^{-3} for L12 and D12.

Cr.	Z (m)	Chl *a*	Chl *a* STD	Phaeo	Phaeo STD	L12 rep #1	L12 rep #2	L12 rep #3	D12 rep #1	D12 rep #2	D12 rep #3
94	45	0.072	0.001	0.066	0.001	7.19	7.34	6.58	0.20	0.21	NA
94	75	0.133	0.001	0.121	0.000	4.92	4.93	5.04	0.18	0.18	0.18
94	100	0.226	0.010	0.245	0.020	2.89	3.05	3.13	0.09	0.09	0.10
94	125	0.251	0.001	0.459	0.014	1.22	1.37	1.27	0.07	0.07	0.06
94	150	0.108	0.009	0.294	0.020	0.43	0.33	0.35	0.08	0.06	0.06
94	175	0.052	0.007	0.123	0.005	0.06	0.07	0.09	0.06	0.07	0.07
95	5	0.093	0.000	0.083	NA	9.36	9.01	8.61	0.18	0.17	0.16
95	25	0.076	0.005	0.066	0.000	7.31	8.86	9.43	0.19	0.18	0.17
95	45	0.079	0.007	0.063	0.008	6.64	6.61	7.42	0.21	0.20	0.00
95	75	0.130	0.008	0.129	0.005	3.96	4.03	4.38	0.12	0.11	0.12
95	100	0.192	0.012	0.284	0.011	2.42	2.55	2.46	0.05	0.06	0.06
95	125	0.198	0.005	0.542	0.017	1.18	1.20	1.07	0.04	0.03	0.05
95	150	0.078	0.004	0.284	0.017	0.19	0.20	0.20	0.03	0.03	0.04
95	175	0.033	0.002	0.094	0.003	0.04	0.06	0.04	0.03	0.03	0.04
96	5	0.173	0.005	0.124	0.011	14.60	4.82	18.73	0.29	0.23	0.28
96	25	0.192	0.014	0.155	0.005	12.61	12.00	7.32	0.27	0.29	0.26
96	45	0.107	0.003	0.108	0.010	4.96	4.73	3.47	0.16	0.21	0.17
96	75	0.163	0.002	0.181	0.004	1.81	1.90	1.85	NA	0.15	0.10
96	100	0.184	0.004	0.458	0.005	1.10	1.31	1.06	0.09	0.09	0.09
96	125	0.175	0.020	0.445	0.018	0.42	0.43	0.48	0.09	0.09	0.07
96	150	0.100	0.011	0.333	0.045	0.18	0.17	0.18	0.09	0.08	0.13
96	175	0.093	0.005	0.193	0.005	0.12	0.10	0.10	0.08	0.08	0.08
97	5	0.055	0.000	0.039	0.002	4.54	4.42	NA	0.17	0.15	NA
97	25	0.055	0.000	0.045	0.002	4.69	4.48	NA	0.18	0.25	NA
97	45	0.052	0.001	0.038	0.000	4.18	4.03	NA	0.23	0.20	NA
97	75	0.133	0.000	0.126	0.002	3.04	3.02	NA	NA	0.23	NA
97	100	0.190	0.010	0.213	0.014	1.22	1.21	NA	0.12	0.12	NA
97	125	0.209	0.002	0.499	0.003	0.58	0.26	NA	NA	0.12	NA
97	150	0.074	0.001	0.248	0.010	0.15	0.14	NA	0.06	0.05	NA
97	175	0.046	0.002	0.091	0.001	NA	0.11	NA	NA	NA	NA
98	5	0.076	0.003	0.071	0.004	4.61	4.76	NA	0.15	0.15	NA
98	25	0.072	0.001	0.055	0.008	5.59	5.24	NA	0.18	0.18	NA
98	45	0.068	0.002	0.048	0.004	4.59	4.77	NA	0.16	0.15	NA
98	75	0.176	0.001	0.189	0.004	3.72	3.64	NA	NA	0.13	NA
98	100	0.232	0.005	0.364	0.002	1.33	1.21	NA	0.04	0.05	NA
98	125	0.177	0.008	0.423	0.043	0.36	0.57	NA	NA	0.06	NA

TABLE 4.1. Primary production and Pigment summary. The first two columns are cruise number and sample depth. Units are mg m^{-3} for Chl *a* and Phaeo; and mgC m^{-3} for L12 and D12.

Cr.	Z (m)	Chl *a*	Chl *a* STD	Phaeo	Phaeo STD	L12 rep #1	L12 rep #2	L12 rep #3	D12 rep #1	D12 rep #2	D12 rep #3
98	150	0.120	0.004	0.328	0.049	0.10	0.11	NA	0.05	0.03	NA
98	175	0.096	0.010	0.230	0.006	0.08	0.07	NA	0.07	0.06	NA
99	5	0.091	0.006	0.073	0.005	6.96	7.18	NA	0.07	0.07	NA
99	25	0.091	0.000	0.073	0.003	6.15	5.97	NA	0.07	0.07	NA
99	45	0.090	0.002	0.075	0.000	4.12	3.99	NA	0.06	0.07	NA
99	75	0.214	0.000	0.236	0.002	2.09	1.94	NA	0.07	0.09	NA
99	100	0.142	0.002	0.366	0.006	0.58	0.61	NA	0.05	0.06	NA
99	125	0.085	0.001	0.244	0.013	0.18	0.20	NA	0.04	0.05	NA
99	150	0.039	0.001	0.122	0.003	0.07	0.07	NA	0.03	0.03	NA
99	175	0.059	0.002	0.109	0.006	0.02	0.02	NA	0.02	0.04	NA
100	5	0.102	0.006	0.093	0.007	2.79	1.02	NA	0.06	0.06	NA
100	25	0.103	0.003	0.099	0.002	4.42	5.67	NA	0.06	0.06	NA
100	45	0.098	0.002	0.100	0.000	1.57	1.96	NA	0.06	0.09	NA
100	75	0.140	0.004	0.153	0.013	0.48	0.53	NA	0.05	0.06	NA
100	100	0.117	0.000	0.129	0.001	0.20	0.25	NA	0.03	0.04	NA
100	125	0.092	0.002	0.282	0.004	0.16	0.18	NA	0.02	0.03	NA
100	150	0.097	0.003	0.101	0.001	0.06	0.05	NA	0.02	0.03	NA
100	175	0.107	0.005	0.130	0.007	0.03	0.03	NA	0.02	0.02	NA

TABLE 4.2. Primary production and pigment summary integrated values (0-200 m)

	Incident Irradiance	Pigments (mg m^{-2})		Incubation Duration	Assimilation Rates (mg C m^{-2} d^{-1})	
Cruise	(E m^{-2} d^{-1})	Chl *a*	Phaeo	(hrs)	Light	Dark
89	37.57	23.7	37.2	12.25	382	15
90	38.40	29.0	40.7	12.00	454	21
91	49.97	24.1	40.8	00375	579	20
92	61.58	25.8	28.9	13.50	613	23
93	59.15	27.5	43.1	14.50	657	24
94	53.70	24.6	36.8	13.75	676	25
95	61.66	21.4	39.0	13.00	689	17
96	53.70	28.6	50.8	14.00	613	26
97	51.66	20.4	33.3	13.75	393	26
98	43.68	25.9	45.1	12.00	446	19
99	23.64	20.2	33.3	12.50	406	10
100	8.65	21.6	27.8	8.50	200	8

4.7.2 Particle Flux

Particulate carbon (PC), nitrogen (PN) and phosphorus (PP) fluxes at 150 m are presented in Table 4.3 and Figures 6.5.12 for the ten years of the program. PC flux displays an annual cycle with peaks in both the early spring and in the late summer months. The magnitude of particle flux varies by a factor of approximately three. With the exception of anomalous PP fluxes measured on the first two HOT cruises, temporal variability in PN and PP show similar trends and also vary between cruises by about a factor of three. Elemental ratios of carbon-to-nitrogen (atom:atom) at 150 m are typically between 6-10 and show no obvious temporal pattern. These particle flux measurements and elemental ratios are consistent with those measured in the central North Pacific Ocean during the VERTEX program (Martin et al. 1987; Knauer et al. 1990).

TABLE 4.3. Station ALOHA sediment trap flux data

	PC Flux ($mg\ m^{-2}\ d^{-1}$)			PN Flux ($mg\ m^{-2}\ d^{-1}$)			PP Flux ($mg\ m^{-2}\ d^{-1}$)		
Cruise	**Mean**	**SD**	**n**	**Mean**	**SD**	**n**	**Mean**	**SD**	**n**
89	25.4	3.7	3	3.6	0.50	3	0.33	0.09	3
90	22.7	7.0	3	3.4	0.80	3	0.28	0.04	3
91	38.4	7.1	3	5.4	0.80	3	0.58	0.02	3
92	36.2	0.8	3	5.3	0.18	3	0.32	0.03	3
93	56.1	3.5	3	8.2	0.30	3	0.57	0.17	3
94	24.3	2.4	3	3.7	0.43	3	0.33	0.14	3
95	24.9	4.0	3	3.6	0.55	3	0.48	0.06	3
96	39.1	5.3	3	5.1	0.85	3	0.32	0.04	3
97	17.1	1.1	3	2.7	NA	1	0.41	0.03	3
98	25.3	0.6	3	4.0	0.21	3	0.34	0.12	3
99	30.6	3.7	3	4.1	0.64	3	0.43	0.33	3
100	19.9	2.0	3	2.7	0.22	3	0.33	0.07	3

4.8 Microbial Community Structure

Depth profiles of counts of heterotrophic and photosynthetic bacteria for each cruise are presented in Figure 6.5.13. At the surface, heterotrophic bacterial number range from 4 to 6 x 10^5 cells ml^{-1}. In some cases bacterial number decrease with depth although there are some profiles where the numbers remain fairly constant with depth. Prochlorococcus -like cells about 2 x 10^5 ml^{-1} at the surface and usually decrease with depth but with a subsurface maximum between 50 and 100 m.

5. REFERENCES

Bidigare, R.R., J. Marra, T.J. Dickey, R. Iturriaga, K.S. Baker, R.C. Smith and H. Pak. 1990. Evidence for phytoplankton succession and chromatic adaptation in the Sargasso Sea during Spring 1985. Marine Ecology Progress Series, 60, 113-122.

Brewer, P.G., K.W. Bruland, R.W. Eppley and J.J. McCarthy. 1986. The Global Ocean Flux Study (GOFS): Status of the US-GOFS program. EOS, Transactions of the American Geophysical Union, 67, 827-832.

Campbell, L., H. Nolla and D. Vaulot. 1994. The importance of Prochlorococcus to community structure in the central North Pacific Ocean. Limnology and Oceanography, 39, 954-961.

Chiswell, S.M. 1996. Intra-annual oscillations at Station ALOHA, north of Oahu, Hawaii. Deep-Sea Research II, 43, 305-319.

Chiswell, S.M., E. Firing, D. Karl, R. Lukas, C. Winn. 1990. Hawaii Ocean Time-series Program Data Report 1, 1988-1989. School of Ocean and Earth Science and Technology, University of Hawaii, SOEST 90-1, 269 pp.

Clayton, T.D. and R.H. Byrne. 1993. Spectrophotometric seawater pH measurements: total hydrogen ion concentration scale calibration of m-cresol purple and at-sea results. Deep-Sea Research, 40, 2115-2129.

Cox, R.D. 1980. Determination of nitrate at the parts per billion level by chemiluminescence. Analytical Chemistry, 52, 332-335.

Dore, J.E. and D.M. Karl. 1996. Nitrite distributions and dynamics at Station ALOHA. Deep-Sea Research, 43, 385-402.

Dore, J.E., T. Houlihan, D.V. Hebel, G. Tien, L.M. Tupas and D.M. Karl. 1996. Freezing as a method of seawater preservation for the analysis of dissolved inorganic nutrients. Marine Chemistry, 53, 173-185.

Garside, C. 1982. A chemiluminescent technique for the determination of nanomolar concentrations of nitrate and nitrite in seawater. Marine Chemistry, 11, 159-167.

Hayward, T.L. 1987. The nutrient distribution and primary production in the central North Pacific. Deep-Sea Research, 34, 1593-1627.

Johnson, D.L. 1971. Simultaneous determination of arsenate and phosphate in natural waters. Environmental Science and Technology, 5, 411-414.

Karl, D.M., J.R. Christian, J.E. Dore, D.V. Hebel, R.M Letelier, L.M. Tupas and C.D. Winn. 1996a. Seasonal and interannual variability in primary production and particle flux at Station ALOHA. Deep-Sea Research, 43, 539-568.

Karl, D.M. and O. Holm-Hansen. 1978. Methodology and measurement of adenylate energy charge ratios in environmental samples. Marine Biology, 48, 185-197.

Karl, D.M., R. Letelier, D. Hebel, L. Tupas, J. Dore, J. Christian and C. Winn. 1995 Ecosystem changes in the North Pacific subtropical gyre attributed to the 1991-92 El Niño. Nature, 373, 230-234.

Karl, D.M., R. Letelier, L. Tupas, J. Dore, J. Christian and D. Hebel. 1997. The role of nitrogen fixation in biogeochemical cycling in the subtropical North Pacific Ocean. Nature, 388, 533-538.

Karl, D.M. and R. Lukas. 1996. The Hawaii Ocean Time-series (HOT) program: Background, rationale and field implementation. Deep-Sea Research, 43, 129-156.

Karl, D.M. and G. Tien. 1992. MAGIC: A sensitive and precise method for measuring dissolved phosphorus in aquatic environments. Limnology and Oceanography, 37, 105-116.

Karl, D.M. and G. Tien. 1997. Temporal variability in dissolved phosphorus concentrations at Station ALOHA (22˚45'N, 158˚W). Marine Chemistry, 56, 77-96.

Karl, D., L. Tupas, F. Santiago-Mandujano, C. Nosse, D. Hebel, E. Firing and R. Lukas, 1996b. Hawaii Ocean Time-series Program Data Report 7, 1995. School of Ocean and Earth Science and Technology, University of Hawaii, SOEST 96-09, 228 pp.

Karl, D.M. and C.D. Winn, 1991. A sea of change: Monitoring the oceans carbon cycle. Environmental Science and Technology, 25, 1967-1981.

Kennan, S.C. and R. Lukas. 1995. Saline intrusions in the intermediate waters north of Oahu, Hawaii. Deep-Sea Research, 43, 215-241.

Knauer, G.A., J.H. Martin and K.W. Bruland. 1979. Fluxes of particulate carbon, nitrogen and phosphorus in the upper water column of the northeast Pacific. Deep-Sea Research, 26, 97-108.

Knauer, G.A., D.G. Redalje, W.G. Harrison and D.M. Karl. 1990. New production at the VERTEX time-series site. Deep-Sea Research, 37, 1121-1134.

Larson, N. and A.M. Pederson. 1996. Temperature measurements in flowing water: Viscous heating of sensor tips. 1st International Group for Hydraulic Efficiency Measurements (IGHEM) Meeting, Montreal, Canada, June 1996.

Laws, E.A., G.R. DiTullio, P.R. Betzer, D.M. Karl and R.L. Carder. 1989. Autotrophic production and elemental fluxes at 26(N, 155(W in the North Pacific subtropical gyre. Deep-Sea Research, 36, 103-120.

Lukas, R. and S. Chiswell. 1991. Submesoscale water mass variations in the salinity minimum of the north Pacific near Hawaii. WOCE Notes, 3(1), 6-8.

Lukas, R., F. Santiago-Mandujano, F. Bingham and A. Mantyla. Cold water events observed in the Hawaii Ocean Time-series: Implications for vertical mixing. Submitted to Deep Sea Research.

Martin, J.H., G.A. Knauer, D.M. Karl and W.W. Broenkow. 1987. VERTEX: Carbon cycling in the northeast Pacific. Deep-Sea Research, 34, 267-285.

Michaels, A. and A. Knap. 1996. Overview of the U.S.-JGOFS Bermuda Atlantic Time-series Study and Hydrostation S program. Deep-Sea Research, 43, 157-198.

Monger, B,C, and M.R. Landry. 1993. Flow cytometry analysis of marine Bacteria with Hoechst 3342. Applied and Environmental Microbiology, 59, 905-911.

National Research Council. 1984a. Global Observations and Understanding of the General Circulation of the Oceans: Proceedings of a Workshop, National Academy Press, Washington, DC, 418 pp.

National Research Council. 1984b. Global Ocean Flux Study: Proceedings of a Workshop, National Academy Press, Washington, DC, 360 pp.

Ortner, P.B. E.M. Hulbert and P.H. Wiebe. 1979. Gulf Stream rings, phytohydrography and herbivore habitat contrasts. Journal of Experimental Marine Biology and Ecology, 39, 101-124.

Owens, W.B. and R.C. Millard. 1985. A new algorithm for CTD oxygen calibration. Journal of Physical Oceanography, 15, 621-631.

Qian, J. and K. Mopper. 1996. Automated high-performance, high-temperature combustion total organic carbon analyzer. Analytical Chemistry, 68, 3090-3097.

Quay, P.D., B. Tilbrook and C.S. Wong. 1992. Oceanic uptake of fossil fuel CO_2: Carbon-13 evidence. Science, 256, 74-79.

Ryther, J.H. 1969. Photosynthesis and fish production in the sea. The production of organic matter and its conversion to higher forms of life vary throughout the world ocean. Science, 166, 72-76.

Scientific Committee on Oceanic Research. 1990. The Joint Global Ocean Flux Study (JGOFS) Science Plan. JGOFS Report No. 5. International Council of Scientific Unions, 61 pp.

Strickland, J.D.H. and T.R. Parsons. 1972. A Practical Handbook of Seawater Analysis. Fisheries Research Board of Canada, 167 pp.

Tsuchiya, M. 1968. Upper Waters of the Intertropical Pacific Ocean. Johns Hopkins Oceanographic Studies, 4, 49 pp.

Tupas, L., F. Santiago-Mandujano, D. Hebel, E. Firing, F. Bingham, R. Lukas and D. Karl. 1994. Hawaii Ocean Time-series Program Data Report 5, 1993. School of Ocean and Earth Science and Technology, University of Hawaii, 156 pp.

Tupas, L., F. Santiago-Mandujano, D. Hebel, E. Firing, R. Lukas and D. Karl. 1995. Hawaii Ocean Time-series Data Report 6: 1994. School of Ocean and Earth Science and Technology, University of Hawaii, 199 pp.

Tupas, L., F. Santiago-Mandujano, D. Hebel, R. Lukas, D. Karl and E. Firing. 1993. Hawaii Ocean Time-series Program Data Report 4, 1992. School of Ocean and Earth Science and Technology, University of Hawaii, 248 pp.

Tupas, L., F. Santiago-Mandujano, D. Hebel, C. Nosse, L. Fujieki, E. Firing, R. Lukas and D. Karl. 1997. Hawaii Ocean Time-series Program Data Report 8, 1996. School of Ocean and Earth Science and Technology, University of Hawaii, SOEST 96-4, 296 pp.

UNESCO. 1981. Tenth Report of the Joint Panel on Oceanographic Tables and Standards. UNESCO Technical Papers in Marine Science, No. 36., UNESCO, Paris.

Vaulot, D. 1989. CYTOPC: Processing software for flow cytometric data. Signal and Noise, 2, 8.

Weiss, R.F., R.A. Jahnke and C.D. Keeling. 1982. Seasonal effects of temperature and salinity on the partial pressure of CO_2 in seawater. Nature, 300, 511-513.

Winn, C.D., L. Campbell, J.R. Christian, R.M. Letelier, D.V. Hebel, J.E. Dore, L. Fujieki and D.M. Karl. 1995. Seasonal variability in the phytoplankton community of the North Pacific subtropical gyre. Global Biogeochemical Cycles, 9, 605-620.

Winn, C., S.M. Chiswell, E. Firing, D. Karl, R. Lukas. 1991. Hawaii Ocean Time-series Program Data Report 2, 1990. School of Ocean and Earth Science and Technology, University of Hawaii, SOEST 92-01, 175 pp.

Winn, C., R. Lukas, D. Karl, E. Firing. 1993. Hawaii Ocean Time-series Program Data Report 3, 1991. School of Ocean and Earth Science and Technology, University of Hawaii, SOEST 93-3, 228 pp.

Wright, S.W., S.W. Jeffrey, R.F.C. Mantoura, C.A. Llewellyn, T. Bjornland, D. Repeta and N. Welschmeyer. 1991. Improved HPLC method for the analysis of chlorophylls and carotenoids from marine phytoplankton. Marine Ecology Progress Series, 77, 183-196.

6. FIGURES

6.1 Hydrography

Figure 6.1.1a-l: [Upper left panel] Temperature, salinity, oxygen and potential density σ_θ as a function of pressure for the WOCE deep cast at Station ALOHA for each HOT cruise. [Upper right panel] Plot of [nitrate + nitrite], soluble reactive phosphorus, silicate, and bottle dissolved oxygen as a function of potential temperature for all water samples. [Lower left panel] CTD temperature and salinity plotted as a function of pressure to 1000 dbar. [Lower right panel] Salinity and oxygen from CTD and water samples plotted as a function of potential temperature. Only the CTD oxygen traces in which bottle oxygens were sampled are included.

Figure 6.1.2a-l: [1st panel] Stack plots of temperature versus pressure to 1000 dbar at Station ALOHA. Offset is 2 °C. [2nd panel] Stack plots of salinity versus pressure to 1000 dbar at Station ALOHA. Offset is 0.1.

Figure 6.1.3a-l: [Upper left panel] Temperature, salinity, oxygen and σ_θ as a function of pressure for the cast at Station Kahe for each HOT cruise. [Upper right panel] Plot of [nitrate + nitrite], soluble reactive phosphorus, silicate, and CTD bottle dissolved oxygen and salinity as a function of potential temperature for all water samples. [Lower left panel] Plot of temperature, salinity, oxygen and σ_θ as a function of pressure at Station HALE ALOHA. [Lower right panel] Plot of CTD and bottle salinity and oxygen as a function of potential temperature at Station HALE ALOHA. Station HALE ALOHA was not occupied during HOT-99 (see text).

Figure 6.1.4: [Upper panel] Potential temperature versus pressure for all deep casts in 1998. [Lower panel]: Potential temperature versus pressure deeper than 2500 dbar for all deep casts in 1998.

Figure 6.1.5: [Upper panel] Salinity versus potential temperature for all deep casts in 1998. [Lower panel]: Salinity versus potential temperature for all deep casts in 1998 in the 1-5 °C range.

Figure 6.1.6: [Upper panel] Oxygen concentrations from calibrated oxygen sensor data versus potential temperature for all deep casts in 1998. [Lower panel] Oxygen versus potential temperature for all deep casts in 1998 in the 1-5 °C range.

Figure 6.1.7: Contour plot of CTD potential temperature versus pressure for HOT cruises 1-100.

Figure 6.1.8: Contour plot of σ_θ, calculated from CTD pressure, temperature and salinity, versus pressure for HOT cruises 1-100.

Figure 6.1.9: Contour plot of CTD salinity versus pressure for HOT cruises 1-100.

Figure 6.1.10: Contour plot of CTD salinity versus σ_θ to 27.5 kg m^{-3} for HOT cruises 1-100. The average σ_θ of the sea surface is connected by the heavy line.

Figure 6.1.11: Contour plot of bottle salinity versus pressure for HOT cruises 1-100. Location of samples in the water column are indicated by the solid circles.

Figure 6.1.12: Contour plot of bottle salinity versus σ_θ to 27.5 kg m^{-3} for HOT cruises 1-100. The average σ_θ of the sea surface is connected by the heavy line.

Figure 6.1.13: Contour plot of bottle oxygen versus pressure for HOT cruises 1-100. Location of samples in the water column are indicated by the solid circles.

Figure 6.1.14: Contour plot of bottle oxygen versus σ_θ to 27.5 kg m^{-3} for HOT cruises 1-100. The average σ_θ of the sea surface is connected by the heavy line.

Figure 6.1.15: Contour plot of [nitrate + nitrite] versus pressure for HOT cruises 1-100. Location of samples in the water column are indicated by the solid circles.

Figure 6.1.16: Contour plot of [nitrate+nitrite] versus σ_θ to 27.5 kg m^{-3} for HOT cruises 1-100. The average σ_θ of the sea surface is connected by the heavy line.

Figure 6.1.17: Contour plot of [nitrate + nitrite] versus σ_θ from 27.0 to 27.8 kg m^{-3} for HOT cruises 1-100.

Figure 6.1.18: Contour plot of soluble reactive phosphorus versus σ_θ from 27.0 to 27.8 kg m^{-3} for HOT cruises 1-100.

Figure 6.1.19: Contour plot of soluble reactive phosphorus versus pressure for HOT cruises 1-100. Location of samples in the water column are indicated by the solid circles.

Figure 6.1.20: Contour plot of soluble reactive phosphorus versus σ_θ to 27.5 kg m^{-3} for HOT cruises 1-100.

Figure 6.1.21: Contour plot of silicate versus pressure for HOT cruises 1-100. Location of samples in the water column are indicated by the solid circles.

Figure 6.1.22: Contour plot of silicate versus σ_θ to 27.5 kg m^{-3} for HOT cruises 1-100. The average σ_θ of the sea surface is connected by the heavy line.

Figure 6.1.23: Time series of mean bottle dissolved oxygen (upper panel), [nitrate + nitrite] (middle panel) and soluble reactive phosphorus (lower panel) between 27.0 and

27.8 kg m^{-3} isopycnals. The smooth line is the spline fit to the data. The asterisks indicate the annual mean.

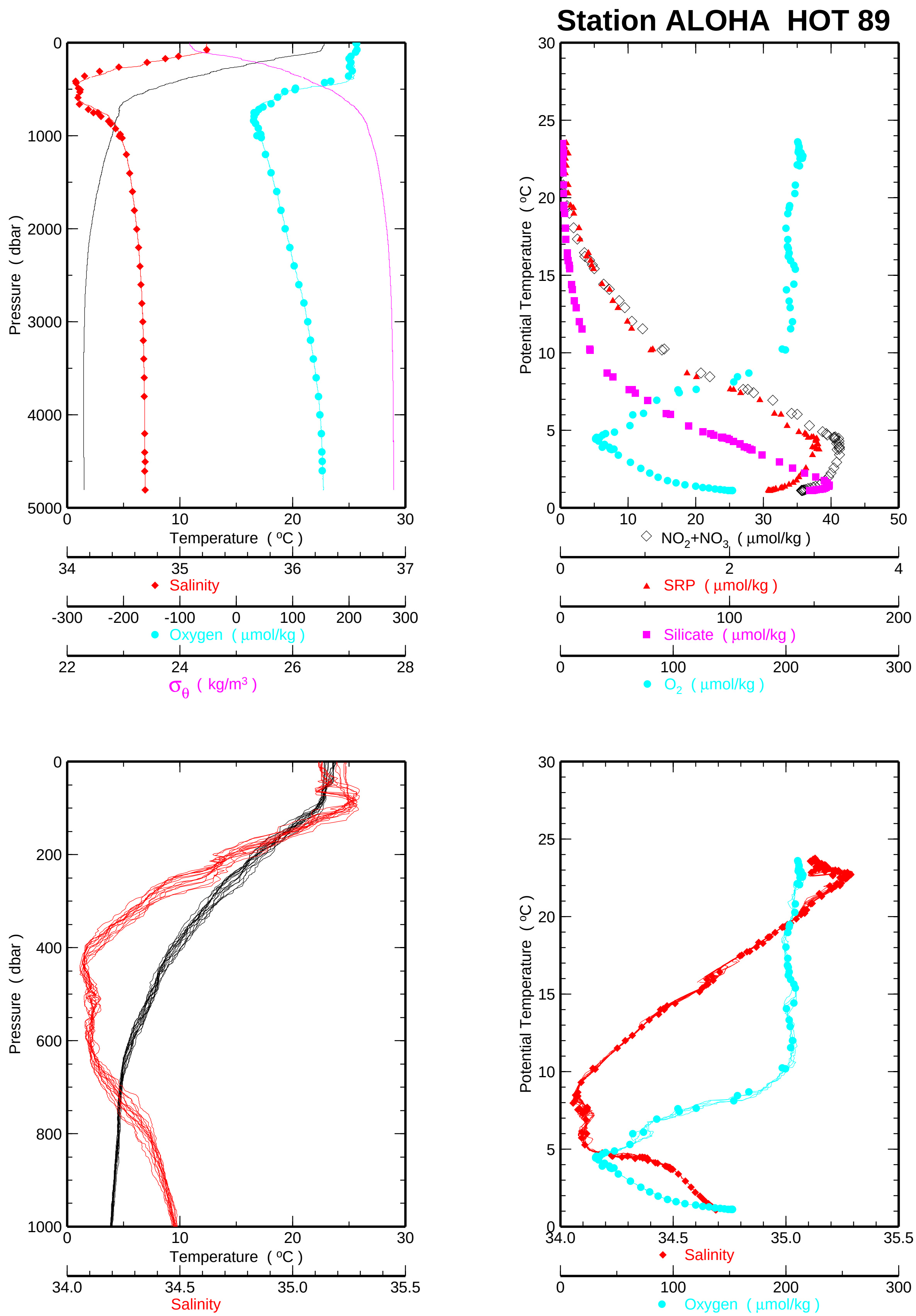

Station ALOHA HOT 89
Pressure (dbar)
Temperature (°C)
Salinity
Oxygen (µmol/kg)
σθ (kg/m3)
Potential Temperature (°C)
NO2+NO3 (µmol/kg)
SRP (µmol/kg)
Silicate (µmol/kg)
O2 (µmol/kg)

FIGURE 6.1.1a.

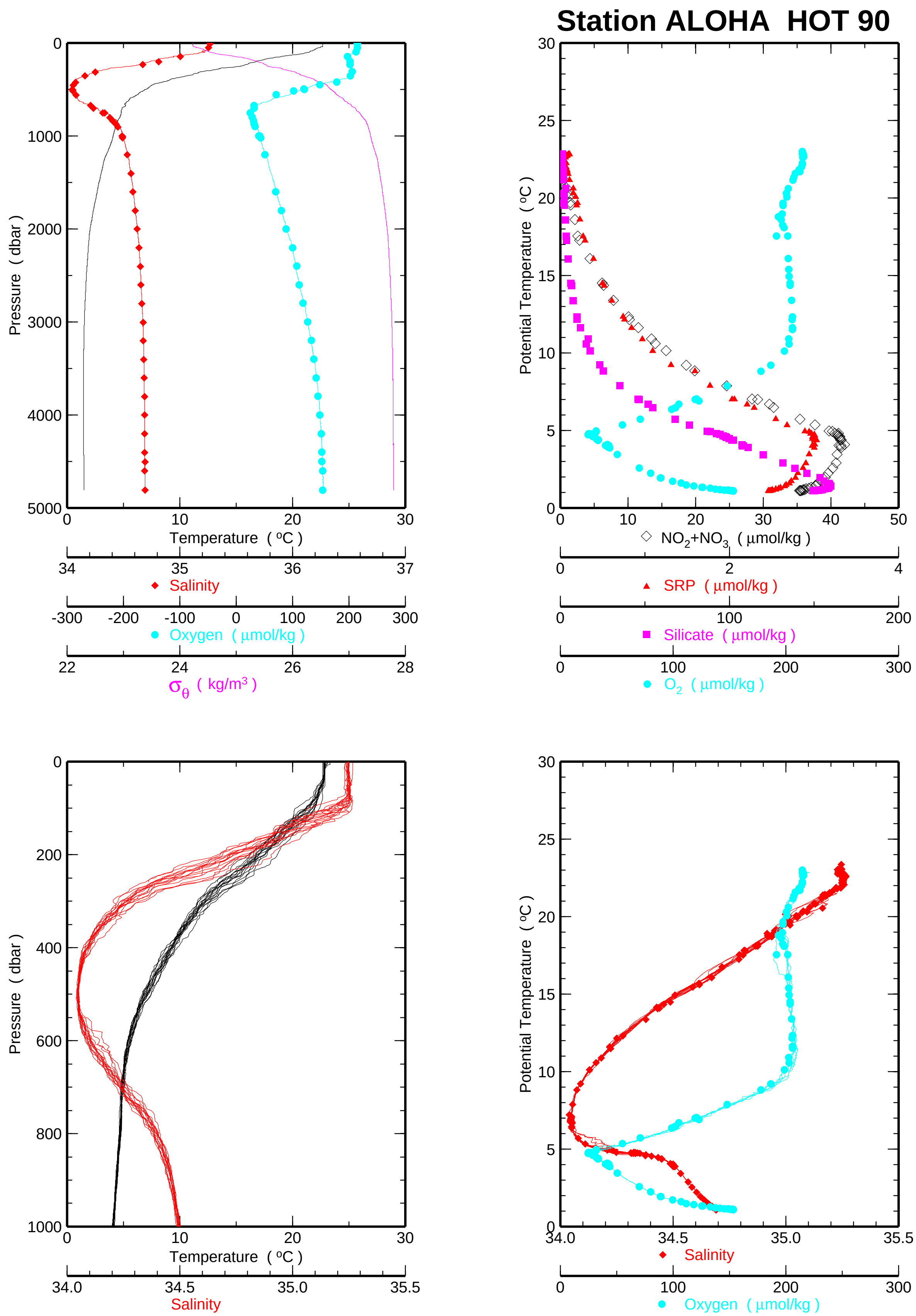

Station ALOHA HOT 90
Pressure (dbar)
Temperature (°C)
Salinity
Oxygen (µmol/kg)
σ_θ (kg/m³)
Potential Temperature (°C)
NO_2+NO_3 (µmol/kg)
SRP (µmol/kg)
Silicate (µmol/kg)
O_2 (µmol/kg)

FIGURE 6.1.1b.

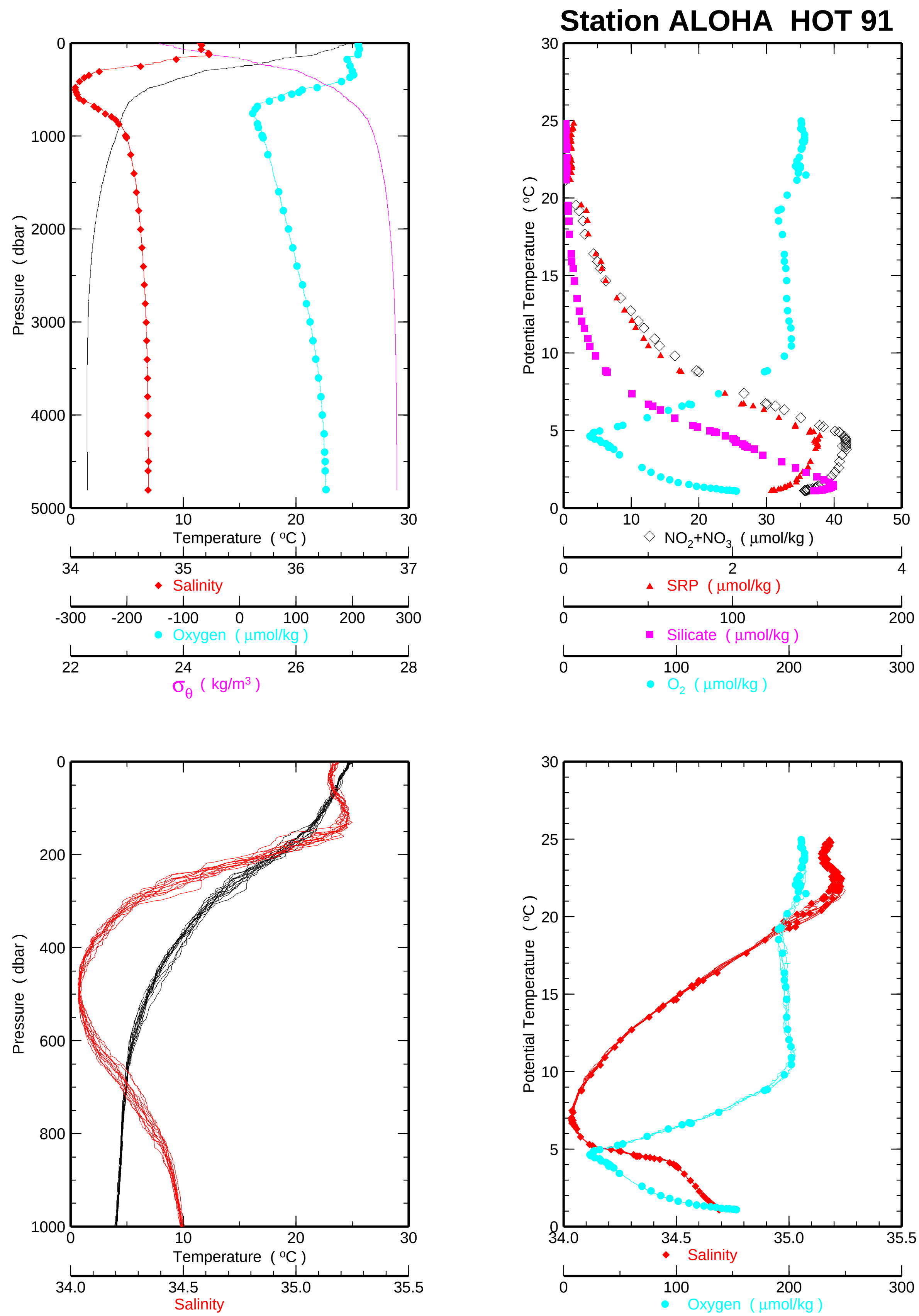

Station ALOHA HOT 91
Pressure (dbar)
Temperature (ºC)
Salinity
Oxygen (µmol/kg)
σθ (kg/m³)
Potential Temperature (ºC)
NO2+NO3 (µmol/kg)
SRP (µmol/kg)
Silicate (µmol/kg)
O2 (µmol/kg)

FIGURE 6.1.1c.

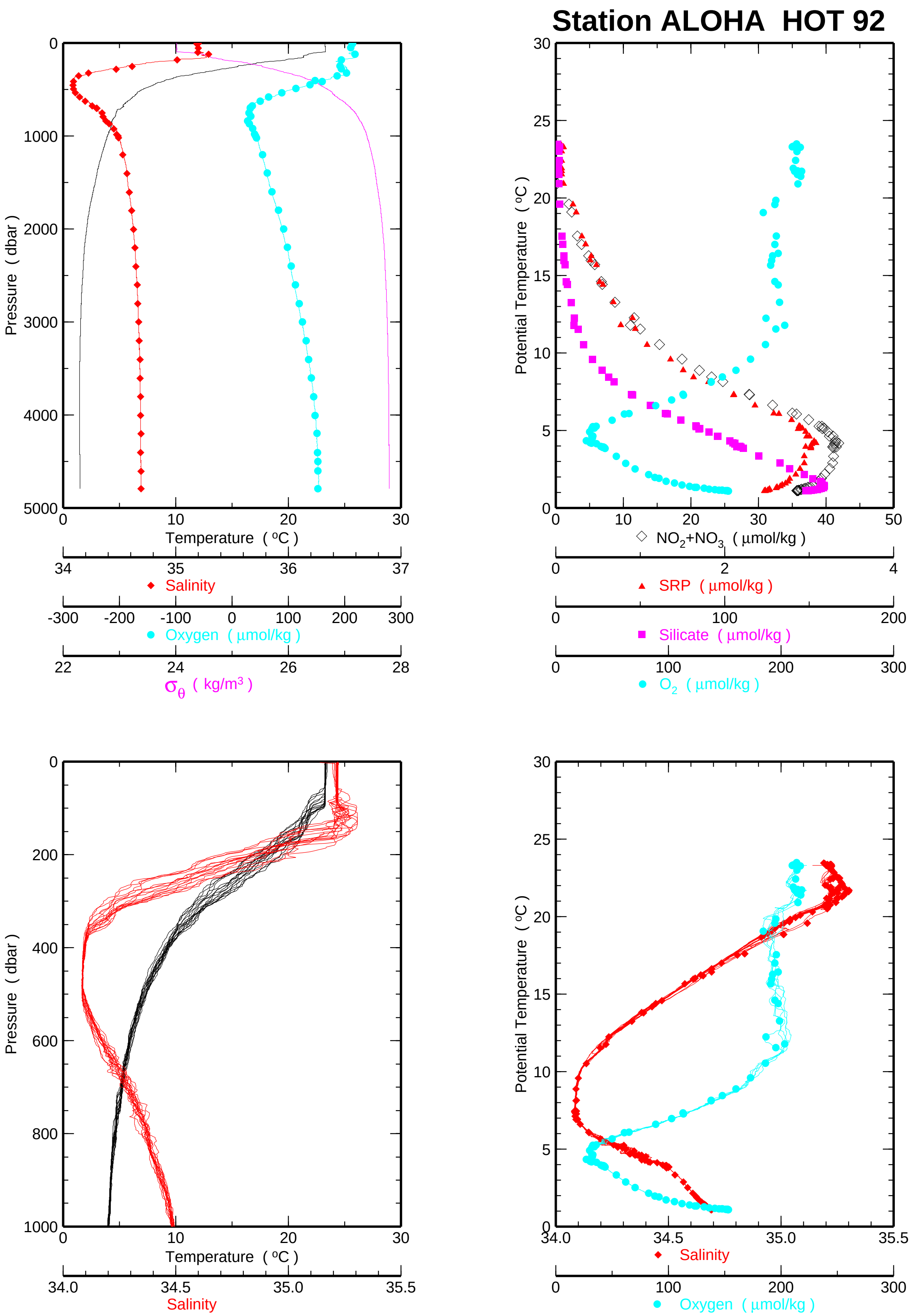

Station ALOHA HOT 92
Pressure (dbar)
Temperature (ºC)
Salinity
Oxygen (µmol/kg)
σ_θ (kg/m^3)
Potential Temperature (ºC)
NO_2+NO_3 (µmol/kg)
SRP (µmol/kg)
Silicate (µmol/kg)
O_2 (µmol/kg)

FIGURE 6.1.1d.

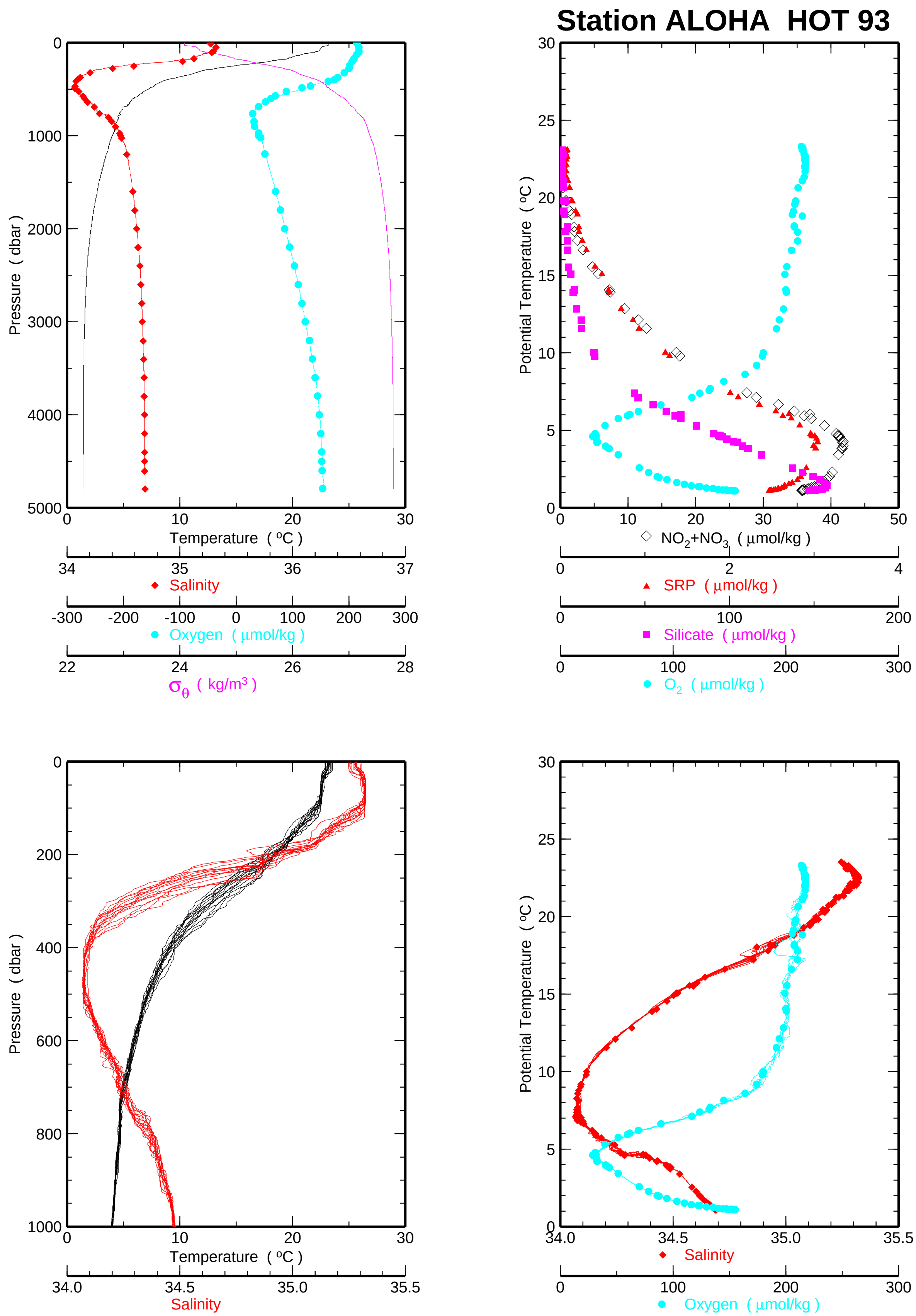

Station ALOHA HOT 93
Pressure (dbar)
Temperature (ºC)
Salinity
Oxygen (µmol/kg)
σ_θ (kg/m³)
Potential Temperature (ºC)
NO₂+NO₃ (µmol/kg)
SRP (µmol/kg)
Silicate (µmol/kg)
O₂ (µmol/kg)

FIGURE 6.1.1e.

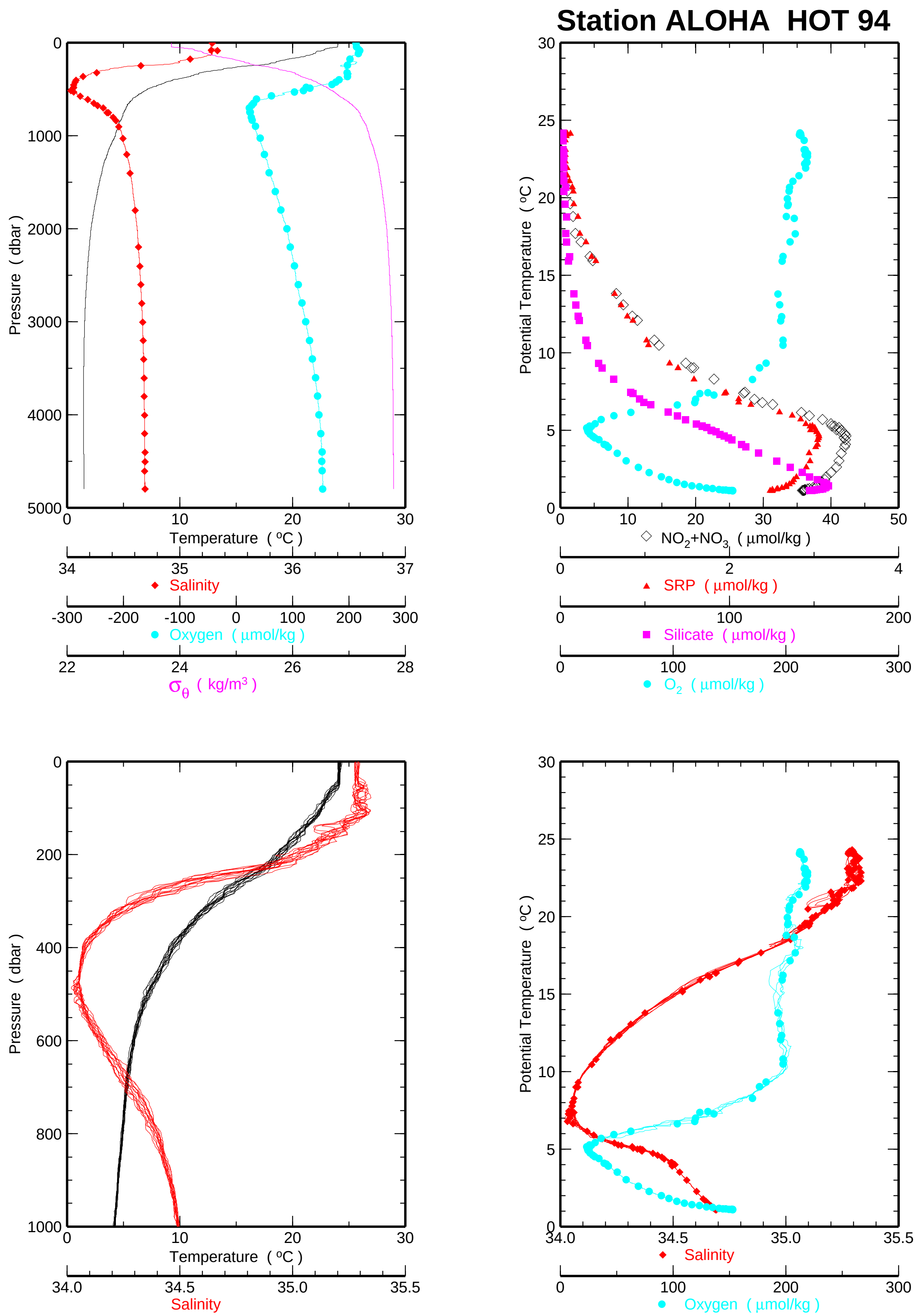
Station ALOHA HOT 94
Pressure (dbar)
Temperature (ºC)
Salinity
Oxygen (µmol/kg)
σθ (kg/m3)
Potential Temperature (ºC)
NO2+NO3 (µmol/kg)
SRP (µmol/kg)
Silicate (µmol/kg)
O2 (µmol/kg)

FIGURE 6.1.1f.

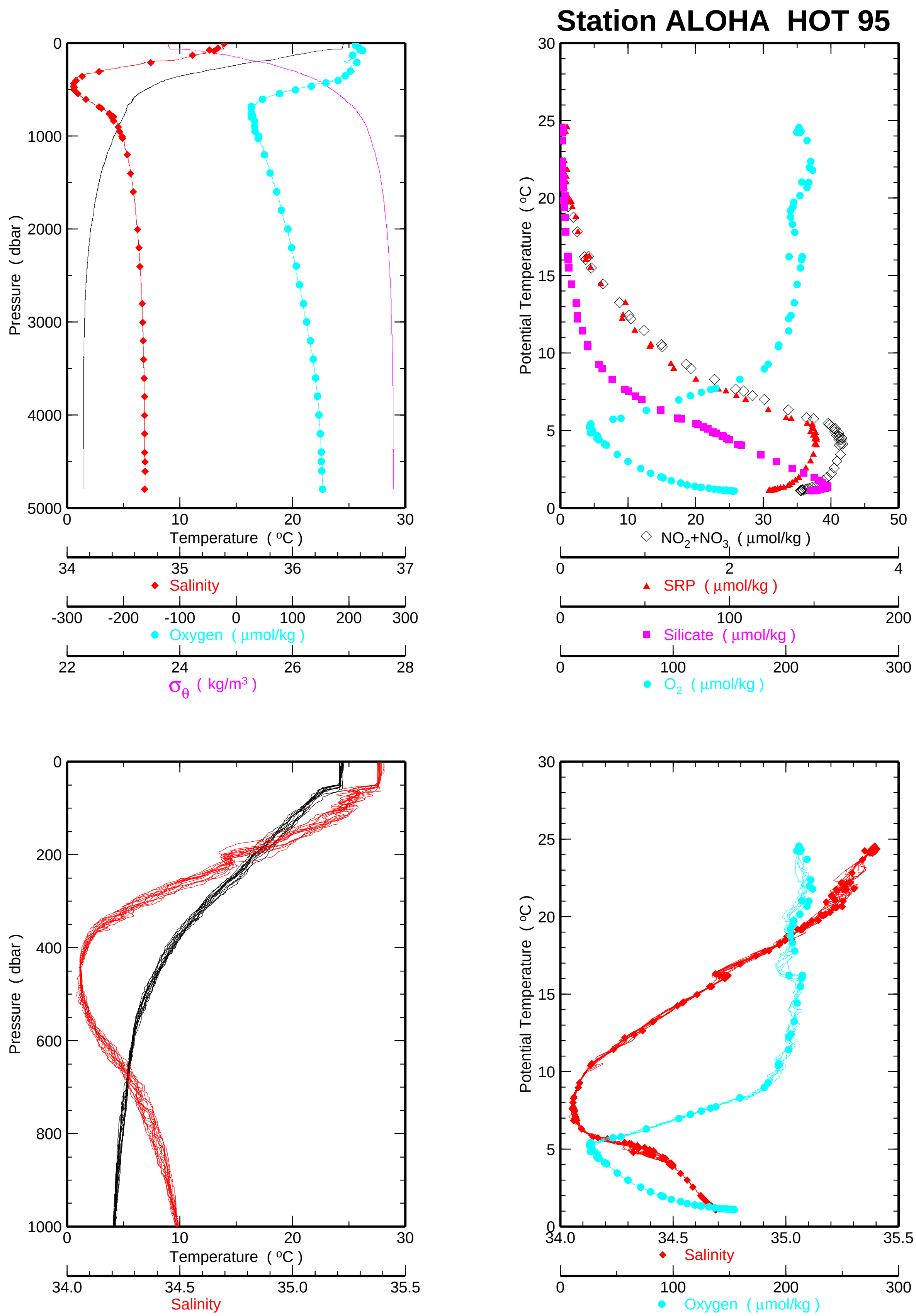
Station ALOHA HOT 95
Pressure (dbar)
Temperature (°C)
Salinity
Oxygen (µmol/kg)
σθ (kg/m3)
Potential Temperature (°C)
NO2+NO3 (µmol/kg)
SRP (µmol/kg)
Silicate (µmol/kg)
O2 (µmol/kg)
Pressure (dbar)
Temperature (°C)
Salinity
Potential Temperature (°C)
Salinity
Oxygen (µmol/kg)

FIGURE 6.1.1g.

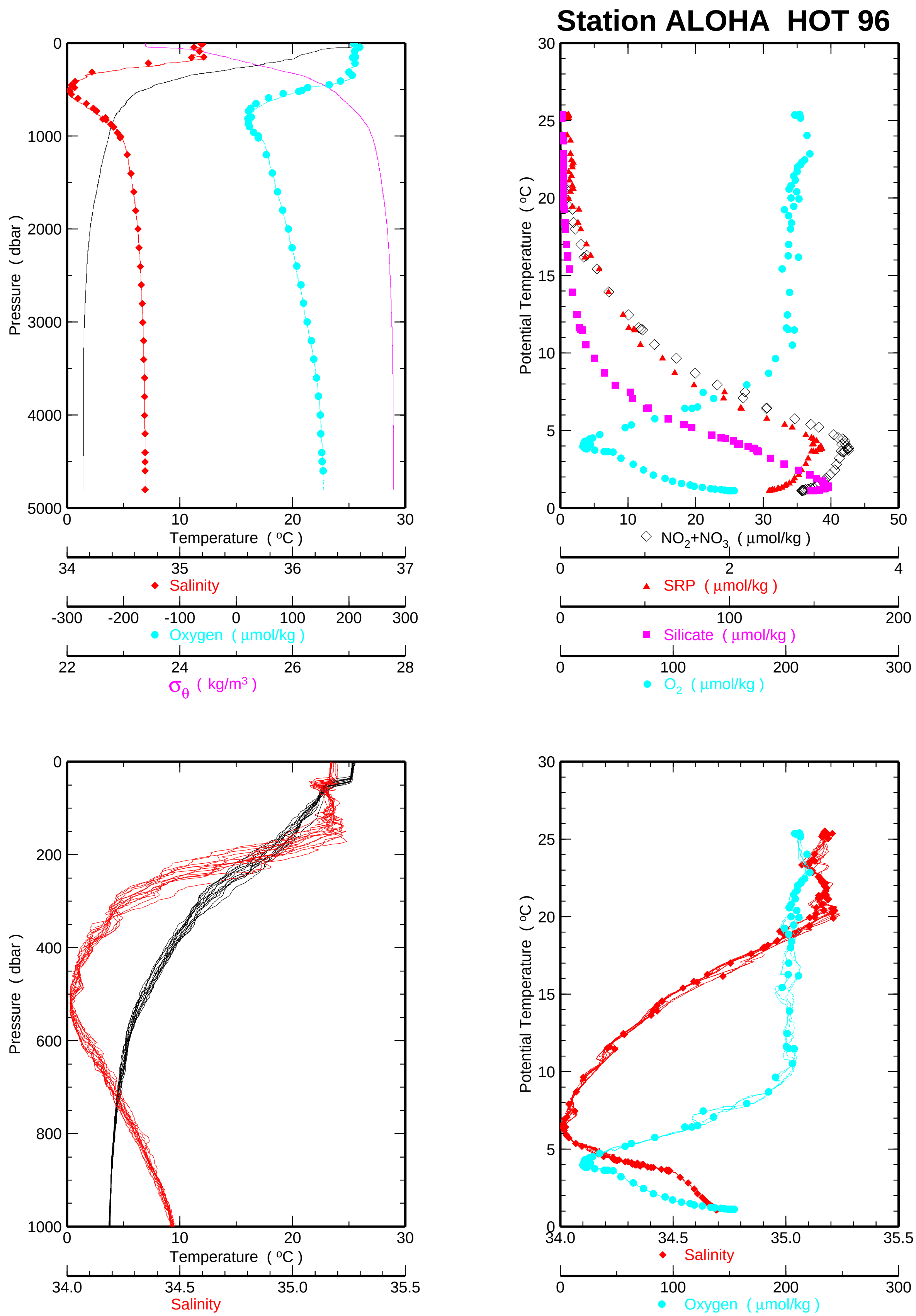
Station ALOHA HOT 96
Pressure (dbar)
Temperature (ºC)
Salinity
Oxygen (µmol/kg)
σθ (kg/m3)
Potential Temperature (ºC)
NO2+NO3 (µmol/kg)
SRP (µmol/kg)
Silicate (µmol/kg)
O2 (µmol/kg)

FIGURE 6.1.1h.

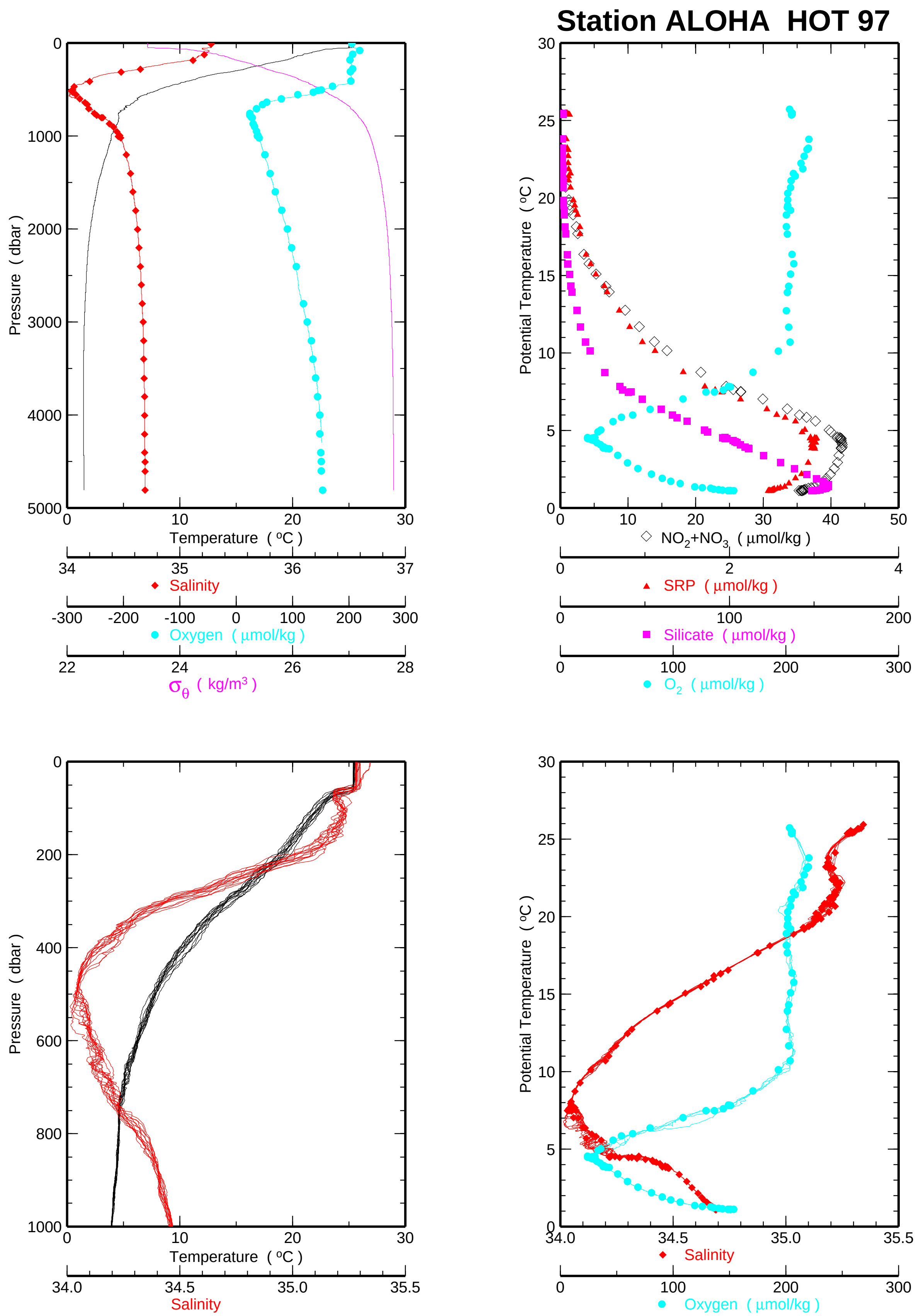

Station ALOHA HOT 97
Pressure (dbar)
Temperature (ºC)
Salinity
Oxygen (µmol/kg)
σθ (kg/m3)
Potential Temperature (ºC)
NO2+NO3 (µmol/kg)
SRP (µmol/kg)
Silicate (µmol/kg)
O2 (µmol/kg)

FIGURE 6.1.1i.

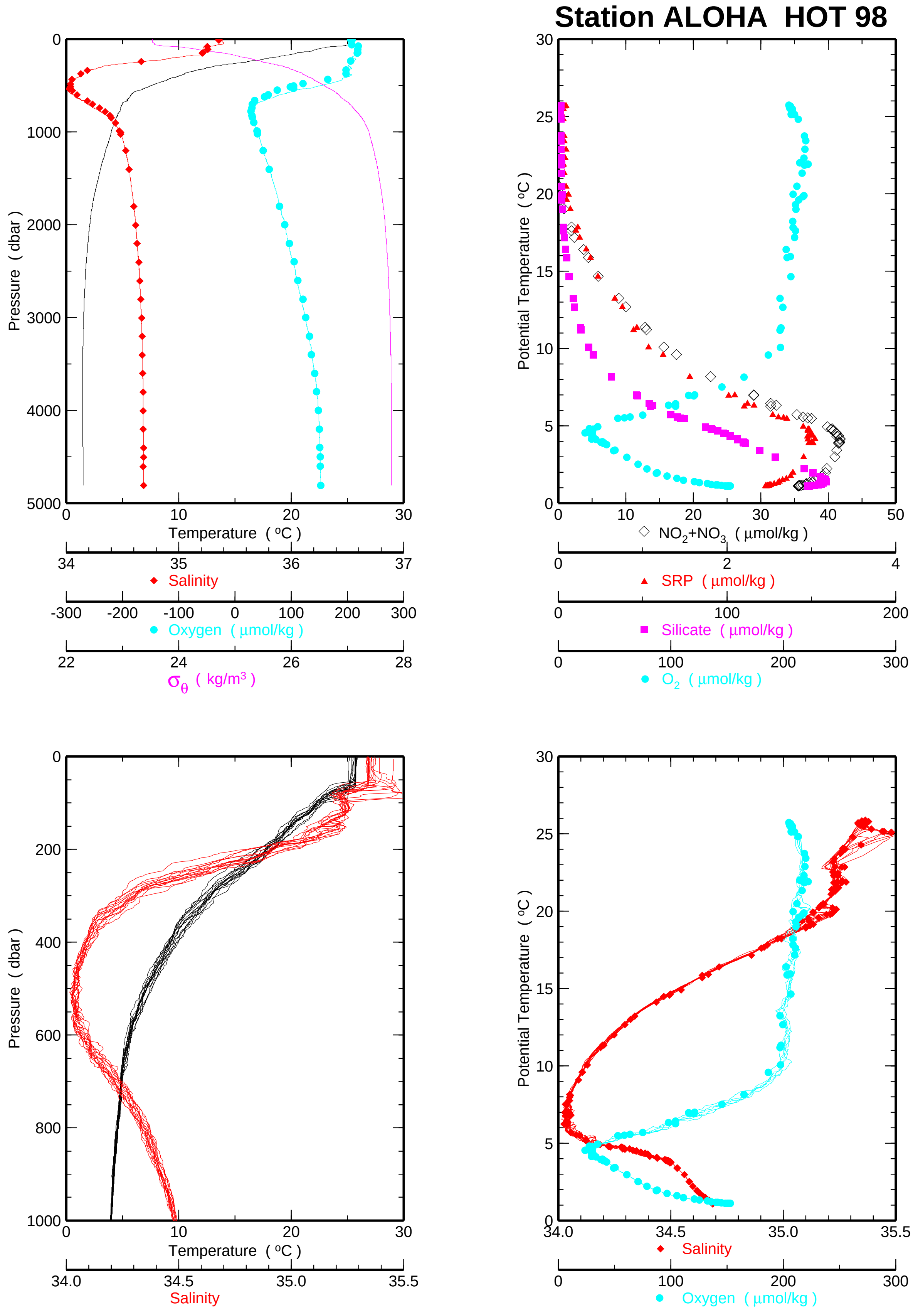
Station ALOHA HOT 98
Pressure (dbar)
Temperature (ºC)
Salinity
Oxygen (µmol/kg)
σθ (kg/m³)
Potential Temperature (ºC)
NO2+NO3 (µmol/kg)
SRP (µmol/kg)
Silicate (µmol/kg)
O2 (µmol/kg)
Pressure (dbar)
Temperature (ºC)
Salinity
Potential Temperature (ºC)
Salinity
Oxygen (µmol/kg)

FIGURE 6.1.1j.

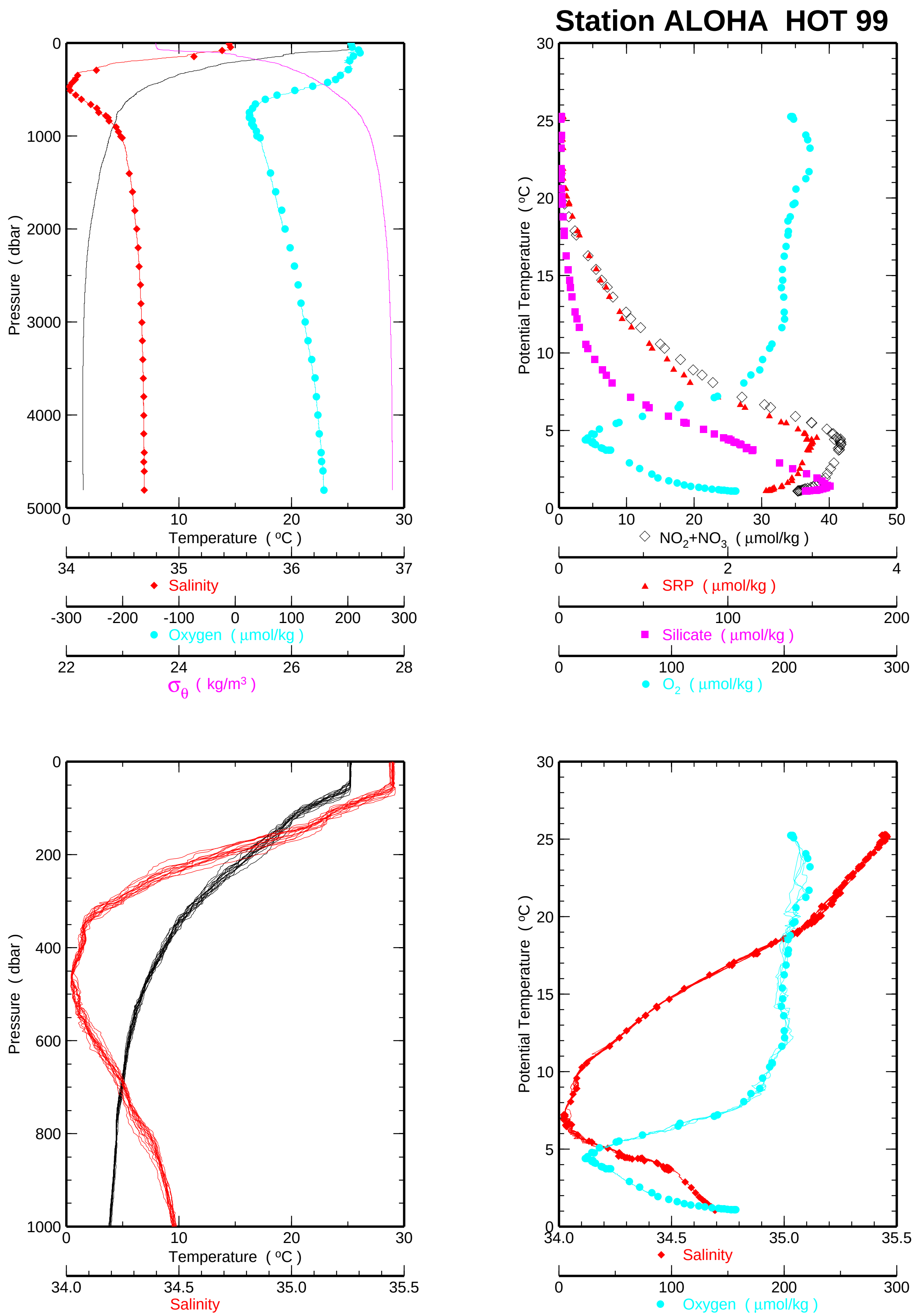

Station ALOHA HOT 99
Pressure (dbar)
Temperature (°C)
Salinity
Oxygen (µmol/kg)
σθ (kg/m³)
Potential Temperature (°C)
NO2+NO3 (µmol/kg)
SRP (µmol/kg)
Silicate (µmol/kg)
O2 (µmol/kg)

FIGURE 6.1.1k.

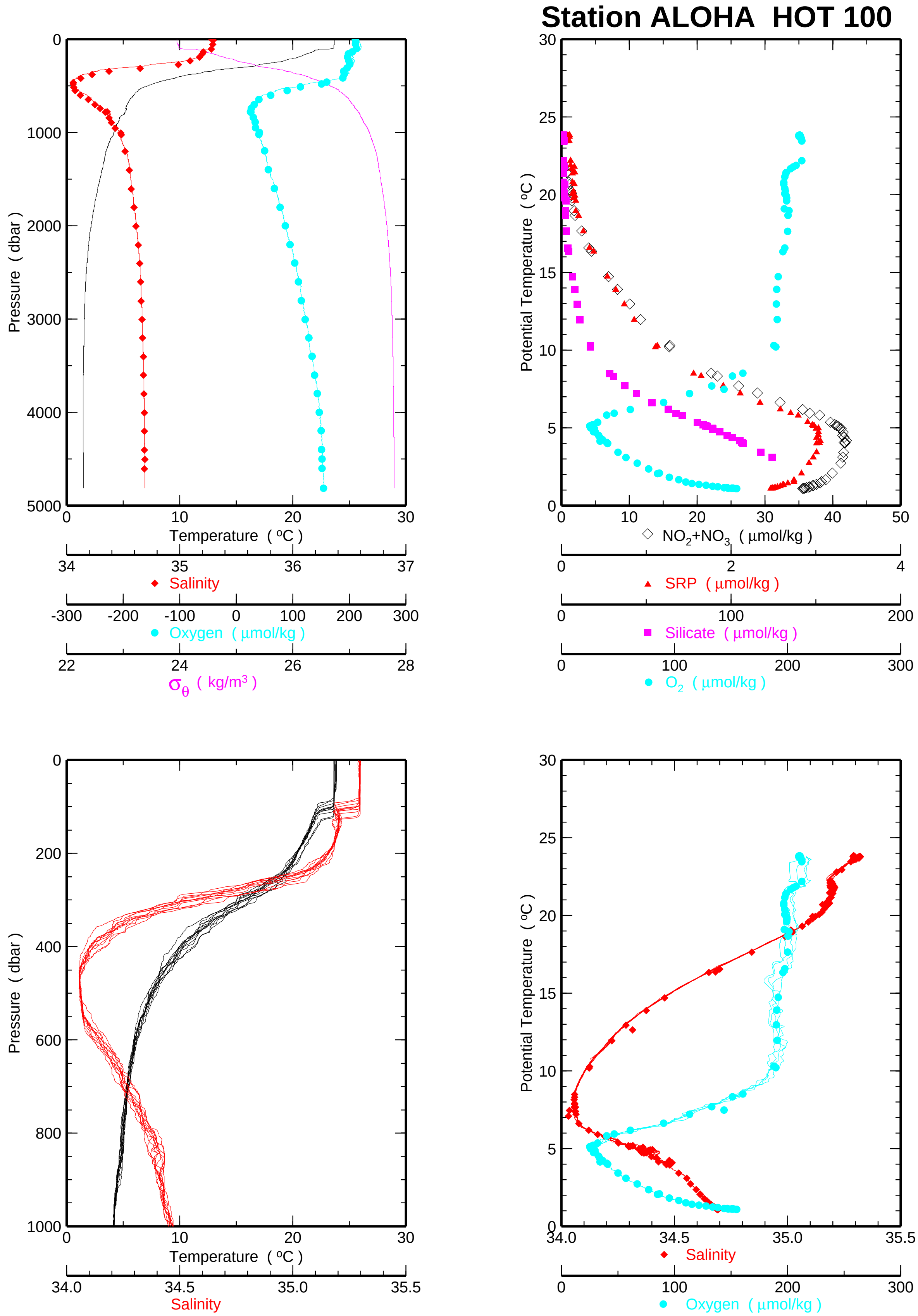

Station ALOHA HOT 100
Pressure (dbar)
Temperature (°C)
Salinity
Oxygen (µmol/kg)
σθ (kg/m³)
Potential Temperature (°C)
NO2+NO3 (µmol/kg)
SRP (µmol/kg)
Silicate (µmol/kg)
O2 (µmol/kg)

FIGURE 6.1.1a.

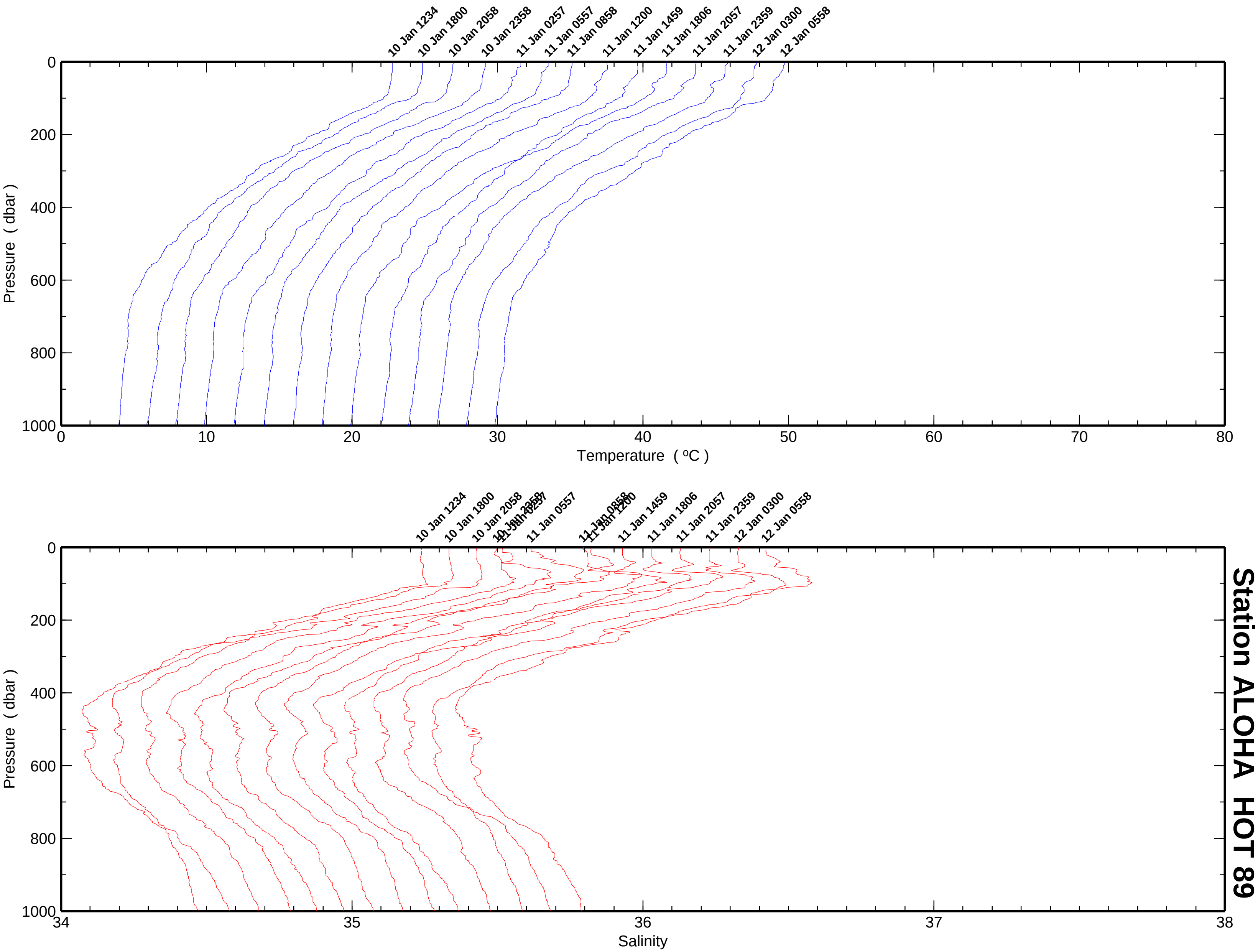
Station ALOHA HOT 89
10 Jan 1234
10 Jan 1800
10 Jan 2058
10 Jan 2358
11 Jan 0257
11 Jan 0557
11 Jan 0858
11 Jan 1200
11 Jan 1459
11 Jan 1806
11 Jan 2057
11 Jan 2359
12 Jan 0300
12 Jan 0558
Pressure (dbar)
Temperature (ºC)
Salinity
0
200
400
600
800
1000
10
20
30
40
50
60
70
80
34
35
36
37
38

FIGURE 6.1.2a.

FIGURE 6.1.2b.

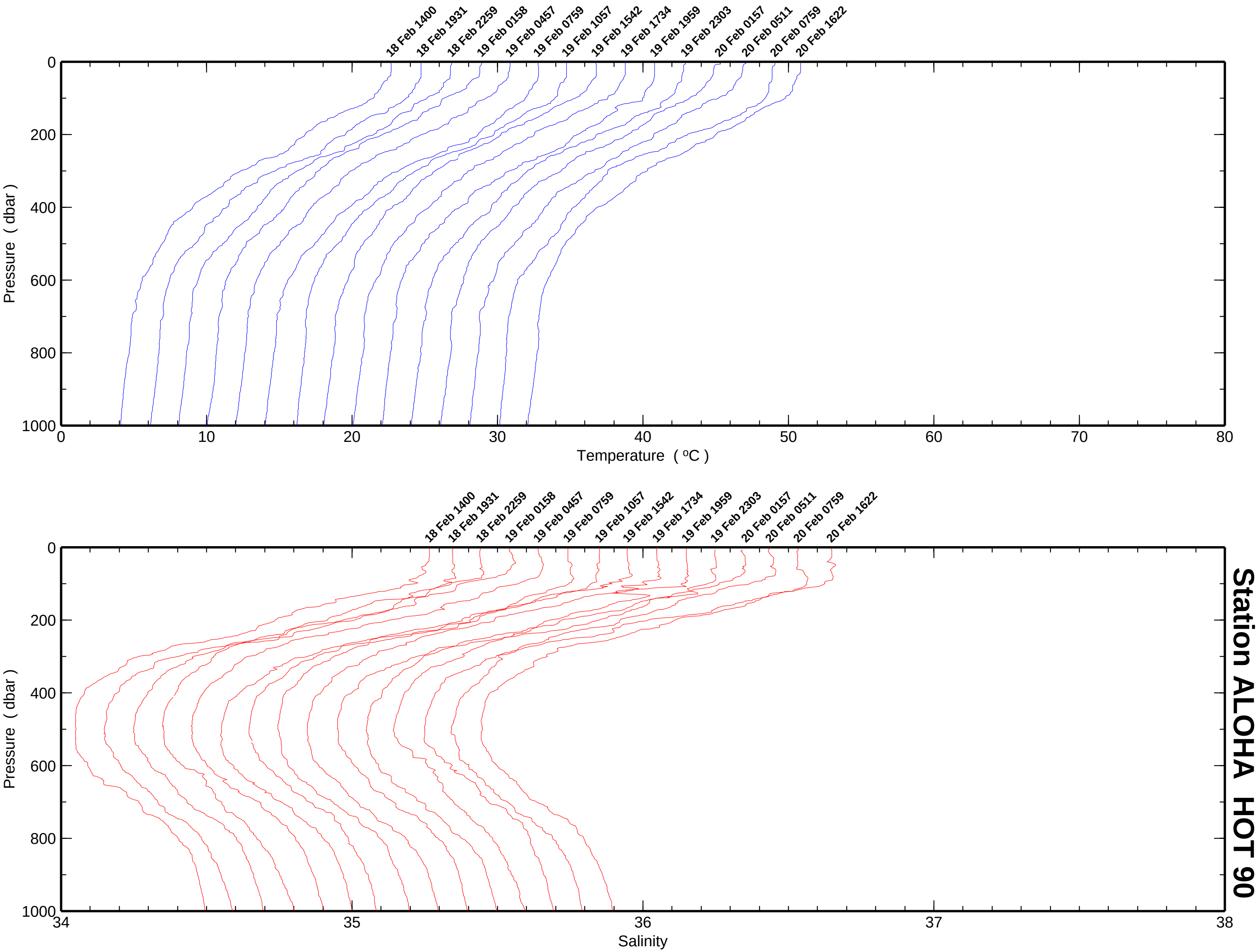

18 Feb 1400
18 Feb 1931
18 Feb 2259
19 Feb 0158
19 Feb 0457
19 Feb 0759
19 Feb 1057
19 Feb 1542
19 Feb 1734
19 Feb 1959
19 Feb 2303
20 Feb 0157
20 Feb 0511
20 Feb 0759
20 Feb 1622
Pressure (dbar)
0
200
400
600
800
1000
0
10
20
30
40
50
60
70
80
Temperature (ºC)
Pressure (dbar)
34
35
36
37
38
Salinity
Station ALOHA HOT 90

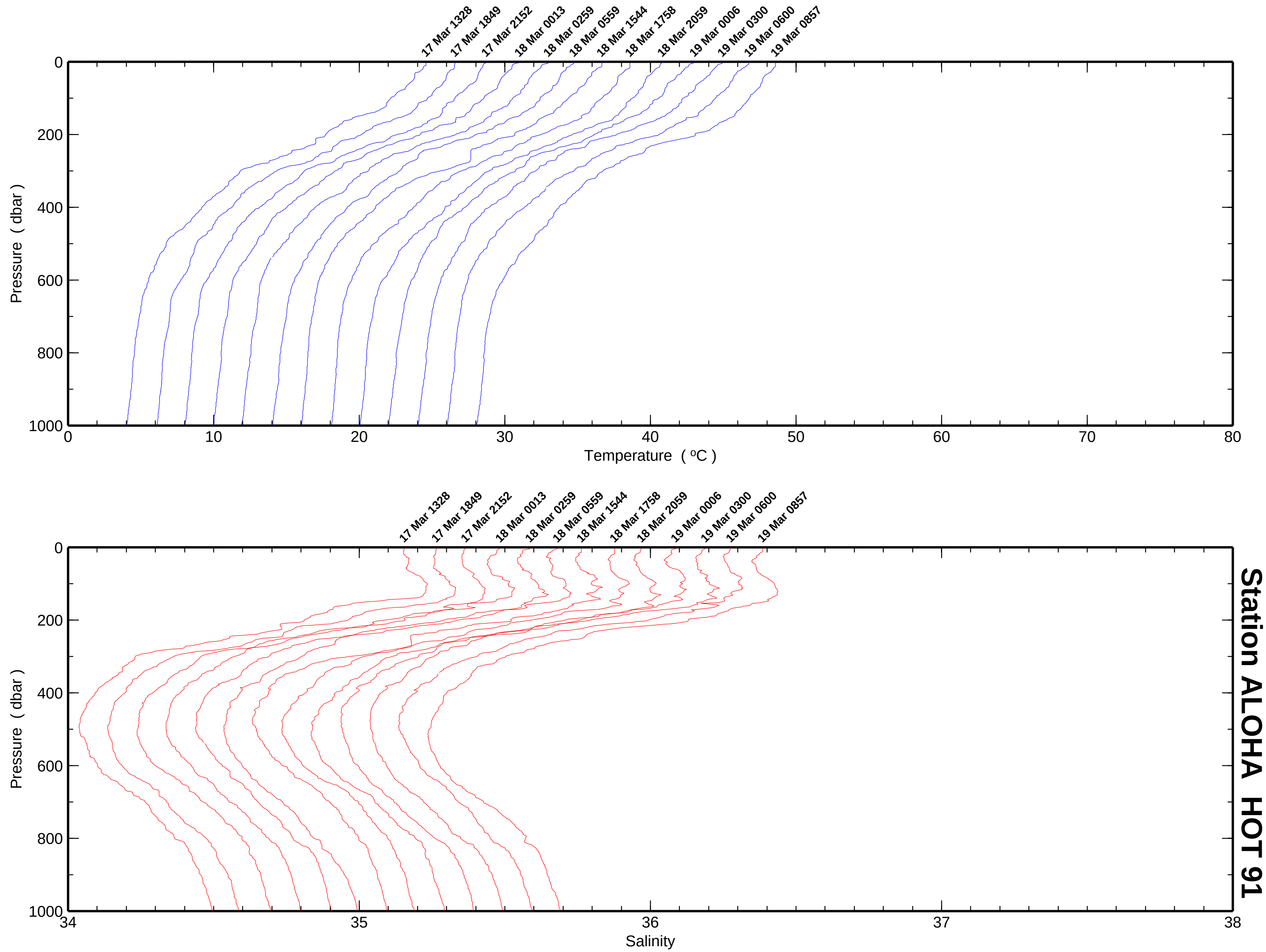
17 Mar 1328
17 Mar 1849
17 Mar 2152
18 Mar 0013
18 Mar 0259
18 Mar 0559
18 Mar 1544
18 Mar 1758
18 Mar 2059
19 Mar 0006
19 Mar 0300
19 Mar 0600
19 Mar 0857
Pressure (dbar)
0
200
400
600
800
1000
0
10
20
30
40
50
60
70
80
Temperature (ºC)
Salinity
34
35
36
37
38
Station ALOHA HOT 91

FIGURE 6.1.2c.

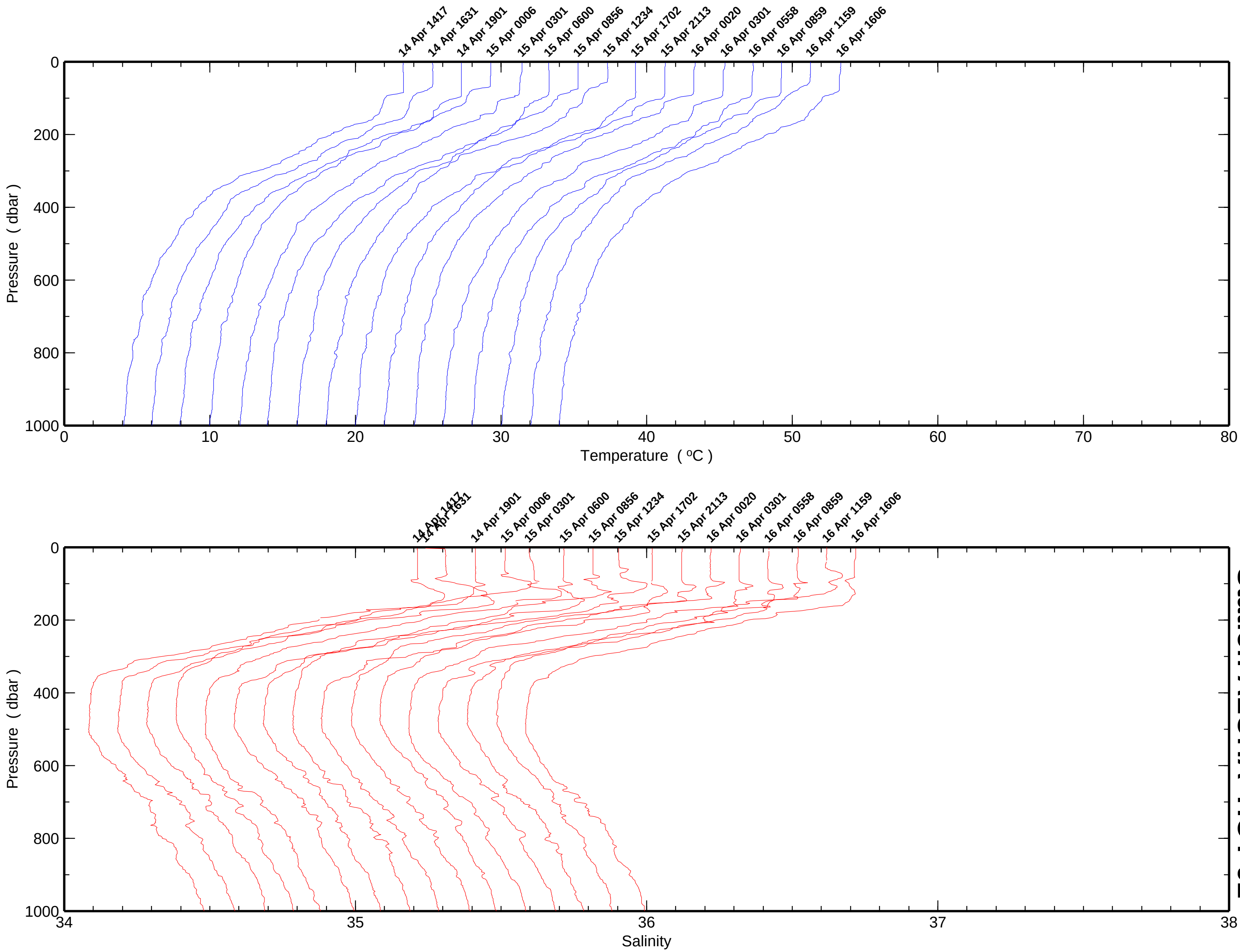

Station ALOHA HOT 92

FIGURE 6.1.2d.

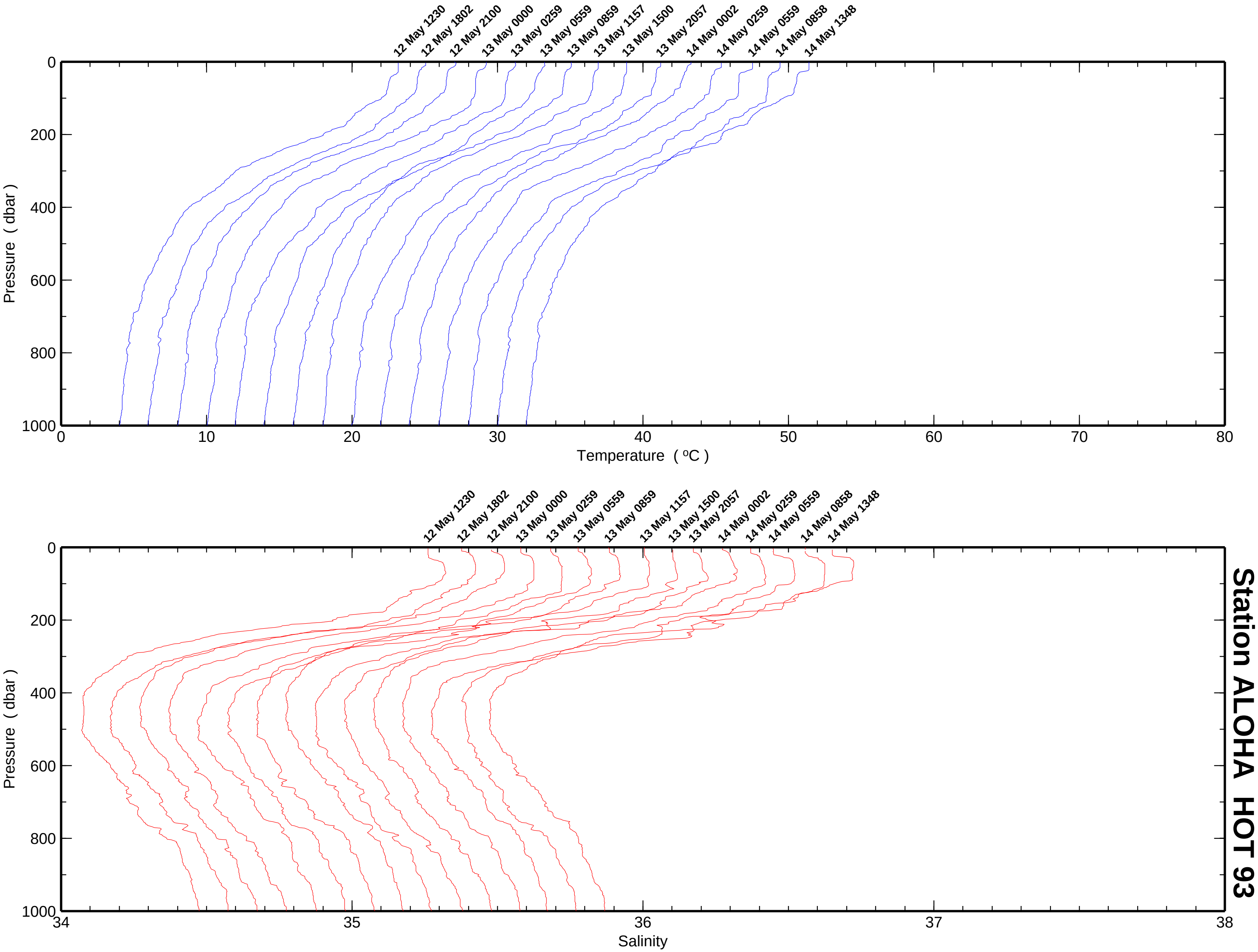
Station ALOHA HOT 93
12 May 1230
12 May 1802
12 May 2100
13 May 0000
13 May 0259
13 May 0559
13 May 0859
13 May 1157
13 May 1500
13 May 2057
14 May 0002
14 May 0259
14 May 0559
14 May 0858
14 May 1348
Pressure (dbar)
Temperature (ºC)
Salinity

FIGURE 6.1.2e.

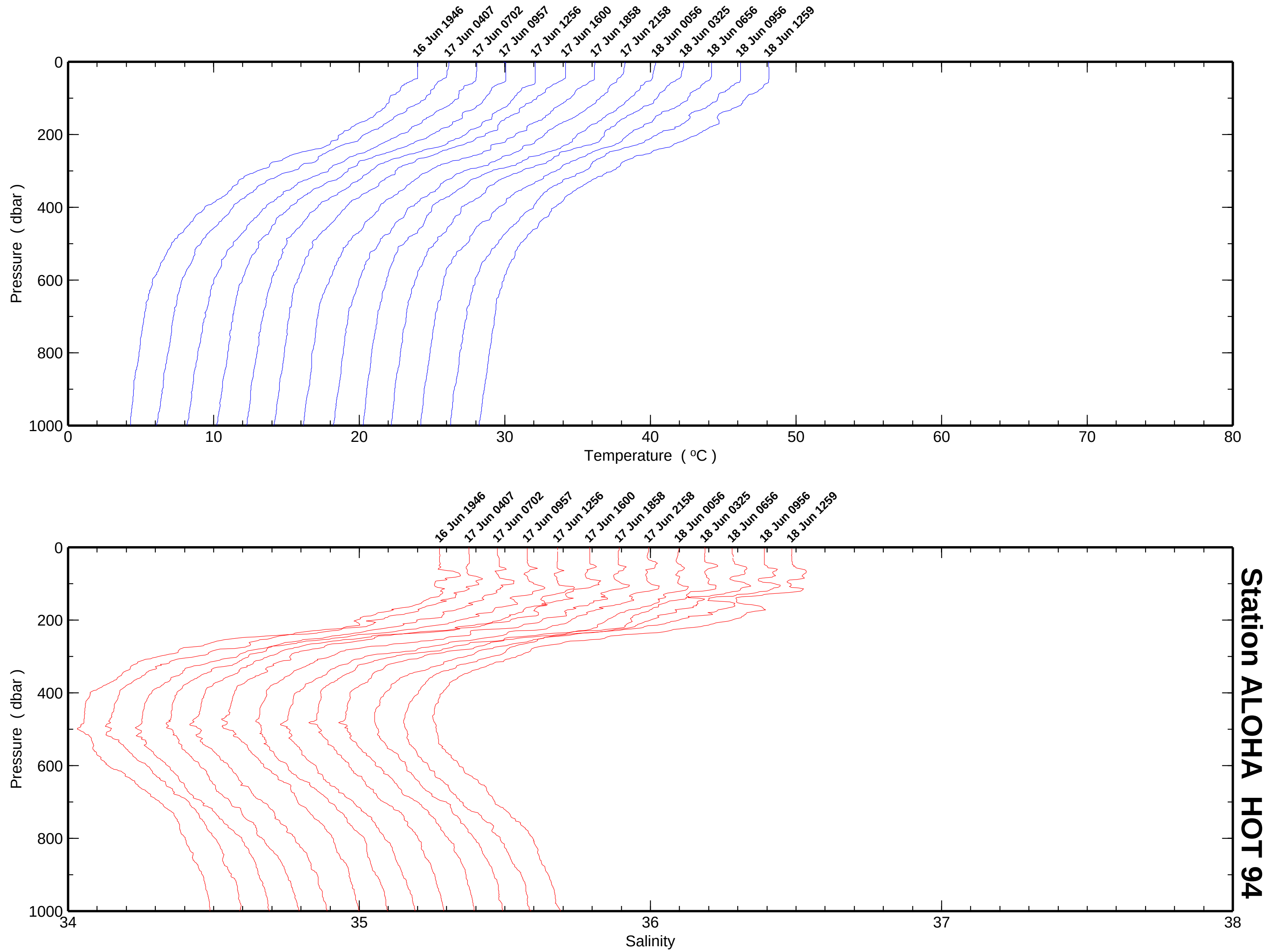
Station ALOHA HOT 94
16 Jun 1946
17 Jun 0407
17 Jun 0702
17 Jun 0957
17 Jun 1256
17 Jun 1600
17 Jun 1858
17 Jun 2158
18 Jun 0056
18 Jun 0325
18 Jun 0656
18 Jun 0956
18 Jun 1259
Pressure (dbar)
0
200
400
600
800
1000
Temperature (ºC)
0
10
20
30
40
50
60
70
80
Salinity
34
35
36
37
38

FIGURE 6.1.2f.

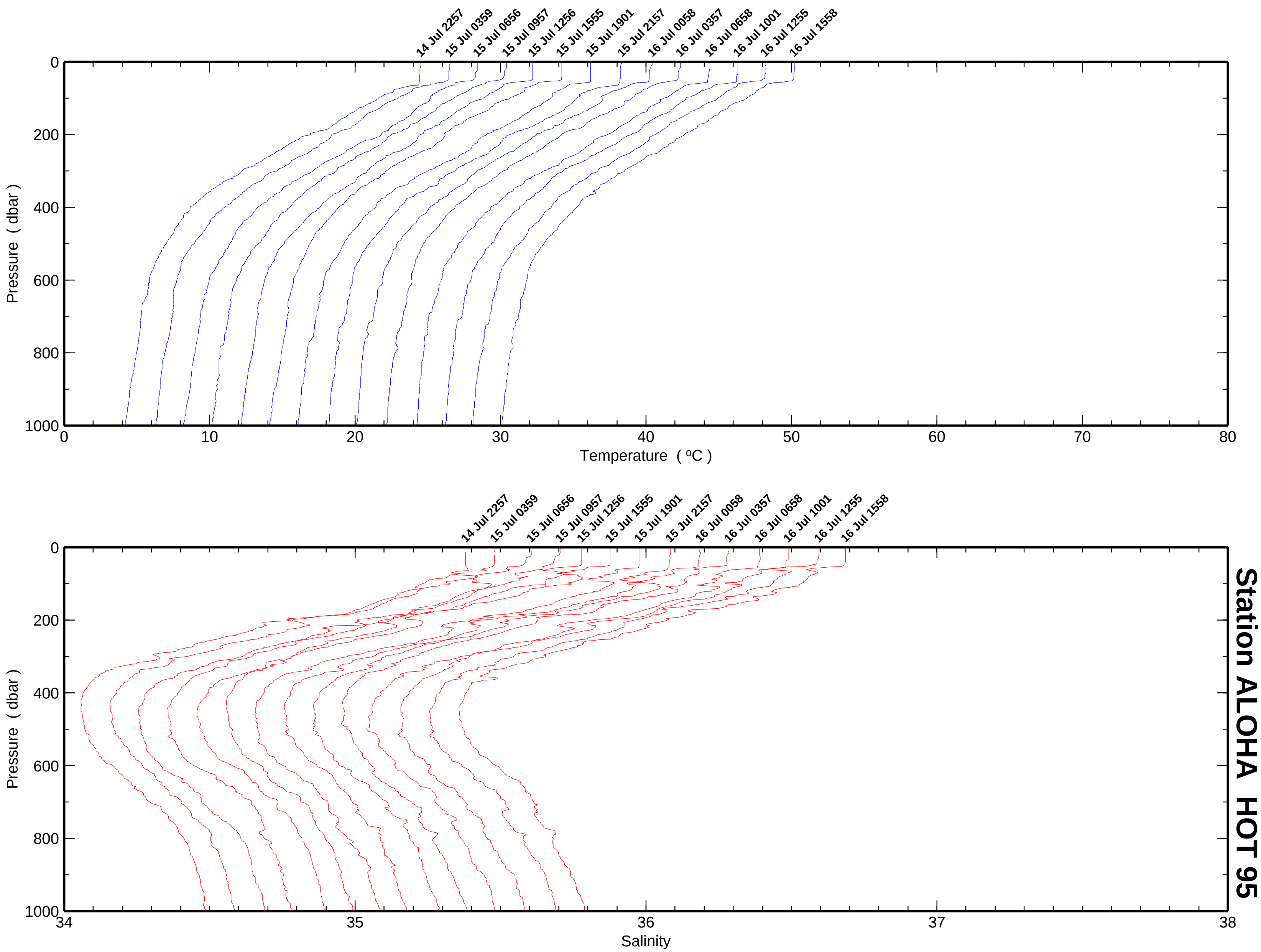
Station ALOHA HOT 95
14 Jul 2257
15 Jul 0359
15 Jul 0656
15 Jul 0957
15 Jul 1256
15 Jul 1555
15 Jul 1901
15 Jul 2157
16 Jul 0058
16 Jul 0357
16 Jul 0658
16 Jul 1001
16 Jul 1255
16 Jul 1558
Pressure (dbar)
Temperature (ºC)
Salinity

FIGURE 6.1.2g.

FIGURE 6.1.2h.

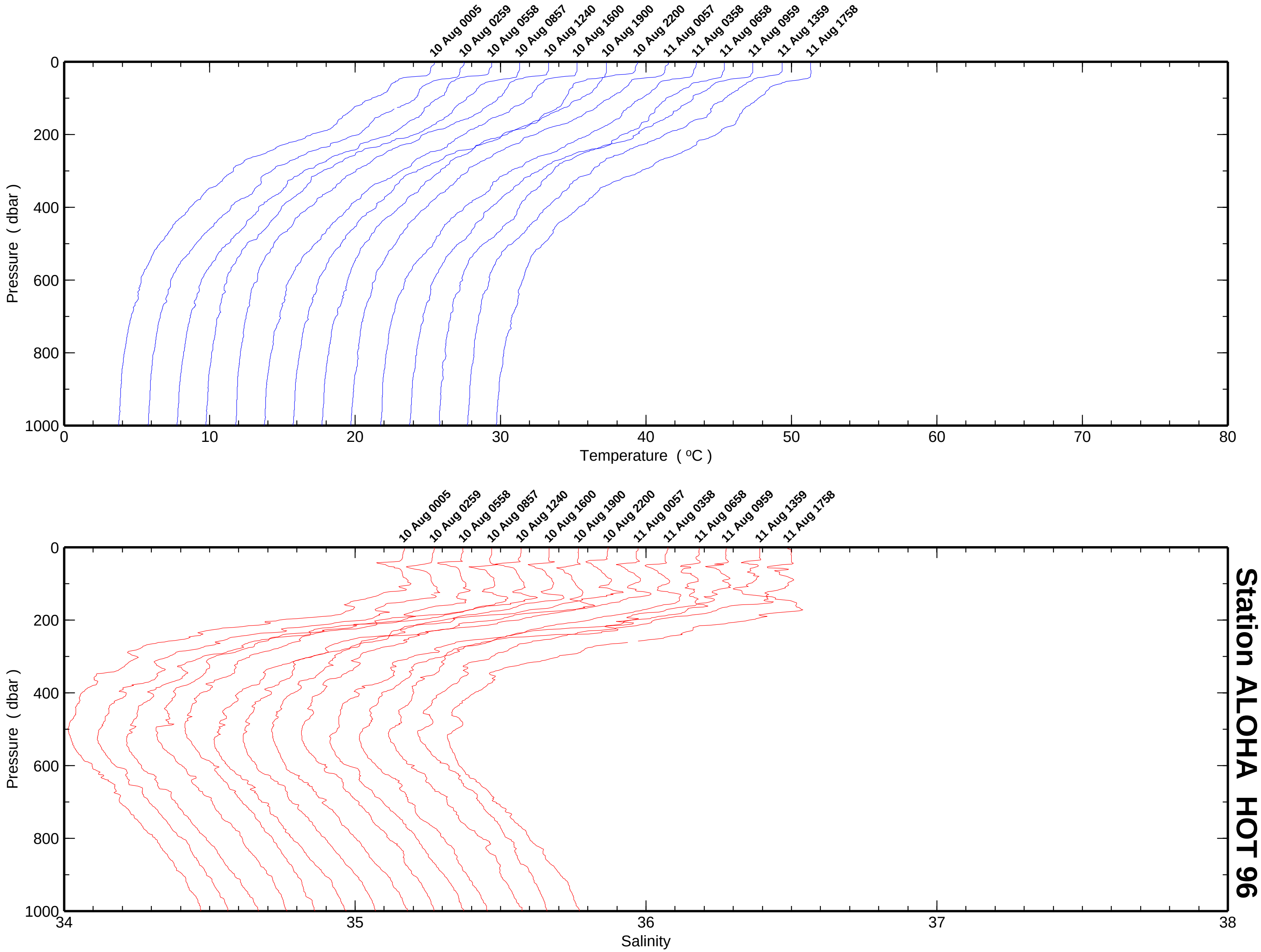
Station ALOHA HOT 96
10 Aug 0005
10 Aug 0259
10 Aug 0558
10 Aug 0857
10 Aug 1240
10 Aug 1600
10 Aug 1900
10 Aug 2200
11 Aug 0057
11 Aug 0358
11 Aug 0658
11 Aug 0959
11 Aug 1359
11 Aug 1758
Pressure (dbar)
0
200
400
600
800
1000
0
10
20
30
40
50
60
70
80
Temperature (ºC)
34
35
36
37
38
Salinity

FIGURE 6.1.2i.

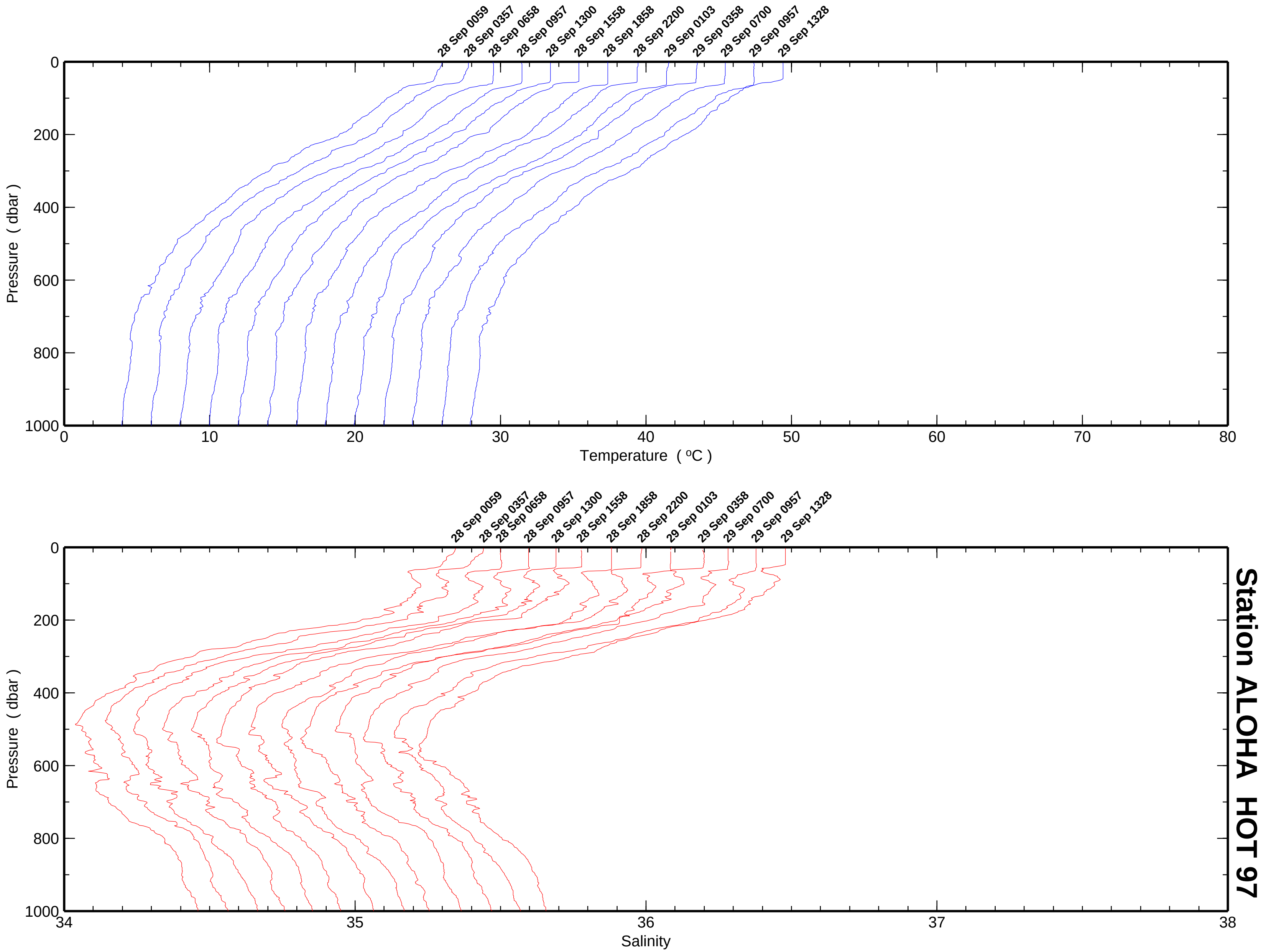

28 Sep 0059
28 Sep 0357
28 Sep 0658
28 Sep 0957
28 Sep 1300
28 Sep 1558
28 Sep 1858
28 Sep 2200
29 Sep 0103
29 Sep 0358
29 Sep 0700
29 Sep 0957
29 Sep 1328
Pressure (dbar)
0
200
400
600
800
1000
Temperature (ºC)
0
10
20
30
40
50
60
70
80
Salinity
34
35
36
37
38
Station ALOHA HOT 97

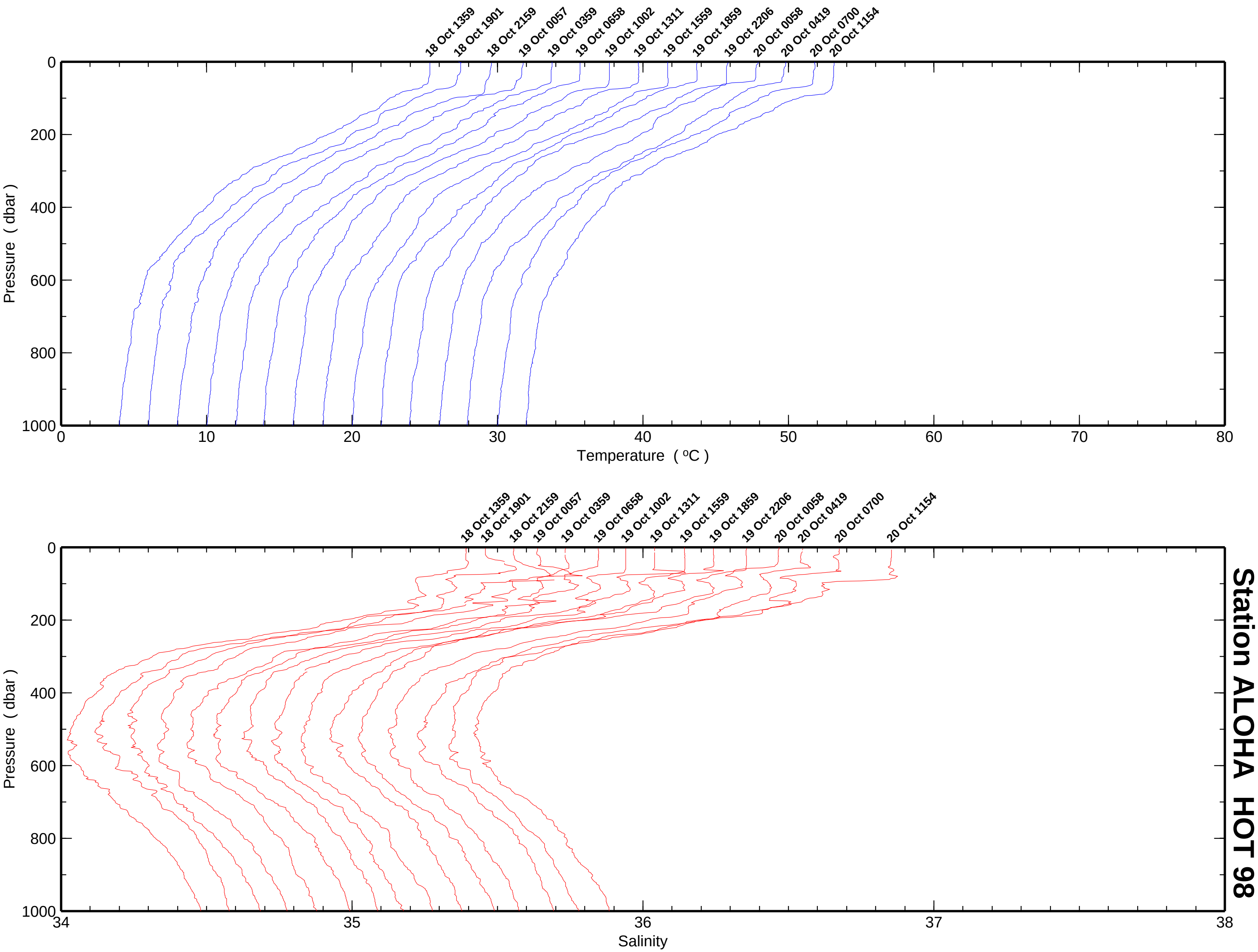
Station ALOHA HOT 98
18 Oct 1359
18 Oct 1901
18 Oct 2159
19 Oct 0057
19 Oct 0359
19 Oct 0658
19 Oct 1002
19 Oct 1311
19 Oct 1559
19 Oct 1859
19 Oct 2206
20 Oct 0058
20 Oct 0419
20 Oct 0700
20 Oct 1154
Pressure (dbar)
Temperature (ºC)
Salinity

FIGURE 6.1.2j.

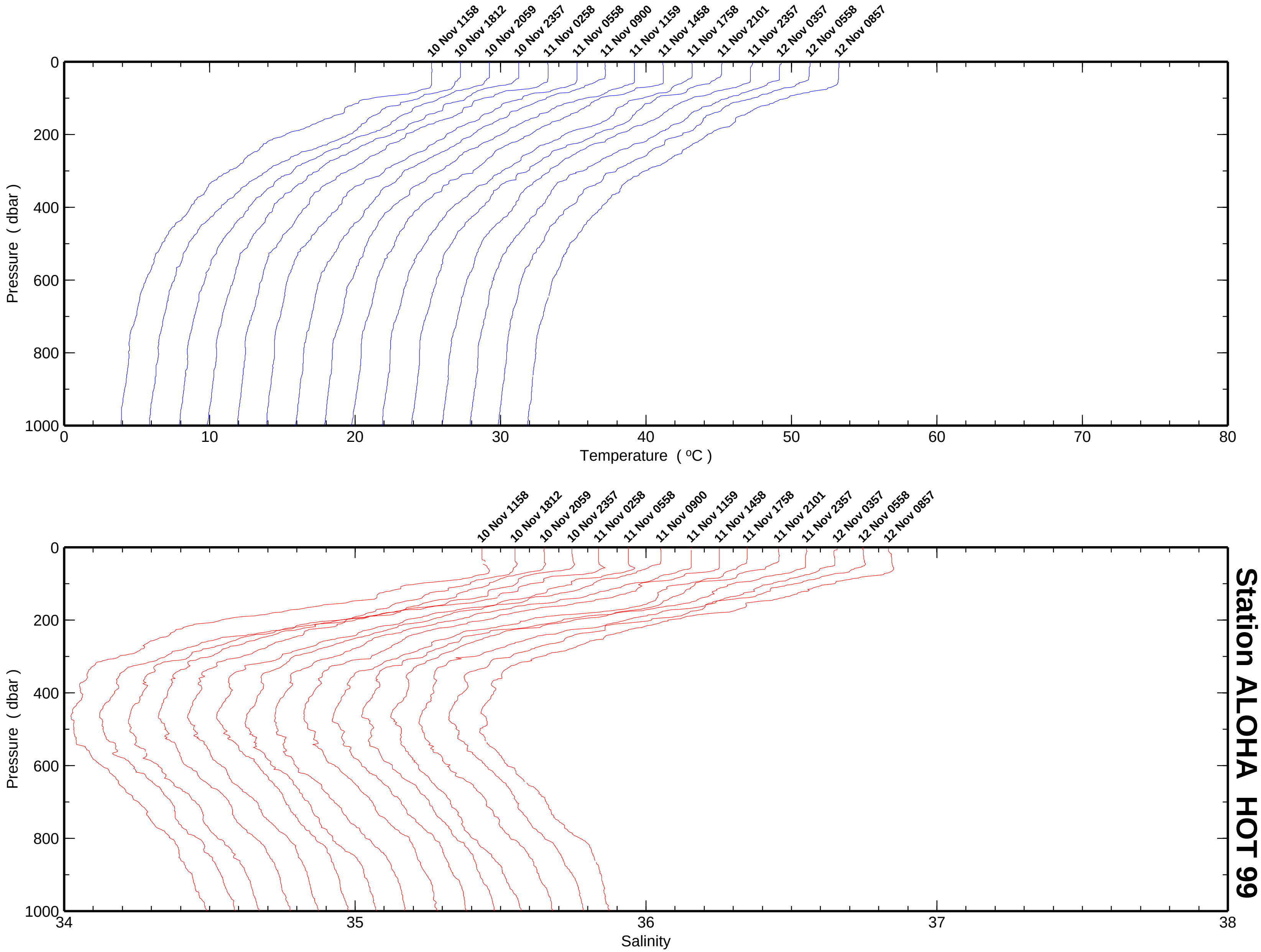
Station ALOHA HOT 99
10 Nov 1158
10 Nov 1812
10 Nov 2059
10 Nov 2357
11 Nov 0258
11 Nov 0558
11 Nov 0900
11 Nov 1159
11 Nov 1458
11 Nov 1758
11 Nov 2101
11 Nov 2357
12 Nov 0357
12 Nov 0558
12 Nov 0857
Pressure (dbar)
Temperature (ºC)
Salinity
0
200
400
600
800
1000
10
20
30
40
50
60
70
80
34
35
36
37
38

FIGURE 6.1.2k.

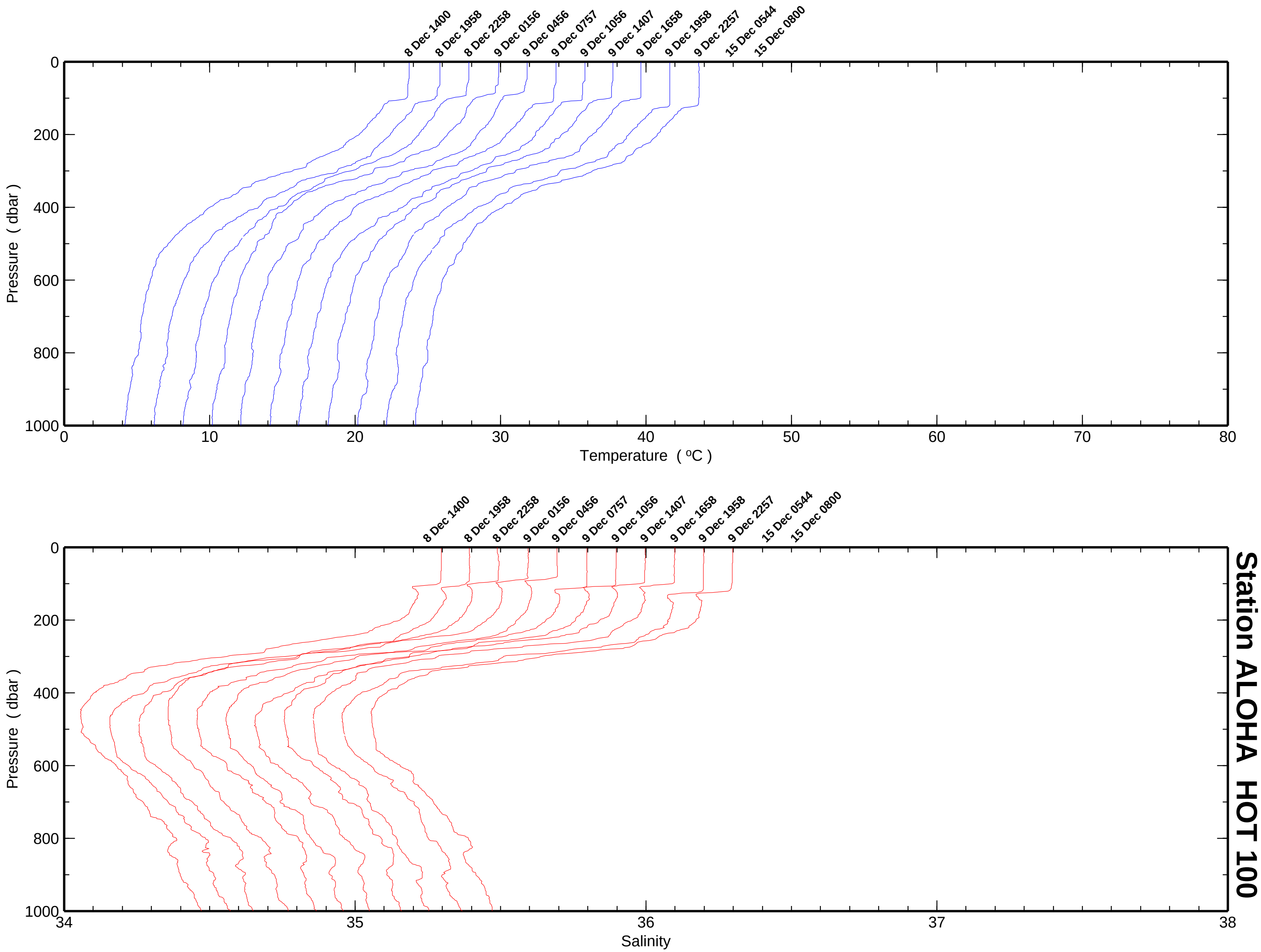
Station ALOHA HOT 100
8 Dec 1400
8 Dec 1958
8 Dec 2258
9 Dec 0156
9 Dec 0456
9 Dec 0757
9 Dec 1056
9 Dec 1407
9 Dec 1658
9 Dec 1958
9 Dec 2257
15 Dec 0544
15 Dec 0800
Pressure (dbar)
0
200
400
600
800
1000
Temperature (ºC)
0
10
20
30
40
50
60
70
80
Salinity
34
35
36
37
38

FIGURE 6.1.2l.

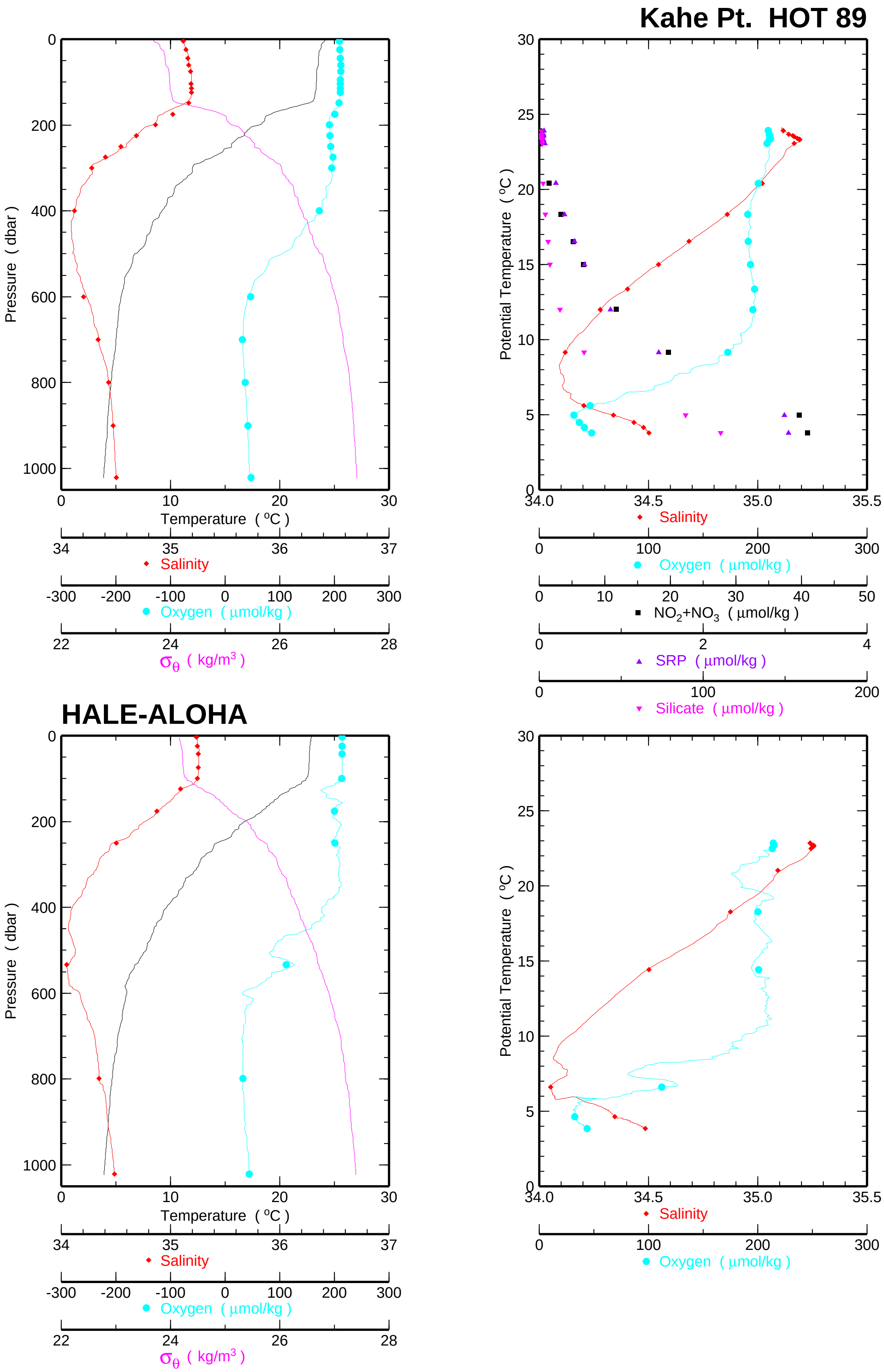

Kahe Pt. HOT 89
HALE-ALOHA
Pressure (dbar)
Temperature (°C)
Salinity
Oxygen (µmol/kg)
σθ (kg/m³)
Potential Temperature (°C)
NO2+NO3 (µmol/kg)
SRP (µmol/kg)
Silicate (µmol/kg)

FIGURE 6.1.3a.

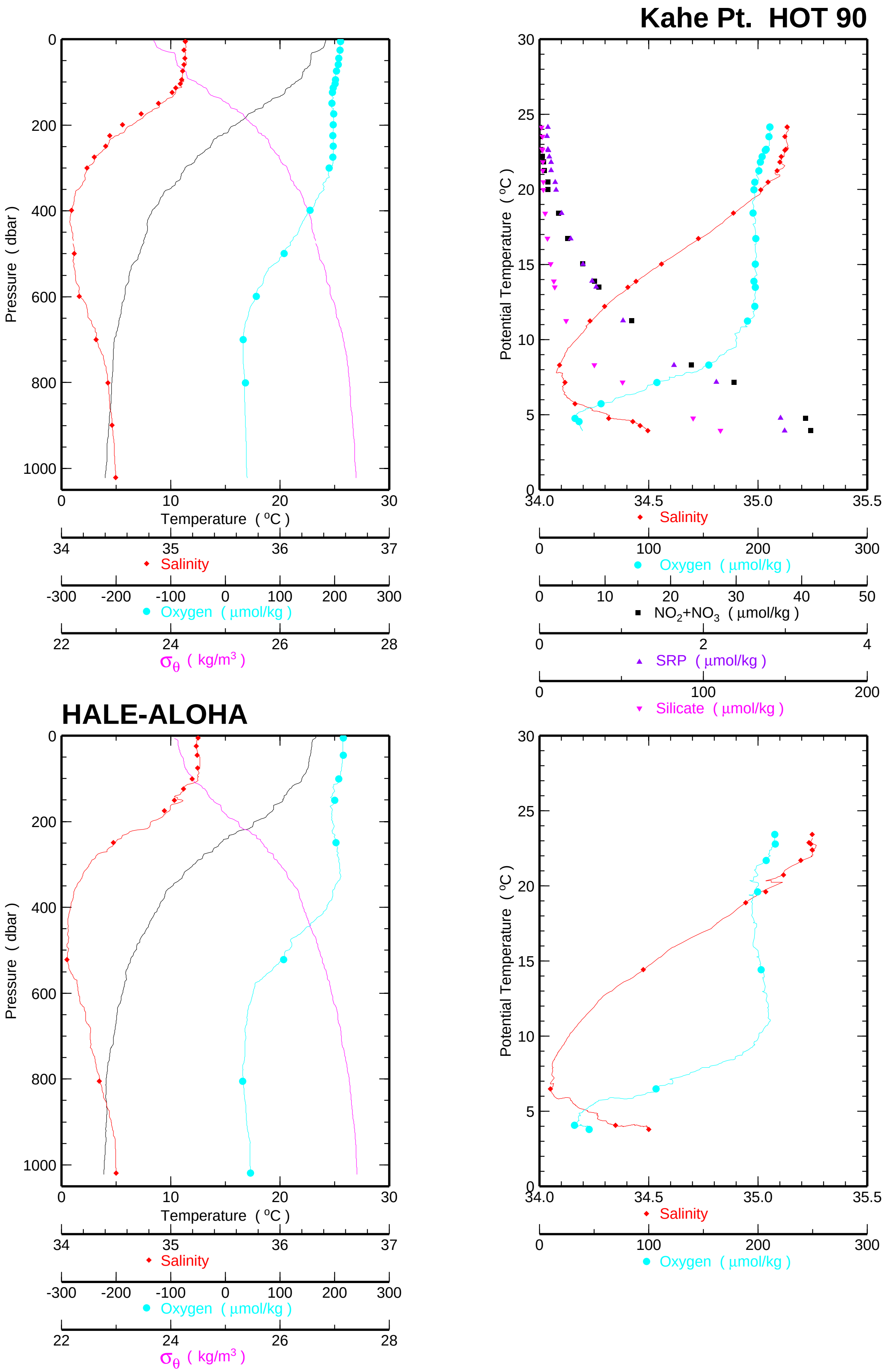

Kahe Pt. HOT 90
HALE-ALOHA
Pressure (dbar)
Temperature (°C)
Salinity
Oxygen (µmol/kg)
σθ (kg/m³)
Potential Temperature (°C)
NO2+NO3 (µmol/kg)
SRP (µmol/kg)
Silicate (µmol/kg)

FIGURE 6.1.3b.

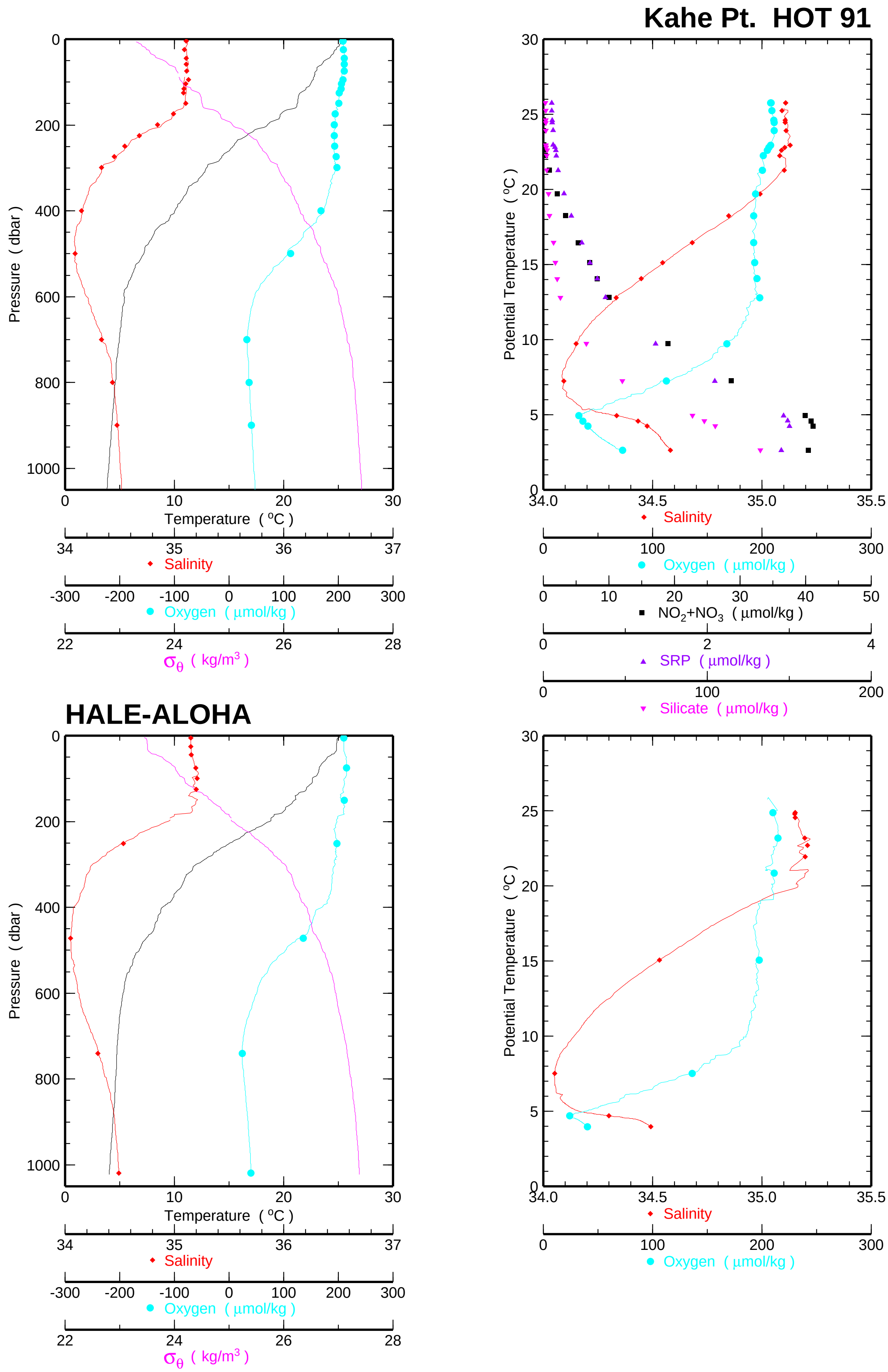
Kahe Pt. HOT 91
HALE-ALOHA
Pressure (dbar)
Temperature (°C)
Salinity
Oxygen (µmol/kg)
σθ (kg/m³)
Potential Temperature (°C)
NO2+NO3 (µmol/kg)
SRP (µmol/kg)
Silicate (µmol/kg)

FIGURE 6.1.3c.

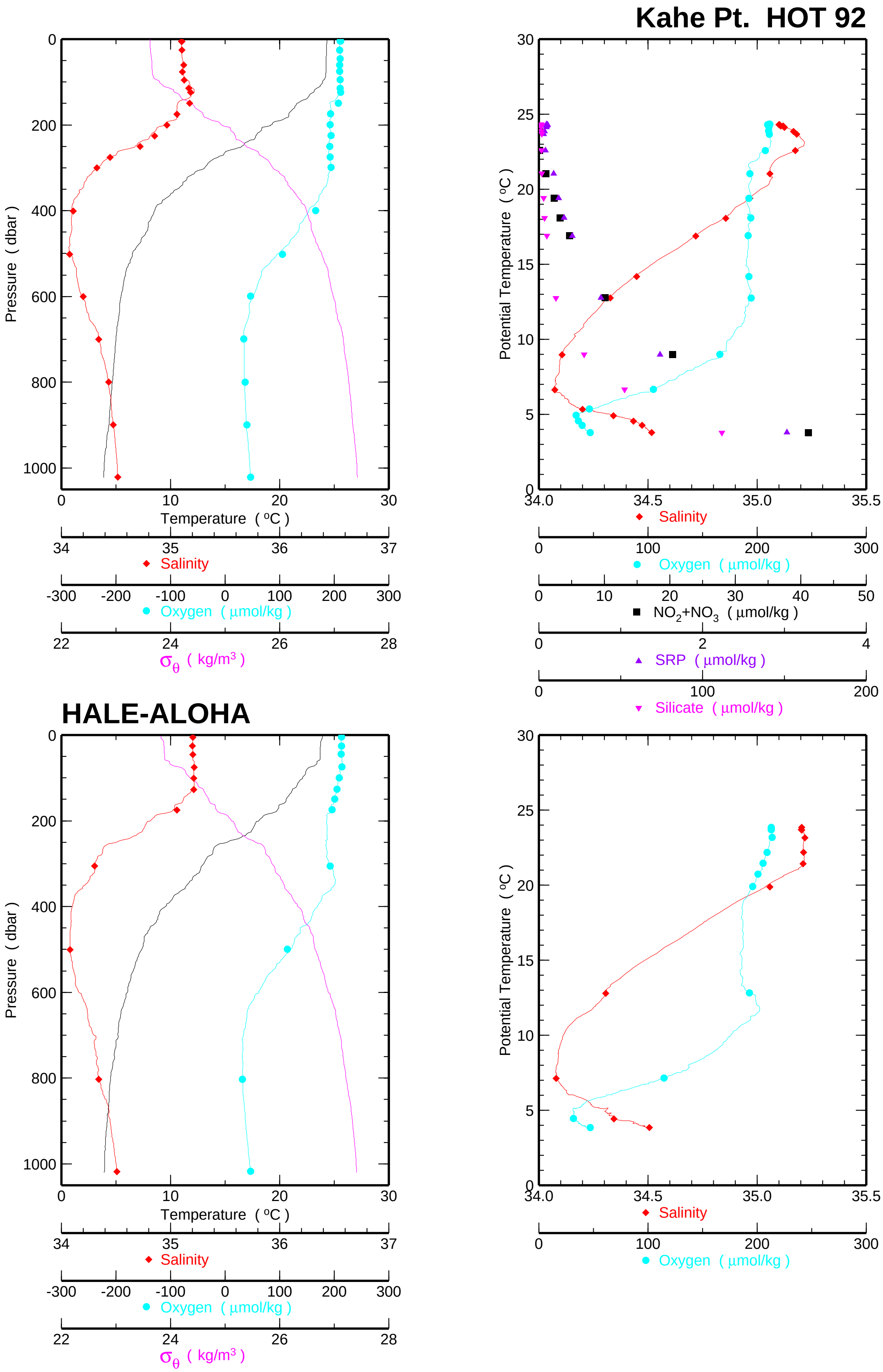
Kahe Pt. HOT 92
HALE-ALOHA
Pressure (dbar)
Temperature (°C)
Salinity
Oxygen (µmol/kg)
σθ (kg/m³)
Potential Temperature (°C)
NO2+NO3 (µmol/kg)
SRP (µmol/kg)
Silicate (µmol/kg)

FIGURE 6.1.3d.

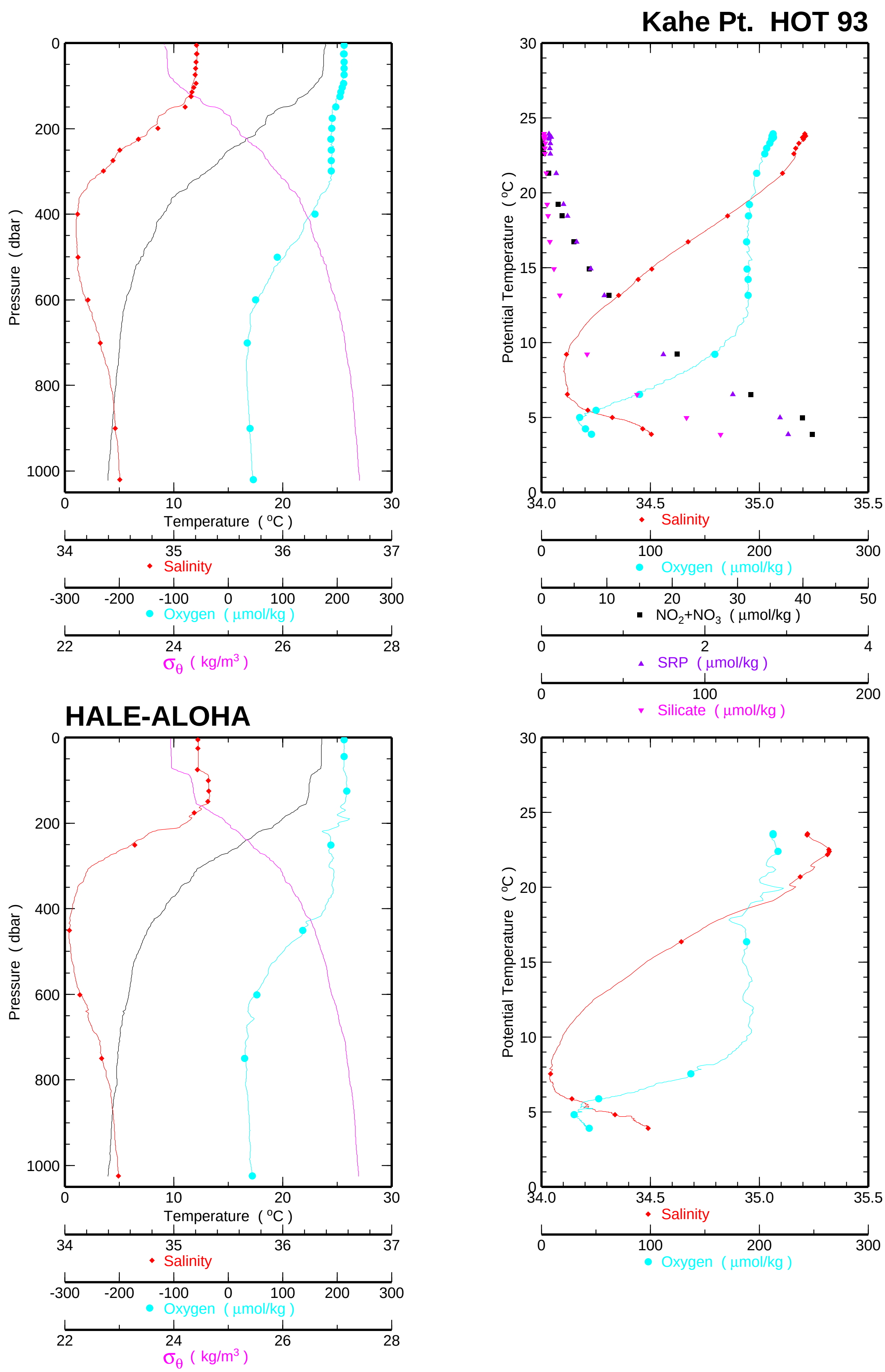
Kahe Pt. HOT 93
HALE-ALOHA
Pressure (dbar)
Temperature (°C)
Salinity
Oxygen (µmol/kg)
σθ (kg/m³)
Potential Temperature (°C)
NO2+NO3 (µmol/kg)
SRP (µmol/kg)
Silicate (µmol/kg)

FIGURE 6.1.3e.

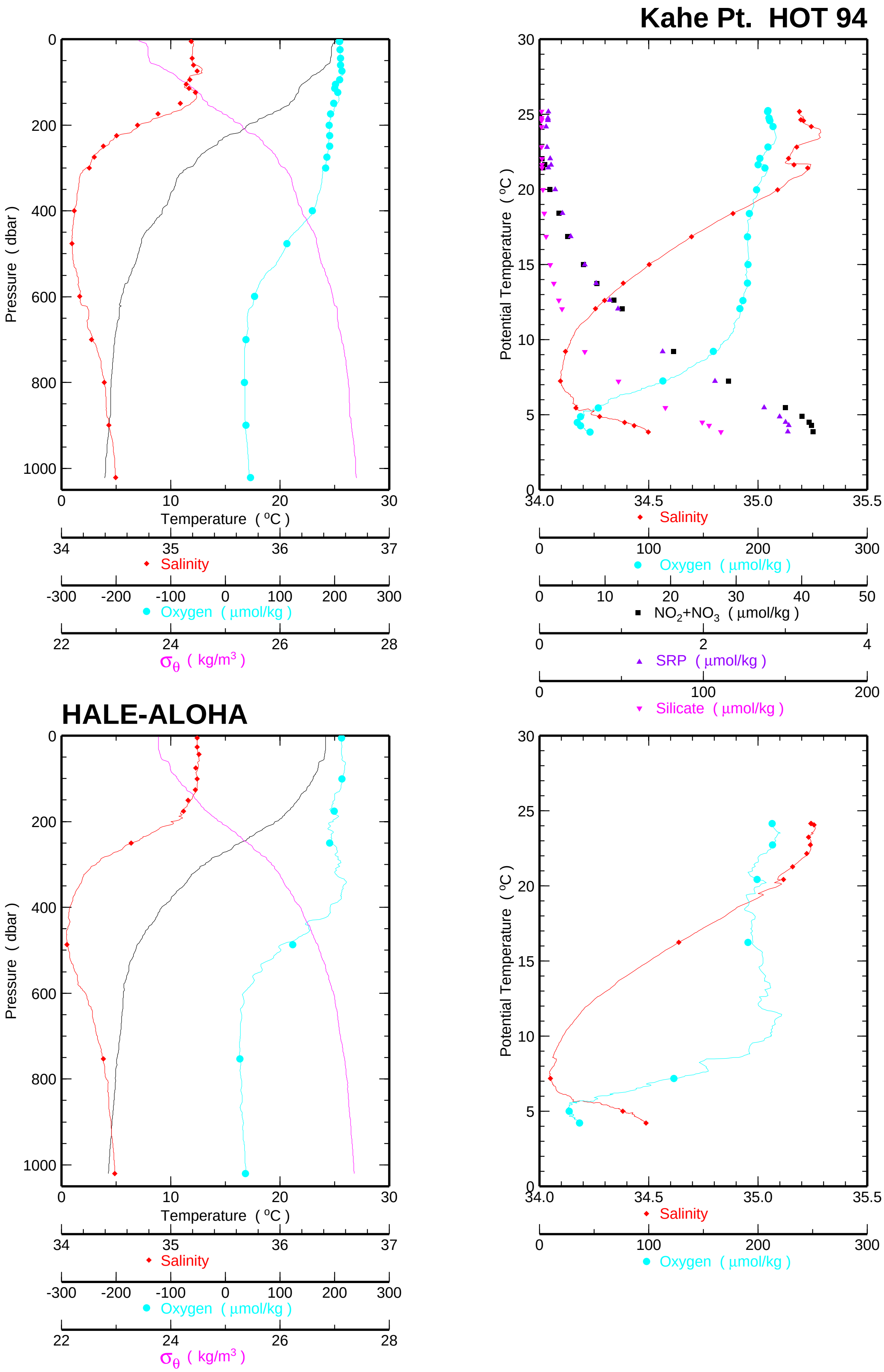
Kahe Pt. HOT 94
HALE-ALOHA
Pressure (dbar)
0
200
400
600
800
1000
Temperature (°C)
0
10
20
30
Salinity
34
35
36
37
Oxygen (µmol/kg)
-300
-200
-100
0
100
200
300
σθ (kg/m3)
22
24
26
28
Potential Temperature (°C)
0
5
10
15
20
25
30
34.0
34.5
35.0
35.5
NO2+NO3 (µmol/kg)
0
10
20
30
40
50
SRP (µmol/kg)
0
2
4
Silicate (µmol/kg)
0
100
200

FIGURE 6.1.3f.

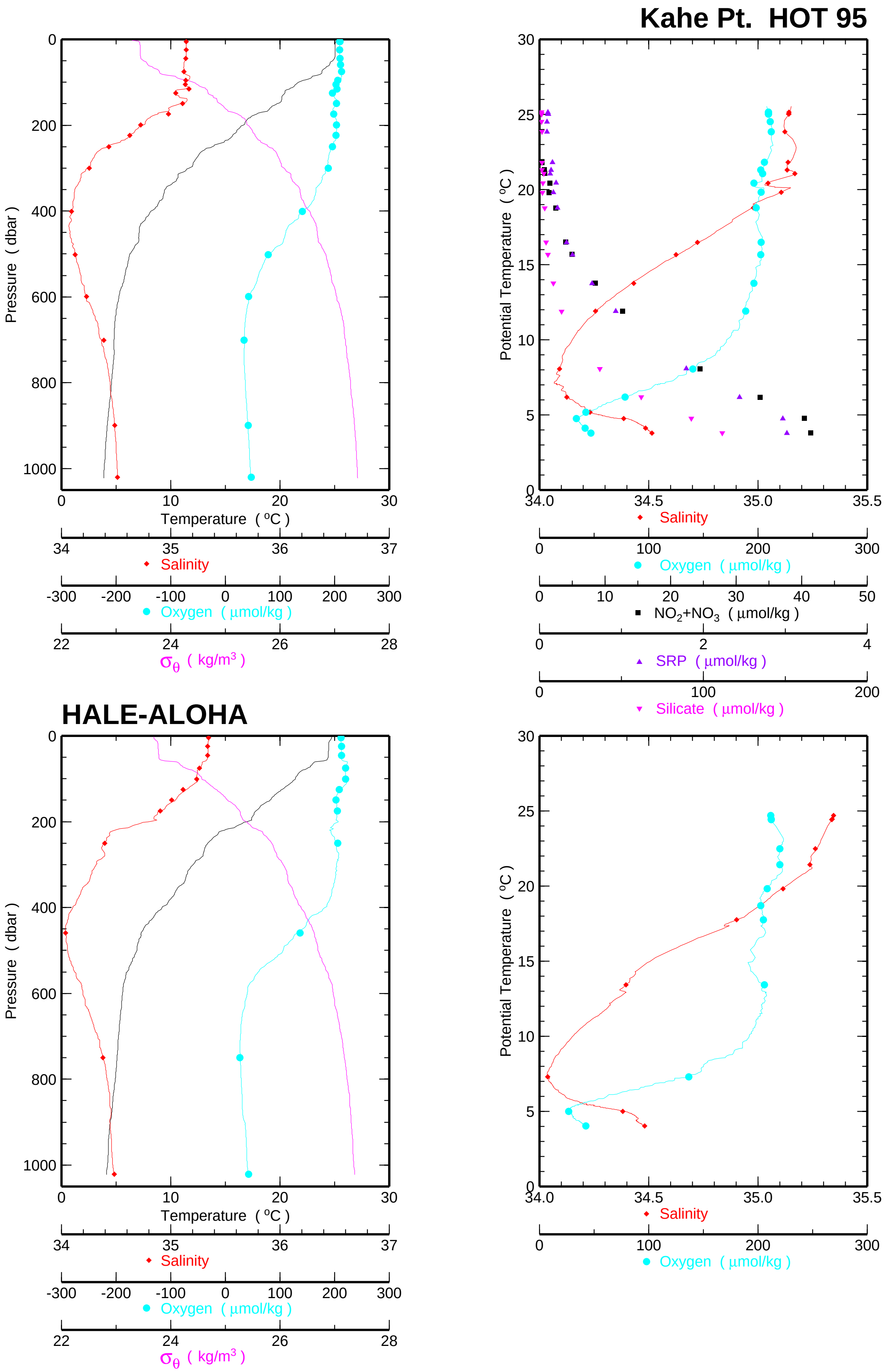
Kahe Pt. HOT 95
HALE-ALOHA
Pressure (dbar)
Temperature (°C)
Salinity
Oxygen (µmol/kg)
σθ (kg/m3)
Potential Temperature (°C)
NO2+NO3 (µmol/kg)
SRP (µmol/kg)
Silicate (µmol/kg)

FIGURE 6.1.3g.

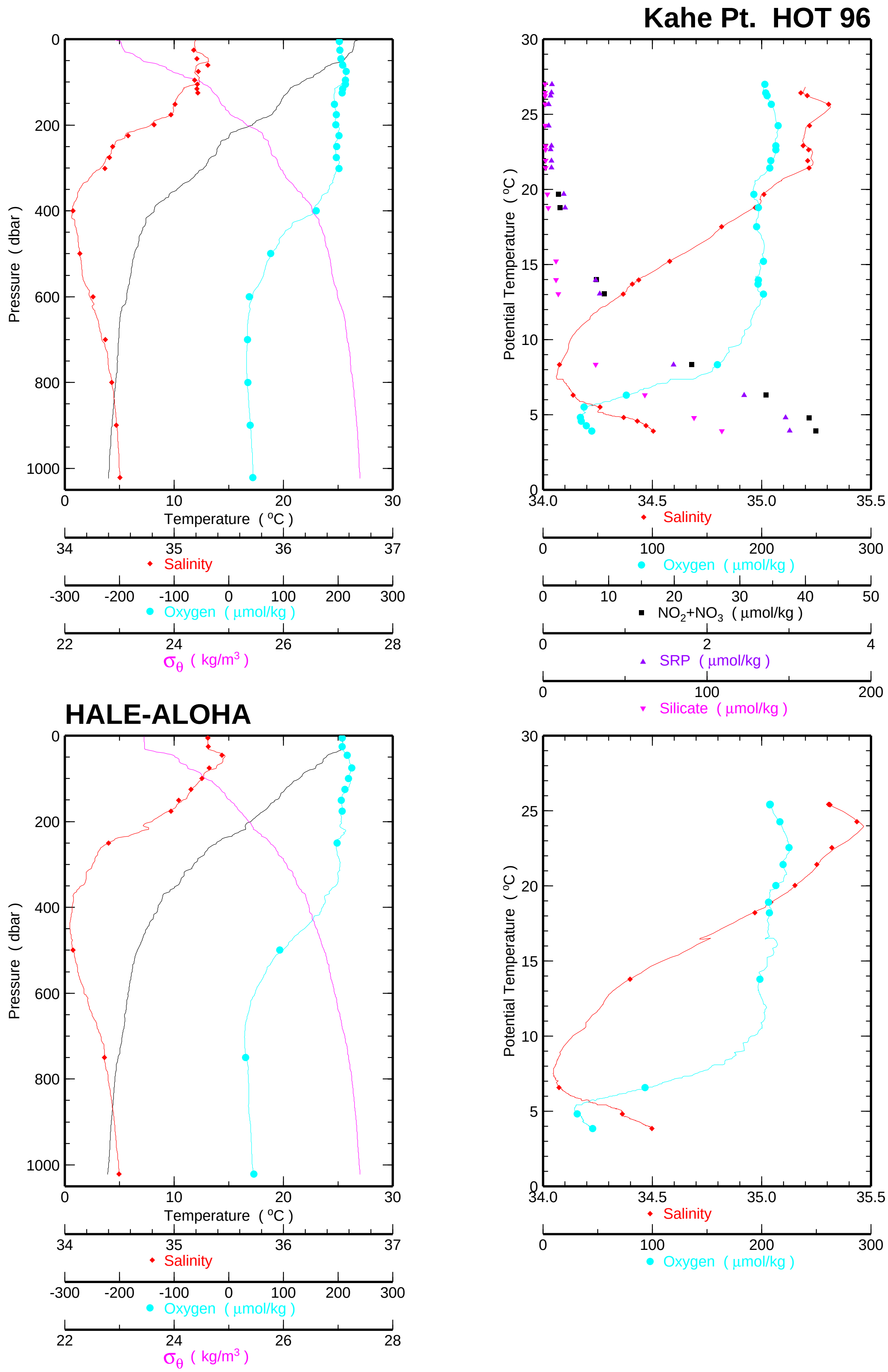
Kahe Pt. HOT 96
HALE-ALOHA
Pressure (dbar)
Temperature (°C)
Salinity
Oxygen (µmol/kg)
σθ (kg/m³)
Potential Temperature (°C)
NO2+NO3 (µmol/kg)
SRP (µmol/kg)
Silicate (µmol/kg)

FIGURE 6.1.3h.

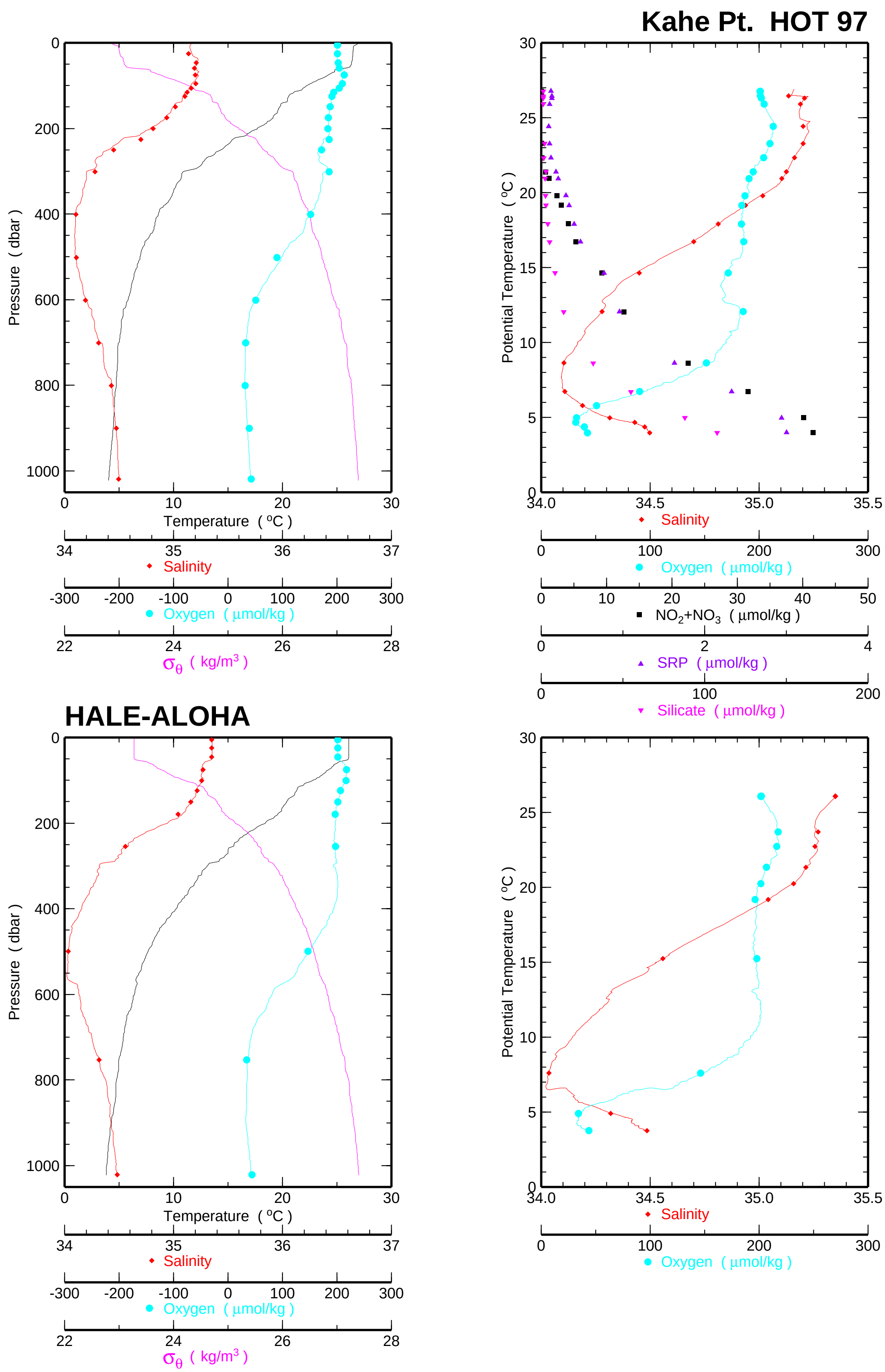

Kahe Pt. HOT 97
Pressure (dbar)
Temperature (°C)
Salinity
Oxygen (µmol/kg)
σθ (kg/m3)
Potential Temperature (°C)
NO2+NO3 (µmol/kg)
SRP (µmol/kg)
Silicate (µmol/kg)
HALE-ALOHA

FIGURE 6.1.3i.

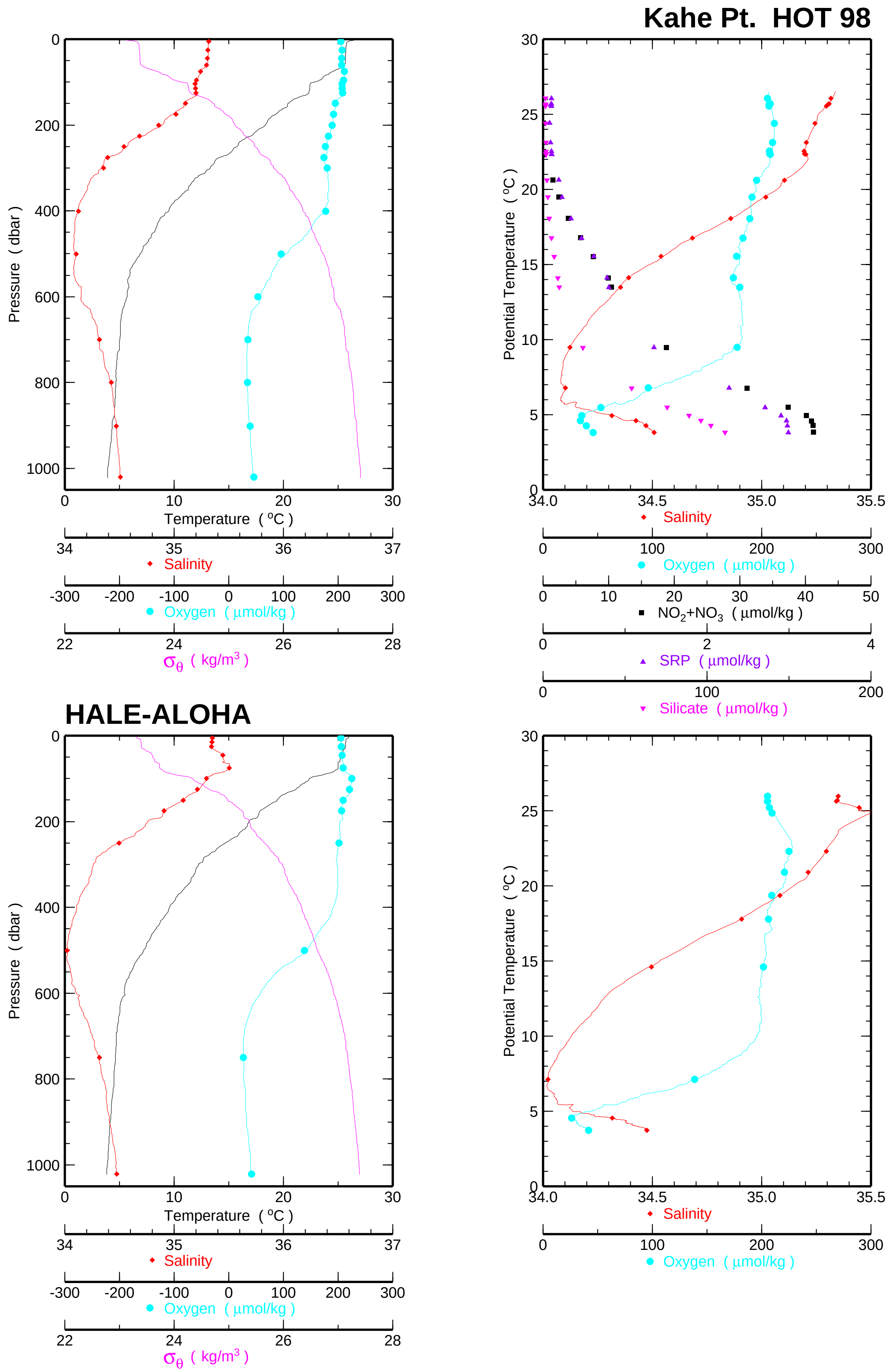
Kahe Pt. HOT 98
HALE-ALOHA
Pressure (dbar)
Temperature (°C)
Salinity
Oxygen (µmol/kg)
σθ (kg/m³)
Potential Temperature (°C)
NO2+NO3 (µmol/kg)
SRP (µmol/kg)
Silicate (µmol/kg)

FIGURE 6.1.3j.

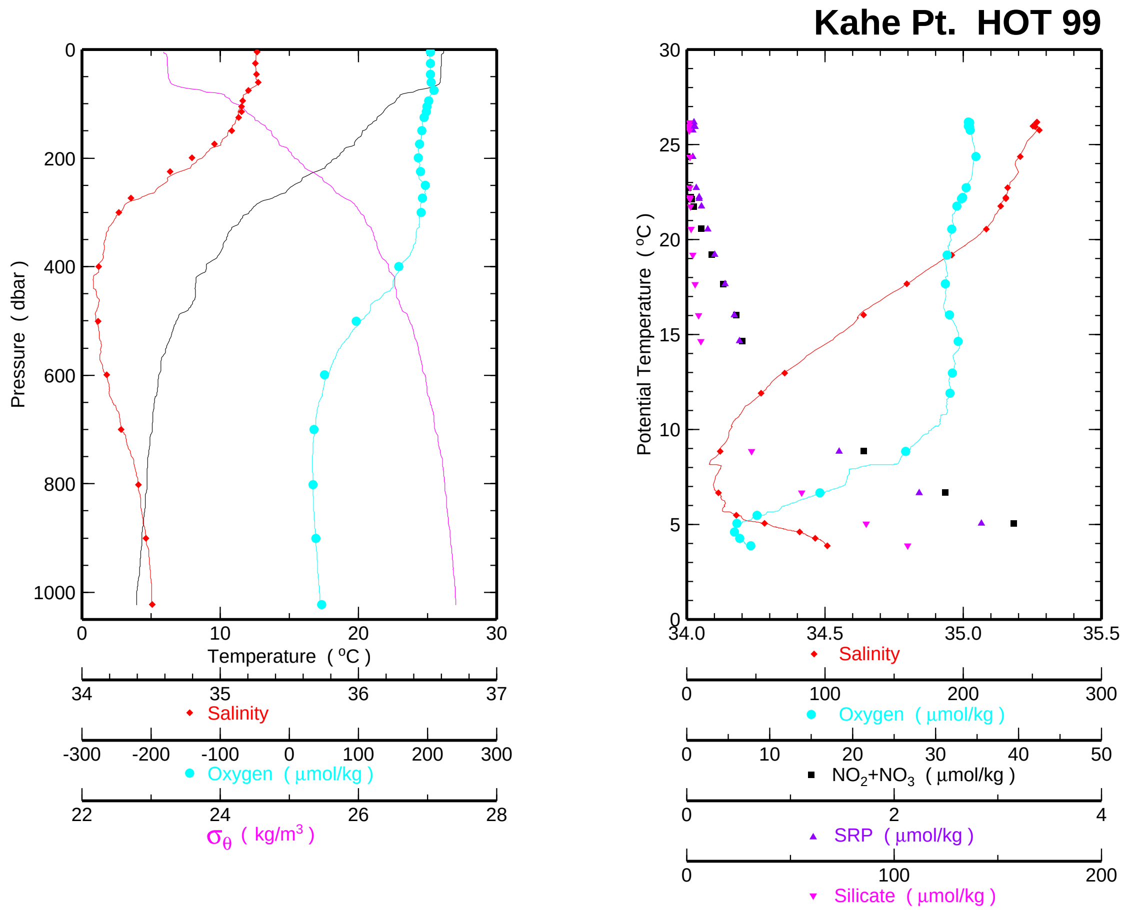

Kahe Pt. HOT 99
Pressure (dbar)
Temperature (°C)
Salinity
Oxygen (µmol/kg)
σθ (kg/m3)
Potential Temperature (°C)
Salinity
Oxygen (µmol/kg)
NO2+NO3 (µmol/kg)
SRP (µmol/kg)
Silicate (µmol/kg)

FIGURE 6.1.3k.

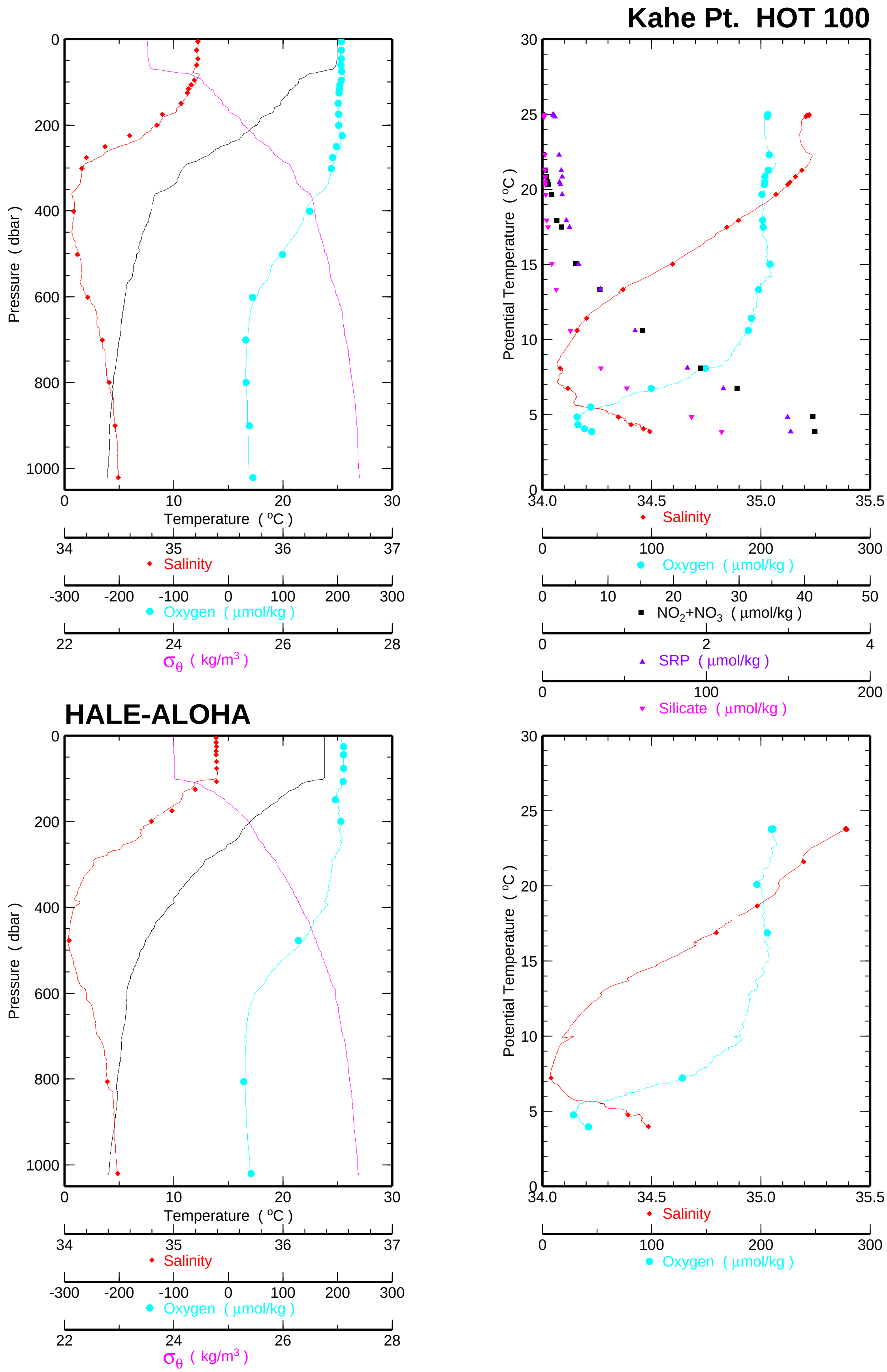
Kahe Pt. HOT 100
HALE-ALOHA
Pressure (dbar)
Temperature (°C)
Salinity
Oxygen (µmol/kg)
σθ (kg/m³)
Potential Temperature (°C)
NO2+NO3 (µmol/kg)
SRP (µmol/kg)
Silicate (µmol/kg)

FIGURE 6.1.3l.

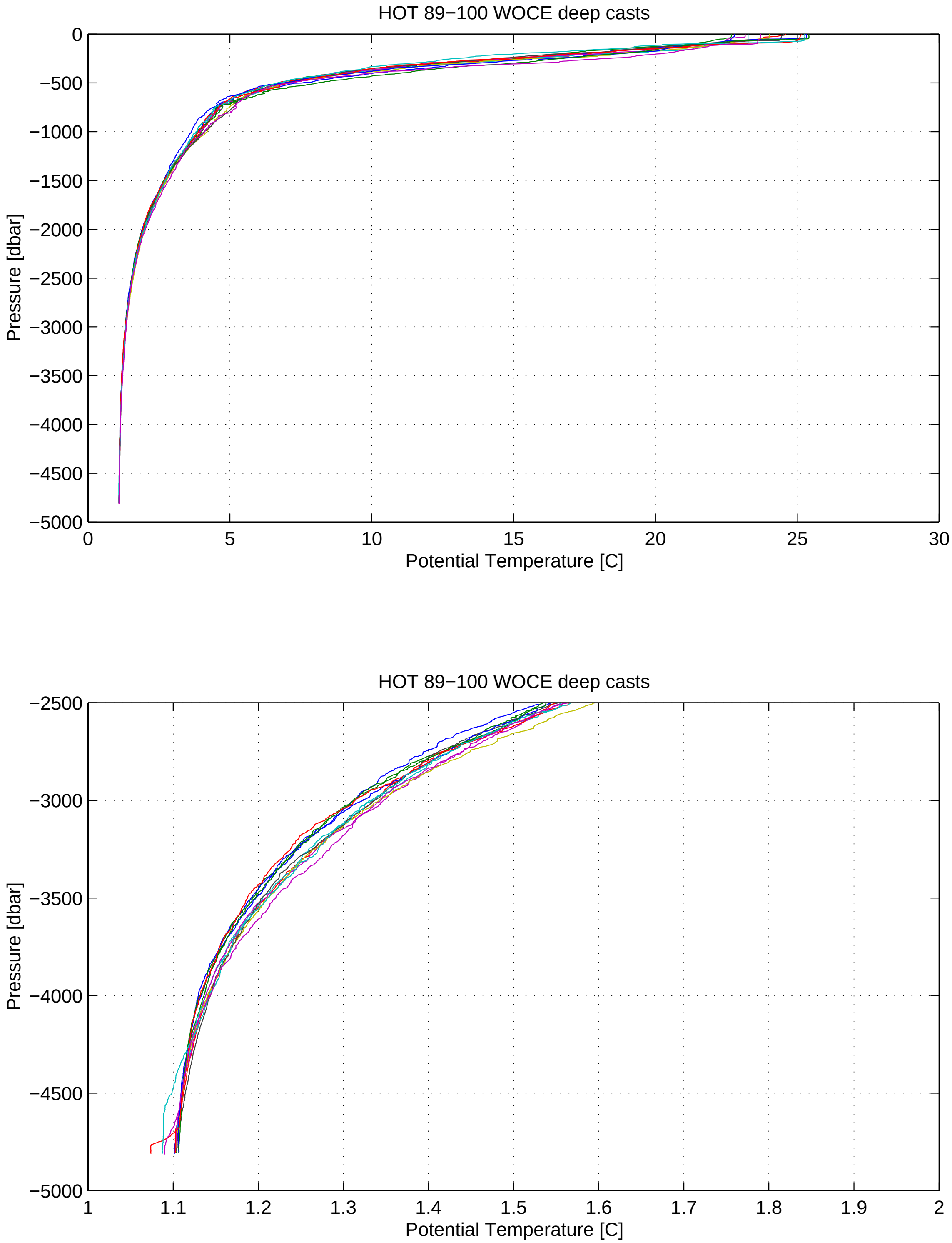
HOT 89−100 WOCE deep casts
Pressure [dbar]
Potential Temperature [C]
0
−500
−1000
−1500
−2000
−2500
−3000
−3500
−4000
−4500
−5000
0
5
10
15
20
25
30
HOT 89−100 WOCE deep casts
Pressure [dbar]
Potential Temperature [C]
−2500
−3000
−3500
−4000
−4500
−5000
1
1.1
1.2
1.3
1.4
1.5
1.6
1.7
1.8
1.9
2

FIGURE 6.1.4.

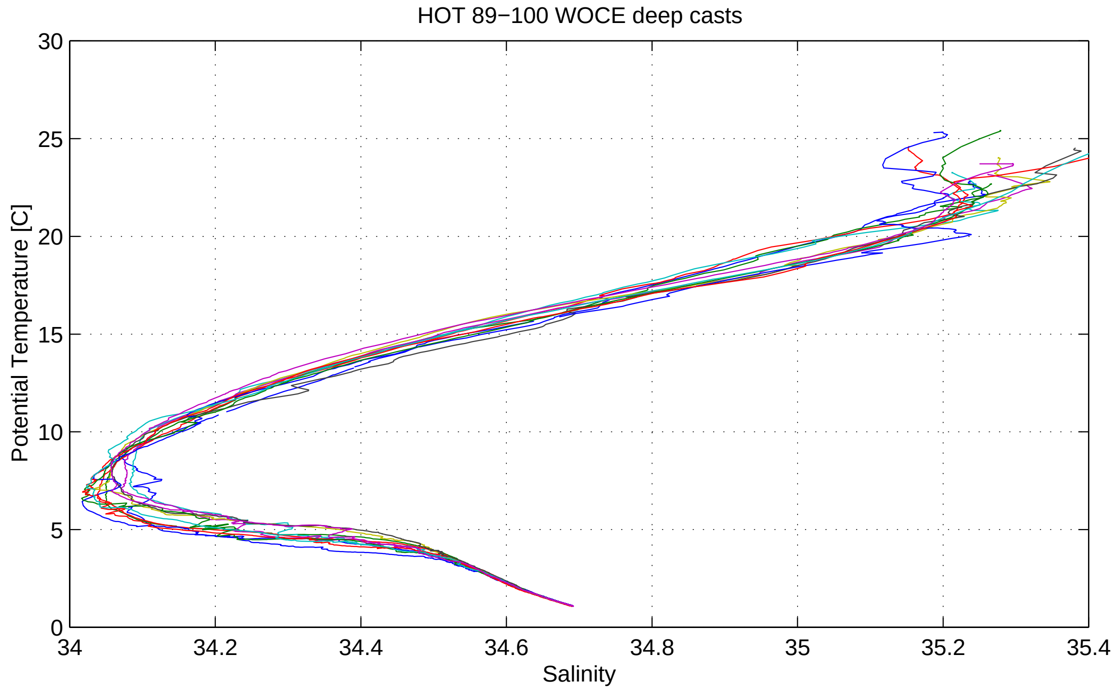
HOT 89−100 WOCE deep casts
Potential Temperature [C]
Salinity
30
25
20
15
10
5
0
34
34.2
34.4
34.6
34.8
35
35.2
35.4

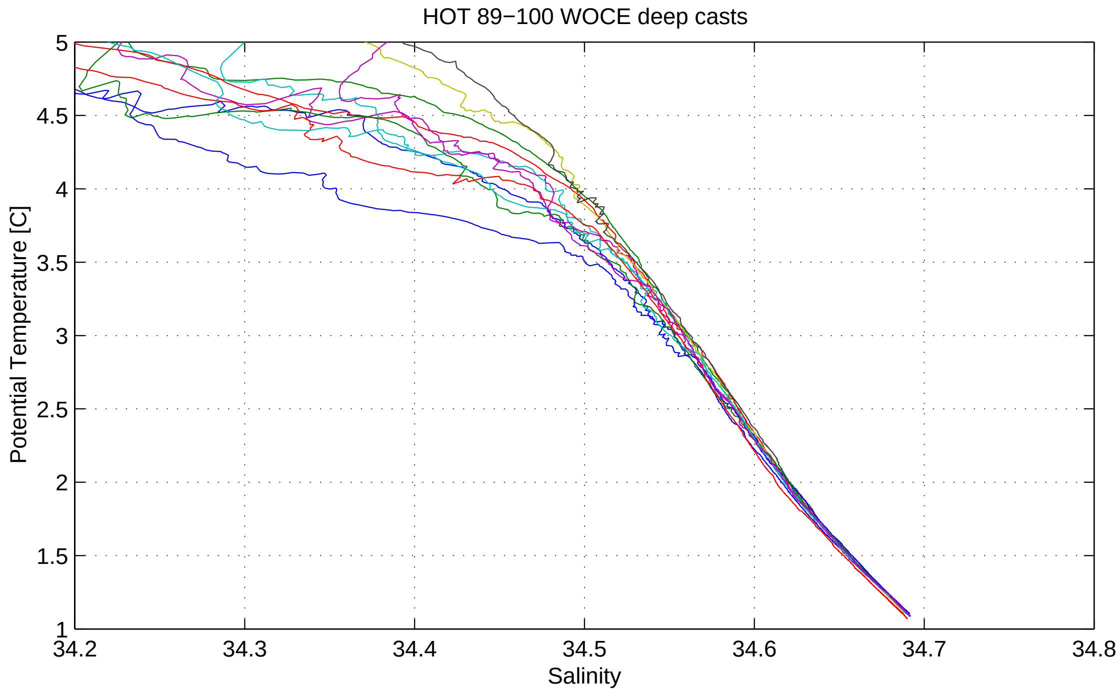
HOT 89−100 WOCE deep casts
Potential Temperature [C]
Salinity
5
4.5
4
3.5
3
2.5
2
1.5
1
34.2
34.3
34.4
34.5
34.6
34.7
34.8

FIGURE 6.1.5.

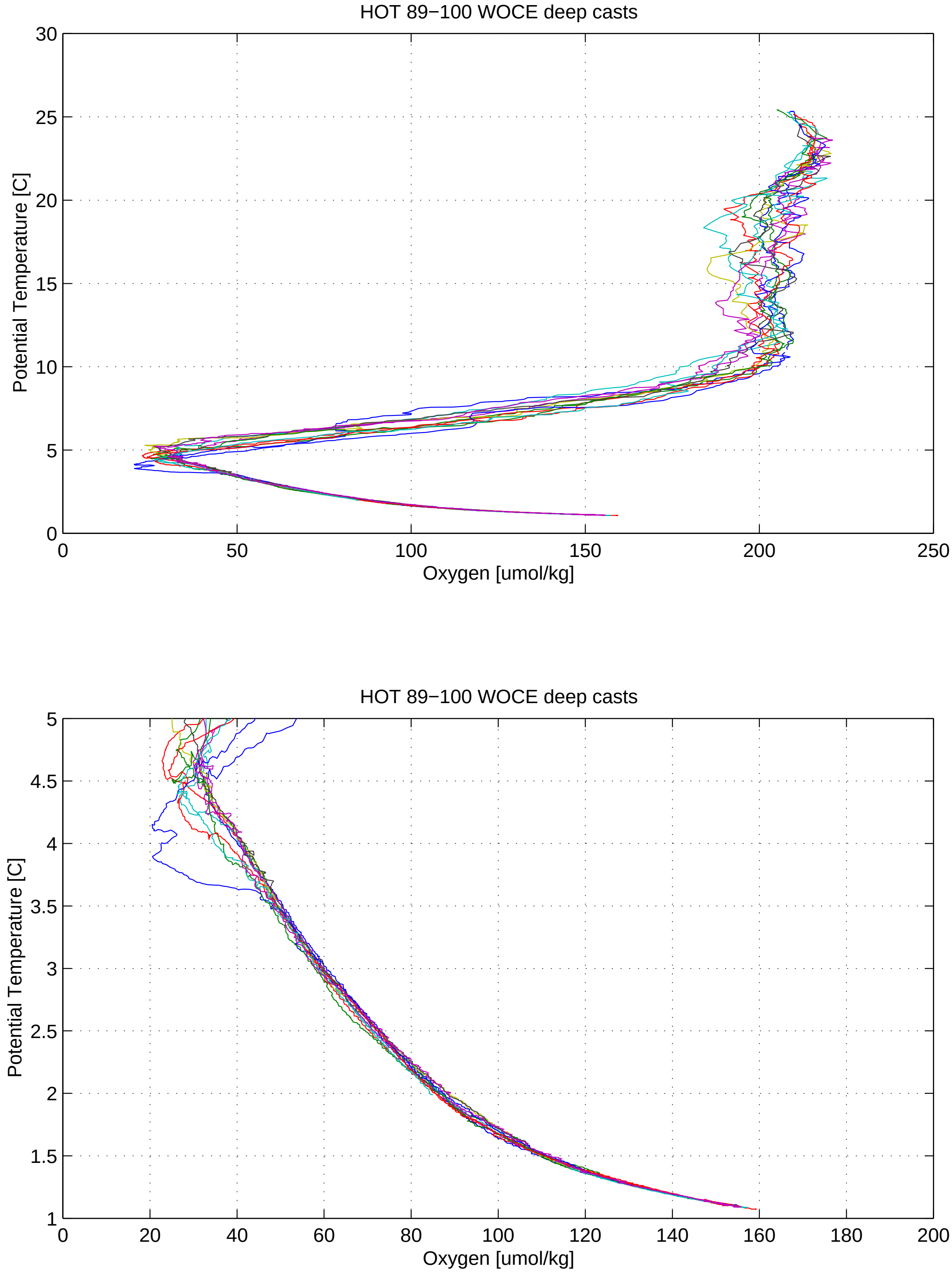

HOT 89−100 WOCE deep casts
Potential Temperature [C]
Oxygen [umol/kg]
30
25
20
15
10
5
0
0
50
100
150
200
250
HOT 89−100 WOCE deep casts
Potential Temperature [C]
Oxygen [umol/kg]
5
4.5
4
3.5
3
2.5
2
1.5
1
0
20
40
60
80
100
120
140
160
180
200

FIGURE 6.1.6.

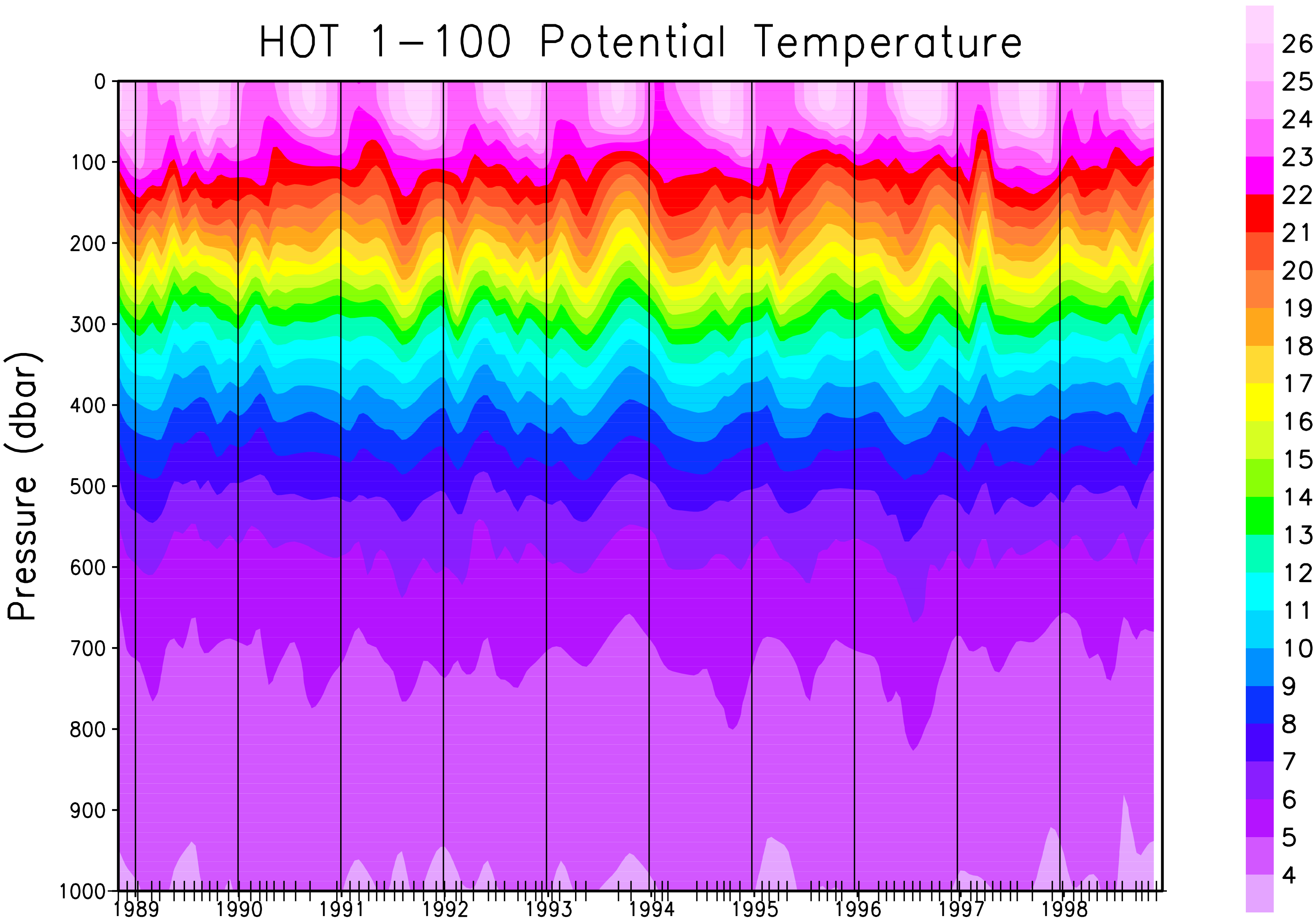
HOT 1-100 Potential Temperature
Pressure (dbar)
0
100
200
300
400
500
600
700
800
900
1000
1989
1990
1991
1992
1993
1994
1995
1996
1997
1998
26
25
24
23
22
21
20
19
18
17
16
15
14
13
12
11
10
9
8
7
6
5
4

FIGURE 6.1.7.

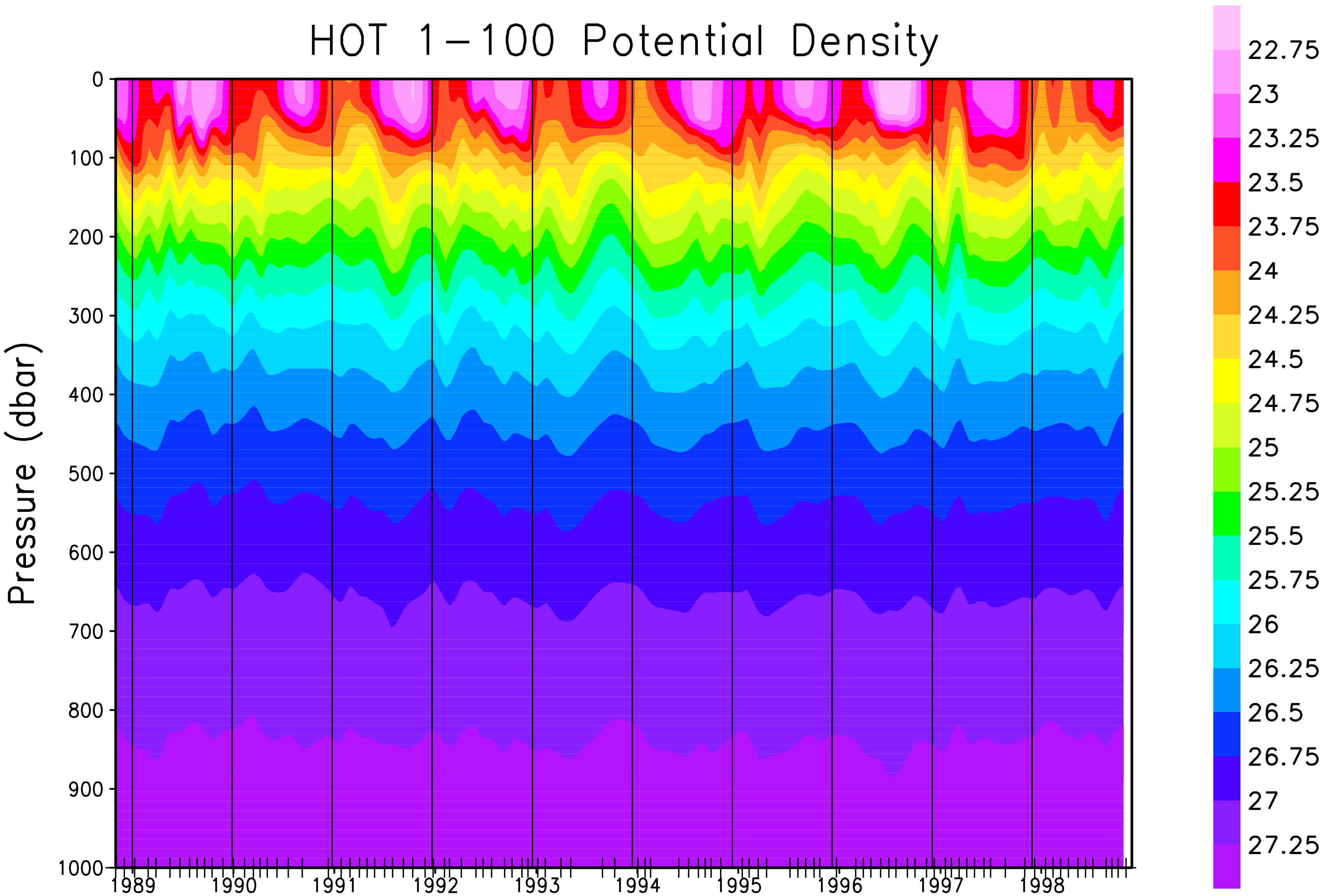
HOT 1-100 Potential Density
Pressure (dbar)
0
100
200
300
400
500
600
700
800
900
1000
1989
1990
1991
1992
1993
1994
1995
1996
1997
1998
22.75
23
23.25
23.5
23.75
24
24.25
24.5
24.75
25
25.25
25.5
25.75
26
26.25
26.5
26.75
27
27.25

FIGURE 6.1.8.

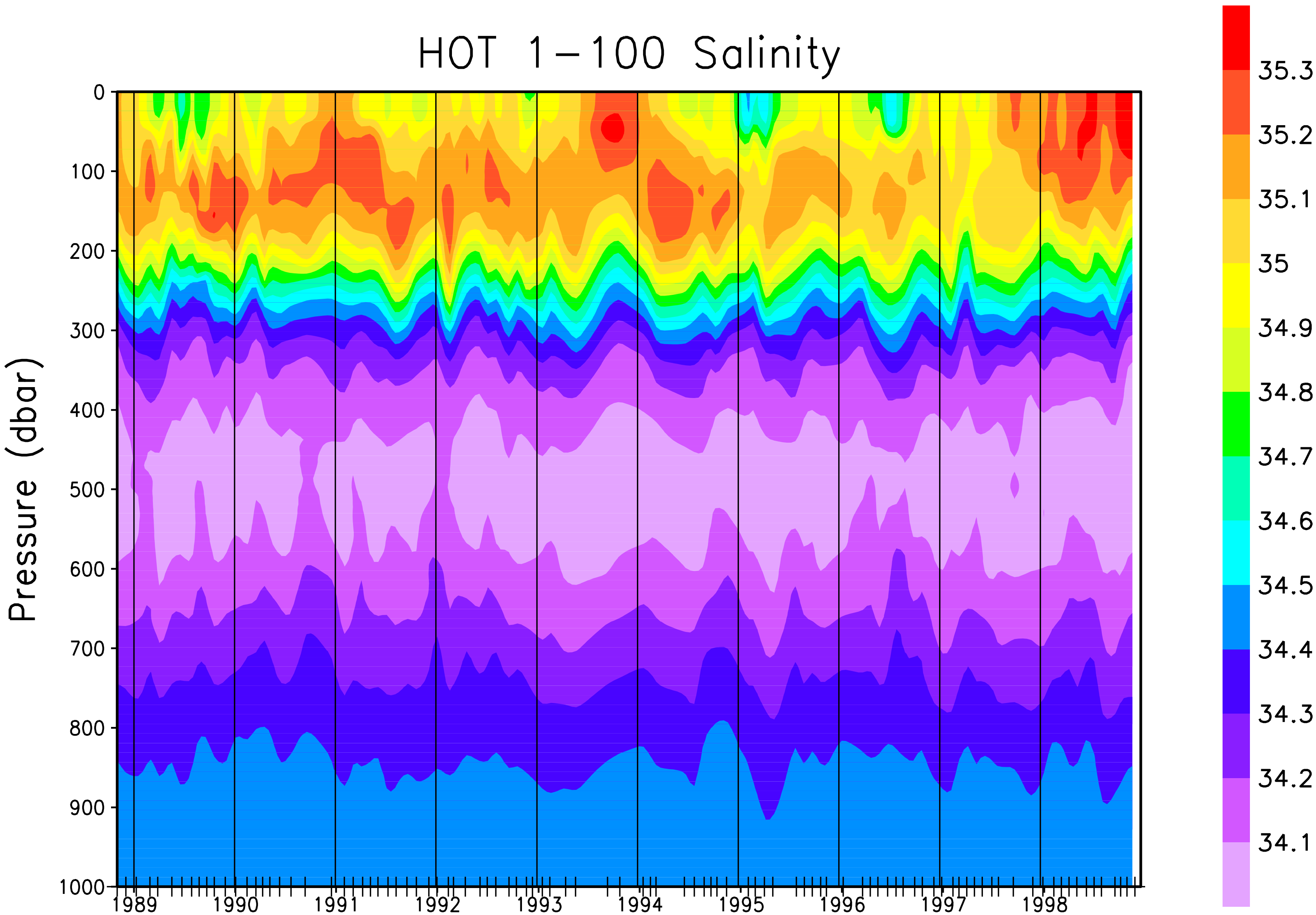
HOT 1-100 Salinity
Pressure (dbar)
0
100
200
300
400
500
600
700
800
900
1000
1989
1990
1991
1992
1993
1994
1995
1996
1997
1998
35.3
35.2
35.1
35
34.9
34.8
34.7
34.6
34.5
34.4
34.3
34.2
34.1

FIGURE 6.1.9.

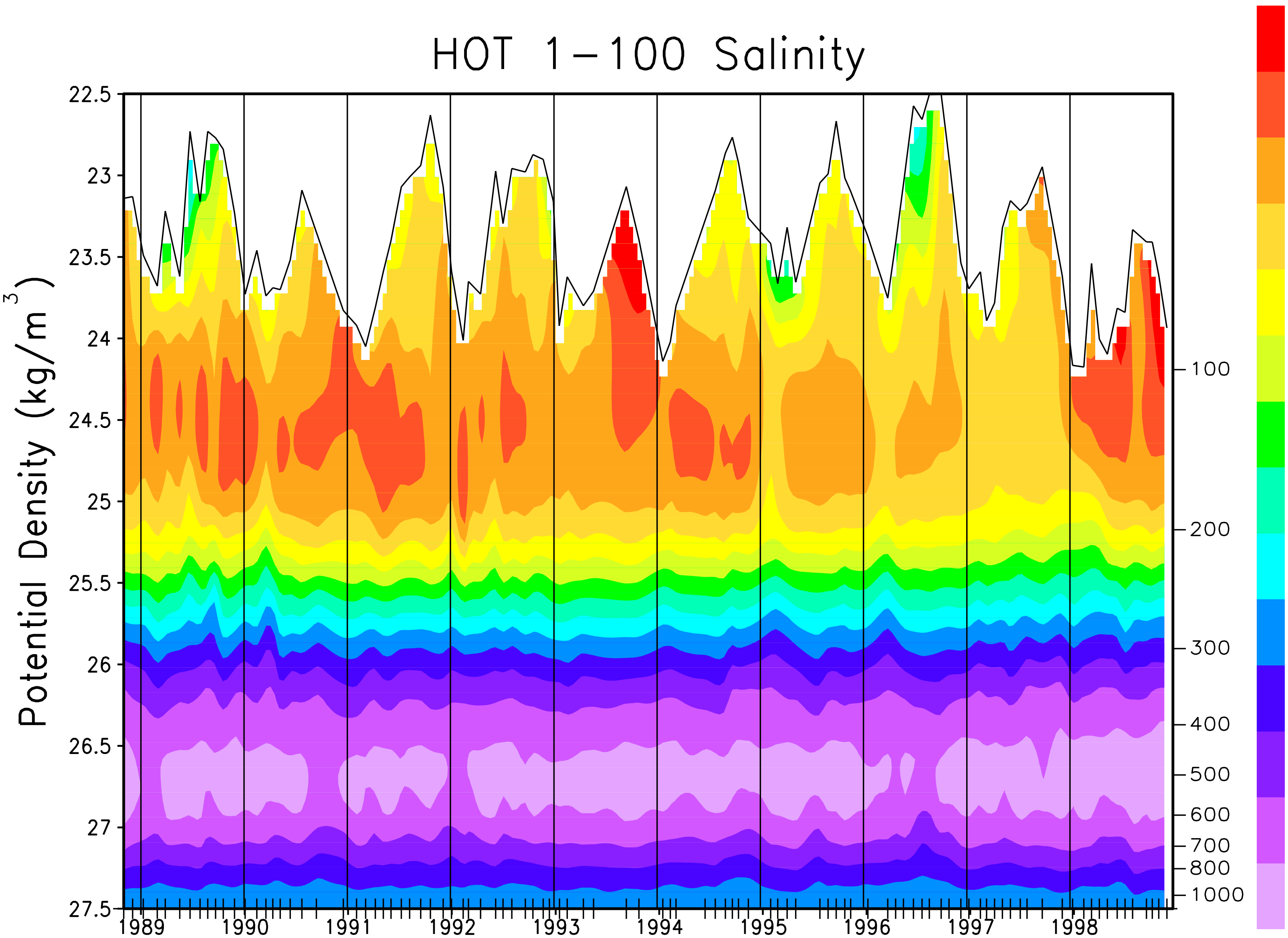
HOT 1-100 Salinity
Potential Density (kg/m^3)
22.5
23
23.5
24
24.5
25
25.5
26
26.5
27
27.5
100
200
300
400
500
600
700
800
1000
1989
1990
1991
1992
1993
1994
1995
1996
1997
1998
35.3
35.2
35.1
35
34.9
34.8
34.7
34.6
34.5
34.4
34.3
34.2
34.1

FIGURE 6.1.10.

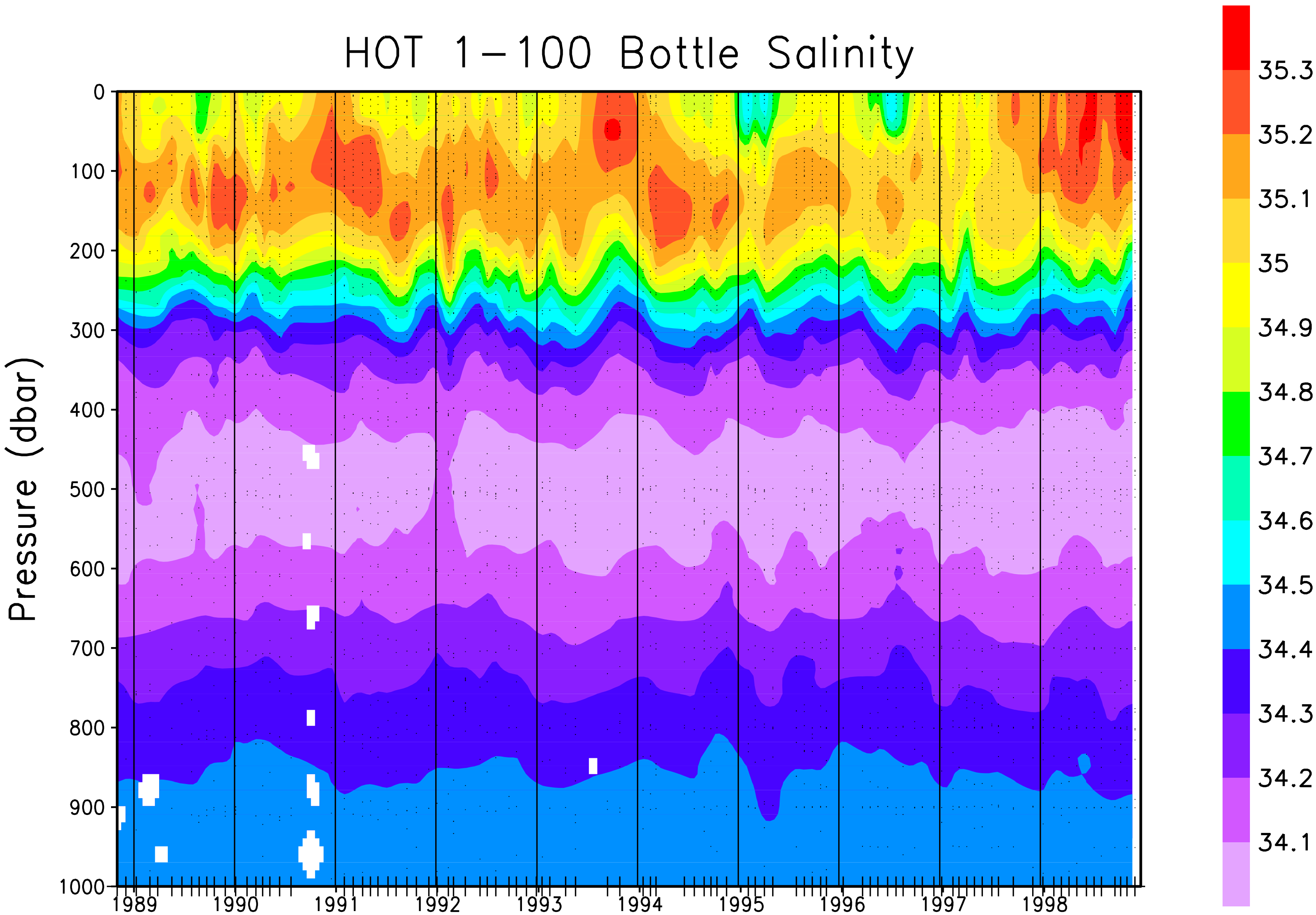
HOT 1-100 Bottle Salinity
Pressure (dbar)
0
100
200
300
400
500
600
700
800
900
1000
1989
1990
1991
1992
1993
1994
1995
1996
1997
1998
35.3
35.2
35.1
35
34.9
34.8
34.7
34.6
34.5
34.4
34.3
34.2
34.1

FIGURE 6.1.11.

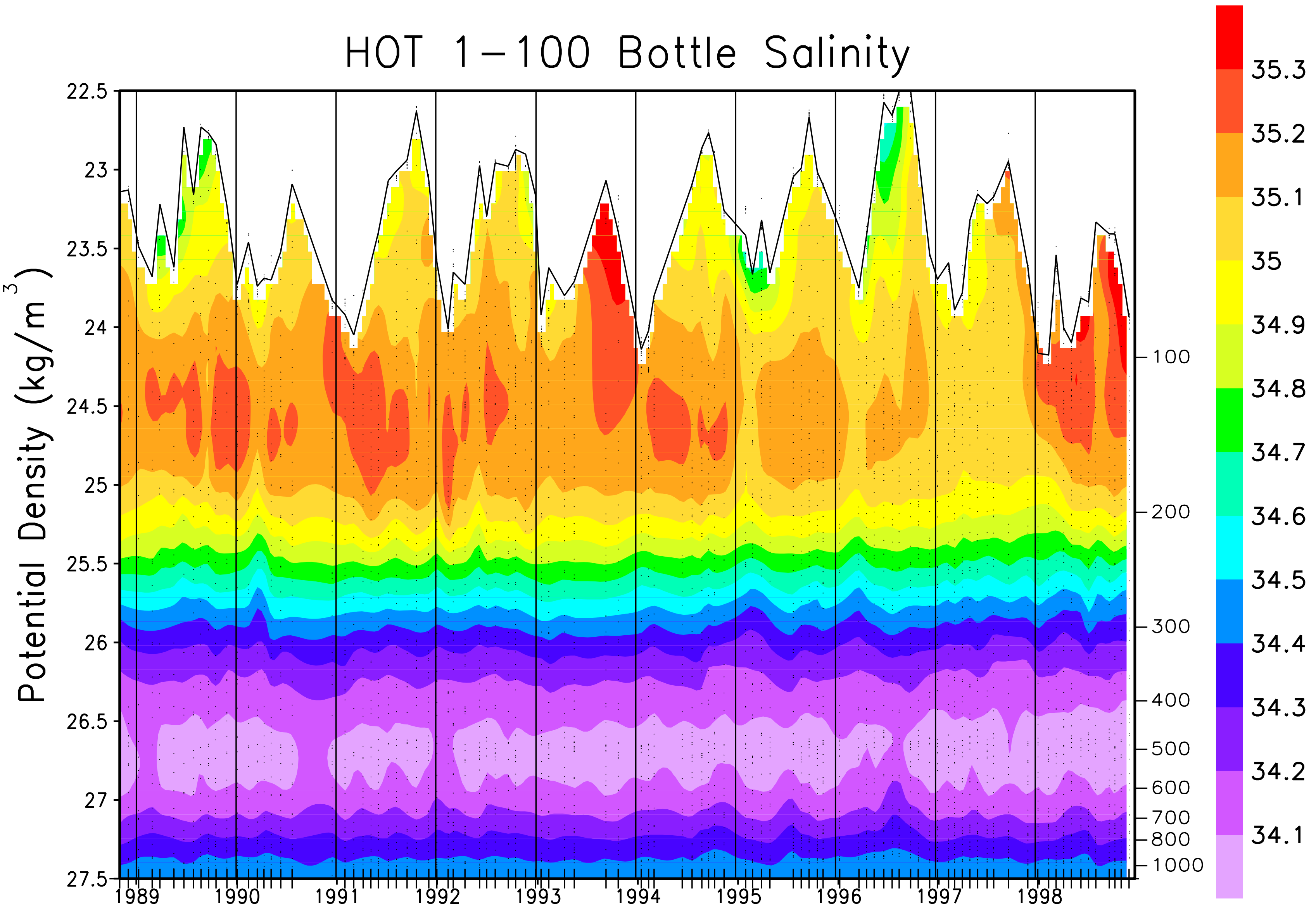
HOT 1-100 Bottle Salinity
Potential Density (kg/m^3)
22.5
23
23.5
24
24.5
25
25.5
26
26.5
27
27.5
1989
1990
1991
1992
1993
1994
1995
1996
1997
1998
100
200
300
400
500
600
700
800
1000
35.3
35.2
35.1
35
34.9
34.8
34.7
34.6
34.5
34.4
34.3
34.2
34.1

FIGURE 6.1.12.

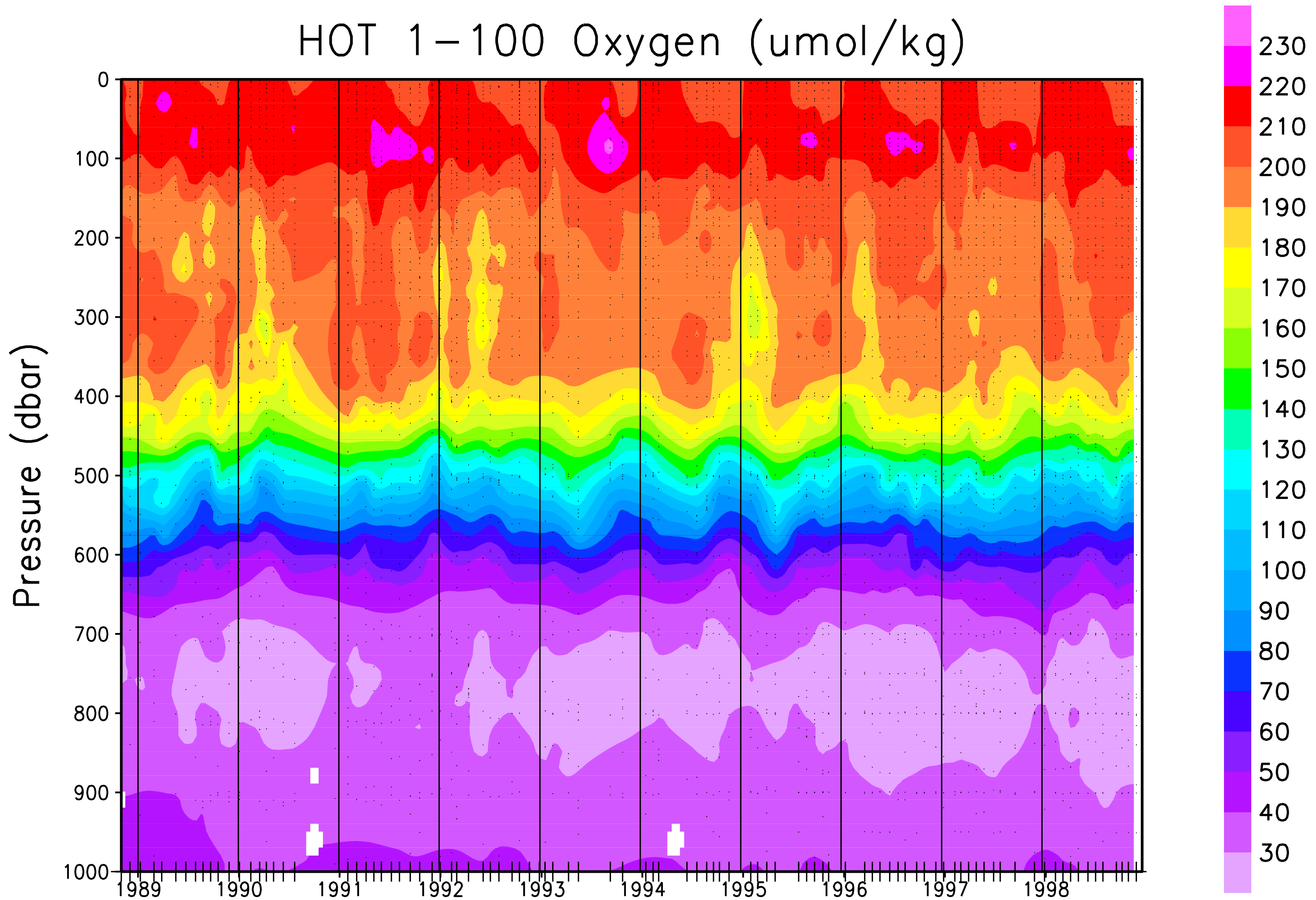
HOT 1-100 Oxygen (umol/kg)
Pressure (dbar)
0
100
200
300
400
500
600
700
800
900
1000
1989
1990
1991
1992
1993
1994
1995
1996
1997
1998
230
220
210
200
190
180
170
160
150
140
130
120
110
100
90
80
70
60
50
40
30

FIGURE 6.1.13.

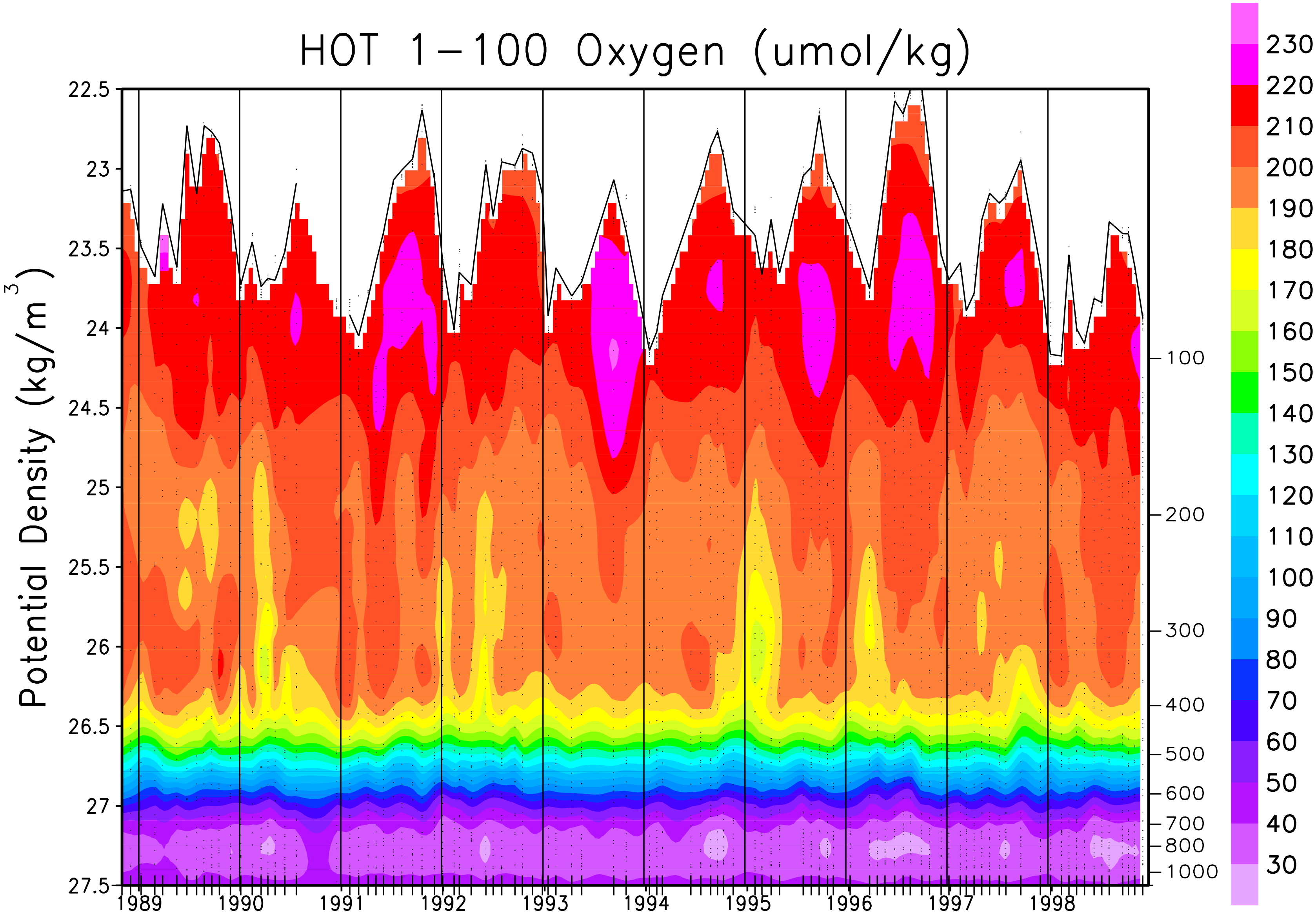
HOT 1-100 Oxygen (umol/kg)
Potential Density (kg/m³)
22.5
23
23.5
24
24.5
25
25.5
26
26.5
27
27.5
1989
1990
1991
1992
1993
1994
1995
1996
1997
1998
100
200
300
400
500
600
700
800
1000
230
220
210
200
190
180
170
160
150
140
130
120
110
100
90
80
70
60
50
40
30

FIGURE 6.1.14.

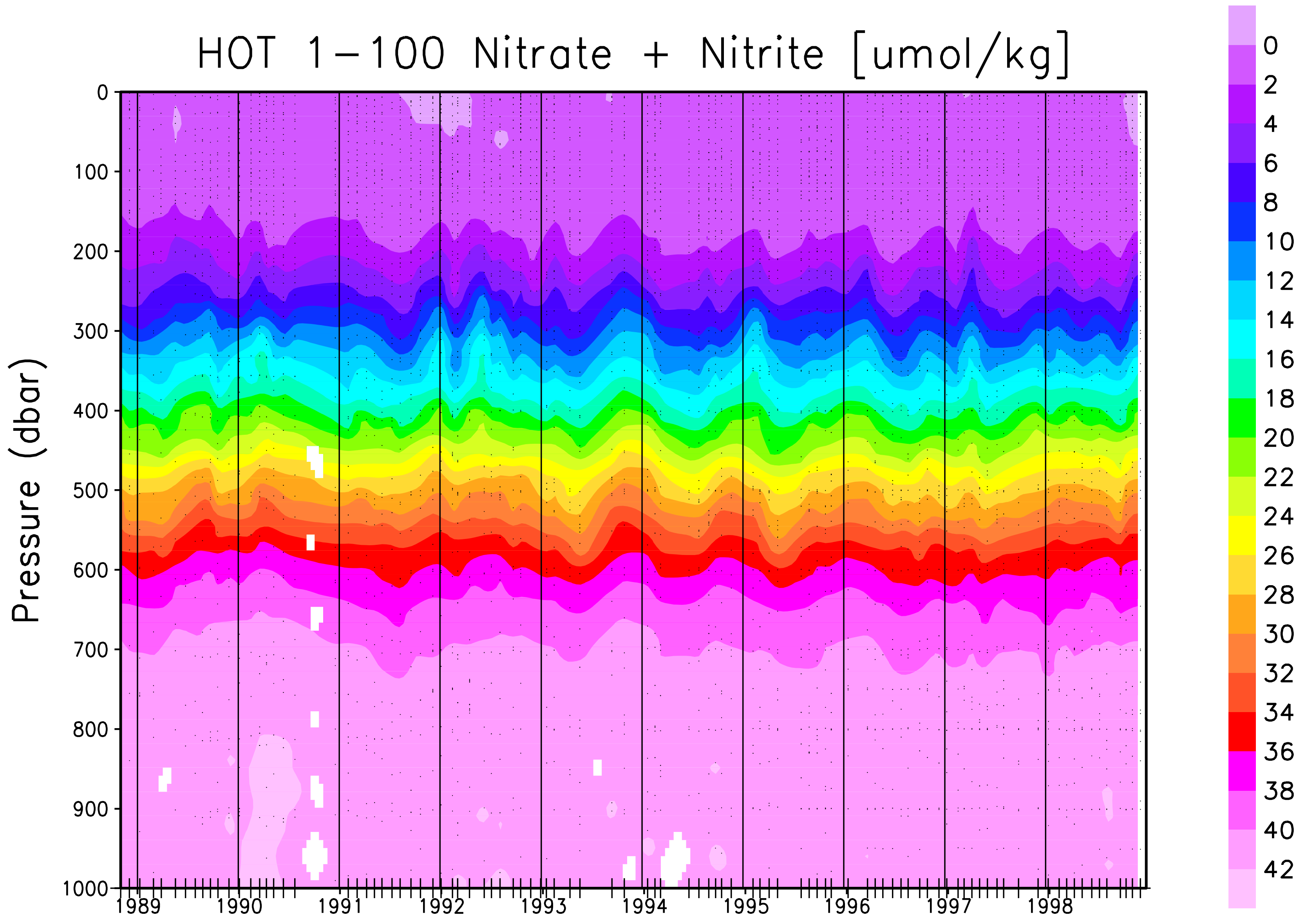
HOT 1-100 Nitrate + Nitrite [umol/kg]
Pressure (dbar)
0
100
200
300
400
500
600
700
800
900
1000
1989
1990
1991
1992
1993
1994
1995
1996
1997
1998
0
2
4
6
8
10
12
14
16
18
20
22
24
26
28
30
32
34
36
38
40
42

FIGURE 6.1.15.

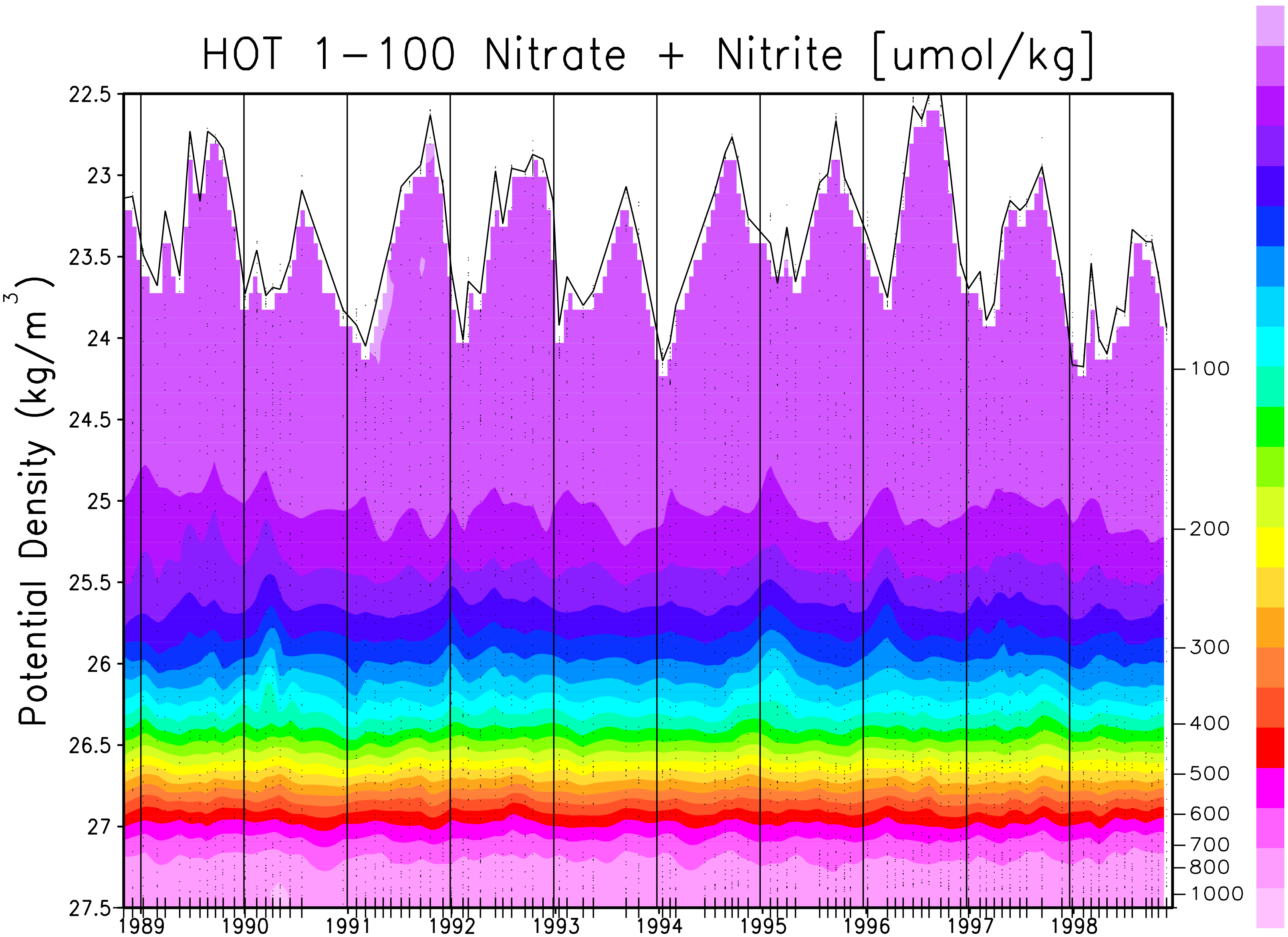
HOT 1-100 Nitrate + Nitrite [umol/kg]
Potential Density (kg/m3)
22.5
23
23.5
24
24.5
25
25.5
26
26.5
27
27.5
100
200
300
400
500
600
700
800
1000
1989
1990
1991
1992
1993
1994
1995
1996
1997
1998
0
2
4
6
8
10
12
14
16
18
20
22
24
26
28
30
32
34
36
38
40
42

FIGURE 6.1.16.

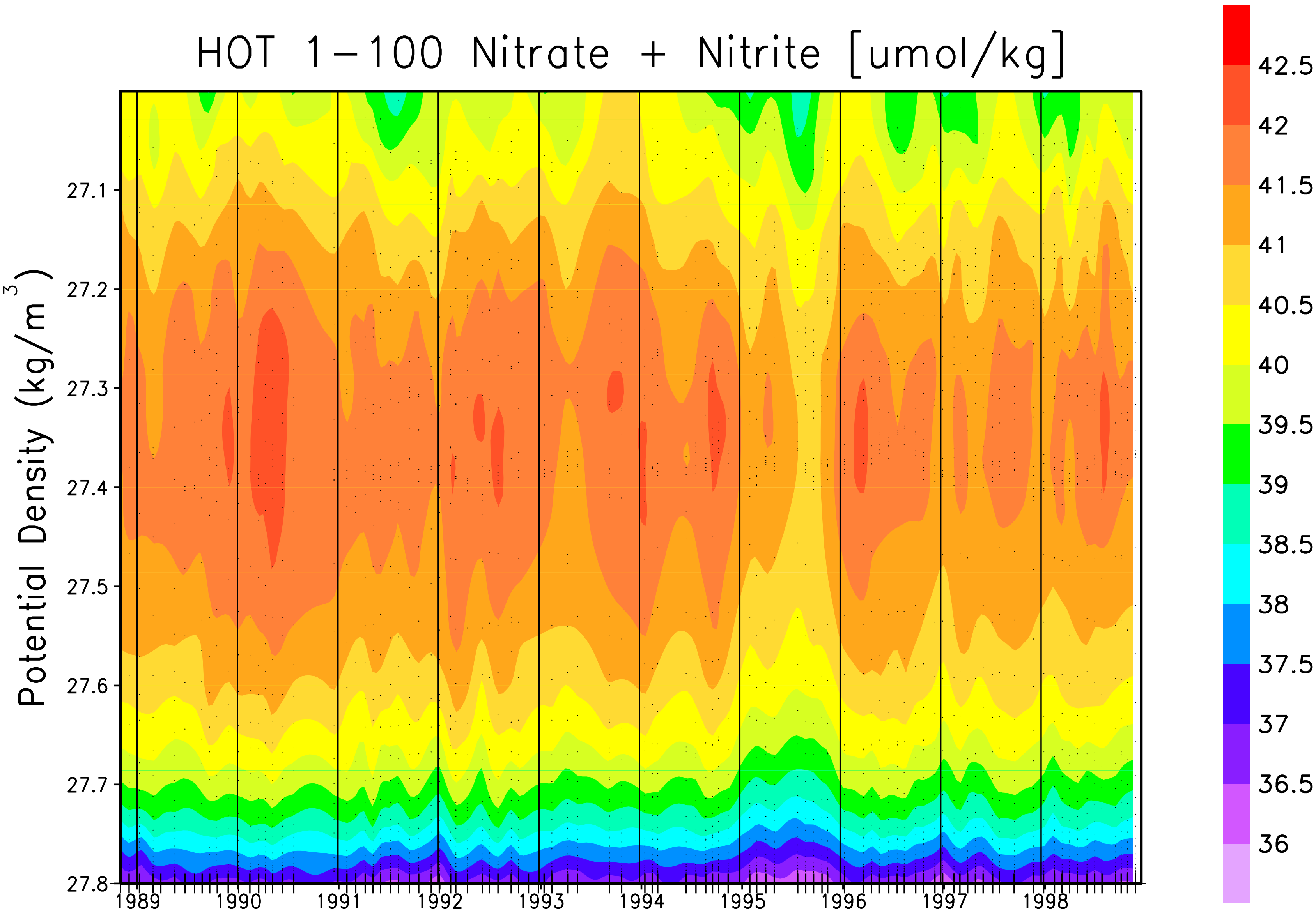
HOT 1-100 Nitrate + Nitrite [umol/kg]
Potential Density (kg/m 3)
27.1
27.2
27.3
27.4
27.5
27.6
27.7
27.8
1989
1990
1991
1992
1993
1994
1995
1996
1997
1998
42.5
42
41.5
41
40.5
40
39.5
39
38.5
38
37.5
37
36.5
36

FIGURE 6.1.17.

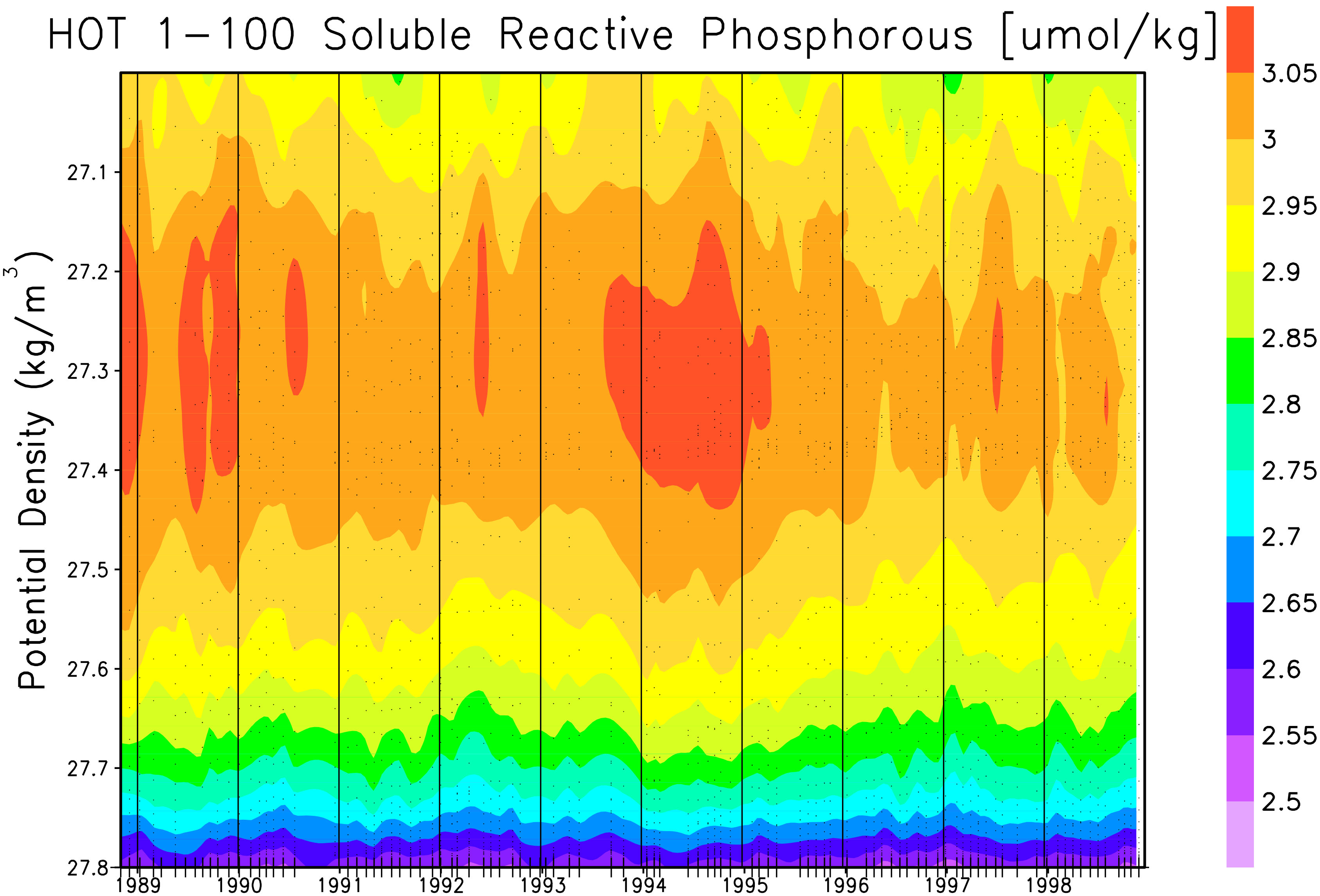

HOT 1-100 Soluble Reactive Phosphorous [umol/kg]
Potential Density (kg/m^3)
27.1
27.2
27.3
27.4
27.5
27.6
27.7
27.8
1989
1990
1991
1992
1993
1994
1995
1996
1997
1998
3.05
3
2.95
2.9
2.85
2.8
2.75
2.7
2.65
2.6
2.55
2.5

FIGURE 6.1.18.

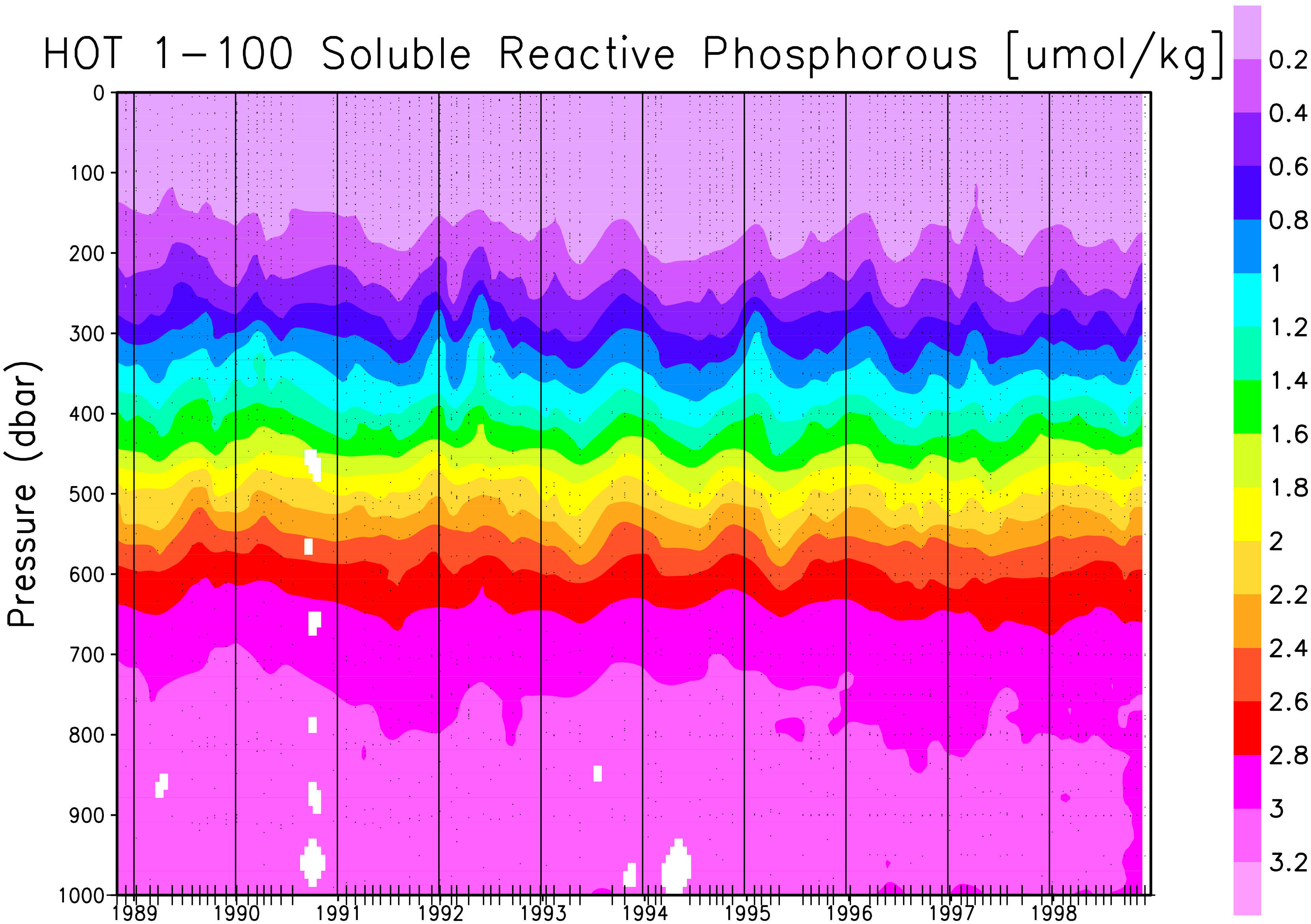

HOT 1-100 Soluble Reactive Phosphorous [umol/kg]
Pressure (dbar)
0
100
200
300
400
500
600
700
800
900
1000
1989
1990
1991
1992
1993
1994
1995
1996
1997
1998
0.2
0.4
0.6
0.8
1
1.2
1.4
1.6
1.8
2
2.2
2.4
2.6
2.8
3
3.2

FIGURE 6.1.19.

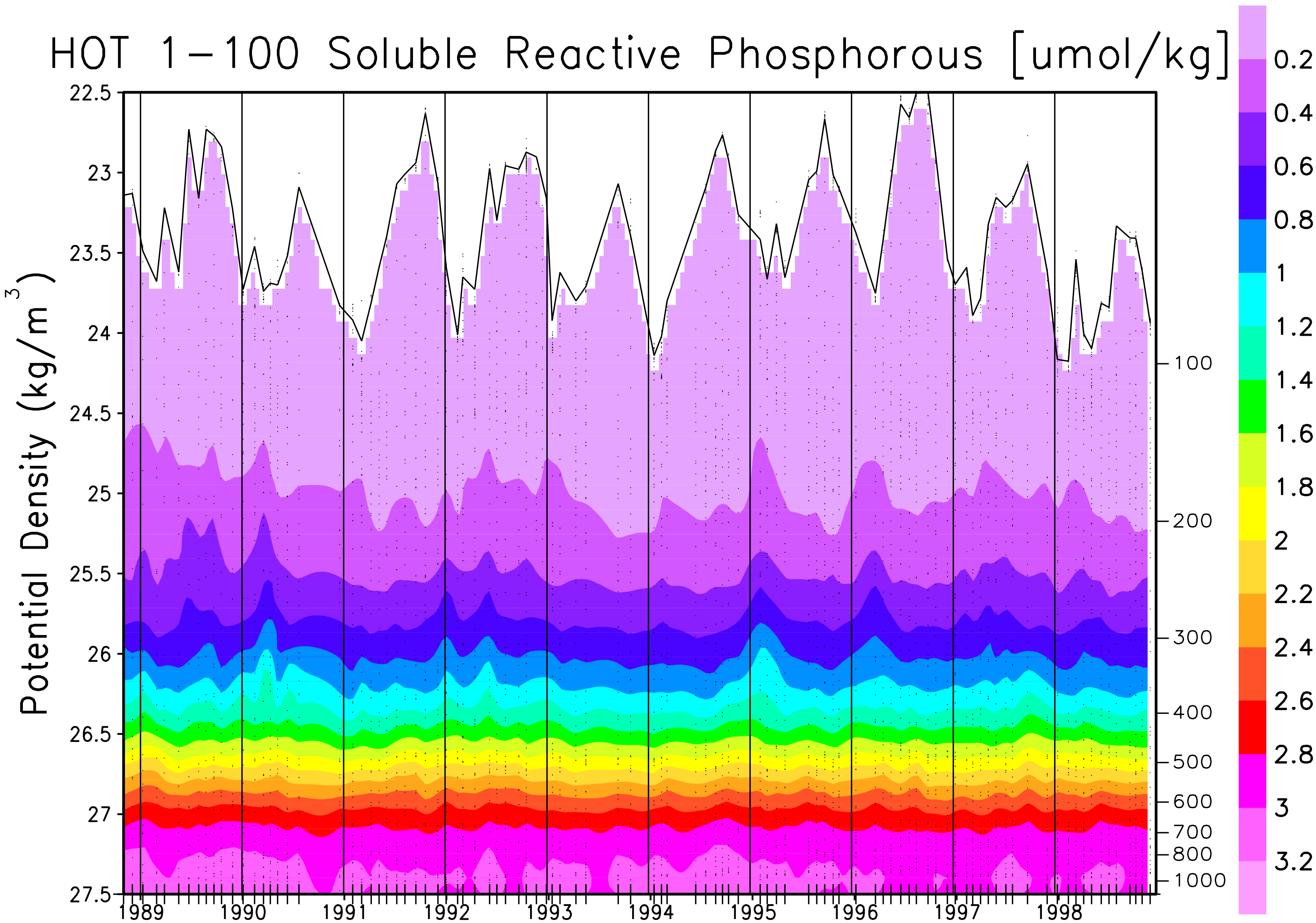
HOT 1-100 Soluble Reactive Phosphorous [umol/kg]
Potential Density (kg/m 3)
22.5
23
23.5
24
24.5
25
25.5
26
26.5
27
27.5
1989
1990
1991
1992
1993
1994
1995
1996
1997
1998
100
200
300
400
500
600
700
800
1000
0.2
0.4
0.6
0.8
1
1.2
1.4
1.6
1.8
2
2.2
2.4
2.6
2.8
3
3.2

FIGURE 6.1.20.

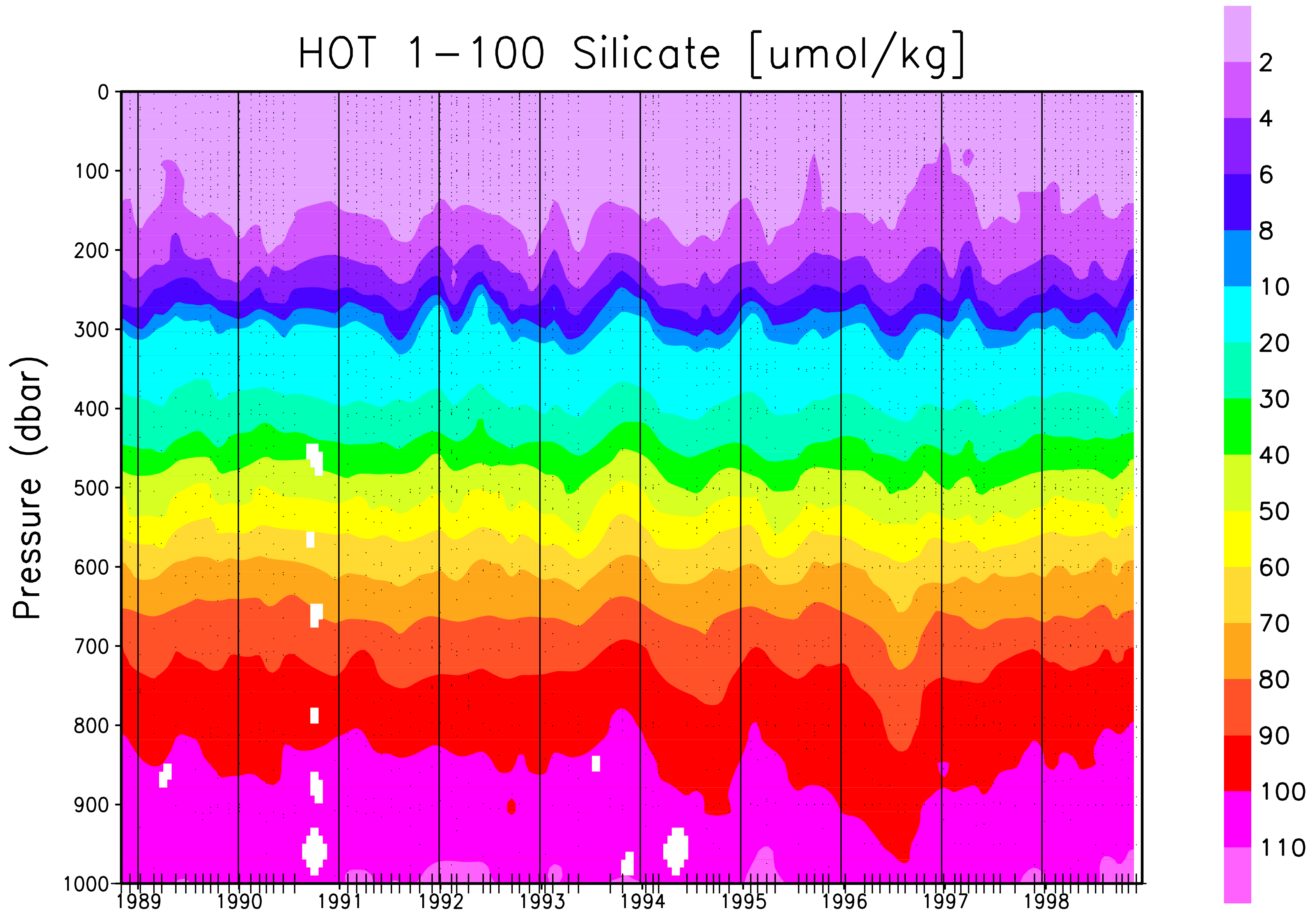

HOT 1-100 Silicate [umol/kg]
Pressure (dbar)
0
100
200
300
400
500
600
700
800
900
1000
1989
1990
1991
1992
1993
1994
1995
1996
1997
1998
2
4
6
8
10
20
30
40
50
60
70
80
90
100
110

FIGURE 6.1.21.

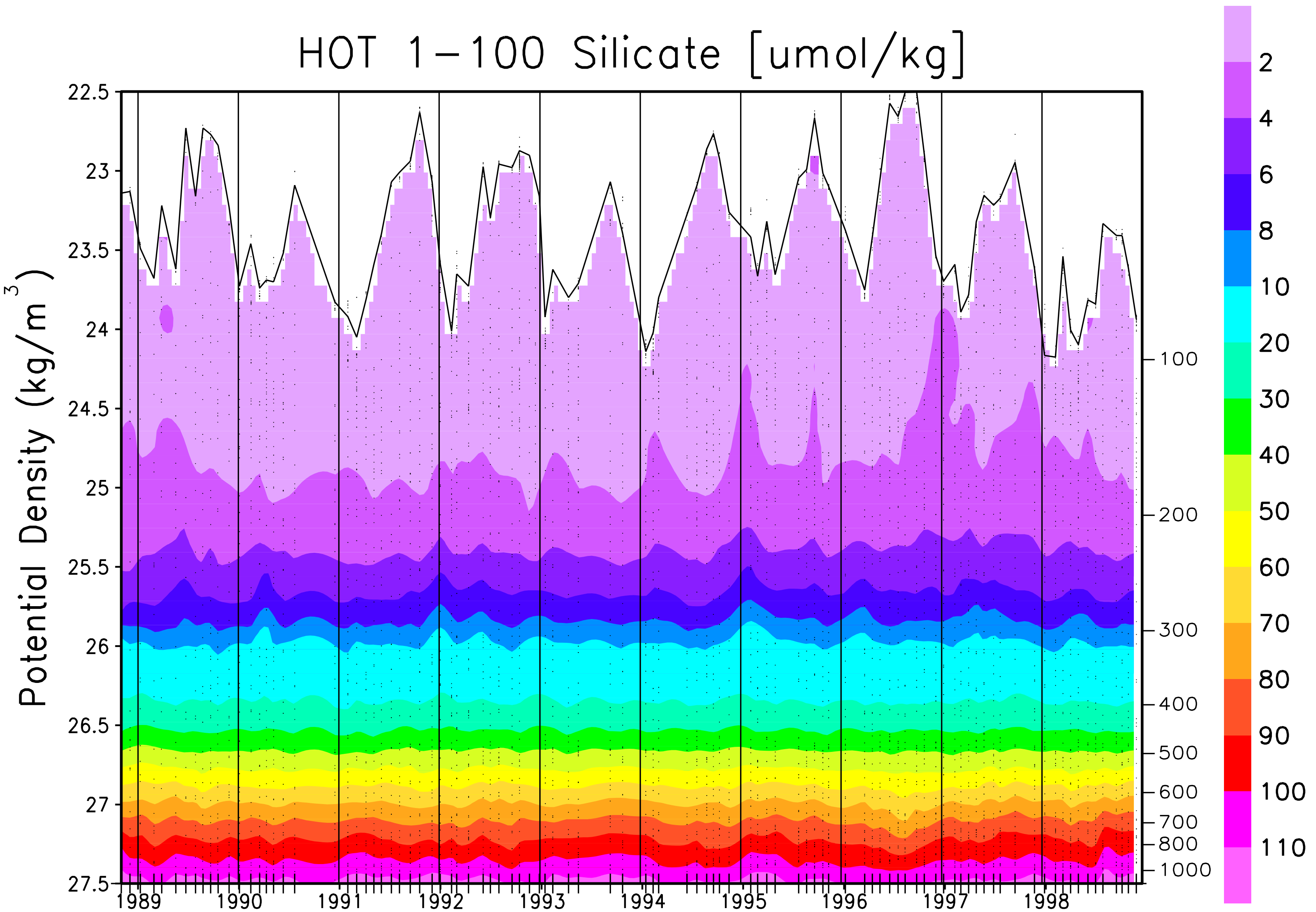

HOT 1-100 Silicate [umol/kg]
Potential Density (kg/m 3)
22.5
23
23.5
24
24.5
25
25.5
26
26.5
27
27.5
1989
1990
1991
1992
1993
1994
1995
1996
1997
1998
100
200
300
400
500
600
700
800
1000
2
4
6
8
10
20
30
40
50
60
70
80
90
100
110

FIGURE 6.1.22.

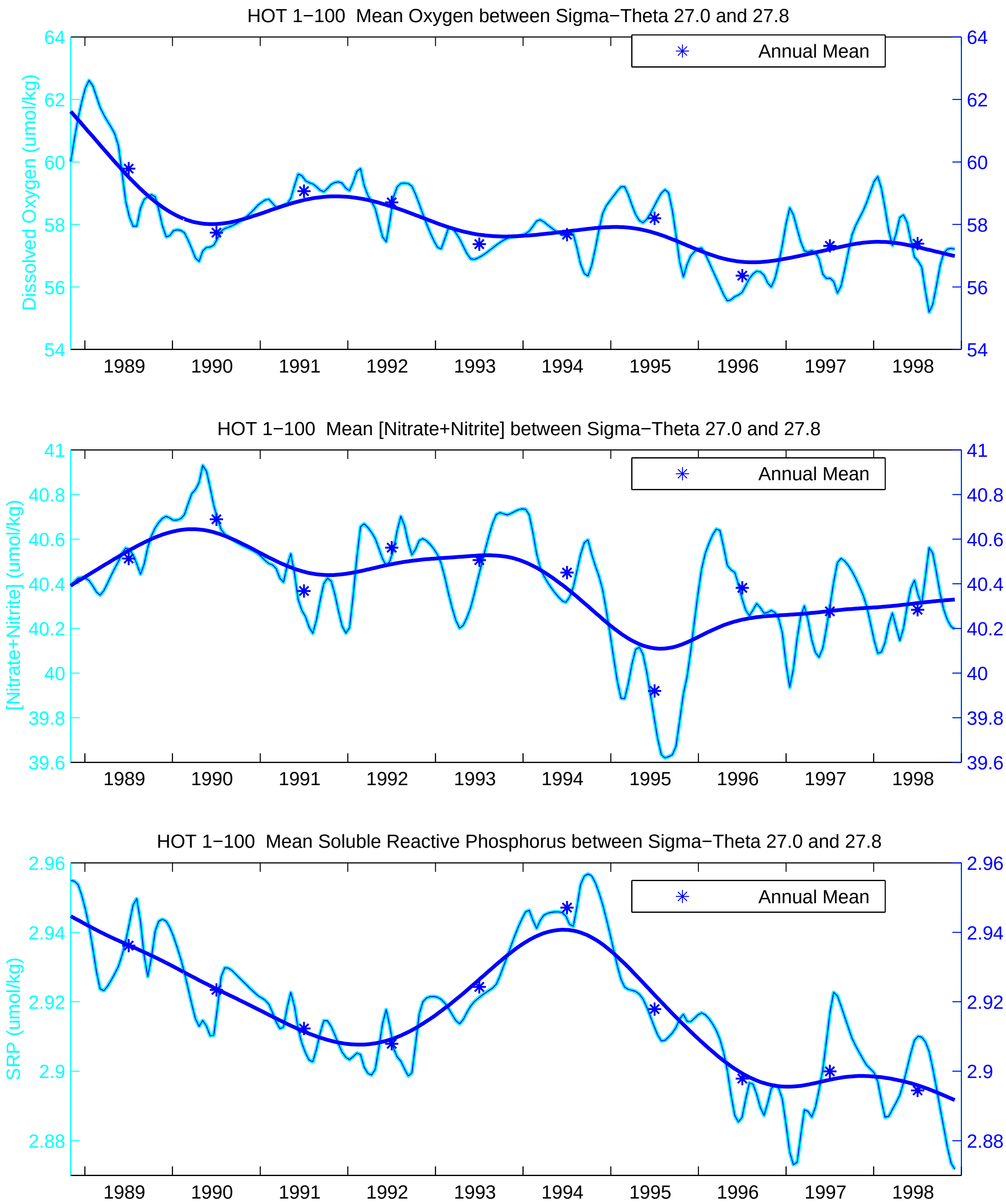
HOT 1−100 Mean Oxygen between Sigma−Theta 27.0 and 27.8
Annual Mean
Dissolved Oxygen (umol/kg)
64
62
60
58
56
54
1989
1990
1991
1992
1993
1994
1995
1996
1997
1998
HOT 1−100 Mean [Nitrate+Nitrite] between Sigma−Theta 27.0 and 27.8
Annual Mean
[Nitrate+Nitrite] (umol/kg)
41
40.8
40.6
40.4
40.2
40
39.8
39.6
HOT 1−100 Mean Soluble Reactive Phosphorus between Sigma−Theta 27.0 and 27.8
Annual Mean
SRP (umol/kg)
2.96
2.94
2.92
2.9
2.88

FIGURE 6.1.23.

6.2 Thermosalinograph

Figure 6.2.1a-q: Thermosalinograph data for each HOT and HALE-ALOHA cruises in 1998, [Upper panel per cruise] Continuous surface salinity (upper line) and surface temperature (lower line). [Lower panel per cruise] Navigation (upper line: longitude, lower line: latitude) over time during the cruise. For the HOT cruises the vertical lines indicate the sampling period while at Station ALOHA.

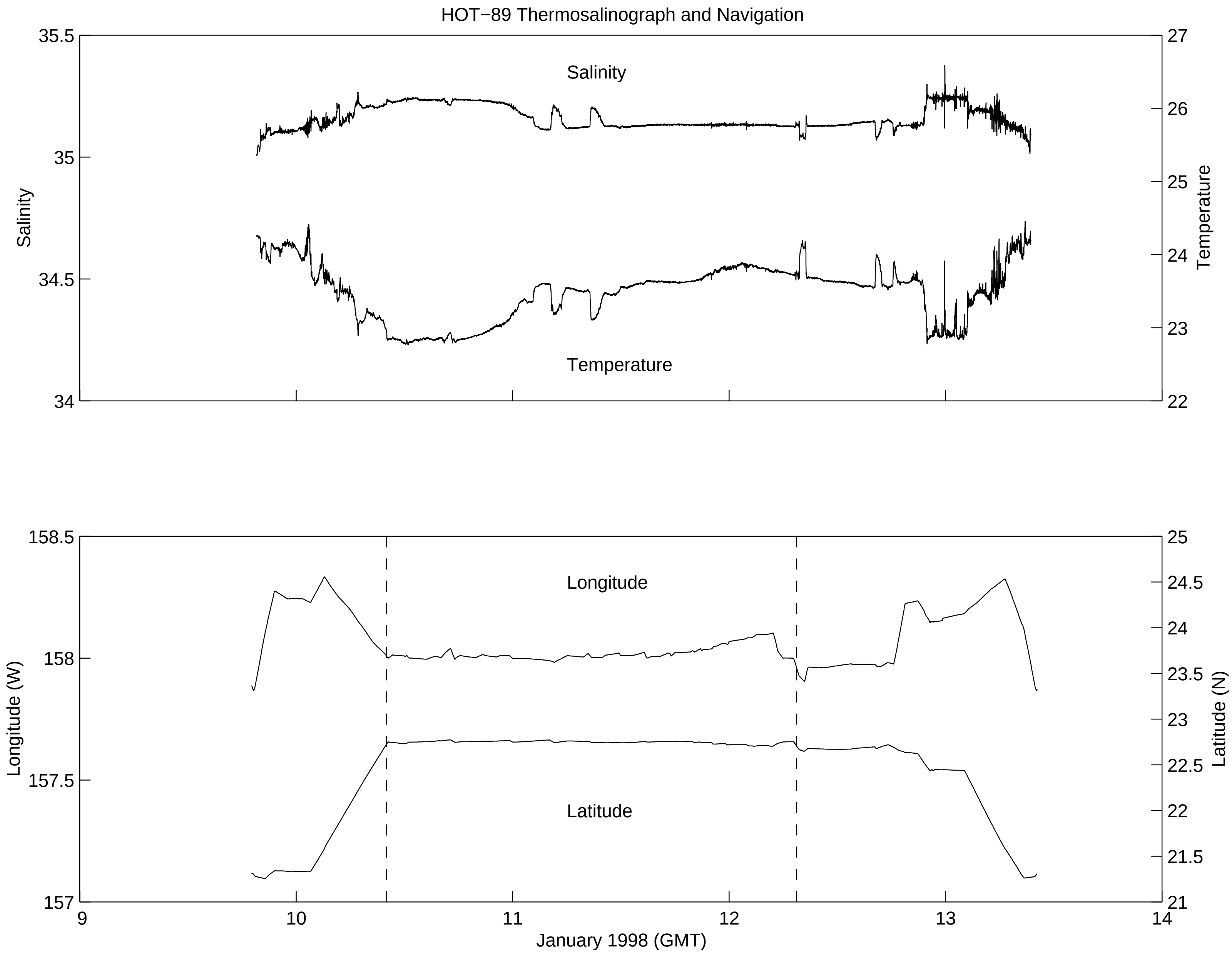
HOT−89 Thermosalinograph and Navigation
Salinity
Temperature
Salinity
Temperature
35.5
35
34.5
34
27
26
25
24
23
22
Longitude
Latitude
Longitude (W)
Latitude (N)
158.5
158
157.5
157
25
24.5
24
23.5
23
22.5
22
21.5
21
9
10
11
12
13
14
January 1998 (GMT)

FIGURE 6.2.1a.

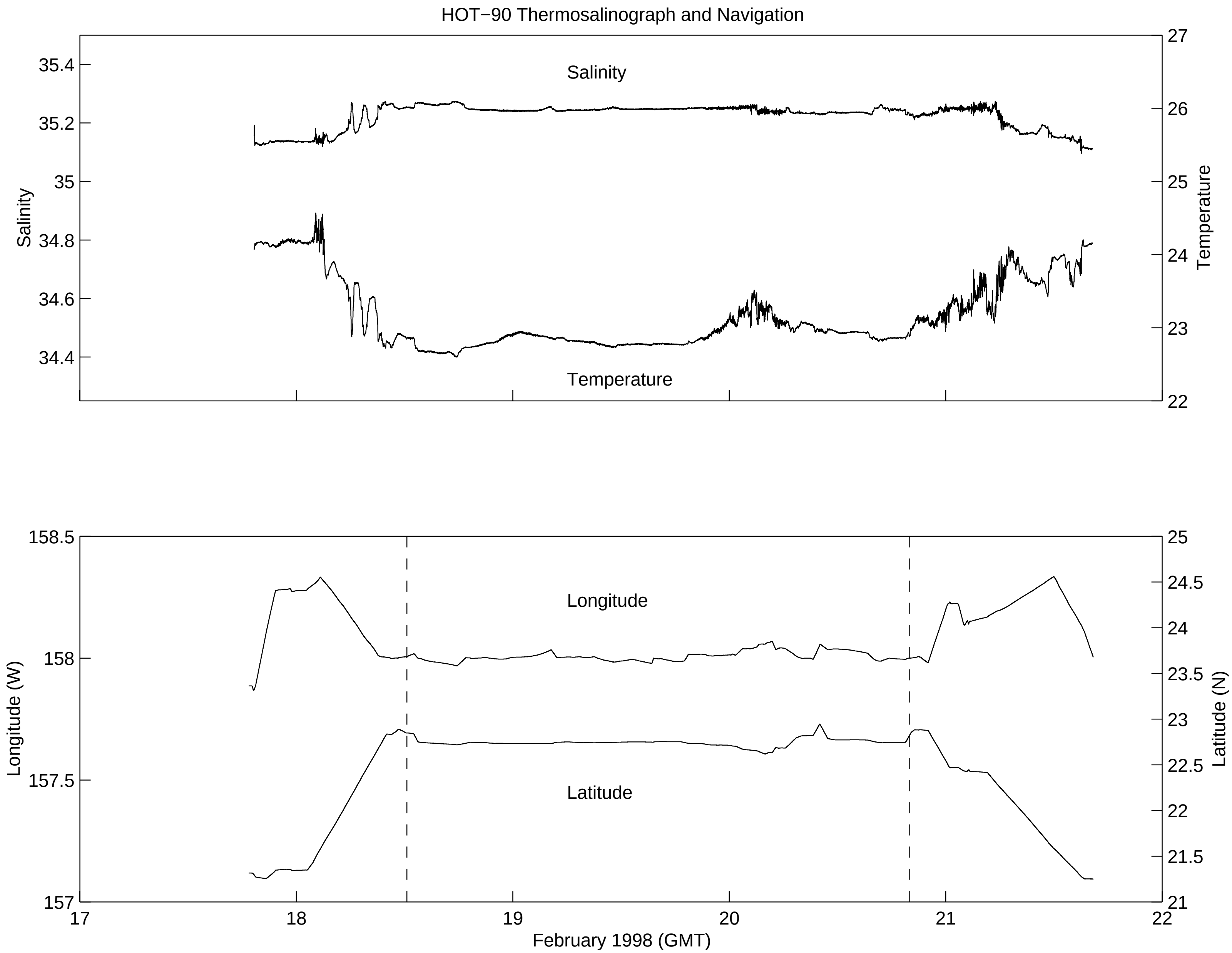
HOT−90 Thermosalinograph and Navigation
Salinity
Temperature
35.4
35.2
35
34.8
34.6
34.4
27
26
25
24
23
22
Longitude
Latitude
Longitude (W)
Latitude (N)
158.5
158
157.5
157
25
24.5
24
23.5
23
22.5
22
21.5
21
17
18
19
20
21
22
February 1998 (GMT)

FIGURE 6.2.1b.

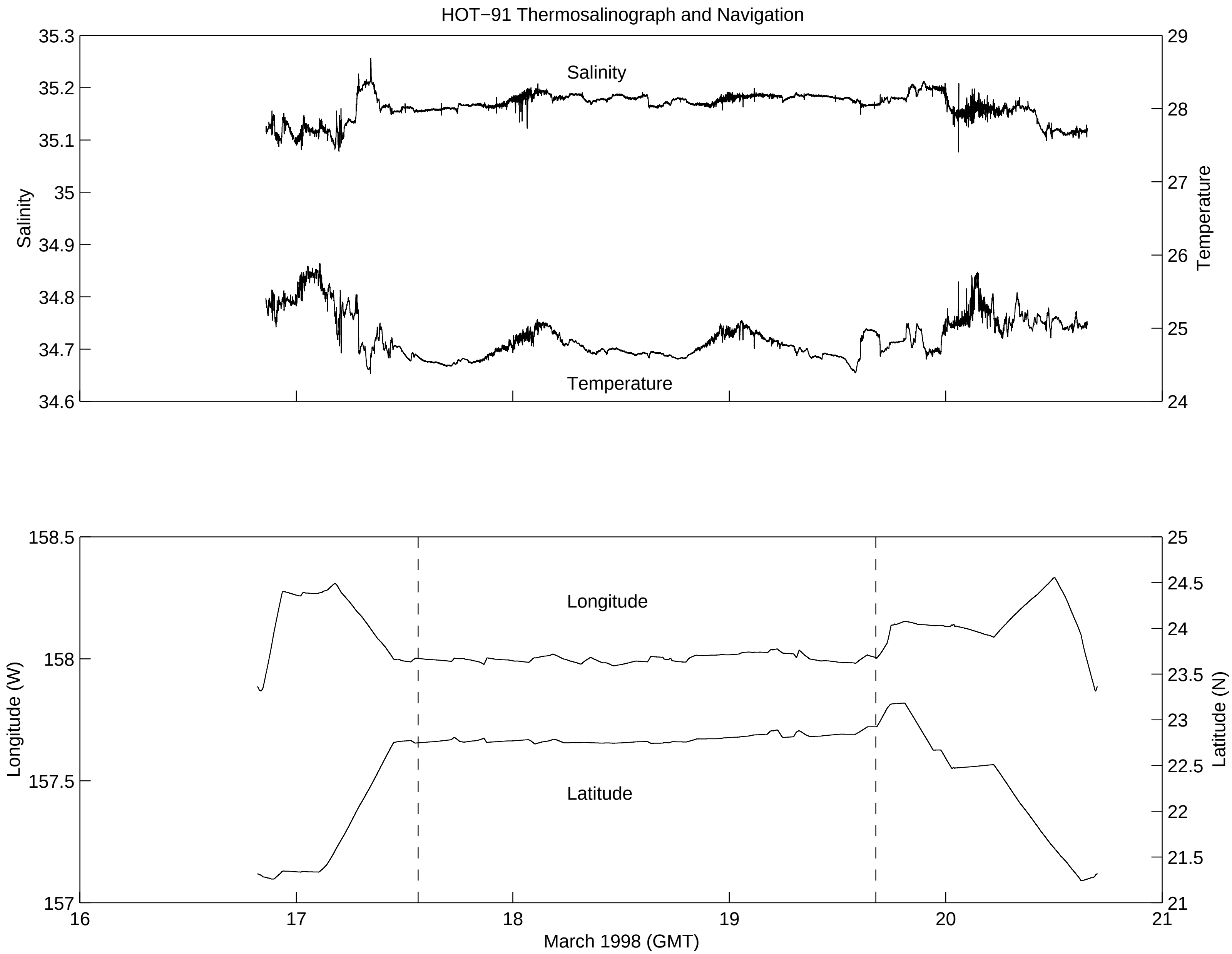

HOT−91 Thermosalinograph and Navigation
Salinity
Temperature
35.3
35.2
35.1
35
34.9
34.8
34.7
34.6
29
28
27
26
25
24
Longitude
Latitude
Longitude (W)
Latitude (N)
158.5
158
157.5
157
25
24.5
24
23.5
23
22.5
22
21.5
21
16
17
18
19
20
21
March 1998 (GMT)

FIGURE 6.2.1c.

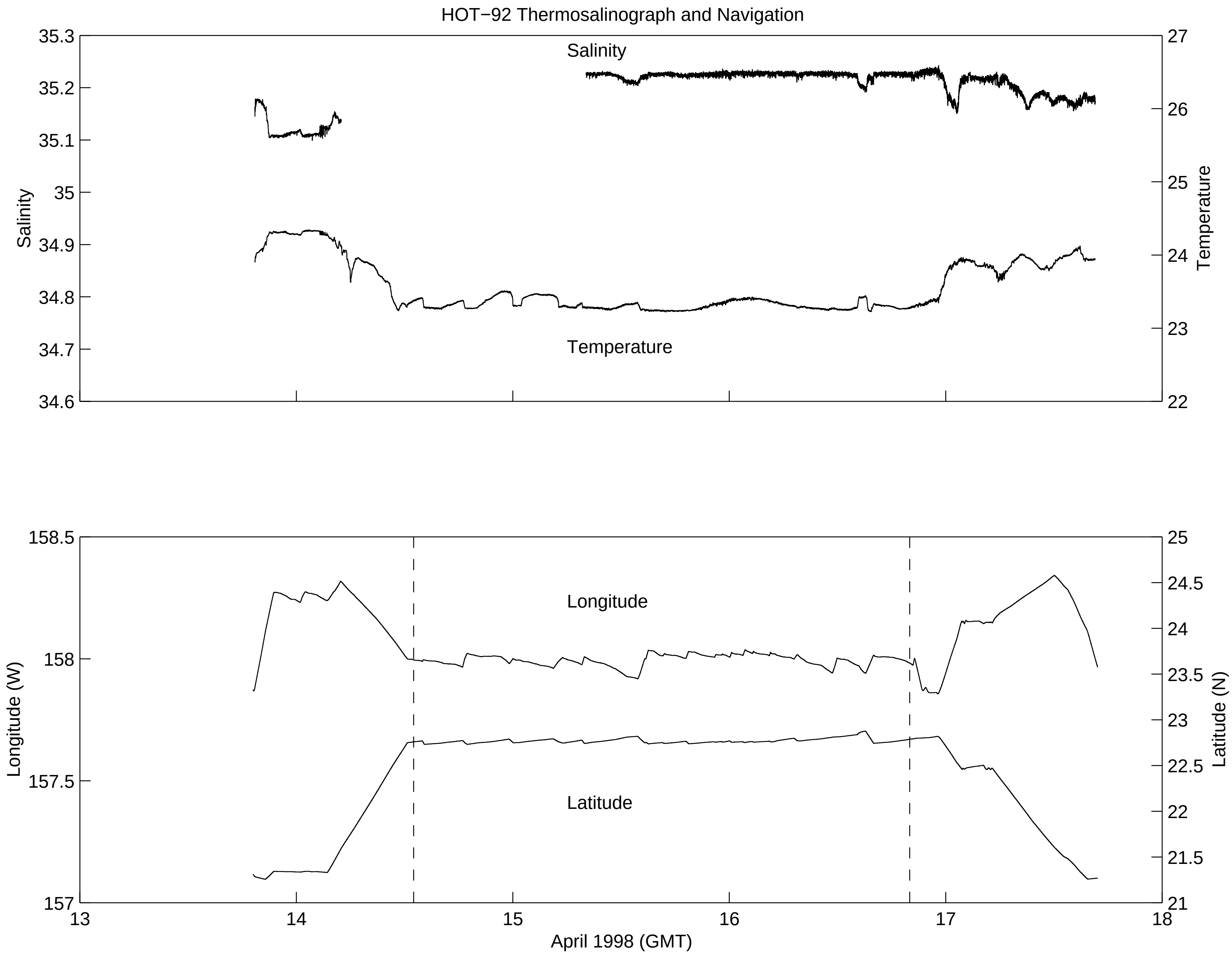

HOT−92 Thermosalinograph and Navigation
Salinity
Temperature
Salinity
Temperature
35.3
35.2
35.1
35
34.9
34.8
34.7
34.6
27
26
25
24
23
22
Longitude
Latitude
Longitude (W)
Latitude (N)
158.5
158
157.5
157
25
24.5
24
23.5
23
22.5
22
21.5
21
13
14
15
16
17
18
April 1998 (GMT)

FIGURE 6.2.1d.

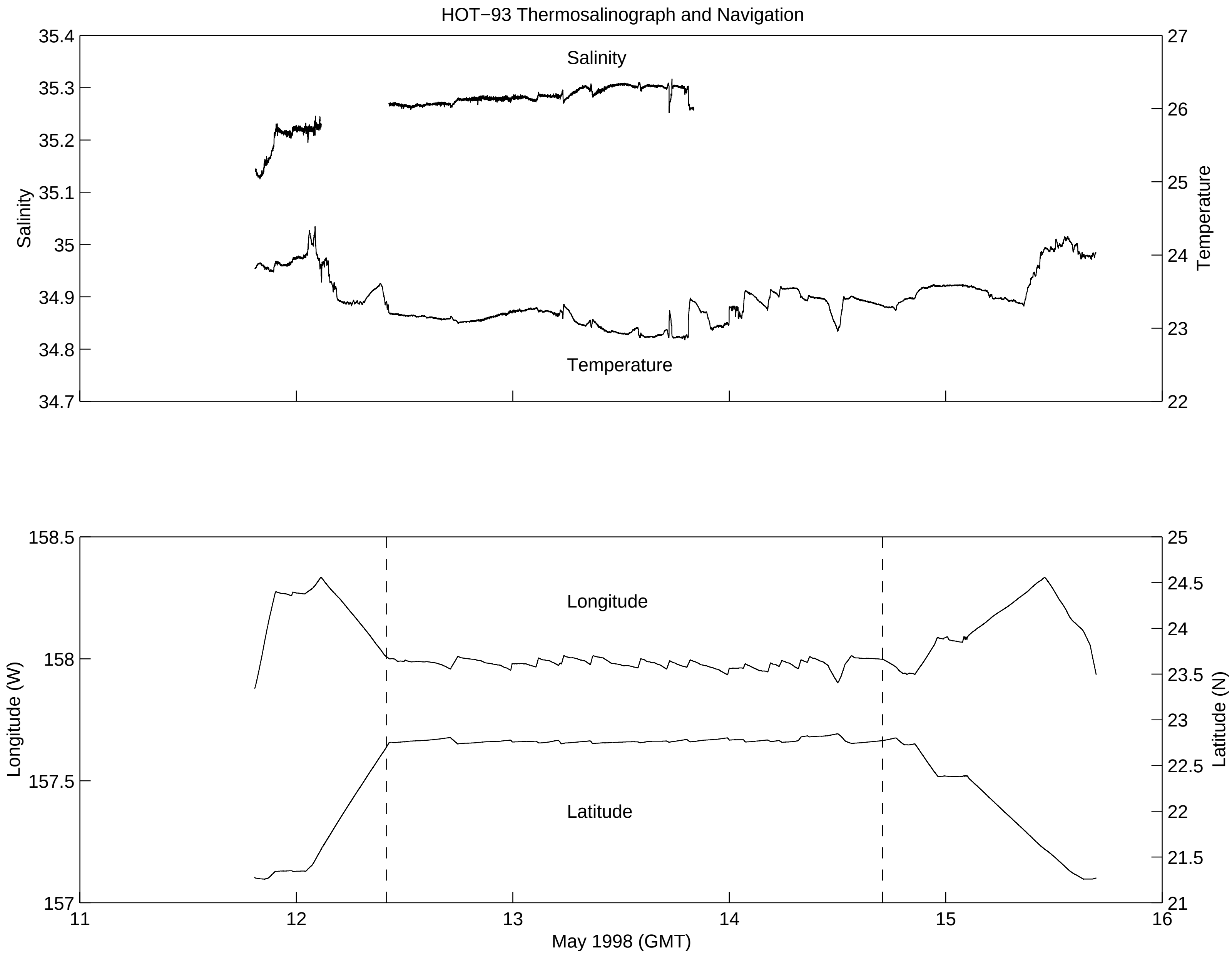
HOT−93 Thermosalinograph and Navigation
Salinity
Temperature
Salinity
Temperature
35.4
35.3
35.2
35.1
35
34.9
34.8
34.7
27
26
25
24
23
22
Longitude
Latitude
Longitude (W)
Latitude (N)
158.5
158
157.5
157
25
24.5
24
23.5
23
22.5
22
21.5
21
11
12
13
14
15
16
May 1998 (GMT)

FIGURE 6.2.1e.

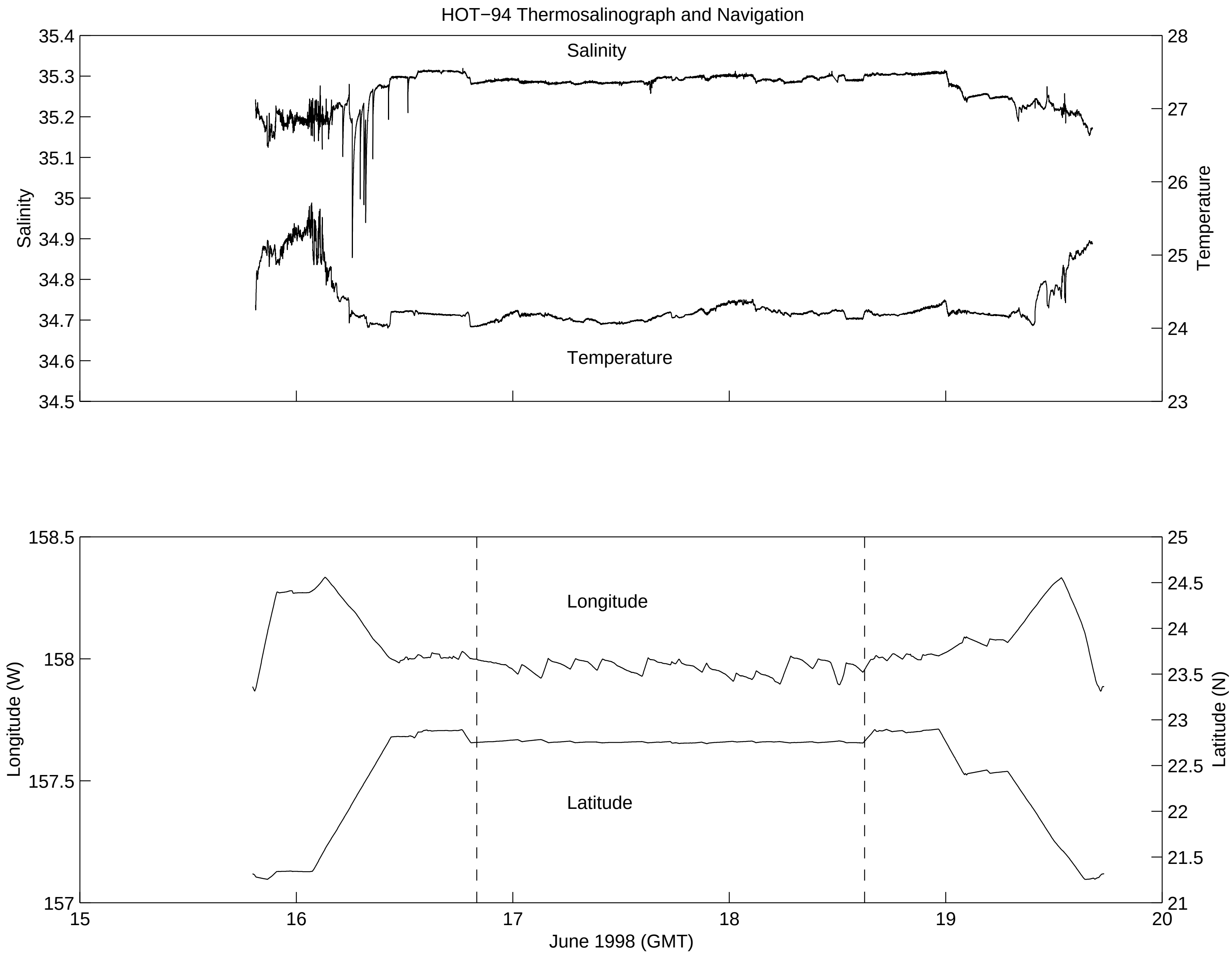
HOT−94 Thermosalinograph and Navigation
Salinity
Temperature
Longitude
Latitude
Salinity
Temperature
Longitude (W)
Latitude (N)
June 1998 (GMT)
35.4
35.3
35.2
35.1
35
34.9
34.8
34.7
34.6
34.5
28
27
26
25
24
23
158.5
158
157.5
157
25
24.5
24
23.5
23
22.5
22
21.5
21
15
16
17
18
19
20

FIGURE 6.2.1f.

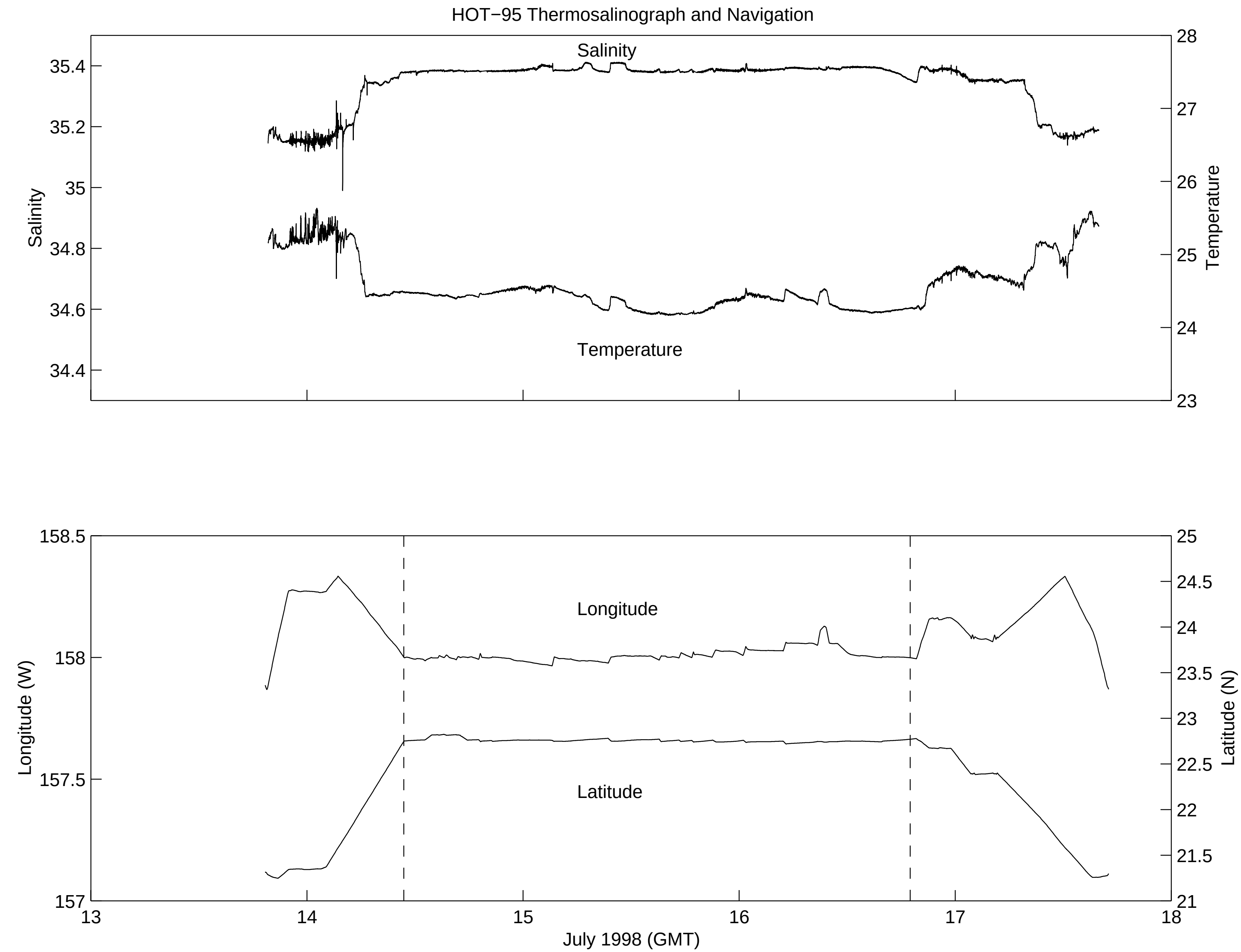

HOT−95 Thermosalinograph and Navigation
Salinity
Temperature
Salinity
Temperature
35.4
35.2
35
34.8
34.6
34.4
28
27
26
25
24
23
Longitude
Latitude
Longitude (W)
Latitude (N)
158.5
158
157.5
157
25
24.5
24
23.5
23
22.5
22
21.5
21
13
14
15
16
17
18
July 1998 (GMT)

FIGURE 6.2.1g.

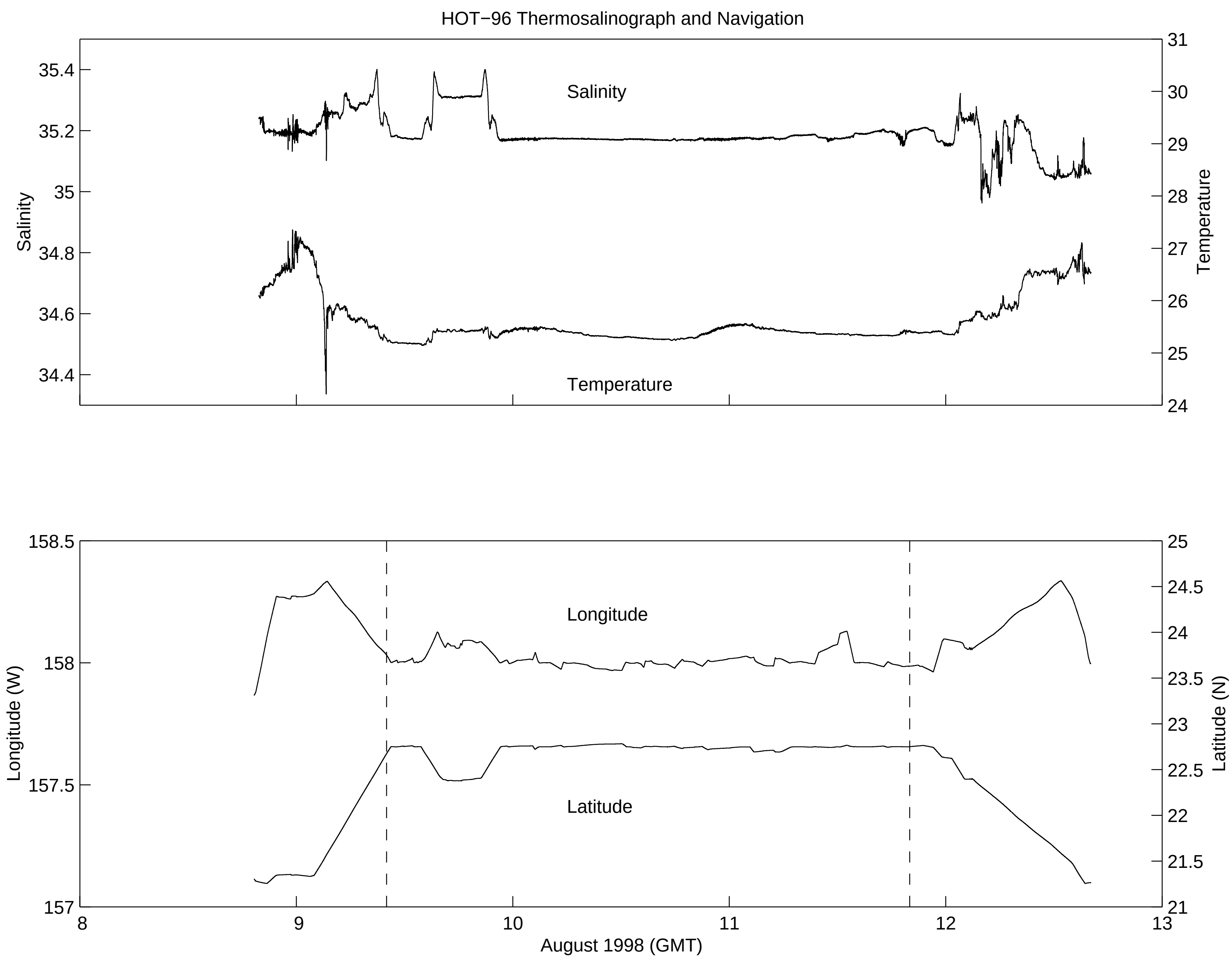
HOT−96 Thermosalinograph and Navigation
Salinity
Temperature
35.4
35.2
35
34.8
34.6
34.4
31
30
29
28
27
26
25
24
Longitude
Latitude
Longitude (W)
Latitude (N)
158.5
158
157.5
157
25
24.5
24
23.5
23
22.5
22
21.5
21
8
9
10
11
12
13
August 1998 (GMT)

FIGURE 6.2.1h.

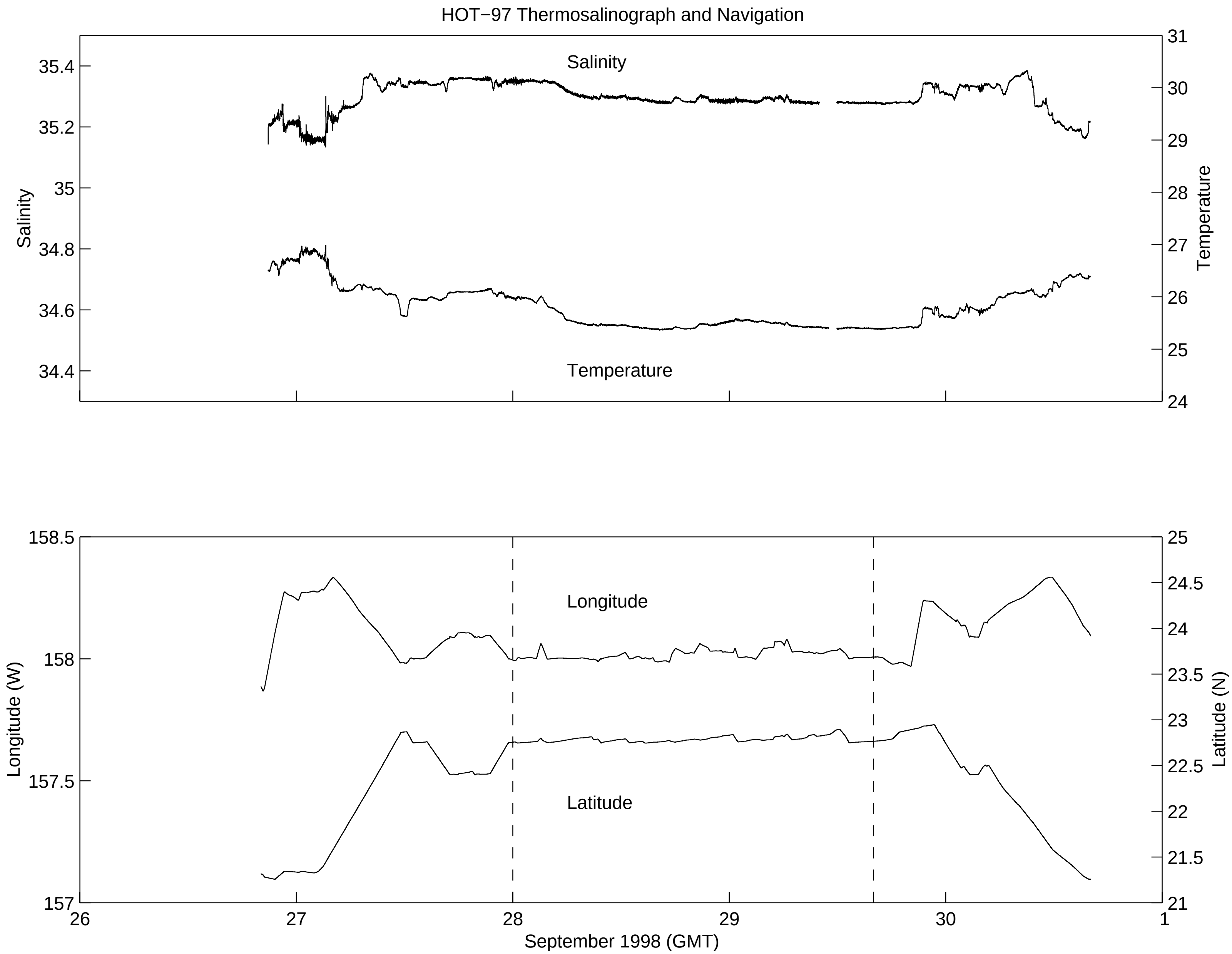
HOT−97 Thermosalinograph and Navigation
Salinity
Temperature
Salinity
Temperature
35.4
35.2
35
34.8
34.6
34.4
31
30
29
28
27
26
25
24
Longitude
Latitude
Longitude (W)
Latitude (N)
158.5
158
157.5
157
25
24.5
24
23.5
23
22.5
22
21.5
21
26
27
28
29
30
1
September 1998 (GMT)

FIGURE 6.2.1i.

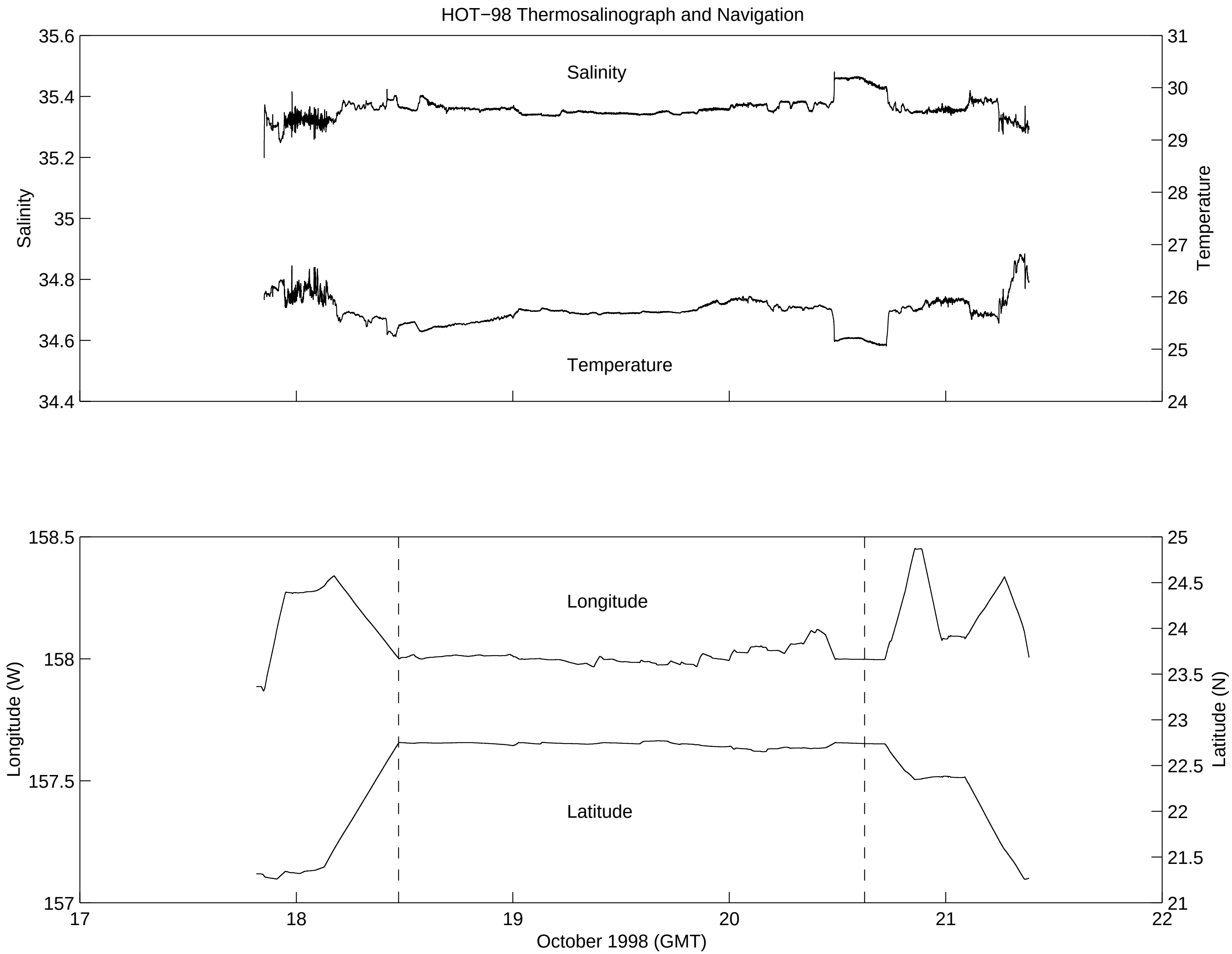
HOT−98 Thermosalinograph and Navigation
Salinity
Temperature
35.6
35.4
35.2
35
34.8
34.6
34.4
31
30
29
28
27
26
25
24
Longitude
Latitude
Longitude (W)
Latitude (N)
158.5
158
157.5
157
25
24.5
24
23.5
23
22.5
22
21.5
21
17
18
19
20
21
22
October 1998 (GMT)

FIGURE 6.2.1j.

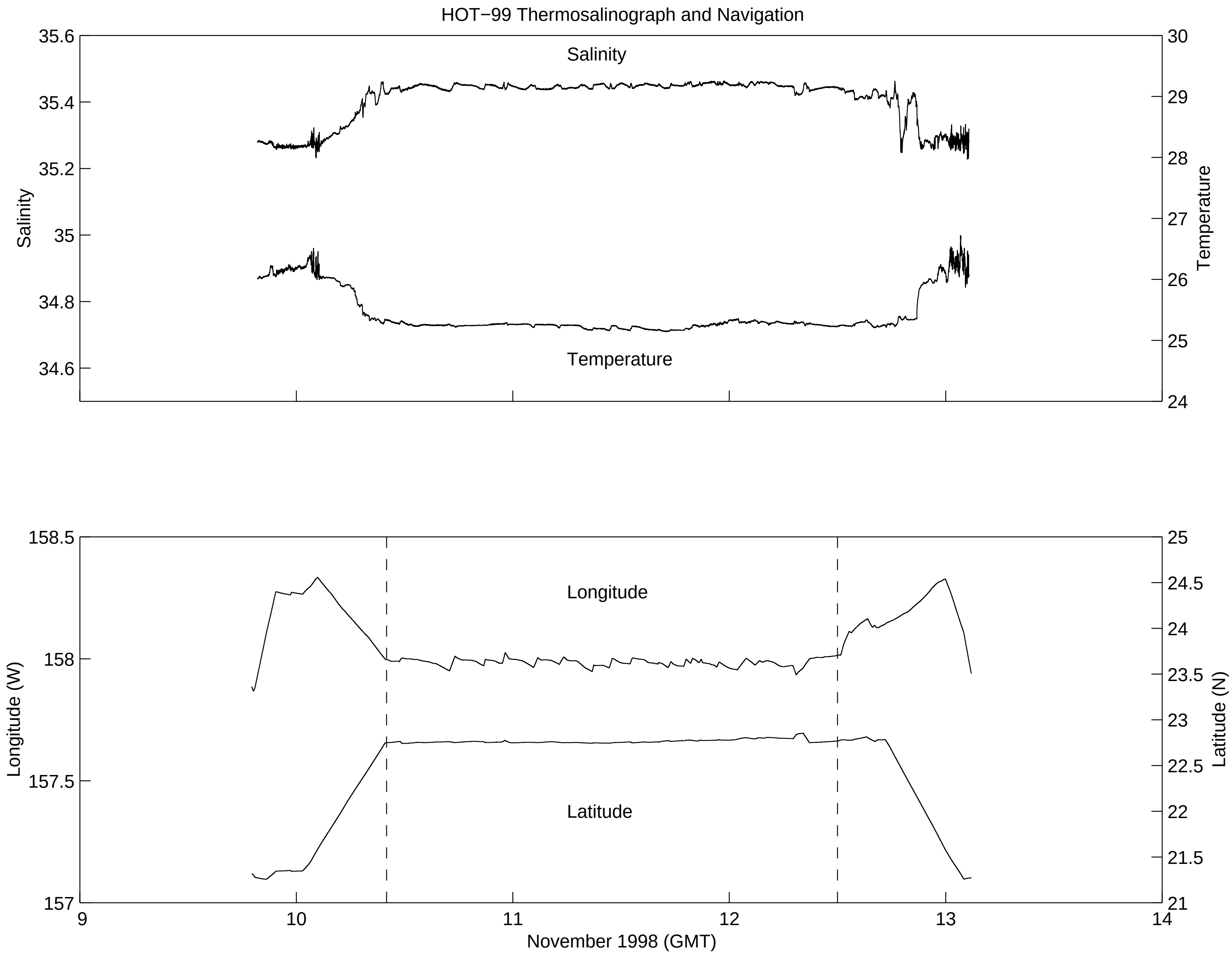
HOT−99 Thermosalinograph and Navigation
Salinity
Temperature
35.6
35.4
35.2
35
34.8
34.6
30
29
28
27
26
25
24
Longitude
Latitude
Longitude (W)
Latitude (N)
158.5
158
157.5
157
25
24.5
24
23.5
23
22.5
22
21.5
21
9
10
11
12
13
14
November 1998 (GMT)

FIGURE 6.2.1k.

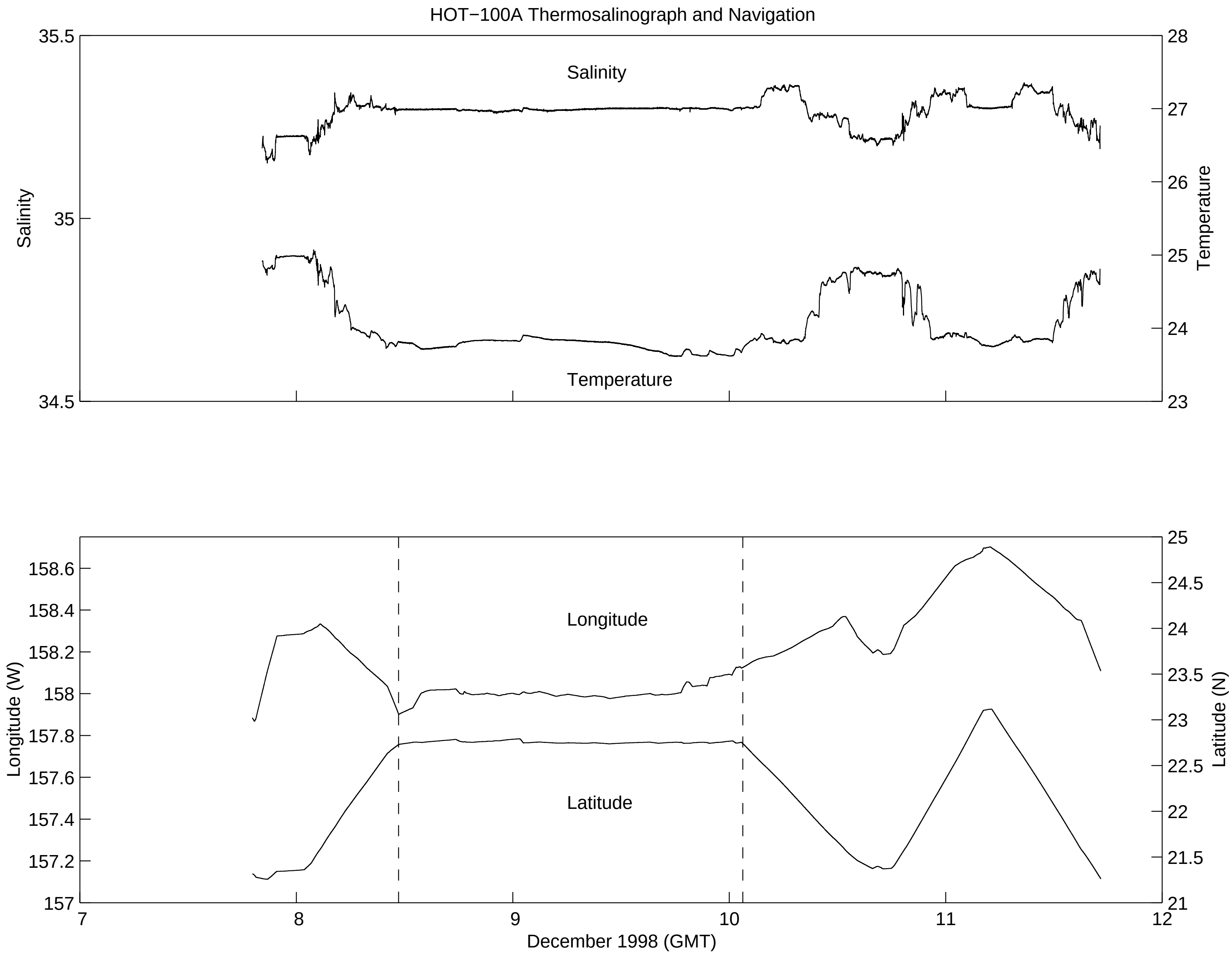
HOT−100A Thermosalinograph and Navigation
Salinity
Temperature
35.5
35
34.5
28
27
26
25
24
23
Longitude
Latitude
Longitude (W)
Latitude (N)
158.6
158.4
158.2
158
157.8
157.6
157.4
157.2
157
25
24.5
24
23.5
23
22.5
22
21.5
21
7
8
9
10
11
12
December 1998 (GMT)

FIGURE 6.2.1l.

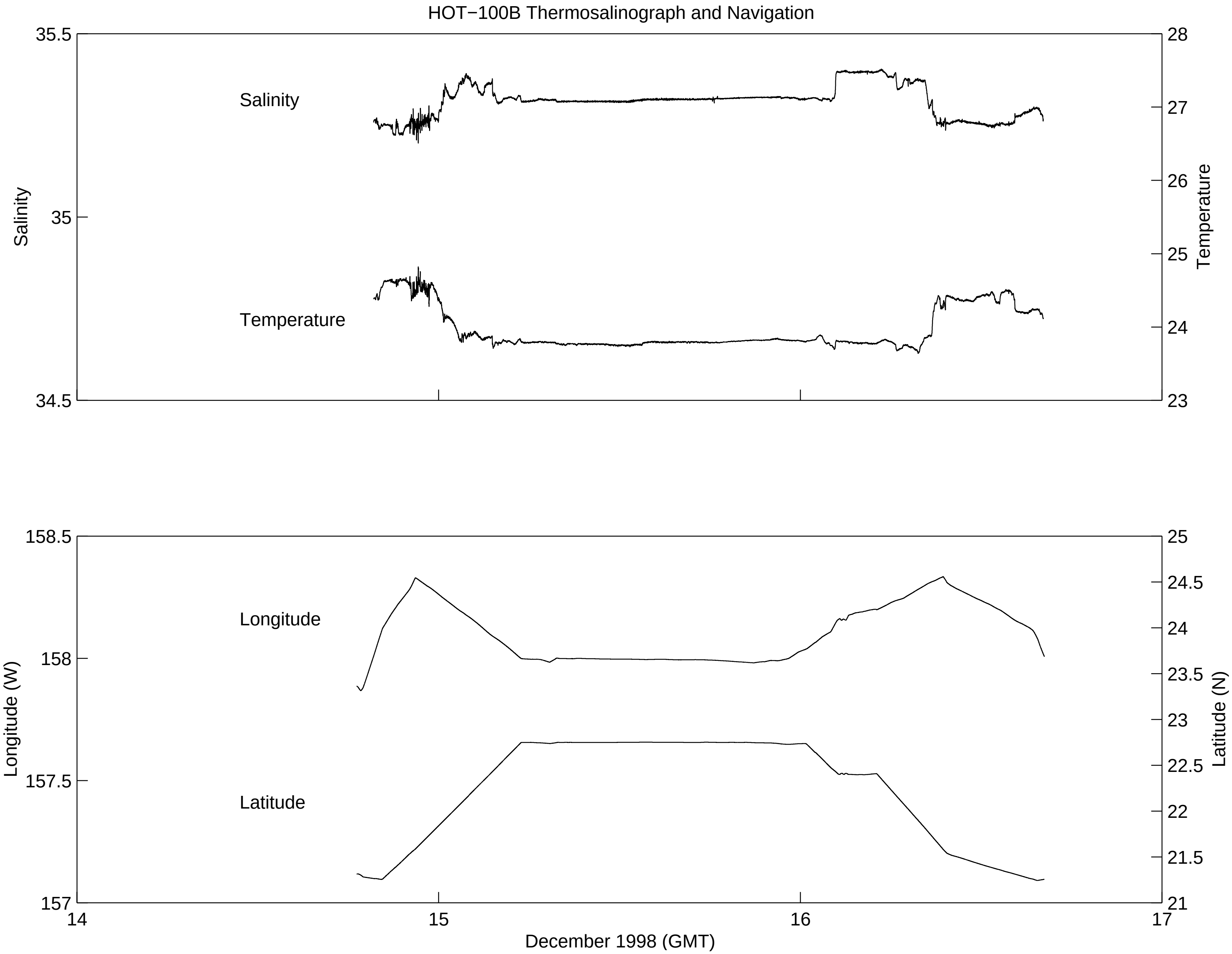
HOT−100B Thermosalinograph and Navigation
Salinity
Temperature
Salinity
Temperature
35.5
35
34.5
28
27
26
25
24
23
Longitude
Latitude
Longitude (W)
Latitude (N)
158.5
158
157.5
157
25
24.5
24
23.5
23
22.5
22
21.5
21
14
15
16
17
December 1998 (GMT)

FIGURE 6.2.1m.

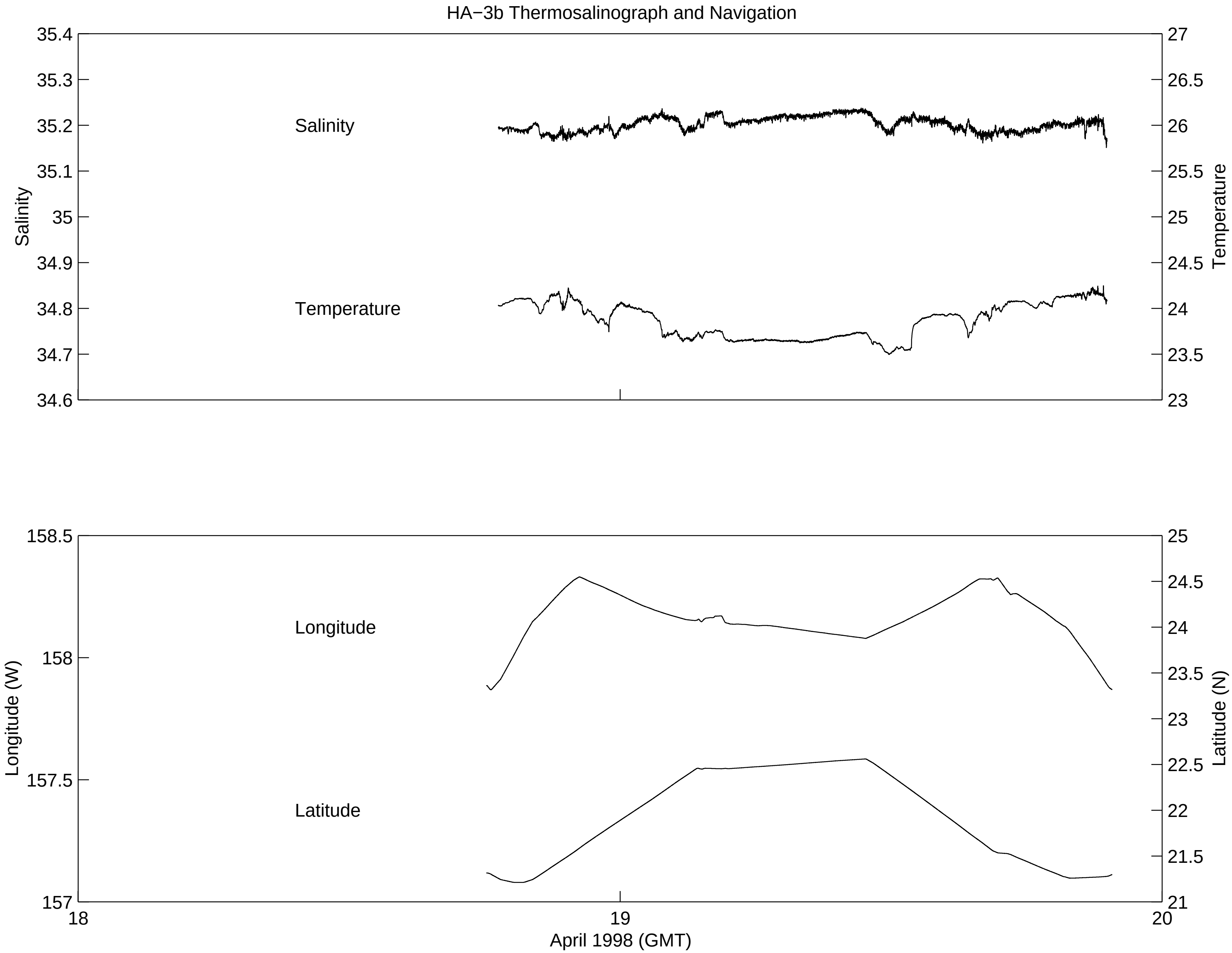
HA−3b Thermosalinograph and Navigation
Salinity
Temperature
35.4
35.3
35.2
35.1
35
34.9
34.8
34.7
34.6
27
26.5
26
25.5
25
24.5
24
23.5
23
Longitude
Latitude
Longitude (W)
Latitude (N)
158.5
158
157.5
157
25
24.5
24
23.5
23
22.5
22
21.5
21
18
19
20
April 1998 (GMT)

FIGURE 6.2.1n.

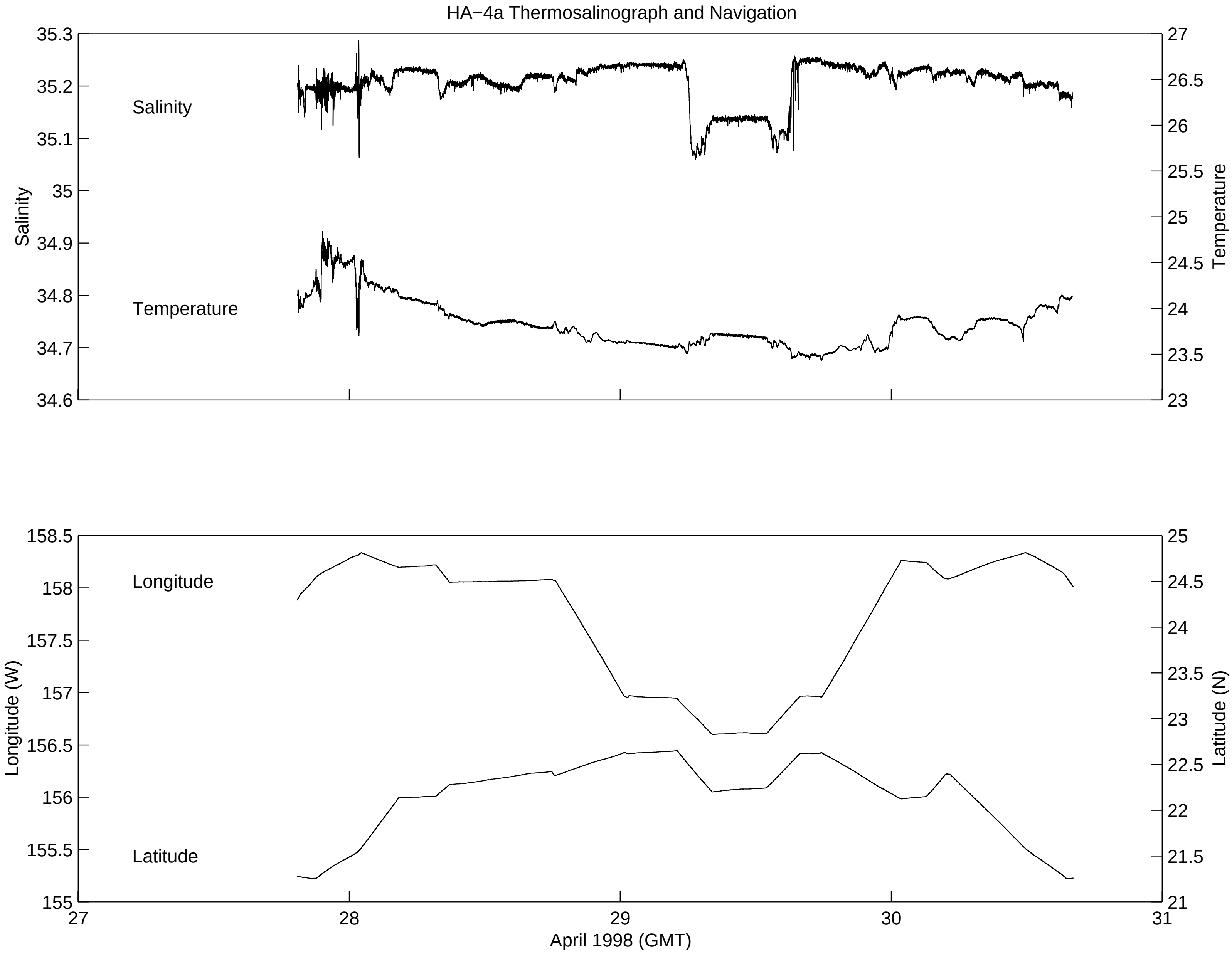
HA−4a Thermosalinograph and Navigation
Salinity
Temperature
35.3
35.2
35.1
35
34.9
34.8
34.7
34.6
27
26.5
26
25.5
25
24.5
24
23.5
23
Longitude
Latitude
Longitude (W)
Latitude (N)
158.5
158
157.5
157
156.5
156
155.5
155
25
24.5
24
23.5
23
22.5
22
21.5
21
27
28
29
30
31
April 1998 (GMT)

FIGURE 6.2.1o.

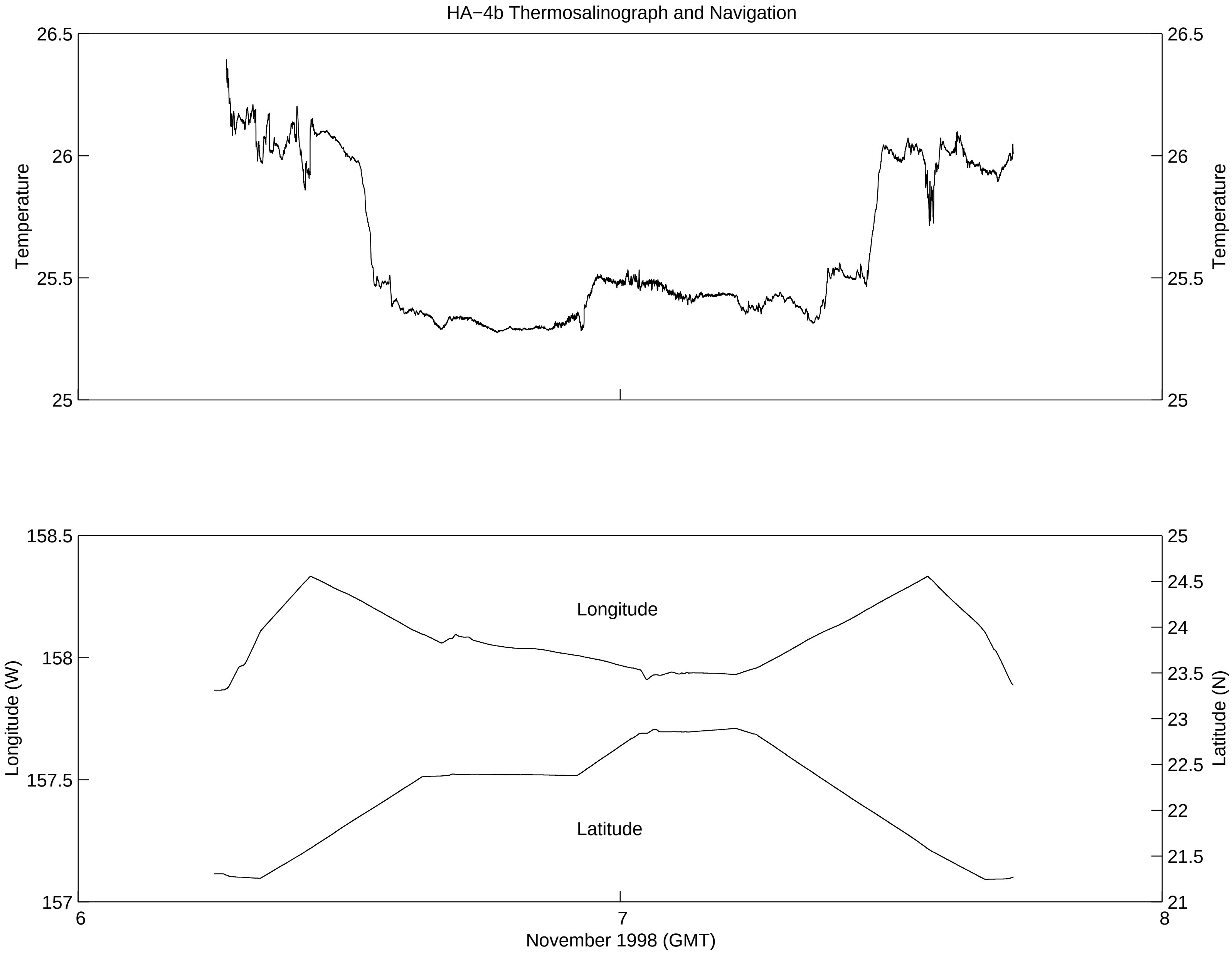
HA−4b Thermosalinograph and Navigation
Temperature
26.5
26
25.5
25
Longitude
Latitude
Longitude (W)
158.5
158
157.5
157
Latitude (N)
24.5
24
23.5
23
22.5
22
21.5
21
6
7
8
November 1998 (GMT)

FIGURE 6.2.1p.

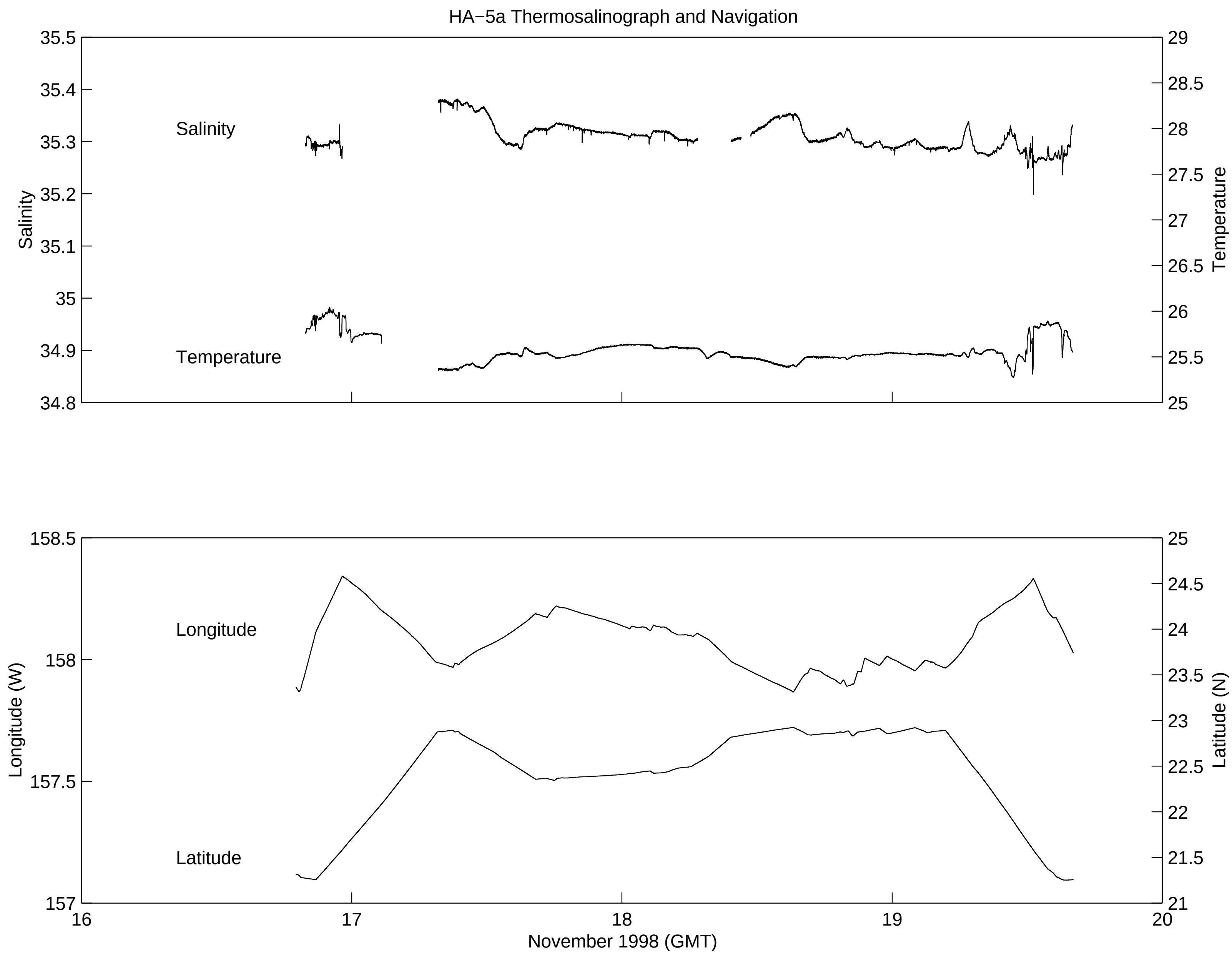
HA−5a Thermosalinograph and Navigation
Salinity
Temperature
Salinity
Temperature
35.5
35.4
35.3
35.2
35.1
35
34.9
34.8
29
28.5
28
27.5
27
26.5
26
25.5
25
Longitude
Latitude
Longitude (W)
Latitude (N)
158.5
158
157.5
157
25
24.5
24
23.5
23
22.5
22
21.5
21
16
17
18
19
20
November 1998 (GMT)

FIGURE 6.2.1q.

6.3 Meteorology

Figure 6.3.1: [Upper panel] Atmospheric pressure while at Station ALOHA for 1998 HOT cruises (open circles), and NDBC buoy #51001 hourly measurements throughout the year (thin line). [Lower panel] Sea surface temperature measured from a bucket sample while at Station ALOHA for 1998 HOT cruises (open circles), NDBC buoy #51001 hourly measurements throughout the year (thin line), and sea temperatures at 3 m from the thermosalinograph while at Station ALOHA during HOT cruises (thick line). The buoy was not operational during January and part of February.

Figure 6.3.2: [Upper panel] Dry bulb air temperature while at Station ALOHA for 1998 HOT cruises (open circles), and NDBC buoy #51001 hourly measurements throughout the year (thin line). [Lower panel] Wet bulb air temperature while at Station ALOHA for 1998 HOT cruises.

Figure 6.3.3: [Upper panel] Sea surface temperature minus dry air temperature while at Station ALOHA for 1998 HOT cruises (open circles), and NDBC buoy #51001 hourly measurements throughout the year (thin line). [Lower panel] Relative humidity while at Station ALOHA for 1998 HOT cruises.

Figures 6.3.4a to l: [Upper panel] True winds measured at Station ALOHA. [Lower panel] True winds measured by NDBC buoy #51001. The orientation of the arrows indicate the wind direction; up is northward, right is eastward.

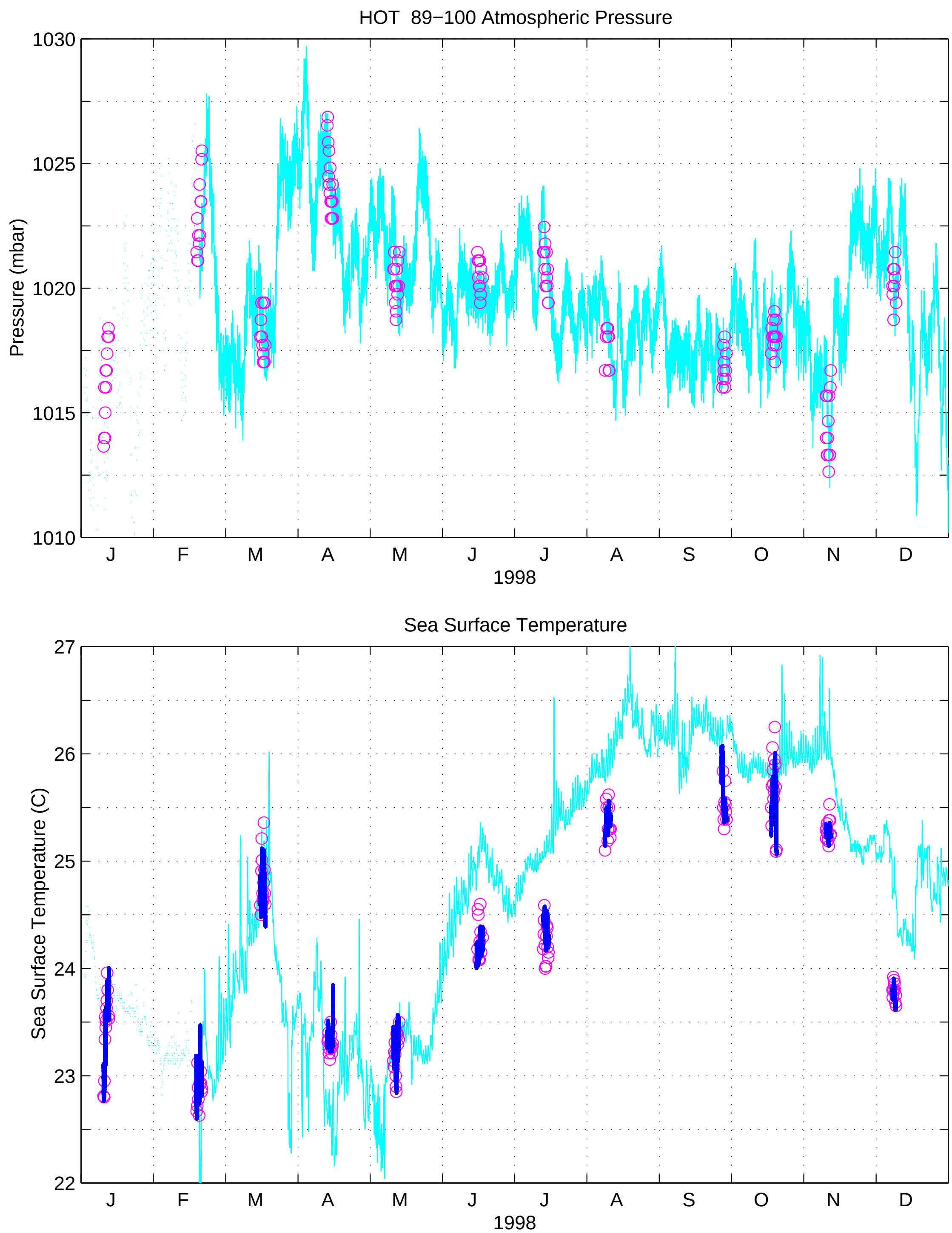

HOT 89−100 Atmospheric Pressure
Pressure (mbar)
1030
1025
1020
1015
1010
J
F
M
A
M
J
J
A
S
O
N
D
1998
Sea Surface Temperature
Sea Surface Temperature (C)
27
26
25
24
23
22
J
F
M
A
M
J
J
A
S
O
N
D
1998

FIGURE 6.3.1.

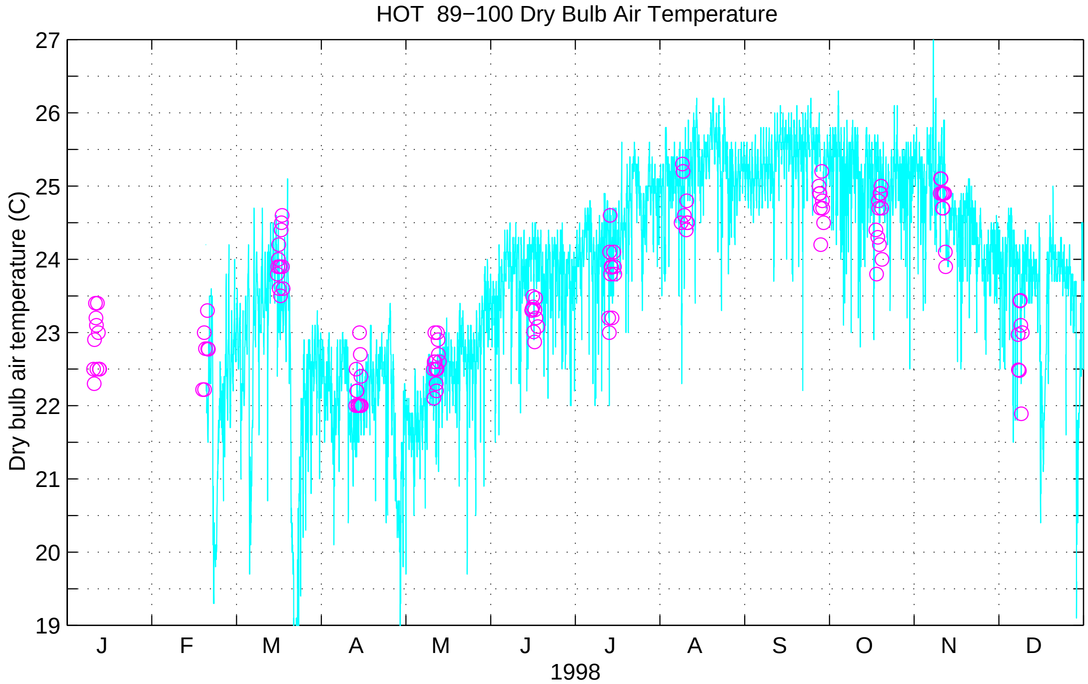
HOT 89−100 Dry Bulb Air Temperature
Dry bulb air temperature (C)
27
26
25
24
23
22
21
20
19
J F M A M J J A S O N D
1998

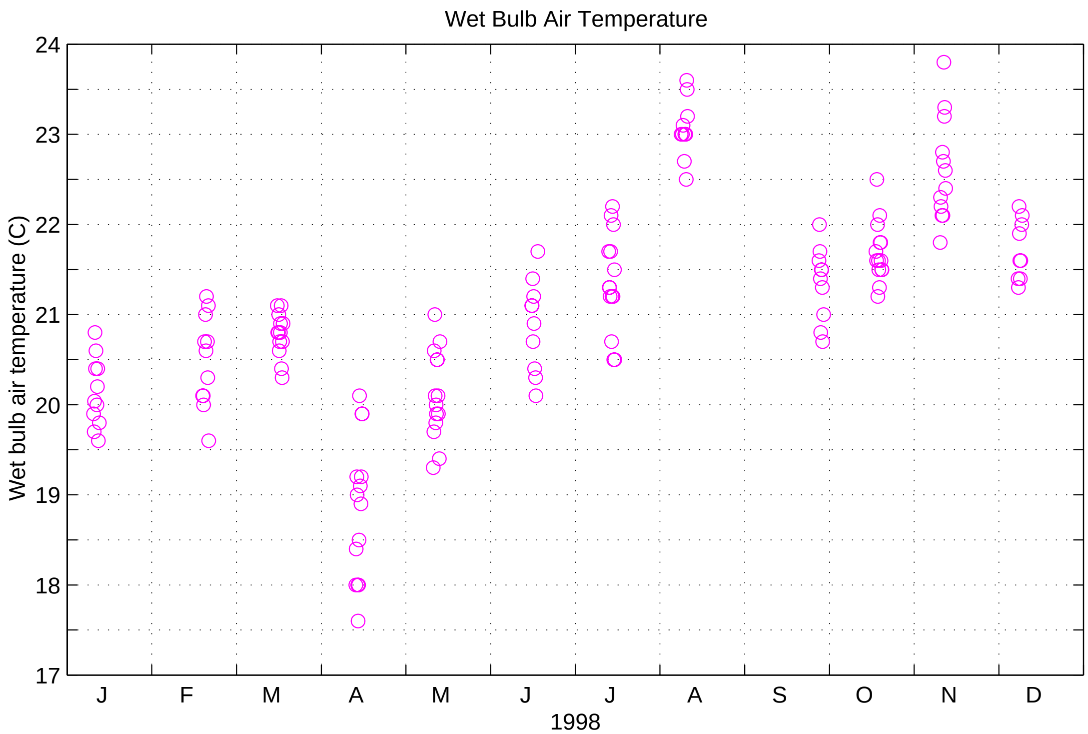
Wet Bulb Air Temperature
Wet bulb air temperature (C)
24
23
22
21
20
19
18
17
J F M A M J J A S O N D
1998

FIGURE 6.3.2.

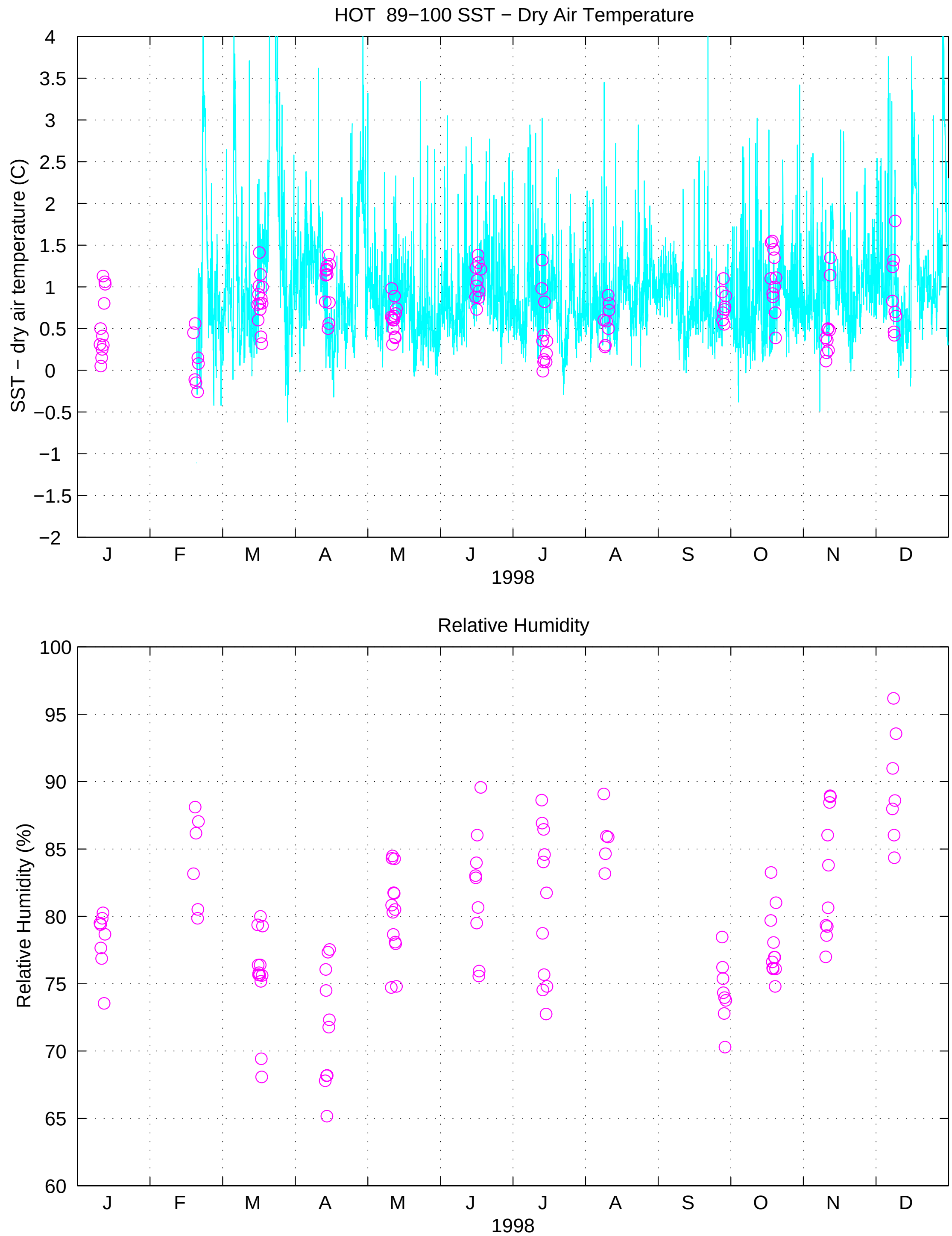
HOT 89−100 SST − Dry Air Temperature
SST − dry air temperature (C)
4
3.5
3
2.5
2
1.5
1
0.5
0
−0.5
−1
−1.5
−2
J F M A M J J A S O N D
1998
Relative Humidity
Relative Humidity (%)
100
95
90
85
80
75
70
65
60
J F M A M J J A S O N D
1998

FIGURE 6.3.3.

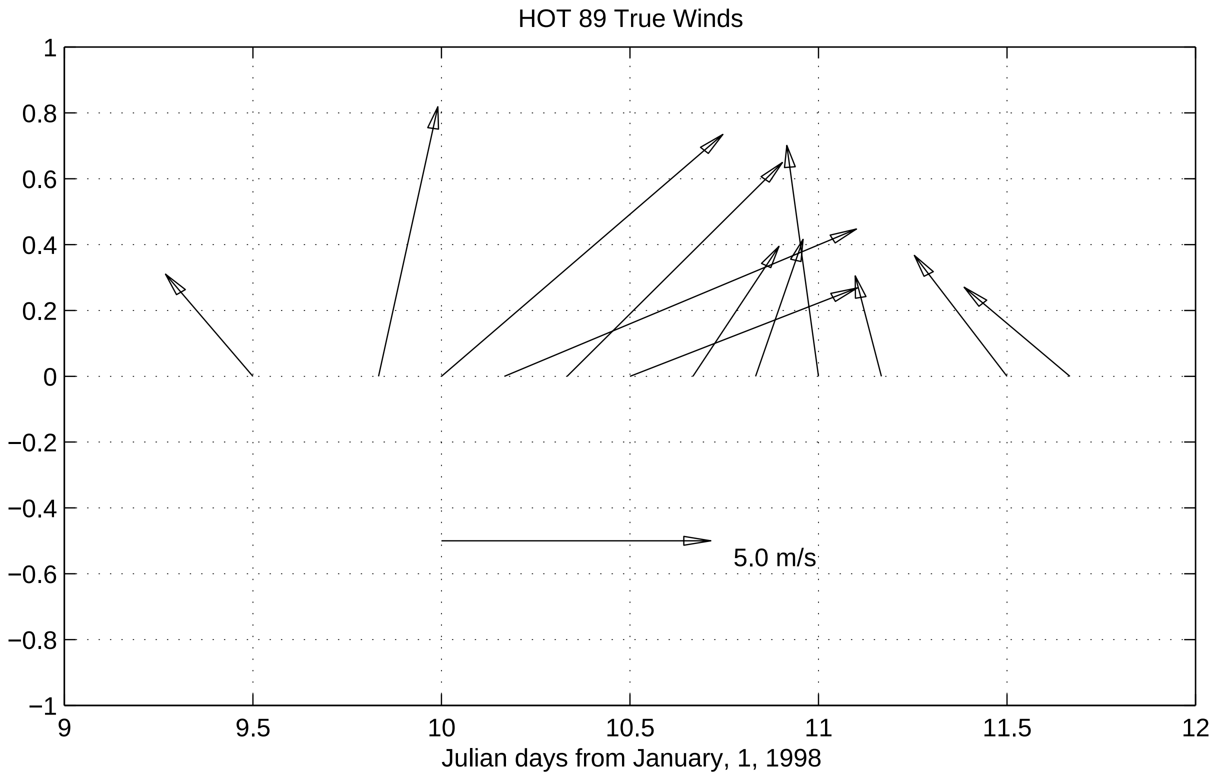
HOT 89 True Winds
1
0.8
0.6
0.4
0.2
0
−0.2
−0.4
−0.6
−0.8
−1
9
9.5
10
10.5
11
11.5
12
Julian days from January, 1, 1998
5.0 m/s

FIGURE 6.3.4a.

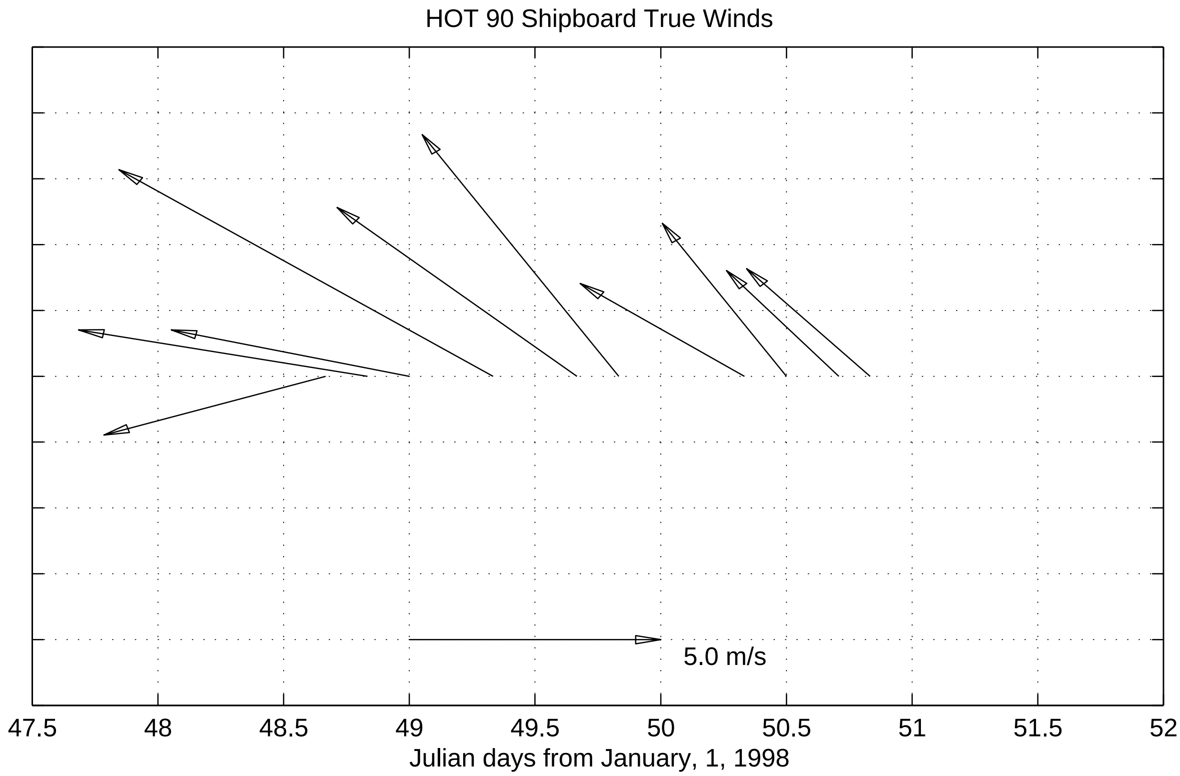
HOT 90 Shipboard True Winds
5.0 m/s
47.5
48
48.5
49
49.5
50
50.5
51
51.5
52
Julian days from January, 1, 1998

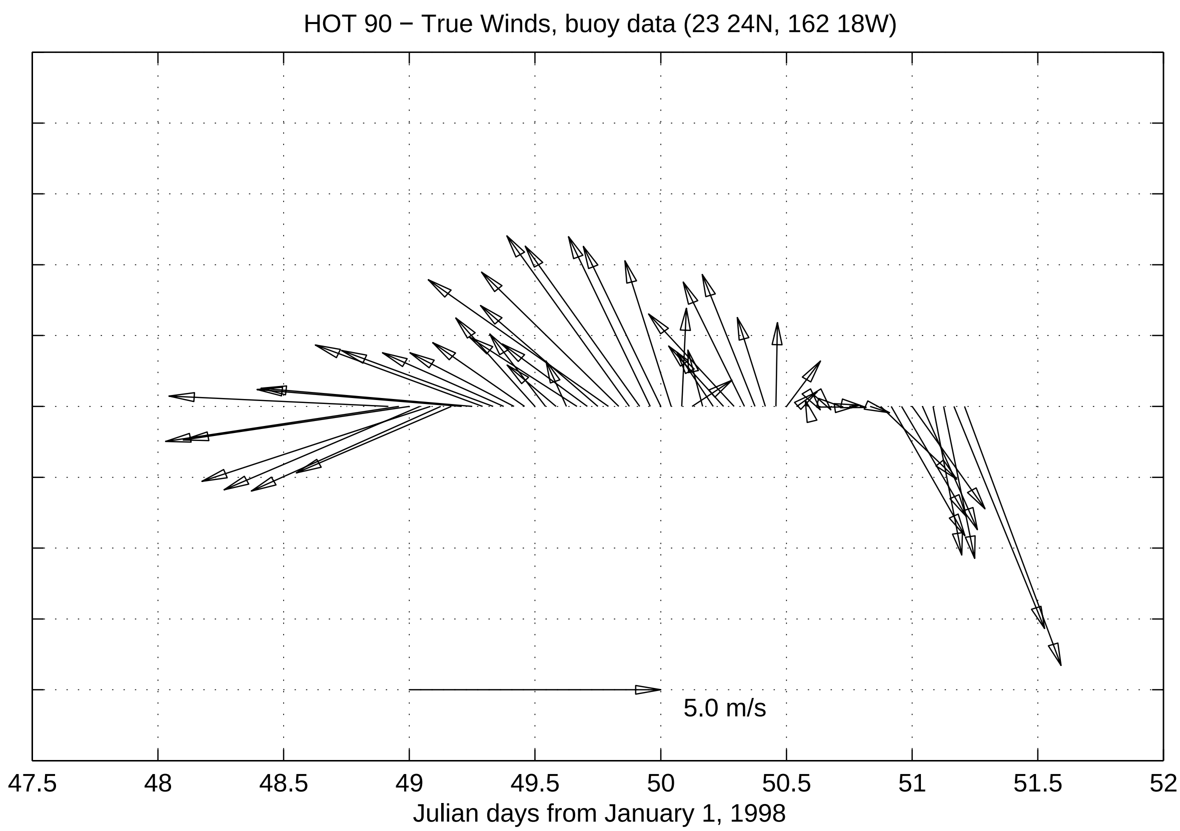
HOT 90 − True Winds, buoy data (23 24N, 162 18W)
5.0 m/s
47.5
48
48.5
49
49.5
50
50.5
51
51.5
52
Julian days from January 1, 1998

FIGURE 6.3.4b.

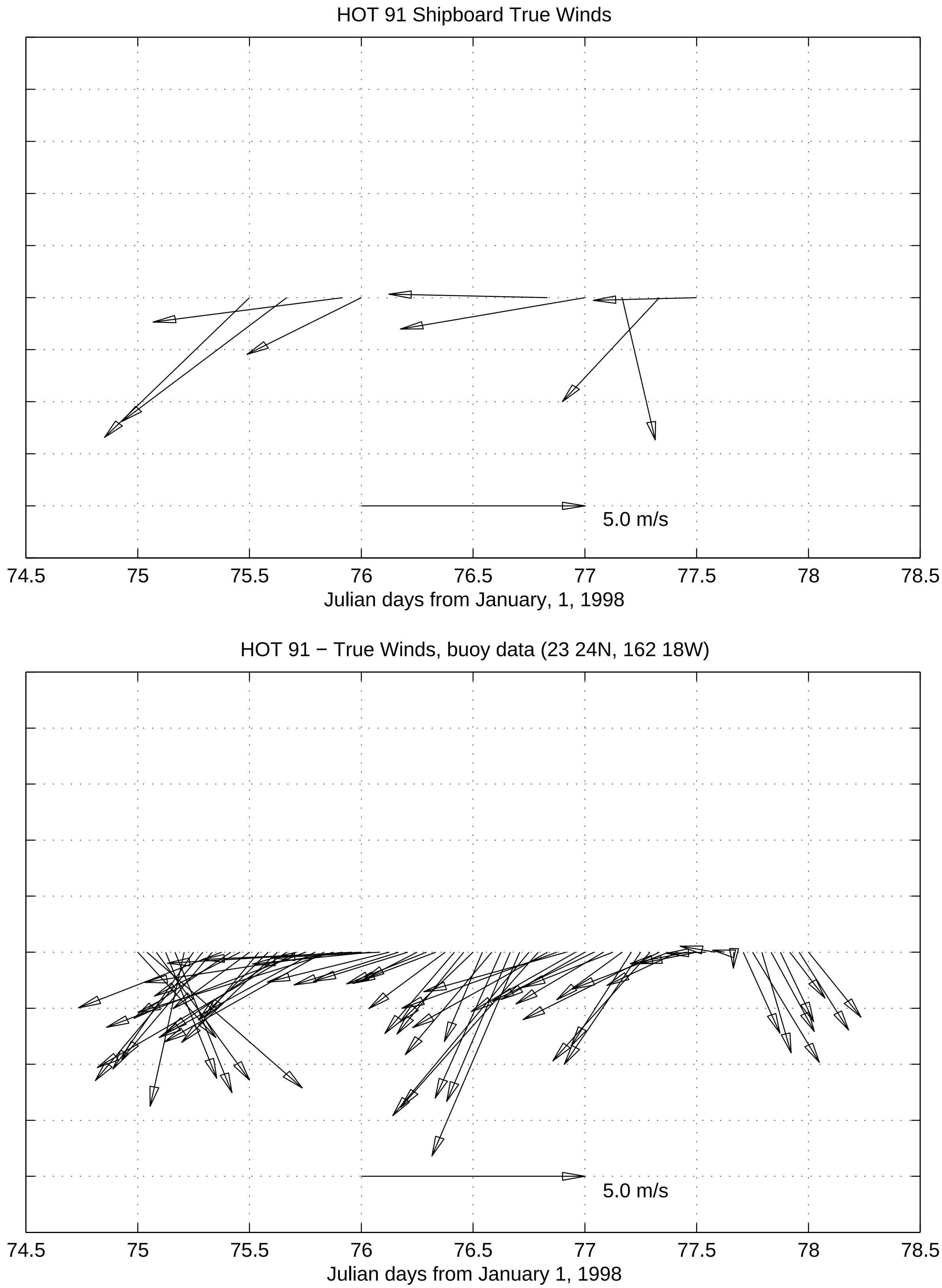
HOT 91 Shipboard True Winds
5.0 m/s
74.5
75
75.5
76
76.5
77
77.5
78
78.5
Julian days from January, 1, 1998
HOT 91 − True Winds, buoy data (23 24N, 162 18W)
5.0 m/s
74.5
75
75.5
76
76.5
77
77.5
78
78.5
Julian days from January 1, 1998

FIGURE 6.3.4c.

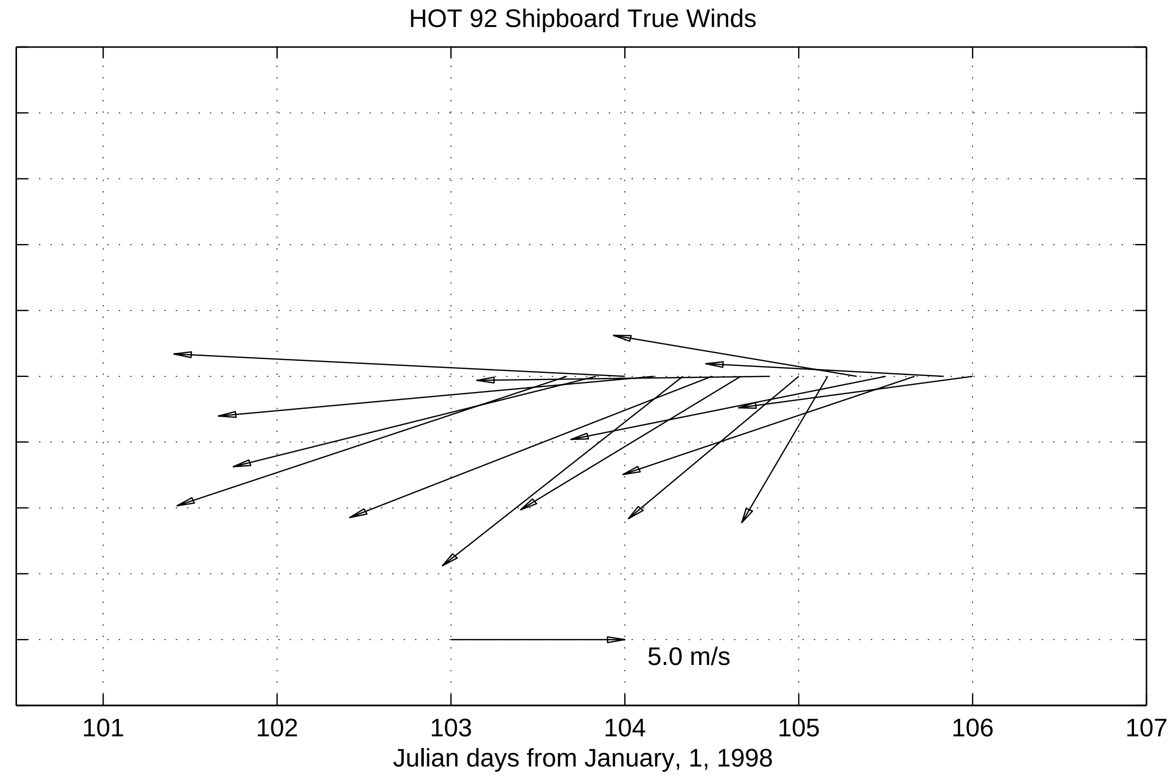
HOT 92 Shipboard True Winds
5.0 m/s
101
102
103
104
105
106
107
Julian days from January, 1, 1998

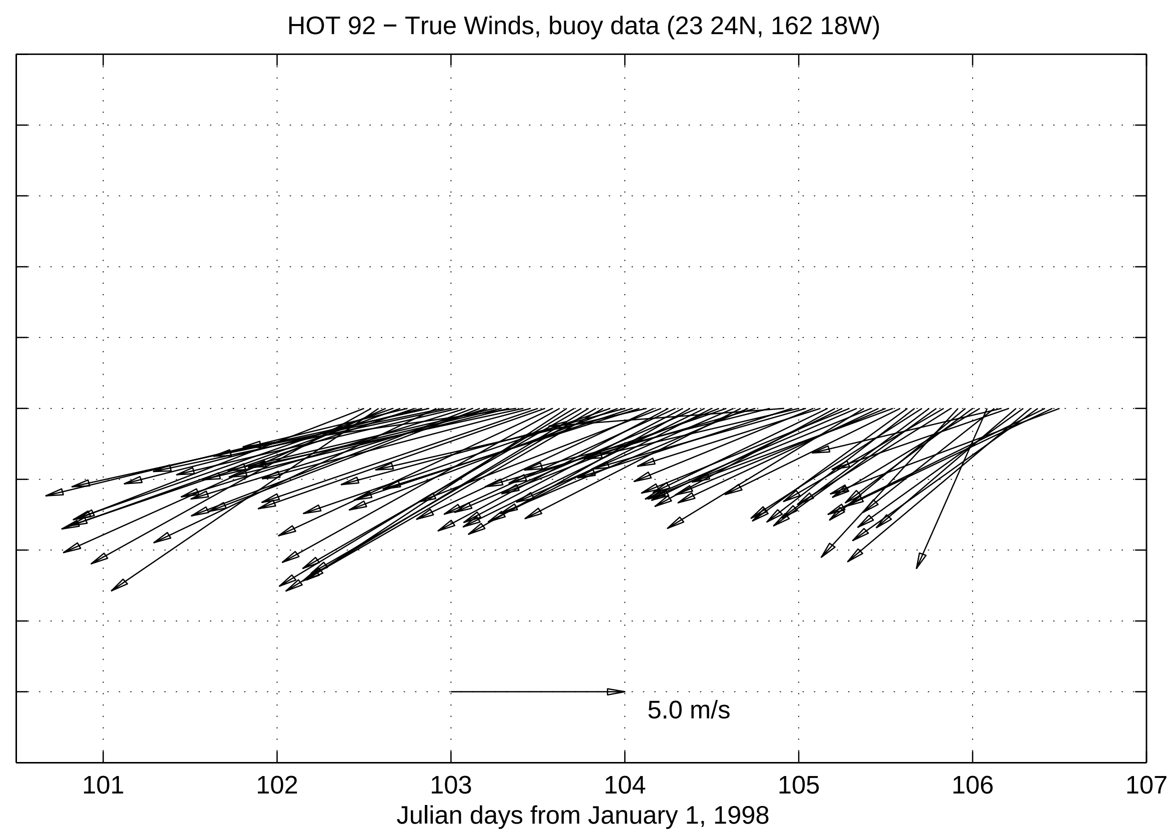
HOT 92 − True Winds, buoy data (23 24N, 162 18W)
5.0 m/s
101
102
103
104
105
106
107
Julian days from January 1, 1998

FIGURE 6.3.4d.

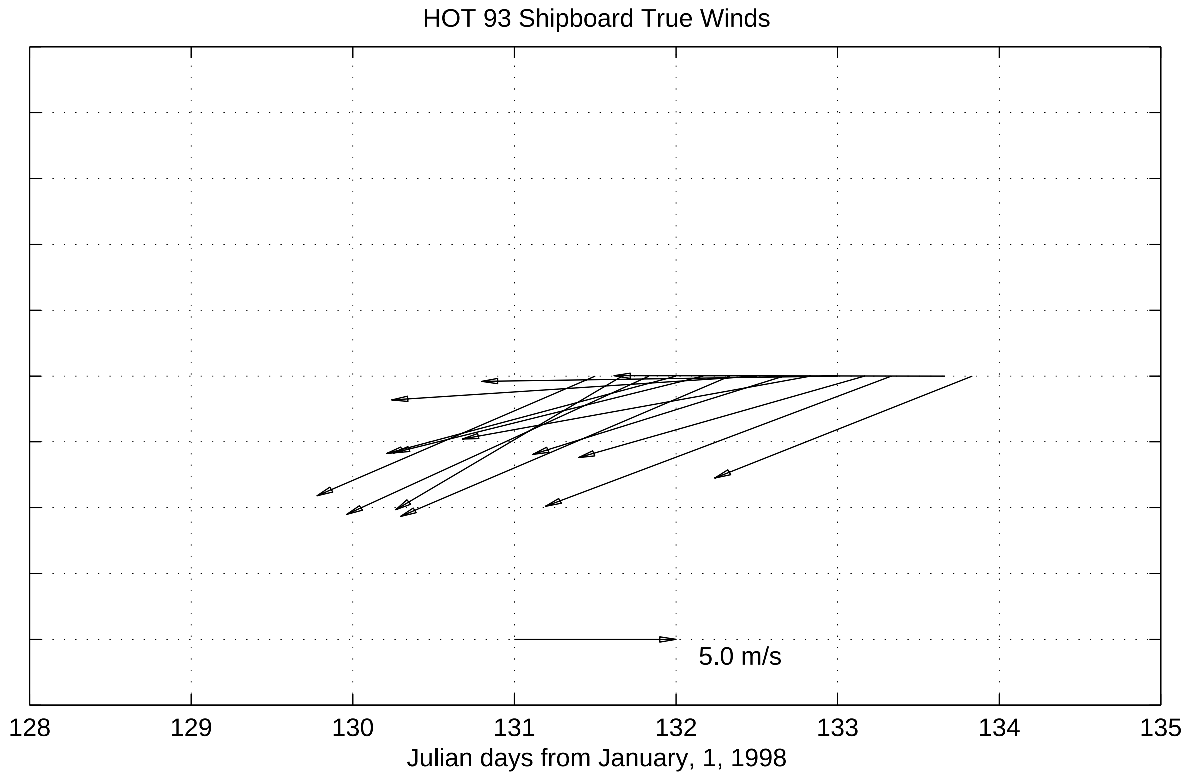
HOT 93 Shipboard True Winds
5.0 m/s
128
129
130
131
132
133
134
135
Julian days from January, 1, 1998

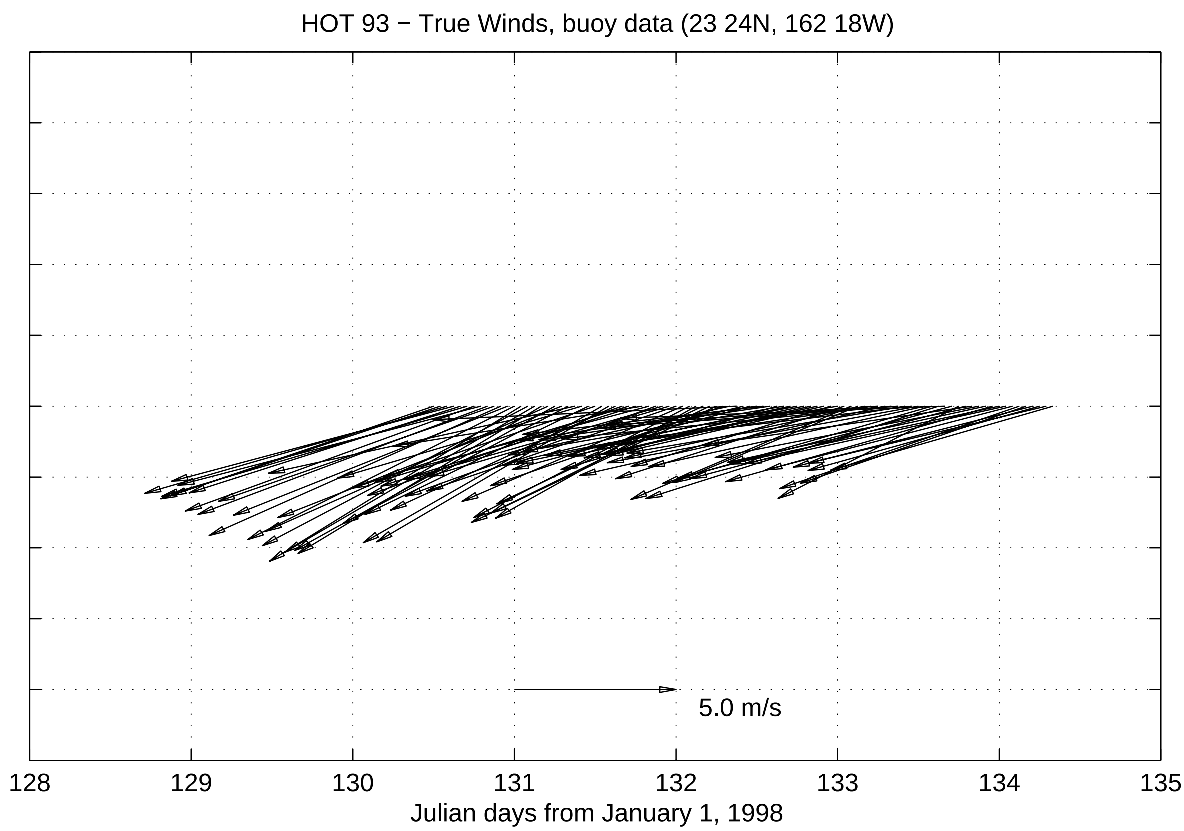
HOT 93 − True Winds, buoy data (23 24N, 162 18W)
5.0 m/s
128
129
130
131
132
133
134
135
Julian days from January 1, 1998

FIGURE 6.3.4e.

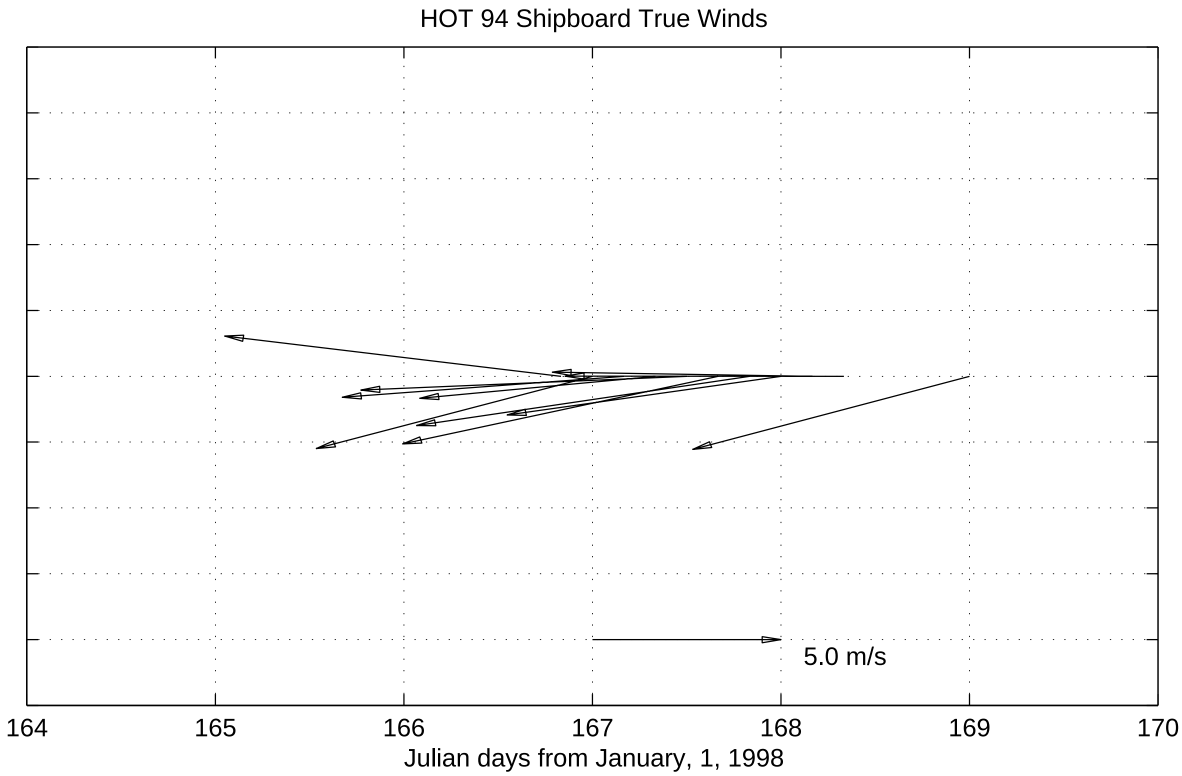
HOT 94 Shipboard True Winds
5.0 m/s
164
165
166
167
168
169
170
Julian days from January, 1, 1998

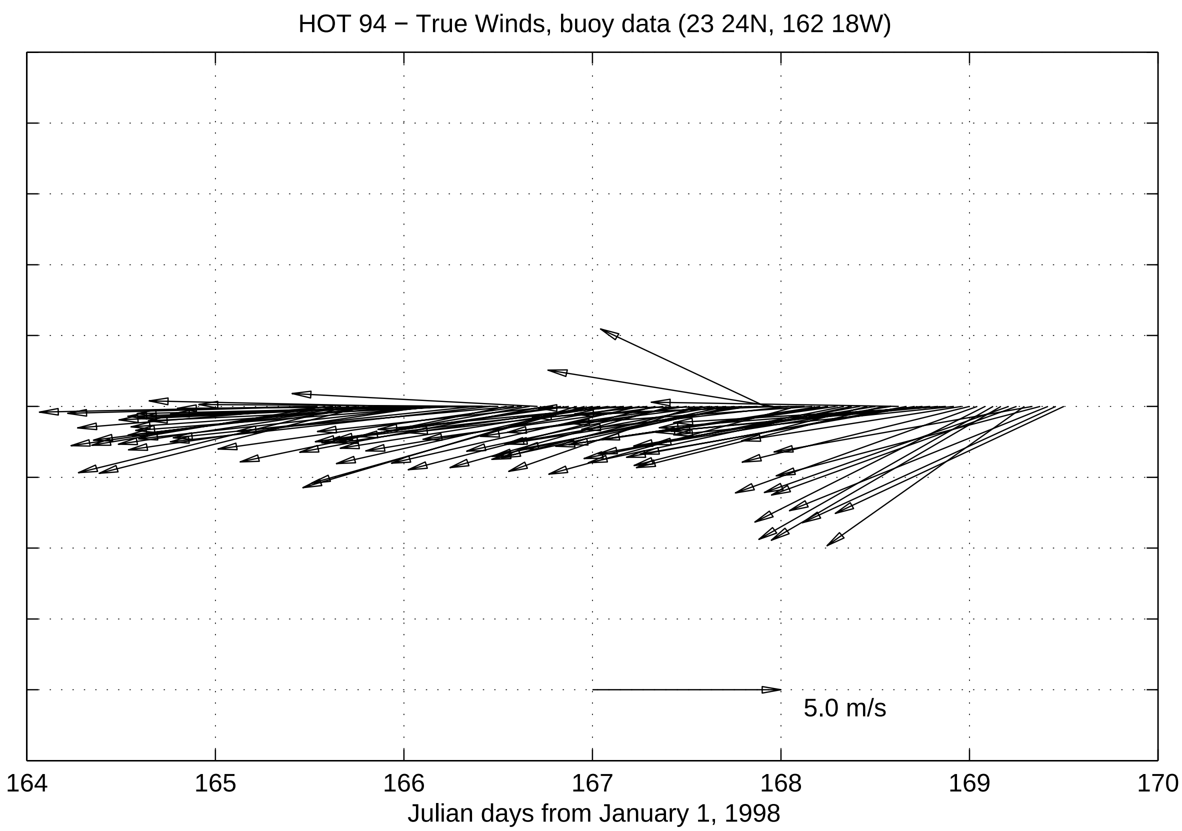
HOT 94 − True Winds, buoy data (23 24N, 162 18W)
5.0 m/s
164
165
166
167
168
169
170
Julian days from January 1, 1998

FIGURE 6.3.4f.

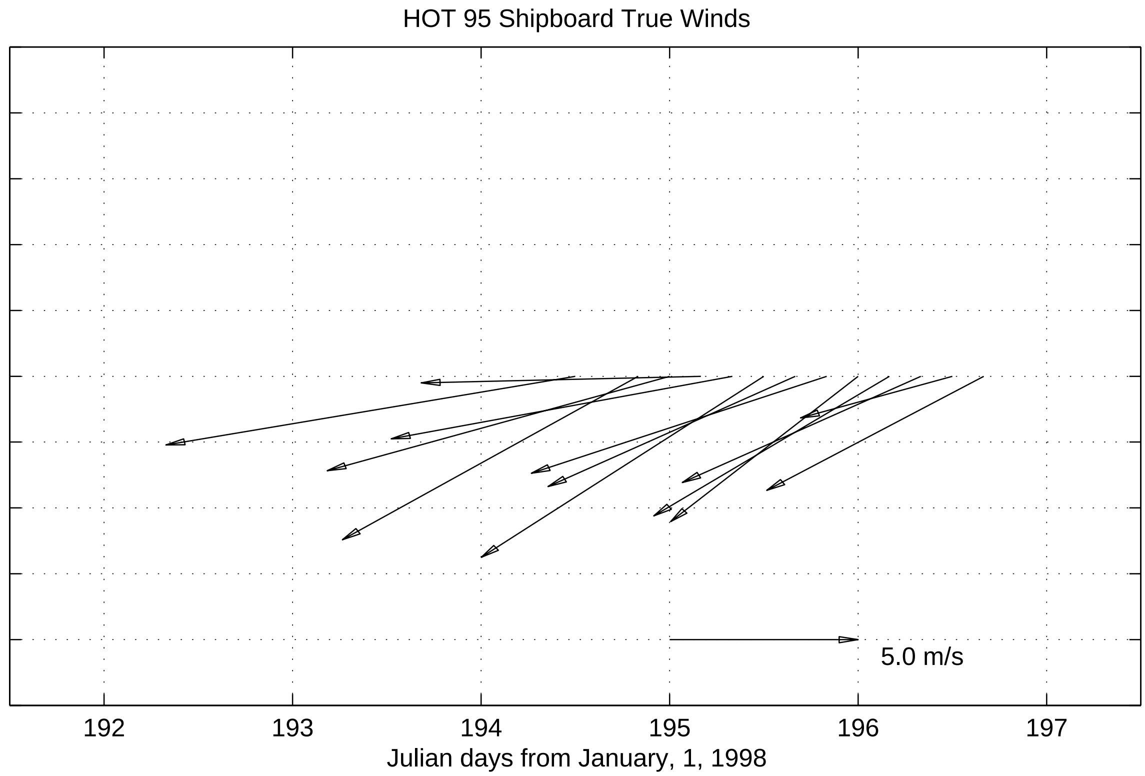
HOT 95 Shipboard True Winds
5.0 m/s
192
193
194
195
196
197
Julian days from January, 1, 1998

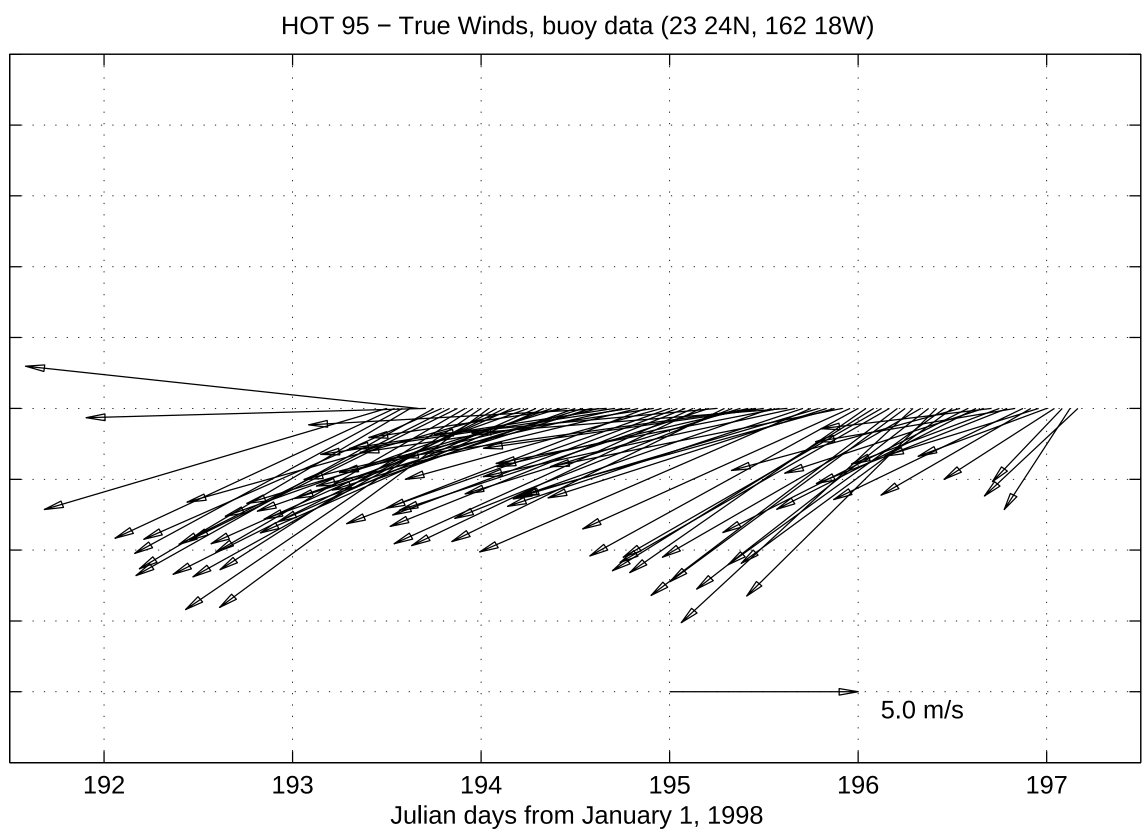
HOT 95 − True Winds, buoy data (23 24N, 162 18W)
5.0 m/s
192
193
194
195
196
197
Julian days from January 1, 1998

FIGURE 6.3.4g.

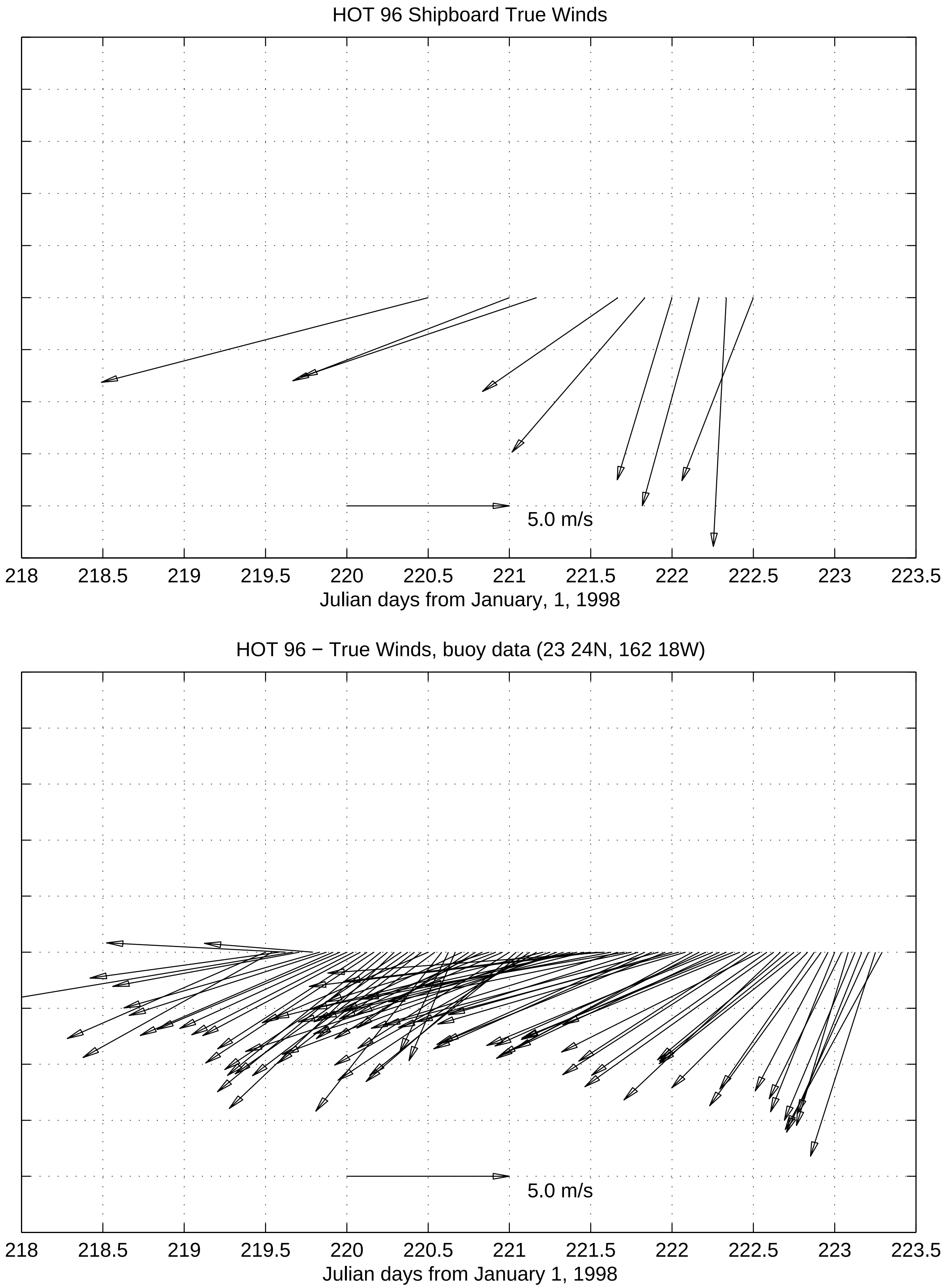
HOT 96 Shipboard True Winds
5.0 m/s
218
218.5
219
219.5
220
220.5
221
221.5
222
222.5
223
223.5
Julian days from January, 1, 1998
HOT 96 − True Winds, buoy data (23 24N, 162 18W)
5.0 m/s
218
218.5
219
219.5
220
220.5
221
221.5
222
222.5
223
223.5
Julian days from January 1, 1998

FIGURE 6.3.4h.

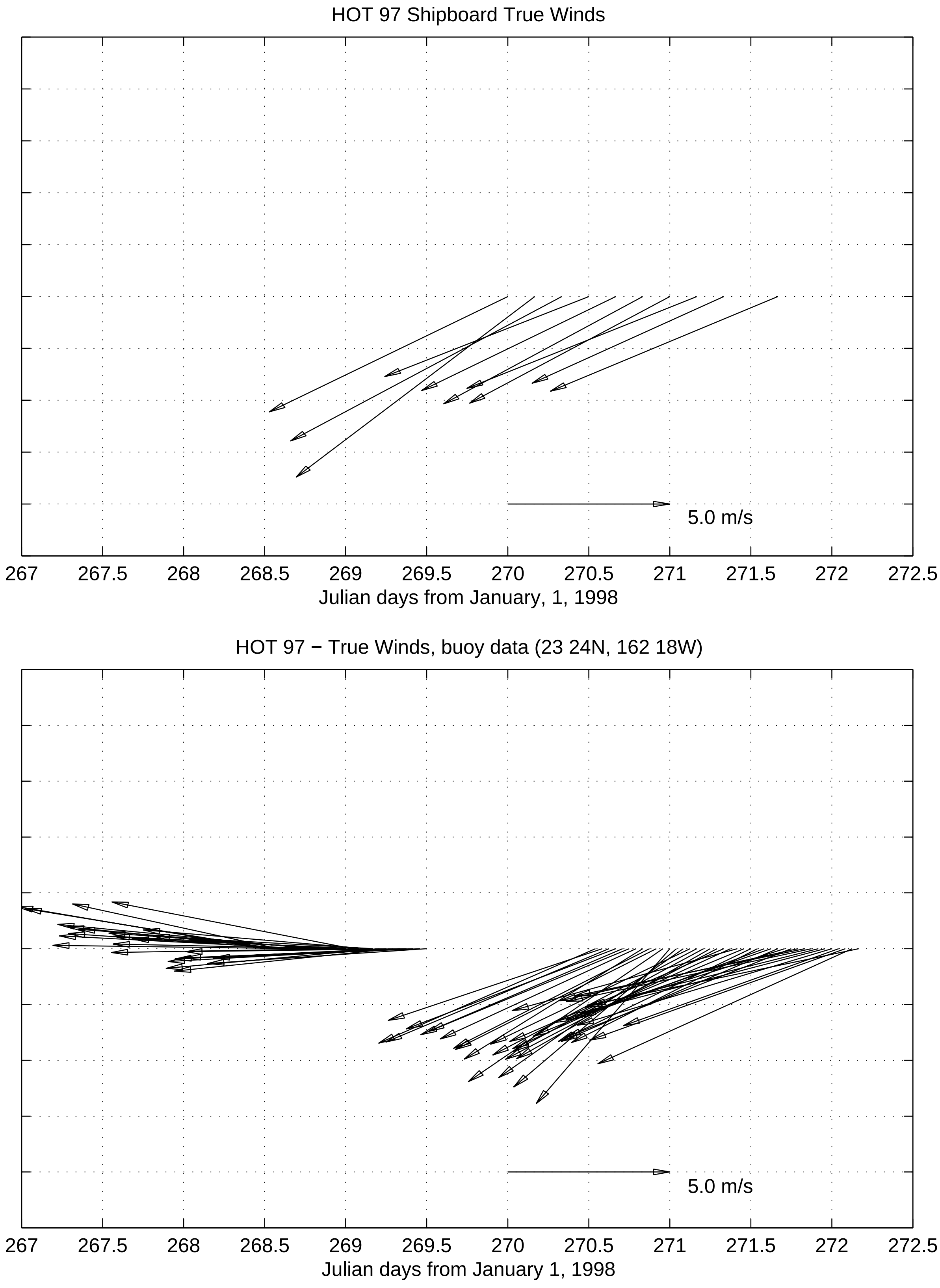
HOT 97 Shipboard True Winds
5.0 m/s
267
267.5
268
268.5
269
269.5
270
270.5
271
271.5
272
272.5
Julian days from January, 1, 1998
HOT 97 − True Winds, buoy data (23 24N, 162 18W)
5.0 m/s
267
267.5
268
268.5
269
269.5
270
270.5
271
271.5
272
272.5
Julian days from January 1, 1998

FIGURE 6.3.4i.

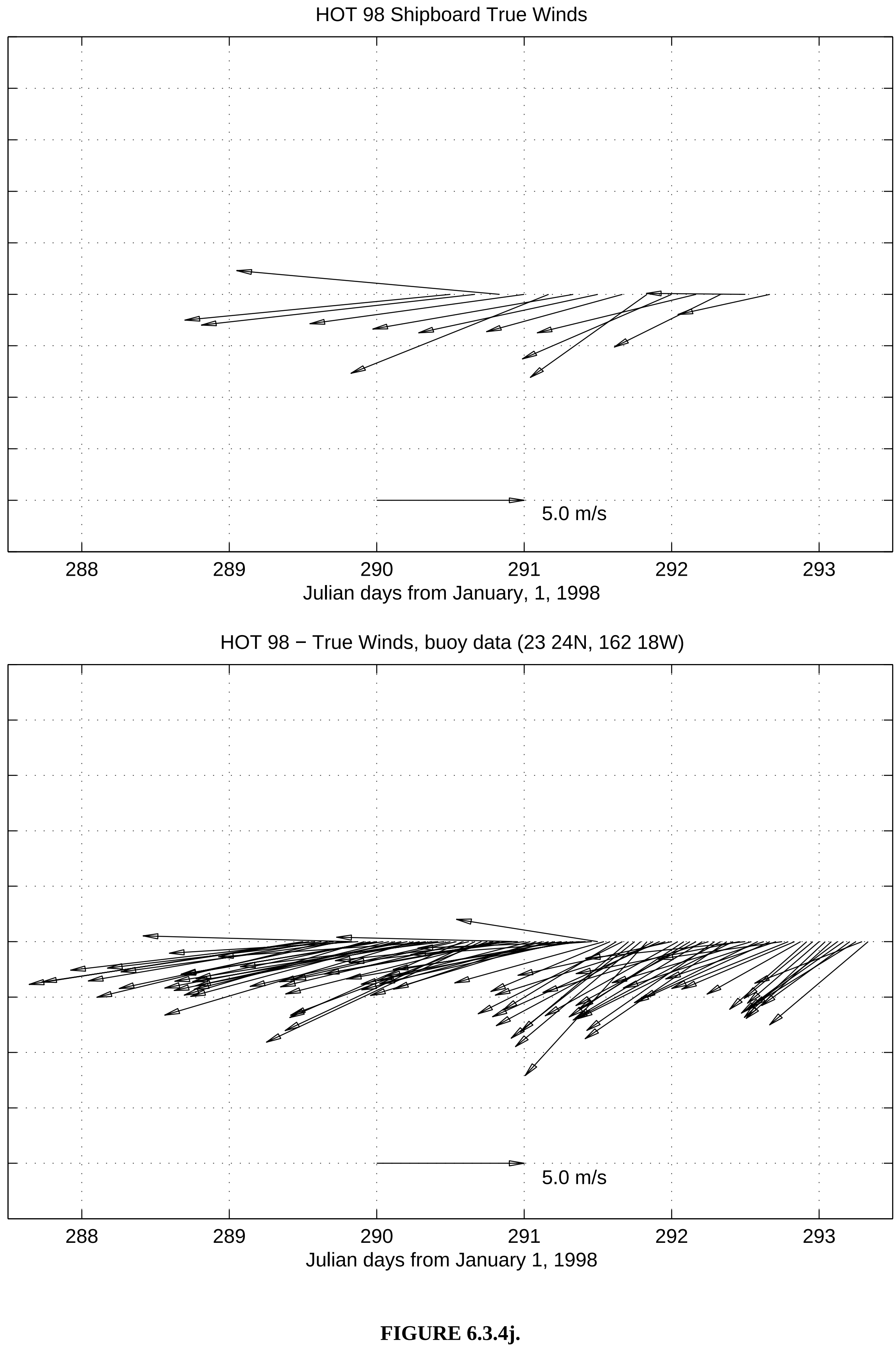
HOT 98 Shipboard True Winds
5.0 m/s
288
289
290
291
292
293
Julian days from January, 1, 1998
HOT 98 − True Winds, buoy data (23 24N, 162 18W)
5.0 m/s
288
289
290
291
292
293
Julian days from January 1, 1998

FIGURE 6.3.4j.

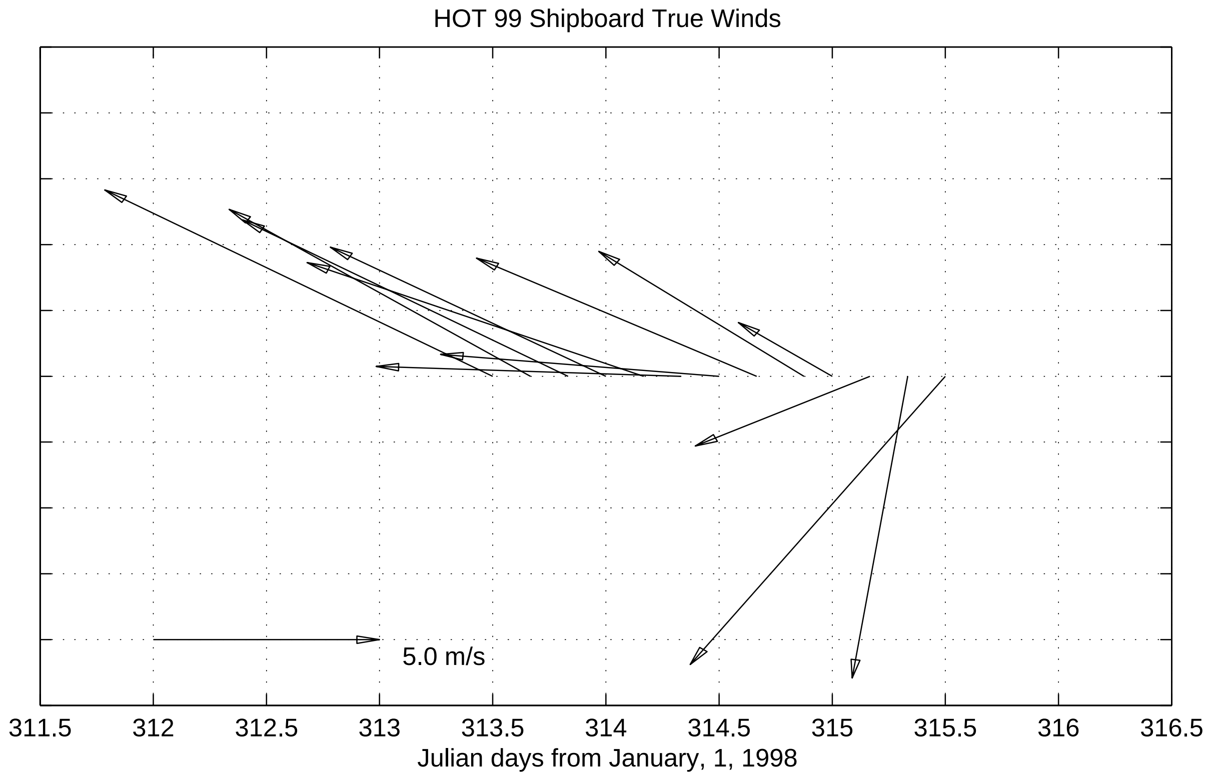
HOT 99 Shipboard True Winds
5.0 m/s
311.5
312
312.5
313
313.5
314
314.5
315
315.5
316
316.5
Julian days from January, 1, 1998

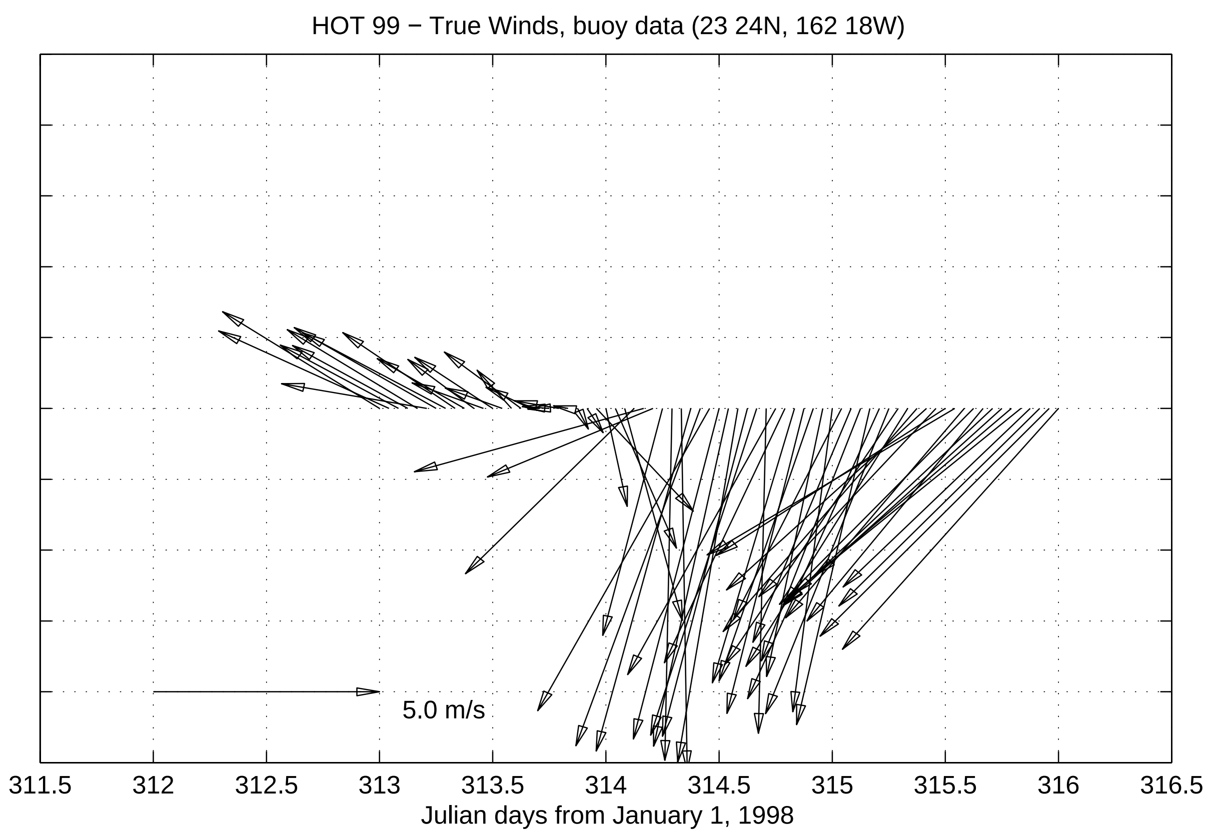
HOT 99 − True Winds, buoy data (23 24N, 162 18W)
5.0 m/s
311.5
312
312.5
313
313.5
314
314.5
315
315.5
316
316.5
Julian days from January 1, 1998

FIGURE 6.3.4k.

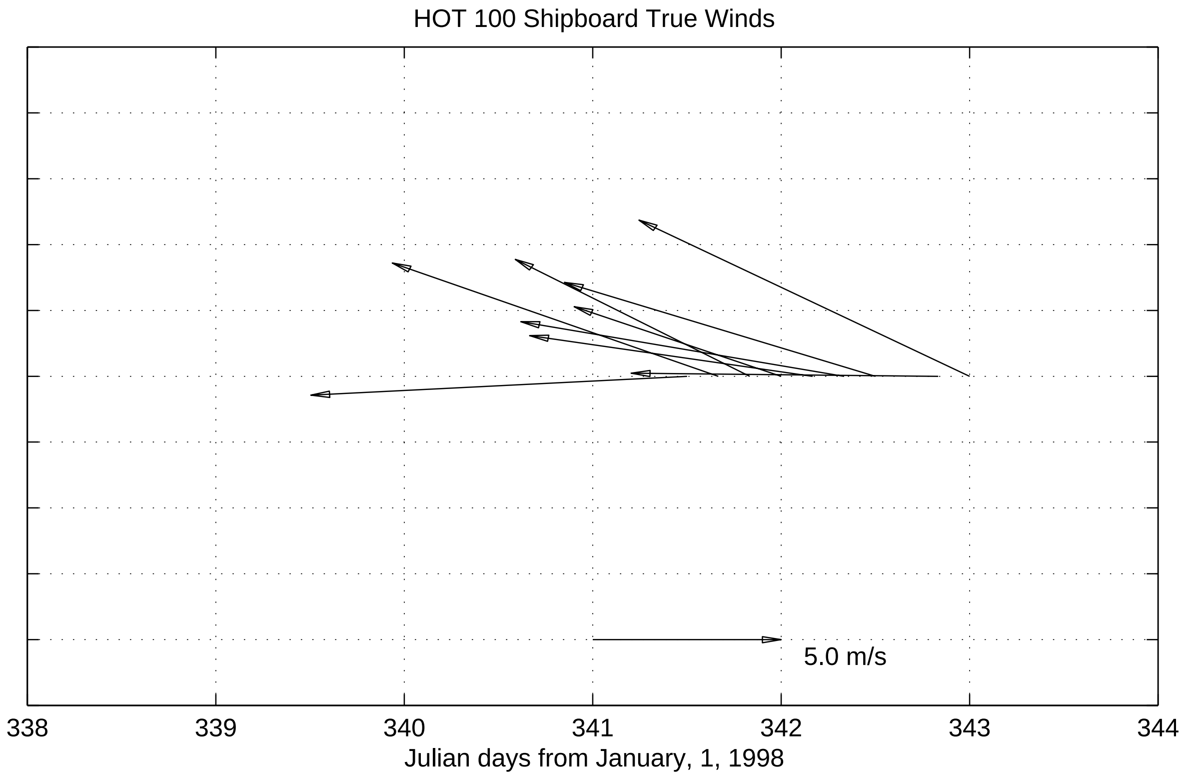
HOT 100 Shipboard True Winds
5.0 m/s
338
339
340
341
342
343
344
Julian days from January, 1, 1998

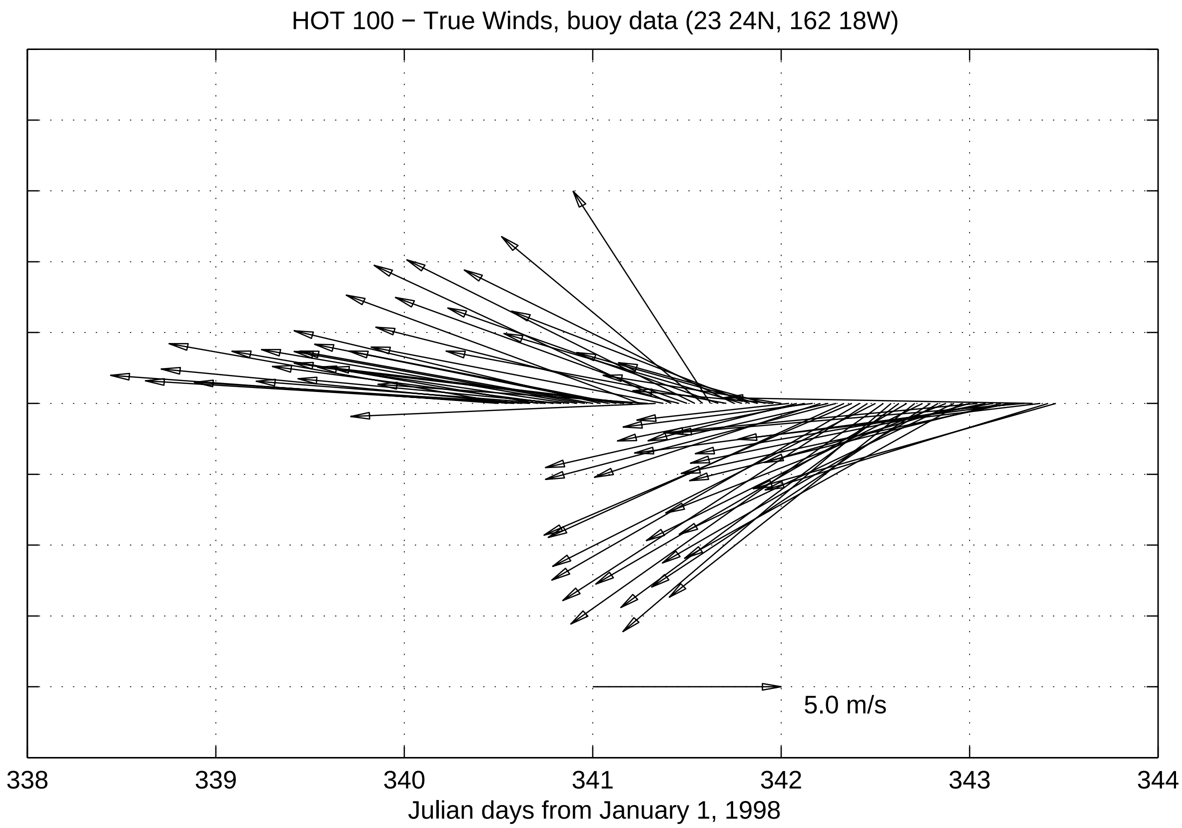
HOT 100 − True Winds, buoy data (23 24N, 162 18W)
5.0 m/s
338
339
340
341
342
343
344
Julian days from January 1, 1998

FIGURE 6.3.4l.

6.4 ADCP Measurements

Figures 6.4.1a-m: Velocity fields at Station ALOHA. Top panel shows hourly averages at 20-m depth intervals while the ship was on station. the orientation of each stick gives the direction of the current: up is northward and to the right is eastward. The bottom panel shows the results of a least-squares fit of hourly averages to a mean, trend, semi-diurnal and diurnal tides; the on-station time-series were not long enough to fit an inertial cycle. In the first column the arrow show the mean current and the headless stick shows the sum of the mean plus the trend at the end of the station. For each harmonic the current ellipse is shown in the first column. the orientation of the stick in the second column shows the direction of the harmonic component of the current at the beginning of the station and the arrowhead at the end of the stick shows the direction of rotation of the current vector around the ellipse. The gaps in the station data of HOT-96 and HOT-97 are due to excursions to retrieve the primary productivity array and floating sediment traps. Cruise HOT-100B was an extension of HOT-100 (see Section 3.12 in the text).

Figures 6.4.2a-m: Velocity fields on the transits to and from Station ALOHA and Station 8. Velocity is shown as a function of latitude averaged in 10-minute intervals.

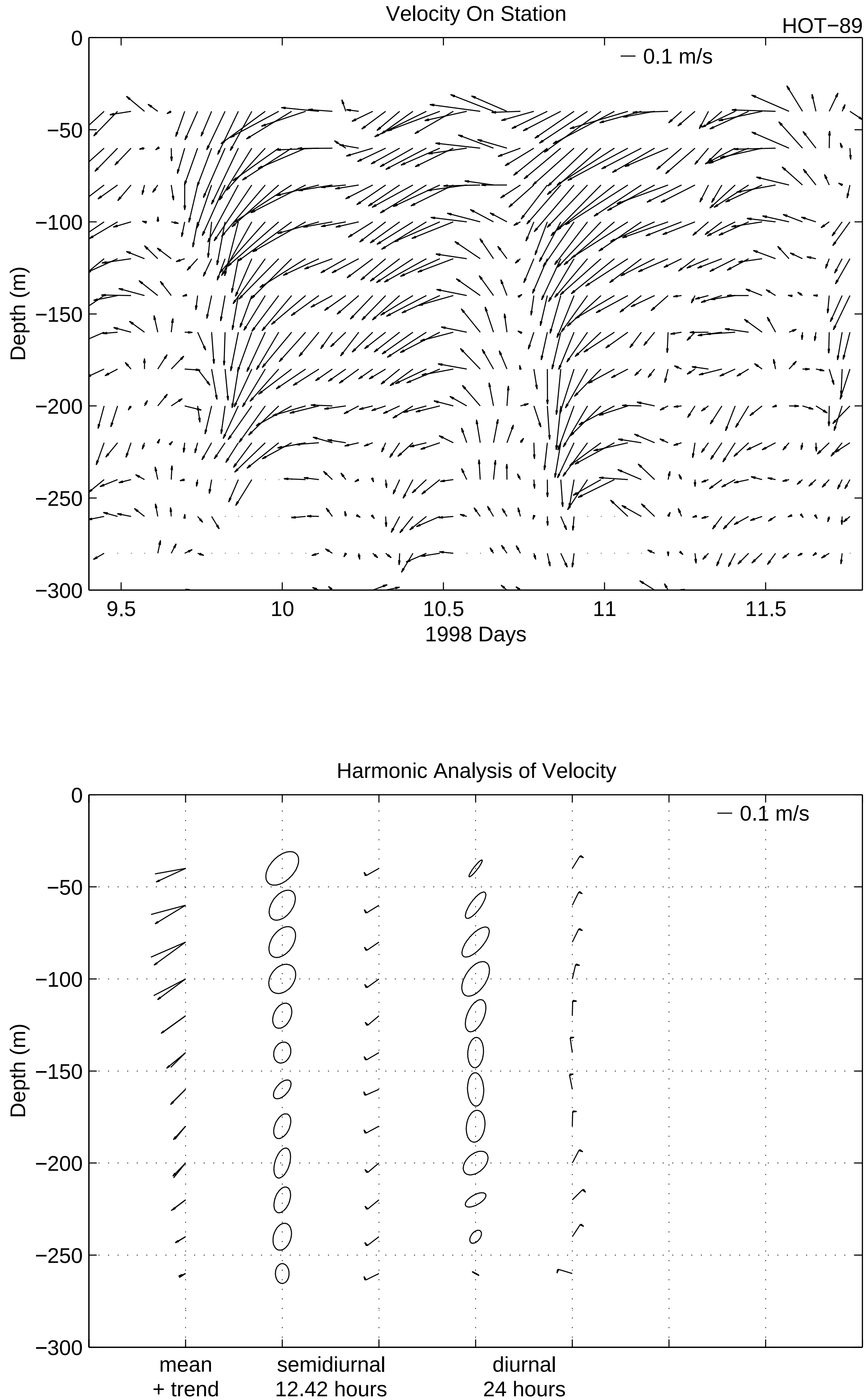
Velocity On Station
HOT−89
0.1 m/s
Depth (m)
0
−50
−100
−150
−200
−250
−300
9.5
10
10.5
11
11.5
1998 Days
Harmonic Analysis of Velocity
0.1 m/s
Depth (m)
mean
+ trend
semidiurnal
12.42 hours
diurnal
24 hours

FIGURE 6.4.1a.

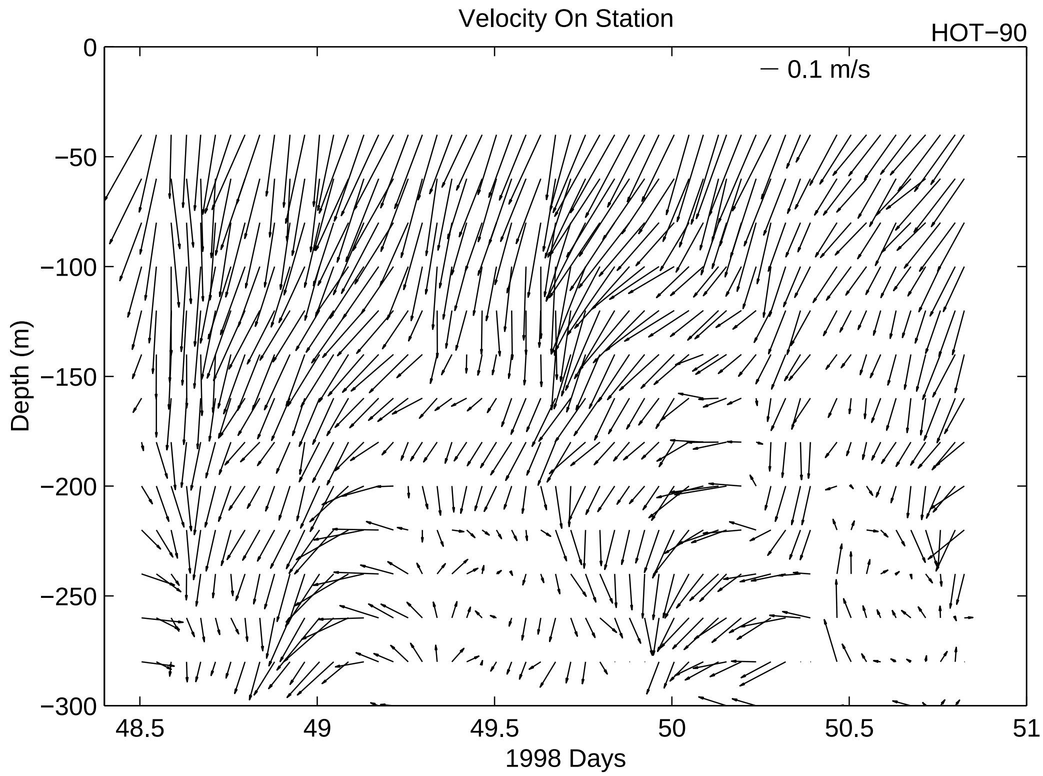

Velocity On Station
HOT−90
0.1 m/s
Depth (m)
0
−50
−100
−150
−200
−250
−300
48.5
49
49.5
50
50.5
51
1998 Days

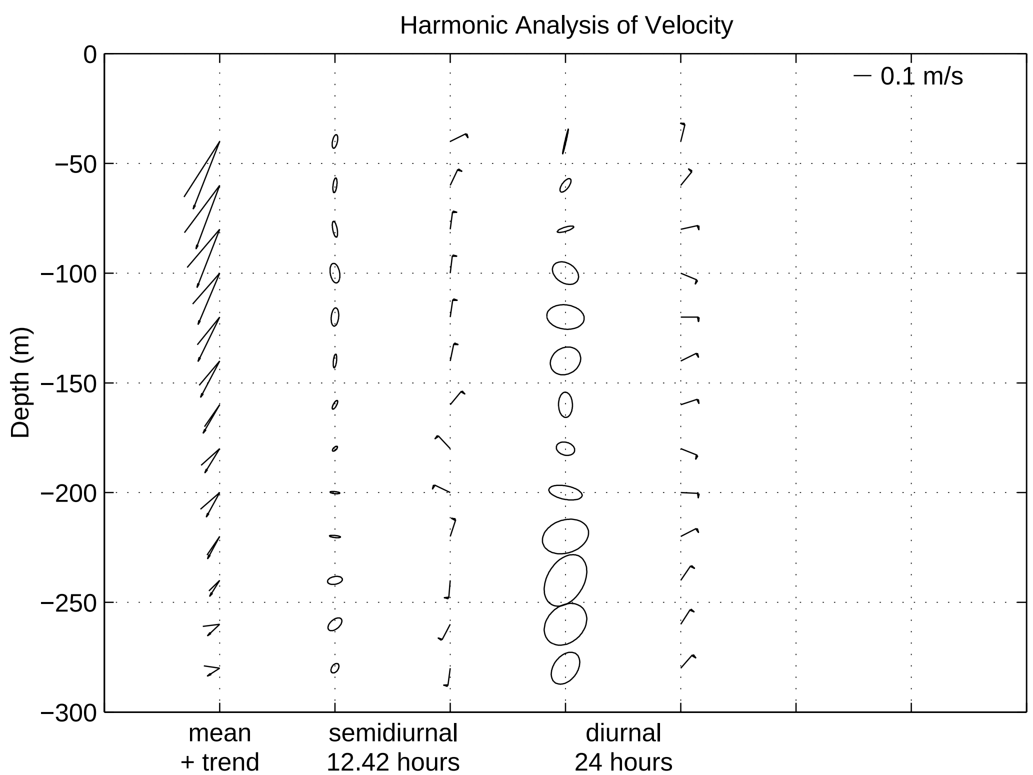

Harmonic Analysis of Velocity
0.1 m/s
Depth (m)
0
−50
−100
−150
−200
−250
−300
mean
+ trend
semidiurnal
12.42 hours
diurnal
24 hours

FIGURE 6.4.1b.

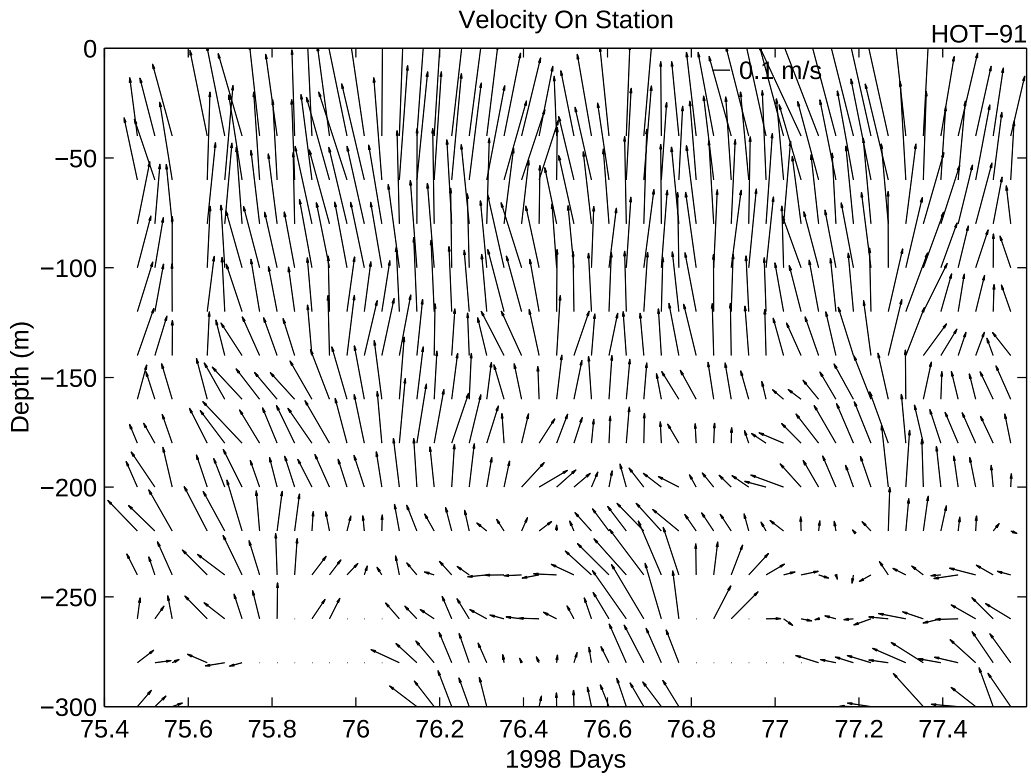
Velocity On Station
HOT−91
0.1 m/s
Depth (m)
0
−50
−100
−150
−200
−250
−300
75.4
75.6
75.8
76
76.2
76.4
76.6
76.8
77
77.2
77.4
1998 Days

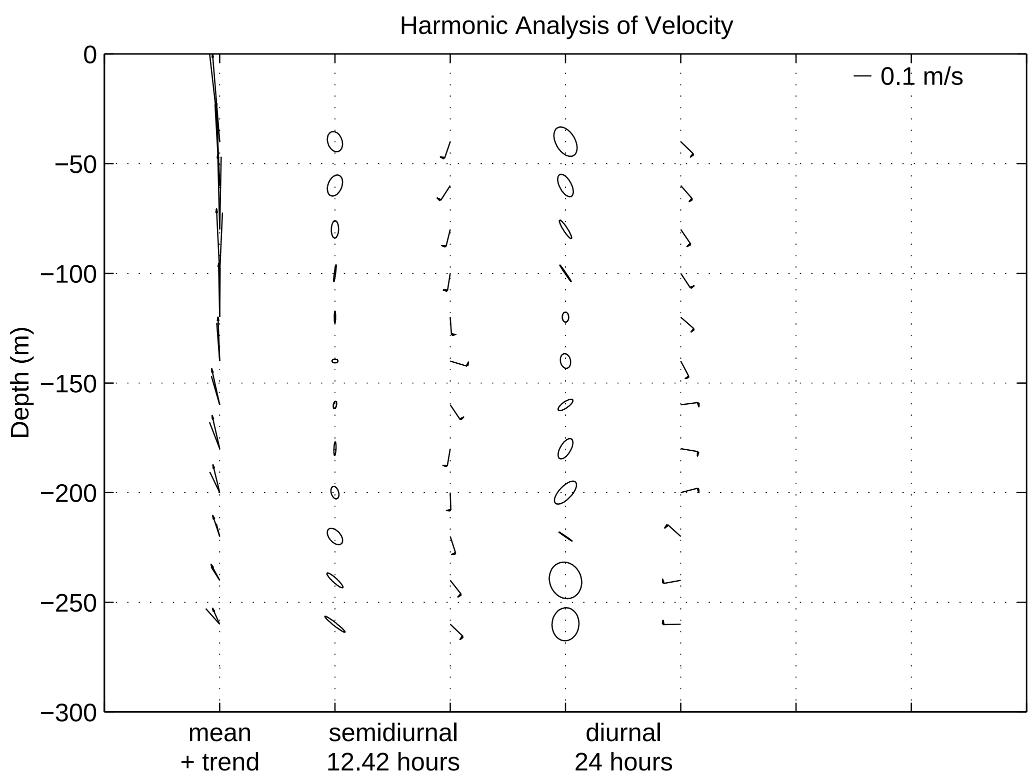
Harmonic Analysis of Velocity
0.1 m/s
Depth (m)
0
−50
−100
−150
−200
−250
−300
mean
+ trend
semidiurnal
12.42 hours
diurnal
24 hours

FIGURE 6.4.1c.

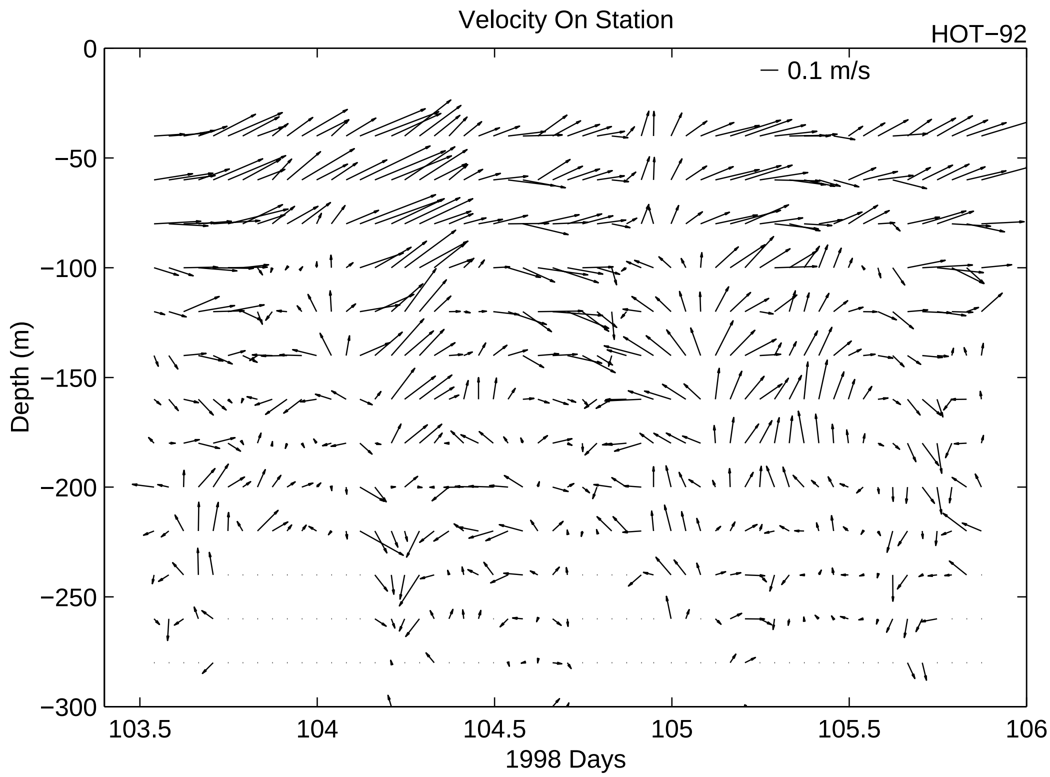

Velocity On Station
HOT−92
0.1 m/s
Depth (m)
0
−50
−100
−150
−200
−250
−300
103.5
104
104.5
105
105.5
106
1998 Days

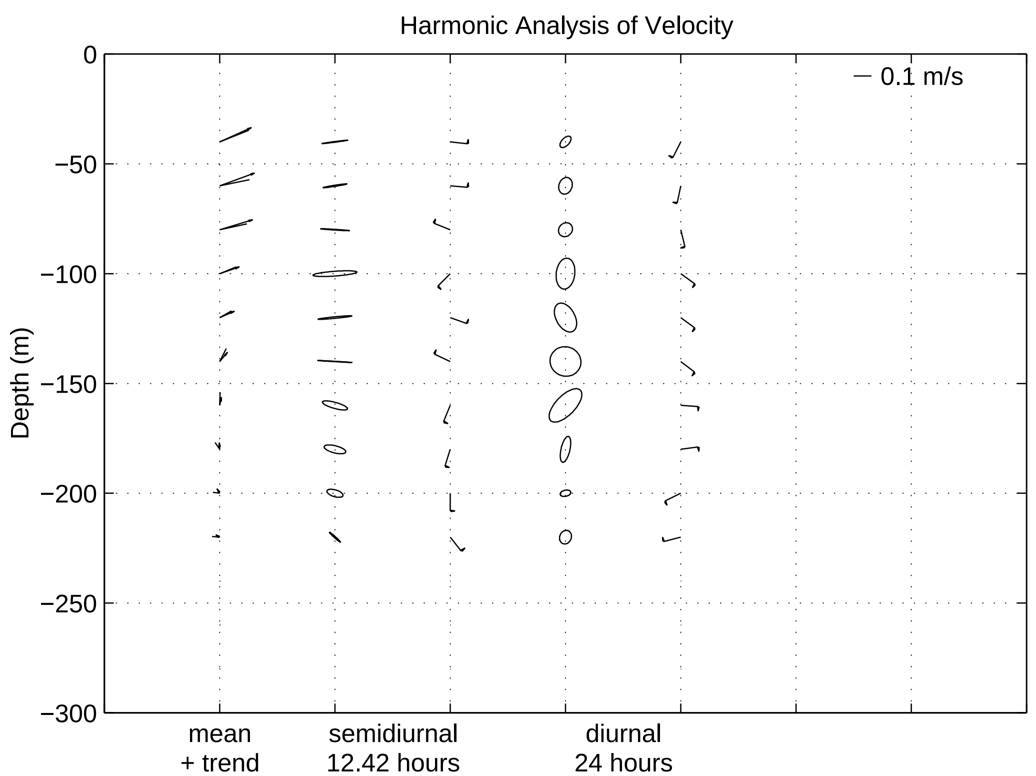

Harmonic Analysis of Velocity
0.1 m/s
Depth (m)
0
−50
−100
−150
−200
−250
−300
mean
+ trend
semidiurnal
12.42 hours
diurnal
24 hours

FIGURE 6.4.1d.

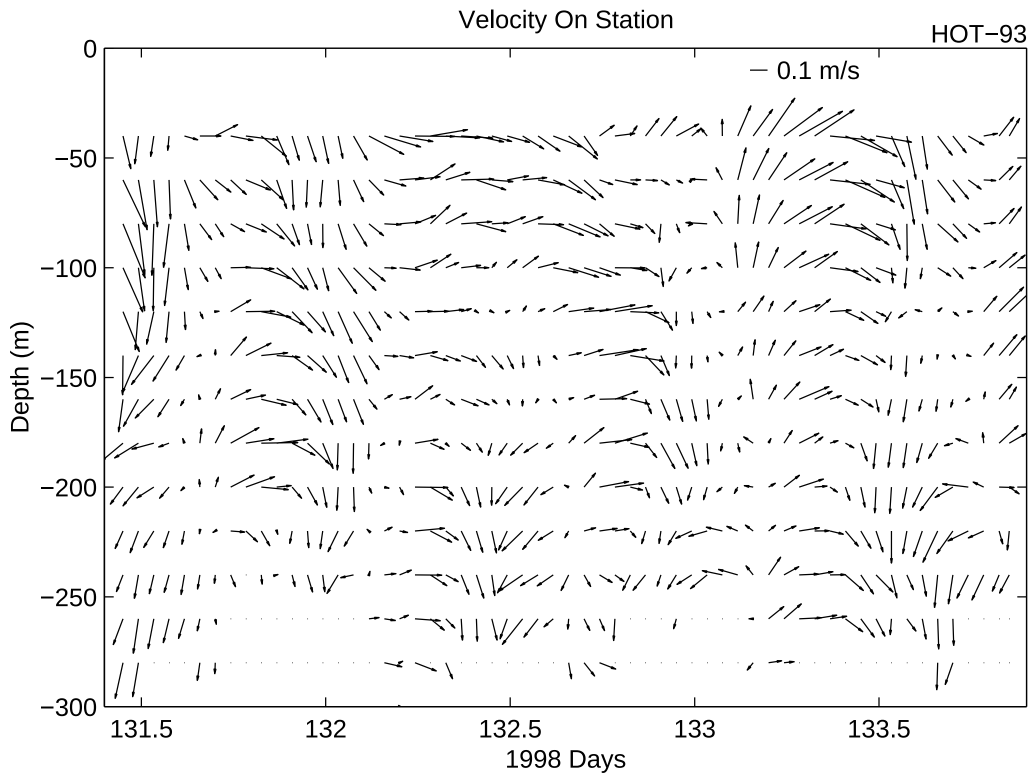
Velocity On Station
HOT−93
0.1 m/s
0
−50
−100
−150
−200
−250
−300
Depth (m)
131.5
132
132.5
133
133.5
1998 Days

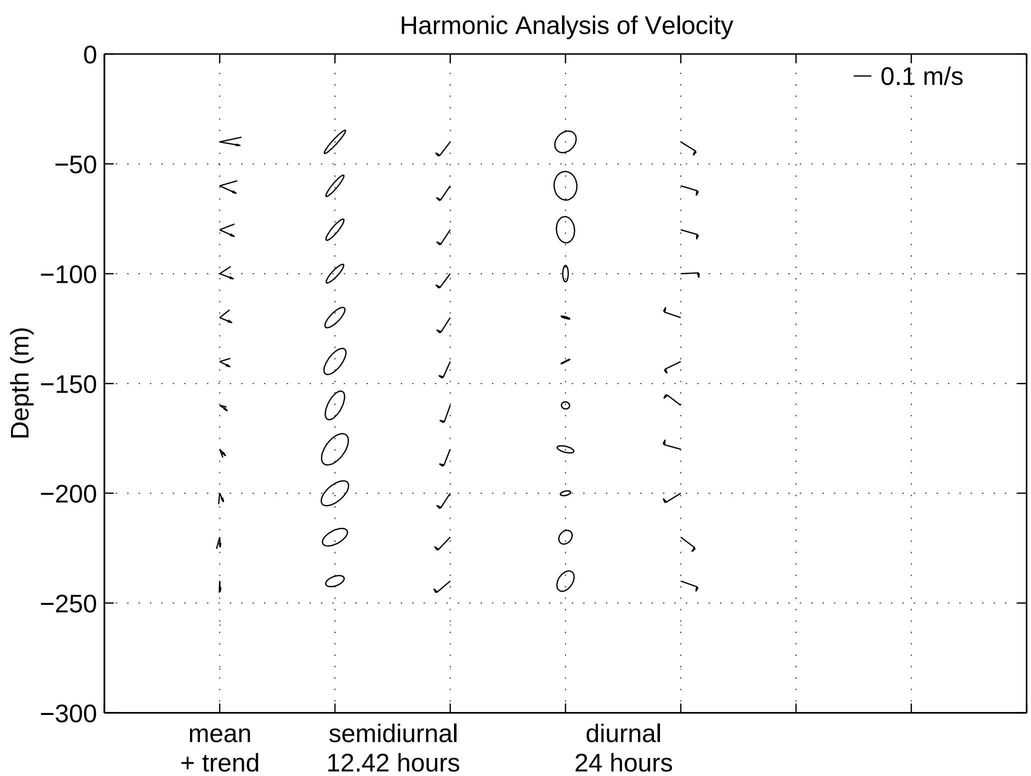
Harmonic Analysis of Velocity
0.1 m/s
0
−50
−100
−150
−200
−250
−300
Depth (m)
mean
+ trend
semidiurnal
12.42 hours
diurnal
24 hours

FIGURE 6.4.1e.

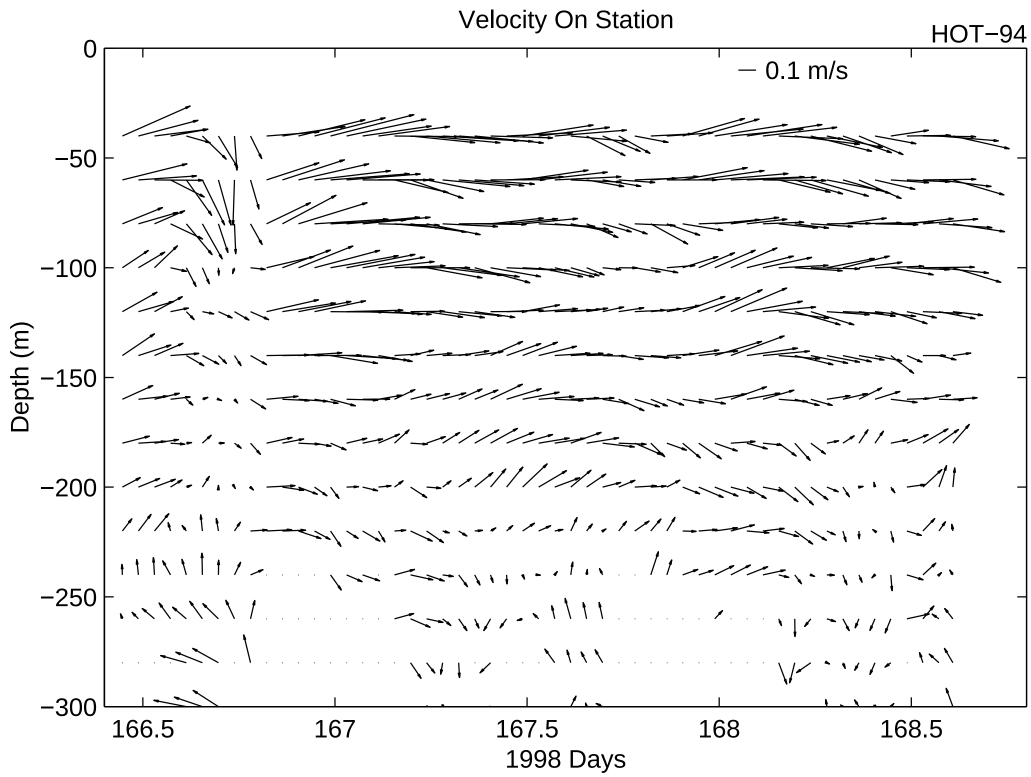
Velocity On Station
HOT−94
0.1 m/s
Depth (m)
0
−50
−100
−150
−200
−250
−300
166.5
167
167.5
168
168.5
1998 Days

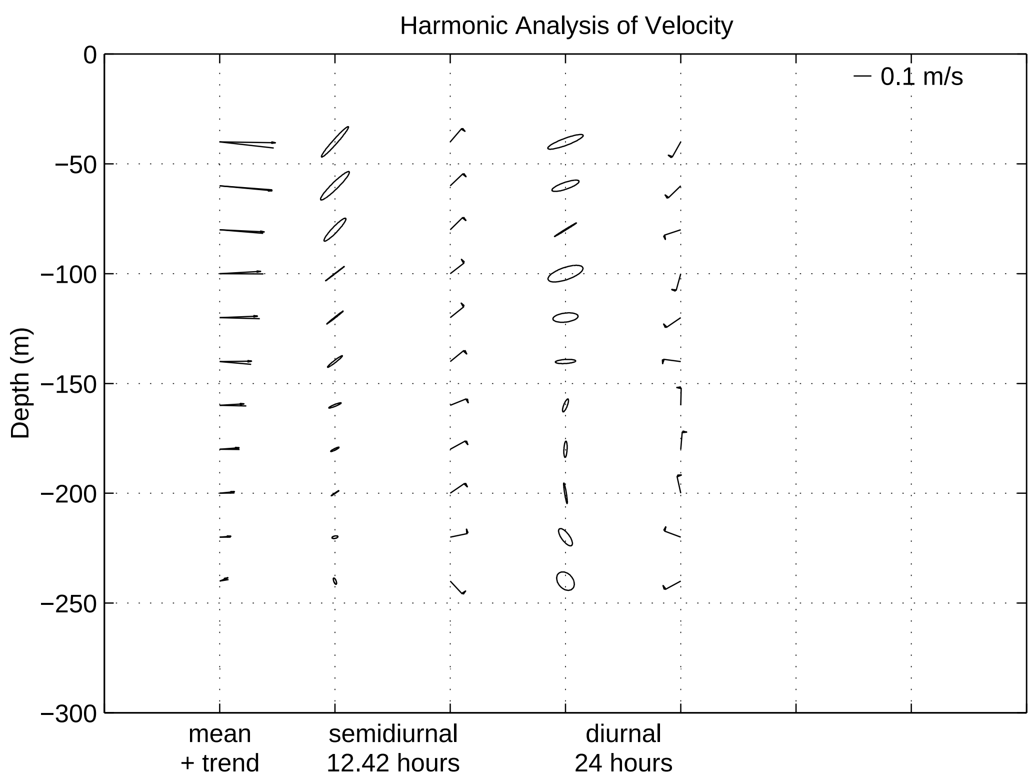
Harmonic Analysis of Velocity
0.1 m/s
Depth (m)
0
−50
−100
−150
−200
−250
−300
mean
+ trend
semidiurnal
12.42 hours
diurnal
24 hours

FIGURE 6.4.1f.

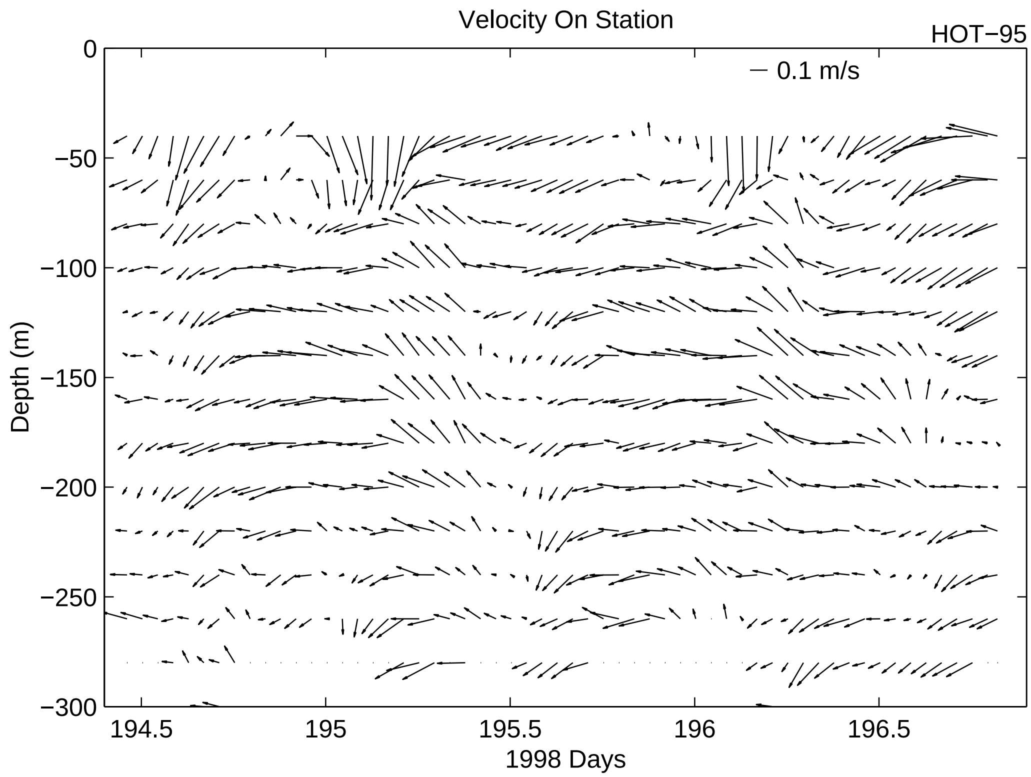
Velocity On Station
HOT−95
0.1 m/s
0
−50
−100
−150
−200
−250
−300
Depth (m)
194.5
195
195.5
196
196.5
1998 Days

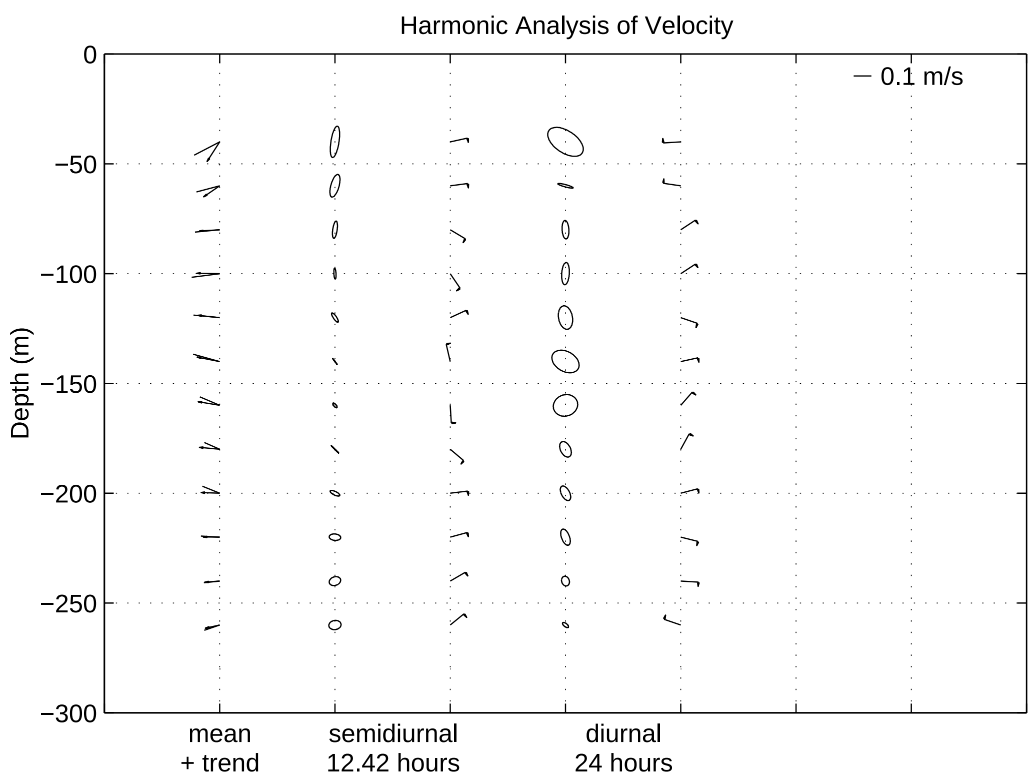
Harmonic Analysis of Velocity
0.1 m/s
0
−50
−100
−150
−200
−250
−300
Depth (m)
mean
+ trend
semidiurnal
12.42 hours
diurnal
24 hours

FIGURE 6.4.1g.

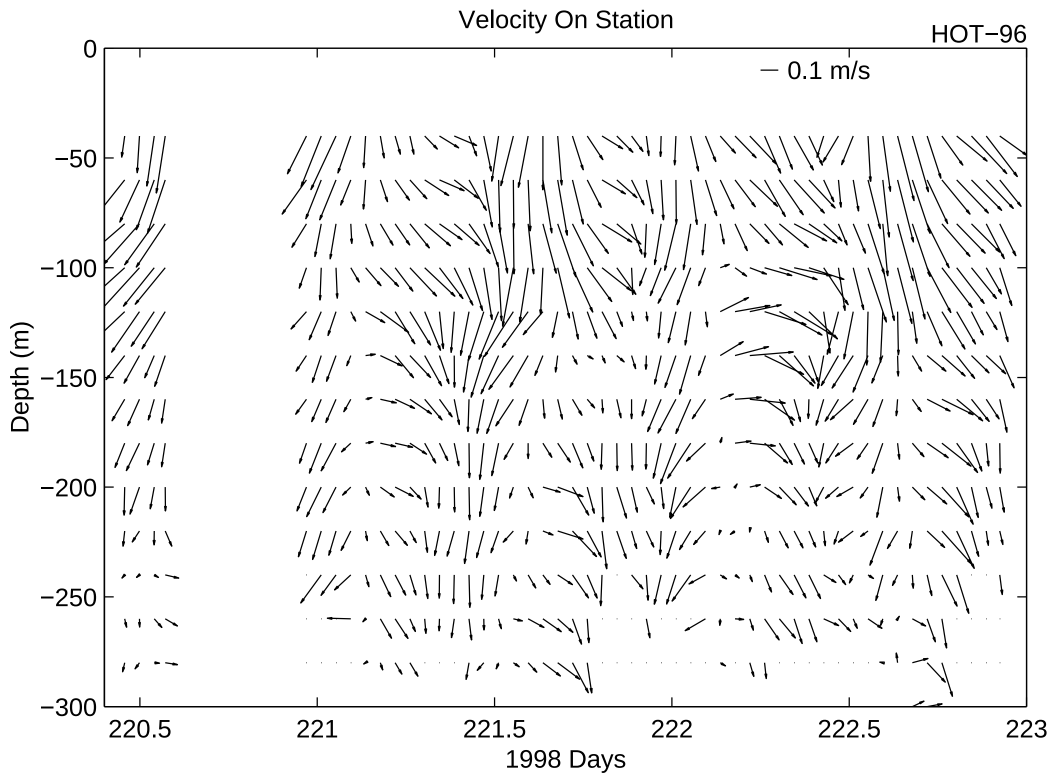
Velocity On Station
HOT−96
0.1 m/s
0
−50
−100
−150
−200
−250
−300
Depth (m)
220.5
221
221.5
222
222.5
223
1998 Days

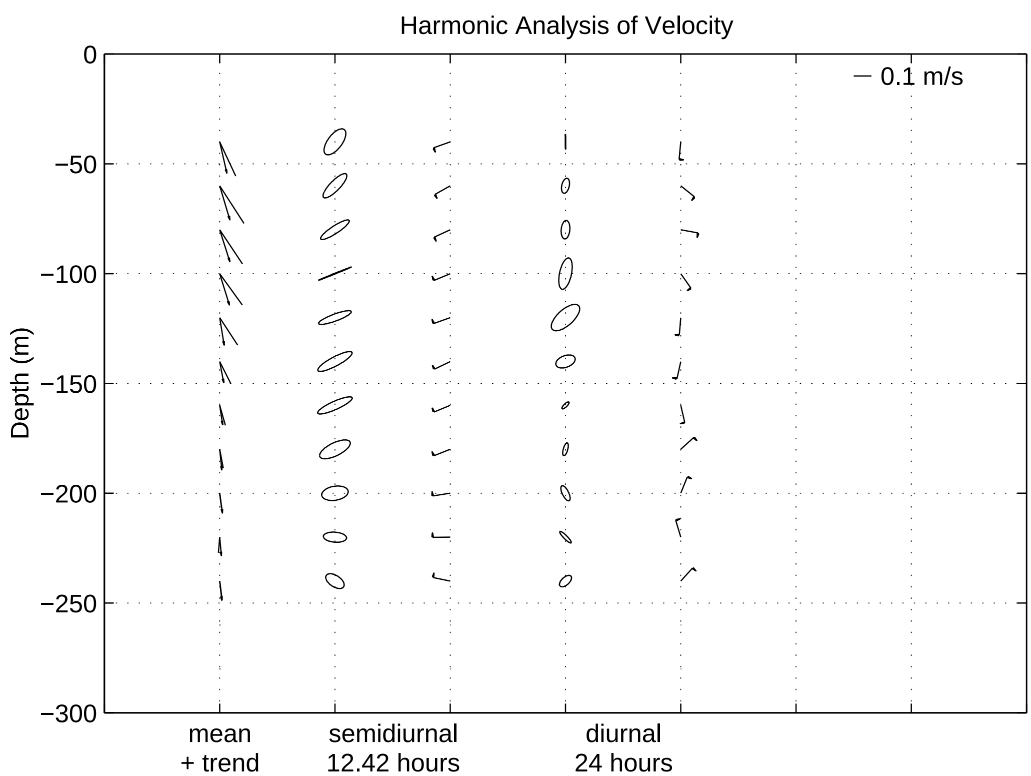
Harmonic Analysis of Velocity
0.1 m/s
0
−50
−100
−150
−200
−250
−300
Depth (m)
mean
+ trend
semidiurnal
12.42 hours
diurnal
24 hours

FIGURE 6.4.1h.

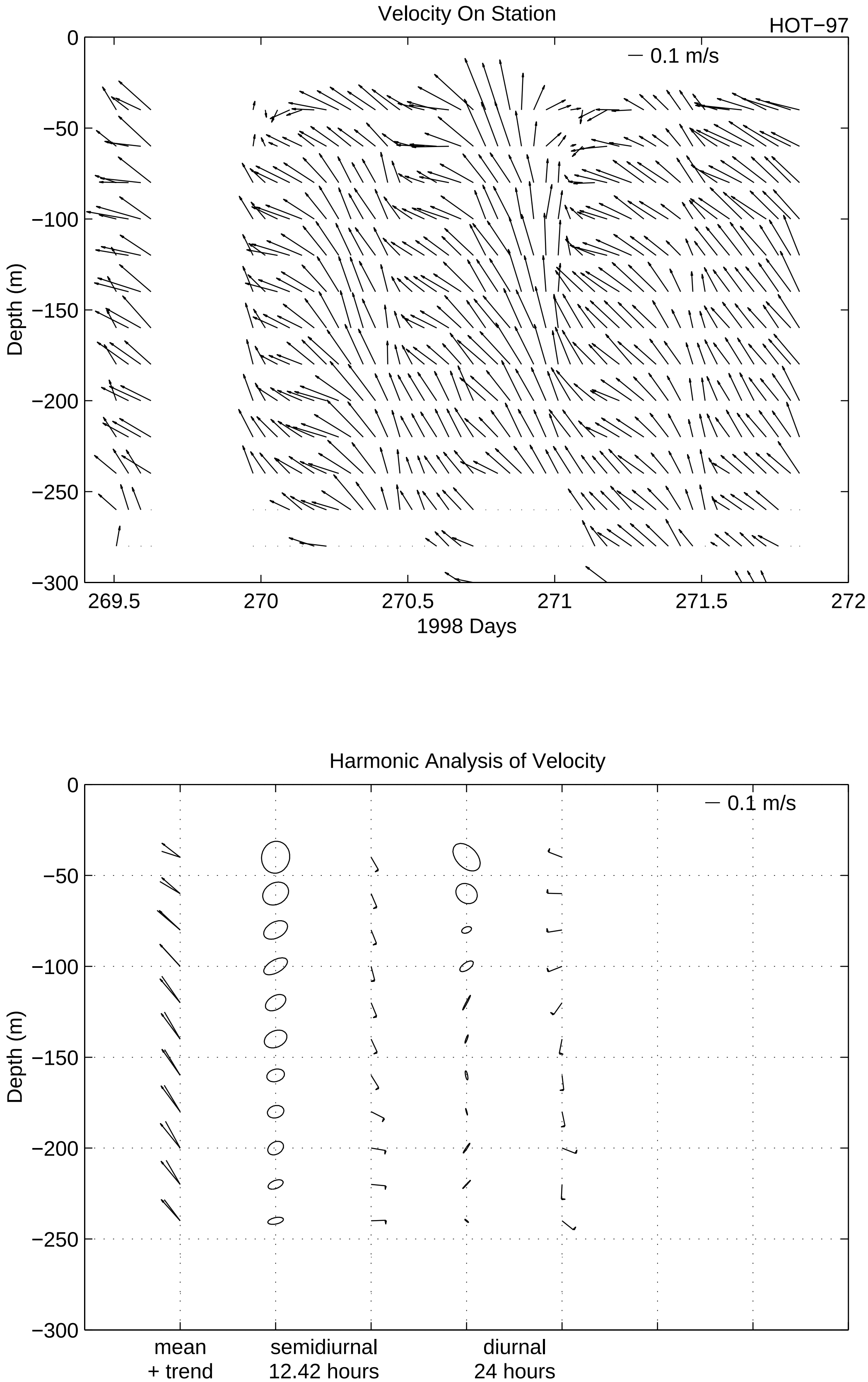

Velocity On Station
HOT−97
0.1 m/s
0
−50
−100
−150
−200
−250
−300
Depth (m)
269.5
270
270.5
271
271.5
272
1998 Days
Harmonic Analysis of Velocity
0.1 m/s
0
−50
−100
−150
−200
−250
−300
Depth (m)
mean
+ trend
semidiurnal
12.42 hours
diurnal
24 hours

FIGURE 6.4.1i.

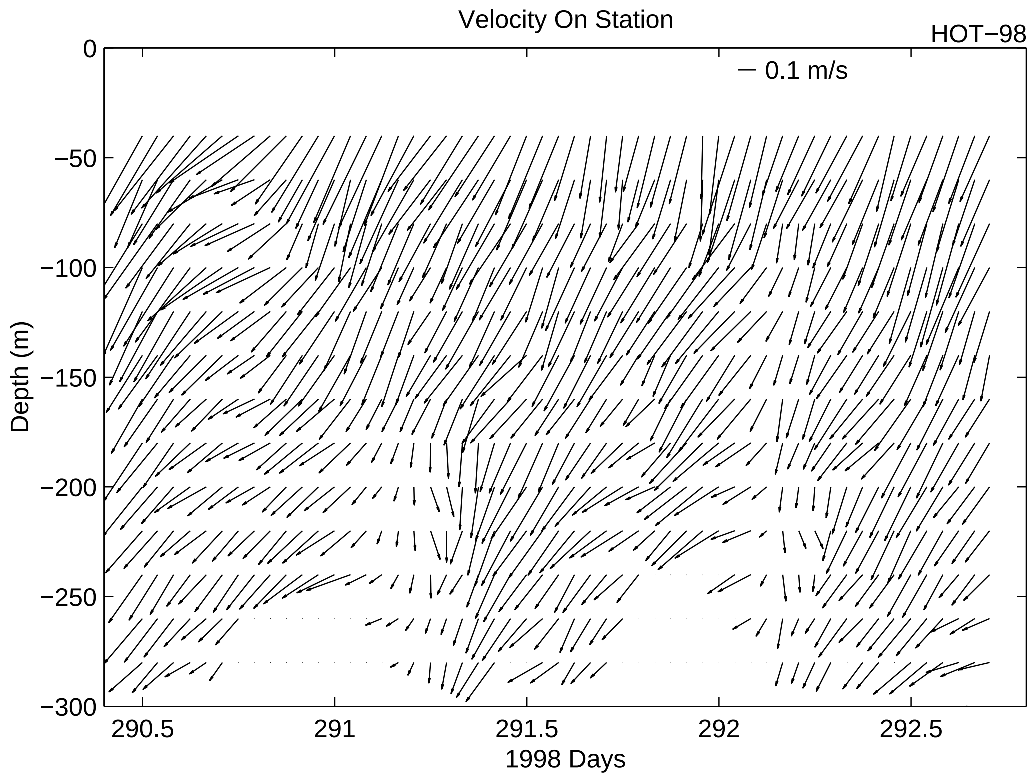
Velocity On Station
HOT−98
0.1 m/s
0
−50
−100
−150
−200
−250
−300
Depth (m)
290.5
291
291.5
292
292.5
1998 Days

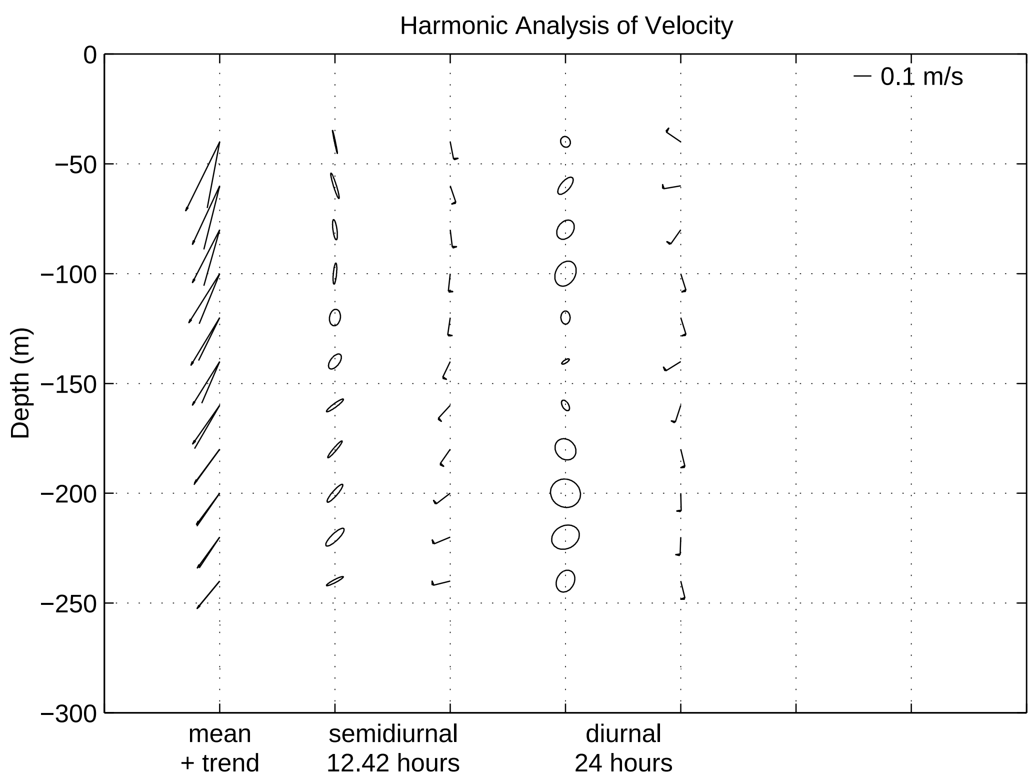
Harmonic Analysis of Velocity
0.1 m/s
0
−50
−100
−150
−200
−250
−300
Depth (m)
mean
+ trend
semidiurnal
12.42 hours
diurnal
24 hours

FIGURE 6.4.1j.

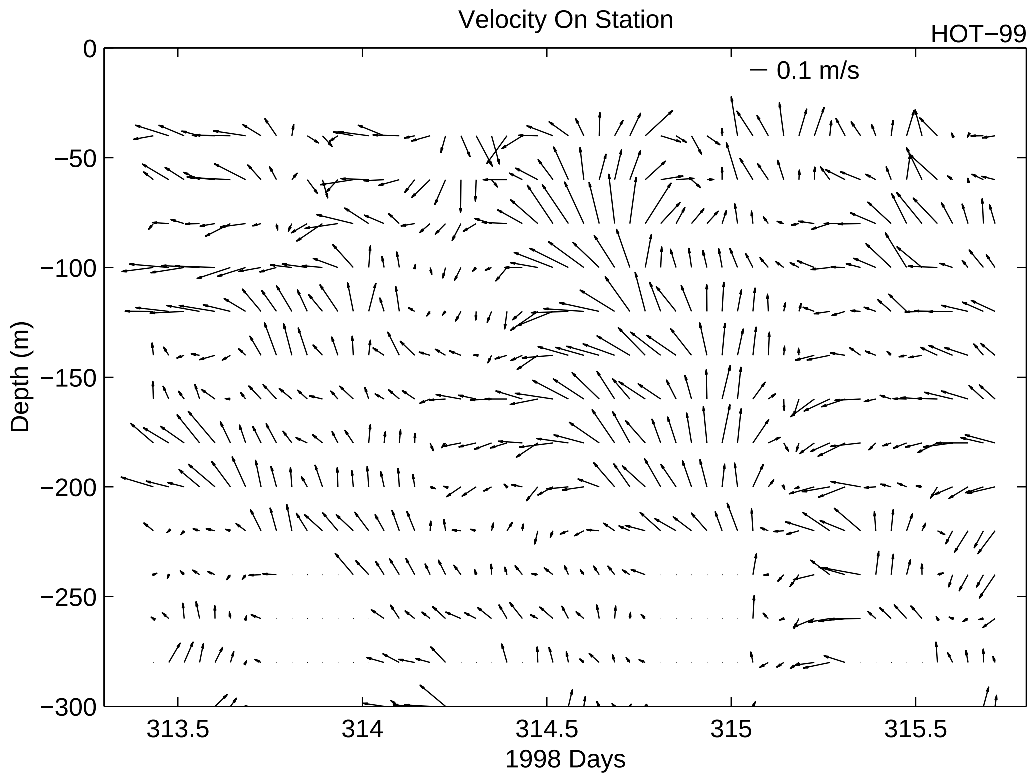

Velocity On Station
HOT−99
0.1 m/s
Depth (m)
0
−50
−100
−150
−200
−250
−300
313.5
314
314.5
315
315.5
1998 Days

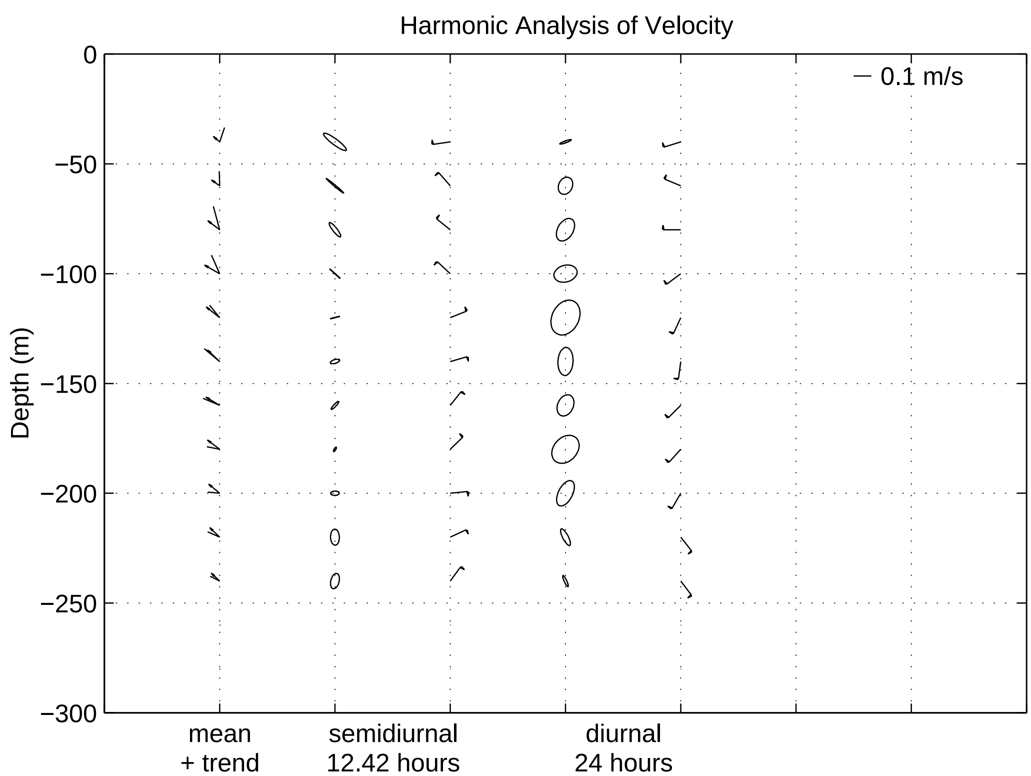

Harmonic Analysis of Velocity
0.1 m/s
Depth (m)
0
−50
−100
−150
−200
−250
−300
mean
+ trend
semidiurnal
12.42 hours
diurnal
24 hours

FIGURE 6.4.1k.

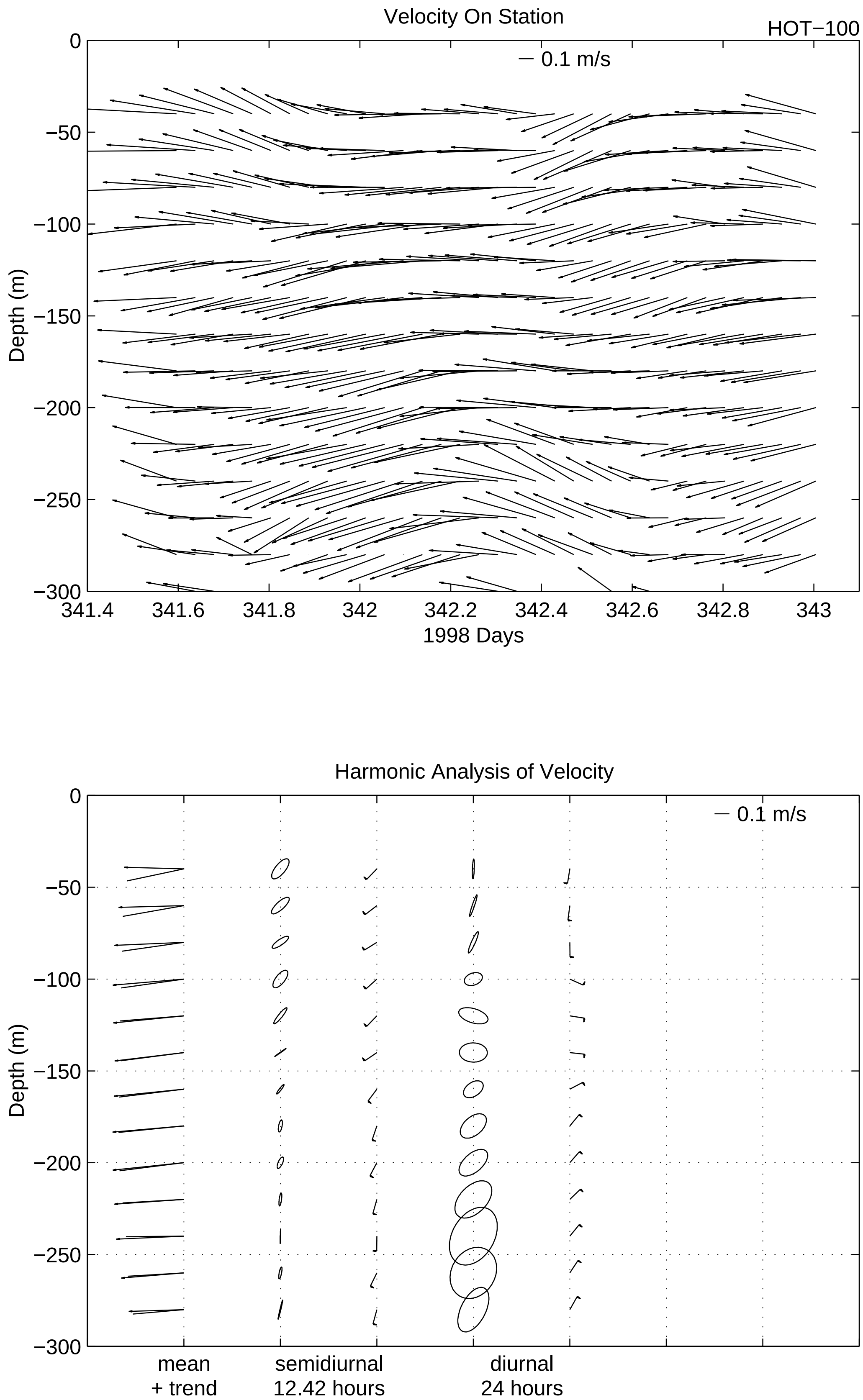
Velocity On Station
HOT−100
0.1 m/s
Depth (m)
0
−50
−100
−150
−200
−250
−300
341.4
341.6
341.8
342
342.2
342.4
342.6
342.8
343
1998 Days
Harmonic Analysis of Velocity
0.1 m/s
Depth (m)
mean
+ trend
semidiurnal
12.42 hours
diurnal
24 hours

FIGURE 6.4.1l.

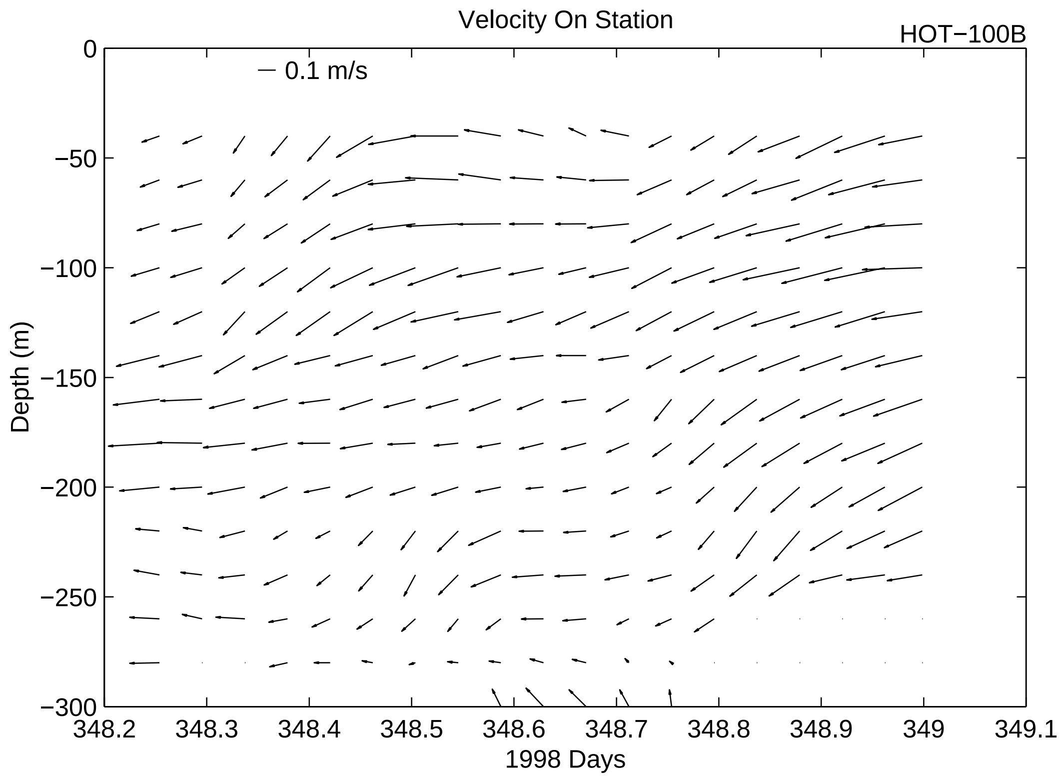
Velocity On Station
HOT−100B
0.1 m/s
Depth (m)
0
−50
−100
−150
−200
−250
−300
348.2
348.3
348.4
348.5
348.6
348.7
348.8
348.9
349
349.1
1998 Days

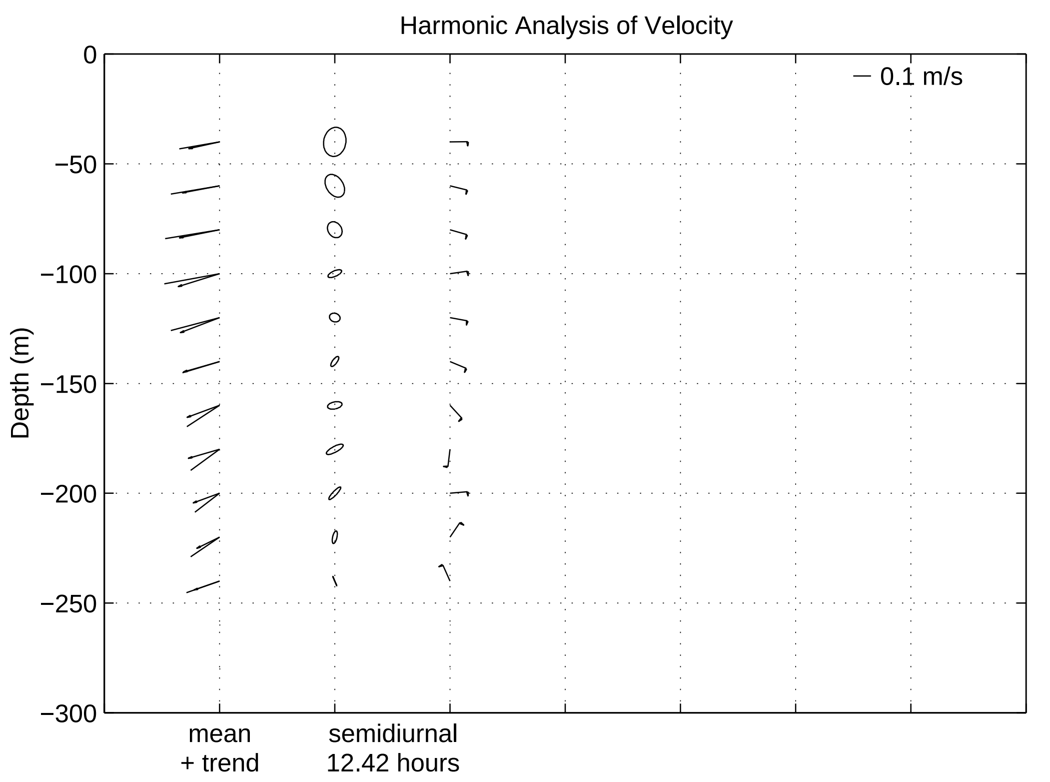
Harmonic Analysis of Velocity
0.1 m/s
Depth (m)
0
−50
−100
−150
−200
−250
−300
mean
+ trend
semidiurnal
12.42 hours

FIGURE 6.4.1m.

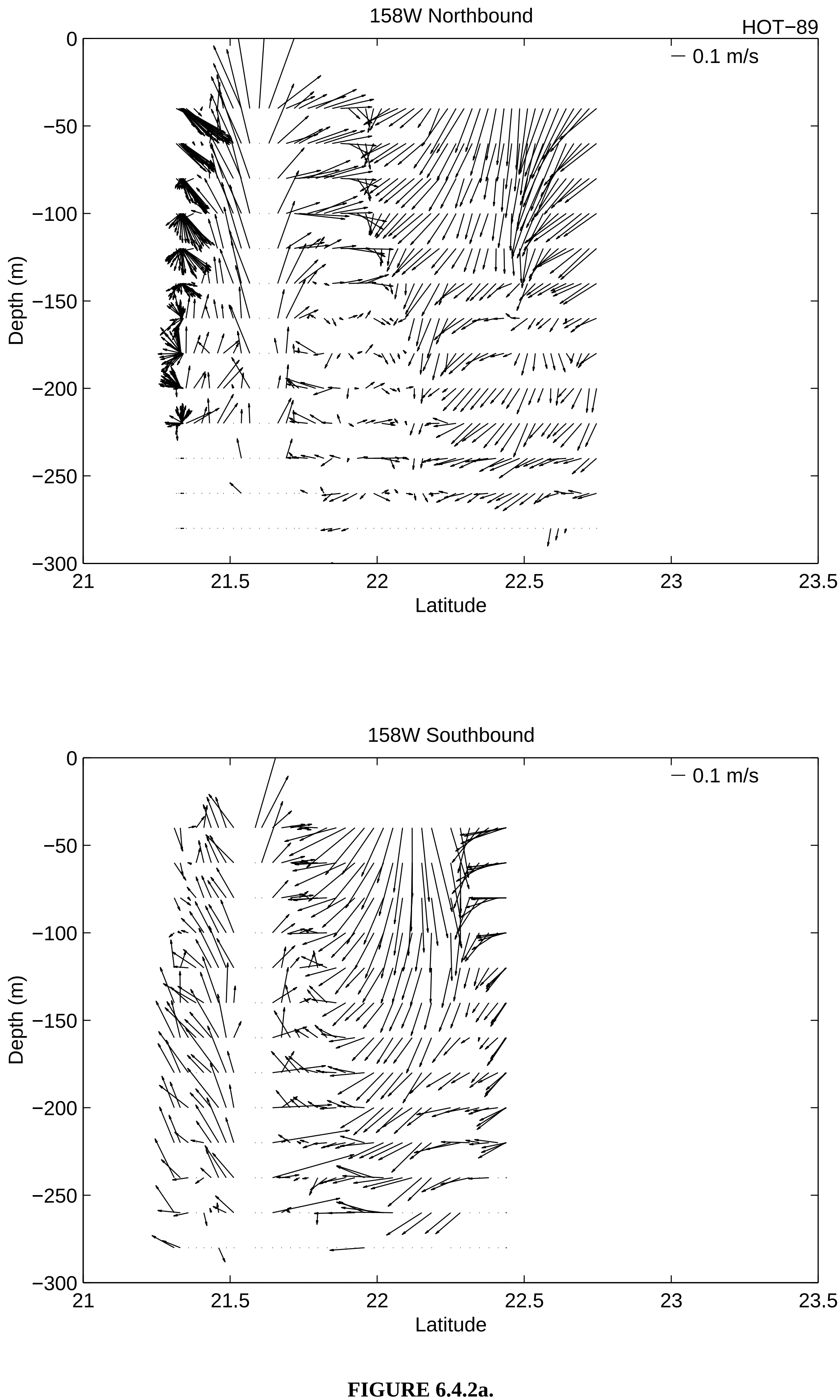
158W Northbound
HOT−89
0.1 m/s
0
−50
−100
−150
−200
−250
−300
Depth (m)
21
21.5
22
22.5
23
23.5
Latitude
158W Southbound
0.1 m/s
0
−50
−100
−150
−200
−250
−300
Depth (m)
21
21.5
22
22.5
23
23.5
Latitude

FIGURE 6.4.2a.

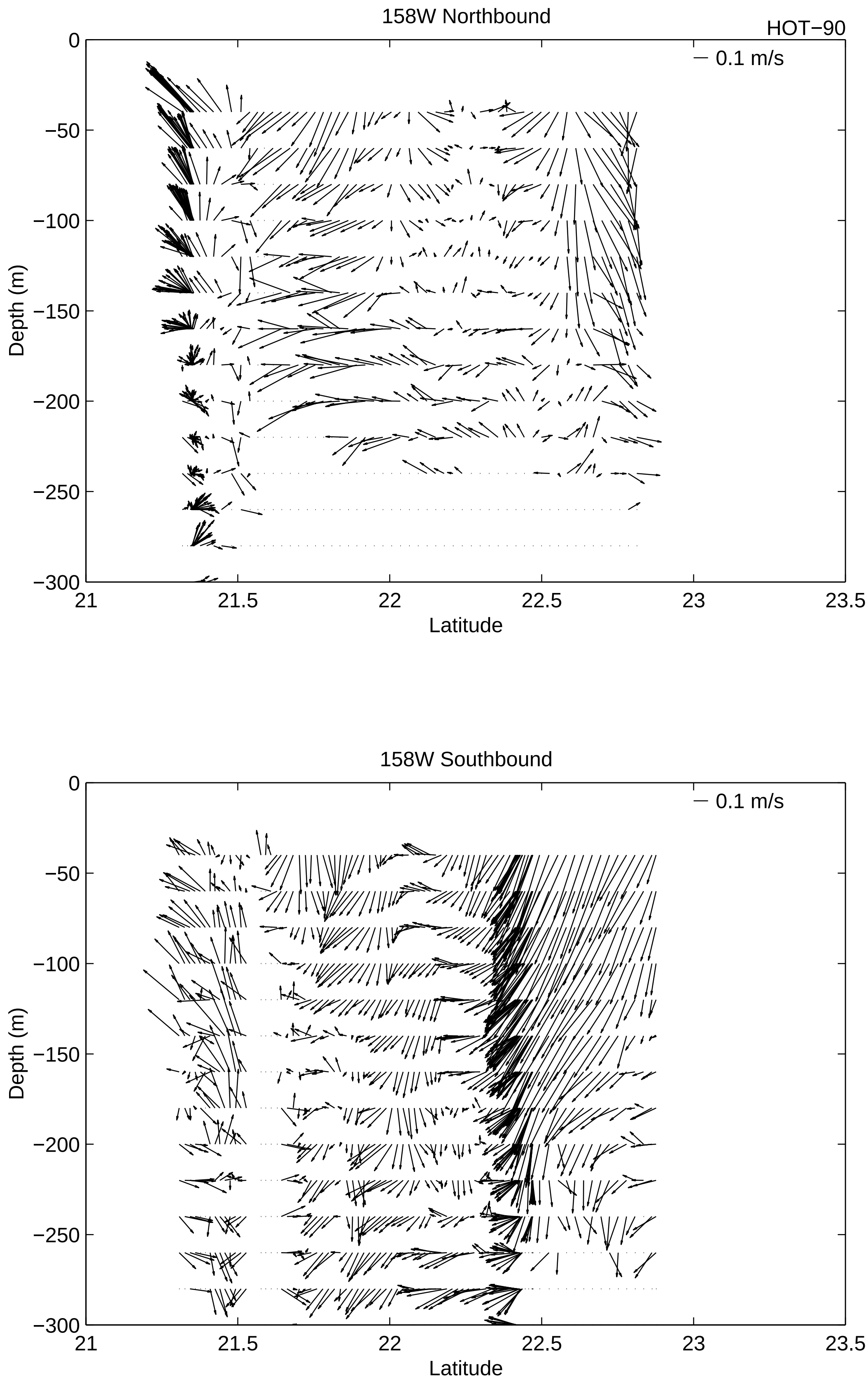
158W Northbound
HOT−90
0.1 m/s
Depth (m)
0
−50
−100
−150
−200
−250
−300
21
21.5
22
22.5
23
23.5
Latitude
158W Southbound
0.1 m/s
Depth (m)
0
−50
−100
−150
−200
−250
−300
21
21.5
22
22.5
23
23.5
Latitude

FIGURE 6.4.2b.

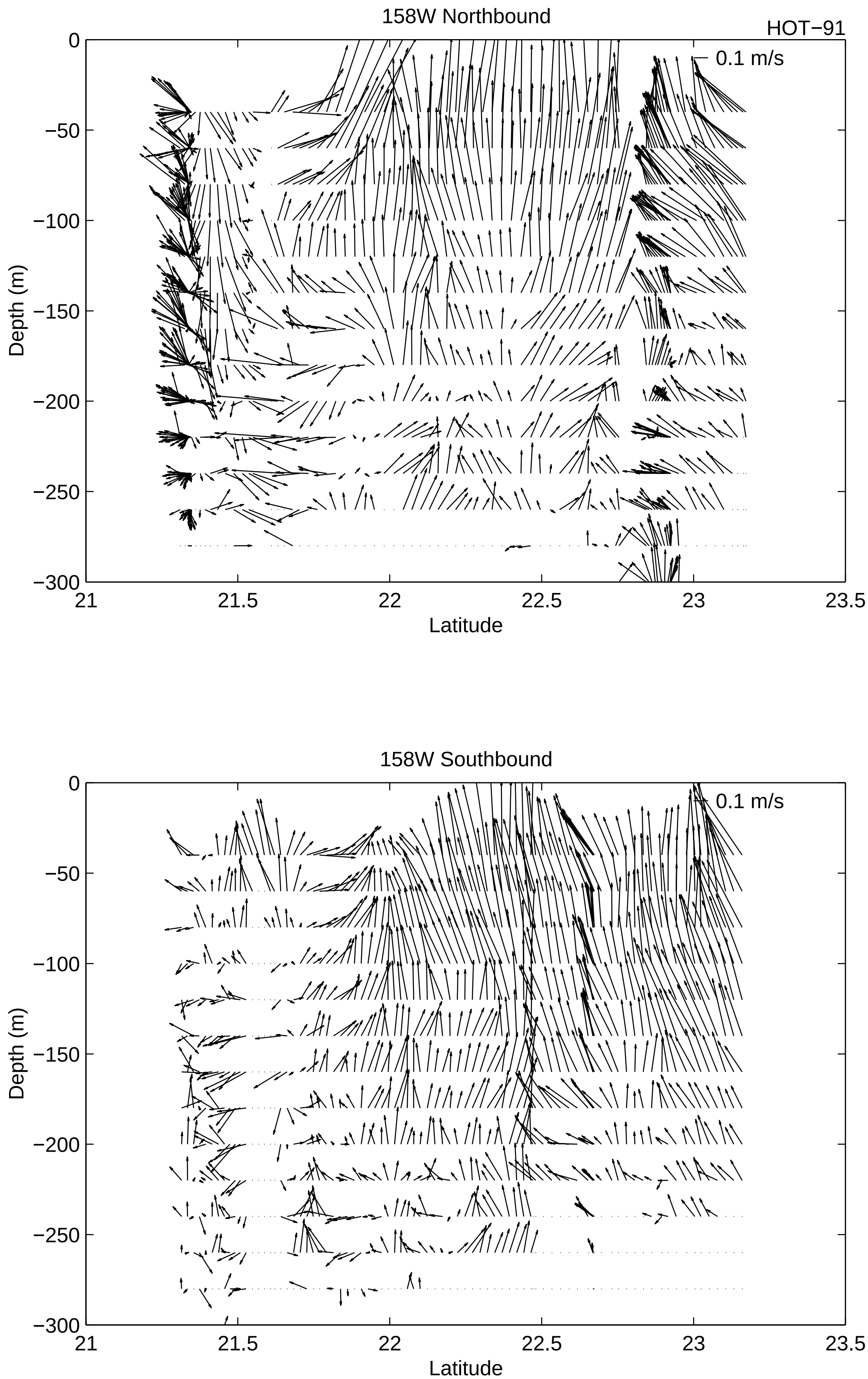
158W Northbound
HOT−91
0.1 m/s
Depth (m)
0
−50
−100
−150
−200
−250
−300
21
21.5
22
22.5
23
23.5
Latitude
158W Southbound
0.1 m/s
Depth (m)
Latitude

FIGURE 6.4.2c.

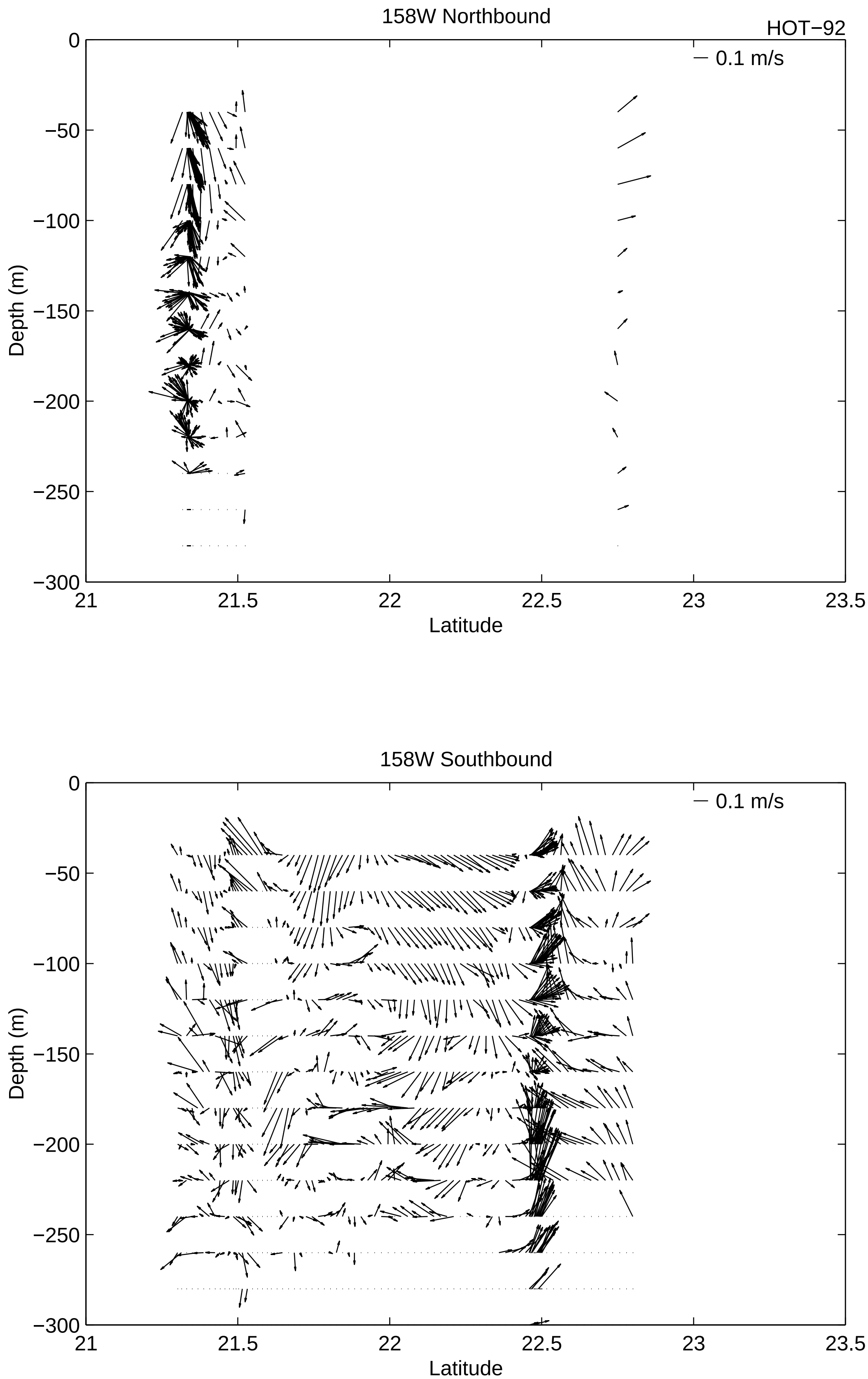
158W Northbound
HOT−92
0.1 m/s
Depth (m)
0
−50
−100
−150
−200
−250
−300
21
21.5
22
22.5
23
23.5
Latitude
158W Southbound
0.1 m/s
Depth (m)
0
−50
−100
−150
−200
−250
−300
21
21.5
22
22.5
23
23.5
Latitude

FIGURE 6.4.2d.

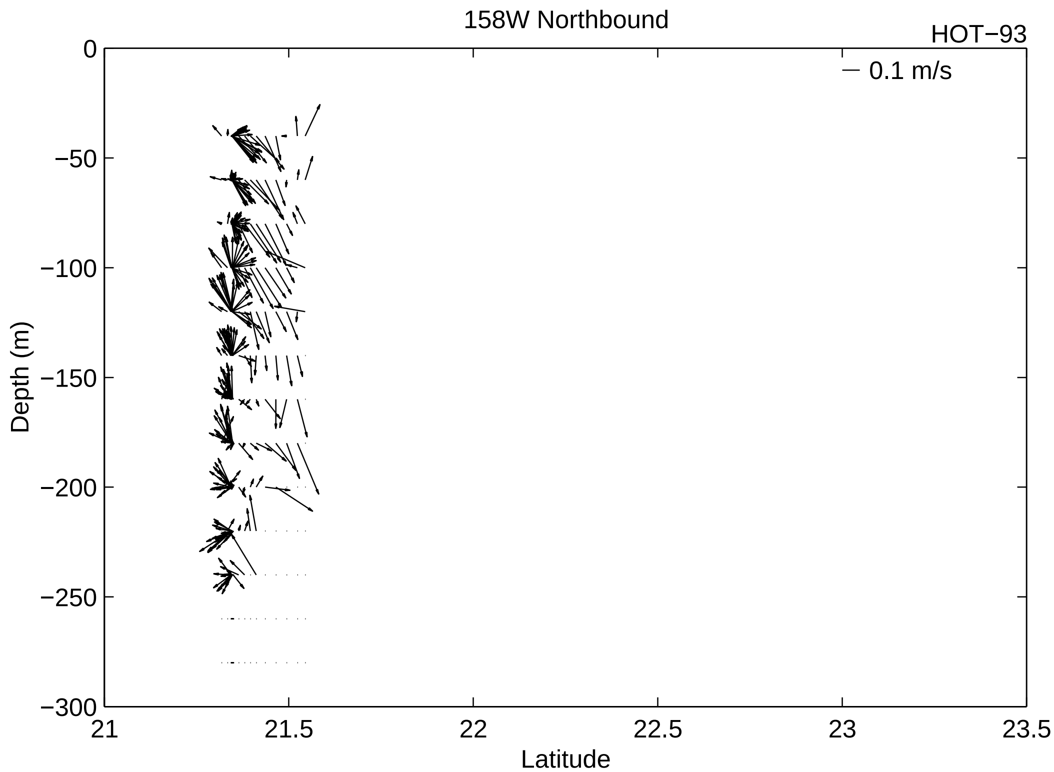

158W Northbound
HOT−93
0.1 m/s
Depth (m)
0
−50
−100
−150
−200
−250
−300
21
21.5
22
22.5
23
23.5
Latitude

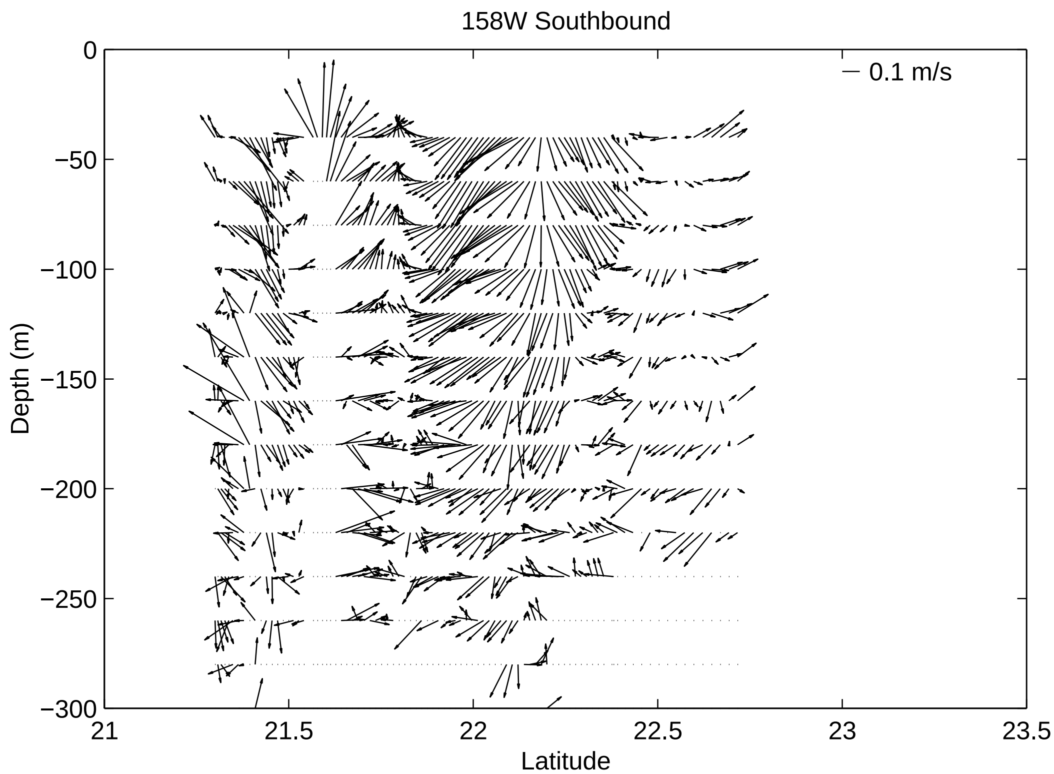

158W Southbound
0.1 m/s
Depth (m)
0
−50
−100
−150
−200
−250
−300
21
21.5
22
22.5
23
23.5
Latitude

FIGURE 6.4.2e.

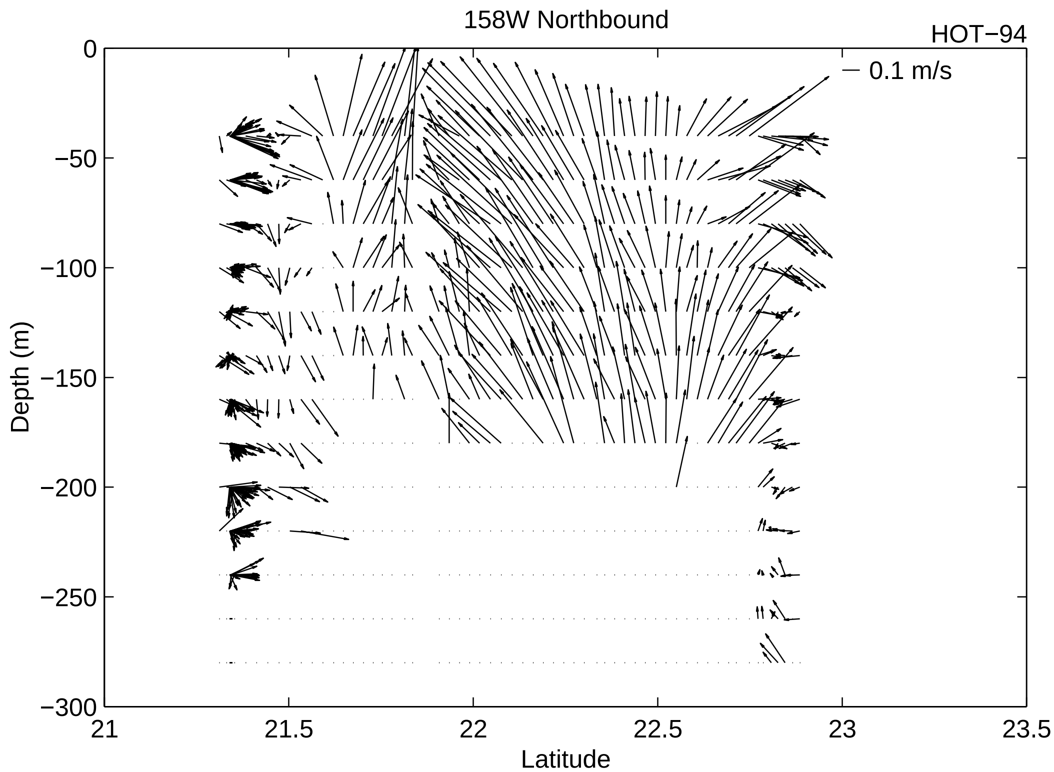
158W Northbound
HOT−94
0.1 m/s
Depth (m)
Latitude
0
−50
−100
−150
−200
−250
−300
21
21.5
22
22.5
23
23.5

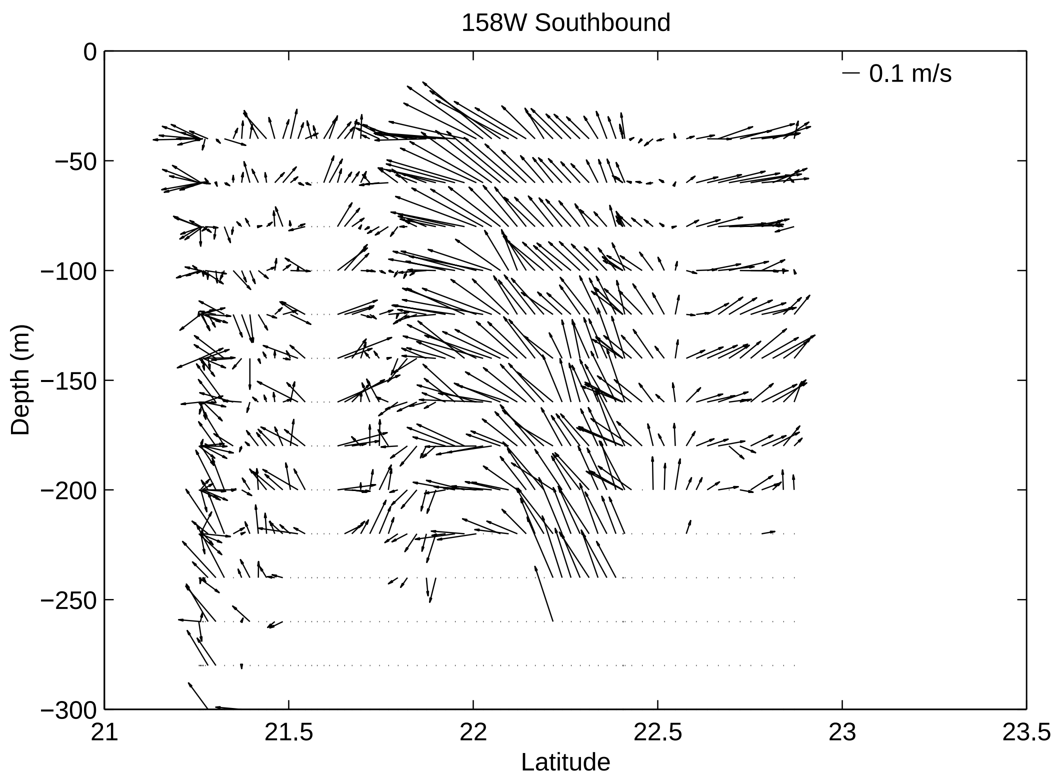
158W Southbound
0.1 m/s
Depth (m)
Latitude
0
−50
−100
−150
−200
−250
−300
21
21.5
22
22.5
23
23.5

FIGURE 6.4.2f.

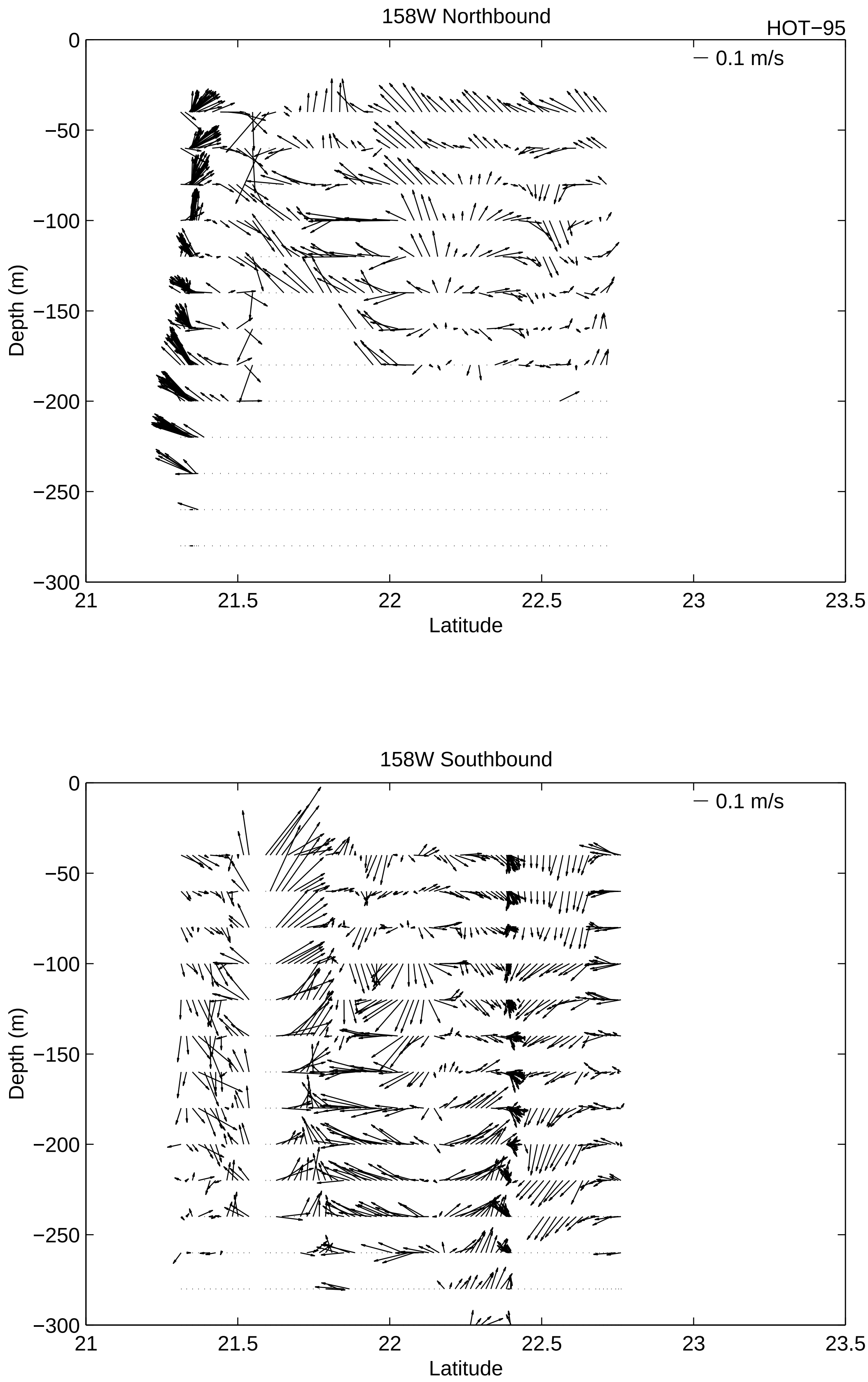
158W Northbound
HOT−95
0.1 m/s
Depth (m)
0
−50
−100
−150
−200
−250
−300
21
21.5
22
22.5
23
23.5
Latitude
158W Southbound
0.1 m/s
Depth (m)
0
−50
−100
−150
−200
−250
−300
21
21.5
22
22.5
23
23.5
Latitude

FIGURE 6.4.2g.

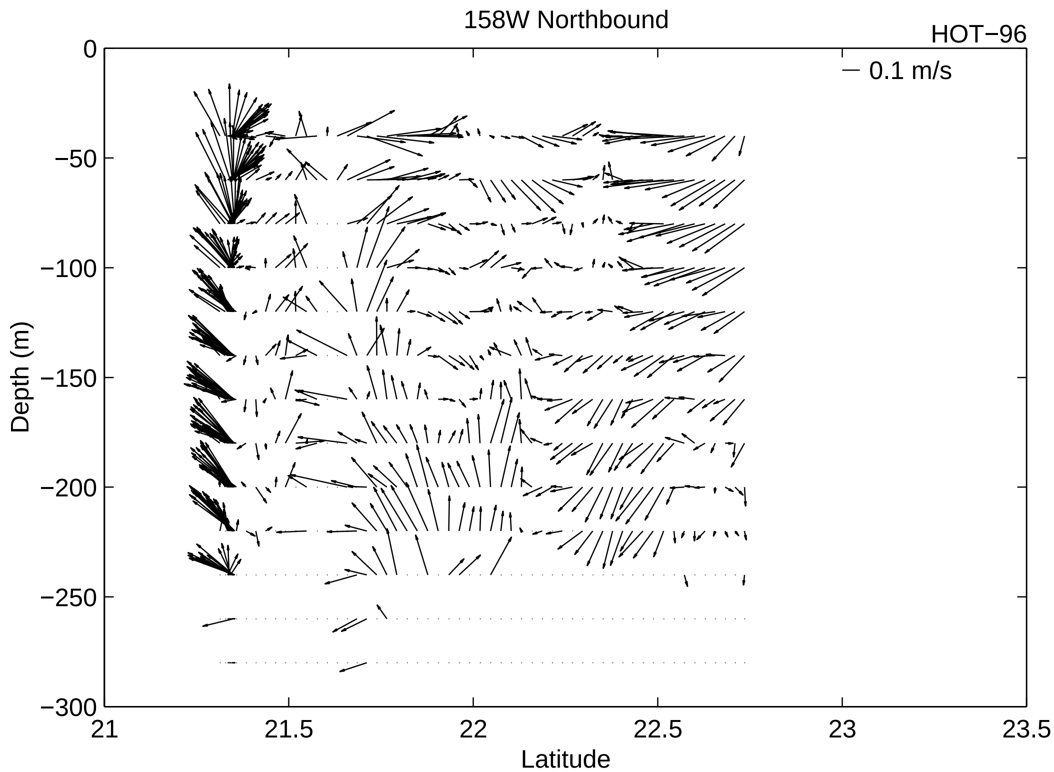
158W Northbound
HOT−96
0.1 m/s
Depth (m)
Latitude
0
−50
−100
−150
−200
−250
−300
21
21.5
22
22.5
23
23.5

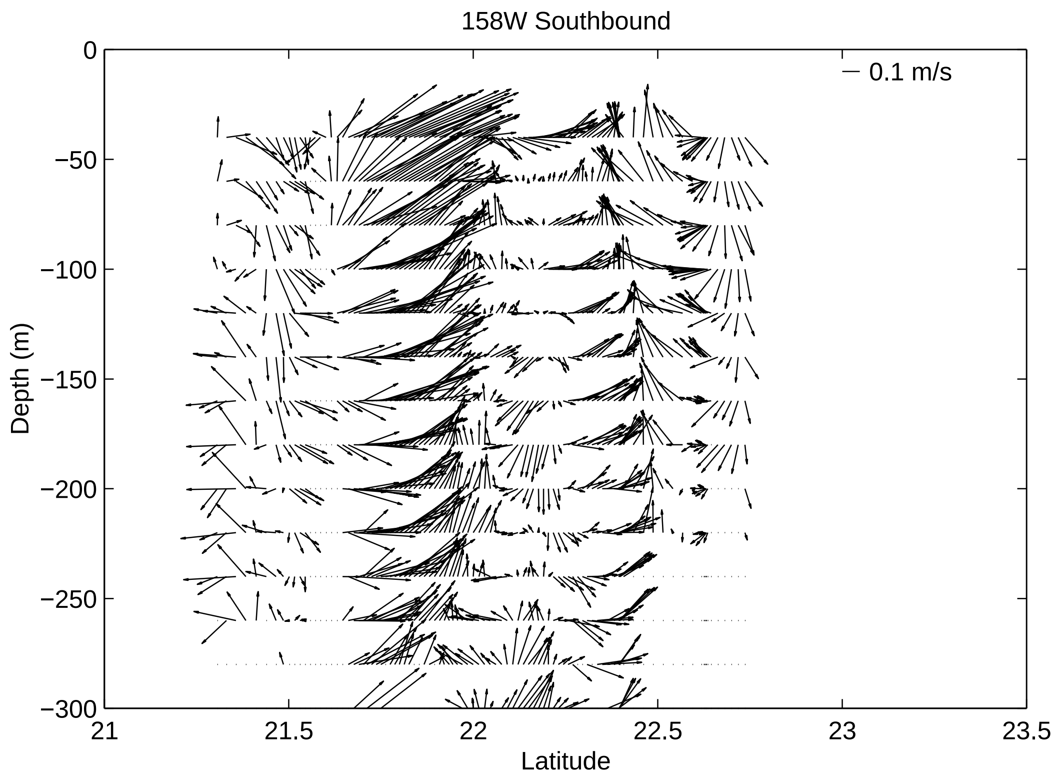
158W Southbound
0.1 m/s
Depth (m)
Latitude
0
−50
−100
−150
−200
−250
−300
21
21.5
22
22.5
23
23.5

FIGURE 6.4.2h.

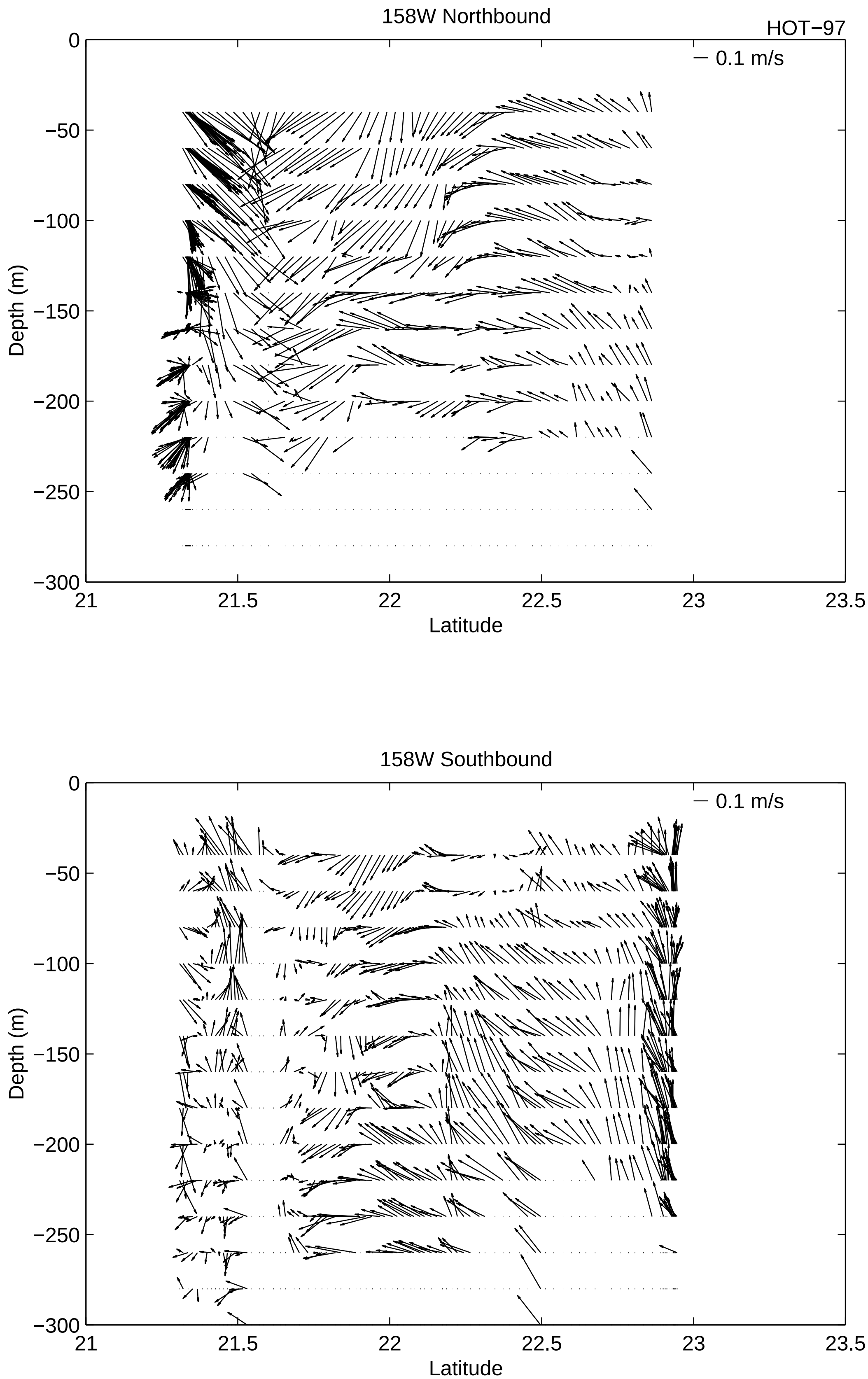
158W Northbound
HOT−97
0.1 m/s
Depth (m)
0
−50
−100
−150
−200
−250
−300
21
21.5
22
22.5
23
23.5
Latitude
158W Southbound
0.1 m/s
Depth (m)
0
−50
−100
−150
−200
−250
−300
21
21.5
22
22.5
23
23.5
Latitude

FIGURE 6.4.2i.

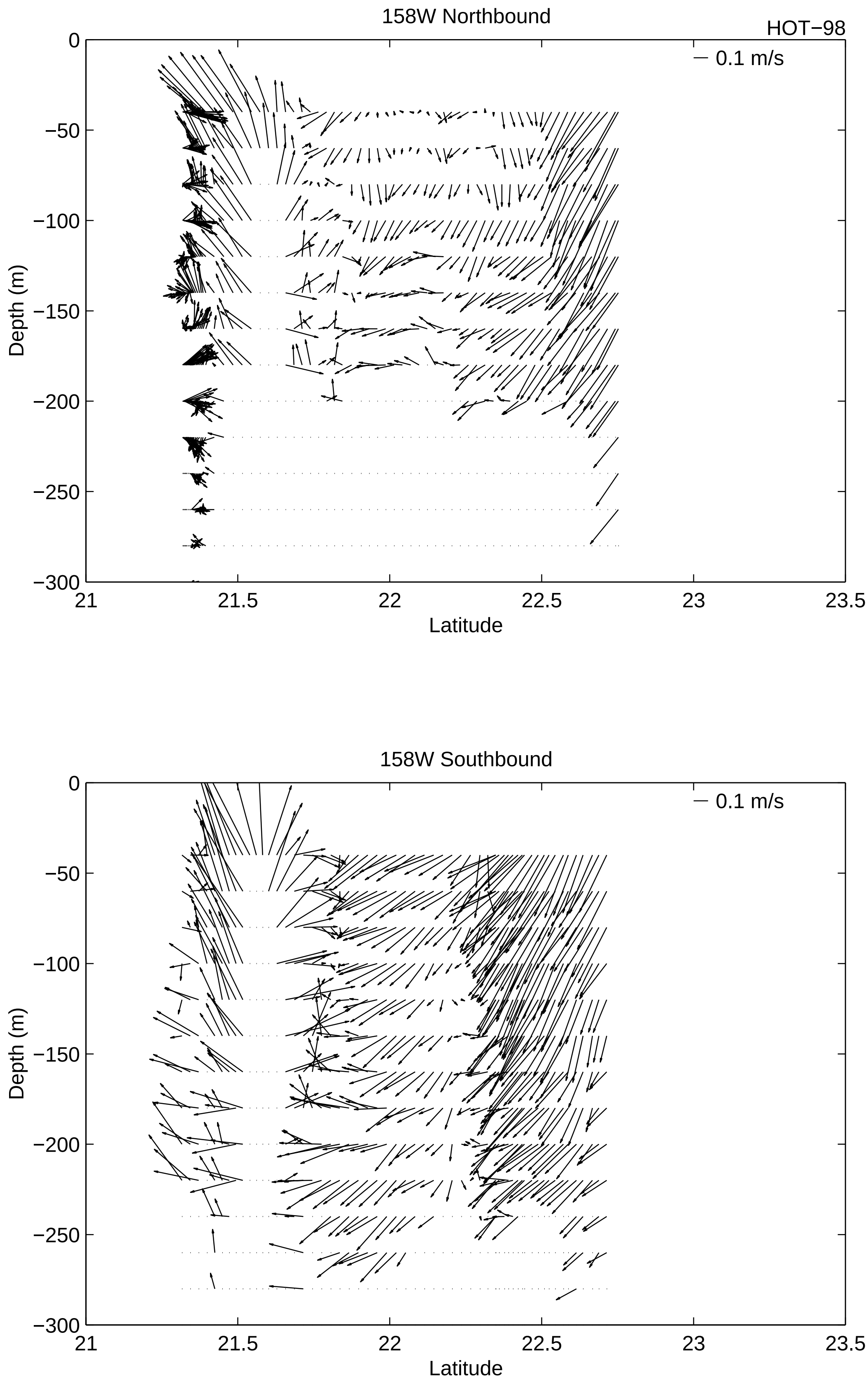
158W Northbound
HOT−98
0.1 m/s
Depth (m)
0
−50
−100
−150
−200
−250
−300
21
21.5
22
22.5
23
23.5
Latitude
158W Southbound
0.1 m/s
Depth (m)
0
−50
−100
−150
−200
−250
−300
21
21.5
22
22.5
23
23.5
Latitude

FIGURE 6.4.2j.

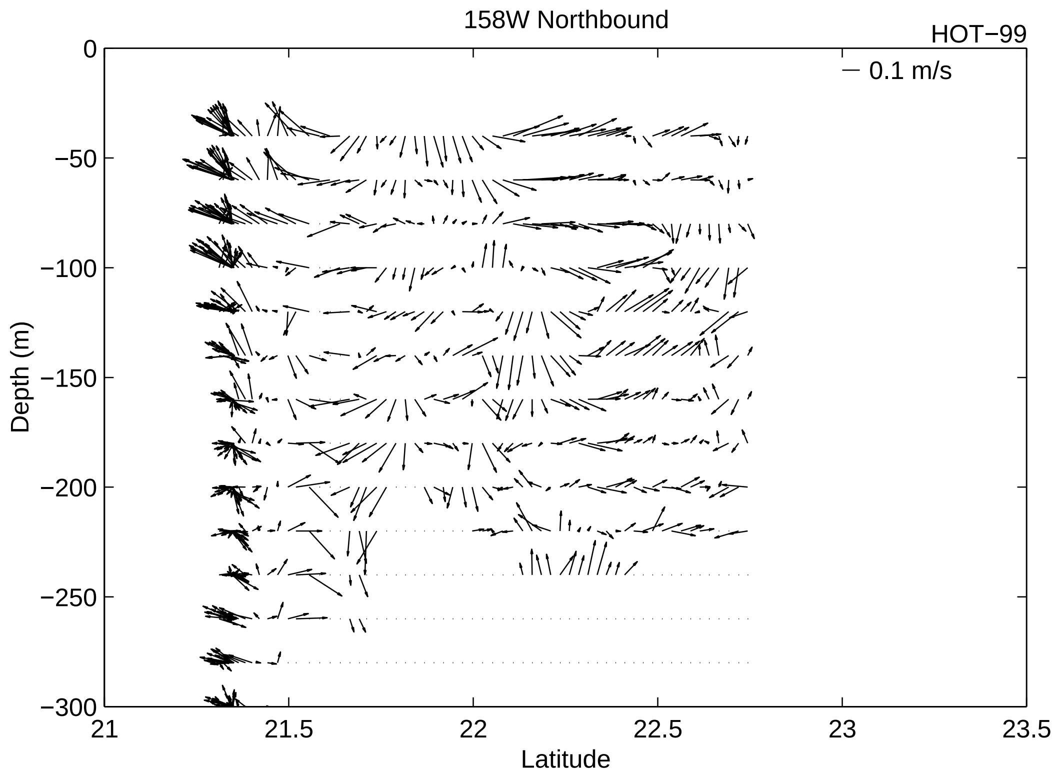
158W Northbound
HOT−99
0.1 m/s
Depth (m)
0
−50
−100
−150
−200
−250
−300
21
21.5
22
22.5
23
23.5
Latitude

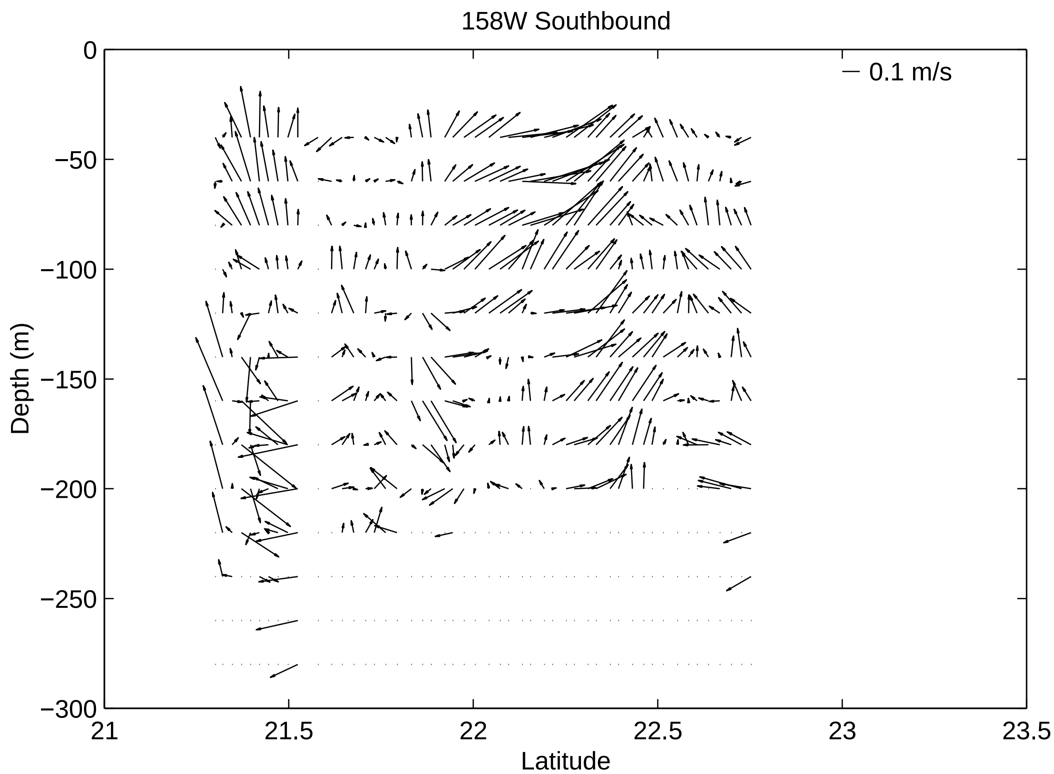
158W Southbound
0.1 m/s
Depth (m)
0
−50
−100
−150
−200
−250
−300
21
21.5
22
22.5
23
23.5
Latitude

FIGURE 6.4.2k.

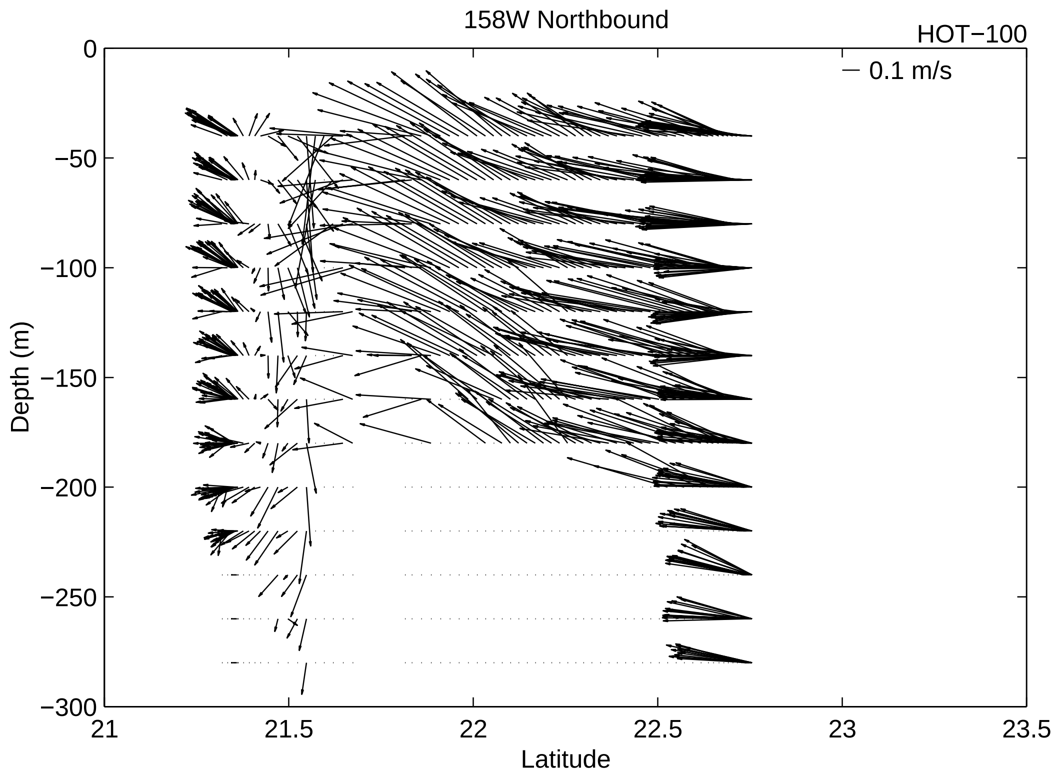

158W Northbound
HOT−100
0.1 m/s
0
−50
−100
−150
−200
−250
−300
Depth (m)
21
21.5
22
22.5
23
23.5
Latitude

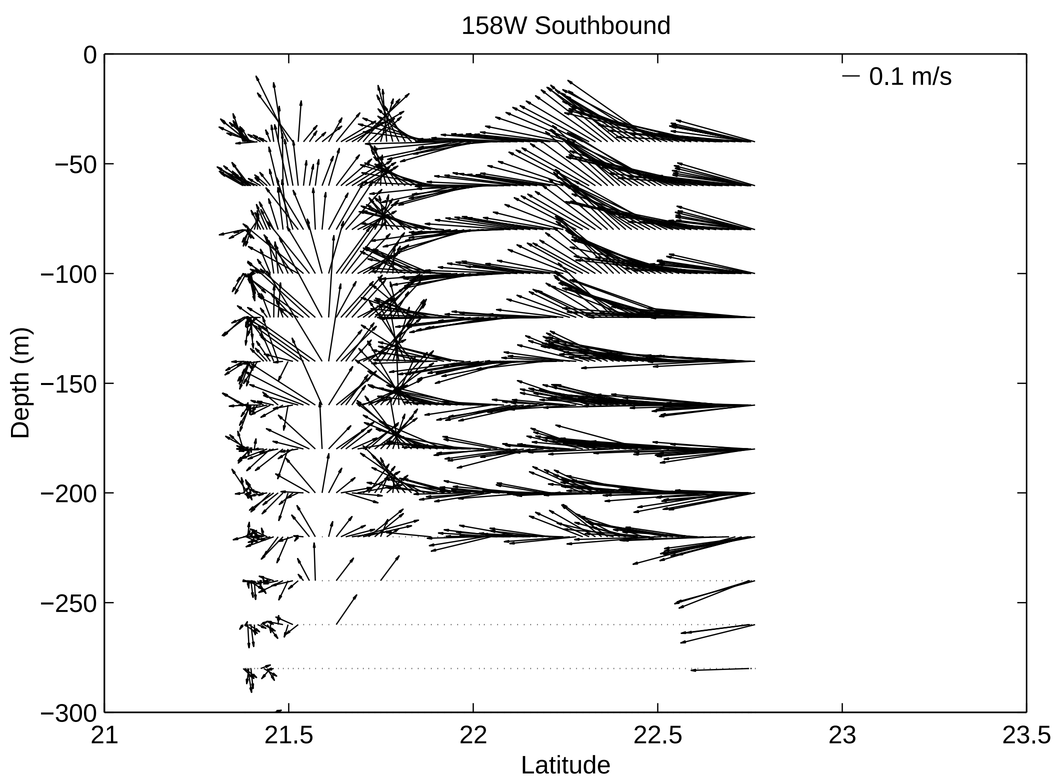

158W Southbound
0.1 m/s
0
−50
−100
−150
−200
−250
−300
Depth (m)
21
21.5
22
22.5
23
23.5
Latitude

FIGURE 6.4.2l.

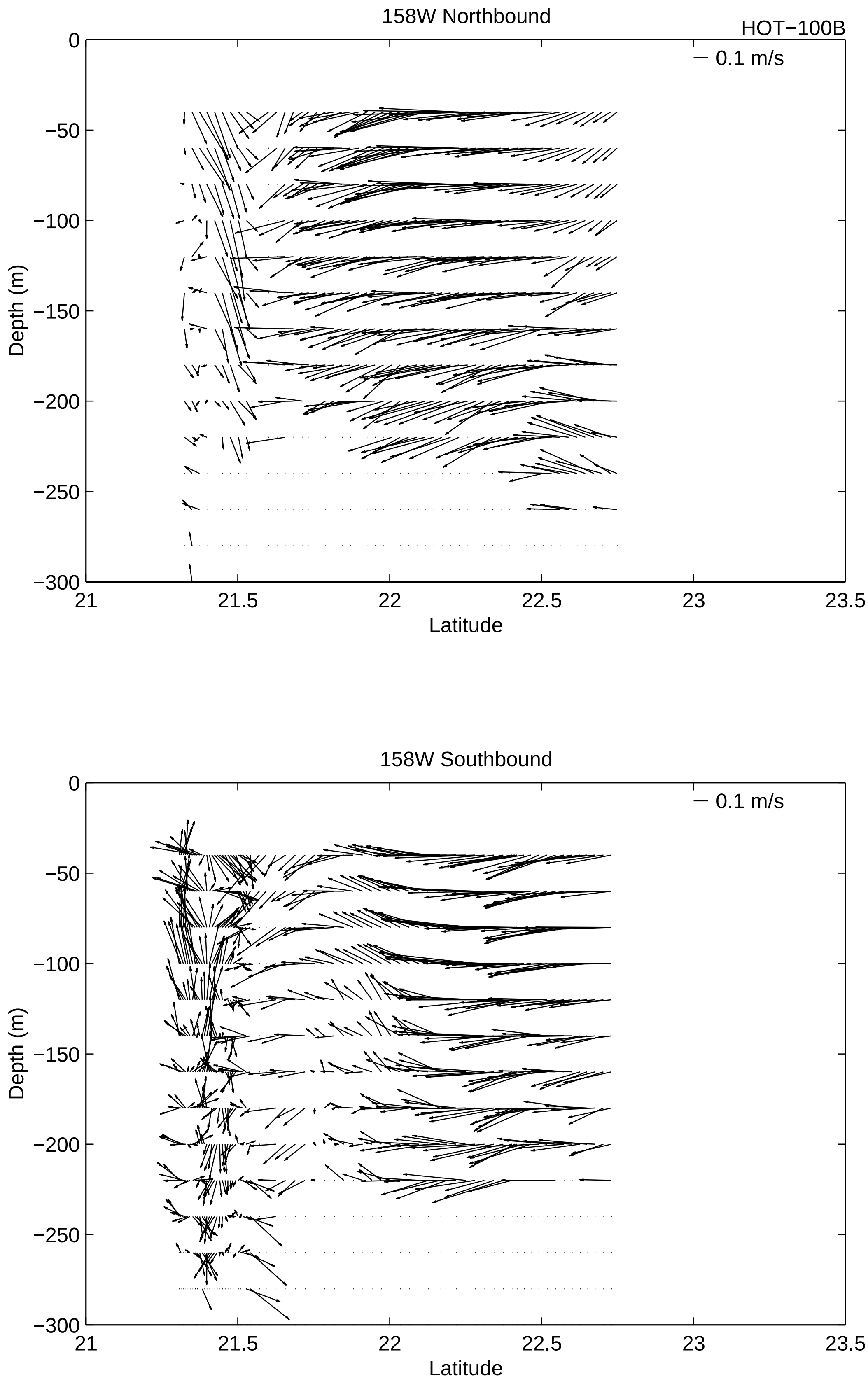
158W Northbound
HOT−100B
0.1 m/s
Depth (m)
0
−50
−100
−150
−200
−250
−300
21
21.5
22
22.5
23
23.5
Latitude
158W Southbound
0.1 m/s
Depth (m)
0
−50
−100
−150
−200
−250
−300
21
21.5
22
22.5
23
23.5
Latitude

FIGURE 6.4.2m.

6.5 Biogeochemistry

Figure 6.5.1: Contour plot of bottle dissolved oxygen versus pressure for HOT cruises 1-100 from 0-200 m. Location of samples in the water column are indicated by the solid circles.

Figure 6.5.2a: Contour plot of dissolved inorganic carbon versus pressure for HOT cruises 1-100 from 0-200 m. Location of samples in the water column are indicated by the solid circles.

Figure 6.5.2b: Contour plot of alkalinity versus pressure for HOT cruises 1-100 from 0-200 m. Location of samples in the water column are indicated by the solid circles.

Figure 6.5.2c: [Upper panel] Time series of mean titration alkalinity for HOT cruises 1-100. [Lower panel] Dissolved inorganic carbon for HOT cruises 1-100. Error bars represent standard deviation of pooled samples collected between 0 and 50 dbar.

Figure 6.5.3a: Depth profile from 0-150 m of [nitrate + nitrite] at Station ALOHA for 1998 HOT cruises by the chemiluminescence method.

Figure 6.5.3b: Depth profile from 0-150 m of [nitrate + nitrite] at Station HALE ALOHA for 1998 HOT cruises by the chemiluminescence method.

Figure 6.5.4: Depth profile from 0-250 m of soluble reactive phosphorus at Station ALOHA for 1998 HOT cruises by the magnesium induced coprecipitation (MAGIC) method.

Figure 6.5.5: Contour plot from 0-1000 m of dissolved organic carbon at Station ALOHA for HOT cruises 49-100.

Figure 6.5.6: Contour plot from 0-1000 m of dissolved organic nitrogen at Station ALOHA for HOT cruises 1-100.

Figure 6.5.7: Contour plot from 0-1000 m of dissolved organic phosphorus at Station ALOHA for HOT cruises 1-100.

Figure 6.5.8a: Mean concentrations of particulate carbon at Station ALOHA for HOT cruises 1-100 from 0-50 dbar [Upper panel], and 50-100 dbar [Lower panel]. Error bars represent standard deviation of pooled samples.

Figure 6.5.8b: Mean concentrations of particulate nitrogen at Station ALOHA for HOT cruises 1-100 from 0-50 dbar [Upper panel], and 50-100 dbar [Lower panel]. Error bars represent standard deviation of pooled samples.

Figure 6.5.8c: Mean concentrations of particulate phosphorus at Station ALOHA for HOT cruises 1-100 from 0-50 dbar [Upper panel], and 50-100 dbar [Lower panel]. Error bars represent standard deviation of pooled samples.

Figure 6.5.9: Contour plot from 0-200 m of fluorometric chlorophyll *a* concentrations at Station ALOHA for HOT cruises 1-100.

Figure 6.5.10: Contour plot from 0-500 m of adenosine 5' triphosphate concentrations at Station ALOHA for HOT cruises 1-100.

Figure 6.5.11: [Upper panel] Integrated (0-200 m) primary production rates from 1988-1998. Solid line represents the average production (477 mg C m-2 d-1), dashed line is one standard deviation (122 mg C m-2 d-1). [Lower panel] 3-point running mean of integrated primary production rates.

Figure 6.5.12: [Upper panel] Carbon flux at 150 m measured on all HOT cruises from 1988-1998. [Middle panel] Nitrogen flux at 150 m measured on all HOT cruises from 1988-1998. [Lower panel] Phosphorus flux at 150 m measured on all HOT cruises from 1988-1998. Error bars represent the standard deviation of replicate determinations.

Figure 6.5.13: Depth profile of heterotrophic bacteria and Prochlorococcus numbers measured by flow cytometry at Station ALOHA for 1998 .

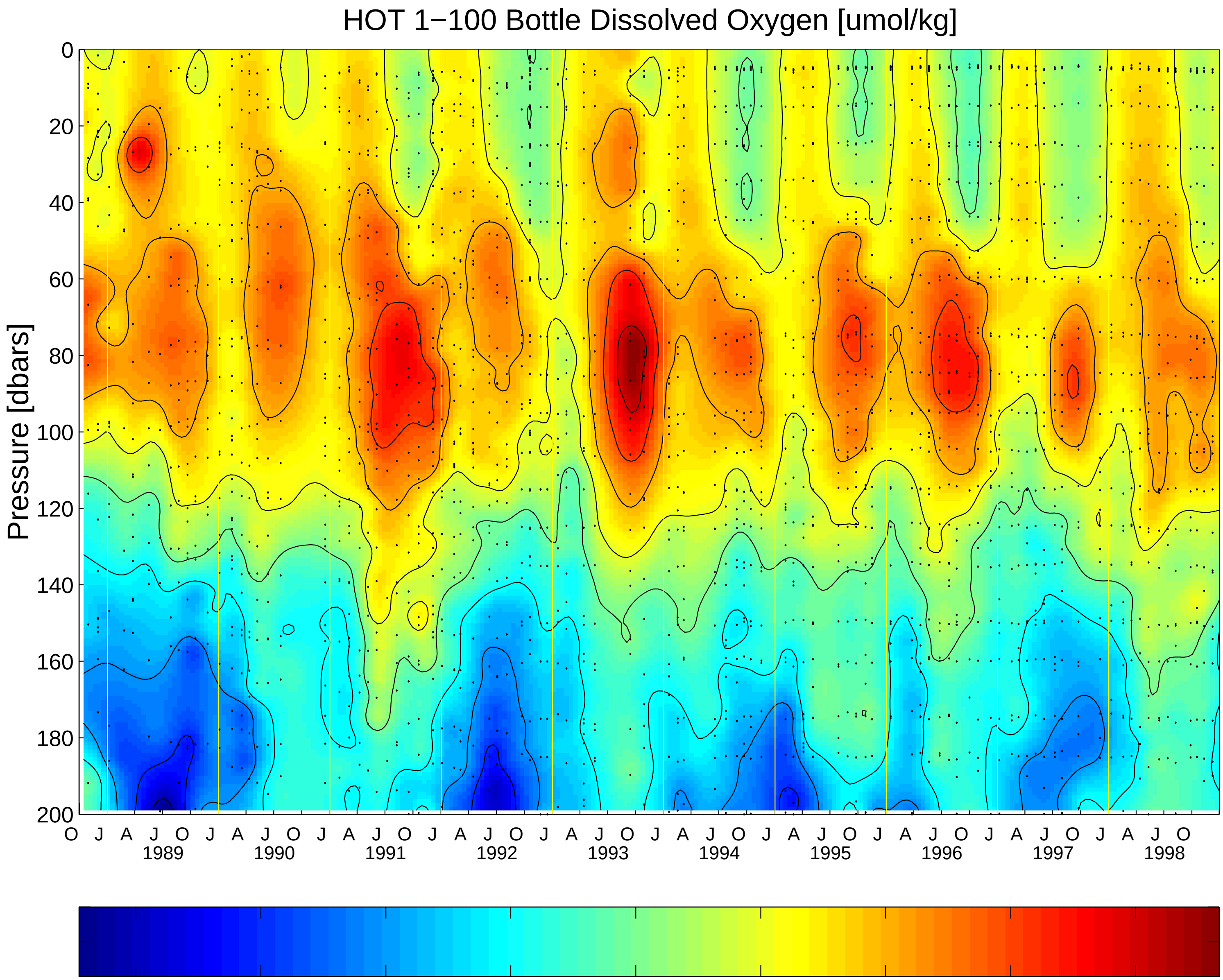

HOT 1−100 Bottle Dissolved Oxygen [umol/kg]
Pressure [dbars]
0
20
40
60
80
100
120
140
160
180
200
O J A J O J A J O J A J O J A J O J A J O J A J O J A J O J A J O J A J O J A J O
1989
1990
1991
1992
1993
1994
1995
1996
1997
1998
185
190
195
200
205
210
215
220
225

FIGURE 6.5.1.

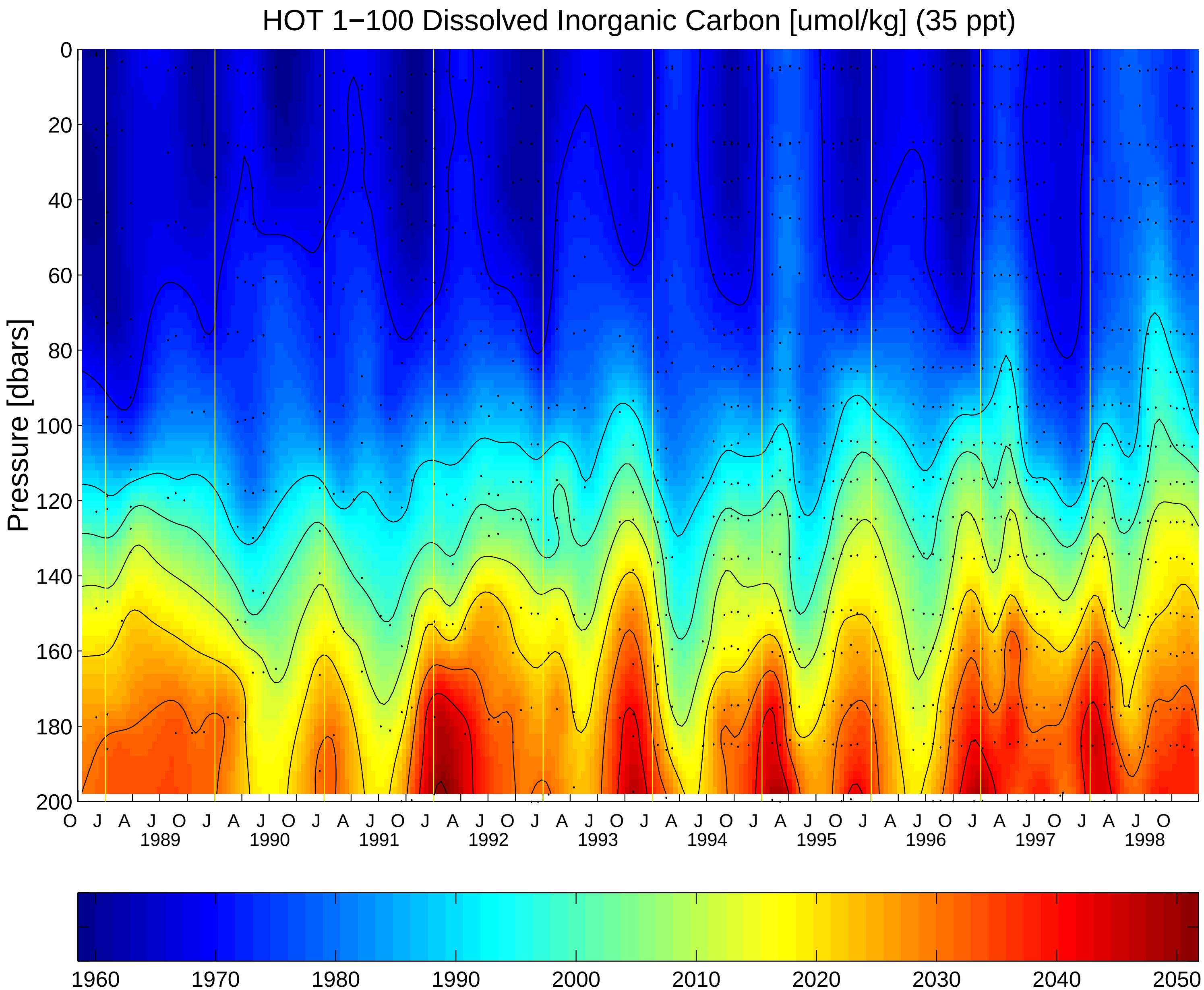
HOT 1−100 Dissolved Inorganic Carbon [umol/kg] (35 ppt)
Pressure [dbars]
0
20
40
60
80
100
120
140
160
180
200
O J A J O J A J O J A J O J A J O J A J O J A J O J A J O J A J O J A J O J A J O
1989
1990
1991
1992
1993
1994
1995
1996
1997
1998
1960
1970
1980
1990
2000
2010
2020
2030
2040
2050

FIGURE 6.5.2a.

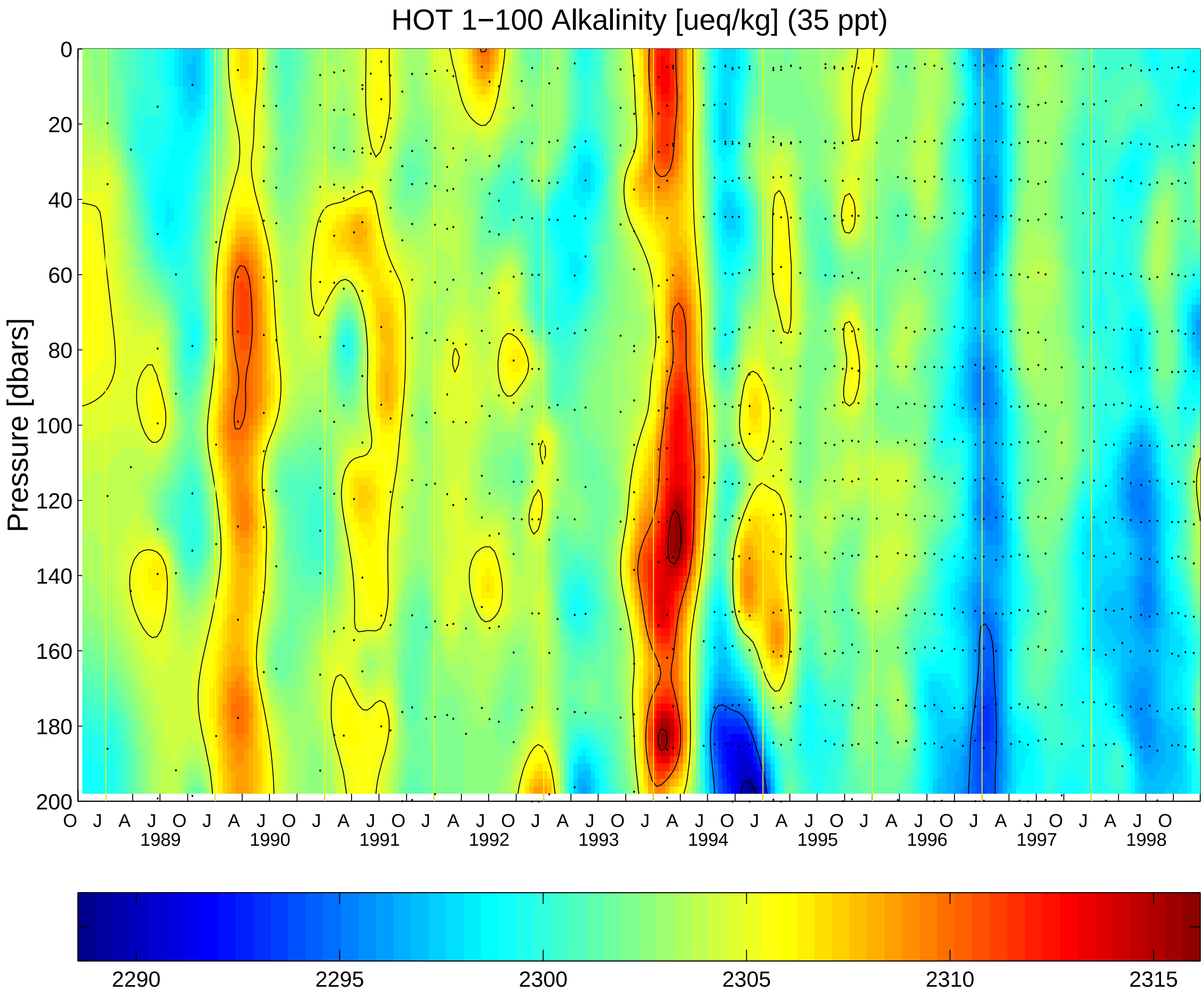
HOT 1−100 Alkalinity [ueq/kg] (35 ppt)
Pressure [dbars]
0
20
40
60
80
100
120
140
160
180
200
O J A J O J A J O J A J O J A J O J A J O J A J O J A J O J A J O J A J O J A J O
1989
1990
1991
1992
1993
1994
1995
1996
1997
1998
2290
2295
2300
2305
2310
2315

FIGURE 6.5.2b.

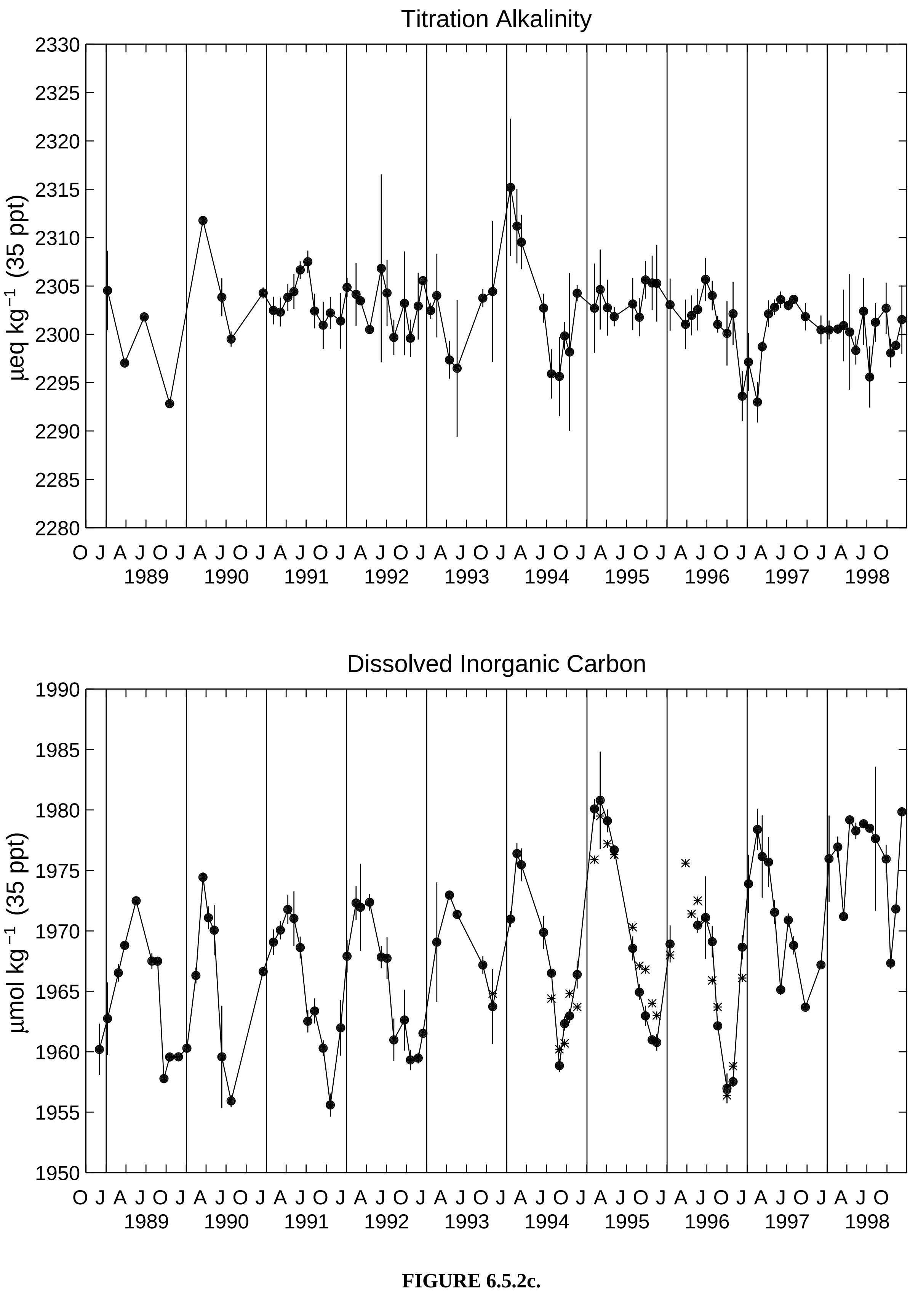

Titration Alkalinity
μeq kg⁻¹ (35 ppt)
2330
2325
2320
2315
2310
2305
2300
2295
2290
2285
2280
O J A J O J A J O J A J O J A J O J A J O J A J O J A J O J A J O J A J O J A J O
1989 1990 1991 1992 1993 1994 1995 1996 1997 1998
Dissolved Inorganic Carbon
μmol kg⁻¹ (35 ppt)
1990
1985
1980
1975
1970
1965
1960
1955
1950
O J A J O J A J O J A J O J A J O J A J O J A J O J A J O J A J O J A J O J A J O
1989 1990 1991 1992 1993 1994 1995 1996 1997 1998

FIGURE 6.5.2c.

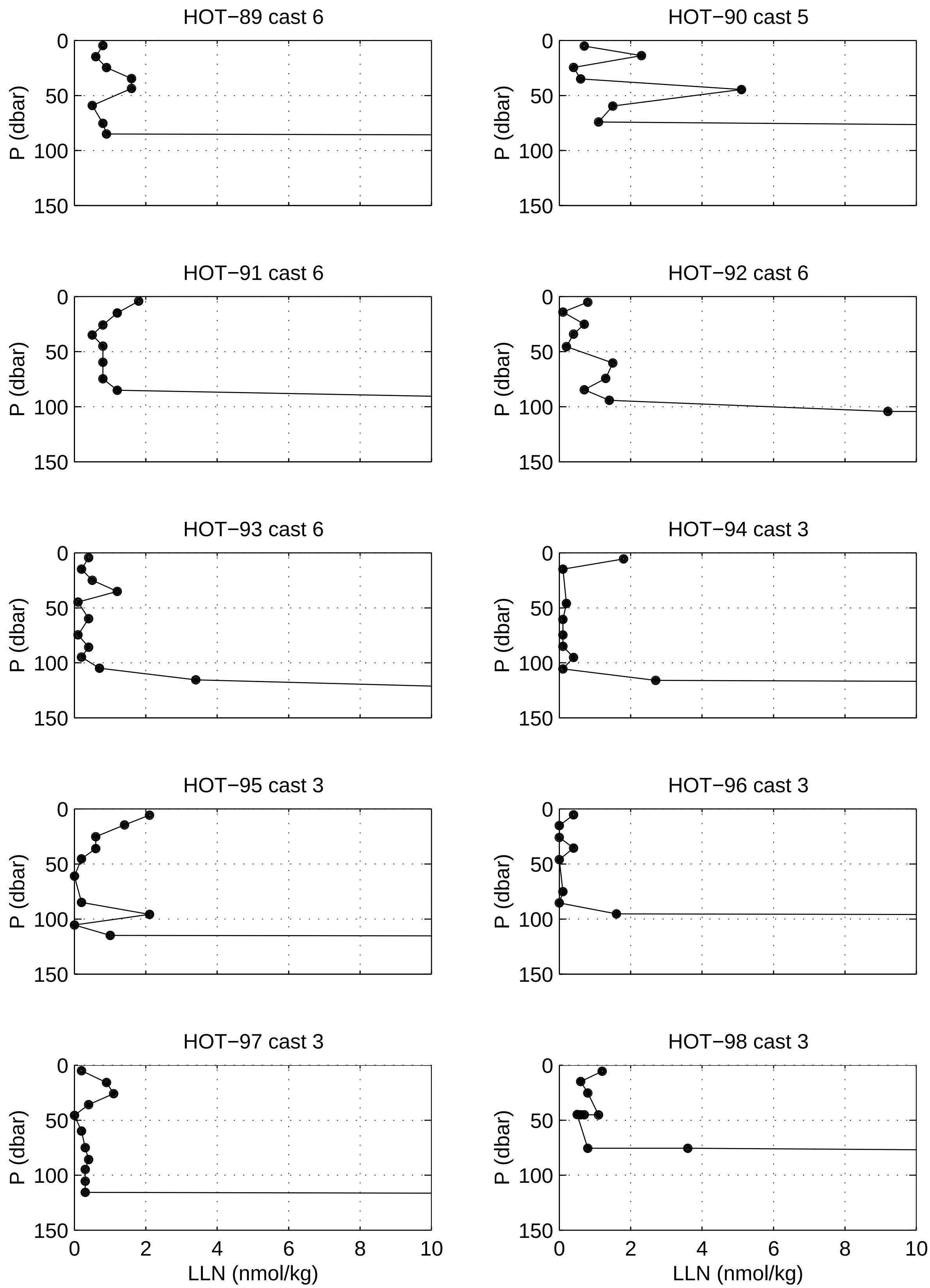
HOT−89 cast 6
HOT−90 cast 5
HOT−91 cast 6
HOT−92 cast 6
HOT−93 cast 6
HOT−94 cast 3
HOT−95 cast 3
HOT−96 cast 3
HOT−97 cast 3
HOT−98 cast 3
P (dbar)
0
50
100
150
0
2
4
6
8
10
LLN (nmol/kg)

FIGURE 6.5.3a.

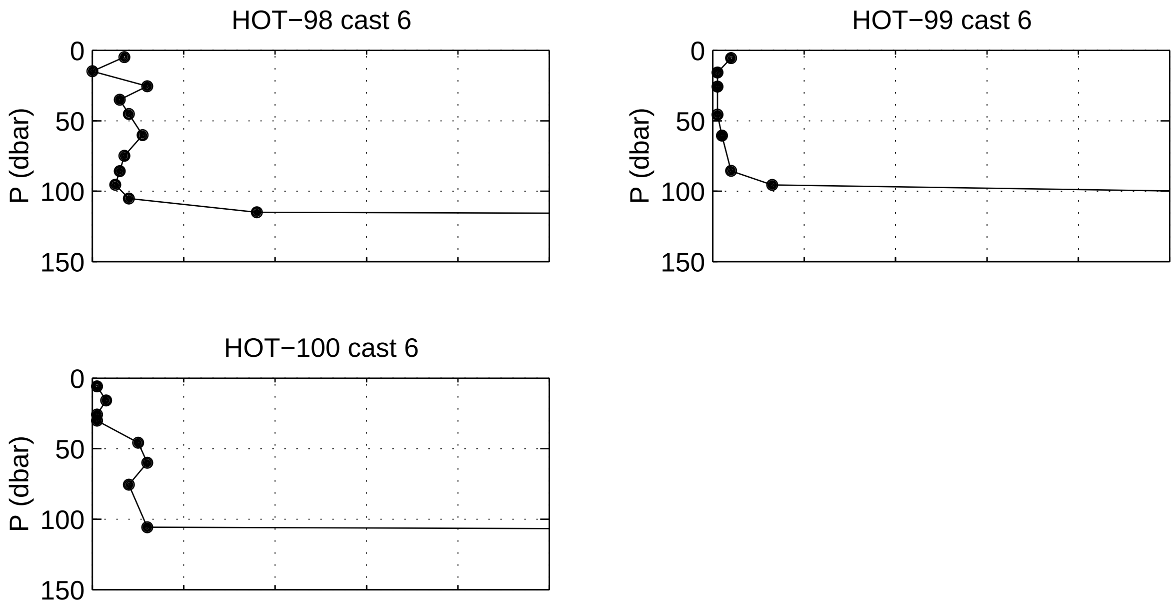

FIGURE 6.5.3a continued.

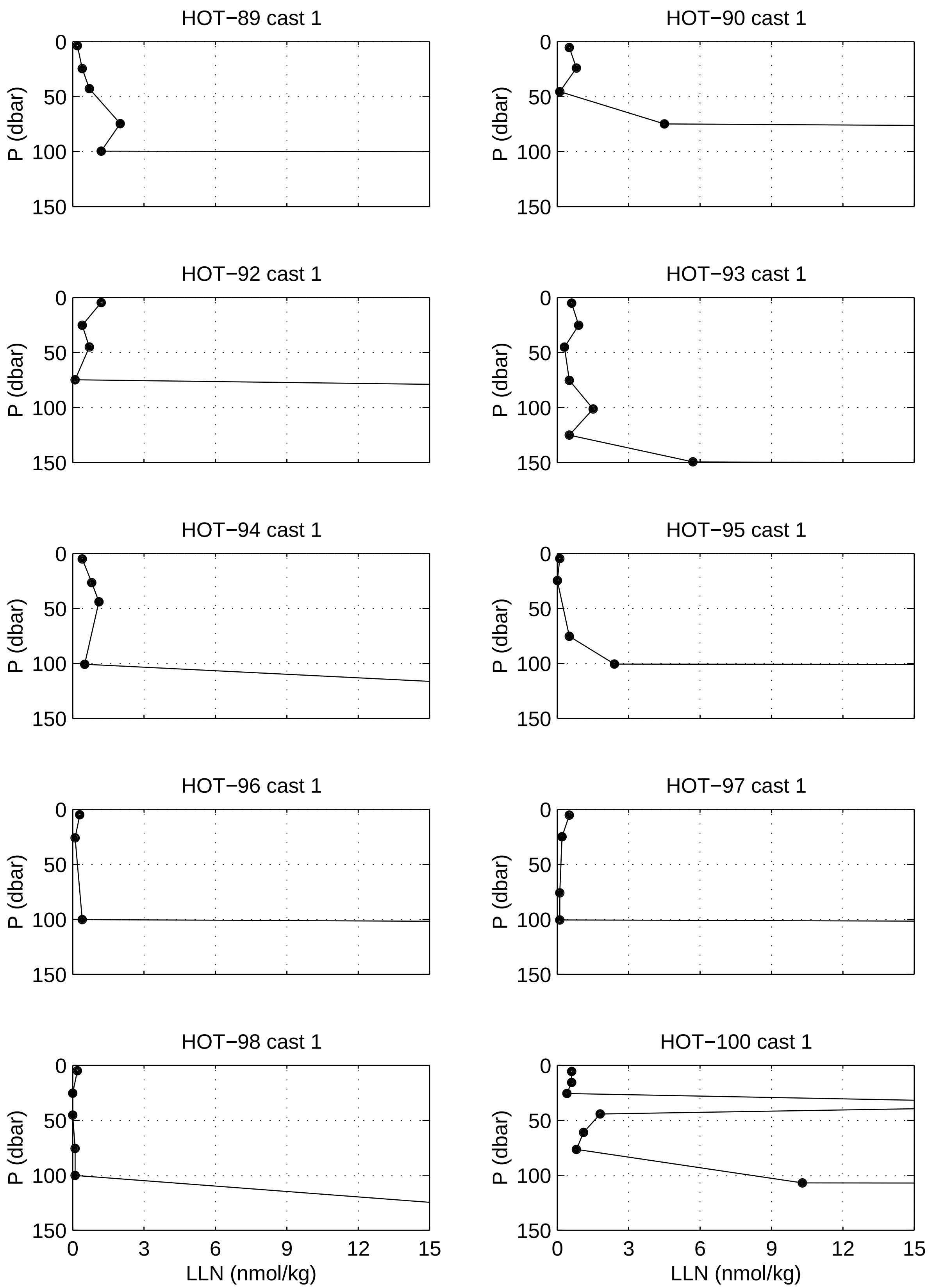

HOT−89 cast 1
HOT−90 cast 1
HOT−92 cast 1
HOT−93 cast 1
HOT−94 cast 1
HOT−95 cast 1
HOT−96 cast 1
HOT−97 cast 1
HOT−98 cast 1
HOT−100 cast 1
P (dbar)
0
50
100
150
0
3
6
9
12
15
LLN (nmol/kg)

FIGURE 6.5.3b.

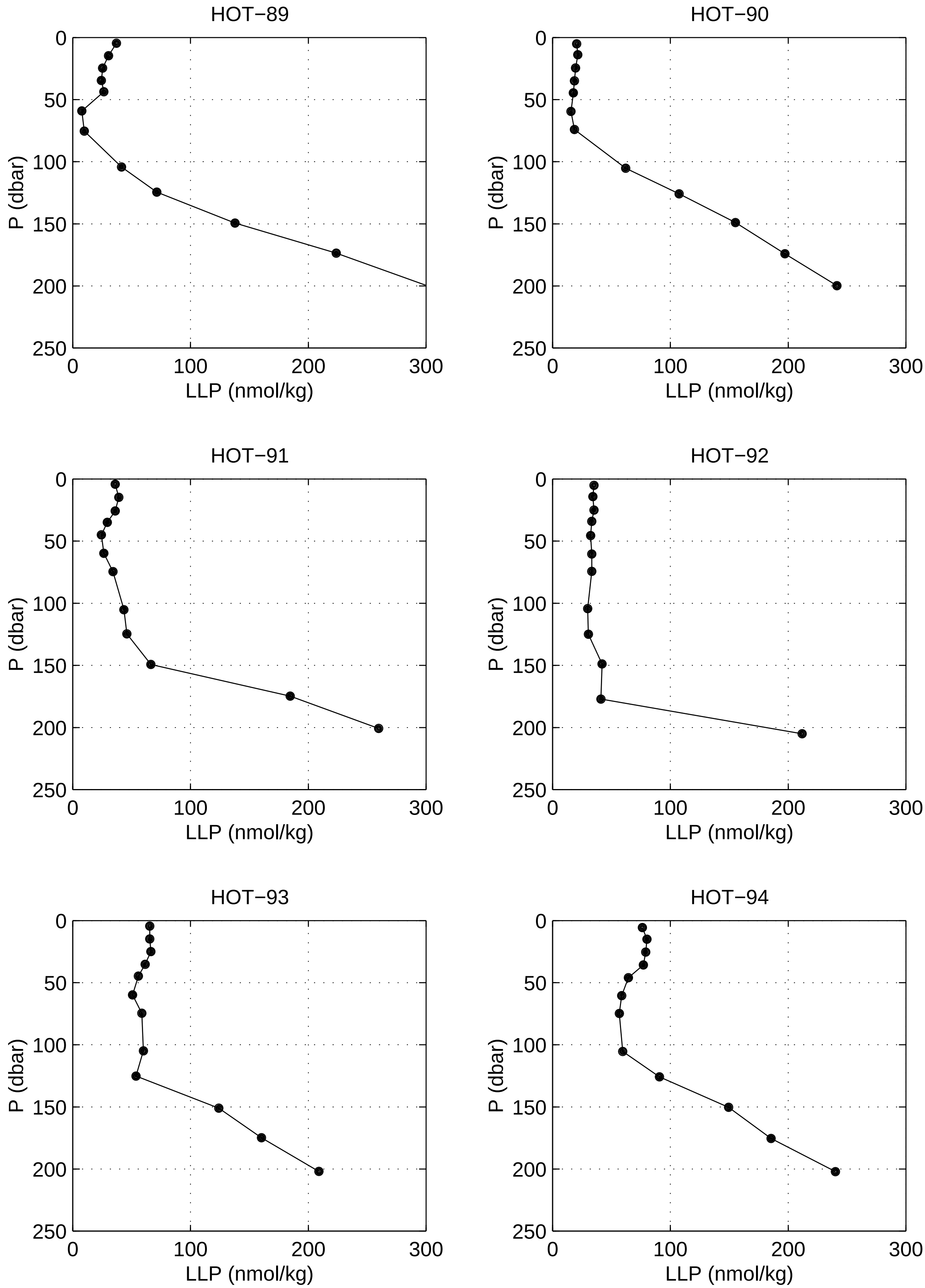

FIGURE 6.5.4.

FIGURE 6.5.5.

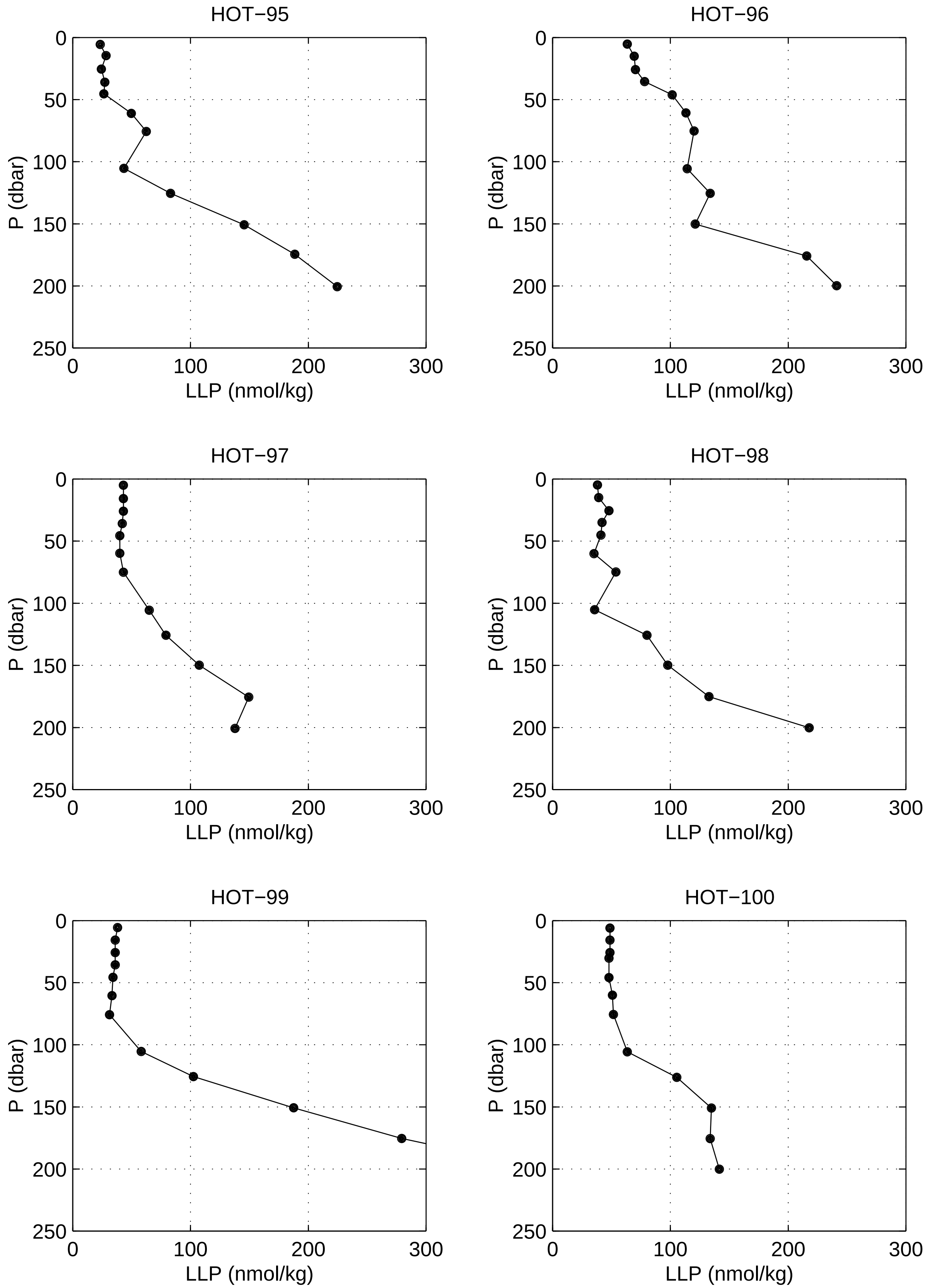

FIGURE 6.5.6.

FIGURE 6.5.4 continued

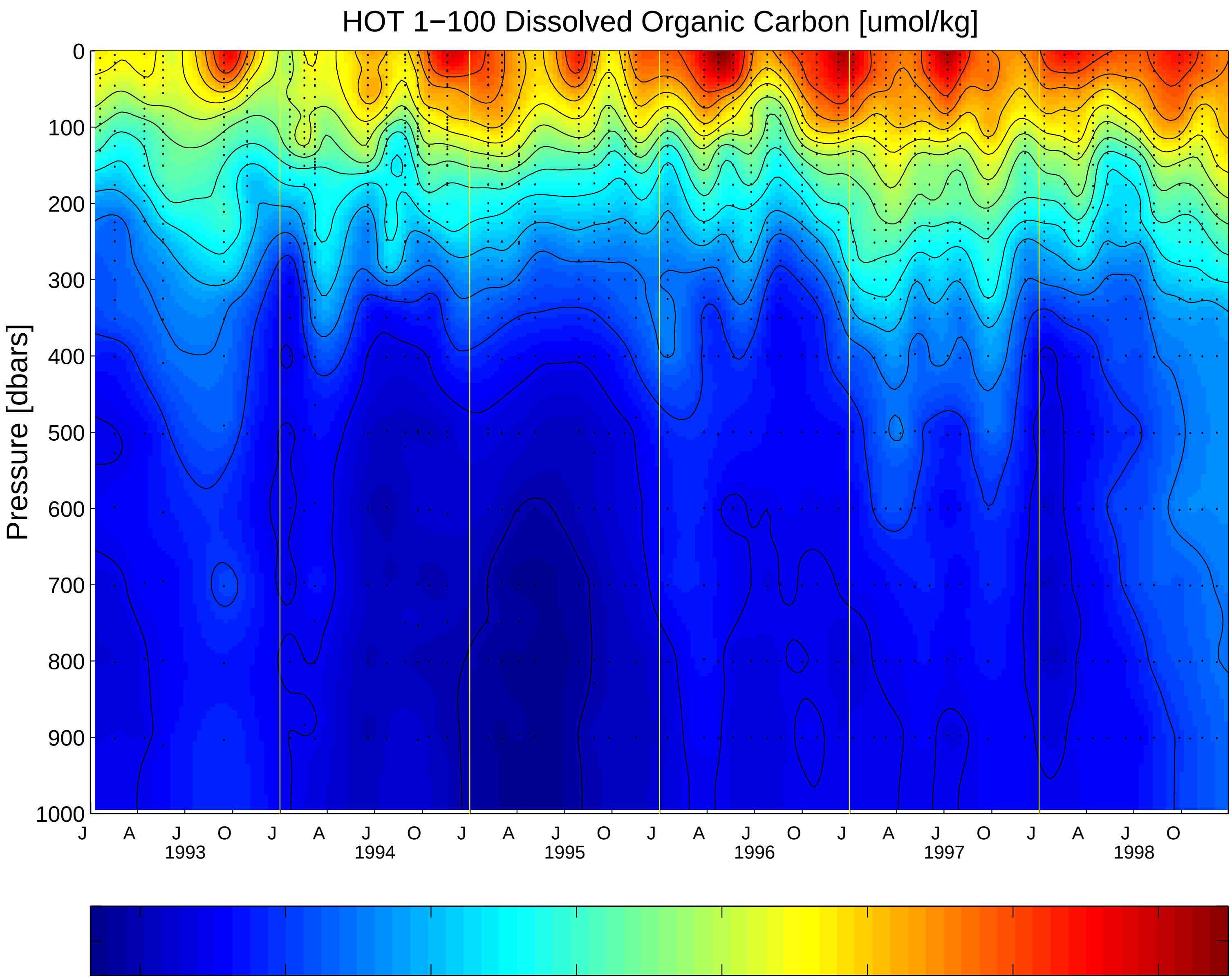
HOT 1−100 Dissolved Organic Carbon [umol/kg]
Pressure [dbars]
0
100
200
300
400
500
600
700
800
900
1000
J A J O J A J O J A J O J A J O J A J O J A J O
1993
1994
1995
1996
1997
1998
40
50
60
70
80
90
100
110

FIGURE 6.5.7.

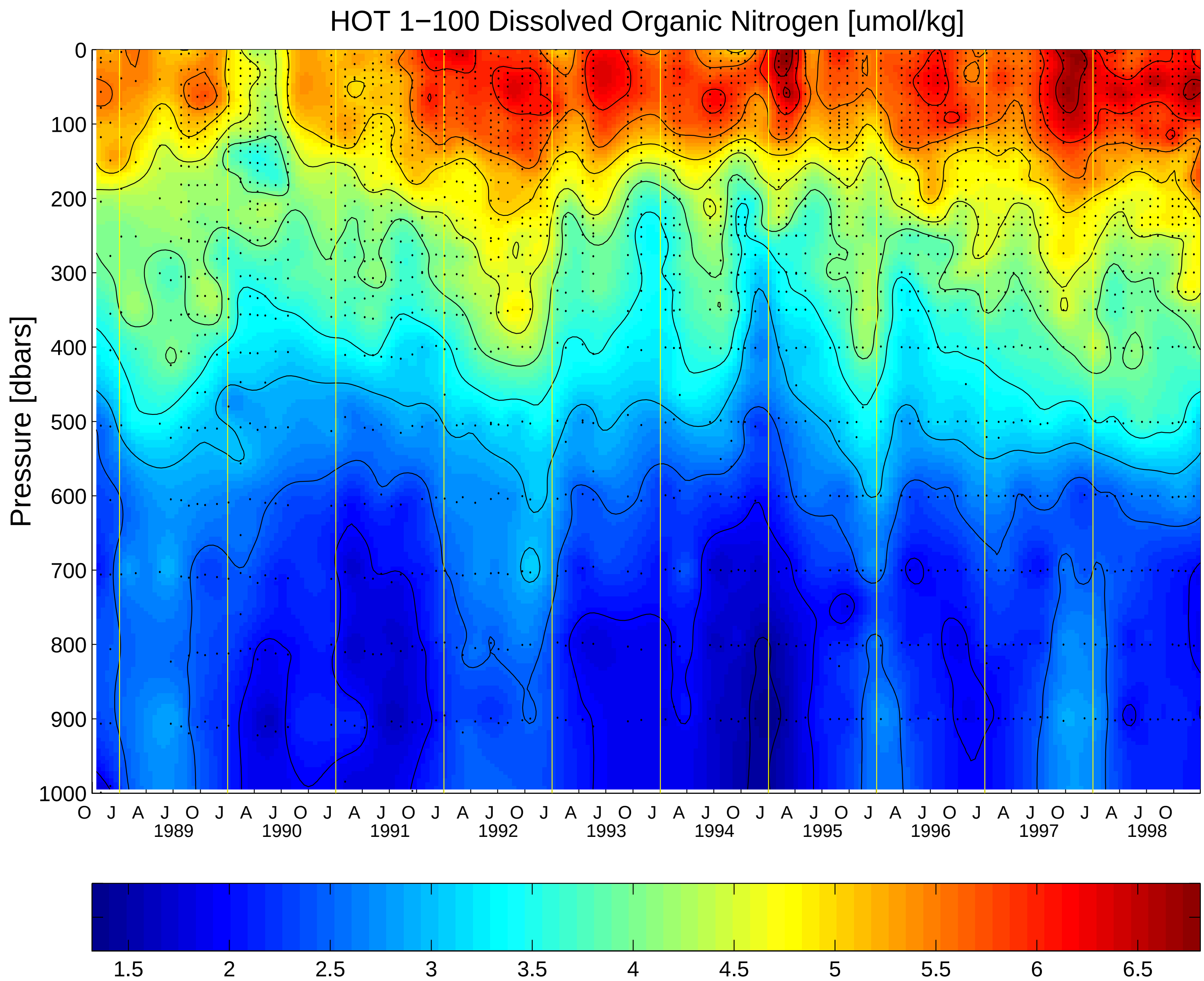
HOT 1−100 Dissolved Organic Nitrogen [umol/kg]
Pressure [dbars]
0
100
200
300
400
500
600
700
800
900
1000
O J A J O J A J O J A J O J A J O J A J O J A J O J A J O J A J O J A J O J A J O
1989
1990
1991
1992
1993
1994
1995
1996
1997
1998
1.5
2
2.5
3
3.5
4
4.5
5
5.5
6
6.5

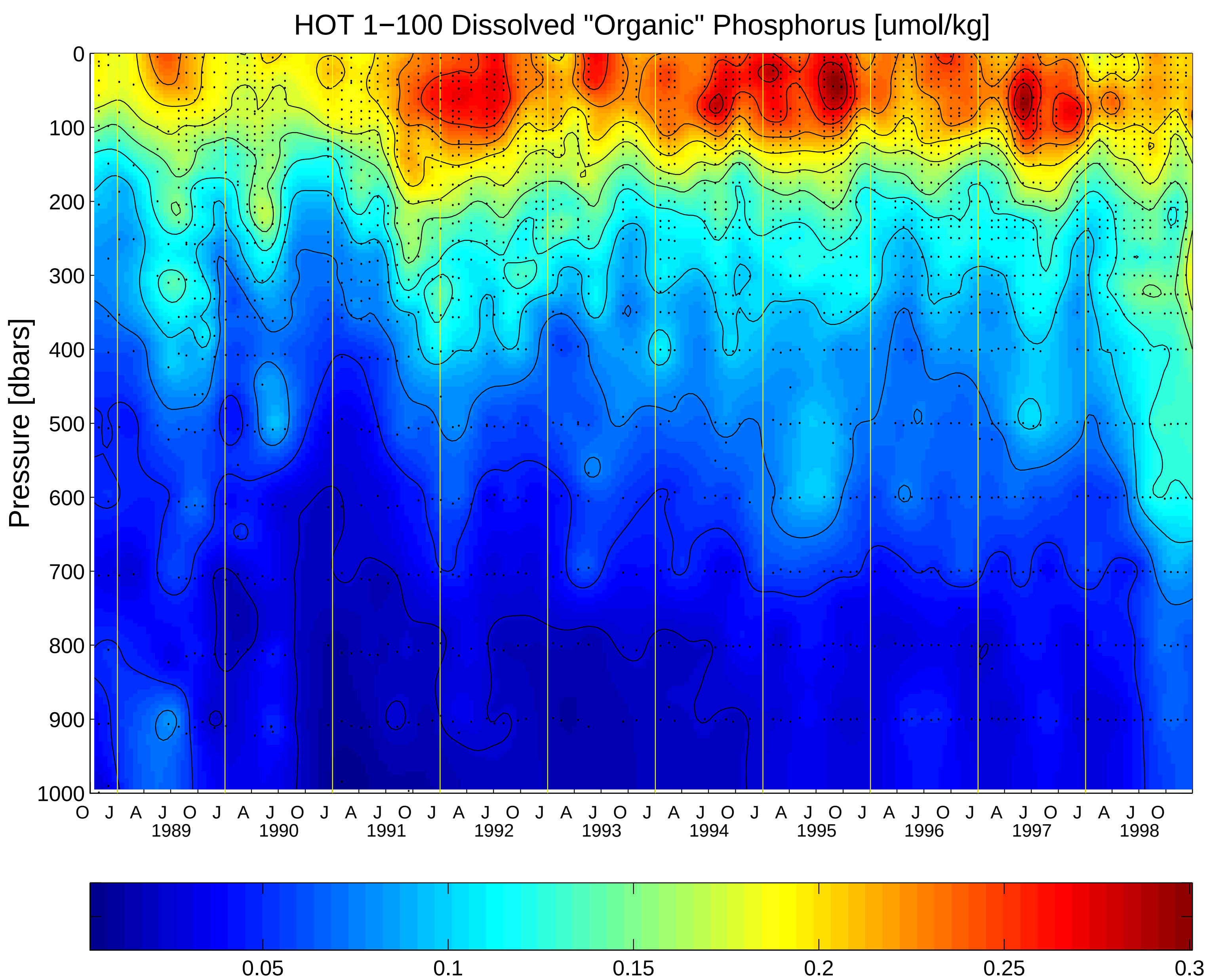

HOT 1−100 Dissolved "Organic" Phosphorus [umol/kg]
Pressure [dbars]
0
100
200
300
400
500
600
700
800
900
1000
O J A J O J A J O J A J O J A J O J A J O J A J O J A J O J A J O J A J O J A J O
1989
1990
1991
1992
1993
1994
1995
1996
1997
1998
0.05
0.1
0.15
0.2
0.25
0.3

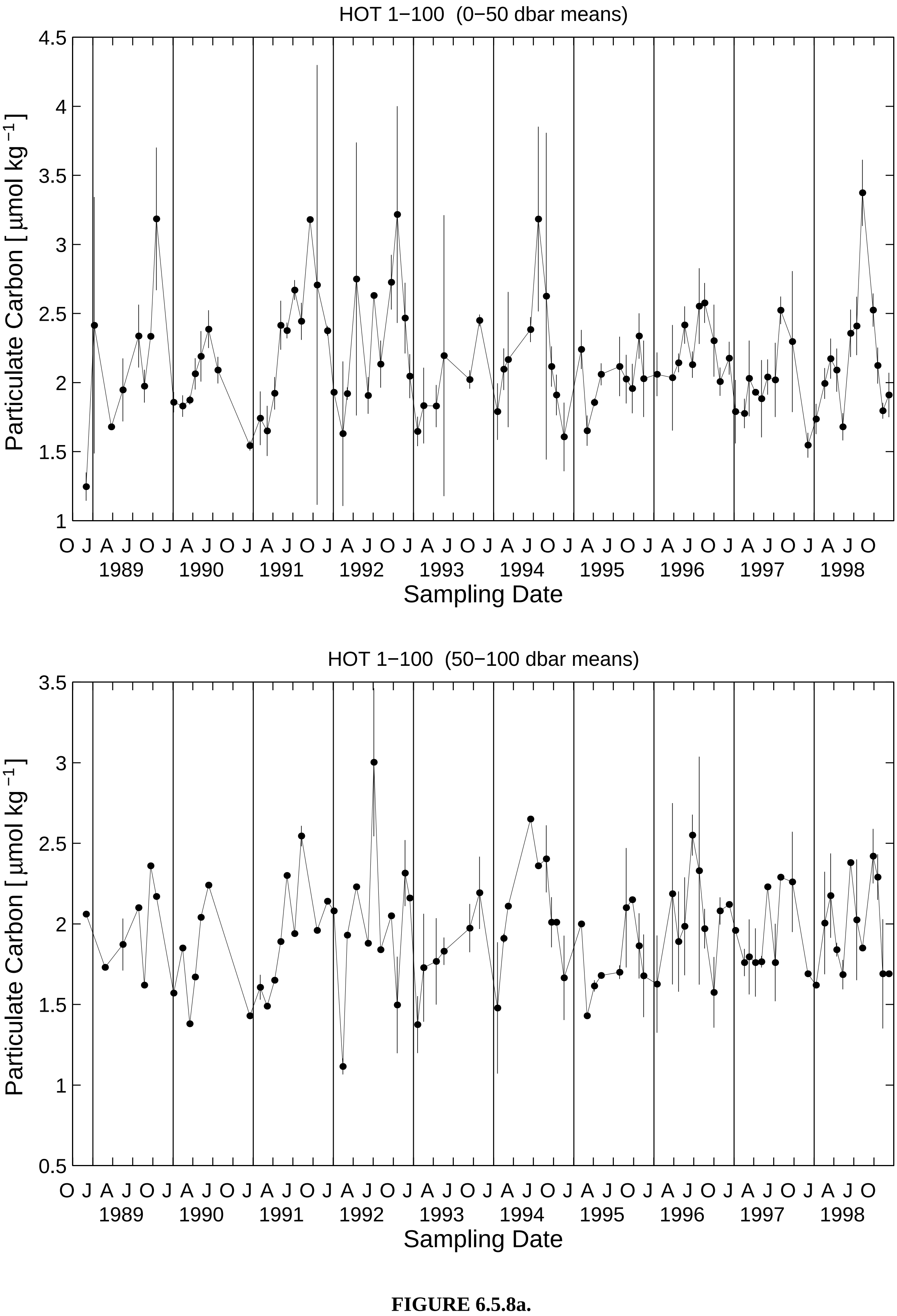
HOT 1−100 (0−50 dbar means)
Particulate Carbon [µmol kg⁻¹]
4.5
4
3.5
3
2.5
2
1.5
1
O J A J O J A J O J A J O J A J O J A J O J A J O J A J O J A J O J A J O J A J O
1989 1990 1991 1992 1993 1994 1995 1996 1997 1998
Sampling Date
HOT 1−100 (50−100 dbar means)
Particulate Carbon [µmol kg⁻¹]
3.5
3
2.5
2
1.5
1
0.5
O J A J O J A J O J A J O J A J O J A J O J A J O J A J O J A J O J A J O J A J O
1989 1990 1991 1992 1993 1994 1995 1996 1997 1998
Sampling Date

FIGURE 6.5.8a.

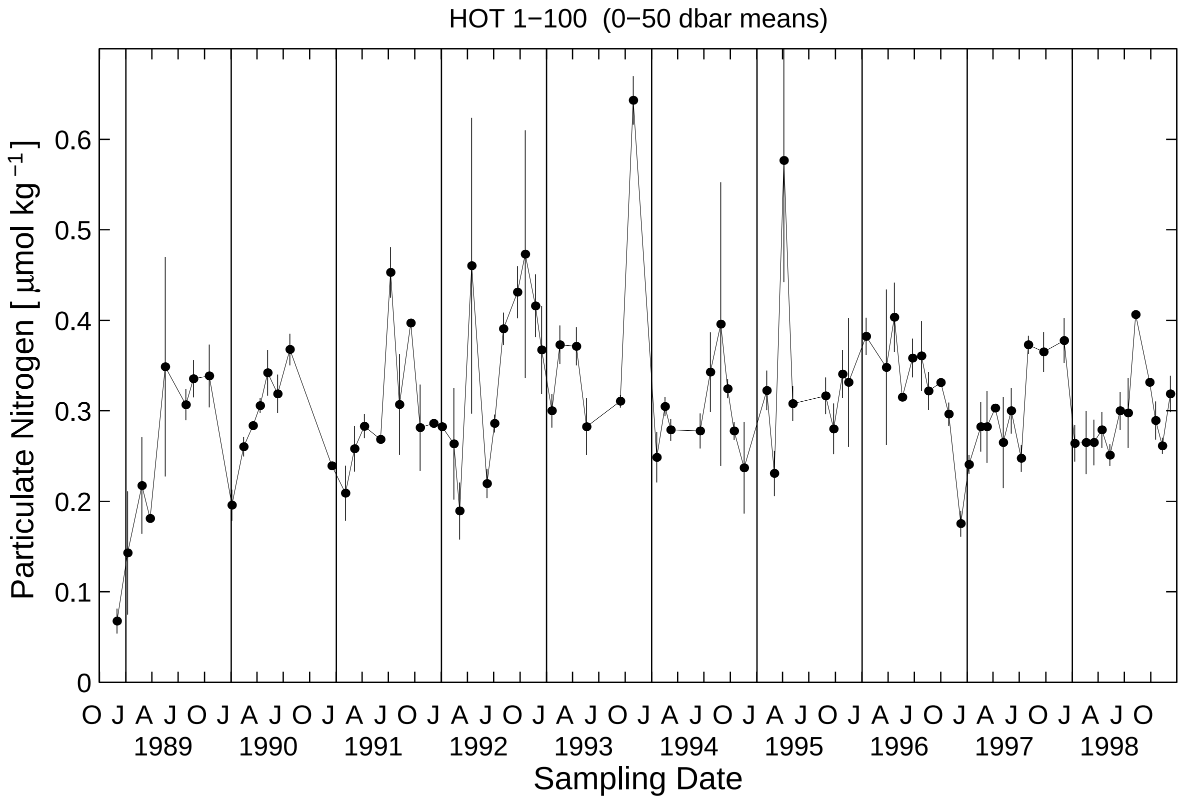

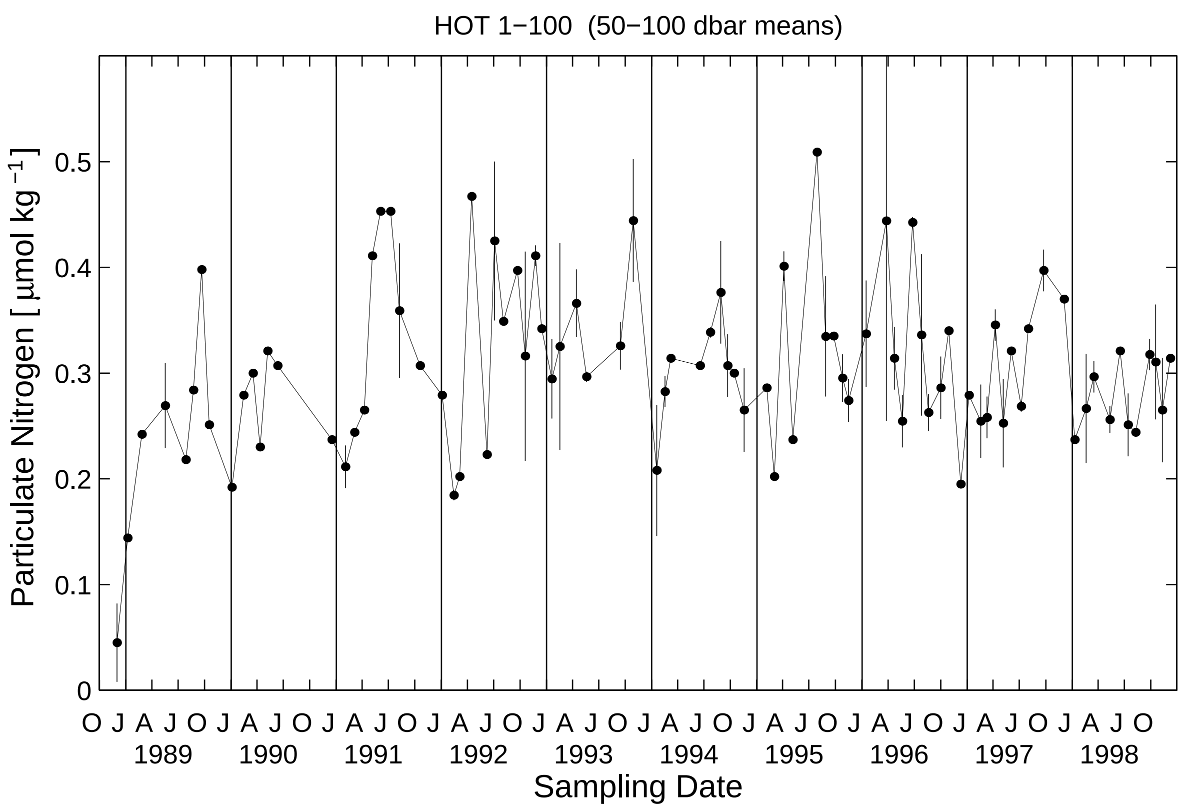

FIGURE 6.5.8b.

FIGURE 6.5.9.

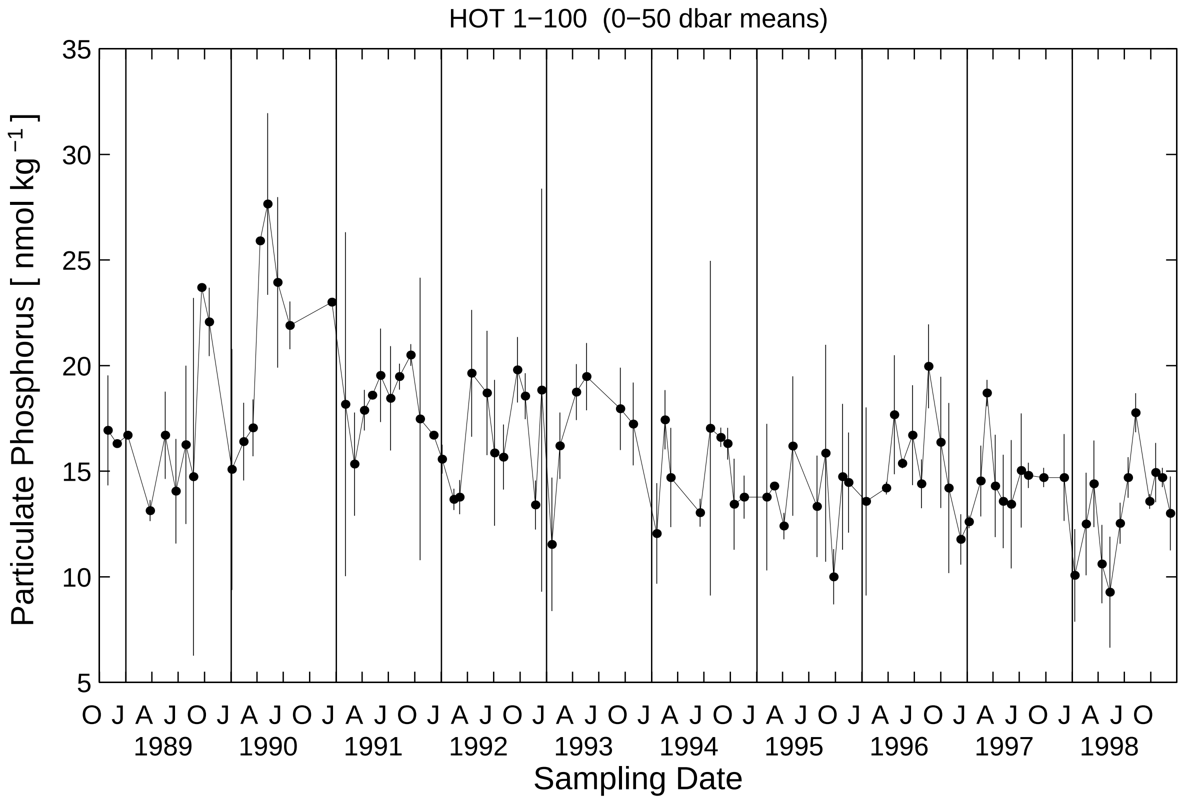

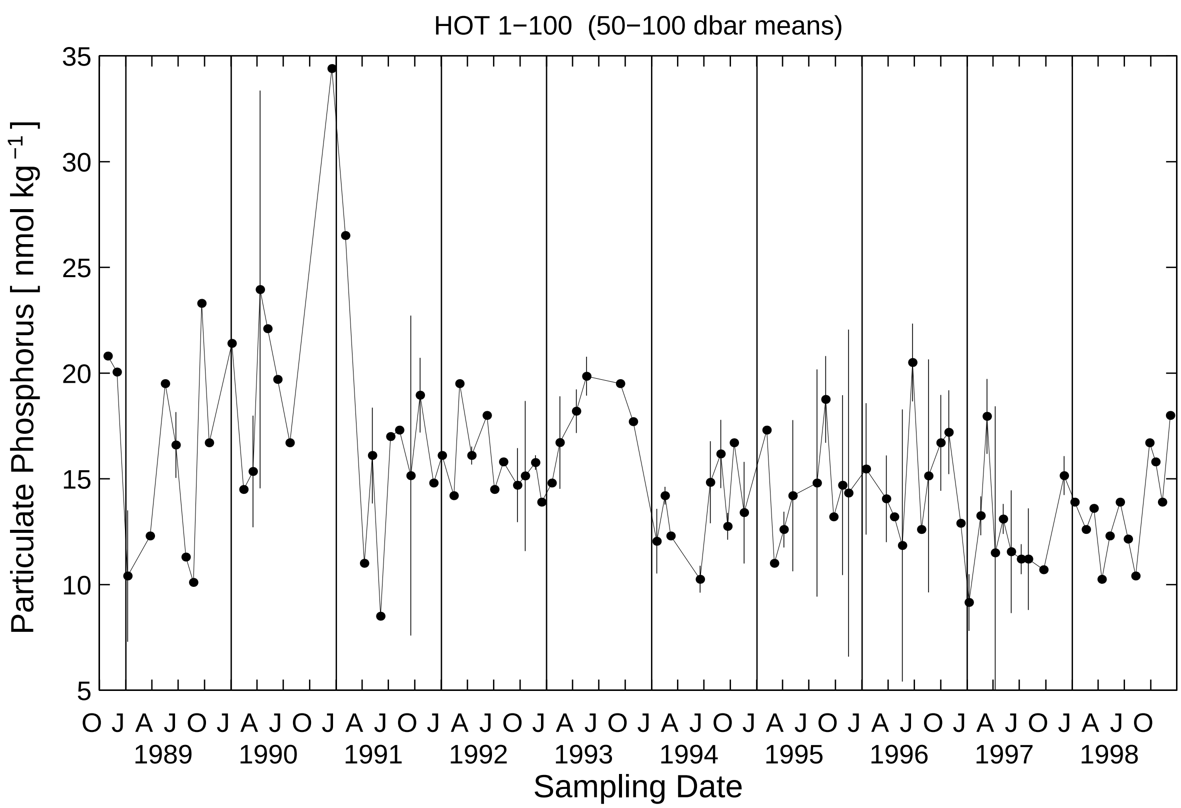

FIGURE 6.5.10.

FIGURE 6.5.8c.

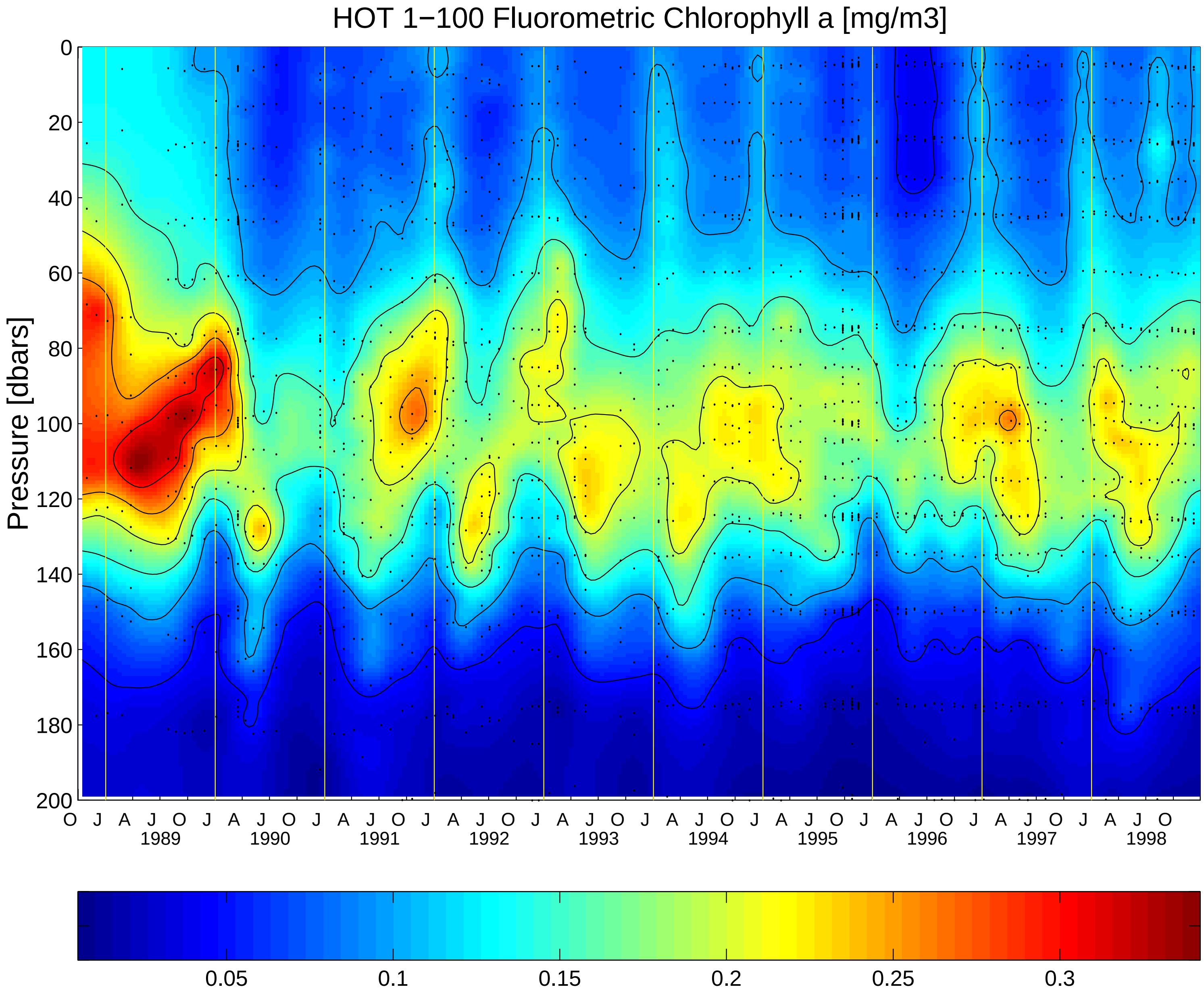

HOT 1−100 Fluorometric Chlorophyll a [mg/m3]
Pressure [dbars]
0
20
40
60
80
100
120
140
160
180
200
O J A J O J A J O J A J O J A J O J A J O J A J O J A J O J A J O J A J O J A J O
1989
1990
1991
1992
1993
1994
1995
1996
1997
1998
0.05
0.1
0.15
0.2
0.25
0.3

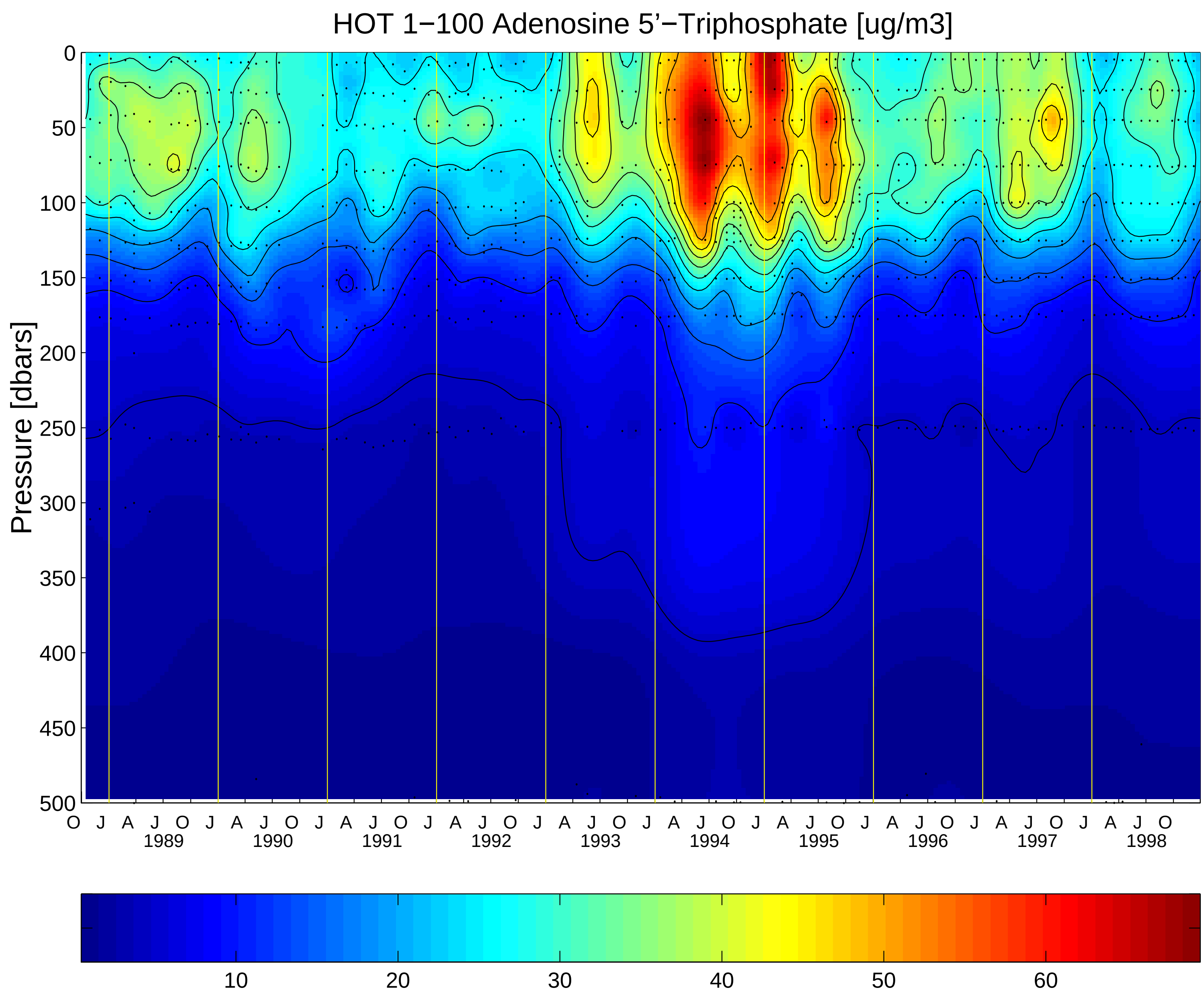
HOT 1−100 Adenosine 5’−Triphosphate [ug/m3]
Pressure [dbars]
0
50
100
150
200
250
300
350
400
450
500
O J A J O J A J O J A J O J A J O J A J O J A J O J A J O J A J O J A J O J A J O
1989
1990
1991
1992
1993
1994
1995
1996
1997
1998
10
20
30
40
50
60

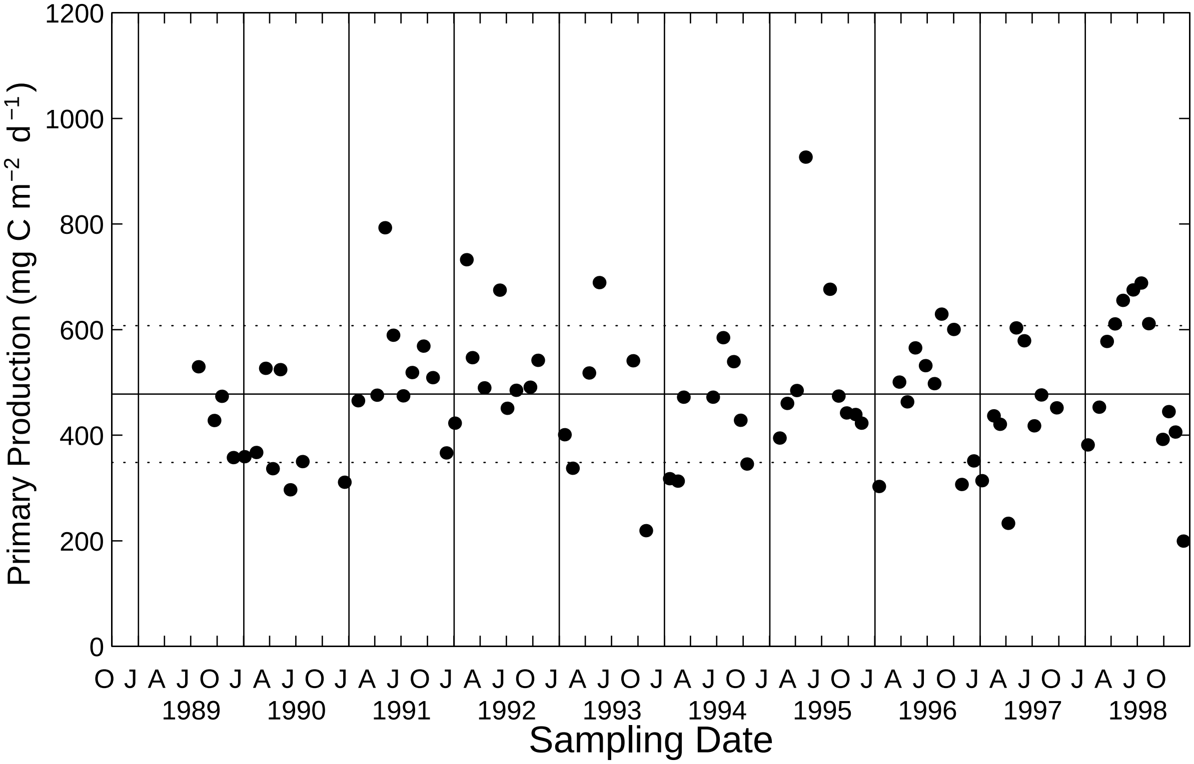
Primary Production (mg C m^{-2} d^{-1})
0
200
400
600
800
1000
1200
O J A J O J A J O J A J O J A J O J A J O J A J O J A J O J A J O J A J O J A J O
1989
1990
1991
1992
1993
1994
1995
1996
1997
1998
Sampling Date

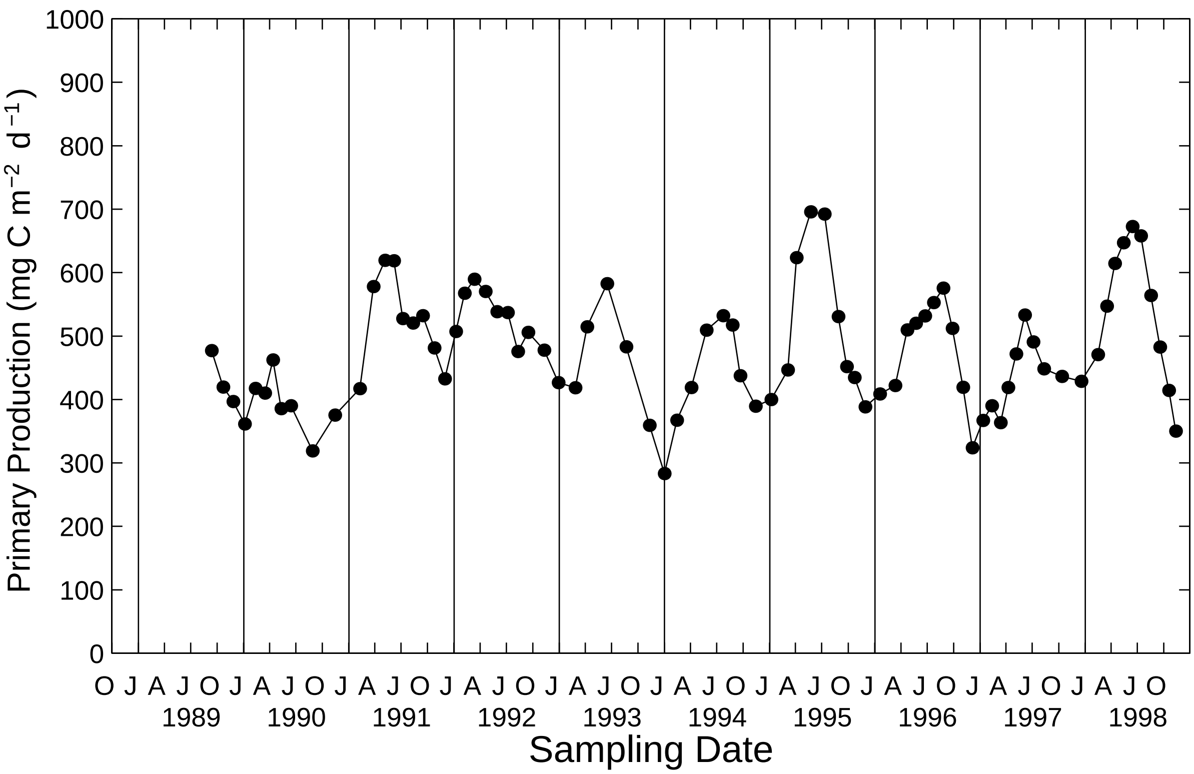
Primary Production (mg C m^{-2} d^{-1})
0
100
200
300
400
500
600
700
800
900
1000
O J A J O J A J O J A J O J A J O J A J O J A J O J A J O J A J O J A J O J A J O
1989
1990
1991
1992
1993
1994
1995
1996
1997
1998
Sampling Date

FIGURE 6.5.11.

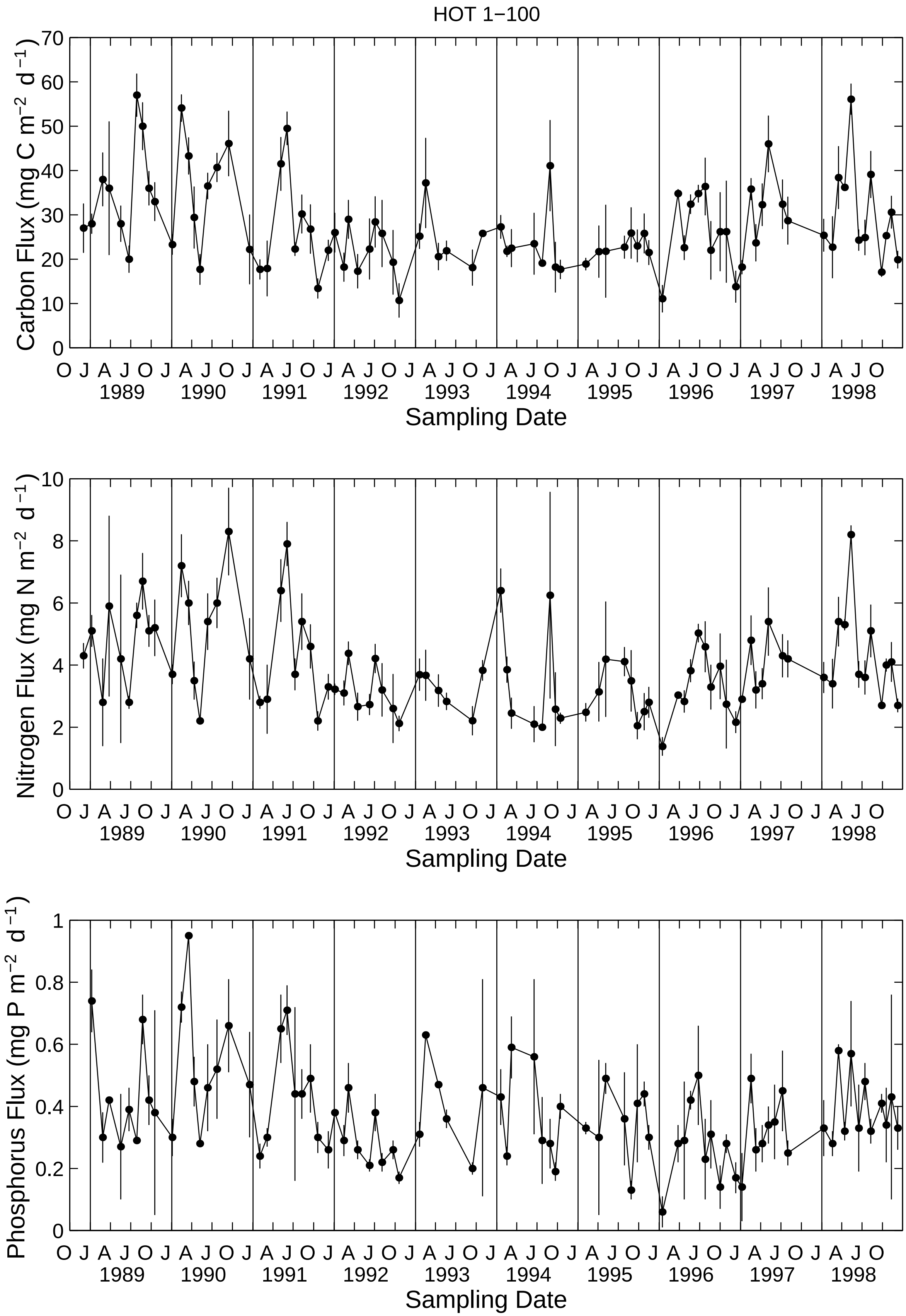
HOT 1−100
Carbon Flux (mg C m−2 d−1)
0
10
20
30
40
50
60
70
O J A J O J A J O J A J O J A J O J A J O J A J O J A J O J A J O J A J O J A J O
1989 1990 1991 1992 1993 1994 1995 1996 1997 1998
Sampling Date
Nitrogen Flux (mg N m−2 d−1)
0
2
4
6
8
10
O J A J O J A J O J A J O J A J O J A J O J A J O J A J O J A J O J A J O J A J O
1989 1990 1991 1992 1993 1994 1995 1996 1997 1998
Sampling Date
Phosphorus Flux (mg P m−2 d−1)
0
0.2
0.4
0.6
0.8
1
O J A J O J A J O J A J O J A J O J A J O J A J O J A J O J A J O J A J O J A J O
1989 1990 1991 1992 1993 1994 1995 1996 1997 1998
Sampling Date

FIGURE 6.5.12.

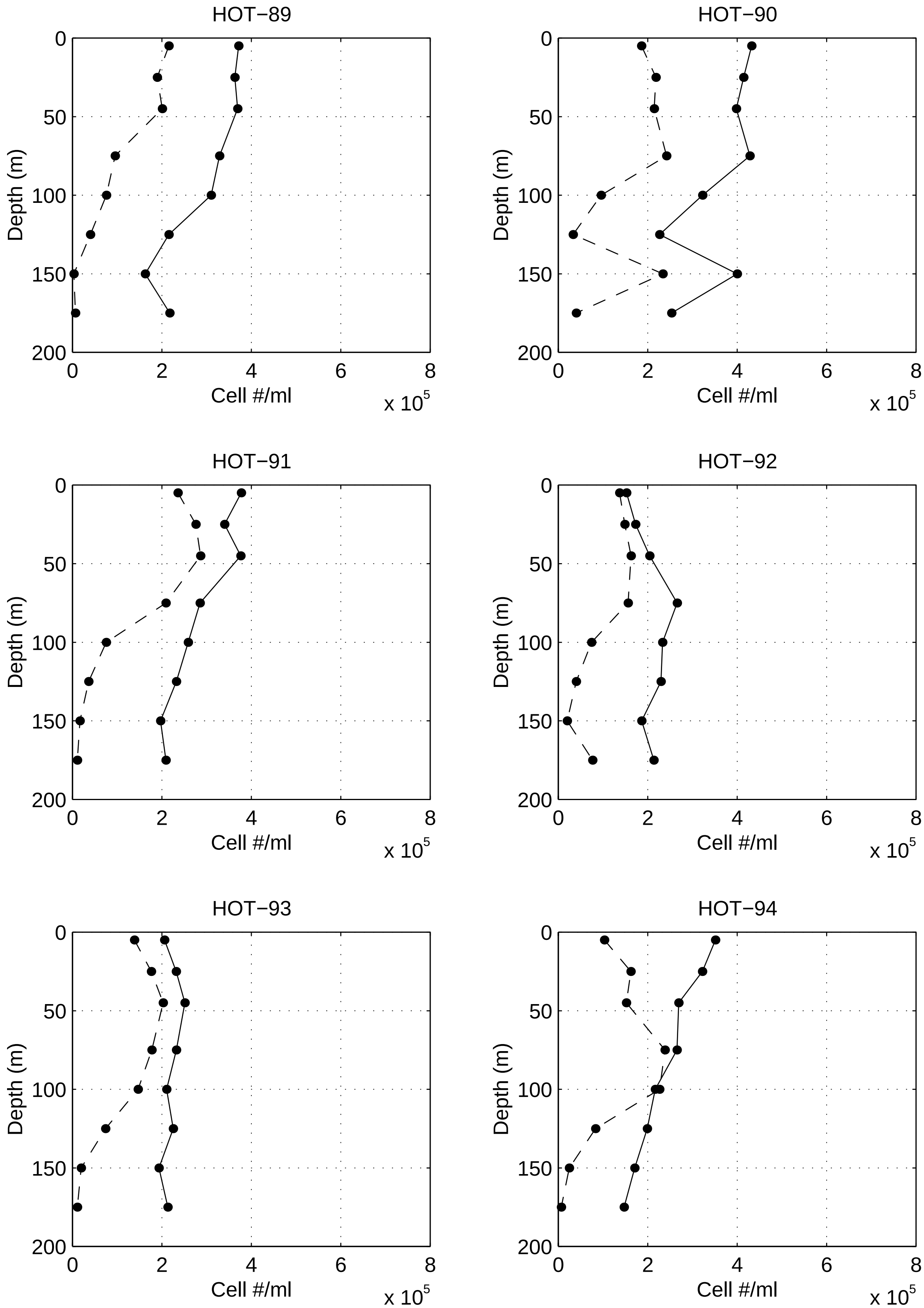
HOT−89
HOT−90
HOT−91
HOT−92
HOT−93
HOT−94
Depth (m)
Cell #/ml
x 10^5
0
50
100
150
200
0
2
4
6
8

FIGURE 6.5.13.

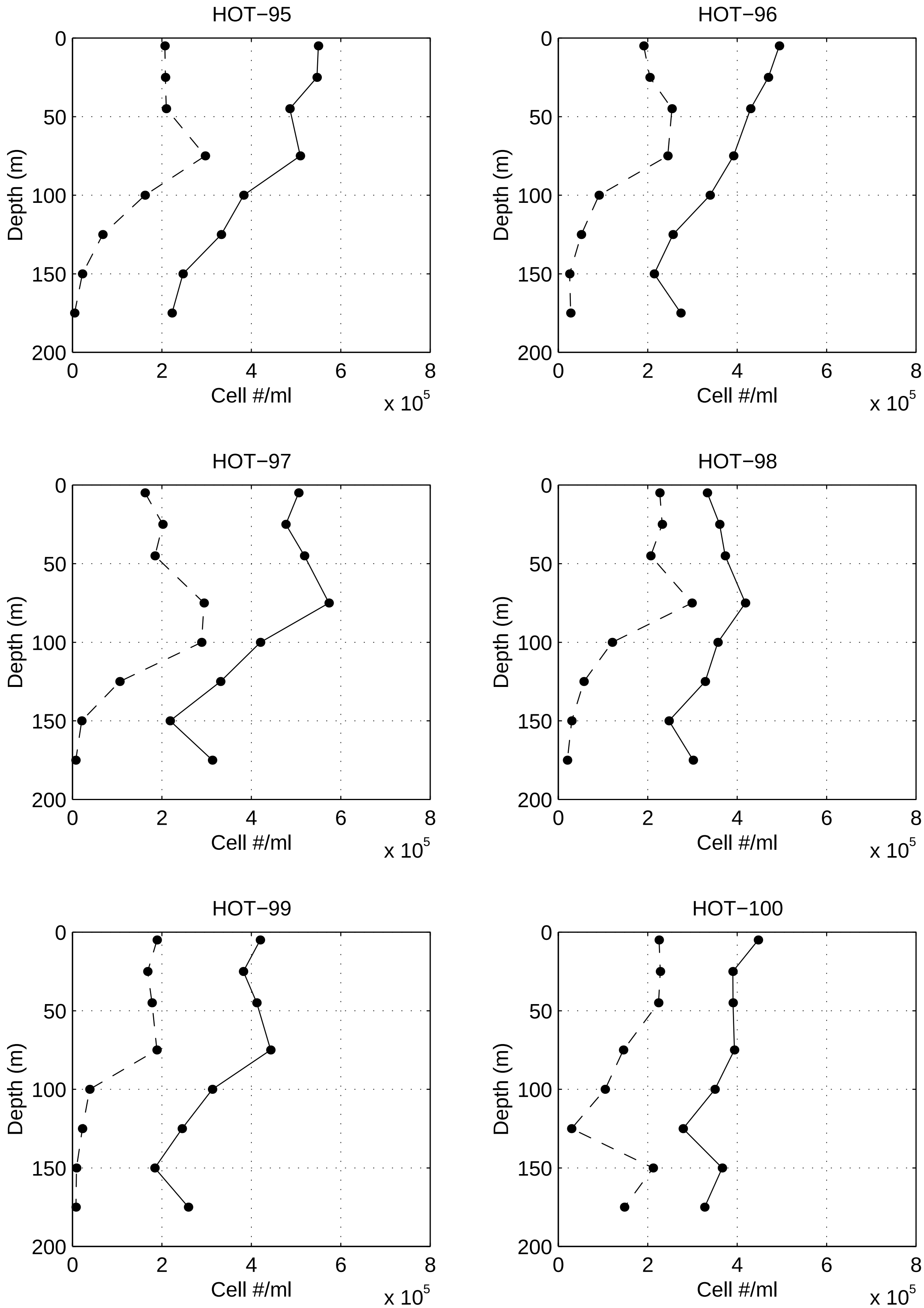

FIGURE 6.5.13 continued

7. HOT PROGRAM PRESENTATIONS AND PUBLICATIONS

I. Invited Presentations and Published Abstracts

I.1.1988 Karl, D. NSF-sponsored symposium on Dissertations in Chemical Oceanography, "Research opportunities in Hawaiian waters", Honolulu, Hawaii, November 1988.

I.2.1988 Karl, D. NSF/GOFS-sponsored workshop on sediment traps, "Determination of total C, N, P flux" and "Screens: A potential solution to the problem of swimmers", Gulf Coast Research Laboratory, Mississippi, November 1988.

I.3.1989 Winn, C.D., S. Chiswell, D.M. Karl and R. Lukas. Long time-series research in the Central Pacific Ocean. The Oceanography Society 1st Annual Meeting, Monterey, California.

I.4.1990 Karl, D., R. Letelier, D. Bird, D. Hebel, C. Sabine and C. Winn. An Oscillatoria bloom in the oligotrophic North Pacific Ocean near the GOFS station ALOHA. EOS, Transactions of the American Geophysical Union 71, 177-178.

I.5.1990 Winn, C.D., D. Hebel, R. Letelier, D. Bird and D. Karl. Variability in biogeochemical fluxes in the oligotrophic central Pacific: Results of the Hawaii Ocean Time- Series Program. EOS, Transactions of the American Geophysical Union 71, 190.

I.6.1990 Chiswell, S.M. and R. Lukas. The Hawaii Ocean Time-series (HOT). EOS, Transactions of the American Geophysical Union 71, 1397.

I.7.1990 Karl, D. "JGOFS time-series programs," San Francisco, California, December 1990.

I.8.1991 Winn, C., C. Sabine, D. Hebel, F. Mackenzie and D.M. Karl. Inorganic carbon system dynamics in the central Pacific Ocean: Results of the Hawaii Ocean Time-series program. EOS, Transactions of the American Geophysical Union 72, 70.

I.9.1991 Lukas, R. Water mass variability observed in the Hawaii Ocean Time Series. EOS, Transactions of the American Geophysical Union 72, 70.

I.10.1991 Letelier, R., D. Karl, R. Bidigare, J. Christian, J. Dore, D. Hebel and C. Winn. Temporal variability of phytoplankton pigments at the U.S.-JGOFS station ALOHA (22˚45'N, 158˚W). EOS, Transactions of the American Geophysical Union 72, 74.

I.11.1991 Karl, D. "The Hawaii Ocean Time-series program: Carbon production and particle flux", The Oceanography Society 2nd Annual Meeting, St. Petersburg, Florida, March 1991.

I.12.1991 Karl, D. NATO symposium on Biology and Ecology of Diazotrophic Marine Organisms, "Trichodesmium blooms and new nitrogen in the North Pacific gyre", Bamberg, Germany, May 1991.

I.13.1992 Anbar, A. D. Rhenium in seawater: Confirmation of generally conservative behavior. EOS, Transactions of the American Geophysical Union 73, 278.

I.14.1992 Schudlich, R. and S. R. Emerson. Modeling dissolved gases in the subtropical upper ocean: JGOFS/WOCE Hawaiian Ocean Time-series. EOS, Transactions of the American Geophysical Union 73, 287.

I.15.1992 Tupas, L.M., B.N. Popp and D.M. Karl. Dissolved organic carbon in oligotrophic waters: experiments on sample preservation, storage and analysis. EOS, Transactions of the American Geophysical Union 73, 287.

I.16.1992 Karl, D., C. Winn, D. Hebel, R. Letelier, J. Dore and J. Christian. The U.S.-JGOFS Hawaii Ocean Time-Series (HOT) program. American Society for Limnology and Oceanography Aquatic Sciences Meeting, Santa Fe, NM, February 1992.

I.17.1992 Campbell, L., R. R. Bidigare, R. Letelier, M. Ondrusek, S. Hall, B. Tsai and C. Winn. Phytoplankton population structure at the Hawaii Ocean Time-series station. American Society for Limnology and Oceanography Aquatic Sciences Meeting, Santa Fe, NM, February 1992.

I.18.1992 Karl, D. NSF-sponsored GLOBEC scientific steering committee meeting, "Hawaii Ocean Time-series (HOT) program: A GLOBEC 'Blue Water' initiative", Honolulu, Hawaii, March 1992.

I.19.1992 Karl, D. IGBP International Symposium on Global Change, "Oceanic ecosystem variability: Initial results from the JGOFS Hawaii Ocean Time-series (HOT) experiment", Tokyo, Japan, March 1992.

I.20.1992 Karl, D. Conoco HOT Topics Seminar Series, "The U.S.-JGOFS Hawaii Ocean Time- Series (HOT) Program: Biogeochemical Vignettes from the Oligotrophic North Pacific Ocean" and "Temporal Variability in Bioelement Flux at Station ALOHA (22˚45'N, 158˚W)", Woods Hole, Massachusetts, May 1992

I.21.1992 Bidigare, R. R., L. Campbell, M. Ondrusek, R. Letelier and D. Vaulot. Characterization of picophytoplankton at Station ALOHA (22˚45'N, 158˚W) using HPLC, flow cytometry and immunofluorescence techniques. PACON 1992 Meeting, June 1992.

I.22.1992 Winn, C.D., D. Hebel, R. Letelier, J. Christian, J. Dore, R. Lukas and D.M. Karl. Long time-series measurements in the central North Pacific: Results of the Hawaii Ocean Time-series program. PACON conference, Kona, Hawaii, June 1992.

I.23.1993 Atkinson, M. J. A potentiometric solid state sensor for oceanic CTDs, Abstract of The Oceanography Society Annual Meeting, Seattle, Washington, April 1993.

I.24.1993 Campbell, L., H.A. Nolla and D. Vaulot. Microbial biomass in the subtropical central North Pacific Ocean (Station ALOHA): The importance of Prochlorococcus, Abstract of The Oceanography Society Annual Meeting, Seattle, Washington, April 1993.

I.25.1993 Emerson, S., P. Quay, C. Stump, D. Wilbur and R. Schudlich. Oxygen cycles and productivity in the oligotrophic subtropical Pacific Ocean. Abstract of The Oceanography Society Annual Meeting, Seattle, Washington, April 1993.

I.26.1993 Sharp, J. H., R. Benner, L. Bennett, C.A. Carlson, S.E. Fitzwater, E.T. Peltzer, and L. Tupas. Dissolved organic carbon: Intercalibration of analyses with equatorial Pacific samples. Abstract of The Oceanography Society Annual Meeting, Seattle, Washington, April 1993.

I.27.1993 Winn, C.D., C.J. Carrillo, F.T. Mackenzie and D.M. Karl. Variability in the inorganic carbon system parameters in the North Pacific subtropical gyre. Abstract of The Oceanography Society Annual Meeting, Seattle, Washington, April 1993.

I.28.1993 Yanagi, K. and D.M. Karl. Note on the fractional determination of TDP in seawater by an UV-irradiation method combined with the MAGIC procedure. Abstract of the Oceanography Society of Japan annual meeting, Tokyo, Japan, April 1993.

I.29.1993 Campbell, L., H. Liu, R. R. Bidigare and D. Vaulot. Immunochemical characterization of Prochlorococcus. Abstract of the American Society of Limnology and Oceanography 1993 Annual Meeting, Edmonton, Alberta, Canada, May 1993.

I.30.1993 Christian, J. R. and D.M. Karl. Bacterial exoenzymes in marine waters: Implications for global biogeochemical cycles. Abstract of the American Society of Limnology and Oceanography 1993 Annual Meeting, Edmonton, Alberta, Canada, May 1993.

I.31.1993 Moyer, C.L., L. Campbell, D.M. Karl and J. Wilcox. Restriction fragment length polymorphism (RFLP) and DNA sequence analysis of PCR-generated clones to assess diversity of picoeukaryotic algae in the subtropical central North Pacific Ocean (Station ALOHA). Abstract of the American Society of Limnology and Oceanography 1993 Annual Meeting, Edmonton, Alberta, Canada, May 1993.

I.32.1993 Sharp, J.H., R. Benner, L. Bennett, C.A. Carlson, S.E. Fitzwater and L. Tupas. The equatorial Pacific intercalibration analyses of dissolved organic carbon in seawater. Abstract of the American Society of Limnology and Oceanography 1993 Annual Meeting, Edmonton, Alberta, Canada, May 1993.

I.33.1994 Yuan, J., C. I. Measures and J. A. Resing. Rapid determination of iron in seawater: In-line preconcentration flow injection analysis with spectrophotometric detection. EOS, Transactions of the American Geophysical Union 75, 25.

I.34.1994 Smith, C.R., S. Garner, D. Hoover and R. Pope. Macrobenthos, mechanisms of bioturbation and carbon flux proxies at the abyssal seafloor along the JGOFS Equatorial Pacific Transect. EOS, Transactions of the American Geophysical Union 75, 70.

I.35.1994 Farrenkopf, A.M., G.W. Luther, III and C.H. Van Der Weijden. Vertical distribution of dissolved iodine species in the northwest Indian Ocean. EOS, Transactions of the American Geophysical Union 75, 78.

I.36.1994 Campbell, L., C.D. Winn, R. Letelier, D. Hebel and D.M. Karl. Temporal variability in phytoplankton fluorescence at Station ALOHA. EOS, Transactions of the American Geophysical Union 75, 100.

I.37.1994 Winn, C., F.T. Mackenzie, C. Carrillo, T. Westby and D.M. Karl. Air-sea carbon dioxide exchange at Station ALOHA. EOS, Transactions of the American Geophysical Union 75, 112.

I.38.1994 Lukas, R., F. Bingham and A. Mantyla. An anomalous cold event in the bottom water observed north of Oahu. EOS, Transactions of the American Geophysical Union 75, 205.

I.39.1994 Tupas, L.M., B.N. Popp and D.M. Karl. Dissolved organic carbon in oligotrophic waters; experiments on sample preservation, storage and analysis. EOS, Transactions of the American Geophysical Union 75, 287.

I.40.1994 Bingham, F.M. Drifter observations of the North Hawaiian Ridge Current. EOS, Transactions of the American Geophysical Union 75, 307.

I.41.1994 HOT Program P.I.s, staff and students. The Hawaii Ocean Time-series (HOT) program: The first five years, p. 59. Abstract of The Oceanography Society Pacific Basin Meeting, Honolulu, Hawaii, July 1994.

I.42.1994 HOT Program P.I.s, staff and students. HOT: a time-series study of carbon cycling in the oligotrophic North Pacific, p. 24. Abstract of The Oceanography Society Pacific Basin Meeting, Honolulu, Hawaii, July 1994.

I.43.1994 Bidigare, R.R., L. Campbell, M.E. Ondrusek, R. Letelier, D. Vaulot and D.M. Karl. Phytoplankton community structure at station ALOHA (22˚45'N, 158˚W) during fall 1991, p. 58. Abstract of The Oceanography Society Pacific Basin Meeting, Honolulu, Hawaii, July 1994.

I.44.1994 Bingham, F.M. and B. Qiu. Interannual variability of surface and mixed layer properties observed in the Hawaii Ocean Time-series, p. 89. Abstract of The Oceanography Society Pacific Basin Meeting, Honolulu, Hawaii, July 1994.

I.45.1994 Bingham, F.M. and R. Lukas. Seasonal cycles of temperature, salinity and dissolved oxygen observed in the Hawaii Ocean Time-series, p. 90. Abstract of The Oceanography Society Pacific Basin Meeting, Honolulu, Hawaii, July 1994.

I.46.1994 Christian, J. Vertical fluxes of carbon and nitrogen at Station ALOHA, p. 61. Abstract of The Oceanography Society Pacific Basin Meeting, Honolulu, Hawaii, July 1994.

I.47.1994 Dore, J.E. and D.M. Karl. Nitrite distributions and dynamics at Station ALOHA, p. 60. Abstract of The Oceanography Society Pacific Basin Meeting, Honolulu, Hawaii, July 1994.

I.48.1994 Firing, E. Currents observed north of Oahu during the first five years of HOT, p. 90. Abstract of The Oceanography Society Pacific Basin Meeting, Honolulu, Hawaii, July 1994.

I.49.1994 Fujieki, L.A., D.V. Hebel, L.M. Tupas and D.M. Karl. Hawaii Ocean Time-series Data Organization and Graphical System (HOT-DOGS), p. 61. Abstract of The Oceanography Society Pacific Basin Meeting, Honolulu, Hawaii, July 1994.

I.50.1994 Hebel, D.V., F.P. Chavez, K.R. Buck, R.R. Bidigare, D.M. Karl, M. Latasa, M.E. Ondrusek, L. Campbell and J. Newton. Do GF/F filters underestimate particulate chlorophyll a and primary production in the oligotrophic ocean?, p. 62. Abstract of The Oceanography Society Pacific Basin Meeting, Honolulu, Hawaii, July 1994.

I.51.1994 Houlihan, T., J.E. Dore, L. Tupas, D.V. Hebel, G. Tien and D.M. Karl. Freezing as a method of preservation for seawater dissolved nutrient and organic carbon samples, p. 62. Abstract of The Oceanography Society Pacific Basin Meeting, Honolulu, Hawaii, July 1994.

I.52.1994 Kennan, S.C. and R. Lukas. Saline intrusions in the intermediate waters north of Oahu, p. 91. Abstract of The Oceanography Society Pacific Basin Meeting, Honolulu, Hawaii, July 1994.

I.53.1994 Letelier, R.M., J. Dore, C.D. Winn and D.M. Karl. Temporal variations in photosynthetic carbon assimilation efficiencies at Station ALOHA (22˚45'N; 158˚00'W), p. 60. Abstract of The Oceanography Society Pacific Basin Meeting, Honolulu, Hawaii, July 1994.

I.54.1994 Liu, H. and L. Campbell. Growth and grazing rates of Prochlorococcus and Synechococcus at Station ALOHA measured by the selective inhibitor technique, p. 59. Abstract of The Oceanography Society Pacific Basin Meeting, Honolulu, Hawaii, July 1994.

I.55.1994 Lukas, R. Interannual variability of Pacific deep and bottom waters observed in the Hawaii Ocean Time-series, p. 91. Abstract of The Oceanography Society Pacific Basin Meeting, Honolulu, Hawaii, July 1994.

I.56.1994 Lukas, R., F. Bingham and E. Firing. Seasonal-to-interannual variability observed in the Hawaii Ocean Time-series, p. 28. Abstract of The Oceanography Society Pacific Basin Meeting, Honolulu, Hawaii, July 1994.

I.57.1994 Tupas, L.M., B.N. Popp, D.V. Hebel, G. Tien and D.M. Karl. Dissolved organic carbon measurements at Station ALOHA measured by high temperature catalytic oxidation: Characteristics and variation in the water column, p. 63. Abstract of The Oceanography Society Pacific Basin Meeting, Honolulu, Hawaii, July 1994.

I.58.1994 Winn, C.D., F. T. Mackenzie, C. Carrillo and D.M. Karl. Air-sea carbon dioxide exchange at Station ALOHA, p. 58. Abstract of The Oceanography Society Pacific Basin Meeting, Honolulu, Hawaii, July 1994.

I.59.1994 Liu, H. and L. Campbell. Measurement of growth and mortality rate of Prochlorococcus and Synechococcus at Station ALOHA using a new selective inhibitor technique. Fifth International Phycological Congress, Qingdao, China, July 1994.

I.60.1994 Winn, C., F. T. Mackenzie, C. Carrillo, T. Westby and D.M. Karl. Air-sea carbon dioxide exchange at Station ALOHA, p. 112. Abstract of the American Society of Limnology and Oceanography 1994 Ocean Sciences Meeting, San Diego, California.

I.61.1994 Measures, C.I., J. Yuan and J.A. Resing. The rapid determination of iron in seawater at sub-nanomolar concentrations using in-line preconcentration and spectrophotometric detection. Sixth Winter Conference on Flow Injection Analysis, San Diego, CA.

I.62.1994 Measures, C.I., J. Yuan and J.A. Resing. Determination of iron in seawater using in-line preconcentration and spectrophotometric detection. Workshop on Iron Speciation and its Biological Activity, Bermuda Biological Station for Research, Bermuda.

I.63.1995 Cortés, M.Y. and H.R. Thierstein. Coccolithophore dynamics during 1994 at the JGOFS time series Station ALOHA, Hawaii. 5th International Conference on Paleoceanography, Halifax, Canada, Abstract, p. 121.

I.64.1995 Campos, M.L.A.M., T.D. Jickells, A.M. Farrenkopf and G.W. Luther, III. A comparison of dissolved iodine cycling at the Bermuda Atlantic Time Series station and Hawaii Ocean Time-series station. EOS, Transactions of the American Geophysical Union 76, S175.

I.65.1995 Yuan, J. Collecting iron samples from well mounted on CTD rosette. EOS, Transactions of the American Geophysical Union 76, S175.

I.66.1995 Michaels, A.F., D. Karl and A.H. Knap. Insights on ocean variability from the JGOFS time-series stations. Invited plenary lecture, The Oceanography Society Biennial Meeting, April 1995.

I.67.1995 Emerson, S., P. Quay, L. Tupas and D. Karl. Chemical tracers of productivity and respiration in the upper ocean at US JGOFS station ALOHA, 10th Anniversary JGOFS Science Conference, Villefranche, France, May 1995.

I.68.1995 Michaels, A.F., D. Karl and A.H. Knap. Insights on ocean variability from the JGOFS time-series stations. Invited lecture, 10th Anniversary JGOFS Science Conference, Villefranche, France, May 1995.

I.69.1995 Karl, D.M. Oceanic carbon cycle and global environmental change: A microbiological perspective. Invited plenary talk, 7th International Symposium on Microbial Ecology, Santos, Brazil, August 1995.

I.70.1995 Winn, C., D. Sadler and D.M. Karl. Carbon dioxide dynamics at the Hawaii JGOFS/WOCE time-series station. International Association for the Physical Sciences of the Oceans, Honolulu, Hawaii, August 1995.

I.71.1996 Campbell, L., H. Liu and H.A. Nolla. Picophytoplankton population dynamics at Station ALOHA, p. OS65. AGU-ASLO Ocean Sciences Meeting, San Diego, CA, February 1996.

I.72.1996 Christian, J.R., J.E. Dore and D.M. Karl. Mixing and nutrient fluxes at the US-JGOFS Station ALOHA ((22˚45'N, 158˚00'W), p. OS65. AGU-ASLO Ocean Sciences Meeting, San Diego, CA, February 1996.

I.73.1996 Dulaney, T.S. and L.R. Sautter. Sedimentation of planktonic foraminifera: Seasonal changes in shell flux north of Oahu, Hawaii, p. OS85. AGU-ASLO Ocean Sciences Meeting, San Diego, CA, February 1996.

I.74.1996 Emerson, S. Chemical tracers of biological processes: O2, Ar and N2 mass balance in the subtropical Pacific at the HOT station, p. OS85. AGU-ASLO Ocean Sciences Meeting, San Diego, CA, February 1996.

I.75.1996 Hebel, D.V., D.M. Karl, J.R. Christian, J.E. Dore, R.M. Letelier, L.M. Tupas and C.D. Winn. Seasonal and interannual variability in primary production and particle flux at Station ALOHA, p. OS85. AGU-ASLO Ocean Sciences Meeting, San Diego, CA, February 1996.

I.76.1996 Karl, D.M.. Alternation of N and P control of new and export production in the North Pacific gyre: A hypothesis based on the HOT program data set, p. OS86. AGU-ASLO Ocean Sciences Meeting, San Diego, CA, February 1996.

I.77.1996 Lawson, L.M. and E.E. Hofmann. Time series sampling and data assimilation in a simple marine ecosystem model, p. OS86. AGU-ASLO Ocean Sciences Meeting, San Diego, CA, February 1996.

I.78.1996 Lopez, M.D.G., Y. Zhu and M.E. Huntley. Space-time variability of zooplankton-sized particle concentrations at the Hawaii Ocean Time-series station (Station ALOHA), p. OS85. AGU-ASLO Ocean Sciences Meeting, San Diego, CA, February 1996.

I.79.1996 Quay, P.D. and H. Anderson. Organic carbon export rates in the subtropical N. Pacific, p. OS85. AGU-ASLO Ocean Sciences Meeting, San Diego, CA, February 1996.

I.80.1996 Richman, J.G., R.M. Letelier, M.R. Abbott and D. Pillsbury. Expandable optical mooring test at Station ALOHA (22˚45'N; 158˚00'W), p. OS64. AGU-ASLO Ocean Sciences Meeting, San Diego, CA, February 1996.

I.81.1996 Scharek, R., M. Latasa, D.M. Karl and R.R. Bidigare Diatom abundance and vertical flux at the US-JGOFS/WOCE Station "ALOHA" in the oligotrophic North Pacific gyre, p. OS85. AGU-ASLO Ocean Sciences Meeting, San Diego, CA, February 1996.

I.82.1996 Selph, K.E., M.R. Landry, R.J. Miller and H.A. Al-Mutairi. Temporal variability in the mesozooplankton community at ocean Station ALOHA, p. OS85. AGU-ASLO Ocean Sciences Meeting, San Diego, CA, February 1996.

I.83.1996 Tersol, V., S. Vink, J. Yuan and C.I. Measures. Variations in iron, aluminum and berylium concentrations in surface waters at Station ALOHA, p. OS65. AGU-ASLO Ocean Sciences Meeting, San Diego, CA, February 1996.

I.84.1996 Tupas, L.M., MP. Sampson and D.M. Karl. Stable nitrogen isotopic analysis of sinking particulate matter at the Hawaii Ocean Time-series site, p. OS86. AGU-ASLO Ocean Sciences Meeting, San Diego, CA, February 1996.

I.85.1996 Venrick, E.L. A comparison between the phytoplankton species from Station ALOHA and from the Climax region, p. OS65. AGU-ASLO Ocean Sciences Meeting, San Diego, CA, February 1996.

I.86.1996 Winn, C.D. Carbon dioxide dynamics at the Hawaii JGOFS/WOCE time-series station: Annual and interannual variability, p. OS64. AGU-ASLO Ocean Sciences Meeting, San Diego, CA, February 1996.

I.87.1996 Lukas, R. Low-frequency climate signals emerge in the Hawaii Ocean Time-series. WOCE Pacific Workshop. Hyatt Newporter, Newport Beach, CA, 19-23 August 1996.

I.88.1996 Santiago-Mandujano, F. Cold bottom water events observed in the Hawaii Ocean Time-series. WOCE Pacific Workshop. Hyatt Newporter, Newport Beach, CA, 19-23 August 1996.

I.89.1997 Lukas, R. Physical studies at the Hawaii Ocean Time-series (HOT) Station. Ocean Climate Time-Series Workshop. Johns Hopkins University, Baltimore, MD, 18-20 March 1997.

I.90.1997 Bird, D.F., R. Maranger and D.M. Karl. The importance of bacterial consumption by algae to marine systems. ASLO-Aquatic Sciences Meeting, Santa Fe, NM, February 1997.

I.91.1997 Karl, D.M., D.V. Hebel and L.M. Tupas. Biogeochemical studies at the Hawaii Ocean Time- series (HOT) station ALOHA. Joint GCOS GOOS WCRP Ocean Observations Panel for Climate (OOPC), GCOS Report No. 41.

I.92. 1998 Letelier, R.M., M.R. Abbott, M.H. Freilich, D.M. Karl, P.J. Flament and R. Lukas. Euphotic zone biogeochemical response to a wind-induced upwelling event in the North Pacific subtropical gyre. AGU-Ocean Sciences Meeting, San Diego, CA, February 1998.

I.93. 1998 Letelier, R.M. and D.M. Karl. The US-JGOFS Hawaii ocean Time-series (HOT) Program; What we have learned over the first decade. AGU-Ocean Sciences Meeting, San Diego, CA, February 1998.

I.94.1998 Karl, D. The subtropical North Pacific: New views on an old ocean. Ocean Optics XIV Meeting, Kailua-Kona, HI, November 1998.

I.95.1998 Ondrusek, M.E., R.R. Bidigare, D. M. Karl and K. Waters. Predictive models for estimating rates of primary production in the subtropical North Pacific Ocean. Ocean Optics XIV Meeting, Kailua-Kona, HI, November 1998.

I. 96.1999 Karl, D.M., K. Bjorkman, D. Hebel, T. Houlihan and L. Tupas. Seasonal and interannual variability in C-N-P stoichiometry of dissolved and particulate matter in the subtropical North Pacific Ocean. ASLO Aquatic Sciences meeting, Santa Fe, NM, February 1999.

I.97. 1999 Karner, M.B., L.T. Taylor, E.F. DeLong and D.M. Karl. Bacterial and archaeal distributions at the Hawaii Ocean Time-series Station, ALOHA, in the North Pacific Ocean. ASLO Aquatic Sciences meeting, Santa Fe, NM, February 1999.

II. Invited/Contributed Book Chapters and Refereed Publications

II.1.1990 Firing, E. and R.L. Gordon. Deep ocean acoustic Doppler current profiling. In: G. F. Appell and T. B. Curtin (eds.), Proceedings of the Fourth IEEE Working Conference on Current Measurements, pp. 192-201. IEEE, New York.

II.2.1990 Giovannoni, S.J., E.F. DeLong, T.M. Schmidt and N.R. Pace. Tangential flow filtration and preliminary phylogenetic analysis of marine picoplankton. Applied and Environmental Microbiology 56, 2572-2575.

II.3.1991 Chiswell, S. M. Dynamic response of CTD pressure sensors to temperature. Journal of Atmospheric and Oceanic Technology 8, 659-668.

II.41991 Karl, D.M., J.E. Dore, D.V. Hebel and C. Winn. Procedures for particulate carbon, nitrogen, phosphorus and total mass analyses used in the US-JGOFS Hawaii Ocean Time- Series Program. In: D. Spencer and D. Hurd (eds.), Marine Particles: Analysis and Characterization, pp. 71-77. American Geophysical Union, Geophysical Monograph 63.

II.5.1991 Karl, D.M., W.G. Harrison, J. Dore et al. Chapter 3. Major bioelements workshop report. In: D.C. Hurd and D.W. Spencer (eds.), Marine Particles: Analysis and Characterization, pp. 33-42. American Geophysical Union, Geophysical Monograph 63.

II.6.1991 Karl, D.M. and C.D. Winn. A sea of change: Monitoring the oceans' carbon cycle. Environmental Science & Technology 25, 1976-1981.

II.7.1991 Laws, E.A. Photosynthetic quotients, new production and net community production in the open ocean. Deep-Sea Research 38, 143-167.

II.8.1991 Sabine, C.L. and F.T. Mackenzie. Oceanic sinks for anthropogenic CO2. International Journal of Energy, Environment, Economics 1, 119-127.

II.9.1991 Schmidt, T.M., E.F. DeLong and N.R. Pace. Analysis of a marine picoplankton community by 16S rRNA gene cloning and sequencing. Journal of Bacteriology 173, 4371- 4378.

II.10.1992 Benner, R., J.D. Pakulski, M. McCarthy, J.I. Hedges and P.G. Hatcher. Bulk chemical characteristics of dissolved organic matter in the ocean. Science 255, 1561-1564.

II.11.1992 Chen, R. F. and J.L. Bada. The fluorescence of dissolved organic matter in seawater. Marine Chemistry 37, 191-221.

II.12.1992 Karl, D.M. The oceanic carbon cycle: Primary production and carbon flux in the oligotrophic North Pacific Ocean. In: Y. Oshima (ed.), Proceedings of the IGBP Symposium on Global Change, pp. 203-219. Japan National Committee for the IGBP, Waseda University, Tokyo, Japan.

II.13.1992 Karl, D.M., R. Letelier, D.V. Hebel, D.F. Bird and C.D. Winn. Trichodesmium blooms and new nitrogen in the North Pacific gyre. In: E. J. Carpenter et al. (eds.), Marine Pelagic Cyanobacteria: Trichodesmium and Other Diazotrophs, pp. 219-237. Kluwer Academic Publishers, Netherlands.

II.14.1992 Karl, D.M. and G. Tien. MAGIC: A sensitive and precise method for measuring dissolved phosphorus in aquatic environments. Limnology and Oceanography 37, 105-116.

II.15.1992 Quay, P.D., B. Tilbrook and C.S. Wong. Oceanic uptake of fossil fuel CO2: Carbon- 13 evidence. Science 256, 74-78.

II.16.1993 Anbar, A.D., R.A. Creaser, D.A. Papanastassiou and G.J. Wasserburg. Rhenium in seawater: Confirmation of generally conservative behavior. Geochimica et Cosmochimica Acta 56, 4099-4103.

II.17.1993 Campbell, L. and D. Vaulot. Photosynthetic picoplankton community structure in the subtropical North Pacific Ocean near Hawaii (station ALOHA). Deep-Sea Research 40, 2043- 2060.

II.18.1993 Coble, P.G., C.A. Schultz and K. Mopper. Fluorescence contouring analysis of DOC intercalibration experiment samples: a comparison of techniques. Marine Chemistry 41, 173-178.

II.19.1993 Emerson, S., P. Quay, C. Stump, D. Wilbur and R. Schudlich. Determining primary production from the mesoscale oxygen field. ICES Marine Science Symposium 197, 196-206.

II.20.1993 Hedges, J.I., B.A. Bergamaschi and R. Benner. Comparative analyses of DOC and DON in natural waters. Marine Chemistry 41, 121-134.

II.21.1993 Karl, D.M. Total microbial biomass estimation derived from the measurement of particulate adenosine-5'-triphosphate. In: P. F. Kemp, B. F. Sherr, E. B. Sherr and J. J. Cole (eds.), Current Methods in Aquatic Microbial Ecology, pp. 359-368. Lewis Publishers, Boca Raton.

II.22.1993 Karl, D.M., G. Tien, J. Dore and C.D. Winn. Total dissolved nitrogen and phosphorus concentrations at US-JGOFS Station ALOHA: Redfield reconciliation. Marine Chemistry 41, 203-208.

II.23.1993 Keeling, C.D. Lecture 2: Surface ocean CO2. NATO ASI Series I(15), 413-429.

II.24.1993 Letelier, R.M., R.R. Bidigare, D.V. Hebel, C.D. Winn and D.M. Karl. Temporal variability study of the phytoplankton community structure at the US-JGOFS Time-series Station ALOHA (22˚45'N, 158˚00'W) based on pigment analyses. Limnology and Oceanography 38, 1420-1437.

II.25.1993 Mopper, K. and C.A. Schultz. Fluorescence as a possible tool for studying the nature and water column distribution of DOC components. Marine Chemistry 41, 229-238.

II.26.1993 Selph, K.E., D.M. Karl and M.R. Landry. Quantification of chemiluminescent DNA probes using liquid scintillation counting. Analytical Biochemistry 210, 394-401.

II.27.1993 Sharp, J.H., E.T. Peltzer, M.J. Alperin, G. Cauwet, J.W. Farrington, B. Fry, D.M. Karl, J.H. Martin, A. Spitzy, S. Tugrul and C.A. Carlson. Procedures subgroup report. Marine Chemistry 41, 37-49.

II.28.1993 Winn, C.D., R. Lukas, D. Hebel, C. Carrillo, R. Letelier and D.M. Karl. The Hawaii Ocean Time-series program: Resolving variability in the North Pacific. In: N. Saxena (ed.), Recent Advances in Marine Science and Technology, pp. 139-150. Proceedings of the Pacific Ocean Congress (PACON).

II.29.1994 Baines, S.B., M.L. Pace and D.M. Karl. Why does the relationship between sinking flux and planktonic primary production differ between lakes and ocean? Limnology and Oceanography 39, 213-226.

II.30.1994 Björkman, K. and D.M. Karl. Bioavailability of inorganic and organic phosphorus compounds to natural assemblages of microorganisms in Hawaiian coastal waters. Marine Ecology Progress Series 111, 265-273.

II.31.1994 Campbell, L., H.A. Nolla and D. Vaulot. The importance of photosynthetic prokaryote biomass in the subtropical central North Pacific Ocean (Station ALOHA). Limnology and Oceanography 39, 954-961.

II.32.1994 Campbell, L., L.P. Shapiro and E.M. Haugen. Immunochemical characterization of the eukaryotic ultraplankton in the Atlantic and Pacific Oceans. Journal of Plankton Research 16, 35-51.

II.33.1994 Christian, J.R. and D.M. Karl. Microbial community structure at the U.S.-Joint Global Ocean Flux Study Station ALOHA: Inverse methods for estimating biochemical indicator ratios. Journal of Geophysical Research 99, 14,269-14,276.

II.34.1994 Karl, D.M. Accurate estimation of microbial loop processes and rates. Microbial Ecology 28, 147-150.

II.35.1994 Karl, D.M. and B.D. Tilbrook. Production and transport of methane in oceanic particulate organic matter. Nature 368, 732-734.

II.36.1994 Tupas, L.M., B.N. Popp and D.M. Karl. Dissolved organic carbon in oligotrophic waters: experiments on sample preservation, storage and analysis. Marine Chemistry 45, 207- 216.

II.37.1994 Winn, C.D., F.T. Mackenzie, C.J. Carrillo, C. L. Sabine and D.M. Karl. Air-sea carbon dioxide exchange in the North Pacific subtropical gyre: Implications for the global carbon budget. Global Biogeochemical Cycles 8, 157-163.

II.38.1994 Chiswell, S. Using an array of inverted echo sounders to measure dynamic height and geostrophic current in the North Pacific subtropical gyre. Journal of Atmospheric and Oceanic Technology 11, 1420-1430.

II.39.1995 Atkinson, M.A., F.I.M. Thomas, N. Larson, E. Terrill, K. Morita and C. Liu. A micro-hole potentiostatic oxygen sensor for oceanic CTDs. Deep-Sea Research 42, 761-771.

II.40.1995 Chavez, F.P., K.R. Buck, R.R. Bidigare, D.M. Karl, D. Hebel, M. Latasa, M. E. Ondrusek, L. Campbell and J. Newton. On the chlorophyll a retention properties of glass- fiber GF/F filters. Limnology and Oceanography 40, 428-433.

II.41.1995 Christian, J.R. and D.M. Karl. Bacterial exocellular enzymes in marine waters: activity ratios and temperature kinetics in three oceanographic provinces. Limnology and Oceanography 40, 1042-1049.

II.42.1995 Christian, J.R. and D.M. Karl. Measuring bacterial ectoenzyme activities in marine waters using mercuric chloride as a preservative and a control. Marine Ecology Progress Series 123, 217-224.

II.43.1995 Emerson, S., P.D. Quay, C. Stump, D. Wilbur and R. Schudlich. Chemical tracers of productivity and respiration in the subtropical Pacific Ocean. Journal of Geophysical Research 100, 15,873-15,887.

II.44.1995 Jones, D. R., D.M. Karl and E.A. Laws. DNA:ATP ratios in marine microalgae and bacteria: Implications for growth rate estimates based on rates of DNA synthesis. Journal of Phycology 31, 215-223.

II.45.1995 Karl, D.M. A reply to a comment by J.A. McGowan "HOT and the North Pacific gyre." Nature 378, 21-22.

II.46.1995 Karl, D.M., R. Letelier, D. Hebel, L. Tupas, J. Dore, J. Christian and C. Winn. Ecosystem changes in the North Pacific subtropical gyre attributed to the 1991-92 El Niño. Nature 373, 230-234.

II.47.1995 Liu, H., L. Campbell and M.R. Landry. Growth and mortality rates of Prochlorococcus and Synechococcus measured with a selective inhibitor technique. Marine Ecology Progress Series 116, 277-287.

II.48.1995 Maranger, R. and D.F. Bird. Viral abundance in aquatic systems: a comparison between marine and fresh waters. Marine Ecology Progress Series 121, 217-226.

II.49.1995 Sabine, C.L. and F.T. Mackenzie. Bank-derived carbonate sediment transport and dissolution in the Hawaiian Archipelago. Aquatic Geochemistry 1, 189-230.

II.50.1995 Sabine, C.L., F.T. Mackenzie, C. Winn and D.M. Karl. Geochemistry of particulate and dissolved inorganic carbon at the Hawaii Ocean Time-series station, ALOHA. Journal of Biogeochemical Cycles 9, 637-651.

II.51.1995 Sharp, J.H., R. Benner, L. Bennett, C.A. Carlson, S.E. Fitzwater, E.T. Peltzer and L.M. Tupas. Analyses of dissolved organic carbon in seawater: the JGOFS EqPac methods comparison. Marine Chemistry 48, 91-108.

II.52.1995 Thomas, F.I.M. and M.J. Atkinson. Field calibration of a microhole potentiostatic oxygen sensor for oceanic CTDs. Journal of Atmospheric and Oceanic Technology 12, 390-394.

II.53.1995 Thomas, F.I.M., S.A. McCarthy, J. Bower, S. Krothapalli, M.J. Atkinson and P. Flament. Response characteristics of two oxygen sensors for oceanic CTDs. Journal of Atmospheric and Oceanic Technology 12, 687-690.

II.54.1995 Tilbrook, B.D. and D.M. Karl. Methane sources, distributions and sinks from California coastal waters to the oligotrophic North Pacific gyre. Marine Chemistry 49, 51-64.

II.55.1995 Winn, C.D., L. Campbell, R. Letelier, D. Hebel, L. Fujieki and D.M. Karl. Seasonal variability in chlorophyll concentrations in the North Pacific subtropical gyre. Global Biogeochemical Cycles 9, 605-620.

II.56.1996 Andersen, R., R. Bidigare, M. Keller and M. Latasa. A comparison of HPLC pigment signatures and electron microscopic observations for oligotrophic waters of the North Atlantic and Pacific Oceans. Deep-Sea Research 43, 517-537.

II.57.1996 Atkinson, M., F. Thomas and N. Larson. Effects of pressure on oxygen sensors. Journal of Atmospheric and Oceanic Technology 13, 1267-1277.

II.58.1996 Bingham, F. and R. Lukas Seasonal cycles of temperature, salinity and dissolved oxygen observed in the Hawaii Ocean Time-series. Deep-Sea Research 43, 199-213.

II.59.1996 Campos, M. L., A. Farrenkopf, T. Jickells and G. Luther. A comparison of dissolved iodine cycling at the Bermuda Atlantic Time-series Study station and Hawaii Ocean Time-series station. Deep-Sea Research 43, 455-466.

II.60.1996 Chiswell, S. Intraseasonal oscillations at Station ALOHA, north of Oahu, Hawaii. Deep-Sea Research 43, 305-319.

II.61.1996 Dore, J.E., T. Houlihan, D.V. Hebel, G. Tien, L.M. Tupas and D.M. Karl. Freezing as a method of seawater preservation for the analysis of dissolved inorganic nutrients in seawater. Marine Chemistry 53, 173-185.

II.62.1996 Dore, J.E. and D.M. Karl. Nitrification in the euphotic zone as a source for nitrite, nitrate and nitrous oxide at Station ALOHA. Limnology and Oceanography 41, 1619-1628.

II.63.1996 Dore, J.E. and D.M. Karl. Nitrite distributions and dynamics at Station ALOHA. Deep-Sea Research 43, 385-402.

II.64.1996 Feller, R. J. and D.M. Karl. The National Association of Marine Laboratories: A connected web for studying long-term changes in US coastal and marine waters. Biological Bulletin 190, 269-277.

II.65.1996 Firing, E. Currents observed north of Oahu during the first 5 years of HOT. Deep-Sea Research 43, 281-303.

II.66.1996 Jones, D.R., D.M. Karl and E.A. Laws. Growth rates and production of heterotrophic bacteria and phytoplankton in the North Pacific subtropical gyre. Deep-Sea Research 43, 1567-1580.

II.67.1996 Karl, D.M., J.R. Christian, J.E. Dore, D.V. Hebel, R.M Letelier, L.M. Tupas and C.D. Winn. Seasonal and interannual variability in primary production and particle flux at Station ALOHA. Deep-Sea Research 43, 539-568.

II.68.1996 Karl, D.M. and A.F. Michaels. Preface: The Hawaiian Ocean Time-series (HOT) and the Bermuda Atlantic Time-series study (BATS). Deep-Sea Research 43, 127-128..

II.69.1996 Karl, D.M. and R. Lukas. The Hawaii Ocean Time-series (HOT) program: Background, rationale and field implementation. Deep-Sea Research 43, 129-156.

II.70.1996 Karl, D.M. and G. Tien. Temporal variability in dissolved phosphorus concentrations at Station ALOHA (22˚45'N, 158˚W). Marine Chemistry 56, 77-96.

II.71.1996 Kennan, S.C. and R. Lukas. Saline intrusions in the intermediate waters north of Oahu, Hawaii. Deep-Sea Research 43, 215-241.

II.72.1996 Latasa, M., R.R. Bidigare, M.E. Ondrusek and M.C. Kennicutt II. HPLC analysis of algal pigments: a comparison exercise among laboratories and recommendations for improved analytical performance. Marine Chemistry 51, 315-324.

II.73.1996 Lawson, L., Y. Spitz and E. Hofmann. Time series sampling and data assimilation in a simple marine ecosystem model. Deep-Sea Research 43, 625-651.

II.74.1996 Letelier, R.M., J.E. Dore, C.D. Winn and D.M. Karl. Temporal variations in photosynthetic carbon assimilation efficiencies at Station ALOHA. Deep-Sea Research 43, 467-490.

II.75.1996 Letelier, R.M. and D.M. Karl. The role of Trichodesmium spp. in the productivity of the subtropical North Pacific Ocean. Marine Ecology Progress Series 133, 263-273.

II.76.1996 Lukas, R. and F. Santiago-Mandujano. Interannual variability of Pacific deep and bottom waters observed in the Hawaii Ocean Time-series. Deep-Sea Research 43, 243-255.

II.77.1996 Mitchum, G. On using satellite altimetric heights to provide a spatial context for the Hawaii Ocean Time-series measurements. Deep-Sea Research 43, 257-280.

II.78.1996 Moyer, C.L., J.M. Tiedje, F.C. Dobbs and D.M. Karl. A computer-simulated restriction fragment length polymorphism analysis of bacterial small-subunit rRNA genes: Efficacy of selected tetrameric restriction enzymes for studies of microbial diversity in nature. Applied and Environmental Microbiology 62, 2501-2507.

II.791996 Roy-Barman, M., J.H. Chen and G.J. Wasserburg. 230Th-232Th systematics in the central Pacific Ocean: The sources and the fates of thorium. Earth and Planetary Science Letters 139, 351-363.

II.80.1996 Schudlich, R. and S. Emerson. Gas saturation in the surface ocean: The roles of heat flux, gas exchange and bubbles. Deep-Sea Research 43, 569-589.

II.811996 Anbar, A.D., G.J. Wasserburg, D.A. Papanastassiou and P.S. Andersson. Iridium in natural waters. Science 273, 1524-1528.

II.821996 De La Rocha, C.L. and M.A. Brzezinski. Purification, recovery, and laser-driven fluorination of silicon from dissolved and particulate silica for the measurement of natural stable isotope abundances. Analytical Chemistry 68, 3746-3750.

II.83.1997 Campbell, L., H. Liu, H.A. Nolla and D. Vaulot. Annual variability of phytoplankton and bacteria in the subtropical North Pacific Ocean at Station ALOHA during the 1991-1994 ENSO event. Deep-Sea Research 44, 167-192.

II.84.1997 Liu, H., L. Campbell and H.A. Nolla. Prochlorococcus growth rate and contribution to primary production in the equatorial and subtropical North Pacific Ocean. Aquatic Microbial Ecology 12, 39-42.

II.85.1997 Sansone, F.J., B.N. Popp and T.M. Rust. Stable carbon isotopic analysis of low-level methane in water and gas. Analytical Chemistry 69, 40-44.

II.86.1997 Troy, P.J., Y.H. Li and F.T. Mackenzie. Changes in surface morphology of calcite exposed to the oceanic water column. Aquatic Geochemistry 3, 1-20.

II.87.1997 Christian, J.R., M. R. Lewis and D.M. Karl. Vertical fluxes of carbon, nitrogen and phosphorus in the North Pacific subtropical gyre. Journal of Geophysical Research 102, 15,667-15,677.

II.88.1997 Karl, D.M., R. Letelier, L. Tupas, J. Dore, J. Christian and D. Hebel. The role of nitrogen fixation in biogeochemical cycling in the subtropical North Pacific Ocean. Nature 388, 533-538.

II.89.1997 Emerson, S., P. Quay, D. Karl, C. Winn, L. Tupas and M. Landry. Experimental determination of the organic carbon flux from open-ocean surface waters. Nature 389: 951-954.

II.90.1997 Winn, C.D., Y.H. Li, F.T. Mackenzie and D.M. Karl. Rising surface ocean total dissolved inorganic carbon at the Hawaii Ocean Time-series site. Marine Chemistry 60, 33-47.

II.91.1997 Karl, D.M. and K. Yanagi. Partial characterization of the dissolved organic phosphorus pool in the oligotrophic North Pacific Ocean. Limnology and Oceanography 42, 1398-1405.

II.92.1997 Karl, D.M. and F. C. Dobbs. Molecular approaches to microbial biomass estimation in the sea. Molecular Approaches to the Study of the Ocean (K. E. Cooksey, Ed.), pp. 29-89.

II.93.1997 Karl, D.M. Oceanic carbon cycle and global environmental change: A microbiological perspective. In: M. T. Martins (ed.), Progress in Microbial Ecology. Proceedings of Seventh International Symposium on Microbial Ecology, Santos, Sao Paulo, Brazil, 1995. Sociedade Brasileira de Microbiologia / International Committee of Microbial Ecology, Brazil, pp. 163-172.

II.94.1997 Letelier, R.M. and D.M. Karl. Trichodesmium spp. physiology and nutrient fluxes in the North Pacific subtropical gyre. Aquatic Microbial Ecology 15, 265-276.

II.95.1997 Karl, D.M. and G. Tien. Temporal variability in dissolved phosphorus concentrations in the subtropical North Pacific Ocean. Marine Chemistry 56, 77-96.

II.96. 1997 Benner, R., B. Biddanda, B. Black and M. McCarthy. Abundance, size distribution and stable carbon and nitrogen isotopic composition of marine organic matter isolated by tangential-flow ultrafiltration. Marine Chemistry 57, 243-263.

II.97.1997 Venrick, E.L. Comparison of the phytoplankton species composition and structure in the Climax area (1973-1985) with that of Station ALOHA (1994). Limnology and Oceanography 42, 1643-1648.

II.98. 1997 Lukas, R., F. Santiago-Mandujano and E. Firing. Long-term hydrographic variations observed in the Hawaii Ocean Time-series. in proceedings of the OOPC Ocean Climate Time-series Workshop, The Johns Hopkins University, Baltimore, Maryland, 18-20 March, 1997. GCOS Rept. No. 41, Annex XX.

II.99. 1998 Lukas, R. A Freshening of the Upper Pycnocline in the North Pacific Subtropical Gyre. In Proceedings of The International Symposium TRIANGLE '98, September 29-October 2, 1998. Japan Marine Science and Technology Center, Yokosuka, Japan, 294-303.

II.100.1998 Loisel, H. and A. Morel. Light scattering and chlorophyll concentration in case 1 waters: A reexamination. Limnology and Oceanography 43, 847-858.

II.101.1998 Karl, D.M., D.V. Hebel, K. Bjorkman and R.M. Letelier. The role of dissolved organic matter fluxes in the productivity of the oligotrophic North pacific Ocean. Limnology and Oceanography 43, 1270-1286.

II.102. 1998 Zehr, J.P., M.T. Mellon and S. Zani. New nitrogen-fixing microorganisms detected in oligotrophic oceans by amplification of nitrogenase (nifH) genes. Applied and Environmental Microbiology 64, 3444-3450.

II.103.1998 Dore, J.E., B.N. Popp, D.M. Karl and F.J. Sansone. A large source of atmospheric nitrous oxide from subtropical North Pacific surface waters Nature 396, 63-66.

II.104.1998 Thomson-Bulldis, A. and D. Karl. Application of a novel method for phosphate and non-phosphate phosphorus determinations in the oligotrophic North Pacific Ocean. Limnology and Oceanography, 43:1565-1577.

II.105.1999 Scharek, R., M. Latasa, D.M. KARL and R.R. Bidigare. Temporal variations in diatom abundance and downward vertical flux in the oligotrophic North Pacific gyre. Deep-Sea Research I, 46:1051-1075.

II.106.1999 Scharek, R., D.M. Karl and L. Tupas. Diatom sinking to the deep sea at U.S.-JGOFS/WOCE Station 'ALOHA' in the oligotrophic North Pacific Gyre. Marine Ecology Progress Series, 182: 55-67.

II.107. 1999 Karl, D.M. A sea of change: Biogeochemical variability in the North Pacific subtropical gyre. Ecosystems, 2:181-214.

II.108.1999 Calbet, A. and M.R. Landry. Mesozooplankton influences on the microbial food web: Direct and indirect trophic interactions in the oligotrophic open ocean. Limnology and Oceanography, 44:1370-1380.

II.109.1998 Michaels, A.F., D.M. Karl and A.H. Knap. Biogeochemical dynamics in oligotrophic oceans: The U.S. JGOFS time-series stations. In R. Hanson, H. Ducklow and J. Field (eds.), The Changing Carbon Cycle in the Sea, Cambridge Univ. Press, in press.

III. Submitted Papers

III.1.Li, Y. H., D. Karl, C. Winn, F. Mackenzie and K. Gans. Remineralization ratios and preformed nutrients in the subtropical North Pacific Gyre. Submitted to Aquatic Geochemistry.

III.2.Karl, D.M., R.R. Bidigare and R.M. Letelier. Climate-related, long-term changes in plankton community structure and productivity in the subtropical North Pacific Ocean. Submitted to Nature.

III.3.Ondrusek, M.E., R.R. Bidigare, K. Waters and D.M. Karl. Predictive models for estimating rates of primary production in the subtropical North Pacific Ocean. Submitted to Deep-Sea Research.

III.4.Lukas, R., F. Santiago-Mandujano , F. Bingham and A. Mantyla. Cold bottom water events observed in the Hawaii Ocean Time-series: Implications for vertical mixing. Submitted to Deep-Sea Research.

III.5.Hebel, D.V. and D.M. Karl. Seasonal, interannual and decadal variations in particulate matter concentrations and composition in the subtropical North Pacific Ocean. Submitted to Deep-Sea Research.

III.6.Donachie, S.P., J.R. Christian and D.M. Karl. Nutrient regulation of bacterial production and ectoenzyme activities in the subtropical North Pacific Ocean. Submitted to Deep-Sea Research.

III.7.Karl, D.M., K.M. Bjorkman, J.E. Dore, L. Fujieki, D.V. Hebel, T. Houlihan, R.M. Letelier and L.M. Tupas. Ecological nitrogen-to-phosphorus stoichiometry at Station ALOHA. Submitted to Deep-Sea Research.

III.8.Letelier, R.M., D.M. Karl, M.R. Abbott, P. Flament, M. Freilich, R. Lukas and T. Strub. Integration of research vessel, autonomous mooring and satellite time-series data to resolve biogeochemical variability in the North Pacific subtropical gyre. Submitted to Journal of Geophysical Research.

III.9.Emerson, S., J. Abell, C. Stump and D. Karl. The marine carbon pump: Mechanisms of phosphorus supply to the surface subtropical oceans. Submitted to Science.

III.10.Bjorkman, K., A.L. Thomson-Bulldis and D.M. Karl. Phosphorus dynamics in the North Pacific subtropical gyre. Submitted to Aquatic Microbial Ecology.

III.11.Ostrom, N.E., M.E. Russ, B. Popp, T.M. Rust and D.M. Karl. Mechanisms of N2O production in the subtropical North Pacific based on determinations of the isotopic abundances of N2O and O2. Submitted to Chemosphere.

III.12.Lukas, R. Freshening of the upper pycnocline near Hawaii. Submitted to Science.

III.13. Bell, J., Betts, J. Boyle, E. MITESS: a Moored In-situ Trace Elemental Serial Sampler for Deep Sea Moorings. Submitted to Deep-Sea Research.

IV. Theses and Dissertations

IV.1.1992 Sabine, C. L. Geochemistry of particulate and dissolved inorganic carbon in the central North Pacific. Ph.D. Dissertation, May 1992

IV.2.1993 Kennan, S. Variability of the intermediate water north of Oahu. M.S. Thesis, December 1993.

IV.3.1994 Letelier, R. M. Studies on the ecology of Trichodesmium spp. (Cyanophyceae) in the central North Pacific gyre. Ph.D. Dissertation, April 1994.

IV.4.1994 Liu, H. B. Growth and mortality rates of Prochlorococcus and Synechococcus measured by a selective inhibitor technique. M.S. Thesis, May 1994.

IV.5.1995 Dore, J. E. Microbial nitrification in the marine euphotic zone: Rates and relationships with nitrite distributions, recycled production and nitrous oxide generation. Ph.D. Dissertation, May 1995.

IV.6.1995 Christian, J. R. Biochemical mechanisms of bacterial utilization of dissolved and particulate organic matter in the upper ocean. Ph.D. Dissertation, December 1995.

V. Data Reports and Manuals

V.1.1990 Karl, D.M., C.D. Winn, D.V. W. Hebel and R. Letelier. Hawaii Ocean Time-series Program Field and Laboratory Protocols, September 1990. School of Ocean and Earth Science and Technology, Univ. of Hawaii, Honolulu, HI, 72 pp.

V.2.1990 Collins, D. J., W. J. Rhea and A. Van Tran. Bio-optical profile data report: HOT-3. National Aeronautics and Space Administration JPL Publ. #90-36.

V.3.1990 Chiswell, S., E. Firing, D. Karl, R. Lukas and C. Winn. Hawaii Ocean Time-series Program Data Report 1: 1988-1989. SOEST Tech. Report 90-1, School of Ocean and Earth Science and Technology, Univ. of Hawaii, Honolulu, HI, 269 pp.

V.4.1992 Winn, C., S. Chiswell, E. Firing, D. Karl and R. Lukas. Hawaii Ocean Time-series Program Data Report 2: 1990. SOEST Tech. Report 92-1, School of Ocean and Earth Science and Technology, Univ. of Hawaii, Honolulu, HI, 175 pp.

V.5.1993 Winn, C., R. Lukas, D. Karl and E. Firing. Hawaii Ocean Time-series Program Data Report 3: 1991. SOEST Tech. Report 93-3, School of Ocean and Earth Science and Technology, Univ. of Hawaii, Honolulu, HI, 228 pp.

V.6.1993 Tupas, L., F. Santiago-Mandujano, D. Hebel, R. Lukas, D. Karl and E. Firing. Hawaii Ocean Time-series Program Data Report 4: 1992. SOEST Tech. Report 93-14, School of Ocean and Earth Science and Technology, Univ. of Hawaii, Honolulu, HI, 248 pp.

V.7.1994 Tupas, L., F. Santiago-Mandujano, D. Hebel, E. Firing, F. Bingham, R. Lukas and D. Karl. Hawaii Ocean Time-series Program Data Report 5: 1993. SOEST Tech. Report 94-5, School of Ocean and Earth Science and Technology, Univ. of Hawaii, Honolulu, HI, 156 pp.

V.8.1994 Voss, C. I. and W. W. Wood Synthesis of geochemical, isotopic and groundwater modeling analysis to explain regional flow in a coastal aquifer of Southern Oahu, Hawaii. In: Mathematical Models and Their Applications to Isotope Studies in Ground-water Hydrology, pp. 147-178, International Atomic Energy Agency, Vienna, Austria.

V.9.1995 Tupas, L., F. Santiago-Mandujano, D. Hebel, E. Firing, R. Lukas and D. Karl. Hawaii Ocean Time-series Program Data Report 6: 1994. SOEST Tech. Report 95-6, School of Ocean and Earth Science and Technology, Univ. of Hawaii, Honolulu, HI, 199 pp.

V.10.1996 Karl, D., L. Tupas, F. Santiago-Mandujano, C. Nosse, D. Hebel, E. Firing and R. Lukas. Hawaii Ocean Time-series Program Data Report 7: 1995. SOEST Tech. Report 96-9, School of Ocean and Earth Science and Technology, Univ. of Hawaii, Honolulu, HI, 228 pp.

V.11.1997 Tupas, L., F. Santiago-Mandujano, D. Hebel, C. Nosse, L. Fujieki, E. Firing, R. Lukas and D. Karl. Hawaii Ocean Time-series Program Data Report 8: 1996. SOEST Tech. Report 97-3, School of Ocean and Earth Science and Technology, Univ. of Hawaii, Honolulu, HI, 296 pp.

V.12.1998 Tupas, L., F. Santiago-Mandujano, D. Hebel, C. Nosse, L. Fujieki, R. Lukas and D. Karl. Hawaii Ocean Time-series Program Data Report 9: 1997. SOEST Tech. Report 98-3, School of Ocean and Earth Science and Technology, Univ. of Hawaii, Honolulu, HI, 159 pp.

VI. Newsletters

VI.1.1989 Karl, D.M. Hawaiian Ocean Time-series program: It's HOT. GOFS Newsletter 1(2), 1-3.

VI.2.1990 Karl, D.M. HOT Stuff: An update on the Hawaiian Ocean Time-series program. US JGOFS Newsletter 2(1), 6,9.

VI.3.1990 Karl, David M. HOT Stuff: Rescue at sea. US JGOFS Newsletter 2(2), 8.

VI.4.1991 Karl, D.M. HOT Stuff: Retrospect and prospect. US JGOFS Newsletter 2(3), 10.

VI.5.1991 Karl, D.M. HOT Stuff: Hectic spring schedule keeps HOT team hustling. US JGOFS Newsletter 2(4), 9-10.

VI.6.1991 Lukas, R. and S. Chiswell. Submesoscale water mass variations in the salinity minimum of the North Pacific. WOCE Notes, 3(1), 6-8.

VI.7.1992 Karl, D.M. Hawaii Time-series program: Progress and prospects. US JGOFS Newsletter 3(4), 1,15.

VI.8.1992 Michaels, A. F. Time-series programs compare results, methods and plans for future. US JGOFS Newsletter 4(1), 7,9.

VI.9.1992 Winn, C. W. HOT program builds time-series set of carbon measurements for central Pacific. US JGOFS Newsletter 4(2), 7.

VI.10.1992 Dickey, T. D. Oversight committee reviews time-series programs, issues recommendations. US JGOFS Newsletter 4(2), 14-15.

VI.11.1992 Firing, E. and P. Hacker. ADCP results from WHP P16/P17. WOCE Notes, 4(3), 6- 12.

VI.12.1992 Chiswell, S. Inverted echo sounders at the WOCE deep-water station. WOCE Notes, 4(4), 1, 3-6.

VI.13.1993 Karl, D.M. HOT Stuff: The five-year perspective. US JGOFS Newsletter 5(1), 6,15.

VI.14.1994 Karl, D.M. HOT Stuff: Surprises emerging from five years' worth of data. US JGOFS Newsletter 5(4), 9-10.

VI.15.1994 Tupas, L. M. Euphotic zone nitrate variability in the central North Pacific gyre at the Hawaii Ocean Time-series Station ALOHA. International WOCE Newsletter 17, 21-23.

VI.16.1994 Lukas, R. HOT results show interannual variability of Pacific Deep and Bottom waters. WOCE Notes 6(2), 1, 3, 14-15.

VI.17.1995 Karl, D.M. HOT and COLD: A trapper's tale of two oceans. US JGOFS Newsletter 6(2): 7, 15.

VI.18.1995 Karl, D.M. HOT Stuff: New hypotheses and projects evolve from growing data set. US JGOFS Newsletter 7(1): 11.

VI.19.1996 Winn, C.D. and P. G. Driscoll. Hawaii Time-series data reveal rising ocean CO2 levels. US JGOFS Newsletter 7(4): 7-8.

VI.20.1996 Karl, D.M. The Hawaii Ocean Time-series study: Still HOT at 75. US JGOFS Newsletter 7(4): 8-9.

VI.21.1997 Karl, D.M. HOT scientists deploy mooring at Station ALOHA. US JGOFS Newsletter 8(2): 4.

VI.22. 1997 Karl, D.M. Ocean time-series meetings explore new collaboration for future. US JGOFS Newsletter 8(3): 15.

VI.23.1998 Karl, D.M. The changing sea: Long-term biogeochemical variability in the subtropical North pacific. US JGOFS Newsletter 9(3): 7-9.

VI.24.1999 Karl, D.M. Wave goodbye: HOT flagship retires from UNOLS fleet. US JGOFS Newsletter 10(1): 6.

VII. HOT symposiums

VII.1.Presentations from the "HOT Program: Progress and Prospectus" symposium, 3-4 June 1992, East-West Center, Honolulu, HI

Campbell, L. Bacterial numbers by flow cytometry: A new approach

Chiswell, S. Results from the inverted echo sounder network

Christian, J. Biomass closure in the epipelagic zone

Christian, J. Exoenzymatic hydrolysis of high molecular weight organic matter

Dore, J. Annual and short-term variability in the distribution of nitrite at the US-JGOFS time-series station ALOHA

Dore, J. and D. Hebel. Low-level nitrate and nitrite above the nutricline at Station ALOHA

Firing, E. Ocean currents near ALOHA

Hebel, D., R. Letelier and J. Dore. Evaluation of the depth dependence and temporal variability of primary production at Station ALOHA

Hebel, D., R. Letelier and J. Dore. Past and present dissolved oxygen trends, methodology, and quality control during the Hawaii Ocean Time series

Hebel, D. and U. Magaard. Structure and temporal variability in biomass estimates at Station ALOHA

Houlihan, T. and D. Hebel. Organic and inorganic nutrients: Water column structure and usefulness in time-series analysis

Karl, D. Carbon utilization in the mesopelagic zone: AOU-DOC relationships

Karl, D. HOT/JGOFS program objectives: A brief overview

Karl, D. P-control of N2 fixation: An ecosystem model

Karl, D. Primary production and particle flux

Karl, D. et al. Review and re-assessment of core measurements: Suggestions for refinement and improvement

Karl, D. and G. Tien. Low-level SRP above the nutricline at Station ALOHA

Karl, D., L. Tupas, G. Tien and B. Popp. "High-temperature" DOC: Pools and implications

Karl, D., K. Yanagi and K. Bjorkman. Composition and turnover of oceanic DOP

Letelier, R. Temporal variability of algal accessory pigments at Station ALOHA: What does it tell about the phytoplankton community structure at the DCML?

Letelier, R. and D. Hebel. Evaluation of fluorometric and HPLC chlorophyll a measurements at Station ALOHA

Letelier, R. and F. Santiago-Mandujano. Wind, sea surface temperature and significant wave height records from NDBC buoy #51001 compared to ship observations at Station ALOHA

Lukas, R. Water mass variability observed in the Hawaii Ocean Time-series

Sadler, D., C. Winn and C. Carrillo. Time-series measurements of pH: A new approach for HOT

Schudlich, R. Upper ocean gas modeling at Station ALOHA

Winn, C. DIC variability

Winn, C. and C. Carrillo. DIC and alkalinity profiles and elemental ratios

VII.2.Presentations from the "HOT Golden Anniversary Science Symposium," 16 November 1993, East-West Center, Honolulu, HI

Bingham, F. M. The oceanographic context of HOT

Campbell, L., H. Nolla, H. Liu and D. Vaulot. Phytoplankton population dynamics at the Hawaii Ocean Time series Station ALOHA

Campbell, L., H. Nolla and D. Vaulot. The importance of Prochlorococcus to community structure in the central North Pacific Ocean

Christian, J. Vertical fluxes of carbon and nitrogen at Station ALOHA

Dore, J. Nitrate diffusive flux cannot support new production during quiescent periods at Station ALOHA

Dore, J. Nitrification in lower euphotic zone at Station ALOHA: Patterns and significance

Firing, E. The north Hawaiian ridge current and other flows near ALOHA

Hebel, D. Temporal distribution, abundance and variability of suspended particulate matter (particulate carbon, nitrogen and phosphorus) at Station ALOHA -- Observations of a seasonal cycle

Karl, D., D. Hebel, L. Tupas, J. Dore and C. Winn. Station ALOHA particle fluxes and estimates of export production

Karl, D.M., R. Letelier, L. Tupas, J. Dore, D. Hebel and C. Winn. N2 fixation as a contributor to new production at Station ALOHA

Karl, D.M., G. Tien and K. Yanagi. Phosphorus dynamics at Station ALOHA

Kennan, S. C. Possibilities for stirring along the Hawaiian ridge

Krothapalli, S., Y. H. Li and F. T. Mackenzie. What controls the temporal variability of carbon flux at Station ALOHA?

Letelier, R. M. Inorganic carbon assimilation at Station ALOHA: Possible evidence of a change in carbon fluxes

Letelier, R. M. Spatial and temporal distribution of Trichodesmium sp. at Station ALOHA: How important are they?

Liu, H. and L. Campbell. Measurement of growth and mortality rates of Prochlorococcus and Synechococcus at Station ALOHA using a new selective inhibitor technique

Lukas, R. and F. Bingham. Annual and interannual variations of hydrographic properties observed in the Hawaii Ocean Time-series (HOT)

Lukas, R., F. M. Bingham and A. Mantyla An anomalous cold event in the bottom water observed at Station ALOHA

Moyer, C. L., L. Campbell, D.M. Karl and J. Wilcox. Restriction fragment length polymorphism (RFLP) and DNA sequence analysis of PCR-generated clones to assess diversity of picoeukaryotic algae in the subtropical central North Pacific Ocean (Station ALOHA)

Polovina, J. J. and D. R. Kobayashi. HOT and Hawaii's fisheries landings: Complementary or independent time-series?

Sadler, D. Time series measurement of pH at Station ALOHA

Smith, C. R., D. J. DeMaster, R. H. Pope, S. P. Garner, D. J. Hoover and S. E. Doan. Seabed radionuclides, bioturbation and benthic community structure at the Hawaii Ocean Time-series Station ALOHA

Tupas, L. M., B. N. Popp and D.M. Karl. Dissolved organic carbon in oligotrophic waters: Experiments on sample preservation, storage and analysis

Winn, C.D. Air-sea carbon dioxide exchange at Station ALOHA

Yuan, J. and C. I. Measures. Sampling and analysis of dissolved iron

VII.3.Presentations from the "HOT-75 Commemorative Science Symposium," 9 September 1996, East-West Center, Honolulu, HI

Atkinson, M. A Potentiostatic, Solid-state Oxygen Sensor for Oceanic CTDs

Bidigare, R., M. Latasa, R. Andersen and M. Keller. A Comparison of HPLC Pigment Signatures and Electron Microscopic Observations for Oligotrophic Waters of the North Atlantic and North Pacific Oceans

Campbell, L., H. Liu, H. Nolla and D. Vaulot. Annual Variability of Phytoplankton and Bacteria in the Subtropical North Pacific Ocean at Station ALOHA during the 1991-1994 ENSO Event

Christian, J., M. Lewis and D. Karl. Vertical Fluxes of Carbon, Nitrogen and Phosphorus at the US-JGOFS Time-Series Station ALOHA

Dore, J. and D. Karl. Nitrification, New Production and Nitrous Oxide at Station ALOHA

Ducklow, H. Joint Global Ocean Flux Study -- Vision and Progress

Emerson, S., C. Stump and D. Wilber. Inert Gases as Tracers of Diapycnal Mixing in the Upper Ocean

Firing, E. Currents in the Vicinity of Station ALOHA: An Update

Fujieki, L. HOTDOGS: A New Tool for HOT Program Data Base Analysis and Presentation

Hebel, D., L. Tupas and D. Karl. The Importance of Organic Exudates in the Measurement of Oligotrophic Ocean Primary Productivity

Karl, D., D. Hebel and L. Tupas. Regionalization of Station ALOHA

Karl, D., G. Tien, K. Björkman, K. Yanagi, R. Letelier, A. Colman and A. Thomson. The "Forgotten" Open Ocean P-Cycle

Karl, D., L. Tupas, D. Hebel, R. Letelier, J. Christian and J. Dore. Station ALOHA N-Cycle: The Case for N2 Fixation

Landry, M., K. Selph and H. Al-Mutairi. Seasonal and Diurnal Variability of the Mesozooplankton Community at Ocean Station ALOHA

Letelier, R. and M. Abbott. Effects of a Subsurface Trichodesmium spp. Bloom on the Optical Reflectance Measured in the Upper 150 m of the Water Column in the North Pacific Subtropical Gyre

Liu, H., L. Campbell and H. Nolla. Prochlorococcus Growth Rate and Daily Variability at Station ALOHA

Lopez, M. and M. Huntley. Particle Concentrations at the Hawaii Ocean Time-series Station (Station ALOHA) Measured with an Optical Plankton Counter

Michaels, A. and A. Knap. The Bermuda Atlantic Time-Series Study (BATS): A View from the "Other" Ocean

Nolla, H., J. Kirshtein, M. Landry, D. Karl, L. Campbell and D. Pence. Flow Cytometry Correction Factors for Enumeration of Heterotrophic Bacteria and Phytoplankton

Quay, P. and H. Anderson. A Dissolved Inorganic Carbon Budget at Station ALOHA

Santiago-Mandujano, F. and R. Lukas. Cold Bottom Water Events Observed in the Hawaii Ocean Time-Series: Modelling and Implications for Vertical Mixing

Scharek, R., M. Latasa, D. Karl and R. Bidigare. Vertical Flux of Diatoms at the JGOFS/WOCE Station ALOHA

Smith, C., R. Miller, R. Pope and D. DeMaster. Seafloor Inventories of Pb-210, Th-234 and Benthic Biomass as Proxies for Deep POC Flux: Placing Export Production at the HOT Station in a General Oceanic Context

Tien, G., D. Pence and D. Karl. Hydrogen Peroxide Measurements at Station ALOHA

Tupas, L., G. Tien, D. Hebel and D. Karl. Dissolved Organic Carbon Dynamics in the Upper Water Column at Station ALOHA

Vink, S., K. Falkner, V. Tersol, J. Yuan and C. Measures. Variations in Iron, Aluminum, Beryllium and Barium Concentrations in Surface Waters at Station ALOHA

Winn, C. Secular Changes in Inorganic Carbon Parameters at HOT and BATS

8. DATA AVAILABILITY AND DISTRIBUTION

8.1 Hard Copies

Data collected by HOT program scientists are made available to the oceanographic community in various ways as soon after processing as possible. The complete data set, containing data collected since year 1 of the HOT program (1988), as well as 2 dbar averaged CTD data, are available from two sources. The first is through the National Oceanographic Data Center. The second source is from the HOT data base residing in a workstation at the University of Hawaii, and may be accessed using anonymous ftp on the Internet or the World Wide Web (www). Access via ftp or through the web is described in more detail below. Details of each web page are described in the section 8.3.

8.2 File Transfer Protocol

In order to maximize ease of access, the data are in ASCII files. File names are chosen so that they may be copied to DOS machines without ambiguity. (DOS users should be aware that Unix is case-sensitive, and Unix extensions may be longer than 3 characters.)

The data are in a subdirectory called /***pub/hot.*** More information about the data base is given in several files called ***Readme.**** at this level. The file ***Readme.first*** gives general information on the data base; we encourage users to read it first.

The following is an example of how to use ftp to obtain HOT data. The user's command are denoted by bold italicized text. The workstation's Internet address is ***mana.soest.hawaii.edu***, or ***128.171.154.9*** (either address should work). All information, except optical data, reside at this address. Optical data are stored at ***hahana.soest.hawaii.edu***, or ***128. 171. 154. 13***.

1.At the Prompt >, type ***ftp 128.171.154.9*** or ***ftp mana.soest.hawaii.edu***.

2.When asked for your login name, type ***anonymous***.

3.When asked for a password, type ***your email address***.

4.To change to the HOT database, type ***cd /pub/hot***. To view files type ***ls***. A directory of files and subdirectories will appear.

5a.To obtain information about the database type ***get Readme.first***. This will transfer an ASCII file to your system. Use any text editor to view it.

5b.To obtain a list of publications, type ***cd publication-list*** then ***get hotpub.lis***.

5c.To obtain the HOT Field and Laboratory Protocols manual, type ***cd protocols*** then ***get 1142.asc***.

5d.To obtain CTD data, type ***cd ctd/hot-#***, where # is the HOT cruise of interest, then type ***mget *.ctd*** to transfer all the cruise CTD files to your system.

5e.To obtain water column data, type ***cd water***, then ***get <filename>*** where the filename is hot#.gof (JGOFS data) or hot#.sea (WOCE data) and # is the HOT cruise of interest.

6.To exit type ***bye***.

7.Data on optical parameters are located on another server. To obtain light data, at the prompt type ***ftp 128.171.154.13*** or ***ftp hahana.soest.hawaii.edu*** then follow steps 2 to 4.

8.3 World Wide Web

The Hawaii Ocean Time-series Program maintains a site on the world wide web where data and information about the program and its activities can easily be accessed over the Internet. The address is http://hahana.soest.hawaii.edu/hot/hot.html. This web page is the springboard from which the homepages of the WOCE and JGOFS components are accessible. Regardless of which site is accessed, there is only one common data base which is referred to by both components. The first half of the most recent year's data is usually available by July and the second half by January the following year with certain quality control caveats. All data are quality controlled by around April of the following year. Down loading of data is through ftp but the web pages provide a more detailed means of access.

8.3.1 HOT-WOCE Homepage

The World Ocean Circulation Experiment component of the HOT program maintains a web page at http://www.soest.hawaii.edu/HOT_WOCE. This web page includes (underlined items provide access to the specified section):

- Introduction:
    - HOT objectives
    - Site location
    - Observations description
    - HOT-WOCE Hydrographic sampling Procedures Manual
- Cruise Dates and Summaries:
    - Summaries of cruise's CTD station and cast
    - Chief Scientist's Reports
- Data description and Transfer:
    - Current status of HOT database
    - Data format information
    - Data transfer (FTP)
- WOCE Highlights:

Color contour of HOT time-series

Abstracts and figures of published papers from current research

Poster: Ocean Climate Variations in HOT

- Personnel:

  The people that make the WOCE component of HOT possible

Accessing data files from the HOT-WOCE site can be accomplished by going to the Data description and transfer section. This section includes 1) data format and transfer information and 2) ftp data guides to (underlined items provide access to the specified section or operation):

- Current data status
- CTD data
- Bottle data
- Cruise summary
- ADCP data
- XBT data
- Meteorological observations
- Inverted Echo Sounder

8.3.2 HOT-JGOFS Homepage

The Joint Global Ocean Flux Study component of the HOT program maintains a web page at http://hahana.soest.hawaii.edu/hot/hot_jgofs.html. This web page includes (underlined items provide access to the specified section):

What's new (and updated)

Overview

- Introduction

  Ancillary Projects Supported by HOT

  Location of the HOT Water Column and Bottom Stations

  Parameters Measured

- Cruise Schedules and Reports

- Principal Investigators and Staff

  Past Cruise Participants

- HALE ALOHA - physical/biogeochemical mooring

Pictures of the Deployment
Mooring Positions
Bottom Topography
Results

- Special Topics and Events

  Deep-Sea Research Special Volume
  HOT-75 Commemorative Science Symposium

Data Links

- Interactive Access to HOT Data (HOT-DOGS)
- Request sample acquisition &/or Cruise Participation
- Analytical Methods and Results
- Current Data Trends
- References

  Field and Laboratory Protocols
  Publications

8.3.2.1 Data Access.

Accessing of data through the HOT-JGOFS can be accomplished by going to the Analytical Methods and Results section. This section includes:

Status & Summaries

- Current Status of the HOT data base
- Corrections
- Cruise summaries

Methods and Results

- Hydrography

  (includes pressue, temperature, conductivity, oxygen, fluorescence and beam transmission)
- Biogeochemistry

  (includes salinity, oxygen, dissolved inorganic carbon, titration alkalinity, pH, dissolved inorganic nutrients, dissolved organic nutrients, low-level nutrients, particulate matter, pigments, ATP)
- Primary Production

- Particle Flux
- ADCP Measurements
- Meteorology
- Light Measurements
- XBT
- Buoy and shipboard Observations
- Inverted Echo Sounder Observations
- Bottom Moored Sediment Traps
- Macrozooplankton
- Thermosalinograph
- Endeco Towfish

8.3.2.2 HOT-DOGS.

HOT-DOGS is the acronym for HOT Data Organizational and Graphical System. HOT-DOGS is a Matlab based program that displays HOT data in a graphical format, as depth profiles or contour plots, or the numerical data for each parameter measured. All figures can be printed as hard copies or files. In addition to its graphical capabilities, HOT-DOGS provides a means of downloading data of selected parameters during specific years of the program. The program allows the user to perform the following:

Data Extraction

- Bottle
- Particle Flux
- Primary Production

Display (vertical water column)

- Bottle
- CTD
- HPLC Pigments
- Particle Flux
- Primary Production

Standard Depths (vertical water column)

- Bottle
- HPLC Pigments
- Primary Production

Time-series

- Bottle
- HPLC
- Particle Flux
- Primary Production

An advanced version of HOT-DOGS is available but at present only operable in the HOT-JGOFS workstation. This version can do more sophisticated graphical presentations such as contour plots. This software can also do graphical presentations of other JGOFS data bases such as the Bermuda Atlantic Time-series and the JGOFS process studies data bases. Development is underway to make the advanced version available through the world-wide web.